A Zebrafish Model of Ataxia Telangiectasia

by

Mirinda Jane Tattan

A thesis submitted to the University of Sheffield for the degree of Doctor of Philosophy (PhD)

Sheffield Institute of Translational Neuroscience

March 2021

Abstract

Ataxia-Telangiectasia is a life-limiting, neurodegenerative disorder, phenotypically characterised by ataxia, infertility, increased sensitivity to ionising radiation, and an increased incidence of cancers, particularly lymphomas. AT is caused by recessively inherited loss of function mutations in the ATM gene, the product of which primarily functions as a protein kinase that is activated in response to DNA damage. Activated ATM initiates DNA repair, or directs the cell towards apoptosis. While there are currently a number of rodent models that exhibit many of the disease phenotypes, they are not suitable for high throughput screening studies. Therefore, we propose a zebrafish model. Using CRISPR/Cas9, zebrafish with a 5 bp deletion in exon 6 of the ATM gene have been generated (ATM^{sh477}). This results in a frameshift mutation, leading to a predicted premature stop codon. ATM^{sh477} homozygous zebrafish are viable, and have no obvious behavioural abnormalities at the larval, juvenile or adult stages. Clutches of these ATM$^{sh477/sh477}$ zebrafish have abnormal sex ratios with all observed ATM null fish being male. These ATM^{sh477} males are also infertile, a key phenotype shared with AT patients and rodent models. Investigations into this infertility reveal that ATM$^{sh477/sh477}$ zebrafish have atypical testes that contain primarily immature spermatogenic cells. Histological sections of the testes also show them to be neoplastic, containing irregular growth of Sertoli cells (support cells) and disorganisation of the seminiferous tubules. However, ATM$^{sh477/sh477}$ zebrafish exhibit no increased sensitivity to ionising radiation or apparent deficiency in their DNA damage response.

Declaration

I, Mirinda Jane Tattan, confirm that this thesis is my own work and that this work has not previously been presented for an award at this, or any other university. Where work has been performed in collaboration or with the help of someone, it is stated in the text. In short and for clarification;

- Generation of CRIPSR/Cas9 ATM^{sh477} zebrafish was carried out by Dr Ringaile Zaksauskaite (Department of Molecular Biology and Biotechnology), under the supervision of Professor Sherif El-Khamisy (Department of Molecular Biology and Biotechnology) and Dr Freek van Eeden (Department of Biomedical Science).

- Quantification of γH$_2$AX foci from whole mount immunofluorescence of zebrafish larvae with a custom script was carried out by Dr Victor Alfred (Sheffield Institute of Translational Neuroscience).

- Identification of the neoplasia cell type in histological sections of adult zebrafish testes was carried out in collaboration with Dr Clare Muir (Department of Infection, Immunity & Cardiovascular Disease) and Dr Jonathan Griffin (Department of Molecular Biology and Biotechnology).

Dedication

This thesis is dedicated to memory of my late mother, Antoinette Tattan. Her unwavering support and enthusiasm for my education throughout my whole life cannot be overstated. This would have made her proud.

Acknowledgements

First, I would like to sincerely thank my supervisor Dr Andrew Grierson for the opportunity to complete a PhD. I am extremely grateful for the time, commitment and guidance he has shown me over the past 4 years. I would also like to thank Professor Marios Hadjivassiliou for his expertise and encouragement.

Next I would like to thank and recognise Dr Ringaile Zaksauskaite who made the CRISPR/Cas9 ATM^{sh477} model during her PhD. Without her previous work, the work characterising a zebrafish model of AT contained in this thesis would not be as advanced.

This project would not have been as successful without the help of a number of people within the university. I was very fortunate to have the input and expertise of both Professor Kurt De Vos and Professor Sherif El-Khamisy, whose knowledge, time and encouragement was given freely. In addition, I would like to convey my thanks to Dr Victor Alfred, Dr Clare Muir and Dr Jonathan Griffin for their technical expertise. I would also like to give a mention to Grierson and De Vos lab groups and all the people who have come and gone in them over the years. Each and every one of you have helped in the completion of this project in some way.

I cannot overstate my appreciation and love for my friends and colleagues in SITraN, who have provided so much support in every imaginable context along the way. Your readiness to pull me out of a dark hole or your willingness to jump in there with me when needed has been what has got me through. I would especially like to thank Toby, Emily, Charlotte, Matt, Lily, Ale, Katie and Amy.

I would also like to give a special mention to my family, friends and an entire community rooting for me back at home. Being away from you all for four years has been difficult. Thank you for keeping me in the loop and not letting me feel like I was too far away. Your excitement and steadfast conviction that I could achieve this has meant more than you could know.

Finally, I would like to thank my wonderful partner Jon for giving me everything one person could give to another. You have accepted me working early, working late and working weekends without complaint. You have put up with my stress and anxieties, and have done everything in your power to ease them. You have shown me nothing but love and support and from this made the seemingly impossible possible. Because of you, I have been able to achieve my goal.

Table of Contents

Abstract i

Declaration ii

Dedication iii

Acknowledgements iv

List of Figures xiii

List of Tables xv

List of Abbreviations xvi

Chapter 1 1

1.1 Hereditary Cerebellar Ataxias 1

1.1.2 DNA Damage Repair Ataxias 5

1.2 Ataxia Telangiectasia Overview 5

1.2.1 Ataxia Telangiectasia Mutated (ATM) Gene and Protein 8

1.2.2 ATM Structure, Functional Domains and Activation in Response to Double Stranded DNA damage 9

1.2.3 ATM Outside the DDR and its Role in Cellular Homeostasis 16

1.2.4 ATM Genotype vs AT Phenotype 21

1.2.4.1 Immunodeficiency 22

1.2.4.2 Malignancies 25

1.2.4.3 Telangiectasias and Vascular Abnormalities 27

1.2.4.4 Metabolic Dysregulation 28

1.2.4.5 Neurodegeneration 30

1.2.4.6 Infertility 40

1.2.4.7 Premature Ageing 41

1.2.4.8 Radiosensitivity 42

1.2.4.9 ATM mutation carriers 43

1.3 Current Animal Models of Ataxia Telangiectasia 44

1.3.1 Drosophila 48

1.3.2 Zebrafish 49

1.3.3 Mouse 49

1.3.4 Rat 50

1.3.5 Pig 51

1.4 Zebrafish as a Model Organism 52

1.4.1 Zebrafish as a Model for Neurological Disease 54

1.4.2 Zebrafish as a Model for DNA Damage Repair 55

1.4.2.1 Homologous Recombination in Zebrafish 55

1.5 Project Rationale 56

Chapter 2 59

2.1 General Zebrafish Methods 59
2.1.1 Zebrafish Maintenance and Breeding 59
2.1.2 Generation of Mutant Zebrafish 61
2.1.3 Anaesthesia 61
2.1.4 Adult Tail Biopsy 61
2.2 Genotyping of the ATM Allele 61
2.2.1 DNA Extraction 61
2.2.2 Amplification of Zebrafish DNA by Polymerase Chain Reaction 62
2.2.3 Restriction Digest of PCR Products 62
2.2.4 Agarose Gel Electrophoresis 62
2.2.5 Preparation of PCR Products for Sequencing 63
2.3 Measuring Gene Expression by Quantitative Reverse Transcription PCR (RT-qPCR) 63
2.3.1 RNA Extraction 63
2.3.2 Reverse Transcription and Complementary DNA (cDNA) Synthesis 64
2.3.3 RT-qPCR 64
2.3.3.1 Primer Optimisation 64
2.3.3.2 Template Optimisation 65
2.3.3.3 RT-qPCR 65
2.4 Behavioural Analysis 66
2.4.1 Measuring Swimming Defects in Zebrafish Larvae 66
2.4.2 Swimming Endurance Test on Adult Zebrafish 67
2.4.3 Total Motility 68
2.5 Measuring Protein Expression 68
2.5.1 Western Blot 68
2.5.1.1 Protein Extraction 68
2.5.1.2 Immunoprecipitation 69
2.5.1.3 SDS PAGE 69
2.5.1.4 Electroblotting 70
2.5.1.5 Immunodetection of proteins 70
2.5.1.6 Visualisation of Protein Bands 70
2.5.2 Whole Mount Immunofluorescence 70
2.5.2.1 Immunostaining 70
2.5.2.2 Preparation of embryos for imaging 71
2.5.2.3 Confocal Imaging 71
2.5.2.4 Quantification of γH_2AX foci 71
2.6 Histology 73

2.6.1 Preparation and Sectioning of Formalin Fixed Paraffin Embedded (FFPE) Adult Zebrafish 73
2.6.2 Haematoxylin and Eosin (H&E) Staining of Slides 73
2.6.3 Immunohistochemistry 74
2.6.4 Imaging of FFPE Sections 74
2.7 Statistical Analysis 74
Chapter 3 75
3.1 Introduction 75
3.2 Results 76
3.2.1 Expression of ATM in ATM$^{sh477/sh477}$ Zebrafish 76
3.2.1.1 Expression of *ATM* mRNA in ATM$^{sh477/sh47}$ Zebrafish 76
3.2.1.2 Investigation into the Expression of the ATM Protein in ATM$^{sh477/sh477}$ Zebrafish 81
3.2.2 ATM$^{sh477/sh477}$ Zebrafish Develop as Male 88
3.2.3 ATM$^{sh477/sh477}$ Zebrafish Show no Increase in Radiosensitivity or Deficiency in the Somatic DNA Damage Repair Response 91
3.2.3.1 ATM$^{sh477/sh477}$ Zebrafish do not Exhibit any Increase in their Radiosensitivity 91
3.2.3.2 Somatic DDR in ATM$^{sh477/sh477}$ Zebrafish. 96
3.2.3.3 ATM$^{sh477/sh477}$ Zebrafish do not Exhibit an Increase in Senescence 100
3.2.4 Investigations into the Possibility of Genetic Compensation by ATR 104
3.3 Discussion 108
3.3.1 ATM$^{sh477/sh477}$ Zebrafish have Phenotypes that are Consistent with Knockout of ATM Signalling 108
3.3.1.1 Nonsense Mediated Decay of the ATM^{sh477} Transcript 108
3.3.1.2 Detection of the ATM Protein in Zebrafish by Western Blot 109
3.3.1.3 ATM$^{sh477/sh477}$ Zebrafish are All Males, Consistent with Loss of the HR Pathway in Zebrafish 111
3.3.2 Radiosensitivity and the DDR in ATM$^{sh477/sh477}$ Zebrafish 112
3.3.2.1 Measuring the DDR in ATM Mutant Zebrafish 112
3.3.2.2 Compensation in the DDR 114
3.3.2.3 Radiosensitivity in the ATM$^{sh477/sh477}$ KO Model versus the ATM MO Induced KD Model 116
3.3.3 Future Work in the General Characterisation of the ATM$^{sh477/sh477}$ Model 117
3.3.3.1 Further Characterising the DDR in ATM Deficient Zebrafish 117
3.3.3.2 Investigating Compensation in the Model 118
Chapter 4 120
4.1 Introduction 120
4.2 Results 122

4.2.1 ATM$^{sh477/sh477}$ Zebrafish do not Produce Progeny 122
4.2.2 Investigations into ATM$^{sh477/sh477}$ Testes 124
4.2.2.1 ATM$^{sh477/sh477}$ Zebrafish have Neoplastic Testes 124
4.2.2.2 ATM$^{sh477/sh477}$ Zebrafish do not Develop Mature Spermatozoa 130
4.2.2.3 ATM$^{sh477/sh477}$ Zebrafish Exhibit Stalled Spermatogenesis 133
4.2.2.4 The ATM Protein is Highly Expressed in Most Cell Types in the Zebrafish Testes 137
4.3 Discussion 144
4.3.1 Loss of ATM Recapitulates Phenotypes Observed in Other Zebrafish KO Models of DNA damage Repair Genes 144
4.3.1.1 Loss of HR Genes in Zebrafish Results in Incomplete Spermatogenesis due to Failure to Complete Meiosis 144
4.3.1.2 Disruption of Sertoli Cell Homeostatic Proliferation is a Feature of Loss of HR Genes in Zebrafish 147
4.3.2 ATM$^{sh477/sh477}$ Zebrafish May Express a Truncated ATM Protein but Exhibit Phenotypes that are Consistent with loss of ATM Activity 150
4.3.3 ATM is an Essential Component of Meiosis and Loss of ATM Causes Infertility in Animal Models of AT 152
4.3.4 Future Work to Further Characterise the Testicular Phenotype in ATM$^{sh477/sh477}$ Zebrafish 153
4.3.4.1 Determination of When Spermatogenesis Fails in ATM$^{sh477/sh477}$ Zebrafish 153
4.3.4.2 Further Investigations into the Testicular Neoplasia 154
Chapter 5 156
5.1 Introduction 156
5.2 Results 157
5.2.1 ATM$^{sh477/sh477}$ Zebrafish Show no Gross Defects in Larval Swimming 157
5.2.1.1 ATM$^{sh477/sh477}$ Larvae Exhibit no Swimming Abnormalities at 5 dpf 157
5.2.1.2 ATM$^{sh477/sh477}$ Larvae Exhibit no Swimming Abnormalities at 5 dpf After Treatments to Induce DNA Damage 160
5.2.1.3 Treatment of Wild Type and ATM$^{sh477/sh477}$ Zebrafish Larvae with an ATM Inhibitor to Investigate Compensatory Mechanisms 175
5.2.2 Investigations into ATM$^{sh477/sh477}$ Juvenile Zebrafish Swimming with and without Induction of Exogenous DNA Damage 179
5.2.3 Investigations into Adult ATM$^{sh477/sh477}$ Zebrafish Swimming Behaviour 184
5.2.4 Histological Examinations of Adult ATM$^{sh477/sh477}$ Cerebella 188
5.3 Discussion 191
5.3.1 ATM$^{sh477/sh477}$ Zebrafish Larvae Show no Divergence in their Behaviour from Wild Type Controls after Attempts to Induce DNA Damage 191
5.3.1.1 ATM$^{sh477/sh477}$ TDP1$^{sh475/sh475}$ Double Mutants 191

5.3.1.2 Induction of DNA Damage by CPT 192

5.3.1.3. Induction of DNA Damage by Treatment with Ionising Radiation 194

5.3.2 Adult ATM$^{sh477/sh477}$ Zebrafish do not Exhibit any Behavioural Defects that can be used as Therapeutic Target Readout........ **195**

5.3.4 Future Work and Characterisation of Neurodegeneration in the ATM$^{sh477/sh477}$ Zebrafish Model **197**

5.3.4.1 Analysis of Larval and Juvenile Behaviour 197

5.3.4.2 Investigation into Cerebellar Degeneration 198

5.3.4.3 Continued Investigation into Compensation for Loss of ATM at the Protein Level........ 199

Chapter 6 201

6.1 Summary of Key findings 201

6.2 Contribution of the ATM$^{sh477/sh477}$ model 206

6.2.1 ....Limitations in the Characterisation of ATM$^{sh477/sh477}$ Zebrafish **206**

6.2.1.1 It has not been experimentally shown that ATM$^{sh477/sh477}$ zebrafish are a KO model 206

6.2.1.2 Characterisation of the DDR at the Whole Larval/Adult Level 206

6.2.1.3 Radiosensitivity and the DDR has not been Investigated in Adult Zebrafish........ 207

6.2.1.4 Female to Male Sex Reversal in ATM$^{sh477/sh477}$ Zebrafish Limits the Numbers of Fish Available for Experimentation 207

6.2.1.5 Gross Morphological Changes in ATM$^{sh477/sh477}$ Zebrafish Make Characterisation of their Adult Swimming Ambiguous 208

6.2.1.6 The Response of ATM$^{sh477/sh477}$ Zebrafish to Oxidative Stress has not een Characterised 209

6.2.2 The Sex Reversal Exhibited by ATM$^{sh477/sh477}$ Zebrafish has the Potential to be Exploited as an Assay to Determine Approaches to Restore ATM Activity **210**

6.2.3 ....Validity of Modelling DDR Disorders in Zebrafish **210**

6.2.3.1 Comparison of Zebrafish DDR Mutants 210

6.2.3.2 Conservation on DDR genes in Zebrafish 214

6.2.3.3 Considerations When Creating Zebrafish Models of DDR Disorders215

6.2.4 Validity of Modelling Hereditary Cerebellar Ataxia Disorders in Zebrafish **216**

6.2.5 ....Other Uses for the ATM$^{sh477/sh477}$ Zebrafish Model **217**

6.3Future work 217

Bibliography........ 219

Appendix 1 286

***Appendix 1.1 Summary table of hereditary ataxias* 286**

***Appendix 1.2. Table Exhibiting Incidence of presentation/diagnosis of Genetic Ataxias discussed in section 1.1 of the text, seen at the Sheffield Ataxia Centre, UK, over a 20-year period* 318**

***Appendix 1.3 Map summarising ATM effector protein activation/inactivation in the DDR. Map was collated using SPIKE database (331). Protein families are shown in yellow, protein complexes are in green, individual proteins in grey, a microRNA in blue.* 319**

***Appendix 1.4 Clustal Ω Alignment of ATM protein sequences from a selection vertebrates* 320**

Appendix 3 327

***Appendix 3.1 Statisitical Analysis Coresponding to figure 3.2: Expression of ATM mRNA in wild type and ATM$^{sh477/sh477}$ zebrafish* 327**

***Appendix 3.2 Prodiction of zebrafish specific ATM antibody by Proteintech™* 331**

***Appendix 3.3: Optimisation of transfer membrane for detection of zebrafish ATM by zATM antibodies.* 338**

***Appendix 3.4 Statistical Analysis Corresponding to figure 3.6: ATM$^{sh477/sh477}$ zebrafish develop as male when raised at normal densities.* 339**

***Appendix 3.5 Statistical Analysis Corresponding to figure 3.8: ATM$^{sh477/sh477}$ zebrafish morphologically exhibit no increase in their radiosensitivity compared to ATM$^{+/+}$ siblings.* 340**

***Appendix 3.6 Statistical analysis corresponding to figure 3.9: H2AX phosphorylation in ATM$^{+/+}$ and ATM$^{sh477/sh477}$ larval zebrafish* 341**

***Appendix 3.7 Statistical analysis corresponding to figure 3.10: ATM$^{sh477/sh477}$ show no inability to produce immunoglobulins* 342**

***Appendix 3.8 Statistical analysis corresponding to figure 3.11: mRNA expression of senescence markers in adult zebrafish* 343**

***Appendix 3.9 Statistical analysis corresponding to figure 3.13: Expression of ATR mRNA is not upregulated in ATM$^{sh477/sh477}$ zebrafish* 344**

***Appendix 3.10 Statistical analysis corresponding to figure 3.14: Expression of ATR mRNA is not upregulated in ATM$^{sh477/sh477}$ zebrafish after induction of DNA damage* 345**

***Appendix 3.11 RNA-binding protein motifs found 100 nt of the ATM^{sh477} allele premature stop codon* 346**

Appendix 4 347

***Appendix 4.1 Statistical Analysis Corresponding to figure 4.4: Neoplastic Sertoli cell growth disrupts the organisational structure of ATM$^{sh477/sh477}$ testes* 347**

***Appendix 4.2 Method used to quantify the area of H&E stained cells in the testes of ATM$^{+/+}$ and ATM$^{sh477/sh477}$* 348**

Appendix 4.3 Statistical analysis corresponding to figure 4.7: Histological comparison of spermatogenesis between ATM$^{+/+}$ and ATM$^{sh477/sh477}$ zebrafish at 3 months 349

Appendix 5 350

Appendix 5.1 Statistical Analysis Corresponding to Figure 5.1: ATM$^{sh477/sh477}$ zebrafish larvae do no exhibit any detectable swimming abnormalities at 5dpf 350

Appendix 5.2 Statistical Analysis Corresponding to Figure 5.2: ATM$^{sh477/sh477}$ zebrafish larvae on a TDP1$^{sh475/sh475}$ (null) background do no exhibit any detectable swimming abnormalities at 5dpf 352

Appendix 5.3 Statistical Analysis Corresponding to Figure 5.3: Optimisation of DMSO treatment at 48 hpf in a 96 well plate for swimming analysis at 5dpf 354

Appendix 5.4.1 Optimisation 3 of CPT treatment on zebrafish embryos and larvae in a 96 well plate for swimming analysis at 5dpf, distance swum analysis 356

Appendix 5.4.2 Statistical Analysis of figures a.ii-e.ii in appendix 5.5.1: Optimisation 3 of CPT treatment on zebrafish embryos and larvae in a 96 well plate for swimming analysis at 5dpf, distance swum analysis. 358

Appendix 5.4.3 Optimisation 3 of CPT treatment on zebrafish embryos and larvae in a 96 well plate for swimming analysis at 5dpf duration of active swimming analysis. 365

Appendix 5.4.4 Statistical Analysis of figures a.ii-e.ii in appendix 5.5.3: Optimisation 3 of CPT treatment on zebrafish embryos and larvae in a 96 well plate for swimming analysis at 5dpf duration of active swimming analysis 367

Appendix 5.4.5. Survival of CPT treatment Optimisation 3 373

Appendix 5.5 Statistical Analysis Corresponding to Figure 5.4: Optimisation 4 of CPT treatment on wild type (LWT) zebrafish embryos at 48 hpf in a 96 well plate for swimming analysis at 5dpf. 375

Appendix 5.6: Statistical Analysis Corresponding to Figure 5.5: Optimisation 5 of CPT treatment on wild type (LWT) zebrafish embryos at 48 hpf in a 96 well plate for swimming analysis at 5dpf. 378

Appendix 5.7: Statistical Analysis Corresponding to Figure 5.6: ATM$^{sh477/sh477}$ zebrafish larvae exhibit no behavioural abnormalities in response to DNA damaging agent CPT compared to their control siblings. 380

Appendix 5.8: Statistical Analysis Corresponding to Figure 5.7: ATM$^{sh477/sh477}$ zebrafish larvae exhibit no swimming defects in response to exogenous DNA damage induced by IR compared to their control siblings. 383

Appendix 5.9.1 Statistical Analysis Corresponding to figure 5.9: ATM$^{sh477/sh477}$ zebrafish do not exhibit sensitivity to an ATM inhibitor. 386

Appendix 5.9.2 Numbers of fish per treatment group in figure 5.9: ATM$^{sh477/sh477}$ zebrafish do not exhibit sensitivity to an ATM inhibitor. 390

Appendix 5.10: Statistical Analysis Corresponding to Figure 5.10: ATM$^{sh477/sh477}$ zebrafish larvae exhibit no swimming defects at 12 dpf. 391

Appendix 5.11.1: Statistical Analysis Corresponding to Figure 5.11: ATM$^{sh477/sh477}$ zebrafish larvae exhibit no swimming defects at 12 dpf after treatment at 48 hpf with ionising radiation. **393**

Appendix 5.11.2: Number of fish used corresponding to Figure 5.9. **397**

Appendix 5.12 Statistical Analysis Corresponding to Figure 5.11: Adult male ATM$^{sh477/sh477}$ zebrafish show slight differences in their swimming endurance at 7 months of age compared to wild type controls. **398**

Appendix 5.13: Statistical Analysis Corresponding to Figure 5.13: Investigations into Total Motility of ATM$^{sh477/sh477}$ zebrafish. **399**

Appendix 6 400

Appendix 6.1 Protein-Protein Blast Sequence Alignment of the rad51 zebrafish and Human Sequences **400**

Appendix 6.2 Protein-Protein Blast Sequence Alignment of the ATM zebrafish and human sequences **401**

Appendix 6.3 Protein-Protein Blast Sequence Alignment of the TDP1 zebrafish and human sequences **409**

Appendix 6.4 Protein-Protein Blast Sequence Alignment of the ATR zebrafish and human sequences **411**

Appendix 6.5 Protein-Protein Blast Sequence Alignment of the DNA-PKcs zebrafish and human sequences **414**

Appendix Bibliography 419

List of Figures

Figure 1.1 Major symptoms associated with Ataxia Telangiectasia 7

Figure 1.2 Overview of the structure of dimeric closed conformation human ATM protein and its functional domains 12

Figure 1.3 Overlapping phenotypic traits of Ataxia Telangiectasia, Ataxia Telangiectasia-Like, Nijmegen Breakage Syndrome, and Nijmegen Breakage Syndrome–Like disorders. 13

Figure 1.4 Modified/Simplistic overview of the ATM signalling pathway in response to DNA damage. 15

Figure 1.5 ATM mediated redox induces autophagy through mTORC1 during oxidative stress. 20

Figure 1.7 Coronal T2-weighted image of cerebellar atrophy in AT patients 31

Figure 1.8 The accumulated DNA damage model of neurodegeneration 32

Figure 1.9 Overview of overlapping phenotypes exhibited by vertebrate models of AT .. 47

Figure 1.10 Number of zebrafish publications per year from 1990-2020 from a Web of Knowledge database search 53

Figure 2.1 Methods of zebrafish breeding 60

Figure 2.2 Quantification of γH2AX foci by a custom script 72

Figure 3.1 Characterisation of the ATM$^{sh477/sh477}$ mutation 78

Figure 3.2 Expression of ATM mRNA in wild type and ATM$^{sh477/sh477}$ zebrafish 80

Figure 3.3 Epitope to which the zebrafish ATM antibodies were raised, modelled on the human ATM structure 81

Figure 3.4 Optimisation of novel zATM antibodies for detection of full-length endogenous ATM with suitable lysis buffer and antibody concentration 83

Figure 3.5 zATM antibodies do not detect endogenous full-length zebrafish ATM 87

Figure 3.6 ATM$^{sh477/sh477}$ zebrafish develop as male when raised at normal densities 90

Figure 3.7 Optimisation of serial IR treatments for detection of radiosensitivity in wild type zebrafish. 94

Figure 3.8 ATM$^{sh477/sh477}$ zebrafish morphologically exhibit no increase in their radiosensitivity compared to ATM$^{+/+}$ siblings 95

Figure 3.9 H2AX phosphorylation in ATM$^{+/+}$ and ATM$^{sh477/sh477}$ larval zebrafish 97

Figure 3.10 ATM$^{sh477/sh477}$ show no inability to produce immunoglobulins 99

Figure 3.11 mRNA expression of senescence markers in adult zebrafish 102

Figure 3.12 mRNA expression of senescence markers in 12 dpf zebrafish after induction of DNA damage 103

Figure 3.13 Expression of ATR mRNA is not upregulated in ATM$^{sh477/sh477}$ zebrafish 106

Figure 3.14 Expression of ATR mRNA is not upregulated in ATM$^{sh477/sh477}$ zebrafish after induction of DNA damage 107

Figure 4.1 Zebrafish Spermatogenesis. 121

Figure 4.2 ATM$^{sh477/sh477}$ Zebrafish are infertile 123

Figure 4.3 ATM$^{sh477/sh477}$ zebrafish exhibit abnormal gross abdominal morphology 126

Figure 4.4 ATM$^{sh477/sh477}$ zebrafish testes at 12 months old exhibit neoplastic Sertoli cell growth 127

Figure 4.5 Neoplastic Sertoli cell growth disrupts the organisational structure of ATM$^{sh477/sh477}$ testes 128

Figure 4.6 Contribution of Sertoli and Leydig cells to the makeup of 12 month old ATM$^{+/+}$ and ATM$^{sh477/sh477}$ testes 129

Figure 4.7 ATM$^{sh477/sh477}$ testes exhibit large empty seminiferous tubule lumens 131

Figure 4.8 ATM$^{sh477/sh477}$ zebrafish testes do not contain mature sperm 132

Figure 4.9 Histological comparison of spermatogenesis between ATM$^{+/+}$ and ATM$^{sh477/sh477}$ zebrafish at 3 months 135

Figure 4.10 Comparison of spermatogenic cell size in ATM$^{+/+}$ and ATM$^{sh477/sh477}$ testes as a means of define cell type 136

Figure 4.11 Optimisation of antigen retrieval for zATM1 IHC 139

Figure 4.12 Optimisation of zATM1 for IHC on zebrafish FFPE testes sections 140

Figure 4.13 Immunohistochemistry staining with the zATM1 antibody on ATM$^{+/+}$ and ATM$^{sh477/sh477}$ testes 142

Figure 4.14 Cell specific staining of ATM 143

Figure 5.1 ATM$^{sh477/sh477}$ zebrafish larvae do not exhibit any detectable swimming abnormalities at 5dpf 159

Figure 5.2 ATM$^{sh477/sh477}$ zebrafish larvae on a TDP1$^{sh475/sh475}$ (null) background do not exhibit any detectable swimming abnormalities at 5 dpf 162

Figure 5.3 Optimisation of DMSO treatment at 48 hpf in a 96 well plate for swimming analysis at 5dpf 165

Figure 5.4 Optimisation 4 of CPT treatment on wild type (LWT) zebrafish embryos at 48 hpf in a 96 well plate for swimming analysis at 5dpf 169

Figure 5.5 Optimisation 5 of CPT treatment on wild type (LWT) zebrafish embryos at 48 hpf in a 96 well plate for swimming analysis at 5dpf 170

Figure 5.6 ATM$^{sh477/sh477}$ zebrafish larvae exhibit no behavioural abnormalities in response to DNA damaging agent CPT compared to their control siblings 172

Figure 5.7 ATM$^{sh477/sh477}$ zebrafish larvae exhibit no swimming defects in response to exogenous DNA damage induced by IR compared to their control siblings 174

Figure 5.8. Model for the effect of ATMi on DDR in ATM$^{sh477/sh477}$ zebrafish 177

Figure 5.9 ATM$^{sh477/sh477}$ zebrafish do not exhibit sensitivity to an ATM inhibitor 178

Figure 5.10 ATM$^{sh477/sh477}$ zebrafish larvae exhibit no swimming defects at 12 dpf. 182

Figure 5.11 ATM$^{sh477/sh477}$ zebrafish larvae exhibit no swimming defects at 12 dpf after treatment at 48 hpf with ionising radiation 183

Figure 5.12 Adult male ATM$^{sh477/sh477}$ zebrafish show significant differences in their swimming endurance at 7 months of age compared to wild type siblings 186

Figure 5.13 Investigations into Total Motility of ATM$^{sh477/sh477}$ zebrafish 187

Figure 5.14 H&E Stained Sagittal Sections of ATM$^{+/+}$ and ATM$^{sh477/sh477}$ cerebella at 12 months 189

Figure 5.15 H&E Stained sagittal sections of ATM$^{+/+}$ and ATM$^{sh477/sh477}$ cerebella at 12 months (higher power) 190

Figure 6.1 Summary of key findings in the characterisation of the ATM$^{sh477/sh477}$ model 204

Figure 6.1 Summary of key findings in the characterisation of the ATM$^{sh477/sh477}$ model 202

List of Tables

Table 1.1 Genetic classification of Cerebellar Ataxias 3

Table 1.2 Common Pathways of Neurodegeneration in HCAs 4

Table 1.3 Effects of ATM deficiency on Mitochondria 37

Table 1.4 Mechanisms of Neurodegeneration in AT 39

Table 1.5 Animal Models of AT 45

Table 2.1 Genomic DNA PCR Primers 62

Table 2.2 30X Touchdown PCR 62

Table 2.3 qPCR Primers 65

Table 2.4 RT-qPCR Protocol 1 66

Table 2.5 RT-qPCR Protocol 2 66

Table 4.1 Stages of Prophase I 145

Table 5.1 Optimisation of Treatment Time and Dose of CPT 166

Table 6.1 Comparison of key findings of the zebrafish ATM$^{sh477/sh477}$ model and other vertebrate models of AT 205

Table 6.2 Comparison of key findings of the zebrafish ATM$^{sh477/sh477}$ model and other vertebrate models of AT........203

List of Abbreviations

(Alphabetical Order)

ADCAN	Cerebellar Ataxia, Deafness, and Narcolepsy, Autosomal Dominant
AFP	alpha-fetoprotein
ASPA	Animals Scientific Procedures Act
AST	aspartate aminotransferase
AT	Ataxia Telangiectasia
AT-LD	Ataxia Telangiectasia Like Disorder
ALS	Amyotrophic lateral sclerosis
ATM	Ataxia Telangiectasia Mutated
ATMi	Ataxia Telangiectasia Mutated inhibitor
AOA	Ataxia-oculomotor Apraxia
ATR	Ataxia Telangiectasia and Rad3 related
bp	base pair
CA	Cerebellar Ataxia
CAMRQ	Cerebellar Ataxia, Mental Retardation, and Disequilibrium Syndrome
CLN2	classic late infantile neuronal ceroid lipofuscinosis
CPT	Camptothecin
CSR	class switching recombination
DAB	3,3’-diaminobenzidine
DDR	DNA Damage Repair
DMSO	Dimethyl sulfoxide
DNA-PKcs	DNA-dependent Protein Kinase, catalytic subunit
dpf	days post fertilisation
DPRLA	Dentatorubral-Pallidoluysian Atrophy
ds	Double Strand
EA	Episodic Ataxia
EDTA	Ethylenediaminetetraacetic acid
eIF-4E	Eukaryotic Initiation Factor 4E
FAT	FRAP-ATM-TRRAP
FFPE	formalin fixed paraffin embedded
FLAP	FATC, Lst8-binding element (LBE) equivalent region, Activation loop, and the PRD

FLAP-BE	FLAP- Binding Element
FSH	follicle stimulating hormone
FTLD	Frontotemporal Lobar Degeneration
GC	genetic compensation
GGT	gamma-glutamyl-transferase
HCA	Hereditary Cerebellar Ataxias
H&E	Haematoxylin and eosin
HEAT	Huntingtin, elongation factor 3, A subunit of protein phosphatase 2A and TOR1
hpf	hours post fertilisation
HR	homologous recombination
HRE	hypoxia-response elements
ILGF-I	Insulin and insulin-like growth factor-I
ILGR-1R	insulin-like growth factor-I receptor
IP	immunoprecipitation assay
IR	ionising radiation
KD	knockdown
KI	knock in
KinD	Kinase dead
KO	knockout
Ig	Immunoglobulin
LKB1	liver kinase B1 protein
LH	luteinising hormone
MO	morpholino
MRI	Magnetic resonance imaging
mTOR	mammalian Target of Rapamycin
mTORC1	mTOR complex 1
NEB	New Engand Biolabs®
NHEJ	nonhomologous end joining
NMD	nonsense mediated degradation
PC	Purkinje cells
PIKK	phosphatidylinositol 3-kinase-related kinase
PINK1	PTEN-induced putative kinase 1
PCOS	polycystic ovarian syndrome
PRD	PIKK regulatory domain

PVDF	Polyvinylidene difluoride
REDD1	regulated in development and DDR 1
Rheb	Ras homolog enriched in brain
RIPA	Radioimmunoprecipitation assay
ROS	Reactive Oxygen Species
RNS	reactive nitrogen species
SASP	senescence-associated secretory phenotype
SCAs	Spinocerebellar Ataxias
SPAX	Spastic Ataxia, Autosomal Dominant
ss	single strand
SSA	single-strand annealing
STING	stimulator of interferon genes
TAN	Tel1, ATM, N terminus
TOP1	Topoisomerase 1
TOPcc	Topoisomerase cleavage complex
TRAP	Transformation/Transcription Domain-Associated Protein
TSC2	Tuberous Sclerosis 2
U_{Crit}	critical swimming velocity
V(D)J	variability, diversity, and joining
XLF	XRCC4-like factor
ZEG	Zebrafish Embryonic Genotyper
ZFHX3/ATBF1	Zinc Finger Homeobox 3/ (AT-motif binding factor 1
4EBP-1	eIF-4E-binding protein 1

Chapter 1

Introduction

1.1 Hereditary Cerebellar Ataxias

Cerebellar ataxia (CA) is a term used to describe loss of co-ordination, uncontrolled and uncoordinated movements, gait instability, and jerky eye movements, and it is the result of damage to the cerebellum and its connections. Hereditary Cerebellar Ataxias (HCAs) are a group of clinically and genetically diverse diseases where mutations in ~75 genes have been described as the causative factor of cerebellar atrophy **(table 1.1 or see appendix 1.1 for an expanded version)** (Jayadev and Bird, 2013).

HCAs are inherited as autosomal dominant, autosomal recessive, X-linked, mitochondrial, episodic, and sporadic, and can be congenital. Reported mutations include missense, nonsense, deletions and insertions, splice site mutations, and repeat expansions. Genes with mutations that are known to cause CA are summarised in **table 1.1**. While most ataxia genes are functionally distinct, they operate in several shared pathways, principally DNA repair, ion channels, oxidative stress, transcriptional regulation, and cellular trafficking **(see table 1.2 or see appendix 1.1 for an expanded version)**. The disruption of these shared pathways tends to make diagnoses difficult, as mutations in different genes can give rise to a similar phenotype.

The main pathophysiological hallmark of HCAs is the degeneration and death of cerebellar Purkinje cells (PCs) and to some degree the granule layer. Magnetic resonance imaging (MRI) demonstrates atrophy of the cerebellum, sometimes even before the onset of neurological symptoms in some Spinocerebellar Ataxias (SCAs) (Dohlinger et al., 2008, Schulz et al., 2010a). Until recently, there was little epistemological foundation for the exact cause of cell death in this heterogeneous group of diseases, and the mechanisms are only now beginning to be decoded. It is reasonable to assume that the post mitotic nature of cerebellar neurons makes them a vulnerable target for disease.

However, how genes that function in seemingly unrelated pathways all result in HCA is puzzling, but it does appear that these pathways are remarkably selective for the nervous system and in particular for PCs

Table 1.1 Genetic classification of Cerebellar Ataxias

Mutation Type	***Genes***	***Ataxia Disorders***
PolyQ Disorders	*Ataxin-1*	SCA1[1]
	Ataxin-2	SCA2
	Ataxin-3,	SCA3
	CACNA1A	SCA6
	Ataxin-7	SCA7
	TATA- binding protein	SCA17
	Atrophin-1	DRPLA[2]
Intronic Repeats	*Ataxin-10*	SCA10
	*PP2A**	SCA12
	BEAN	SCA31
	NOP56	SCA36
	FXN	Friedreich's Ataxia
Dominantly Inherited Ataxias with Conventional Mutations	*SPTBN2*	SCA5
	TTBK2	SCA11
	KCNC3	SCA13
	PRKCG	SCA14
	ITPR1	SCA15
	IFRD1	SCA18
	KCND3	SCA19/*SCA22*
	TMEM240	SCA21
	PDYN	SCA23
	EEF2	SCA26
	FGF14	SCA27
	AFG3L2	SCA28
	ELOVL4	SCA34
	TGM6	SCA35
	CCDC88C	SCA40
	CACNA1G	SCA42
	DNMT1	ADCAN[3]
	KCNA1	EA1[4]
	CACNA1A	EA2
	CACNB4	EA5
	SLC1A3	EA6
	VAMP1	SPAX1[5]
	Unknown	SPAX7
Recessively Inherited Ataxias with Conventional Mutations	*APTX*	*AOA1*[6]
	SETX	*AOA2*
	PIK3R5	*AOA3*
	PNKP	*AOA4*
	VLDLR	*CAMRQ1*[7]
	WDR81	*CAMRQ2*
	CA8	*CAMRQ3*
	ATP8A2	*CMARQ4*
	PMPCA	*SCAR2*[8]
	Unknown	*SCAR3*
	TPP1	*SCAR7*
	SYNE1	*SCAR8*
	ADCK3	*SCAR9*
	ANO10	*SCAR10*
	SYT14	*SCAR11*
	WWOX	*SCAR12*
	SPTBN2	*SCAR14*
	KIAA0226	*SCAR15*
	STUB1	SCAR16
	CWF19L1	SCAR17
	GRID2	SCAR18
	SLC9A1	SCAR19
	SNX14	SCAR20
	SCYL1	SCAR21
	VWA3B	SCAR22
	TDP2	SCAR23
	UBA5	SCAR24
	ATM	Ataxia-Telangiectasia
	MRE11A	Ataxia-Telangiectasia-Like Disorder-1
	SIL1	Marinesco-Sjogren Syndrome
	KIF1C	SPAX2
	MARS2	SPAX3
	MTPAP	SPAX4
	AFG3L2	SPAX5
	SACS	SPAX6
	Tdp1	SCAN1
A yet undefined	*DAGLA*	SCA20
	Unknown	SCA30
	Unknown	*SCA32*

[1] Spinocerebellar Ataxia
[2] Dentatorubral-Pallidoluysian Atrophy
[3] Cerebellar Ataxia, Deafness, and Narcolepsy, Autosomal Dominant
[4] Episodic Ataxia
[5] Spastic Ataxia, Autosomal Dominant
[6] Ataxia-oculomotor Apraxia
[7] Cerebellar Ataxia, Mental Retardation, and Disequilibrium Syndrome
* Neuronal specific subunit of the protein phosphatase

Table 1.2 Common Pathways of Neurodegeneration in HCAs

Pathway currently indicated by the literature	*Ataxia*	*Gene*
DNA Damage	*AT*	*ATM*
	AT-LD	*MRE11A*
	SCA3	*Ataxin-3*
	AOA1	*APTX*
	AOA2	*SETX*
	AOA4	*PNKP*
	SCAR17	*CWF19L1*
	SCAR22	*VWA3B*
	SCAR23	*TDP2*
Genomic Instability	*SCA1*	*Ataxin-1*
	AT	*ATM*
	AT-LD	*MRE11A*
	SCA3	*Ataxin-3*
	SCA7	*Ataxin-7*
Protein Aggregation	*FA*	*FXN*
	SCA1	*Ataxin-1*
	SCA2	*Ataxin-2*
	SCA3	*Ataxin-3*
	SCA6	*CACNA1A*
	SCA7	*Ataxin-7*
	SCA17	*TATA- binding protein*
	DRPLA	*Atrophin-1*
Transcriptional/Translational Dysregulation	*SCA1*	*Ataxin-1*
	SCA7	*Ataxin-7*
	SCA8	*Ataxin-8*
	SCA10	*ATXN-10*
	SCA17	*TATA- binding protein*
	SCA26	*EEF2*
	SCA28	*AFG3L2*
	SCA31	*BEAN*
	SCA36	*NOP56*
	DRPLA	*Atrophin-1*
	AOA2	*SETX*
	SCAR17	*CWF19L1*
	SPAX3	*MARS2*
	SPAX4	*MTPAP*
Gain of function by RNA Foci	*SCA3*	*Ataxin-3*
	SCA8	*Ataxin-8*
	SCA10	*ATXN-10*
	SCA12	*PP2A*
	SCA31	*BEAN*
	SCA36	*NOP56*
	FA	*FXN*
Primary Channelopathies *	*CAMRQ3*	*CA8*
	CAMRQ4	*ATP8A2*
	EA1	*KCNA1*
	EA2	*CACNA1A*
	EA5	*CACNB4*
	EA6	*SLC1A3*
	SCA6	*CACNA1A*
	SCA13	*KCNC3*
	SCA15	*TPR1*
	SCA19	*KCND3*
	SCA42	*CACNA1G*
Secondary Channelopathies **	*SCA1*	*Ataxin-1*
	SCA2	*Ataxin-2*
	SCA3	*Ataxin-3*
	SCA6	*CACNA1A*
	CAMRQ3	*CA8*

Ataxias are listed in more than one pathway, as the literature suggests that there may be multiple pathways responsible for cerebellar atrophy. *Conditions where there is a mutation in a gene that directly plays a role in the proper functioning of ligand and ion gated channels. **Aggregation of PolyQ proteins co-op components involved in proper functioning of ligand and ion gated channels into their aggregates.

1.1.2 DNA Damage Repair Ataxias

DNA damage is a common theme in many HCA disorders. HCAs such as AT, AT-LD, SCA3, AOA1, AOA2, AOA4, SCAR17, SCAR22, and SCAR23 **(see appendix 1.1)** are caused by mutations in DNA damage repair (DDR) genes. Compromised DDR is thought to be at least partially responsible for pathogenesis in these cases (Savitsky et al., 1995, Zhang et al., 1997, Banin et al., 1998, Ledesma et al., 2009, Gomez-Herreros et al., 2014, Kawarai et al., 2016, Jilani et al., 1999, Stewart et al., 1999). Previously, it was suspected that unrepaired DNA damage may be a relevant factor in the progression of HCAs, but it was not until the causative gene for AT was identified and characterised that a paradigm shift occurred (Gatti et al., 1988, Savitsky et al., 1995). Since this discovery, defective DDR has been implicated in a growing number of neurodegenerative diseases (Jeppesen et al., 2011).

1.2 Ataxia Telangiectasia Overview

Ataxia Telangiectasia (AT) (OMIM#208900) is a life limiting, autosomal recessive cerebellar ataxia. It is caused by homozygous or compound heterozygous loss of function mutations in the *Ataxia Telangiectasia mutated (ATM)* gene (OMIM# 607585). Functional mutations in the gene result in a broad and variant phenotype, of which the primary presentations (in addition to cerebellar ataxia) include telangiectasias, infertility, immunodeficiency, and increased incidence of cancer. These are outlined in **figure 1.1**.

The neurological effects are the first manifestation of the disease, with patients generally presenting at approximately 3 years old with features of progressive cerebellar ataxia, such as deficiency in the extrapyramidal system, and oculomotor defects such as nystagmus and saccades (Boder and Sedgewick, 1958). Patients later develop slurred speech and peripheral neuropathy, and are commonly wheelchair bound by 10 years old. The neurological symptoms are caused by the degeneration of PCs and progressive atrophy of the cerebellum (Tavani et al., 2003, Shaikh et al., 2013). Telangiectasias also occur in early childhood, and their appearance aids in the differential diagnosis to distinguish AT from other HCAs before genetic testing has occurred. AT tends to be fatal in approximately the third decade of life, when patients predominantly succumb to chronic respiratory infections and malignancies (van Os et al., 2017b, Micol et al., 2011b). However, the lifespan of AT sufferers greatly depends on the level of clinical care and management of symptoms (Crawford et al., 2006).

AT is considered a relatively rare disease, with its worldwide incidence difficult to determine. It is estimated to have a prevalence of 1-1.6: 400,000 live births in France and Norway but its incidence appears to be highly dependent on founder effects, with the incidence in Manitoba Canada 20: 400,000 and Hedmark, Norway estimated to be as high as 40: 400,000 (Anheim et al., 2010, Campbell et al., 2003, Erichsen et al., 2009, Salman et al., 2013). It is estimated that 2.8% of the USA population are pathogenic mutation carriers and the incidence appears to be higher in ethnic populations from India and Iran, where consanguinity is more widespread (Swift et al., 1986, Erichsen et al., 2009).

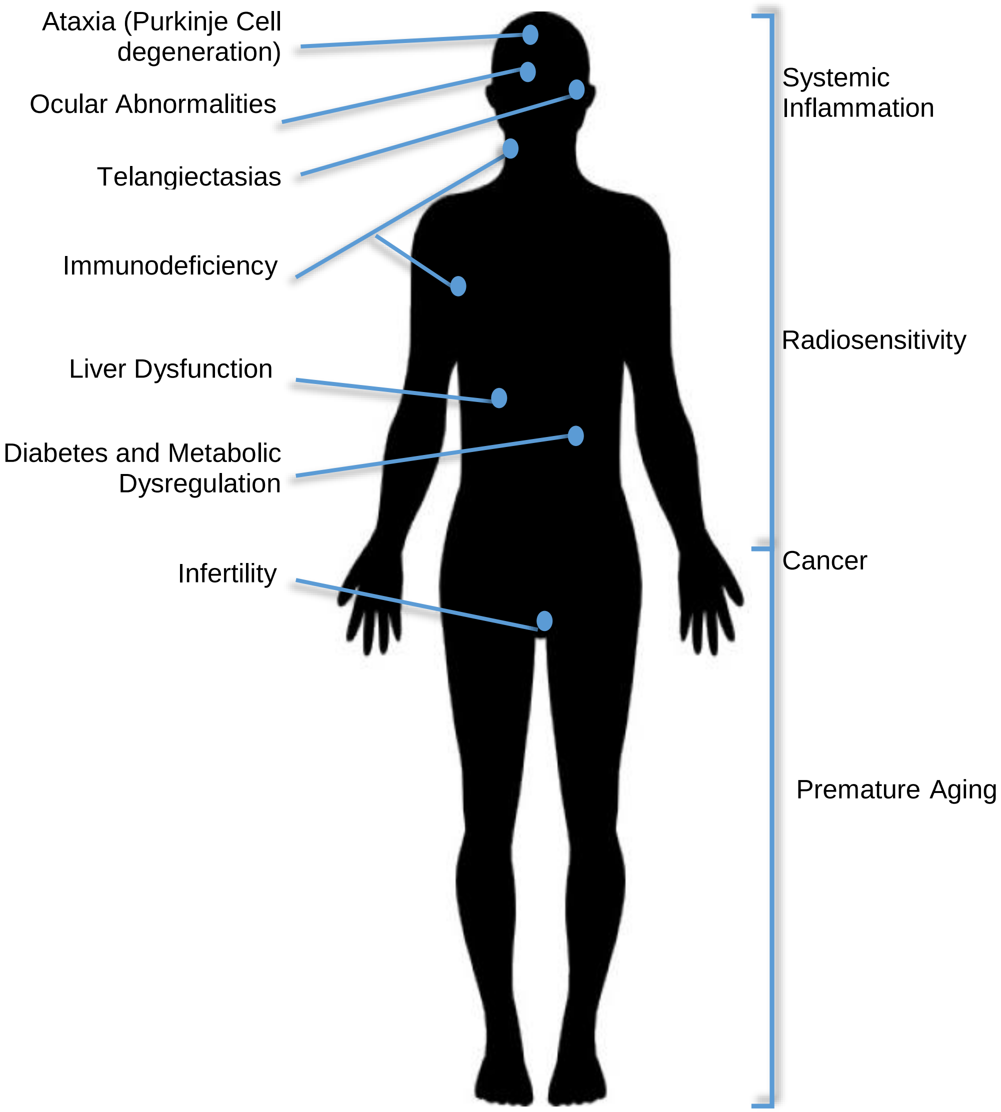
Ataxia (Purkinje Cell degeneration)
Ocular Abnormalities
Telangiectasias
Immunodeficiency
Liver Dysfunction
Diabetes and Metabolic Dysregulation
Infertility
Systemic Inflammation
Radiosensitivity
Cancer
Premature Aging

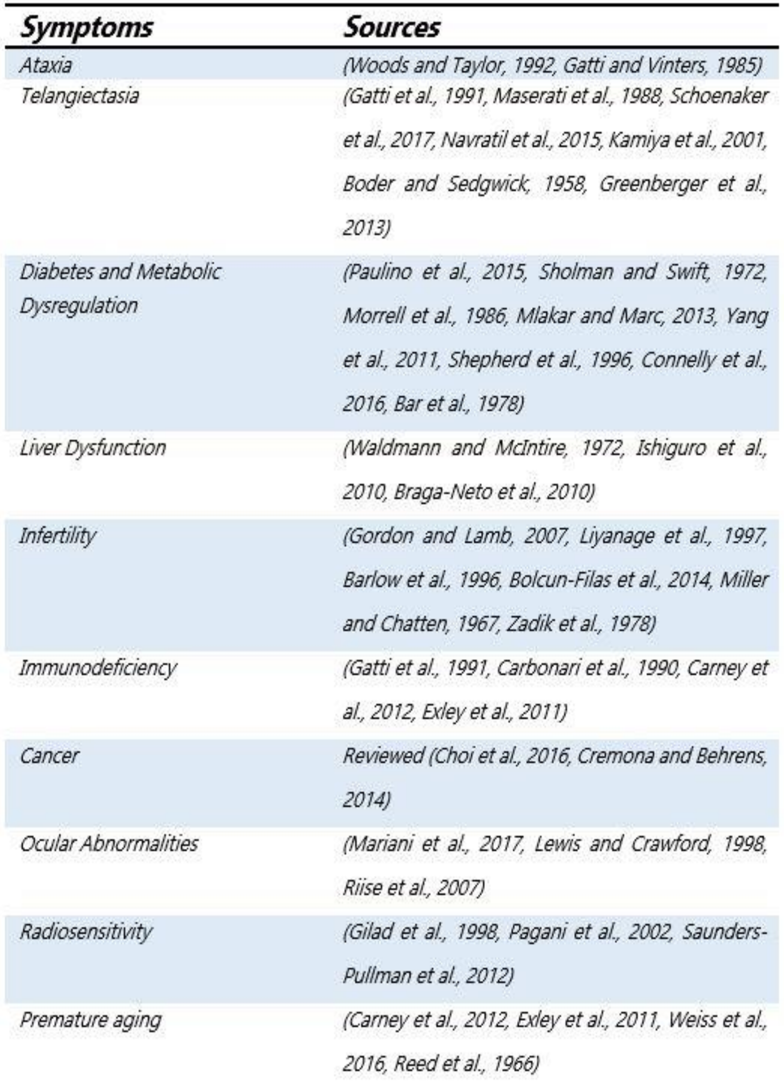

Symptoms	Sources
Ataxia	(Woods and Taylor, 1992, Gatti and Vinters, 1985)
Telangiectasia	(Gatti et al., 1991, Maserati et al., 1988, Schoenaker et al., 2017, Navratil et al., 2015, Kamiya et al., 2001, Boder and Sedgwick, 1958, Greenberger et al., 2013)
Diabetes and Metabolic Dysregulation	(Paulino et al., 2015, Sholman and Swift, 1972, Morrell et al., 1986, Mlakar and Marc, 2013, Yang et al., 2011, Shepherd et al., 1996, Connelly et al., 2016, Bar et al., 1978)
Liver Dysfunction	(Waldmann and McIntire, 1972, Ishiguro et al., 2010, Braga-Neto et al., 2010)
Infertility	(Gordon and Lamb, 2007, Liyanage et al., 1997, Barlow et al., 1996, Bolcun-Filas et al., 2014, Miller and Chatten, 1967, Zadik et al., 1978)
Immunodeficiency	(Gatti et al., 1991, Carbonari et al., 1990, Carney et al., 2012, Exley et al., 2011)
Cancer	Reviewed (Choi et al., 2016, Cremona and Behrens, 2014)
Ocular Abnormalities	(Mariani et al., 2017, Lewis and Crawford, 1998, Riise et al., 2007)
Radiosensitivity	(Gilad et al., 1998, Pagani et al., 2002, Saunders-Pullman et al., 2012)
Premature aging	(Carney et al., 2012, Exley et al., 2011, Weiss et al., 2016, Reed et al., 1966)

Figure 1.1 Major symptoms associated with Ataxia Telangiectasia

1.2.1 Ataxia Telangiectasia Mutated (ATM) Gene and Protein

Ataxia Telangiectasia Mutated (ATM) is a member of the phosphatidylinositol 3-kinase-related kinase (PIKK) family, which also includes *ATR (Ataxia Telangiectasia and Rad3 related)* and *DNA-PKcs (DNA-dependent Protein Kinase, catalytic subunit)* which all function in the DNA damage response (DDR). In addition to these three PIKKs, humans have three others, *mTOR (mammalian Target of Rapamycin), SMG1* and *TRRAP (Transformation/Transcription Domain-Associated Protein),* where *mTOR* functions in cell growth and metabolism, *SMG1* in regulation of nonsense mediated decay of mRNA, and *TRRAP* in chromatin remodelling during transcription (Lovejoy and Cortez, 2009). This family are a group of large, multifunctional, structurally related proteins that share three domains; a kinase domain, which, is sandwiched between a FAT and a FAT C-terminal (FATC) domain (Perry and Kleckner, 2003) **(see fig 1.2).** These proteins are all considered master regulators of the cellular stress response as well as regulators of cell growth and proliferation (Abraham, 1996, Yue et al., 2020).

ATM is a 350 KDa serine/threonine protein kinase located on (Gatti et al., 1988), and is considered an essential signal transducer in the DDR (Savitsky et al., 1995, Sanal et al., 1990, Matsuda et al., 1996). ATM is a constitutively expressed protein and has been found to localise to the nucleus, cytosol, and mitochondria, which is consistent with known ATM substrates (Mu et al., 2007, Matsuoka et al., 2007)**.** ATM acts as a homeostatic master regulator and functional component of many cellular and developmental processes, including, but not limited to, oxidative stress, meiotic recombination, insulin signalling, cell cycle control, telomere maintenance, and genomic stability. However, it is principally regarded as an essential regulator of the DDR (Brown et al., 1997b, Barlow et al., 2000, Watters et al., 1999, Oka and Takashima, 1998, Valentin-Vega et al., 2012, Boehrs et al., 2007, Matsuoka et al., 2007, Shiloh and Ziv, 2013).

1.2.2 ATM Structure, Functional Domains and Activation in Response to Double Stranded DNA damage

Catalytically inactive ATM exists as a dimer, and canonically in the DDR upon activation, becomes a monomer (Bakkenist and Kastan, 2003). The dimerization of the protein is autoinhibitory, as many ATM substrate binding sites are located well within the peptide folds of the dimer (Lau et al., 2016). Like other members of the PIKK family, ATM has three main C terminal domains; a kinase domain sandwiched between a FAT and FATC domain. Along with the other PIKK family members, ATM contains a repeated N terminal HEAT motif and uniquely, it contains a far N terminal TAN domain (Perry and Kleckner, 2003, Seidel et al., 2008) **(figure 1.2 a)**.

The FAT and FATC domains are situated either side of the kinase domain and they interact to ensure proper folding and inhibition of the kinase domain (Bosotti et al., 2000) **(figure 1.2)**. Additionally, serine 1981 found in the FAT domain acts as a marker for monomeric active ATM and it is thought that phosphorylation of this site prevents the protein returning to the dimeric inactive conformation (Bakkenist and Kastan, 2003). The N terminal of the protein is comprised mainly of HEAT (Huntingtin, elongation factor 3, A subunit of protein phosphatase 2A and TOR1) repeats (Andrade and Bork, 1995), which constitute over 50% of the protein **(figure 1.2 a)** (Perry and Kleckner, 2003). The extreme N terminus of the ATM protein contains the TAN (Tel1, ATM, N terminus) domain that has been experimentally shown to function in telomere length maintenance and DNA damage repair through chromatin association (Seidel et al., 2008). It characteristically contains a highly conserved (L/V/I)XXX(R/K)XX(E/D)RXXX(L/V/I) motif as shown in **figure 1.2 a**, and residues 2-40 are crucial for its telomere length maintenance function. Furthermore, the N-terminus of the ATM protein is critical for its proper function as it contains two NLSs (Nuclear Localisation Sequences), made up of clusters of basic amino acids, ^{23}RKK^{25} and ^{385}KRKK^{388}, which are essential for importation of ATM into the nucleus to the site of DNA damage (Young et al., 2005).

Within the closed dimer, the two ATM molecules interact through the FAT domains. In the closed conformation, they inhibit each other when a FLAP motif (FATC, Lst8-binding element (LBE) equivalent region, Activation loop, and the

PRD) in the FAT domain of one molecule is pressed against and obscures the active site of its own protein by a FLAP-BE (FLAP- Binding Element) of the opposite ATM molecule **(figure 1.2 b)** (Imseng et al., 2018, Baretić et al., 2017). In the open conformation, the FLAP-BE rotates outward at a 24° angle, removing the constraints on the PRD (PIKK regulatory domain) region of the opposite molecule's FLAP motif and allowing greater access to the active site (Baretić et al., 2017). Recently, it has been suggested that the ATM dimer is dynamic and moves between a closed and an open conformation. The closed conformation is catalytically inactive while the open conformation, although not considered truly 'active' ATM, has some kinase activity (Baretić et al., 2017).

Several different pathways activating ATM have been described, and these seem to be context dependent. Canonically, ATM is activated in response to double strand DNA (dsDNA) damage (Myers and Cortez, 2006, Zhao et al., 2020b, Sakasai et al., 2010, Canman et al., 1998, Banin et al., 1998, Brown et al., 1997b). In this context, ATM in its inactive state exists as a dimer, and is activated by autophosphorylation at S367, S1893, S1981 and S2996, and dissociates into a monomer (So et al., 2010, Kozlov et al., 2003, Kozlov et al., 2006, Du et al., 2014, Baretić et al., 2017, Bakkenist and Kastan, 2003, Kozlov et al., 2011). While there is some evidence to suggest that ATM is activated to a small extent directly through DNA damage in a dose dependent manner, it is largely activated through the DNA damage sensor MRN (Lee and Paull, 2004, Lee and Paull, 2005, Wang et al., 2014, Dupré et al., 2006). MRN is a DNA-binding-protein complex that consists of three proteins; Mre11, Rad 50, and Nbs1. Holomorphic mutations in these genes cause the autosomal recessive DNA damage repair disorders, Ataxia Telangiectasia- Like disorder, Nijmegen breakage syndrome-like disorder, and Nijmegen breakage syndrome respectively, which all share features with AT **(figure 1.3) (see appendix 1.1)** (Paull and Lee, 2005, Stewart et al., 1999, Waltes et al., 2009, Saar et al., 1997).

Once activated in response to DNA damage, ATM-mediated signal transduction results in one of two cell fates. The first is cell survival, where ATM halts gene transcription/translation, arrests cell cycle, and activates other DNA damage repair proteins. The ATM protein can also bind directly to the site of DNA double strand breaks and attract DNA repair proteins to that site **(see figure 1.4)**.

The second fate is cell death, which occurs if the genomic instability is too great to repair, whereby ATM then directs the cell towards apoptosis (Jang et al., 2010, Kubota et al., 2014, Ma et al., 2013, Pizarro et al., 2009, Meng et al., 1999, Kim et al., 2002, Yazdi et al., 2002, Yukawa et al., 2008, Oleson et al., 2014, Schweikl et al., 2014, Brown et al., 1997a, Shanbhag et al., 2010). A condensed outline of the DDR signalling pathway can be seen in **figure 1.4**.

While it is largely accepted that ATM activation in the context of dsDNA breaks is through the MRN complex for optimum signalling in the DDR, there is still controversy surrounding DNA damage activation of ATM as a whole. As previously stated, dsDNA can activate ATM directly in a dose dependent manner, independent of the MRN complex (Dupré et al., 2006, You et al., 2007). However, it is possible that the conformational change that occurs in chromatin upon double strand breaks may also activate ATM (Bakkenist and Kastan, 2003). Additionally, it has been demonstrated that ATM activation can take place by its effector proteins in the DDR pathway even in the absence of DNA lesions (Soutoglou and Misteli, 2008). In reality, it is likely that there is redundancy in ATM activation and that some combination of these processes occurs together in a complex feedback loop that allows the DDR to be sustained for a number of hours (Andegeko et al., 2001). Differing levels of DNA damage sparks the DDR to differing degrees through many pathways to ensure an adequate but not overly zealous response, that would no doubt be at a high energy cost to the cell. Multiple redundancies of DDR activation is also supported by that fact that expression of kinase dead ATM results in a more severe phenotype than ablation of ATM (Choi et al., 2010, Yamamoto et al., 2012b, Daniel et al., 2012)

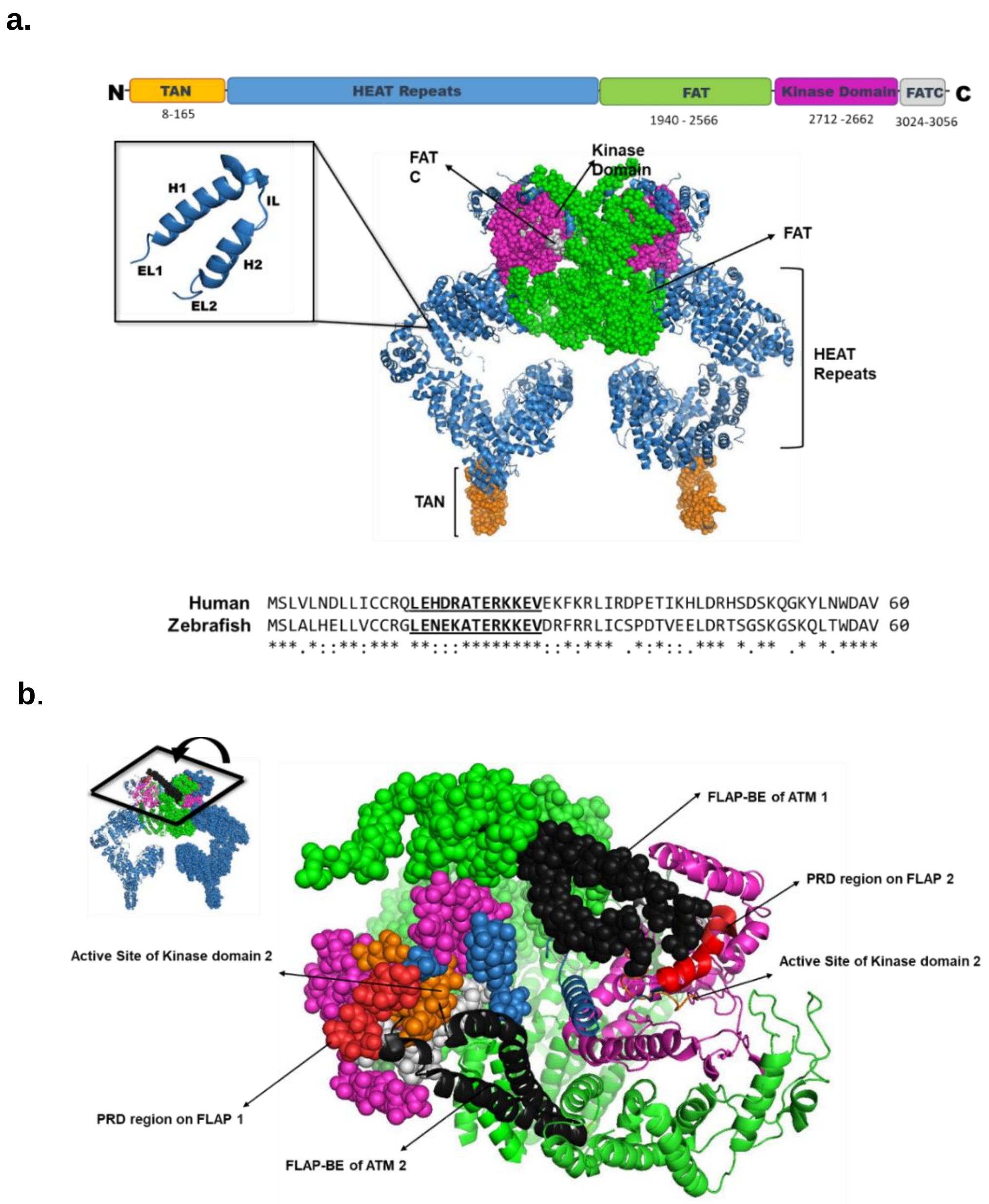
a.
N
TAN
8-165
HEAT Repeats
FAT
1940 - 2566
Kinase Domain
2712 -2662
FATC
3024-3056
C
H1
IL
EL1
H2
EL2
FAT C
Kinase Domain
FAT
HEAT Repeats
TAN
b.
FLAP-BE of ATM 1
PRD region on FLAP 2
Active Site of Kinase domain 2
Active Site of Kinase domain 2
PRD region on FLAP 1
FLAP-BE of ATM 2

```
Human      MSLVLNDLLICCRQLEHDRATERKKEVEKFKRLIRDPETIKHLDRHSDSKQGKYLNWDAV 60
Zebrafish  MSLALHELLVCCRGLENEKATERKKEVDRFRRLICSPDTVEELDRTSGSKGSKQLTWDAV 60
           ***.*::**:*** **:::********::*:*** .*:*::.*** *.** .* *.****
```

Figure 1.2 Overview of the structure of dimeric closed conformation human ATM protein and its functional domains. a) Representation of electron cryomicroscopy structure of closed conformation of ATM submitted to RSCB Protein Data Bank (PDB) - 5NP0 (RCSB, 2017, Baretić et al., 2017). ATM contains a kinase domain (pink) sandwiched between an N terminal FAT (FRAP-ATM-TRRAP) domain (green) and a C-terminal FATC domain (grey). N terminal to the FAT domain is HEAT (Huntingtin, Elongation factor 3, Alpha-regulatory subunit of protein phosphatase 2A and TOR1) domain (blue). At the extreme N terminal is the TAN (Tel1/ATM N-terminal) domain (orange) which functions in telomere maintenance. These domains are thought to regulate the kinase activity through protein-protein interactions and steric hindrance (Lempiäinen and Halazonetis, 2009). The first 60 residues of human and zebrafish ATM showing part of the TAN domain and the highly conserved motif is presented in bold and underscored (Seidel et al., 2008). **b)** ATM molecule 1 of the dimer is shown in spheres; ATM molecule 2 is shown as ribbons. The FLAP-BE (black) of one ATM pushes the PRD region of the FLAP motif (red) of the opposite molecule into its own active site (orange), therefore preventing the access of substrates. Note, the remainder of the HEAT, FAT, Kinase, and FATC domains are shown in blue, green, pink, and grey respectively, as in part **a.**

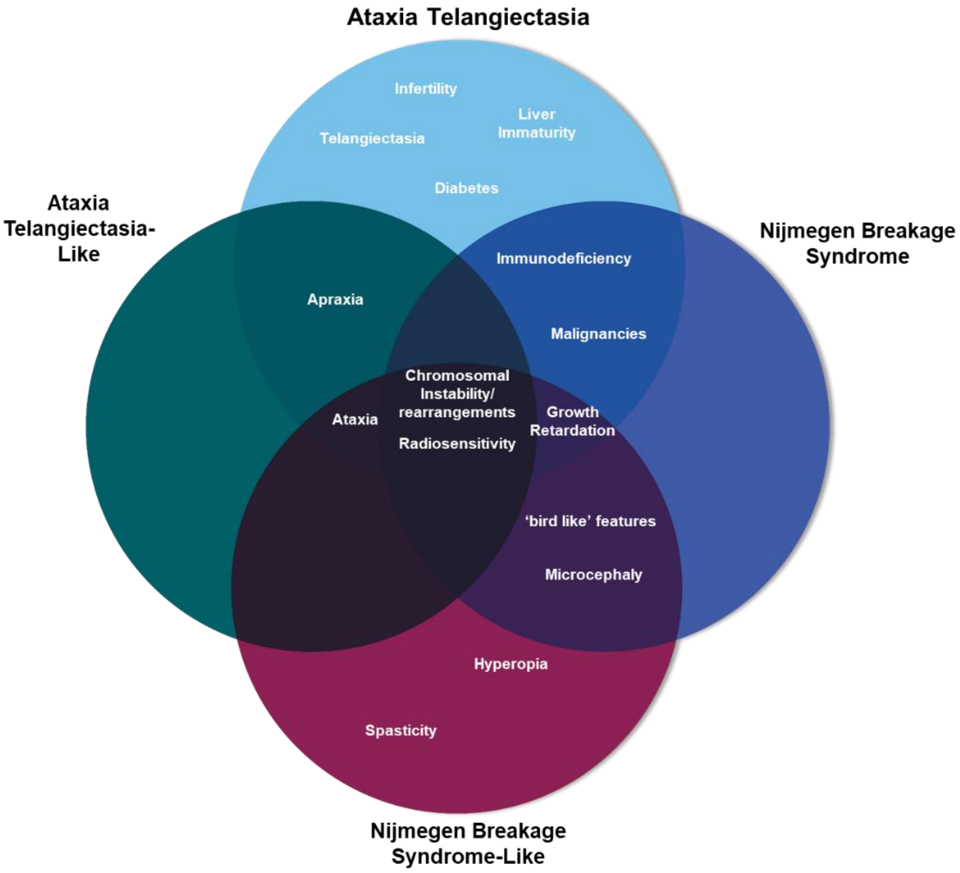
Ataxia Telangiectasia
Infertility
Liver Immaturity
Telangiectasia
Diabetes
Ataxia Telangiectasia-Like
Nijmegen Breakage Syndrome
Immunodeficiency
Apraxia
Malignancies
Chromosomal Instability/ rearrangements
Ataxia
Growth Retardation
Radiosensitivity
'bird like' features
Microcephaly
Hyperopia
Spasticity
Nijmegen Breakage Syndrome-Like

Figure 1.3 Overlapping phenotypic traits of Ataxia Telangiectasia, Ataxia Telangiectasia-Like, Nijmegen Breakage Syndrome, and Nijmegen Breakage Syndrome–Like disorders. These disorders are associated by mutations in the *ATM, Mre11, Nbs1* and *Rad50* genes respectively (Hernandez et al., 1993, Delia et al., 2004, Fernet et al., 2005, Miyamoto et al., 2014, Wegner et al., 1988, Saar et al., 1997, Seemanová et al., 1985, Barbi et al., 1991, Waltes et al., 2009).

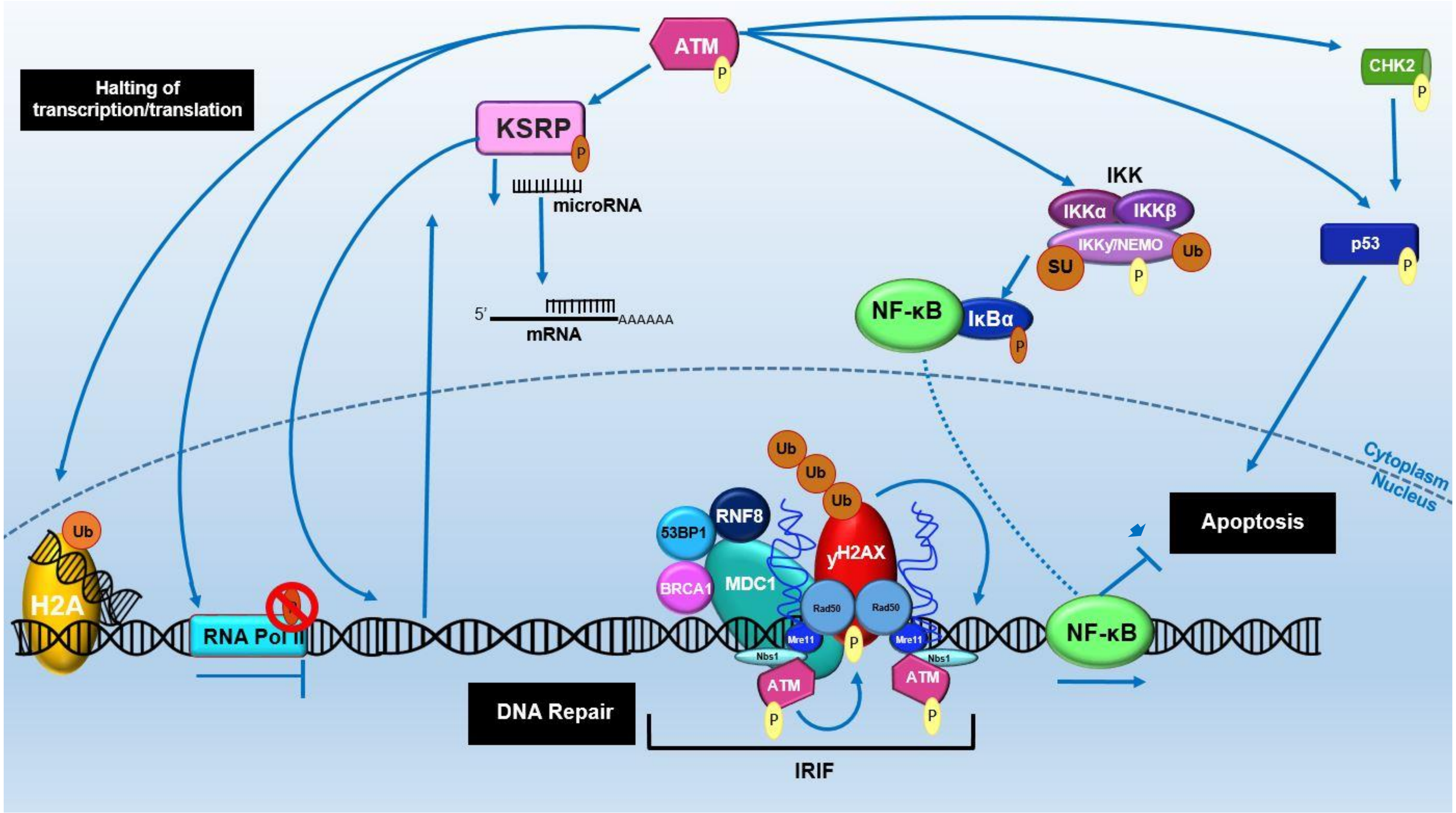
ATM
P
Halting of transcription/translation
KSRP
P
microRNA
5′
mRNA
AAAAAA
CHK2
P
IKK
IKKα
IKKβ
IKKγ/NEMO
SU
Ub
P
NF-κB
IκBα
P
p53
P
Cytoplasm
Nucleus
Apoptosis
Ub
H2A
RNA Pol II
P
Ub
Ub
Ub
RNF8
53BP1
BRCA1
MDC1
γH2AX
Rad50
Rad50
Mre11
Mre11
Nbs1
Nbs1
P
ATM
P
ATM
P
NF-κB
DNA Repair
IRIF

Figure 1.4 Modified/Simplistic overview of the ATM signalling pathway in response to DNA damage. ATM is implicit in the regulation of over 1077 downstream effector proteins (Mu et al., 2007, Matsuoka et al., 2007); the above is an overview of the ATM signalling cascade using specific examples to illustrate the three pronged approach to attenuate DNA damage. **NB Direct phosphorylation targets of ATM are shown in yellow while ATM mediated phosphorylation targets are shown in orange.** Within seconds of dsDNA breaks, the ATM dimer is activated by the MRN complex, monomerises and becomes autophosphorylated at S367, T1885, S1893 and Ser1981, and acetylated at L3016 (Baretić et al., 2017). **1)** The first prong of the response is **DNA Repair** where monomeric ATM interacts with both the Mre11 and Nbs1 subunits of the MRN complex, which bridges the two ends of the damaged DNA. This interaction between ATM and the MRN complex anchors ATM directly to the site of the DNA break which in turn phosphorylates the MRN complex, amplifying the DDR (Lee and Paull, 2004, Lee and Paull, 2005, Dupré et al., 2006). At the site of dsDNA breaks, ATM phosphorylates the c-terminal tail of ƴH2AX. Phosphorylated ƴH2AX interacts with the Nbs1 subunit of the MRN to continuously activate ATM. Additionally, activated ƴH2AX recruits MDC1 protein (mediator of DNA damage checkpoint protein 1) which activates and recruits additional ATM protein to the damaged site. MDC1 has a reciprocal relationship with ATM, where it activates ATM and in turn ATM increases MDC1 oligomerization, snowballing DDR amplification. Moreover, the MDC1 protein also co-recruits further ATM effectors such as RNF8, 53BP1 (p53-Binding Protein 1) and BRCA1 (Breast and Ovarian Cancer Susceptibility Protein 1) (Mochan et al., 2003, Stucki et al., 2005, Lou et al., 2006, Savic et al., 2009, Luo et al., 2011, Liu et al., 2012b, Jungmichel et al., 2012, Yuan et al., 2010, Huen et al., 2007, Kolas et al., 2007, Mailand et al., 2007, Wang and Elledge, 2007, Stucki and Jackson, 2006, Wood et al., 2007). The massive accumulation of proteins at the site of dsDNA breaks are termed ionizing radiation induced foci (IRIF). **2)** The second prong of the approach is to stop erroneous transcript expression from around the site of the damage, therefore ATM reforms the transcriptome by **halting transcription and translation**. One pathway that is suggested for stopping gene transcription is the ubiquitination of Histone 2A (H2A) in an ATM dependent manner. Ubiquitination of H2A prevents chromatin from relaxing and de-condensing to allow transcription. A second ATM pathway that has been described for transcription inactivation is the dephosphorylation, and thus inactivation, of RNA polymerase II (RNA Pol II). To stop translation of mRNA transcripts that may have already been produced from the site of DNA damage or perhaps transcripts promoting the continuation of the cell cycle, ATM has been shown to upregulate the biogenesis and transcription of KSRP (KH-type splicing regulatory protein) dependent microRNAs. These microRNAs bind to mRNA in the cytosol and prevent its translation (Wang et al., 2004, Shanbhag et al., 2010, Müller et al., 2001, Wan et al., 2013, Liu and Liu, 2011, Zhang et al., 2011). **3)** Finally, dependant on whether the cell can repair the DNA damage, the cell survives, or where it cannot overcome the DNA insults, it is removed through apoptosis. ATM antagonistically mediates this. For the **Cell Survival/Apoptosis** axis, cytosolic ATM both directly and indirectly phosphorylates the cell fate protein, p53 through CHK2. Again, this is another example of the redundancy seen in ATM signalling pathways. p53 then phosphorylates its own effector proteins, some of which are also phosphorylated by ATM. Activation of this pathway stalls cell cycle progression and directs the cell towards apoptosis. Conversely, ATM also liberates the transcription factor NF-kB from its inhibitor protein through the IKK complex (IκB kinase), allowing NF-kB to translocate to the nucleus and activate anti-apoptotic genes (Siliciano et al., 1997, Canman et al., 1998, Banin et al., 1998, Rashi-Elkeles et al., 2011, Rashi-Elkeles et al., 2006, Hadian and Krappmann, 2011, McCool and Miyamoto, 2012)

1.2.3 ATM Outside the DDR and its Role in Cellular Homeostasis

There is increasing evidence to suggest that the primary function of ATM is maintaining cellular homeostasis in general, and that it functions in many cellular processes in addition to its role in DDR. Over the past 10 years, there has been a paradigm shift in the way in which ATM is thought to function outside the DDR. Relatively recently it has been shown that ATM is activated differentially in the cytosol in response to oxidative stress, and that it also has a peroxisome localisation sequence in the C-terminal end of the FATC domain (Watters et al., 1999, Zhang et al., 2013). Its activation in the context of oxidative stress is independent of the monomerisation observed in response to DNA damage, and instead employs the use of multiple intermolecular disulfide bonds to produce an active dimer conformation, particularly between C2991 of each ATM molecule (Lee et al., 2018, Guo et al., 2010b, Guo et al., 2010a). In response to ROS, ATM is not only activated in a different manner but also phosphorylates substrates in separate pathways, particularly pathways upregulating autophagy (Guo et al., 2010b, Kim et al., 2010, Guo et al., 2010a, Kozlov et al., 2016, Alexander et al., 2010, Watters et al., 1999, Zhang et al., 2015a, Guo et al., 2020). The functions of ATM in the DDR and in response to oxidative stress are separable, to the extent that one functional pathway can remain uninterrupted even when crucial residues for the other are mutated (Guo et al., 2010b, Lee et al., 2018).

Some consideration should be given to the possibility that the open conformation dimer with some kinase activity, observed by Baretić et al, 2017 **(section 1.2.2)**, may be the same dislufide bond induced active dimer observed by Guo et al, (2010a 2010b) in response to oxidative stress. It is possible that under basal conditions the S-S bond between the two dimeric molecules exists in a redox equilibrium, and then in the presence of ROS the bond becomes oxidised to a stable S-S bond and the 24° rotation of the FLAP-BE remains the activated form.

It appears that the activation of ATM through the oxidative stress pathway functions in maintaining proteostasis by regulating autophagy **(figure 1.5)**. In cells expressing mutant ATM that could not be activated by ROS, or transduce signals through that pathway, but which still maintained its role in the DDR, researchers saw a 100-fold increase in global protein aggregation. Interestingly, the authors saw an increase specifically in the aggregation of CK2, a direct target of ATM, and a mediator of ATM induced autophagy in response to oxidative stress **(see figure 1.5)**. Aggregation of CK2 is known to decrease its signalling, which would suggest that the aggregation of proteins observed in cells unable to mount an ATM dependant oxidative stress pathway is due to a failure to adequately upregulate autophagy (Valero et al., 1995, Hübner et al., 2014, Lolli et al., 2012, Niefind and Issinger, 2005). This protein aggregation was observed to further increased in these mutant ATM cells when they were exposed to low levels of ROS (Lee et al., 2018).

In response to oxidative stress and hypoxia, ATM has also been shown to inhibit mTORC1 (mTOR complex 1) through the tumour suppressor protein TSC2 (Tuberous Sclerosis 2) resulting in an upregulation of autophagy **(see figure 1.5)** (Budanov and Karin, 2008, Alexander et al., 2010, Sarbassov et al., 2005, Olcina et al., 2013, Cam et al., 2010). A similar pathway has also been delineated for the maintenance of proteostasis in response to reactive nitrogen species (RNS) (Tripathi et al., 2013).

ATM has been specifically linked to pexophagy and mitophagy. In the N-terminal FAT domain, ATM contains a peroxisome localisation sequence, which sequesters ATM to the peroxisome membrane via the import receptor PEX5 (Watters et al., 1999, Zhang et al., 2013, Tripathi et al., 2016). ATM is also found to localise to mitochondria and becomes rapidly phosphorylated in response to mitochondrial dysfunction. Cells lacking functional ATM also have a decrease in mitochondrial turnover (Valentin-Vega et al., 2012, Fang and Bohr, 2017, Fang et al., 2016). It is thought that ATM might regulate mitophagy by being an apex signal that regulates the well-studied PINK1/Parkin (PTEN-induced putative kinase 1/Parkin) mitophagy pathway, although the exact mechanism of this has yet to be decoded (Qi et al., 2016, Gu et al., 2018). ATM also functions in the upregulation of antioxidant synthesis through the Pentose Phosphate Pathway, and loss of residues required specifically for the oxidative stress response correlates with decreased levels of the antioxidant glutathione (Zhang et al., 2018, Cosentino et al., 2011).

Outside of cellular stress, ATM functions in maintaining cellular homeostasis by regulating insulin/glucose signalling both directly and indirectly. Insulin and insulin-like growth factor-I (IGF-I) have both been shown to signal through ATM, and in turn, ATM regulates the signalling of ILGF-I by upregulating transcription of the ILGF-I receptor in response to ILGF-1 signalling (Yang and Kastan, 2000, Ching et al., 2013, Peretz et al., 2001). Once activated by insulin signalling, ATM initiates a signalling cascade where it phosphorylates PKB/Akt (Protein Kinase B), which allows its translocation to the membrane, (Viniegra et al., 2005, Halaby et al., 2008), where it regulates glucose entry to the cell by activating GLUT4.

The ability of a cell to adequately uptake glucose in response to insulin signalling is a key mechanism of energy storage and organism survival. Glucose transporter proteins mediate this movement of glucose across the cell membrane, the most insulin dependent of which is GLUT4 (Karlsson et al., 2005, Khayat et al., 2000). ATM functions in regulating both GLUT1 and GLUT4 independent of the PKB/Akt pathway. Through insulin signalling, ATM acts on GLUT4 through the Rab GTPase, AS160, and sequesters it to the cell membrane for glucose translocation (Jeong et al., 2010, Sano et al., 2003). ATM phosphorylates GLUT1, increasing its association with the GTPase activator GIPC1, allowing GLUT1 translocation to the extracellular side of the membrane (Matsuoka et al., 2007, Andrisse et al., 2013). This pathway emphasises genetic compensation that can happen after the loss of ATM, as despite there being a decrease of GLUT1 on the cell membrane there is a compensatory upregulation of GLUT1 translation (Andrisse et al., 2013, Ousset et al., 2010).

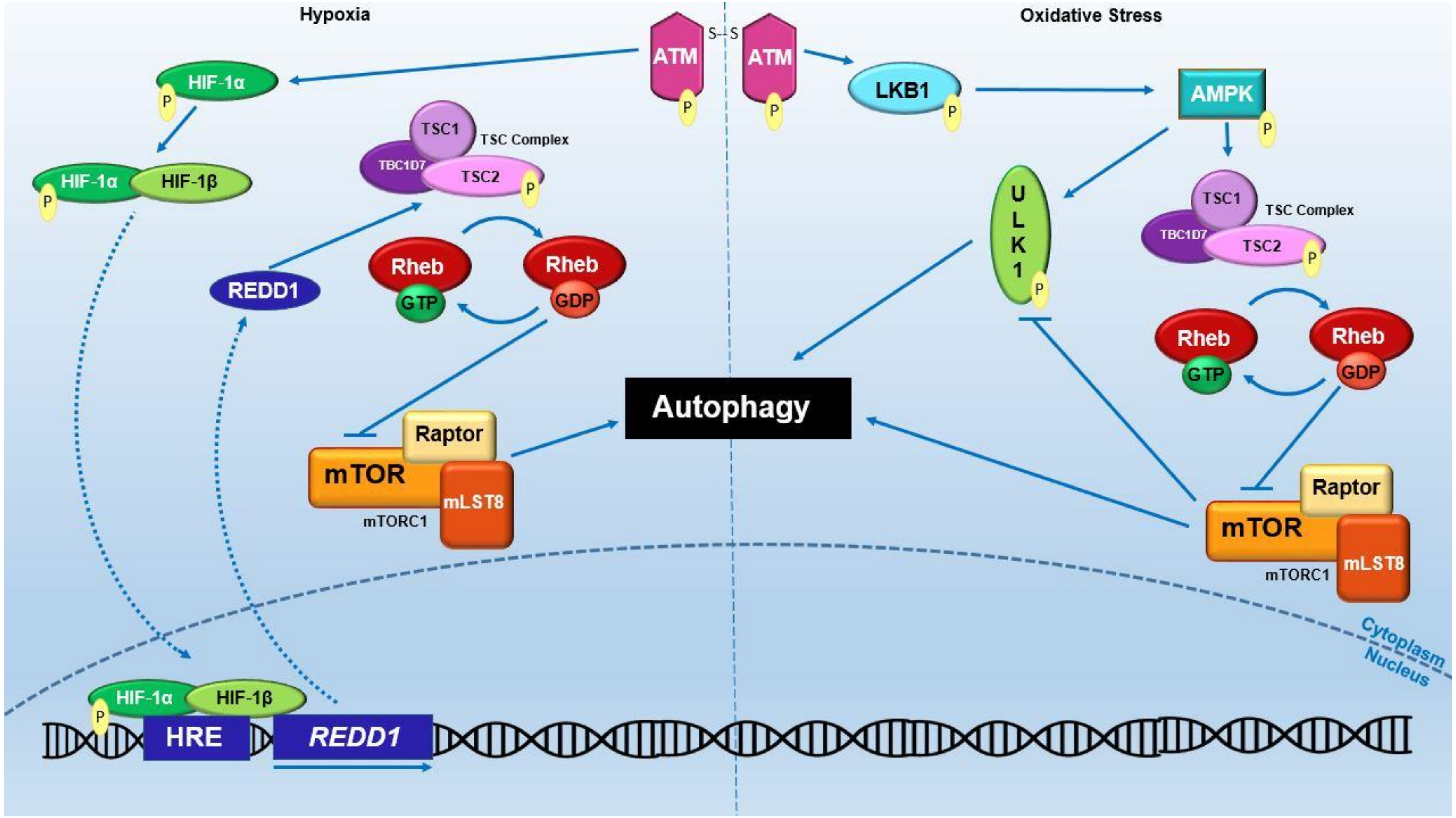
Hypoxia
Oxidative Stress
ATM
S--S
ATM
P
P
HIF-1α
P
LKB1
P
AMPK
P
HIF-1α
HIF-1β
P
TSC1
TSC Complex
TBC1D7
TSC2
P
ULK1
P
TSC1
TSC Complex
TBC1D7
TSC2
P
REDD1
Rheb
GTP
Rheb
GDP
Rheb
GTP
Rheb
GDP
Autophagy
Raptor
mTOR
mLST8
mTORC1
Raptor
mTOR
mLST8
mTORC1
Cytoplasm
Nucleus
HIF-1α
HIF-1β
P
HRE
REDD1

Figure 1.5 ATM mediated redox induces autophagy through mTORC1 during oxidative stress. The ATM dimer is activated through a conformational change from the formation of a number of disulfide bonds, particularly of C2991 in the FATC domain. The autophosphorylation of ATM begins a signalling cascade whereby ATM phosphorylates LKB1 (liver kinase B1 protein) which in turn phosphorylates AMPK (AMP-activated protein kinase). AMPK then phosphorylates TSC2 in the TSC (Tuberous sclerosis complex). The TSC has GTPase activity and inactivates Rheb (Ras homolog enriched in brain) by converting the bound GTP to GDP. mTORC requires active GTP bound Rheb for its activity, therefore the conversion of GTP bound Rheb to GDP bound Rheb inactivates mTOR, which allows for the upregulation of autophagy. Again demonstrating the redundancy in the ATM signalling pathway, ATM mediated activated AMPK also directly phosphorylates and activates ULK1 kinase complex. ULK1 directly upregulates autophagosome biogenesis, and under times of cell growth is directly inhibited by mTORC1 in a feedback mechanism. Conversely, in times of **hypoxia**, ATM also directly upregulates autophagy in a similar pathway. Under low oxygen concentrations, cytosolic ATM has been shown to phosphorylate HIF-1α (hypoxia-inducible factor). Phospho-HIF-1α is then able to bind to HIF-1β, forming the HIF complex. This transcription factor complex translocates to the nucleus where it binds to hypoxia-response elements (HRE) in the promoters of genes that are upregulated to protect the cell against hypoxia. One of these genes is *regulated in development and DDR 1 (REDD1).* The REDD1 protein, once in the cytosol it is then able to activate the TSC complex and suppress mTORC1 activity as seen in the oxidative stress response (Olcina et al., 2013, Cam et al., 2010, Bencokova et al., 2009, Alexander et al., 2010, Dibble et al., 2012, Kim et al., 2011, Di Nardo et al., 2014).

1.2.4 ATM Genotype vs AT Phenotype

The severity of the clinical phenotype can vary significantly from classical AT to a considerably milder phenotype (variant AT). It appears that variant AT is linked to a subset of cases where the mutant ATM protein is present and has some residual activity. Patients with less severe symptoms tend to have compound heterozygous mutations with one allele being a null variant while the other tends to be 'leaky' and to confer some protein functionality (Gilad et al., 1998, Ying and Decoteau, 1981, Saviozzi et al., 2002, Hiel et al., 2006, Verhagen et al., 2009, Verhagen et al., 2012a, Fievet et al., 2019). Genotype/phenotype correlations can be problematic in AT for two reasons; first, there are no mutational hotspots in ATM, therefore due to the size of the ATM gene, identifying novel pathogenic mutations from non-pathogenic variants can be challenging (Mitui et al., 2003). As splice site mutations in AT are common, both coding and noncoding regions of ATM need to be considered. Second, many individuals affected by AT are compound heterozygotes (Mitui et al., 2003, Mitui et al., 2005, Verhagen et al., 2009, Verhagen et al., 2012b, Verhagen et al., 2012a). Therefore, it can be difficult to determine the contribution of each allele to the overall clinical phenotype (Gatti et al., 1999, Meyn, 1999). It is not known in what circumstances ATM dimer exists in heterozygous patients without a null allele, and whether the dimer is comprised of ATM proteins from just one or both alleles (Fievet et al., 2019, Taylor et al., 2015). Finally, individuals with homozygous mutations tend to be from consanguineous families (Shimazaki et al., 2020, Concannon and Gatti, 1997). Such patients will have extensive regions of homozygosity in their genomes, which makes it challenging to rule out the influence of other recessively inherited variants that may influence the phenotypic presentation (Balta et al., 2019).

AT symptoms, and their severity, are dependent on residual levels of ATM kinase activity (Barone et al., 2009, Verhagen et al., 2012a). ATM kinase activity is measured in patient cells by measuring phosphorylation of downstream targets of ATM (Mitui et al., 2005, Paucar et al., 2019, Cummins et al., 2013, Fievet et al., 2019). While this does give an excellent indication of kinase activity, it is only kinase activity for those specific targets, and does not indicate any alteration to protein-protein interactions. For instance, missense mutations have been described which cause ATM to mislocalise in cells, and this is thought to be sufficient to cause AT (Jacquemin et al., 2012, Fievet et al., 2019).

It is thought that the pleiotropic effects of AT can be mostly defined by a perturbation of two main downstream pathways. Disruption to the DDR pathway may lead to immunodeficiency, telangiectasia, and infertility, while metabolic dysregulation may be attributed to the inability to control redox stress. It is not clear from perturbation of which pathway results in ataxia as there is evidence for deregulation of both the DDR and oxidative stress being causative. Malignancy seems to be caused by an overlap of failure in both the DDR and oxidative stress pathways. Evidence for these divergent pathways leading to different AT phenotypes are presented in the following sections.

1.2.4.1 Immunodeficiency

AT is classed as a Primary Immunodeficiency Disorder that affects both cellular and humoral immune function, and over 70-80% of AT patients suffer from severe and often fatal infections as a result (Nowak-Wegrzyn et al., 2004, Buckley, 2004). In the absence of ATM, there is a failure to mount an adequate response to pathogens, including insufficient antigen receptor combinations due to failure in V(D)J (variability, diversity, and joining) recombination, low levels of circulating immunoglobulins (Ig) due to failures in class switching recombination (CSR), and low levels of circulating mature B and T cells, which is a result of incomplete recombination events. Immunodeficiency amongst AT sufferers is variable, and the degree of immunodeficiency suffered by the patients correlates strongly with residual ATM activity, and primarily stems from the inability to repair specific DNA double strand breaks (Bredemeyer et al., 2006b, Reina-San-Martin et al., 2004a, Lumsden et al., 2004, Kracker and Durandy, 2011, Pan-Hammarström et al., 2003, Pan et al., 2002, Staples et al., 2008, Stray-Pedersen et al., 2005, Noordzij et al., 2009, Verhagen et al., 2012a).

Somatic recombination events in the immune system allow a highly varied antibody reaction in response to pathogens. V(D)J recombination takes place in developing B cells and it allows the humoral immune system to create antigen specific recognition sequences to several antigens from the same pathogen. This diversity in antigen recognition sequences is complemented by CSR, which allows these variable regions to be paired in a number of ways with ‘effector’ constant regions of the antibody, e.g. IgM, IgG, IgE, IgD, and IgA (Roth, 2014, de Villartay, 2002, Kracker and Durandy, 2011). These recombination events are highly specific and ATM directly mediates repair of these DNA breaks during both V(D)J and CSR (Perkins et al., 2002, Dujka et al., 2010, Bredemeyer et al., 2006b, Noordzij et al., 2009, Reina-San-Martin et al., 2004b, Amirifar et al., 2020, Meek et al., 2016, Hewitt et al., 2009).

The inability of the adaptive immune system to adequately complete V(D)J recombination leaves AT sufferers with a depleted antibody repertoire, and therefore the inability of the immune system to recognise multiple antigens from the same pathogen. Failure in CSR leads AT patients to have lower overall circulating serum immunoglobulin levels. In a study of 100 AT patients, 65% had a decrease in serum IgG4, 48% had a decrease in IgG2, 63% had a decrease in IgA, and 23% had a decrease in IgE (Nowak-Wegrzyn et al., 2004). As IgM is the ‘default’ immunoglobulin class from which the others are ‘switched’, AT can lead to a serum increase of IgM, often leading to a misdiagnosis of hyper-IgM syndrome (Noordzij et al., 2009). The degree to which immunoglobulins are reduced in patient shows a relationship to residual kinase activity, where variant AT may have inconsistent levels of immunoglobulins but no observed primary immunodeficiency. Classical AT patients generally have very low levels of immunoglobulins, to the point where some individuals may have hypoimmunoglobulinemia (Nowak-Wegrzyn et al., 2004, Fievet et al., 2019).

AT patients also present with excessive translocations and inversions of chromosome 7 and 14 in lymphocytes (Oxford et al., 1975, McCaw et al., 1975, Aurias et al., 1980, Aurias et al., 1986). These are also found in the general population, but at a rate of 1:2000 per lymphocytes surveyed, while in AT patients they are found a rate of 1:60 (Kojis et al., 1989, Kojis et al., 1991). These chromosome breaks are not random and map to sites of genes of the immunoglobulin heavy chain and T cell receptor genes (Kirsch et al., 1982, Aurias and Dutrillaux, 1986, Huang et al., 2007, Bredemeyer et al., 2006b). This suggests that these translocations are a result of unrepaired intermediate ds breaks from somatic recombination events. These cytogenic abnormalities are pathogenic to AT sufferers, as not only do they inhibit the required immune response to infections, they are also associated with increased incidence of AT associated leukaemia and lymphomas. This will be discussed in more detail below in section **1.2.4.2 Malignancies**.

This inability of the AT immune system to form antibodies results in decreased B cell and T cell serum levels. However, the degree to which they are reduced varies from classical AT to variant AT, and very low levels of B cells in classical AT correlate with a decrease in circulating immunoglobulins, signifying that aberrant V(D)J recombination blocks B cell maturation. Classical AT patients also show an increase in naive B cell production as a compensatory mechanism. This compensatory mechanism, as well as IgA deficiency, is likely to underlie the burden of lymphoma in AT patients. It also demonstrates the overlap between immunodeficiency and malignant pathology in AT (Driessen et al., 2013, Suarez et al., 2015). AT variant patients also show an increase in this compensatory mechanism but to a far lesser extent (Driessen et al., 2013).

The decrease in serum T cells in AT patients is likely to be associated with chromosome 7 and 14 translations at the sites of T cell receptor genes (Driessen et al., 2013, Kirsch et al., 1982, Aurias and Dutrillaux, 1986, Aurias et al., 1986, Kojis et al., 1991). Additionally, abnormalities in the thymus, the site of T cell production, are also observed in AT, but these are thought to be linked to dysregulation of the oxidative stress response and an increase in apoptosis, rather than a deficiency in the DDR (Peterson et al., 1964, Schubert et al., 2002, Giovannetti et al., 2002, Bagley et al., 2007, Gatti and Vinters, 1985).

Deficits in the ability of the immune system to induce the required immune response leaves AT patients open to recurrent and severe infections, particularly respiratory infections. These infections make up a significant portion of the morbidity of AT, with up to 50% of AT patients dying during adolescence from respiratory failure (Bott et al., 2007, Crawford et al., 2006, Pagano et al., 1998). Mitigating infections in AT patients is clinically difficult. The inability of some AT patients to mount an antibody response makes vaccination a low yielding avenue of treatment. Prophylactic vaccination may be a viable approach to attenuate infection and boost circulating immunoglobulin levels in variant AT patients.

However, this is far less efficacious for classical AT patients with very low levels of circulating immunoglobulin, particularly in individuals with hypoimmunoglobulinemia (Warren et al., 2019, Stray-Pedersen et al., 2005, Sanal et al., 1999). Therefore, the current best practice for the treatment of immunodeficiency in AT patients is immunoglobulin replacement therapy and management of individual infections. Additionally, viral infections exhibit a unique challenge for a DDR deficient immune system because the cellular defence mechanism to cytosolic nucleic acid may be ATM dependent (Dunphy et al., 2018, Hartlova et al., 2015). Oncogenic viruses pose a particular threat to AT patients, as they can not only cause a primary infection, but can also result in related malignancies (Kulinski et al., 2012, Okano et al., 1993, Rubinstein et al., 2020, Dunphy et al., 2018).

1.2.4.2 Malignancies

AT patients have a significant predisposition to malignancies, and the incidence of malignancies in AT patients is estimated to be as high as 33%. These malignancies tend to be leukaemias, lymphomas and carcinomas (Morrell et al., 1990, Suarez et al., 2015, Reiman et al., 2011, Peterson et al., 1964, Taylor et al., 1996). Malignancies in young and early adult AT patients tend to present as leukaemia and lymphomas which are the result of failure in V(D)J recombination, causing translocations involving chromosomes 7 and 14 in lymphocytes (Taylor et al., 1996, Bredemeyer et al., 2006b, Huang et al., 2007, Vacchio et al., 2007, Hewitt et al., 2009) **(see section 1.2.4.1 Immunodeficiency).** Childhood leukaemias within the general population tend to be pre-B cell and B cell-precursor Acute lymphoblastic leukaemia (ALL), which are formed by cells that have not yet completed V(D)J recombination (Greaves and Wiemels, 2003), whereas AT patients do not show any increase in these type of leukaemias, but do show an increase in B-cell tumours where the cell should have completed V(D)J recombination (Taylor et al., 1996, Gumy-Pause et al., 2004). Lymphoid leukaemias are the main cause of death in patients with homozygous loss of function mutations (Reiman et al., 2011, Suarez et al., 2015, Taylor et al., 1996, Micol et al., 2011a).

Early childhood lymphomas and leukaemias in AT are causally linked to a deficiency in the DDR and the inability to maintain genome integrity, and these types of malignancies affect classical AT patients to a far greater extent than they do variant AT patients (Reiman et al., 2011). Complete loss of function mutations are strongly associated with increased cancer risk and increased morbidity (Micol et al., 2011a). Note that this pattern of variation is similar to that observed in immunodeficiency in variant AT patients **(see 1.2.4.1)**. It is also closely correlated with residual kinase activity, and if variant AT patients do develop leukaemia/lymphoma, it tends to be in adulthood as opposed to early childhood (Reiman et al., 2011). Interestingly, patients with severe IgA deficiency have a higher risk of cancer (Suarez et al., 2015). Although a properly functioning immune system is protective in clearing malignant cells, this correlation is most likely due to a severe attenuation of CSR in these cells (where the IgA locus is last to be cleaved during recombination) and increased genome instability.

AT patients also have an increased risk of carcinomas in late childhood/adulthood, particularly breast, liver and gastrointestinal carcinomas (Micol et al., 2011a). By age 50, AT patients have a 45% risk of developing breast cancer, which is significantly higher than similarly aged patients carrying heterozygous or holomorphic mutations in the DDR genes *BRCA1* or *BRAC2*, which carry a breast cancer risk of 30% and 20% respectively (Antoniou et al., 2008, Reiman et al., 2011). Whether defects in the DDR or unresolved oxidative stress is causative in later onset malignancies in AT is open to debate, and will likely vary from patient to patient due to genetic predisposition and environmental factors.

It should also be noted that dysfunction of ATM has also been shown to play a role in the formation of solid tumours in the general population. De novo somatic mutations in *ATM*, low ATM expression caused by hypermethylation of the *ATM* promoter, and specific SNPs in the ATM gene have all been shown to be causative factors (Choi et al., 2016, Kim et al., 2014a, Kim et al., 2013, Kim et al., 2014b, Suh et al., 2016, Begam et al., 2017, Bolt et al., 2005, Mehdipour et al., 2015, Safar et al., 2005, Vo et al., 2004, Stracker et al., 2013, Weber and Ryan, 2015, Tao et al., 2020).

1.2.4.3 Telangiectasias and Vascular Abnormalities

Telangiectasias, or spider veins, are dilated and broken blood vessels that present as threadlike patterns **(see figure 1.6).** The cause of telangiectasias in AT remains unclear. In AT patients, onset of telangiectasia occurs around 8 years of age and tends to present on the cheeks, ears, legs, arms, trunk, and particularly the bulbar conjunctiva in the eyes. One study estimates that telangiectasias occur in 97% of classical AT cases and therefore they aid in the differential diagnosis of the disease (Greenberger et al., 2013). However, it should be noted that not all patients with a mutation in the *ATM* gene present with this symptom, and this can often result in a diagnostic delay (Cabana et al., 1998, Navratil et al., 2015). These exterior telangiectasias associated with AT appear to be mainly cosmetic, since they are non-progressive and do not usually cause itching or pain to the sufferer. It does appear that the degree to which patients have telangiectasias correlates with the residual kinase activity of the mutant ATM protein. In one study, 100% of patients with no expression of the ATM protein exhibited external telangiectasias, and this decreased to 54% of patients with some residual kinase activity (Schoenaker et al., 2018).

Although there do not seem to be any pathological concerns from these external telangiectasias, there are many reports in which internal telangiectasias and vascular abnormalities have severe consequences for the patient. Several case studies have been reported where AT patients have bladder telangiectasias **(see figure 1.6c)**, which result in significant life threatening haematuria in the individual. In addition to telangiectasias, there are several reported cases of haemorrhagic cysts in the bladder (Micol et al., 2011b, van Os et al., 2017b, Kaymaz et al., 2009, Christmann et al., 2009, Cohen et al., 2008, Aygün et al., 2015, Suzuki et al., 2008).

How loss of ATM function causes telangiectasias, and telangiectasia formation in general, is not well understood, but it is thought to be correlated with ageing; another symptom associated with the AT phenotype. ATM has been implicated in angiogenesis through the oxidative stress pathway (Yun et al., 2009, Okuno et al., 2012).

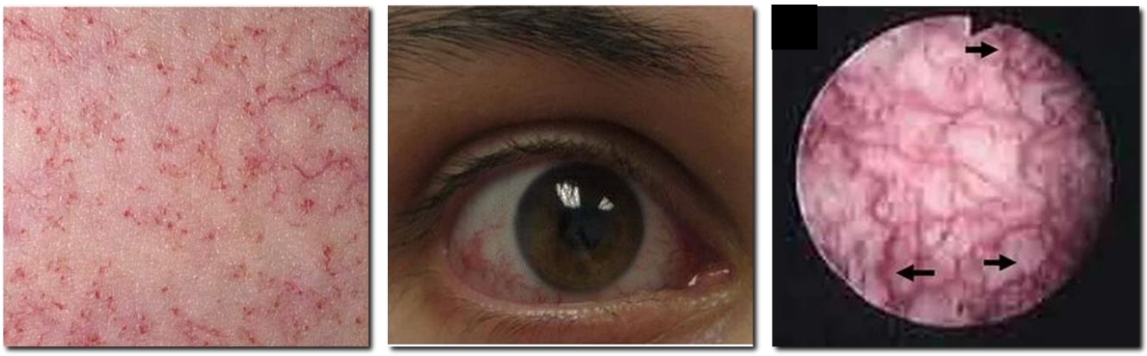

Figure 1.6 Telangiectasias in AT patients a. on the surface of the skin (Fernandez, 2019) and **b.** eyes (Rothblum-Oviatt et al., 2016) https://creativecommons.org/publicdomain/zero/1.0/ and **c.** telangiectasias in the bladder leading to severe haematuria (Suzuki et al., 2008).

1.2.4.4 Metabolic Dysregulation

Elevated levels of AFP (alpha-fetoprotein) is a characteristic finding in AT patients of all ages and often serves as an important biomarker for AT (Waldmann and McIntire, 1972). Normally, AFP is produced at high levels by the fetal liver, and expression steadily decreases over the first few years of life to low ‘adult’ levels at around 2 years old (Bergstrand and Czar, 1956). However, in AT patients AFP levels tend to increase with age (Waldmann and McIntire, 1972, Stray-Pedersen et al., 2007). Concerning genotype/phenotype correlation, all cases of AT appear to have elevated AFP regardless of whether they present as classical or variant AT (Mitui et al., 2005). It is the only symptom of AT that does not correlate to residual kinase activity, and it is not clear yet if the elevated levels of AFP are pathogenic or only serve as a marker for some other pathogeneses, as the mechanism for its elevation is not yet understood. However, the elevation of AFP levels in AT has tentatively been linked to the loss of regulation of an ATM target, the transcription regulatory factor ZFHX3/ATBF1 (Zinc Finger Homeobox 3/ (AT-motif binding factor 1) (Kim et al., 2010, Matsuoka et al., 2007). ZFHX3/ATBF1 binds to A-T rich sequences of the *AFP* gene and inhibits its transcription in conjunction with p53 (Morinaga et al., 1991, Yasuda et al., 1994, Wilkinson et al., 2008). Therefore, loss of ATM signalling is associated with loss of downstream ZFHX3/ATBF1 and p53 signalling, and subsequent aberrant expression of AFP (Kim et al., 2010).

Interestingly, two other autosomal recessive ataxias exhibit elevated AFP levels; AOA2 and AOA3 (Ataxia-Oculomotor Apraxia) **(see appendix 1.1)**. This suggests at least two shared deregulated pathways between these three ASRAs; Purkinje cell death and chronic hepatic dysfunction (Anheim et al., 2009, Le Ber et al., 2004, Al Tassan et al., 2012). AOA2 patients have a loss of function mutation in the *SETX* gene; although not much is known about the SETX protein, it is thought to function in repairing transcription related DNA double strand breaks and possibly prevent R loop formation (Cohen et al., 2018, Suraweera et al., 2009, Zhao et al., 2016, Grunseich et al., 2018). This suggests that the elevated levels of AFP in both diseases may be a result of impaired DNA damage repair in the hepatic tissue, and more specifically, the inability to resolve R loop formation (Marabitti et al., 2019, Sordet et al., 2009, Sordet et al., 2010, Vermeulen and Tresini, 2017).

Due to more advanced care and as management of AT symptoms has improved, patients are living longer than previously, and this leads to an increase of age related liver pathology in AT. Older AT patients have been shown to suffer from hepatic stenosis along with fibrosis and cirrhosis, as well as elevated levels of other liver enzymes such as GGT (gamma-glutamyl-transferase), AST (aspartate aminotransferase), and ALT (alanine aminotransferase) (Paulino et al., 2017, Pillsbury et al., 1985, Caballero et al., 2014, Weiss et al., 2016). In a longitudinal study of AT patients, it seems that severe liver involvement begins around puberty, is progressive, and affects 92% of patients who survive into their 30s (Donath et al., 2019). It has been proposed that these abnormalities seen in the liver are due to the inability to activate the oxidative stress pathway of ATM rather than the DNA damage pathway (Daugherity et al., 2012, Donath et al., 2019).

As AT progresses into adolescence and adulthood, patients begin to exhibit metabolic syndrome, insulin resistance, and type 2 diabetes (Paulino et al., 2015, Yang et al., 2011b, Schalch et al., 1970, Connelly et al., 2016, Schneider et al., 2006), and it has been experimentally shown in mice that activation of ATM is protective against metabolic syndrome (Schneider et al., 2006). Mechanistically, ATM is thought to phosphorylate 4EBP-1 (eIF-4E-binding protein 1) in an insulin dependent manner. This then liberates eIF-4E (Eukaryotic

Initiation Factor 4E) from 4EBP-1, and allows eIF-4E dependent transcription (Yang and Kastan, 2000). A similar eIF-4E pathway has been implicated in cellular growth (Flynn and Proud, 1996) as well as ATM dependent activation of the IGF-IR (insulin-like growth factor-I receptor) (Peretz et al., 2001, Bar et al., 1978). Additionally, disruption of mTORC1 signalling has been implicated in insulin resistance diabetes. mTORC1 is negatively regulated by ATM in the context of the DDR and oxidative stress (Sarbassov et al., 2005, Alexander et al., 2010, Budanov and Karin, 2008). Disruption of these pathways is likely to contribute to insulin resistance, and therefore to the raised insulin levels observed. Additionally, aberrant insulin signalling may cause the short stature and growth retardation seen in AT sufferers.

1.2.4.5 Neurodegeneration

a. Clinical Presentation of Neurodegeneration in AT

Neurological symptoms are usually the first signs of AT and tend to present in infants. Children that suffer with AT tend to initially match normal developmental milestones but then either their gait starts to regress or they do not develop beyond a wobbly toddler gait. Around mid-childhood, an AT gait is progressively ataxic, along with the onset of oculomotor apraxia, nystagmus and saccades. Concurrently, there is an onset of dysarthria, as well as a progressive decrease in fine motor skills along with symptoms associated with deficiencies in the extrapyramidal system, such as chorea, athetosis, dystonia and myoclonic jerks. Patients' intentional movements may be hypokinetic or bradykinetic, and development of facial hypomimea is common. AT patients are generally confined to a wheelchair at approximately 10 years of age, and at around 15 years of age, patients can often enter a plateau stage where the neurological symptoms are severe but no longer progressive (Boder and Sedgwick, 1958, Crawford, 1998, Hoche et al., 2012, Shaikh et al., 2013, Pearson, 2016, Kwast and Ignatowicz, 1990, Rothblum-Oviatt et al., 2016, Lewis and Crawford, 1998, Shaikh et al., 2009).

Neurological symptoms in AT are caused by degeneration of PCs and progressive atrophy of the cerebellum (Tavani et al., 2003, Shaikh et al., 2013).

Figure 1.7 shows MRI scans from three different AT patients aged 5, 13 and 39 years. As can be seen, the cerebellum of the 5 year old is largely intact, with the Purkinje dendritic arbors filling the cerebellar space. However, the 13 year old displays a substantial lessening of dendritic arbors, atrophy of the vermis, and cerebrospinal fluid (white) has infiltrated the molecular layer. In the 39 year old, near total atrophy of the cerebellum can be observed, with major degeneration of PC structure and again extensive intrusion of cerebrospinal fluid (Tavani et al., 2003). It has also been reported that there is an overall increase in microglial activation, suggesting the involvement of neuroinflammation (Verhagen et al., 2012b).

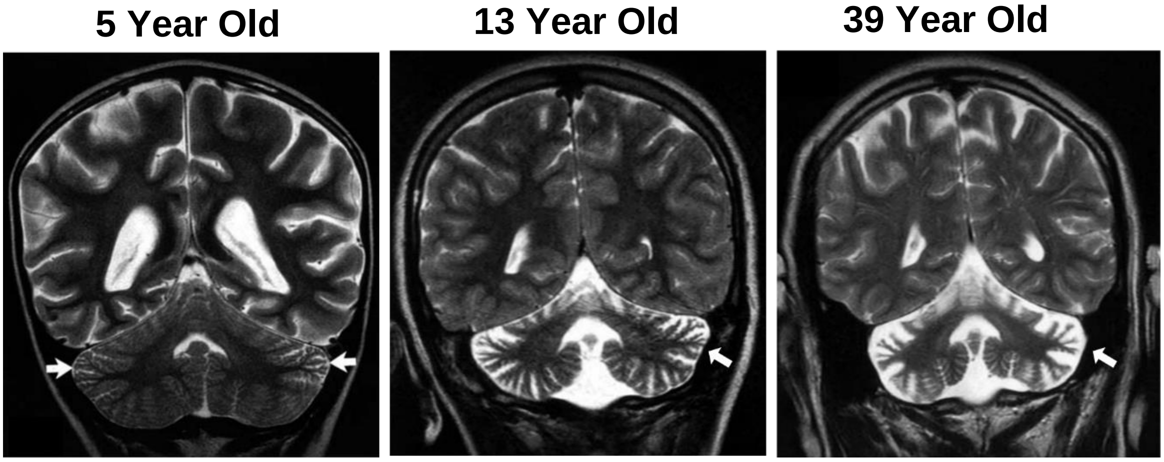

Figure 1.7 Coronal T2-weighted image of cerebellar atrophy in AT patients. White arrows indicate the cerebellar structure. Panels from left to right: 5 year old, 13 year old, 39 year old. Cerebellar atrophy with degeneration of PC dendrites and infiltration of cerebrospinal fluid can be observed in 13 & 39 year olds. Images adapted from (Tavani et al., 2003) and reproduced with permissions from SpringerNature.

The cause of the neurodegeneration observed in AT patients is not well understood, and the exact pathological mechanism responsible is hotly debated. Several potential mechanisms are summarised in **table 1.4** and discussed below. While the neurological symptoms are not a primary life-limiting aspect of AT, they remain the biggest barrier to quality to life for AT patients and contribute to morbidity by increasing food and saliva aspirations that lead to fatal respiratory infections. Therefore, the understanding of the pathological mechanism behind this feature and the ability to reduce and mitigate its severity is an important aspect of AT clinical care.

b. DNA Damage Repair Deficiencies

Although the DDR plays an integral role in the development of the nervous system (Barzilai et al., 2008, Herzog et al., 1998, Lee et al., 2001), AT is degenerative, not developmental, and therefore, the reason that PCs in particular are vulnerable to the effects of DNA damage is not understood. An accumulated DNA damage model was first proposed to be a pathogenic mechanism in neurodegeneration as far back as 1978, and is still accepted today (Andrews et al., 1978). This model proposes that while endogenous neuronal DNA damage occurs in normal individuals, it is constantly being repaired, resulting in an equilibrium of low level damage and subsequent repair which the cells are able to tolerate and allows them to function efficiently. However, in patients with a DNA damage repair deficiency, the non-repaired DNA damage accumulates over time until it reaches a threshold that neuronal cells can no longer tolerate, and they die as a result of abortive transcription **(figure 1.8)**. In the case of AT, this threshold may take years to be reached and may offer an explanation as to why mouse models of AT do not exhibit a strong neuronal phenotype, as their lifespan may not allow for this accumulation.

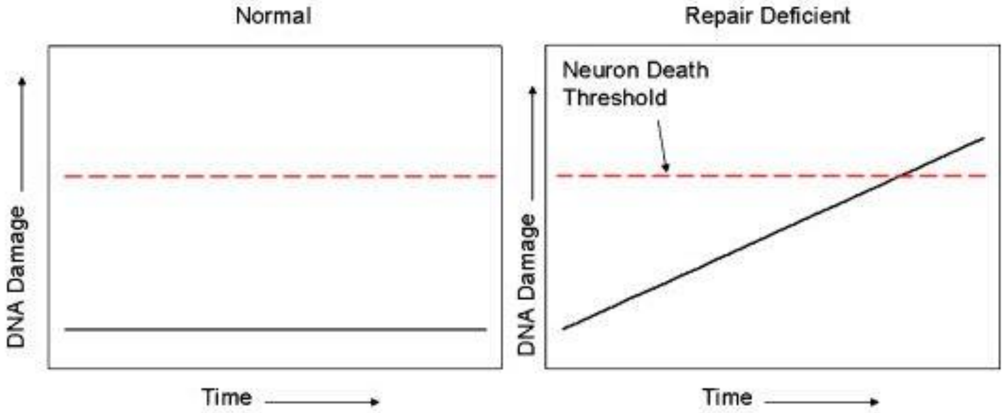

Figure 1.8 The accumulated DNA damage model of neurodegeneration. In normal individuals neuronal cells existed in a low level equilibrium of DNA damage and repair. In patients with a DNA damage repair deficiency, over time the unrepaired DNA damage reaches a threshold level whereby neuronal cell death occurs due to abortive transcription. Reproduced with permissions from (Brooks et al., 2008).

Abortive transcription due to excessive DNA lesions has been specifically implicated in AT. ATM is now known to play a role in repairing double and single strand breaks due to replication fork stalling and transcriptional unwinding, particularly in resolving Top1cc and R loops (Sordet et al., 2009, Sordet et al., 2010, Das et al., 2009, Alagoz et al., 2013, Katyal et al., 2014, Marabitti et al., 2019, Vermeulen and Tresini, 2017). TOP1cc are formed during DNA replication when Topoisomerase 1 (TOP1) binds to DNA and creates a single strand break to allow access of the replication machinery. The composite of TOP1 bound to DNA creates a Topoisomerase cleavage complex (TOPcc) which is generally transient and resolved by the hydrolysis of the shared 3' phosphodiester bond by TDP1 allowing re-ligation of the DNA backbone (Koster et al., 2005, Humbert et al., 2009, Pouliot et al., 1999, Interthal et al., 2001, Takashima et al., 2002). TOP1ccs have been shown to activate ATM in both the presence and absence of TDP1, and ATM deficient cells show a decrease in their ability to resolve these DNA protein linked breaks, as ATM directly phosphorylates TDP1 (Alagoz et al., 2013, Katyal et al., 2014, Das et al., 2009, Humbert et al., 2009, Sordet et al., 2009, Sordet et al., 2010, Lin et al., 2008). Top1ccs have also been observed in ATM-null neuronal cells and animal models (Katyal et al., 2014, Alagoz et al., 2013). Additionally, abortive transcription has also been implicated in two other recessively inherited ataxias, SCAN1 and AOA2, caused by mutations in TDP1 and SETX genes respectively **(see table 1.2 and appendix 1.1)**. While ATM has roles outside of DNA repair, the fact that all three genes function in replication stress-related DNA repair suggests that this may be a shared disease mechanism. However, a caveat to note is that PCs are quiescent and exist in a G_0 state, so it is difficult to determine how replication stress would arise; however, TDP1 is highly expressed in PCs (Gorodetsky et al., 2007, Brooks et al., 2008).

There is also evidence to suggest that, in common with immune cells, neuronal cells also undergo somatic recombination events to maintain neuronal cell diversity (Iourov et al., 2009a, Iourov et al., 2009b, Gao et al., 1998, Wu and Maniatis, 1999). Given the absolute imperative that ATM must be functional for proper recombination events to occur in both the immune and reproductive systems **(see section 1.2.4.1 Immunodeficiency and 1.2.4.6 Infertility)**, it would be reasonable to expect that any recombination events that occur in neuronal cells in the absence of ATM would also be detrimental. Together with endogenous DNA damage, these unrepaired recombination events could lead to disproportionate genomic instability and possible aneuploidy in the AT CNS (Iourov et al., 2009b).

In addition to DNA damage resulting directly in cellular failure, it has been proposed that this excessive unrepaired DNA damage in the CNS causes an immune response similar to that of a severe viral infection, and during the immune response, the affected PCs are cleared (Quek et al., 2016, Quek et al., 2017b, Hartlova et al., 2015). It has been reported that as a result of the loss of ATM, damaged DNA can become cytosolic and activate NFkB and the Type I Interferon System via the STING (stimulator of interferon genes) pathway (Hartlova et al., 2015, Dunphy et al., 2018, Zhang et al., 2019). Concurrently, some vertebrate models of AT also exhibit evidence of cytosolic DNA and a neuroinflammatory phenotype (Quek et al., 2016, Quek et al., 2017a, Quek et al., 2017b), while neuroinflammation is also often observed in AT patients (Verhagen et al., 2012b).

The neurodegeneration observed in DNA damage repair disorders, such as Aicardi-Goutières syndrome and cerebellar ataxias including AOA1, SCAR1 and SCAN1, and Ataxia Telangiectasia-Like disorder, Nijmegen breakage syndrome-like disorder, and Nijmegen breakage syndrome, strongly suggests that DNA damage contributes to AT. Interestingly, the relevant mutated genes in the latter three disorders *MRE11, Rad50,* and *Nbs1,* respectively, all function together as ‘sensors’ of DNA damage directly upstream of ATM in the MRN complex **(appendix 1.1, section 1.2.2 and figure 1.3 and 1.4)**. However, the neurodegeneration in patients suffering from Nijmegen breakage syndrome-like disorder and Nijmegen breakage syndrome tends to be microcephaly and not ataxia, which would suggest a developmental rather than degenerative phenotype (Waltes et al., 2009, Ragamin et al., 2020). Additionally, the ataxia observed in Ataxia Telangiectasia-Like disorder has much later onset, slower progression and is less severe (Taylor et al., 2004, Palmeri et al., 2013, Fiévet et al., 2019). So while the MRN complex is the master ‘sensor’ of DNA damage, and although it does activate ATM, it also activates many other DNA damage repair proteins, while also being active at the site of DNA damage repair **(see section 1.2.2 and figure 1.4)**.

c. Oxidative Stress and Mitochondrial Dysfunction

Evidence for redox stress and mitochondrial dysfunction being the causative mechanisms for neurodegeneration in AT is mounting. These mechanisms have also been implicated in many age-related neurodegenerative diseases, such as Alzheimer's and Parkinson's disease (Lin and Beal, 2006, Halliwell, 2006, Ryter et al., 2007). While the oxidative stress burden of ATM null cells will add to DNA damage experienced by these cells (Tanaka et al., 2006a), oxidative stress is likely pathogenic on its own, as treatment of ATM null models with antioxidants has been shown to lessen the severity of the neurological phenotypes observed (Browne et al., 2004, Reliene et al., 2008, Chen et al., 2003b, Gueven et al., 2006). The ATM R3047X mutation causes loss of only the last 10 amino acid residues of the ATM protein that are required for oxidative stress activation **(see section 1.2.3)**. The ATM protein carrying this mutation can appropriately activate the ATM DDR pathway, but not the oxidative stress pathway (Guo et al., 2010b, Guo et al., 2010a). Furthermore, patients with this mutation are considered AT variants, since they exhibit neurodegeneration but not immunodeficiency, and only small amounts of radiosensitivity (Chessa et al., 1992, Gilad et al., 1998, Toyoshima et al., 1998, Guo et al., 2010b, Guo et al., 2010a). This pattern is consistent with other cases of variant AT, where although some patients may have a less severe or later onset of neurological symptoms, they show no great susceptibility to the other features of AT caused by deficiency in the DDR, such as infertility and immunodeficiency (Reiman et al., 2011, Verhagen et al., 2009, Verhagen et al., 2012b, Verhagen et al., 2012a). Pathological mechanisms of increased oxidative stress in the context of AT are outlined below.

i. Protein Aggregation

As previously described in **section 1.2.3**, un-attenuated oxidative stress in ATM-null cells causes defective protein turnover and aggregation (Guo et al., 2010b, Guo et al., 2010a, Lee et al., 2018), and it appears that ATM deficient cells under increased oxidative stress, decrease their protein production (Wood et al., 2011, Poletto et al., 2017), possibly as a means of tempering this aggregation. Protein aggregation is thought to be a major contributing factor in many neurodegenerative disease, such as Alzheimer’s Disease, Parkinson’s Disease, Huntington’s Disease, Amyotrophic Lateral Sclerosis (ALS) and some SCAs **(see appendix 1.1 and table 1.2)**, (Gandhi et al., 2019).

ii. Mitochondrial Dysfunction

One of the major contributing factors to cellular ROS is mitochondrial oxidation (Nissanka and Moraes, 2018). ATM is localised in the mitochondria during oxidative stress and plays a role in maintaining mitochondrial homeostasis (Valentin-Vega et al., 2012, Morita et al., 2014, Eaton et al., 2007). However, despite the consensus that loss of ATM causes mitochondrial dysfunction, the exact effects of loss of ATM on the mitochondria are not clear. Key findings are outlined in **table 1.3**. Furthermore, mitochondrial dysfunction has been implicated in many other neurodegenerative disorders, such as Charcot-Marie-Tooth type 2A (CMT2A), Parkinson's, Huntington's and Alzheimer's disease (Züchner et al., 2004, Dodson and Guo, 2007, Bossy-Wetzel et al., 2008, Bose and Beal, 2016).

Table 1.3 Effects of ATM deficiency on Mitochondria

Paper	***Nature of ATM Deficiency***	***Key Findings***
ATM directs DNA damage responses and proteostasis via genetically separable pathways (Lee et al., 2018)	*C2991L ATM mutant (loss of ATM oxidation specific pathway)*	*Decreased mitochondrial numbers Decreased mitophagy Aberrant fatty acid oxidation*
Intrinsic mitochondrial dysfunction in ATM-deficient lymphoblastoid cells (Ambrose et al., 2007)	*AT patient lymphoblasts*	*Polarised cellular organisation No difference in mitochondrial number Increased mitochondrial DNA damage Decreased membrane potential Decreased respiration and oxidation rates*
Cancer chemoprevention by the antioxidant tempol in Atm-deficient mice. (Schubert et al., 2004)	*ATM$^{-/-}$ mice thymocytes*	*Decreased membrane potential*
Mitochondrial dysfunction in ataxia-telangiectasia. (Valentin-Vega et al., 2012)	*ATM$^{-/-}$ mice tymocytes*	*Mitochondrial structural abnormalities Increased mitochondrial number Increased mitochondrial mass Increase in ROS Increased membrane potential Decreased mitophagy Decreased ATP levels*
Ataxia-telangiectasia mutated kinase regulates ribonucleotide reductase and mitochondrial homeostasis. (Eaton et al., 2007)	*At patient–derived fibroblasts*	*Decreased mitochondrial DNA levels after IR Decreased ability to increase mitochondrial mass after IR*
Accumulation of DNA Damage and Reduced Levels of Nicotine Adenine Dinucleotide in the Brains of Atm-deficient Mice (Stern et al., 2002)	*ATM$^{-/-}$ mice cerebella*	*Increased respiration rates*
Intrinsic mitochondrial DNA repair defects in Ataxia Telangiectasia. (Sharma et al., 2014)	*A-T patient fibroblast, siRNA KD, ATM$^{-/-}$ mice*	*Increased mitochondrial DNA damage Increased mitochondrial ROS Decreased membrane potential Decreased ATP levels*

d. Energy Deficiency

Neuronal cells affected by loss of ATM, such as PCs and motor and sensory neurons, are some of the largest cells in the body. These larger cells have an increased energy demand (Watts et al., 2018, Angelova and Abramov, 2018), which could put a strain on an ATM-deficient system for several reasons. First, as discussed previously, in an ATM deficient system there is a defect in glucose transportation into the cell **(see section 1.2.3 and section 1.2.4.4 above)**. Second, as outlined in the section above **(1.2.4.5 b ii)**, ATM plays a vital role in mitochondrial function. Loss of ATM in this capacity can have deleterious consequences for the cell, particularly regarding decreased respiration and decreased mitochondrial number, leading to a decrease in ATP levels (Lee et al., 2018, Ambrose et al., 2007, Valentin-Vega et al., 2012, Sharma et al., 2014). Therefore, in addition to having decreased availability of glucose, mitochondria in ATM deficient neurons may not be able to process the energy source sufficiently for these larger cells.

e. Conclusion

The pathogenic mechanism of neurodegeneration in AT remains poorly understood and is still much debated. Although cerebellar atrophy appears to be a relatively early event, the neurological progression of AT is variable in patients, and in some cases other movement defects may be masked by the extent of the ataxia (Churchyard et al., 1991, Willems et al., 1993, Trimis et al., 2004, Teive et al., 2018, van Egmond et al., 2015, Saunders-Pullman et al., 2012, Charlesworth et al., 2013, Klein et al., 1996, Kuhm et al., 2015, Bodensteiner et al., 1980, Nakayama et al., 2015). Current evidence supports a multi-hit model involving several of the mechanisms described above and summarised in **table 1.4**.

Table 1.4 Mechanisms of Neurodegeneration in AT

Mechanism	*References*
Defective DNA damage repair - *Neuroinflammation* - *Abortive Transcription* - *Mitochondrial DNA damage* - *Genomic Instability*	*(McKinnon, 2009, Biton et al., 2006, Hartlova et al., 2015, Dunphy et al., 2018, Zhang et al., 2019, Quek et al., 2016, Quek et al., 2017a, Quek et al., 2017b, Sordet et al., 2009, Sordet et al., 2010, Das et al., 2009, Alagoz et al., 2013, Katyal et al., 2014, Marabitti et al., 2019, Tresini et al., 2016, Vermeulen and Tresini, 2017, Iourov et al., 2009b, Iourov et al., 2009a, Olcina et al., 2013, Fang and Bohr, 2017)*
Oxidative Stress *-Redox stress due to deficiencies in the oxidative stress pathway* *-Increased ROS from mitochondrial dysfunction* *-Decreased autophagy/mitophagy*	*(Tanaka et al., 2006a, Browne et al., 2004, Reliene et al., 2008, Chen et al., 2003b, Gueven et al., 2006, Guo et al., Guo et al., 2010b, Guo et al., 2010a, Hübner et al., 2014, Lolli et al., 2012, Budanov and Karin, 2008, Alexander et al., 2010, Tripathi et al., 2016, Cam et al., 2010, Zhang et al., 2015b, Valentin-Vega and Kastan, 2012, Valentin-Vega et al., 2012, Fang et al., 2016, Qi et al., 2016, Gu et al., 2018)*
Energy Deficiency *-Inability to get sufficient glucose into neuronal cells* *-Mitochondrial dysfunction leading to decreased respiration*	*(Yang and Kastan, 2000, Ching et al., 2013, Peretz et al., 2001, Viniegra et al., 2005, Halaby et al., 2008, Jeong et al., 2010, Sano et al., 2003, Andrisse et al., 2013, Ambrose et al., 2007, Eaton et al., 2007, Sharma et al., 2014, Valentin-Vega and Kastan, 2012, Valentin-Vega et al., 2012, Kamsler et al., 2001, Stern et al., 2002)*

1.2.4.6 Infertility

Infertility in AT exists on a spectrum, ranging from complete infertility and no onset of puberty in classical AT, to a much more diverse presentation in variant AT, where some variant AT patients have fathered offspring or had more than one successful pregnancy (Nissenkorn et al., 2016, Verhagen et al., 2012a, Dawson et al., 2015, Takubo et al., 2006, Strich, 1966). Infertility in classical AT is a symptom of gonadal dysfunction due to meiotic failure, as ATM plays a key role in the DNA repair after meiotic recombination events (Nissenkorn et al., 2016, Paiano et al., 2020, Di Siena et al., 2018, Hamer et al., 2004, Cooper et al., 2014, Lange et al., 2011).

While infertility in classical AT is due to a failure in the DDR and therefore complete arrest in meiosis, infertility in variant AT may be more complex. Variant AT patients exist on a spectrum of fertility that may be unrelated to meiotic failure, particularly in female AT patients. Female AT patients have been shown to have an increase in gonadotropic hormones such as luteinising hormone (LH) and follicle stimulating hormone (FSH) (Nissenkorn et al., 2016, Ammann et al., 1970, Zadik et al., 1978). These patients present on a spectrum, from normal sexual development, to varying degrees of amenorrhea, to no onset of puberty. The elevation of these hormones may be due to primary ovary dysfunction arising from meiotic failure, but may also indicate a role for ATM outside meiosis in reproductive function by mediating sex hormone signalling. Female AT patients have been shown to have low levels of oestrogen (Zadik et al., 1978), and ATM is known to function in other hormone signalling pathways, such as insulin and IGF-I **(see section 1.2.4.4 Metabolic Dysregulation above)**. Additional support for this is provided by the fact that polymorphisms in the ATM gene are thought to be a contributing factor to PCOS (Schweighofer et al., 2014, Ornik and Ferk, 2013). Women with PCOS experience reversible infertility due to high levels of androgens, LH, and circulating insulin due to insulin resistance (Wang et al., 2019, Goodarzi et al., 2011). This perhaps indicates a shared dysregulated pathway and suggests that infertility in variant female AT patients may not be due to a primary failure of meiosis or the resultant secondary irregular hormone levels, but a primary dysregulation in hormone signalling pathways.

It has been noted that AT seems to affect female sufferers more severely, particularly concerning growth retardation. It has been hypothesised that the smaller stature of female AT patients is due to the lack of a growth spurt during puberty. However, as slight differences in size can be detected in mid childhood well before the onset of puberty would be expected, ovarian atrophy cannot account for all of this decrease in size compared to males (Nissenkorn et al., 2016). Therefore, the reason that AT appears to affect female patients to a greater degree than male patients is not yet wholly understood.

Because infertility in AT is not a life-limiting aspect, or a major barrier to quality of life, gonadal dysfunction and hormone dysregulation are not well characterised in AT patients. Gonadal dysfunction has however been well characterised in animal models of the disease, and so will be discussed in more detail in relation to the results in **chapter 4**.

1.2.4.7 Premature Ageing

Premature ageing seems to be an overarching facet of AT since many AT symptoms such as infertility, immune deficiency, fatty liver disease, and cancer are hallmarks of ageing. Additionally, AT patients look physically aged, with features such as greying thinning hair and thinning skin (Reed et al., 1966). Many of the ageing features of AT are attributable to defects in specific systems, such as the immune and reproductive systems. However, there is a particular cellular ageing phenotype associated with AT that is likely to contribute to the less well defined ageing axis. Interestingly, there is evidence suggesting that SNPs in the ATM promoter region which increase ATM expression are associated with increased longevity in Chinese and Italian populations (Piaceri et al., 2013, Chen et al., 2010). This is supported by the finding that increased expression of ATM in a mouse model of ageing increased longevity by prolonging ATM mediated DNA damage repair, which is thought to decline with age (Qian et al., 2018).

Early in the investigation of the AT phenotype, it was noted that AT patients had increased cellular senescence (Shiloh et al., 1982). Senescence is an irreversible cellular protective mechanism that stops the proliferation of damaged cells and is therefore considered to function in tumour suppression, embryonic development, and tissue repair, and is heavily implicated in ageing. In addition to stopping the propagation of the damaged cell, senescence is also associated with the senescence-associated secretory phenotype (SASP), where senescent cells secrete pro-inflammatory and matrix-degrading markers to evoke an immune response and clearing of the damaged cells (Childs et al., 2015, Loaiza and Demaria, 2016). In AT, given the increased level of unresolved cellular stress, due to failures in the DDR and the oxidative stress response, it is not surprising that cells become senescent. Consequently, it is likely that a prolonged SASP is responsible for the aged appearance of AT individuals.

ATM is also a mediator of cellular senescence, however, the precise role of ATM in cellular senescence is still debated, as some studies show that ATM positively regulates senescence, while others argue that it negatively regulates it (Zhan et al., 2010, Nair et al., 2015, Luo et al., 2014, Mallette et al., 2007, Zhao et al., 2020a, Liu et al., 2013, Sasaki et al., 2008, Kuk et al., 2019).

1.2.4.8 Radiosensitivity

Radiosensitivity is an ambiguous term, and from a medical perspective can refer to radiation induced cancers, non-cancerous effects due to cellular transformation, such as cataracts, or non-cancerous tissue events that are due to cellular death, such as skin burns (Britel et al., 2018). AT is considered *the* most radiosensitive human disease, and in the context of discussion of AT, radiosensitivity generally refers to cellular death as a result of ionising radiation (Berthel et al., 2019b, Deschavanne and Fertil, 1996). The best determinant of the radiosensitivity of cells is their survival faction at 2 Gy (SF2) (Deschavanne and Fertil, 1996). Homozygous ATM null human cells have an SF2 between 1-10%, compared to Fanconi anaemia cells, with an SF2 of between 10-50%, and control cells with an SF2 of 50-80% (Berthel et al., 2019b).

Ionising radiation can have many effects on cellular homeostasis, such as production of ROS, disruption of lipid membranes, and the oxidative/reductive posttranslational modification of cytoplasmic proteins (Reisz et al., 2014). However, the area of the cell most sensitive to the effects of ionising radiation is the nucleus and DNA in particular, where ionising radiation causes ds DNA breaks. Therefore, there is a strong inverse correlation between the repair of DNA damage and radiosensitivity, where less DNA repair results in increased radiosensitivity (Berthel et al., 2019a). The consensus on this correlation is so strong that the terms are often used interchangeably.

Individual radiosensitivity is predicted by the RIANS model (Radiation Induced ATM Nucleoshuttling) (Bodgi and Foray, 2016, Granzotto et al., 2016). This model proposes that ATM exists in inactive dimers in the cytoplasm. Ionising radiation then directly triggers the autophosphorylation and subsequent monomersisation of ATM in a dose dependant manner. These active ATM monomers, but not the dimers, are able to diffuse into the nucleus and activate the DDR cascade. Therefore, delays in the nucleoshuttling of ATM to the nucleus, due to causes such as expression levels, delayed activation, or interaction of ATM with cytosolic proteins are thought to determine an individual's radiosensitivity (Granzotto et al., 2016). Consequently, the radiosensitivity exhibited by AT patients is attributed to the deficiency in DNA repair, resulting in cellular death (Foray et al., 1997, Joubert et al., 2008).

While this increased radiosensitivity exhibited by AT patients is pathogenic on its own, it also has serious consequences for the treatment of AT associated malignancies. As radiotherapy and chemotherapeutic DNA damaging drugs are generally the prescribed treatment for malignancies in the general population, the increased sensitivity of AT patients to treatment with these can often cause secondary fatal pathologies (van Os et al., 2017a).

1.2.4.9 ATM mutation carriers

ATM mutation carrier heterozygotes are at an increased risk of heart disease and cancer, with female ATM mutant heterozygotes having a 5-fold increased risk of breast cancer (Swift, 2001, Maillet et al., 2002, d'Almeida et al., 2005, Bubien et al., 2017, van Os et al., 2016). ATM carriers also exhibit abnormal levels of radiosensitivity and chromosomal instability, as evidenced by higher rates of adverse effects during radiotherapy treatment (Chen et al., 1978, Cohen et al., 1975, Cole et al., 1988, Fernet et al., 2004, Neubauer et al., 2002, Pernin et al., 1999, Varghese et al., 1999, Mou et al., 2020).

1.3 Current Animal Models of Ataxia Telangiectasia

To date, a number of animal models of AT have been developed, and these are summarised in **table 1.5,** as well as further delineated in the sections below. Each model organism has advantages and disadvantages as an AT model. Phenotypes which are shared between the vertebrate models are summarised in **figure 1.9**.

Table 1.5 Animal Models of AT

Mutation	*Histology/ Cellular and Molecular Pathology*	*Behavioural Phenotype*
Drosophila		
ATM temperature induced KD by RNAi *(Rimkus et al., 2008, Rimkus et al., 2010)*	*Progressive photoreceptor neuron degeneration by apoptosis due to re-entry into the cell cycle. ATM KD eventually leads to lethality*	*Not studied*
ATM^{8} (Temperature induced loss of kinase activity) *(Petersen et al., 2013, Petersen et al., 2012, Pedersen et al., 2010)*	*Neuroinflammation and apoptotic glia lead to neurodegeneration and lethality*	*Walking, flying and climbing defects. Also inability to right themselves when on their back. The severity of the behavioural defects correlated with reduced kinase activity.*
Zebrafish		
ATM Morpholino (MO) KD	*Radiosensitivity and lethality*	*Not Studied*
Mouse		
ATM-/- (mutation in exons 40/41) *(Barlow et al., 1996)*	*Radiosensitivity and genomic instability but no abnormal cerebellar morphology*	*Motor defects*
ATM-/- (mutation in exon 62/63) (Xu and Baltimore, 1996, Kuljis et al., 1997)	*Subtle lesions in all three cerebellar layers (molecular, Purkinje and granular) by electron microscopy. Purkinje cell dendrites are dystrophic with increased mitochondrial density. Neuroinflammation characterised by microglial activation*	*Not studied*
ATM-/-(deletion of exons 57/58) (Herzog et al., 1998)	*No radiation induced cell death in hippocampal dentate gyrus, retina, cerebellum, and cerebral cortex compared with WT controls*	*Not studied*
ATM-/- (mutation in exon 37) (Elson et al., 1996)	*ATM deficient mice brain 20% smaller than WT controls. Decrease in dopaminergic neurons.*	*Motor defects observed that were corrected with administration of L-dopa. ATM-/- mice are significantly more reactive to amphetamine*
ATM $^{y/y}$ (mutation in exon 51/55) (Borghesani et al., 2000)	*Abnormal pattern of Purkinje dendritic growth and decrease in thickness of the molecular layer with ectopically placed Purkinje cells*	*Motor learning deficits*

ATM $^{\Delta SRI/\Delta SRI}$ Knock in model (Spring et al., 2001)	*No observed effects*	*None*
ATM^{tm1Mmpl} (mutation in exon 4) (Campbell et al., 2015)	*Observed some changes in Purkinje cell number and dendrite morphology but these changes were inconsistent and had no statistical significance.*	*Some motor defects*
ATM$^{KD/KD}$ (Yamamoto et al., 2012b)	*Die in early embryonic development*	*N/A*
ATM$^{KD/KD}$ (Daniel et al., 2012)	*Die in early embryonic development*	*N/A*
Rat		
ATM -/- (mutation in exon 13 (Quek et al., 2016, Quek et al., 2017a, Quek et al., 2017b)	*Progressive loss of motor neurons with remaining neurons positive for cytosolic DNA and apoptosis markers. However, no difference in cerebellum, or Purkinje cell morphology, however Purkinje cells show strong signal for cytoplasmic DNA. Rats also exhibited evidence of neuroinflammation.*	*Loss of use and paralysis of hind limbs*
Porcine		
ATM -/- (mutation in exon 57) (Beraldi et al., 2015, Beraldi et al., 2017)	*Reduced number of Purkinje cells from birth which continues through development. Purkinje cell dendrites were also abnormally angled with respect to the soma in adulthood. No difference observed in granular layer.*	*Unable to fully perform behavioural tests and had severe gait instability*

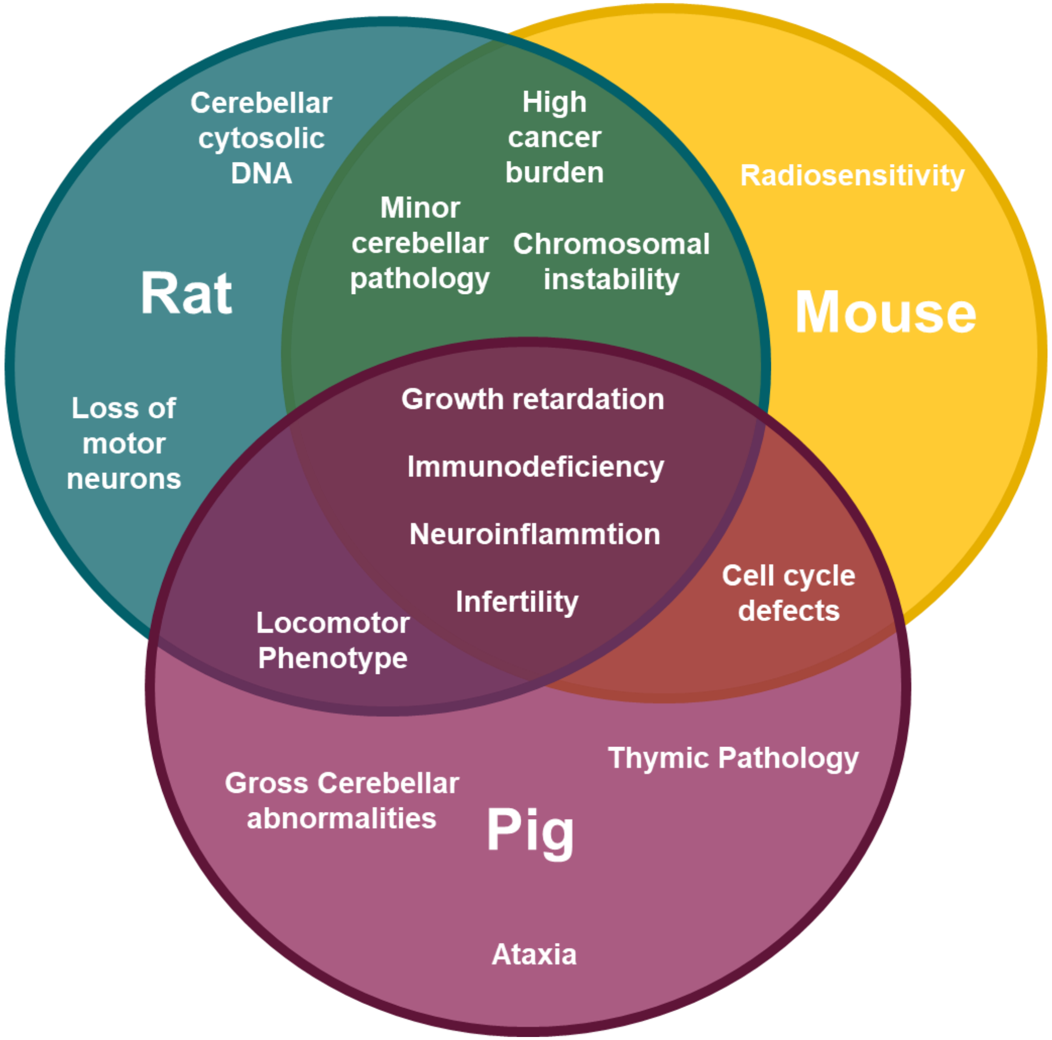
Cerebellar cytosolic DNA
High cancer burden
Radiosensitivity
Minor cerebellar pathology
Chromosomal instability
Rat
Mouse
Loss of motor neurons
Growth retardation
Immunodeficiency
Neuroinflammtion
Infertility
Cell cycle defects
Locomotor Phenotype
Thymic Pathology
Gross Cerebellar abnormalities
Pig
Ataxia

Figure 1.9 Overview of overlapping phenotypes exhibited by vertebrate models of AT. Note that although a vertebrate model, zebrafish are not included as only preliminary investigations up to 3 dpf have been published, and the results sections of this thesis will present new results obtained during this project.

1.3.1 Drosophila

ATM is conserved in Drosophila and its function is crucial for managing DNA damage and telomere length maintenance, as it is in mammals (Song et al., 2004). However, unlike mammals, ATM in drosophila is essential for development, and loss of ATM leads to lethality (Silva et al., 2004, Song et al., 2004, Rimkus et al., 2010, Rimkus et al., 2008). Therefore, AT models in drosophila have utilised conditional knockdown (KD) of the gene, first by temperature dependant RNAi (Rimkus et al., 2010, Rimkus et al., 2008) and secondly by a temperature dependent mutant ATM allele (ATM^8) where the final amino acid of the FATC domain is mutated from a leucine to a phenylalanine causing survival of the pupae at 18°, but loss of ATM activity and subsequent lethality when the temperature is raised to 25° (Pedersen et al., 2010, Petersen et al., 2012, Petersen et al., 2013).

Using the inducible KD, it is possible to generate adult flies and then perform ATM KD. In these animals there is caspase 3 dependent progressive degeneration of photoreceptor neurons that are post mitotic. This apoptotic cell death was associated with prior re-entry into the cell cycle at S phase by these post mitotic neurons (Rimkus et al., 2008). Moreover, this re-entry into the cell cycle was found to be associated with increased DNA damage due to loss of ATM (Rimkus et al., 2010). Importantly, it should be noted that neurodegeneration appeared to be the cause of lethality in this model, as both global and neuron specific induced loss of ATM caused death.

Drosophila with the temperature dependant ATM^8 allele also show progressive caspase 3 mediated apoptotic neuronal death after loss of ATM kinase activity. Moreover, in addition to neuronal death, the majority of caspase 3 positive cells were glia. Neuroinflammation has been associated with neurodegeneration in AT patients **(see section 1.2.4.5)** as well as mouse, rat and pig models of AT **(see below and table 1.3)**. Preceding cell death, neuronal cells in the ATM^8 drosophila model were found to have an increase in expression of innate immune response genes, particularly in glial cells. Furthermore, glial specific KD of ATM by RNAi was enough to induce this neuroinflammation and cause death of neurons, while neuron specific KD of ATM did not cause a neurodegenerative phenotype or increase in inflammation. Loss of ATM kinase activity in drosophila is also associated with a motility defect and decrease longevity, most likely due to neuronal loss (Petersen et al., 2012, Petersen et al., 2013).

1.3.2 Zebrafish

Currently the only published zebrafish model uses a transient morpholino (MO) KD of ATM and this has only been partially characterised within the first few days post fertilisation (dpf). It was found that ATM MO zebrafish are highly sensitive to ionising radiation and die by 72 hpf (Imamura and Kishi, 2005). It should be noted that ATM morphant zebrafish described by Imamura and Kishi (2005) likely express a kinase dead ATM protein and not KD of expression of ATM. The implications of this are discussed in detail in **section 3.3.2.3**.

1.3.3 Mouse

Mice are the most common vertebrate model organism, and within 5 years of the discovery of the *ATM* gene, 6 AT knockout (KO) mouse models had been created (Barlow et al., 1996, Xu et al., 1996, Kuljis et al., 1997, Herzog et al., 1998, Elson et al., 1996, Borghesani et al., 2000). The majority of mouse models of AT are knockouts, aiming to replicate the most common genotype associated with AT (Cardiff, 2017) but there are also some knock in (KI) models (Spring et al., 2001, Chen et al., 2003b, Daniel et al., 2012, Yamamoto et al., 2012b). While the mouse model has vastly aided the study of this disease, and although it recapitulates the pleotropic effects of ATM deficiency relatively well, it fails to exhibit any gross neurological changes.

The formation of tumours, particularly lymphomas, are very prevalent in mouse models and the animal usually succumbs to these at a young age. It had been previously hypothesised that these mouse models may exhibit significant neurological defects at a later stage, but owing to the presence of tumours do not survive that long. However, Campbell et al. (2015) created a mouse model that more accurately represents the tumour rate seen in AT patients (10-20%) and as such, the mice lived significantly longer than previous mouse models.

Nevertheless, these animals also failed to demonstrate any gross cerebellar defects or an obvious locomotor phenotype. However, some mouse models have exhibited slight motor defects, ectopic PC localisation and neuroinflammation (Campbell et al., 2015, Borghesani et al., 2000).

Consistently, ATM KO mouse models exhibit infertility which is a key aspect of AT in patients. ATM deficient testes in mice appear morphologically normal and have evidence of developing sperm having gone through mitosis but not meiosis (Barlow et al., 1996, Elson et al., 1996, Spring et al., 2001, Xu et al., 1996). Similar results were also observed in female mice, with failure to produce mature oocytes in the ovaries. This halting of germ cell development has been attributed to failure of the ATM deficient system to successfully complete meiotic recombination (Xu et al., 1996, Barlow et al., 1998, Di Siena et al., 2018).

1.3.4 Rat

To date, two models of AT in rats have been developed; a KO rat model with an 8 bp deletion mutation (Quek et al., 2017a), and a missense mutation where amino acid 2262 has a leucine to proline mutation and consequently reduced kinase activity (Quek et al., 2017b). While KO rats continue to have a significant tumour burden, particularly T cell lymphomas and leukaemias (Quek et al., 2017a), the model does demonstrate a significant motor defect with progressive hind leg paralysis. This paralysis correlated with a loss of motor neurons and strong evidence of neuroinflammation thought to be brought about by cytosolic DNA (Hartlova et al., 2015). In common with mouse models, no gross defects of the cerebellum were observed, but there was strong evidence of neuroinflammation and PCs contained cytosolic DNA. A with both AT patients and mouse models, the rat KO model of AT also shows infertility, with failure to complete meiosis (Quek et al., 2017a).

In common with the KO model, the missense rat model also exhibited hind leg paralysis, infertility, and a significant T cell derived tumour burden. ATM missense rats also exhibited neuroinflammation due to cytosolic DNA, although not to the same extent as ATM KO (Quek et al., 2017b).

Current vertebrate models recapitulate well most aspects of the AT disease except for gross neurodegeneration. Organisation, cell types, and molecules of the cerebellum are well conserved between rodents and humans (Goldowitz and Hamre, 1998), therefore, it is not known why a similar neuro-phenotype is not observed in AT models. One explanation is that rodents have some sort of redundancy for ATM that is neuroprotective. If this was the case then why does this redundancy not protect them against the other effects of ATM loss; why is it neuro-specific? One of the major differences between rodent and human CNS is the size and volume of the neurons. The lesser demand of a smaller cell on an ATM deficient single nucleus cell in terms of energy demand or redox stress may be the deciding factor in AT neuropathogenesis. Conversely, it may be the comparative life spans of human and rodent, whereby the 2-3 years of a rodent life span may not be enough to pass a threshold level of DNA damage.

1.3.5 Pig

Yucatan pigs are miniature pigs which owing to their small size have been used in research for decades (Kim et al., 2015, Panepinto et al., 1982, Boakye et al., 2020). Recently, a porcine KO AT model has been developed. As a larger vertebrate, this appeared to recapitulate the symptoms of AT better than the rodent models. It does exhibit an ataxia-like phenotype linked to a decrease in PC cell number from birth, and an atypical topology of PCs in adults in ATM-/- mutants. ATM deficient pigs also exhibited a thinning of the motor cortex. Investigation of female KO pigs showed small ovaries, and a halting a follicular development. These animals were unsurprisingly infertile, and had dramatically decreased amounts of circulating oestrogen. Interestingly, male KO pigs did produce mature sperm, although sperm levels in ATM KO pigs were much decreased compared to wild type controls. Additionally, male pigs were able to impregnate females, although the resultant litter sizes were much smaller. However, despite male ATM KO pigs having mature functional sperm, they did exhibit some cytoplasmic morphological abnormalities (Beraldi et al., 2015, Beraldi et al., 2017).

1.4 Zebrafish as a Model Organism

Zebrafish models are a relatively new tool in biological studies. Their use has seen a vast explosion over the past few years (**figure 1.10**), owing to the fact that they share many physiological, genetic, anatomical and biochemical similarities with humans, but particularly since their genome has been fully sequenced (Howe et al., 2013, Kettleborough et al., 2013), and since the introduction of CRISPR technology (Cong et al., 2013, Mali et al., 2013, Chang et al., 2013, Hwang et al., 2013).

Zebrafish as a model organism offer several advantages over conventional models such as rodents. Zebrafish embryos are fertilised and develop externally from the mother, which allows for easy tracking of development, with most organ systems being functional within a few days of fertilisation (Kimmel et al., 1995). Embryos are also transparent, allowing for easy *in vivo* imaging, and can be kept alive in an appropriate mounting media to facilitate live imaging studies. Additionally, zebrafish embryos are genetically tractable, which has allowed for development of a whole range of knockout models to aid in the investigation of many different diseases and developmental processes (Cong et al., 2013, Chang et al., 2013, Hwang et al., 2013, Zhang et al., 2016). Knock in models and transgenic lines can also be created (Thakur and Welford, 2020, Lin et al., 1994, Emelyanov et al., 2006, Armstrong et al., 2016, Prykhozhij et al., 2018). In contrast to rodent and higher vertebrate models, zebrafish are also cheaper to house, require less husbandry, and tend to live longer (Kimmel et al., 1995). Furthermore, from a single pairing of adult zebrafish a large clutch of a few hundred embryos can be gathered. This and their small size makes them ideal for high throughput studies (Cornet et al., 2018, Deveau et al., 2017, Liu et al., 2016a). A further aspect that makes them conducive to high throughput screen studies is that their behaviour has been well characterised, and perturbations of that behaviour can be studied and used as a disease/dysfunction readout out, particularly where neurological diseases are considered (Norton and Bally-Cuif, 2010, Deakin et al., 2019, Plaut, 2000, Basnet et al., 2019).

However, it should be noted that zebrafish do pose some limitations as a model organism. First, they are further away in the evolutionary tree to humans than higher vertebrate models, therefore it should be considered that some biological process and pathways may have been lost or altered. In addition to this, the zebrafish genome underwent a duplication event, and while selective pressure has forced many of the duplications to be lost, about 20% remain (Amores et al., 1998, Christoffels et al., 2004, Meyer and Van de Peer, 2005). Therefore, it should be considered if a particular gene of interest has been duplicated and if so, whether its paralogue maintains the same function (Force et al., 1999, Postlethwait, 2006). Second, one of the major constraints of zebrafish research is the lack of antibodies (Villarreal et al., 2017), which slows progress in research and closes some avenues of investigation.

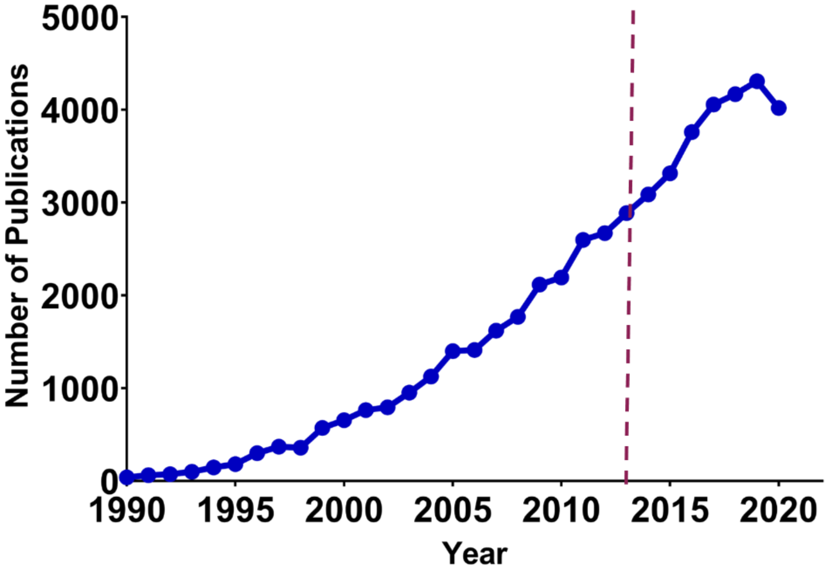

Figure 1.10 Number of zebrafish publications per year from 1990-2020 from a Web of Knowledge database search. Dashed line represents first publications of use of CRISPR in zebrafish (2013).

1.4.1 Zebrafish as a Model for Neurological Disease

Thus far, a number of neurodegenerative disorders have been modelled in zebrafish, such as Frontotemporal Lobar Degeneration (FTLD), ALS, Parkinson's disease, Charcot-Marie-Tooth disease, and Huntington's disease (Kabashi et al., 2010, Schmid et al., 2013, Mori et al., 2013, Ciura et al., 2013, Fett et al., 2010, Sheng et al., 2010, Lumsden et al., 2007, Henshall et al., 2009, Ponomareva et al., 2016). However, modelling of these diseases in zebrafish does have some disadvantages. Most neurodegenerative diseases are late onset and tend to occur due to accumulative pathologies in the cells of the CNS. As the fish ages, recognising subtle phenotypes becomes more difficult and imaging becomes more problematic. Furthermore, adult zebrafish have a remarkable capacity for neurogenesis (Becker et al., 1997, Kizil et al., 2012) which may obscure neurodegeneration.

One of the advantages of modelling neurodegenerative diseases in zebrafish is that gross morphology and cell type within the brain are well conserved between humans and zebrafish (Turner et al., 2014), particularly in the cerebellum which contains a distinct granule cell layer, Purkinje cell layer, and molecular layer (Bae et al., 2009, Hamling et al., 2015).

So far a number of cerebellar degenerative diseases and ataxias have been modelled in zebrafish. A model of Spinocerebellar Ataxia 3 in zebrafish exhibited a motor defect where transgenic zebrafish carrying the mutant human ataxin 3 protein showed a decrease in swimming ability (Watchon et al., 2017). This has also been seen in zebrafish models of ataxias causes by lysosomal storage disorders (Lin et al., 2018), and a zebrafish model of Spinocerebellar Ataxia 13 (Namikawa et al., 2019b, Namikawa et al., 2019a). A zebrafish model of the ataxia causing disease Marinesco-Sjögren Syndrome has shown cerebellar degeneration, as has a model of classic late infantile neuronal ceroid lipofuscinosis (CLN2) (Kawahara and Hayashi, 2016, Mahmood et al., 2013). This evidence suggests that cerebellar degeneration and the resultant ataxia can be modelled using zebrafish.

1.4.2 Zebrafish as a Model for DNA Damage Repair

Zebrafish represent an epitome organism for modelling DNA damage repair mechanisms. In eukaryotes a number of DNA damage repair pathways exist, specifically, direct reversal, base excision repair, mismatch repair, nucleotide excision repair, nonhomologous end joining (NHEJ), homologous recombination, translation synthesis, and p53-mediated surveillance (Pei and Strauss, 2013). Zebrafish have orthologues of genes that function in all these pathways (Zebrafish Genome - GRCz11 Ensembl (last updated Nov 2020)), and some of these repair pathways, such as NHEJ and homologous recombination, are exploited to create CRISPR/Cas9 induced frame shift KO mutations and KI mutants respectively. Furthermore, although the zebrafish genome underwent a duplication event during evolution (Amores et al., 1998, Christoffels et al., 2004, Meyer and Van de Peer, 2005), only ~10% of the 684 DDR associated genes are found to be still duplicated (Cayuela et al., 2019). As ATM primarily functions in homologous recombination (Kocher and Dahm-Daphi, 2010), zebrafish and homologous recombination mutant models will be discussed below.

1.4.2.1 Homologous Recombination in Zebrafish

Homologous Recombination (HR) in zebrafish is only starting to be decoded, and as such only a small number of zebrafish mutants for HR proteins exist (Ramanagoudr-Bhojappa et al., 2018, Rodriguez-Mari et al., 2010, Botthof et al., 2017, Liu et al., 2003, Rodríguez-Marí et al., 2011). However, as HR in general is well conserved in both lower and higher eukaryotes, and as zebrafish have orthologues of most genes associated with HR (Pei and Strauss, 2013), it can be assumed that HR is also well conserved in Zebrafish (Fan et al., 2006).

HR occurs in the S phase of the cell cycle during DNA replication as it requires a sister chromatid to act as a template for repair. However, there is data that suggests that the predominant DNA repair pathway in the very early stages of zebrafish embryogenesis is alternative end joining (alt-EJ) (Thyme and Schier, 2016). This is an error prone repair pathway, which uses some of the components of the HR pathway to resect the 5’ end of the damaged DNA to points of microhomology (2-20 bp), these microhomolgy points are then bridged and the remaining 3’ flap (which is complementary to the resected 5’ end) is cleaved. Therefore, this pathway has the potential to introduce large chromosomal deletions as well as translocations (Sallmyr and Tomkinson, 2018) and the reason that the embryo favours this error prone pathway is not known. It is not lack of maternally contributed HR machinery, as Rad51, which is essential for HR, is expressed in Rad51 KO zebrafish derived from a Rad51 heterozygous in-cross at the one cell stage (Botthof et al., 2017). It could be that the embryo promotes this erroneous DNA repair pathway to espouse rapid cellular proliferation, instead of allowing a temporary halting of the cell cycle and therefore slowing of proliferation to repair the damage in the case of HR. It should be noted that it is not known exactly when this preference stops and HR commences. However, complete abolition of the HR pathway by double KO of *rad51* and r*ad51L1* leads to embryonic lethality before 6 hpf (Botthof et al., 2017), and HR can be forced at the one cell stage (Pi et al., 2020).

In terms of HR zebrafish mutants, the best characterised are zebrafish with mutations in the genes that function in the Fanconi anaemia/BRCA pathway. This pathway has 22 associated genes, and mutations in these genes cause the heterogeneous disease Fanconi anaemia (Mamrak et al., 2017). This pathway includes the brca2 protein which is a direct target of ATM kinase activity (Wang et al., 2010b). Mutation of the 22 genes in this pathway in zebrafish enhances sensitivity to DNA damage and infertility due to failure in meiotic HR and therefore the inability to produce mature gametes. Furthermore, zebrafish in this pathway exhibit an unusual phenotype of female to male sex reversal (Ramanagoudr-Bhojappa et al., 2018, Rodriguez-Mari et al., 2010, Rodríguez-Marí et al., 2011, Shive et al., 2010, Vierstraete et al., 2017).

1.5 Project Rationale

Ataxia Telangiectasia is a juvenile onset, autosomal recessive, life limiting disease that is characterised by progressive ataxia, a high cancer burden, metabolic dysregulation, immunodeficiencies, infertility, radiosensitivity and premature aging. Although AT is associated with a plethora of devastating conditions, progressive ataxia is one of the biggest barriers to quality of life of AT patients. The ataxia exhibited by AT patients is associated with neurodegeneration as a result of Purkinje cell loss in the cerebellum. Despite intensive research, the exact mechanisms of neurodegeneration and Purkinje cells loss in AT are not well understood. This is in large part due to the lack of an appropriate vertebrate AT model that faithfully recapitulates the neurodegenerative phenotype associated with AT and that is conducive to large-scale experimentation. While the porcine model of AT does largely recapitulate the neurodegenerative and behavioural phenotype associated with AT, the cost of large-scale experimentation on this model can be prohibitive. Furthermore, the use of large numbers of higher vertebrates for scientific research where there is an alternative is not in line with the 3Rs principles of Reduction, Refinement, Replacement. Therefore, we propose the development of a zebrafish model of AT, as the DNA damage pathways appears to be well conserved between zebrafish and humans, they have previously been used to model other neurodegenerative disease, and are highly advantageous for high throughput drug screening.

Zebrafish with a predicted truncating mutation in ATM, similar to mutations found in AT patients, had already been created with the use of CRIPSR/Cas9 by Dr Ringaile Zaksauskaite (Department of Molecular Biology and Biotechnology), under the supervision of Professor Sherif El-Khamisy (Department of Molecular Biology and Biotechnology) and Dr Freek van Eeden (Department of Biomedical Science), as part of her PhD. The mutant allele was designated *sh477*. However, these mutant zebrafish remained uninvestigated and uncharacterised. Therefore, our aim was to investigate these fish with respect to the following questions:

- Does the introduction of the *sh477* mutation cause ablation of ATM signalling in zebrafish through either loss of protein expression, or loss of function?

  Do ATM$^{sh477/sh477}$ zebrafish recapitulate any aspects of the AT disease related to defects in DNA damage repair, such as radiosensitivity, immunodeficiencies or infertility?

To determine if ATM$^{sh477/sh477}$ mutant zebrafish exhibit any behavioural abnormalities that may be related to an ataxia like phenotype.

- To determine if ATM$^{sh477/sh477}$ zebrafish exhibit a phenotype due to loss of ATM function that may be exploited as a read out in high throughput drug screening for therapeutic targets.

Chapter 2

Materials and Methods

2.1 General Zebrafish Methods

2.1.1 Zebrafish Maintenance and Breeding

Zebrafish were housed in the Bateson Centre Aquarium at the University of Sheffield. The Zebrafish were maintained at 28 °C in 14 hrs light and 10 hrs dark cycle. All experiments were conducted in line with Home Office guidelines for animal research, in accordance with the Animal Scientific Procedures Act (ASPA) 1986 under the authority of project licences 70/8309 and PP2798691.

For the generation of embryos through mass spawning, the evening prior to spawning, two containers were placed in the home tank, one inside the other, with the inner container containing a mesh bottom and marbles laid on top **(see figure 2.1 a)**. Zebrafish embryos were collected from the group spawning the following morning.

For individual pair mating, one male and one female zebrafish were paired in a tank containing a divider the evening prior to spawning. In the morning, at the beginning of the light cycle, dividers were removed, and the pairing tanks tilted slight to encourage spawning **(see figure 2.1 b)**.

Embryos were collected and sorted into groups of 60 in 10 cm dishes at approximately 4 hours post fertilisation (hpf). Embryos were maintained in E3 medium (NaCl 5mM, 0.17 mM KCl, 0.33 mM CaCl2, 0.33 mM MgSO4, 0.0001% methylene blue) at 28 °C. Zebrafish intended for raising were transferred to aquarium tanks at 5 dpf and maintained as above.

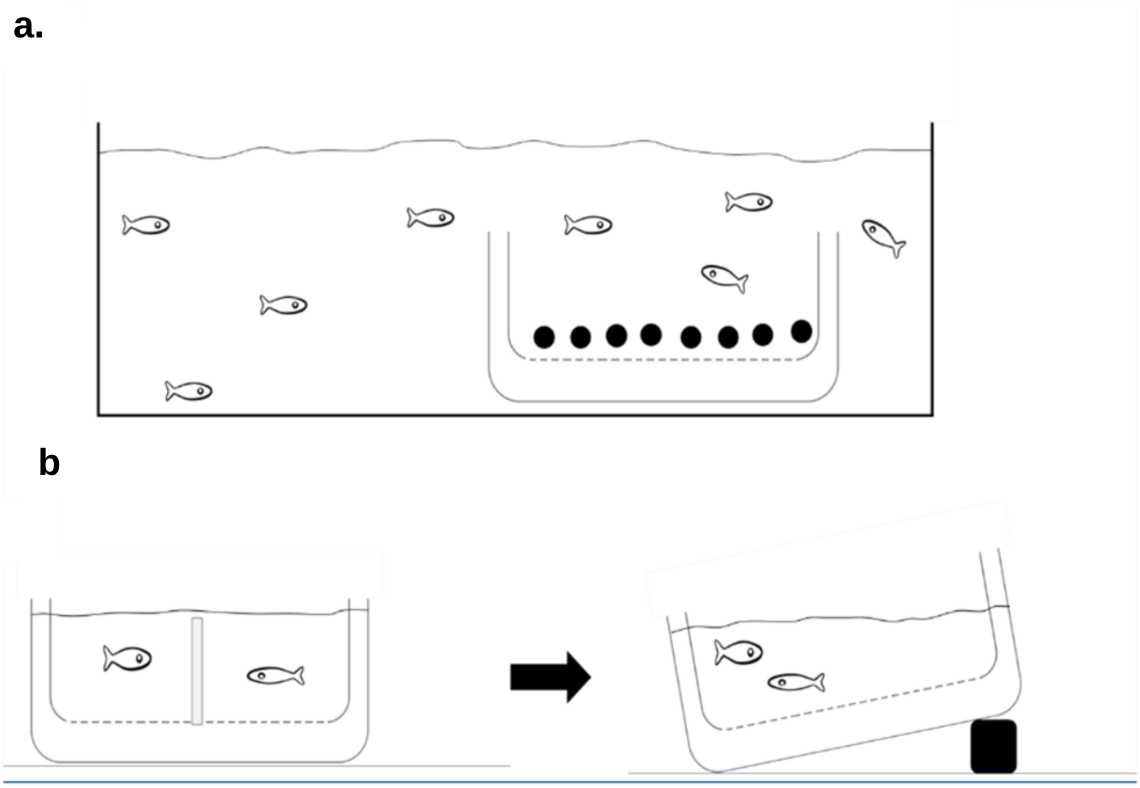

Figure 2.1 Methods of zebrafish breeding a. breeding of zebrafish through group spawning by placing two plastic containers at the bottom of the tank, one inside the other. The inner container has a mesh bottom covered by marbles to allow for protection and easy collection of embryos. **b.** Pair mating of zebrafish, where the evening prior to spawning, a male and female are placed inside a container similar to **a.** with a divider between them. The following morning the divider is removed and the tank tilted slightly to encourage spawning.

2.1.2 Generation of Mutant Zebrafish

ATM$^{sh477/sh477}$ and TDP1$^{sh475/sh475}$ mutant zebrafish were generated using CRISPR/Cas9 by Ringaile Zaksauskaite in the department of Biomedical Sciences at the University of Sheffield. These fish were gifted to our lab at 7 months old. The ATM^{SH477} allele has a 5 base pair (bp) deletion in exon 6, and the TDP1^{SH475} allele has a 4 bp deletion in exon 2. Both deletions result in a frameshift mutation and subsequently to downstream premature stop codons.

2.1.3 Anaesthesia

To terminally anaesthetise, zebrafish were treated with Tricaine (400 mg Tricaine powder (Sigma, #A-5040), 97.9 ml dH2O, ~2.1 ml 1M Tris (pH 9), adjusted if required to pH 7), diluted to 30 ml Tricaine solution per 100 ml of aquarium water for 20 minutes. For use as an anaesthetic, zebrafish larvae and adults were treated with Tricaine diluted to 4.2 ml per 100 ml aquarium water and moved to fresh water after 5 minutes.

2.1.4 Adult Tail Biopsy

Adult Zebrafish were anaesthetised as described above **(section 2.1.3).** While anaesthetised, a small section from the end of the caudal fin was cut using a scalpel blade and transferred to a microliter plate containing 20 µl of QuickExtract™ solution (Epicentre Biotechnologies).

2.2 Genotyping of the ATM Allele

2.2.1 DNA Extraction

Whole embryos/larvae were placed in individual wells of a 96 well plate and 20 µl QuickExtract™ solution was added to each well. Plates were incubated at 65° C for 2 hours and then 99° C for a further 2 mins. When embryos were required for RNA extraction and first required genotyping, under terminal aesthetic, tails were clipped under a dissecting microscope and treated as above. The body was kept for RNA extraction by preserving it at -80° C. For adult genotyping, tail biopsies, as described in **section 2.1.4**, were treated as above.

2.2.2 Amplification of Zebrafish DNA by Polymerase Chain Reaction

A standard PCR was used for genotyping with a reaction mix containing a final concentration of 1X FIREPol® (Solis Biodyne, OÜ, Tartu, Estonia), 1 µM each of forward and reverse primers **(table2.1)** and 1 µl template DNA **(section 2.2.1)**. The reaction was made up to a final volume of 10 µl using dH_2O. The template was amplified using a 30X touchdown PCR programme in **table 2.2**.

Table 2.1 Genomic DNA PCR Primers

ATM	*Forward*	TCAACCAATTCACGTTACACTTT
	Reverse	TTCTTCCAGGGCCCTTACTG

Table 2.2 30X Touchdown PCR

Step	***Temperature °C***	***Time (min:sec)***	***Cycles***
Initial denaturation	*94*	*3:00*	
Touchdown			
Denaturation	*94*	*0:45*	*15X*
Annealing	*65-50 (-1° C/cycle)*	*0:45*	
Elongation	*72° C*	*1:30*	
PCR			
Denaturation	*94° C*	*0:30*	*30X*
Annealing	*58° C*	*0:45*	
Elongation	*72° C*	*1:00*	
Final Elongation:	*72° C*	*10:00*	
Hold	*10° C*	*Infinite*	

2.2.3 Restriction Digest of PCR Products

Digestion mix was added directly to the 10 µl PCR products **(section 2.2.2)**, with a final concentration of 1X CutSmart® (NewEngand Biolabs®) (NEB), 0.4 µl PpuM1 (NEB) to a final volume of 20 µl. Samples were incubated at 37° C for 12 hrs.

2.2.4 Agarose Gel Electrophoresis

Digested PCR products were separated by agarose gel electrophoreses on a 2% gel by loading the entire 20 µl reaction. A voltage of 120 V was applied to the gel for 30 mins and the gel was imaged on a SYNGENE G:Box.

2.2.5 Preparation of PCR Products for Sequencing

PCR products **(section 2.2.2)** of zebrafish from an ATM$^{+/sh477}$ in-cross were prepared for sequencing by removal of excess dNTPs and primers by addition of 0.05 µl Exonuclease I (NEB), 1 µl Shrimp Alkaline Phosphatase (Affymetrix), to 5 µl of PCR product and made up to 10 µl with dH_2O. Samples were then incubated at 37° C for 45 mins, and then incubated at 80° C for a further 15 mins. Samples were sequenced by the Genomic Core Facility at the University of Sheffield.

2.3 Measuring Gene Expression by Quantitative Reverse Transcription PCR (RT-qPCR)

2.3.1 RNA Extraction

Pooled zebrafish larvae were homogenised in 200 µl TRIzol® Reagent (Ambion® Life Technologies) with a handheld homogeniser (Pellet Pestles Cordless Motor-Sigma Aldrich). Dissected brain or muscle samples were homogenised in 1 ml TRIzol® Reagent with a handheld homogeniser. Whole adult zebrafish were flash frozen in liquid nitrogen, ground under liquid nitrogen with a pestle and mortar to a powder, and homogenised in 1 ml of TRIzol® Reagent. Homogenised samples were incubated for 5 mins at room temperature, after which 0.2 mls of chloroform per 1 ml of TRIzol® Reagent was added. Samples were vigorously agitated by shaking for 15 sec and allowed to stand at room temperature for 3 mins. Samples were centrifuged at 12,000 g for 15 mins a 4 °C to separate into 3 phases. The upper (aqueous) phase containing the RNA was removed to an RNase free Eppendorf tube®.

RNA was precipitated by addition of 0.5 ml isopropyl alcohol per 1 ml of TRIzol® Reagent and incubated for 10 mins at room temperature. The sample was again centrifuged at 12,000 g for 10 mins at 4° C to collect the precipitate, and the supernatant removed from the collected pellet. The RNA pellet was washed once by resuspension in 1 ml of 75% ethanol per 1 ml of TRIzol® Reagent. To again collect the pellet, the sample was centrifuged at 7,500 g at 4° C for 5 mins and supernatant removed.

The pellet was air dried for 30 mins. Extract from larvae, and brain and muscle were dissolved in 10 µl of RNase free water, while extracts from whole adult fish were dissolved in 100 µl. Concentration and purity of extracted RNA were determined by spectrophotometry (NanoDrop® - 1000) and the samples stored at -80° C.

2.3.2 Reverse Transcription and Complementary DNA (cDNA) Synthesis

To remove contaminating genomic DNA, RNA samples (1 µg) were incubated with 1 µl DNase I (NEB), 1X DNase I reaction buffer (NEB) and made up to a final volume of 10 µl with RNase free water, at 37° C for 10 mins. Ethylenediaminetetraacetic acid (EDTA) was added to a final concentration of 2.5 mM and the reaction heat inactivated by incubation at 75° C for 10 mins. Samples were then placed on ice.

cDNA synthesis was carried out using Quanta Bioscience qScript™ cDNA Synthesis Kit. Reactions were prepared on ice and each reaction contained 4 µl qScript™ reverse transcriptase mix and 11 µl of cleaned RNA sample mix, to a final volume 20 µl using RNase free water. Reactions were carried out in a thermal cycler under the following conditions: 22° C for 5 mins, 42° C for 30 mins, and 85° C for 5 mins.

2.3.3 RT-qPCR

2.3.3.1 Primer Optimisation

Before performing RT-qPCR on samples, primer concentrations were optimised to eliminate the formation of primer dimers. Both forward and reverse primers (100 µM) were diluted together to 1:10, 1:20, 1:40 and 1:80 in RNAase free water. An RT-qPCR reaction was carried out for each dilution with 1X EvaGreen® qPCR Master Mix (Biotium), 1 µl WT cDNA (diluted 1/5), 1 µl diluted primer pair mix to a final volume of 10 µl, using Bio Rad C100 Touch™ Real Time Thermal Cycler (Bio Rad). Reactions were analysed for amplification curve and Ct values under 35, and the presence of only one melt peak using MxPro v4.10 software.

2.3.3.2 Template Optimisation

Subsequent to primer optimisation, reaction/amplification efficiency (the amount of product increase after each cycle (%)) was determined by serial dilution (5 fold) of the template in triplicate to create a standard curve using WT cDNA in a RT-qPCR reaction outlined in section **2.4.3.1**. Reaction efficiency was calculated by:

$$10^{((-1/\text{slope of standard curve})\ -1)}*100$$

An appropriate reaction efficiency was considered 90-110%.

2.3.3.3 RT-qPCR

1 µl of a 1/5 dilution of each cDNA sample was amplified in triplicate using primers **(outlined in table 2.3)** at their optimised primer concentrations. Levels of mRNA were quantified relative to the reference genes *EF1α* or *β actin* and were amplified by cycling conditions laid out in **table 2.4** and **2.5**.

Table 2.3 qPCR Primers

Primer Name	***Sequences***	***Dilution***	***Protocol***
ATM	*Forward CGGTTCCATTCAGATTGTCTCG*	*1/40* *(2.5μM)*	*1*
	Reverse TTCTGAAGACACCCTCCACCC		
ATR	*Forward TGGAGTAAACCTGTGAAGGGT*	*1/20* *(5 μM)*	*1*
	Reverse CAGAGGCAAGCCCATCACTT		
IgM	*Forward GAAGCCTCCAATTCTGTTGG*	*1/20* *(5 μM)*	*1*
	Reverse CCGGGCTAAACACATGAAG		
IgD	*Forward GACACATTAGCCCATCAGCA*	*1/20* *(5 μM)*	*2*
	Reverse CTGGAGAGCAGCAAAAGGAT		
IgZ/T	*Forward GAACCAAACTCAGGGTTGGA*	*1/20* *(5 μM)*	*2*
	Reverse CACCCAGCATTCTACAGCAA		

	Forward GGATTGCCACACGGCTCACATT	*1/20* *(5 µM)*	*n/a*
Eef1α	*Reverse GGTGGATAGTCTGAGAAGCTCTC*		
	Forward CTCTTCACGCCTTCCTTCCT	*1/10* *(10 µM)*	*n/a*
β actin	*Forward CTCTTCCAGCCTTCCTTCCT*	*1/20* *(5 µM)*	
	Reverse CACCGATCCAGACGGACTAT		

Table 2.4 RT-qPCR Protocol 1

Step	***Temperature °C***	***Time (min:sec)***	***Cycles***
Initial denaturation	*95*	*10:00*	
PCR cycles			
Denaturation	*95*	*0:30*	*39X*
Annealing/Elongation	*65*	*1:00*	
Plate Read			
Denaturation	*95*	*1:00*	*60X*
Annealing	*65*	*0:30*	
Melt curve	*65*	*00:05 (+0.5 °C/cycle)*	

Table 2.5 RT-qPCR Protocol 2

Step	***Temperature °C***	***Time (min:sec)***	***Cycles***
Initial denaturation	*95*	*10:00*	
PCR cycles			
Denaturation	*95*	*0:30*	*39X*
Annealing	*56*	*0:30*	
Elongation	*72*	*1:00*	
Plate Read			
Denaturation	*95*	*1:00*	*60X*
Annealing	*65*	*0:30*	
Melt curve	*65*	*00:05 (+0.5 °C/cycle)*	

2.4 Behavioural Analysis

2.4.1 Measuring Swimming Defects in Zebrafish Larvae

Analysis was carried out at 5 and 12 dpf on a ZebraLab tracking system (Zebrabox, ViewPoint, Behaviour Technology). Zebrafish to be analysed at 5 dpf were arrayed in a 96 well plate (CytoOne®), one larva per well at 4.3 dpf, and allowed to acclimatise overnight. Zebrafish to be analysed at 12 dpf were removed from the aquarium system on the morning of analysis by directly netting them from the tank in a small tea strainer and transferring them to a 10 cm plate. The zebrafish were then transfer to a 12 well plate using a pasture pipette.

For analysis, the ZebraLab tracking system was switched on and the temperature left to equilibrate for 30 mins. The zebrafish were then placed in the ViewPoint chamber for 30 mins in 100% intensity light to let fish acclimatise. Larvae were then subjected to 6 cycles of alternating dark/light (100% intensity) with each interval lasting 5 mins (30 mins total). Zebrafish movement was tracked via an infrared camera and a lower threshold for movement (inactive) set as 2 mm/sec, and an upper threshold for movement (large movements) set at 6.4 mm/sec.

For analysis of ATM$^{+/sh477}$ in-crosses, after ZebraLab tracking, larvae were genotyped as per **section 2.2** above. For analysis of zebrafish treated with CPT, embryos were placed in the 96 well plate at 8 hpf and left to develop in that environment along with the relevant CPT treatment added at the appropriate time point.

For data analysis, movement tracked between the thresholds and above the upper threshold were totalled, and all movement under the lower threshold (2 mm/sec) discarded.

2.4.2 Swimming Endurance Test on Adult Zebrafish

Critical swimming velocity (U_{crit}) is the maximum velocity that the fish can maintain for a set period. It was determined for each fish using a custom-built swim tunnel apparatus (Ramesh et al., 2010, Plaut, 2000, Brett, 1964). Zebrafish at 10 months of age were individually introduced into a plastic tunnel that would allow a variable flow rate of water to pass through. The adult zebrafish were initially subjected to a water velocity of 6.6 cm/sec for 5 mins. The flow rate of water was increased in increments of 6.6 cm/sec every 5 mins to a final velocity of 52.8 cm/sec (40 mins), or until the zebrafish became exhausted and was pushed into a mesh net at the end of the tube. When exhausted, the zebrafish was allowed 30 seconds of recovery by pausing the time and ceasing the flow of water, and was given the chance to re-enter their highest achieved velocity by slowly increasing the flowrate. When zebrafish again became exhausted, the time was recorded. The U_{crit} was calculated by the following formula:

$$U_{crit} = U_i + (U_{ii}(T_i))/T_{ii}$$

U_i = the highest velocity maintained for a whole interval (cm/sec)
U_{ii} = the velocity increment (6.6 cm/sec)
T_i = the time elapsed at fatigue velocity (mins)
T_{ii} = the time interval (5 mins)

2.4.3 Total Motility

In a sound and lightproof box, zebrafish were placed in 0.8 L tanks in aquarium water, with a cold source back light, and allowed to acclimatise for 1 hr. Zebrafish swimming was then tracked from a side view with an infrared camera in conjunction with the ZebraLab: zebrafish behaviour screening software (ViewPoint, Behaviour Technology). A lower threshold for movement (inactive) was set as 25 mm/sec and an upper threshold for movement (large movements) was set at 50 mm/sec. For data analysis, movements tracked between the thresholds and above the upper threshold were totalled, and all movement under the lower threshold (25 mm/sec) discarded.

2.5 Measuring Protein Expression

2.5.1 Western Blot

2.5.1.1 Protein Extraction

Whole zebrafish were sacrificed and snap frozen in liquid nitrogen. For protein extraction, each zebrafish was crushed to a powder with liquid nitrogen with a pestle and mortar. To roughly a third of the crushed fish, 300 µl of ice-cold buffer was added. Buffers used for protein extraction were: Radioimmunoprecipitation assay (RIPA) buffer (-) ‘no salt’ (25 mM Tris pH 7-8, 0.1% SDS, 0.5% sodium deoxycholate, 1% Triton X-100); General Lysis buffer (Tris 50 mM, pH8, NaCl 40 mM, $MgCl_2$ 2 mM, 0.5% Triton, Benzonase 1:1000), Reporter Lysis buffer (Promega), with 1:1000 Benzobnase. To each buffer, 1X proteases inhibitor cocktail (ThermoFisherScientific) was added. Crushed zebrafish were homogenised using a handheld homogeniser and a further 300 µl of the relevant buffer was added. Note: the RIPA buffer that was added at this point was RIPA (+) ‘salt’ (25 mM Tris pH 7-8, 0.1% SDS, 0.5% sodium deoxycholate, 1% Triton X-100, 150 mM NaCl). To this 1X protease inhibitor cocktail was again added. The crushed zebrafish were then sonicated at 40% amplitude, for 5 sec X5, placing on ice between each sonication. Zebrafish were then left to lyse on ice for 30 mins. Samples were centrifuged at 12,000 g for 20 mins at 4° C to remove insoluble debris. The supernatant, containing soluble proteins, was removed to a clean Eppendorf tube, and a Bradford Assay (BioRad) to determine concentration was performed using bovine serum albumin (BSA) to calculate a standard curve.

2.5.1.2 Immunoprecipitation

To 1.5 mg of lysates, the relevant antibody was added at a ratio of 2 µg/500 µg of lysates, and incubated overnight at 4° C. Then, 50 µl of 50% Protein G beads (Mag Sepharose™Xtra, GE Healthcare, Sweden) were added and incubated at 4° C for 2 hrs. The mixture was then spun at 17,000 g for 1 min and the supernatant removed. The beads were washed 3 times in RIPA buffer and washed in TBS once. To the beads, 50 µl of laemmli buffer was added and the samples boiled on a heat block at 100° C for 10 mins.

2.5.1.3 SDS PAGE

Extracted protein was separated by 7.5% SDS-PAGE, (7.5% acrylamide, 0.375 mM Tris-HCl pH 8.8, 0.1% SDS, 0.1% APS, 0.1% TEMED and made up to a total volume of 25 mls with H_2O) and 4% stacking gel (4% acrylamide, 125 mM Tris-HCl pH 6.8, 0.1% SDS, 0.06% APS, 0.3% TEMED and made up to a total volume of 4 mls with H_2O), or with a 4-20% gradient gel (Mini-PROTEAN TGX, #4561096, BioRad). Running buffer was diluted to 1X from a 10X stock (249 mM Tris, 1.918 M Glycine) and 0.1% SDS added.

2.5.1.4 Electroblotting

Polyvinylidene difluoride *(*PVDF*)* membrane (0.45 µm Immobilon®P, Millipore) was soaked in methanol for 30 secs to activate it. Proteins were transferred from the gel to a PVDF or nitrocellulose (Amersham™ Protran™ 0.45 µm, 10600002, GE Healthcare) membrane by wet electroblotting (Mini Trans-Blot® Cell) in transfer buffer, which was made by diluting 10X running buffer **(section 2.5.3)** and adding 20% methanol*.*

2.5.1.5 Immunodetection of proteins

After transfer of proteins, membranes were blocked in 5% solution of powdered skimmed milk (Marvel) in TBST (0.1% Tween-20 in Tris buffered saline (TBS) solution for 1 hr. Primary antibodies to proteins of interest were diluted in the 5% powdered skimmed milk TBST solution. Primary antibodies used, and the concentrations with which they were used, can be found in the text. Membranes were incubated with agitation overnight at 4° C. Membranes were washed three times at room temperature in TBST with agitation, for 10 minutes each wash. Membranes were then incubated with the appropriate horseradish peroxidase (HRP)-conjugated secondary antibody (Polyclonal Goat anti-rabbit immunoglobulin HRP, Dako) diluted to 1:5000 in TBST for 1 hr at room temperature with agitation. Membranes were again washed as above.

2.5.1.6 Visualisation of Protein Bands

Membranes were incubated with SuperSignal West Pico Chemiluminescent Substrate (Thermo Scientific) for 5 mins with agitation, and the chemiluminescent bands detected using autoradiography film (Amersham Hyperfilm™ ECL, GE Healthcare).

2.5.2 Whole Mount Immunofluorescence

2.5.2.1 Immunostaining

Zebrafish embryos were anaesthetised in batches 30 by treatment with 120 µl Tricaine solution (42 ml per 100 ml of E3). Once fish were anaesthetised, the

Tricaine was removed, and the larvae incubated in 4% PFA, at 4° C, with agitation overnight. Zebrafish were washed in PBS once, and washed in PBT (PBS, 1% Triton-X) for 5 min X3. To permeabilise the embryos, they were incubated for 25 mins, with 0.25% Trypsin/PBT at room temperature. To stop the reaction, 1% goat serum/PBT was added at an equal volume to the permeabilisation reaction. Embryos were again washed with PBT and blocked for 3 hrs, rocking at room temperature in blocking buffer (10 % goat serum, 1% BSA, 1% DMSO, in PBT). Primary antibody, rabbit anti γH$_2$AX, Cat No. GTX127342 (GeneTex), was added to the embryos in antibody dilution buffer (5% goat serum, 1% BSA, 1% DMSO, in PBT) at a concentration of 1:1000, and incubated rocking at 4° C, overnight. The following day, embryos were washed in PBT for 5 hrs with 5 changes of PBT. Secondary antibody, goat anti-rabbit, Alexa Flour™568 (Life Technologies), was added at a concentration of 1:1000, along with Hoechst (1:10,000) overnight, rocking at 4° C. Embryos were then washed at room temperature for 5 hrs, with 5 changes of PBT.

2.5.2.2 Preparation of embryos for imaging

In an Eppendorf, embryos were placed in 25% glycerol until they sank to the bottom. Stepwise, the embryos were then placed in 50% glycerol and 75% glycerol, and the same allowed to happen. Under a dissecting microscope, the embryos heads and tails were separated, with the tails being used for genotyping and the heads mounted in 75% glycerol for imaging.

2.5.2.3 Confocal Imaging

Whole mount immunostained larvae were imaged on an SP5 confocal microscope system (Leica). Image analysis was performed using ImageJ (NIH).

2.5.2.4 Quantification of γH$_2$AX foci

Automated quantification of γH$_2$AX foci was performed with a custom MATLAB script. Briefly, maximum projections of Hoechst-marked nuclei and γH2AX foci were binarized by applying an adaptive threshold, and de-noised using a median filter. A threshold based on size and shape (roundness) was applied to the binary nuclei to exclude incomplete or overlapping nuclei **(figure 2.2 a)**. A mask of the selected nuclei was then applied to the binary γH2AX signal to select for only those γH2AX foci that are present in the nuclei of interest **(figure 2.2 b)**. The area of the γH2AX foci in each nucleus was then determined and normalised to the area of the relevant nucleus. Data was expressed as Relative Area γH_2AX foci/cell and used as a measure of γH2AX foci number/cell. Quantification of γH_2AX foci was carried out by Dr Victor Alfred, Grierson Lab, SITraN.

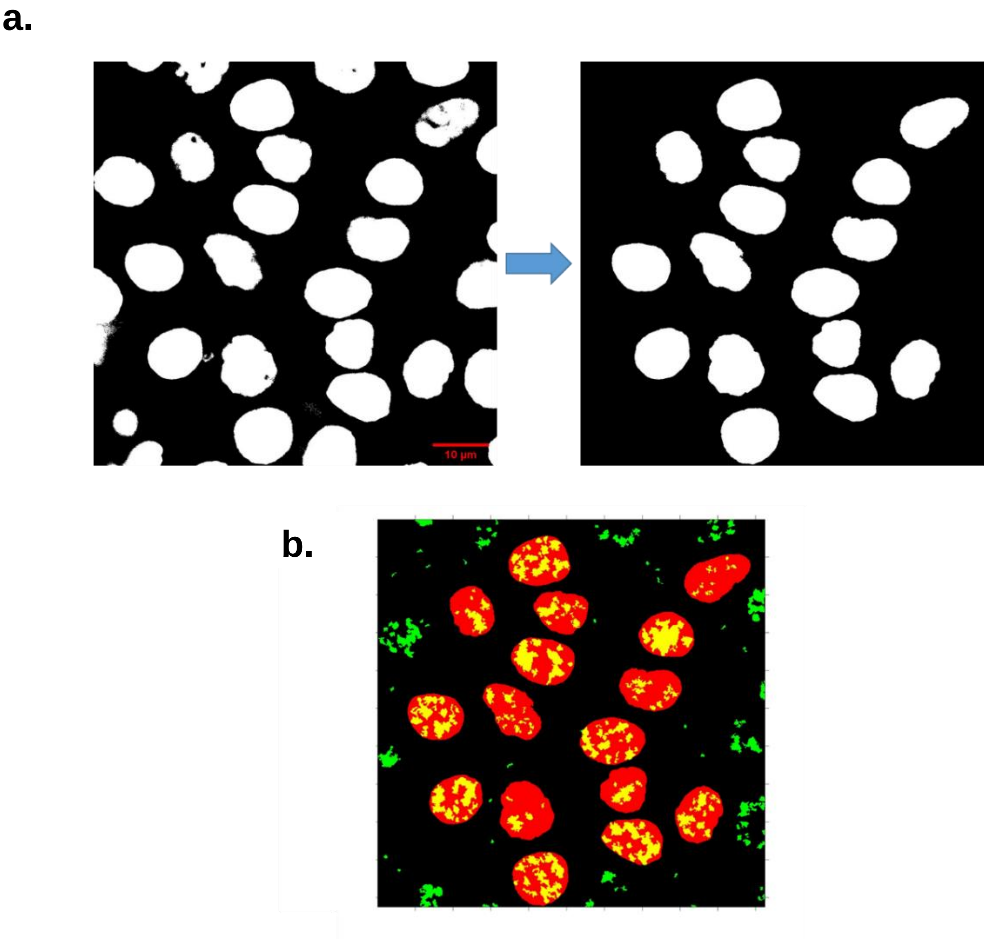

Figure 2.2 Quantification of γH2AX foci by a custom script. a. Nuclei to be analysed were selected based on shape and size to prevent to analysis of overlapping cells. **b.** A binary mask of the selected nuclei was then applied to γH_2AX foci, and the area of the foci within the selected nuclei was measured.

2.6 Histology

2.6.1 Preparation and Sectioning of Formalin Fixed Paraffin Embedded (FFPE) Adult Zebrafish

Adult zebrafish were sacrificed and immersed in 4% PFA. Zebrafish were incubated in the PFA, rocking, at 4° C for 4 days. Zebrafish were briefly washed in PBS and then incubated in 8.5 mM EDTA, pH8, for 7 days, with the EDTA being changed on day 4. Zebrafish were then processed in a tissue processer (Leica TP1020), with the following protocol: 70% ethanol (2 hrs) X3, 95% (2 hrs) X2, 100% ethanol (2 hrs) X2, Xylene (Fisher Scientific, UK) (2 hrs) X2, paraffin with vacuum (2 hrs) X2.

The zebrafish tissue was then microtome sectioned at a thickness of 5 µm and mounted on charged slides (StarFrost, Knittel Glass). Slides were dried overnight in an oven at 37° C.

2.6.2 Haematoxylin and Eosin (H&E) Staining of Slides

To remove the paraffin, slides were placed in xylene, for 5 mins, X2. Slides were then hydrated by placing them sequentially in 100% X2, 95% and 70% ethanol (Fisher Scientific, UK), for 5 mins each. Slides were then quickly washed in tap water and stained in filtered Harris's haematoxylin (Leica, UK), for 2 mins. Slides were quickly washed again in tap water, and then the haematoxylin differentiated by dipping the slides into acid alcohol 3 times, before being washed in tap water again. Slides were then incubated in Scott's tap water until the haematoxylin turned from purple to blue. Slides were incubated in eosin (Leica, UK) for 5 mins, and then washed in tap water. Slides were dehydrated by sequentially washing them in 70%, 95% and 100% X2 ethanol for 1 min each, and finally placing in xylene for 5 mins. Slides were cover slipped (Fisher Scientific, UK) in DPX mounting media (Leica, UK). To set the DPX, slides were dried in an oven overnight at 37° C.

2.6.3 Immunohistochemistry

FFPE slides were deparaffinised and hydrated as outlined above in **section 2.8.2**. After incubation in ethanol, slides underwent peroxidase quenching by incubation in methanol and 3% H_2O_2 for 20 mins. Slides were washed in tap water, and antigen retrieval performed at either pH 6 (Access Revelation, Menapath, Wokingham, United Kingdom) or pH9 (Super RTU antigen retrieval solution, Menarini Diagnostics) by placing the slides in the relevant antigen solution in a pressure cooker, with 500 ml water. The pressure cooker program was set to 300 psi at 125° C for 30 sec. Slides were then immunostained with Vectastain Elite ABC-HRP kits, specific to the species in which the primary antibody was raised, as per their protocol. Slides were incubated in primary antibody overnight at 4° C. For antibody optimisations, a rabbit IgG (Vector Laboratories, UK) was used as a control, at the highest concentration that the primary antibody was used at, to ensure primary antibody specificity. Antibody staining was visualised by 3,3’-diaminobenzidine (DAB) kit (Vector Laboratories) for ~ 6 mins, and the reaction stopped by washing in water. Slides were counterstained with haematoxylin for 1 min, and again washed in tap water. The haematoxylin was differentiated by dipping the slides into acid alcohol X3, before quickly washing in tap water again. Slides were then incubated in Scotts tap water until the haematoxylin turned from purple to blue, and washed again in tap water. Slides were prepared for cover slipping by dehydration in progressively concentrated ethanol, and incubated in xylene as described above in **section 2.8.2**. Slides were then cover slipped as previously described.

2.6.4 Imaging of FFPE Sections

Slides were imaged on NanoZoomer S60 Digital Slide Scanner U12388-01, C13210-01 (Hamamatsu) and analysed using NDP.view2 Viewing software (Hamamatsu).

2.7 Statistical Analysis

Data were analysed using GraphPad Prism software ® and power calculations were carried out using G*Power software.

Chapter 3

Characterisation of the ATM Mutation in ATM$^{sh477/sh477}$ Zebrafish, their Response to Ionising Radiation and Activation of the DDR

3.1 Introduction

As outlined above in **chapter 1, section 1.3**, several animal models of AT already exist. However, most of these, with the exception of the porcine model, fail to faithfully recapitulate the neurodegenerative phenotype seen in AT. Zebrafish are genetically tractable, and generation of an ATM knockout model is relatively quick and inexpensive. Furthermore, zebrafish embryos are conducive to high throughput screening in a way that higher vertebrate models are not. A zebrafish ATM morpholino (MO) KD model has been reported (Imamura and Kishi, 2005). However, investigation into the effects of ablation of ATM have only been made at the embryonic level as MO KD is transient, and since AT is a degenerative disorder it will likely be necessary to look beyond embryonic development to understand the full effects of loss of ATM. Furthermore, MO KD is sometimes associated with off-target effects, such as p53 activation, which is regulated by ATM (Robu et al., 2007, Cheng and Chen, 2010), thus observations made in that model may not be truly representative of loss of ATM. Therefore, we propose use of a KO model carrying a similar type of ATM mutation to that found in classical AT patients.

In order to determine if a zebrafish ATM KO is an appropriate model of AT, characterisation of the effects of loss of ATM in zebrafish must be carried out. In this chapter, we have characterised zebrafish carrying a truncating mutation in ATM and investigated whether this model recapitulates any of the phenotypes observed in AT patients, such as radiosensitivity, deficiencies in the DDR, and immunodeficiency.

3.2 Results

3.2.1 Expression of ATM in ATM$^{sh477/sh477}$ Zebrafish

3.2.1.1 Expression of *ATM* mRNA in ATM$^{sh477/sh47}$ Zebrafish

A potential zebrafish ATM KO model of AT (ATM$^{sh477/sh477}$) had previously been made using CRISPR/Cas9 (Zakšauskaitė, Van Eeden and El Khamisy, Unpublished). These fish were uncharacterised, and the characterisation studies described in this thesis were performed in collaboration with Prof. El Khamisy.

To confirm the mutation in these zebrafish, the CRISPR targeted region of exon 6 was amplified by PCR, and the products sequenced by the University of Sheffield Genomics Core Facility. Chromatograms of the sequences were analysed and ATM$^{sh477/sh477}$ zebrafish were found to have a 5 bp deletion mutation when compared to their wild type siblings **(figure 3.1 a)**. The predicted amino acid sequence results in a frameshift mutation, leading to generation of 18 novel amino acids followed by a premature stop codon **(figure 3.1 b)**.

We predicted that this premature stop codon would either lead to a truncated protein product and loss of the ATM pathway, or loss of the ATM protein via induction of nonsense mediated degradation (NMD) of the mutant mRNA due to the upstream premature stop codon (Hug et al., 2016). To determine if the *ATM*^{sh477} transcript induced NMD, we used reverse transcriptase – quantitative PCR (RT- qPCR) to determine the *ATM* mRNA levels in the mutant zebrafish. We developed a number of primers upstream and downstream of the mutation site, which are outlined in **figure 3.2 a**, and used these to determine *ATM* mRNA expression at a number of different ages. Unless otherwise stated, *ATM* mRNA expression was measured using primers designed against exons 58-59 **(figure 3.2 a)**. This area was selected as it is 3’ of the predicted stop codon in exon 6 and is also within the kinase domain, which is known to be critical for ATM protein function **(see chapter 1, section 1.2.2)**.

ATM$^{sh477/sh477}$ zebrafish are produced from an ATM$^{+/sh477}$ in-cross. Therefore, it is important to determine if there is any maternal contribution of *ATM* mRNA and when it ends. Second, it is useful to know when high levels of *ATM* are expressed, as this may indicate its importance in development of the fish at that time. Thus, *ATM* mRNA expression was measured in wild type zebrafish through the first 28 days of development using RNA extracted from pooled wild type embryos **(figure 3.2 b and c)**. Expression was normalised to *EAF1α*. It appears that there is a strong maternal contribution of *ATM* mRNA as there are significantly higher levels detected ~1.5 hours post fertilisation (hpf), at the 16 cell stage **(figure 3.2 b)**. *ATM* mRNA levels are sharply decreased by ~ 5.25 hpf, at 50% epiboly. While the level of *ATM* mRNA varied over the next 7 days, changes in expression did not reach statistical significance. *ATM* mRNA expression was transiently increased at 14 dpf ($p<0.01$), but decreased again at 21 and 28 dpf **(figure 3.2 c).**

NMD decay is a mechanism by which aberrant mRNA transcripts are degraded to protect the cell. This results in a decrease in, or almost complete ablation of the mutant mRNA expression to prevent the mutant protein from being translated (Lindeboom et al., 2016). To determine if the deletion mutation is associated with NMD of *ATM* mRNA, 5 pooled larvae from each genotype were analysed at 5 dpf, and no significant difference was observed in expression between ATM$^{+/+}$ and ATM$^{sh477/sh477}$ zebrafish **(figure 3.2 d)**. *ATM* expression was further investigated at 21 dpf (3 weeks), as at this point in development maternally contributed mRNA will no longer be detectable. All 3 possible genotypes resulting from an ATM$^{+/sh477}$ in-cross exhibited remarkably similar *ATM* mRNA expression **(figure 3.2 e)**, suggesting that the *ATM* mRNA is not susceptible to NMD.

All expression data gathered thus far used primers amplifying a 3' region of the transcript encoding the kinase coding domain, which is critical for ATM function. However, we hypothesised that alternative *ATM* transcripts with ATG codons 3' of the frame shift mutation may be present. Therefore, RT-qPCR was also carried out at 3 weeks using primers upstream of the mutation site amplifying exons 1-2 and 4-5. No significant differences in mRNA levels were observed with either of the new primer pairs **(figure 3.2 f & g)**.

As a final step, we investigated *ATM* mRNA levels in whole zebrafish extracts and mRNA prepared from adult brains. While there was variation in expression between fish, and there was a trend of decreased expression in ATM$^{sh477/sh477}$ compared to ATM$^{+/+}$ siblings, it was not statistically significant **(figure 3.2 h and i)**.

a.

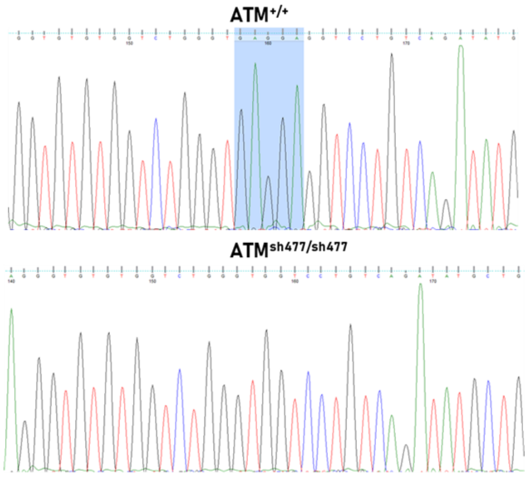

```
                5'                                                           3'
Ensembl         GCTTCTCTCCTGCAGGAAGAGGGTGTGTGGTCTGGGTGAGGAGGTCCTGTCAGATATGCT
Wild Type       GCTTCTCTCCTGCAGGAAGAGGGTGTGTGGTCTGGGTGAGGAGGTCCTGTCAGATATGCT
ATMsh477/sh477  GCTTCTCTCCTGCAGGAAGAGGGTGTGTGGTCTGGGT-----GGTCCTGTCAGATATGCT
                *************************************     ******************
```

b.

```
Ensembl         AEKQLMVLENLVSAVNVFLRSVLLSCRKRVCGLGEEVLSDMLCVYTGMRPSSVLKEELVKFFQIQLFVHHPKGAKTIET

Wild Type       AEKQLMVLENLVSAVNVFLRSVLLSCRKRVCGLGEEVLSDMLCVYTGMRPSSVLKEELVKFFQIQLFVHHPKGAKTIET

ATMsh477/sh477  AEKQLMVLENLVSAVNVFLRSVLLSCRKRVCGLGGPVRYAVRLYWDETQLST*
                **********************************
```

Figure 3.1 Characterisation of the ATM$^{sh477/sh477}$ mutation. a. Chromatogram of partial sequences from wild type and mutant PCR products of exon 6 of *ATM* (deleted bases in blue), along with a partial alignment of the sequence compared with Ensembl (Ensemble, 2017) sequence showing a 5 bp deletion in the mutant zebrafish. **b.** Translated protein sequence of exon 6 showing that the 5 bp deletion in ATM$^{sh477/sh477}$ zebrafish leads to a downstream premature stop codon.

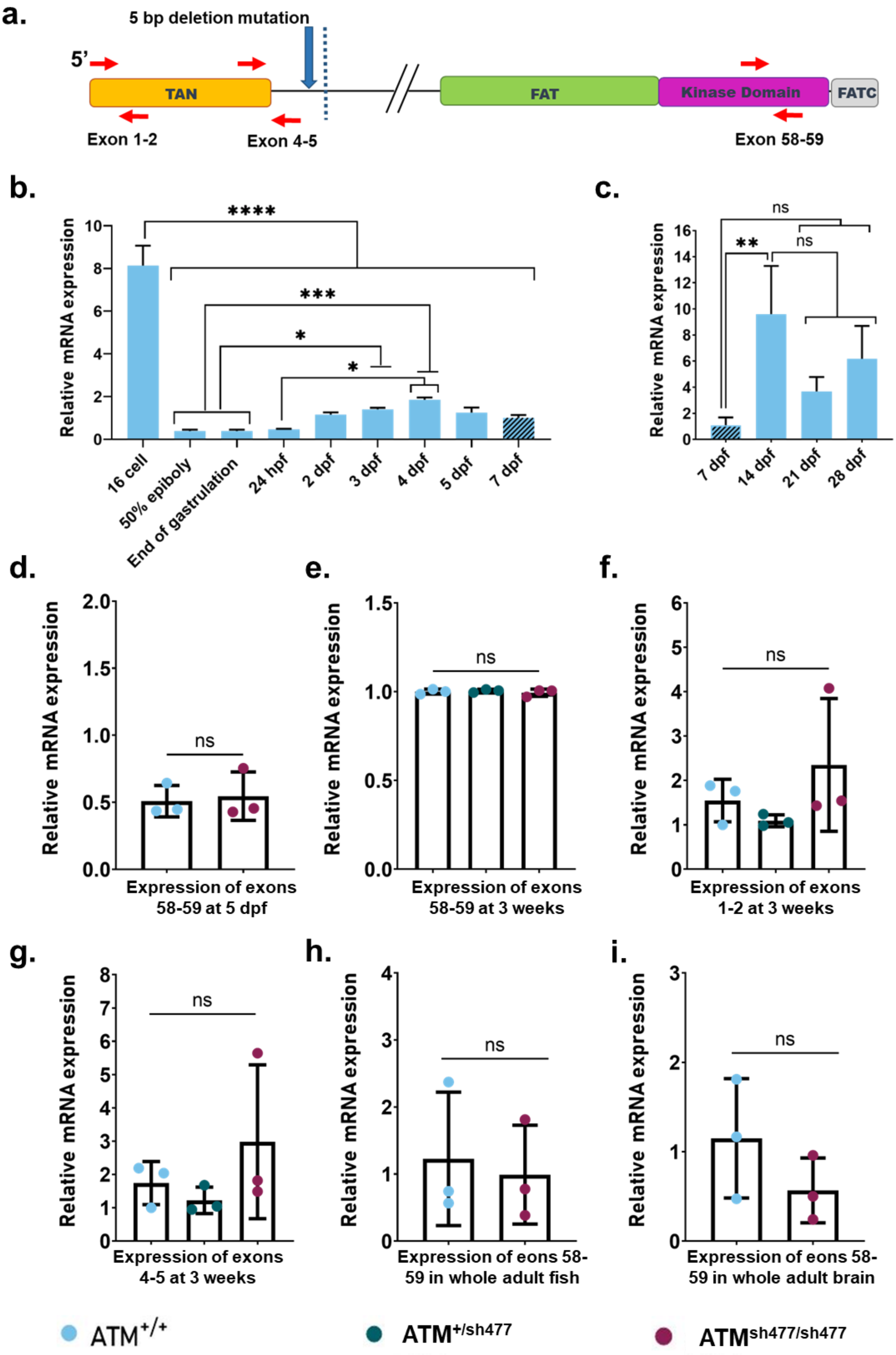
a.
5 bp deletion mutation
5'
TAN
FAT
Kinase Domain
FATC
Exon 1-2
Exon 4-5
Exon 58-59
b.
Relative mRNA expression
0
2
4
6
8
10
****
***
*
*
16 cell
50% epiboly
End of gastrulation
24 hpf
2 dpf
3 dpf
4 dpf
5 dpf
7 dpf
c.
Relative mRNA expression
0
2
4
6
8
10
12
14
16
ns
**
ns
7 dpf
14 dpf
21 dpf
28 dpf
d.
Relative mRNA expression
0.0
0.5
1.0
1.5
2.0
ns
Expression of exons 58-59 at 5 dpf
e.
Relative mRNA expression
0.0
0.5
1.0
1.5
ns
Expression of exons 58-59 at 3 weeks
f.
Relative mRNA expression
0
1
2
3
4
5
6
ns
Expression of exons 1-2 at 3 weeks
g.
Relative mRNA expression
0
1
2
3
4
5
6
7
8
ns
Expression of exons 4-5 at 3 weeks
h.
Relative mRNA expression
0
1
2
3
4
ns
Expression of eons 58-59 in whole adult fish
i.
Relative mRNA expression
0
1
2
3
ns
Expression of eons 58-59 in whole adult brain
● ATM$^{+/+}$
● ATM$^{+/sh477}$
● ATM$^{sh477/sh477}$

Figure 3.2 Expression of ATM mRNA in wild type and ATM$^{sh477/sh477}$ zebrafish. a. Schematic of zebrafish ATM mRNA indicating the encoded protein functional regions and positions of primers used for RT-qPCR analysis (red arrows). Blue arrow indicates position of the deletion mutation and dotted line indicates the resulting downstream stop codon. **b.** Expression of *ATM* mRNA through first 7 days of development. Expression was normalised to *EF1α* levels as a control and then expressed relative to the expression level at 7 dpf. Data were analysed by one-way ANOVA with a *post hoc* Tukey's multiple comparisons test. Each stage assessed represents mRNA expression in a number of pooled embryos (16 cell - end of gastrulation = 100 embryos, 1 and 2 dpf = 50 embryos, 3 – 7 dpf = 25 larvae) with N=3 replicates. **c.** Expression of *ATM* mRNA from 7-28 dpf, normalised to *EF1α* expression and expressed relative to 7 dpf expression. Data were analysed by one-way ANOVA with a *post hoc* Tukey's multiple comparisons test, 7 dpf vs 21 dpf (p= 0.5522), 7 dpf vs 28 dpf (p= 0.1042). Each data point represents 10 pooled fish with N=3 replicates. **d.** Expression of ATM$^{+/+}$ and ATM$^{sh477/sh477}$ at 5dpf. Each data point represents 5 pooled embryos, N=3 replicates. Expression was normalised to *EF1α* levels as a control. Data were analysed by an unpaired t-test (p= 0.7797). **e.** Expression of ATM$^{+/+}$, ATM$^{+/sh477}$ and ATM$^{sh477/sh477}$ at 3 weeks old. Data points represent individual fish. Expression was normalised to *EF1α* levels as a control. Data were analysed by one-way ANOVA with a *post hoc* Tukey's multiple comparisons test**. f.** Expression of exons 1-2 of *ATM* mRNA at 3 weeks. Expression was normalised to *EF1α* levels as a control. Data were analysed by one-way ANOVA with a *post hoc* Tukey's multiple comparisons test**. g.** Expression of exons 4-5 of *ATM* mRNA at 3 weeks. Data were analysed by one-way ANOVA with a *post hoc* Tukey's multiple comparisons test**. h.** Exons 58-59 of *ATM* mRNA global expression in adult zebrafish. Each data point represents an individual fish. Expression was normalised to *EF1α* levels as a control. Note: Individual fish analysed in **e** are the same fish analysed in **f** and **h**. Data were analysed by an unpaired t-test (p= 0.7576). **i.** Exons 58-59 of *ATM* mRNA expression in the brain of adult zebrafish. Each data point represents an individual fish. Data were analysed by an unpaired t-test (p= 0.2549). In all graphs, error bars represent the mean +/- SD. Statistical analysis can be seen in **appendix 3.1**.

3.2.1.2 Investigation into the Expression of the ATM Protein in ATM$^{sh477/sh477}$ Zebrafish

As no difference in the expression level of *ATM* mRNA was observed, we decided to raise an antibody to detect zebrafish ATM protein. The extreme N-terminal of the protein was chosen as the immunogenic sequence (amino acids1-120) **(figure 3.3)**, as it was hoped that if *ATM*^{sh477} mRNA does not undergo NMD and is translated, both the full length and truncated protein might be detected by western blot.

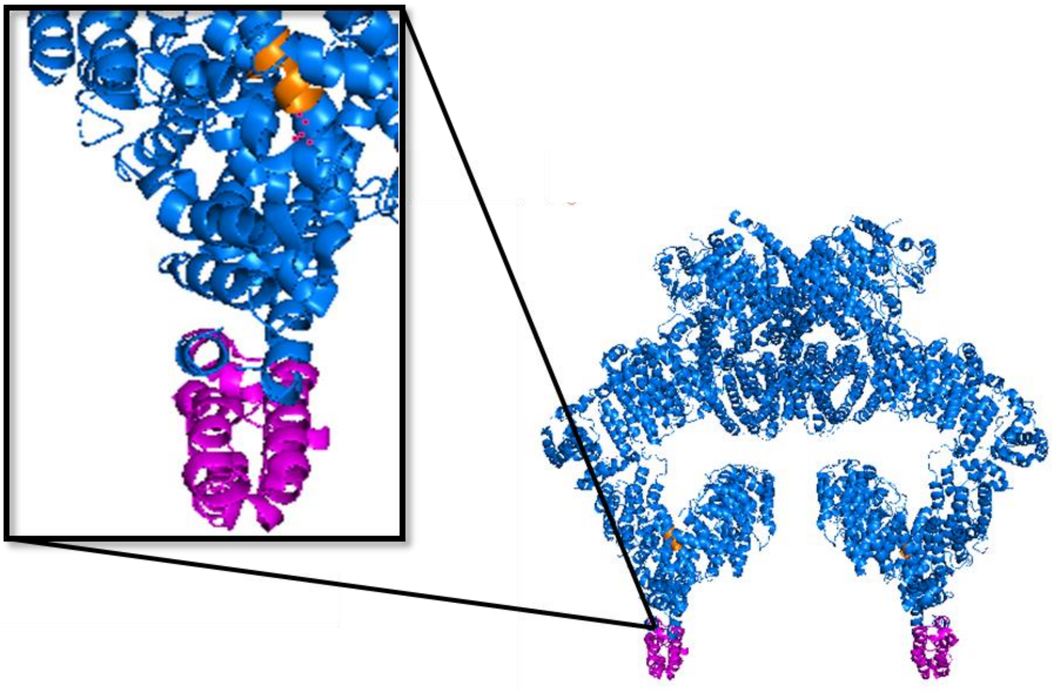

Figure 3.3 Epitope to which the zebrafish ATM antibodies were raised, modelled on the human ATM structure. Pink indicates the recombinant peptide of the N-terminal that was used to raise the antibody (amino acids 1-120). For reference, orange indicates the location of the residues surrounding the premature stop codon in the mutant protein.

Zebrafish specific ATM antibodies were generated by Proteintech™ by inoculation of two rabbits with a GST tagged recombinant peptide corresponding to amino acids 1-120 of the zebrafish ATM protein. The method and production data sheet of the antibodies carried out by Proteintech™ can be observed in **appendix 3.2**. As two rabbits were inoculated, two polyclonal antibodies were received (zATM1 and zATM2) and these were first optimised for detection of full-length endogenous ATM by western blot, and optimised in order to find an appropriate lysis buffer and antibody concentration. Whole adult sexed match fish (12 months/male), were first crushed under liquid nitrogen using a mortar and pestle, and then the powdered tissue was split into 3 aliquots, and lysed in 3 different buffers. The lysis buffers used were Radioimmunoprecipitation assay (RIPA) buffer, a General Lysis (lysis) buffer, and a commercial buffer, Reporter Lysis (Reporter) buffer. As full-length zebrafish ATM is predicted to have a molecular weight of ~350 KDa, lysates were run on 7.5% polyacrylamide gels to allow adequate separation of high molecular weight proteins, and transferred to PVDF membranes. The membranes were then probed with three antibody concentrations (1:100, 1:500 and 1:1000) **(figure 3.4).** On the basis of prominent bands after Ponceau staining of the PVDF membranes, samples collected from the same fish gave distinctly different protein content depending on which buffer was used **(figure 3.4)**. Furthermore, ATM$^{+/+}$ and ATM$^{sh477/sh477}$ zebrafish lysed with the same buffer also gave different Ponceau staining patterns. This is likely due to a testicular pathology that will be discussed in **chapter 4**, causing a difference in the cellular makeup of the tissue that was lysed. These differences in overall protein content make it difficult to know the effect of antibody specificity. This is evident in the reactivity of the antibody, both between the buffers used and the lysates from each genotype, as different banding patterns can be observed on the western blot. This is best observed in **figure 3.4 a iii and b ii**. Both antibodies are reactive even when diluted 1:1000, detecting bands at a number of different sizes, particularly around 50 KDa. However, neither antibody detected anything above 250 KDa that could be considered full length ATM in either ATM$^{+/+}$ or ATM$^{sh477/sh477}$ lysates. In the context of probing with zATM1, lysing with RIPA buffer appeared to give the highest protein content that was reactive with the antibody, whereas probing with zATM2, the general lysis buffer gave the protein content with the greatest reactivity.

In addition to optimisation of lysis buffer and antibody concentration, the type of transfer membrane used was also tested, comparing nitrocellulose and PVDF **(see appendix 3.3)**. No significant differences were observed between the two membranes; therefore PVDF was used for detection of zebrafish ATM.

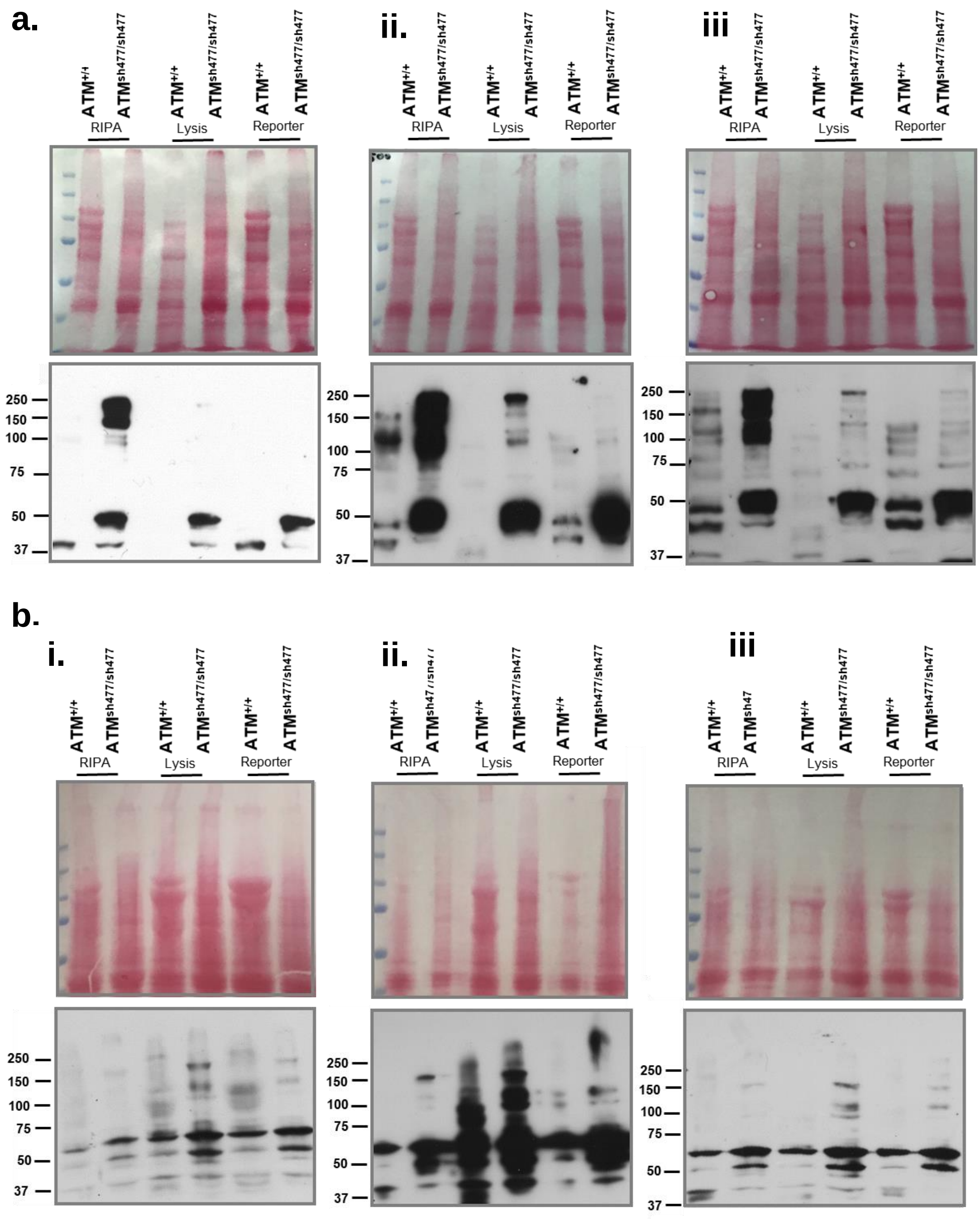
a.
ii.
iii
b.
i.
ii.
iii
ATM+/+
ATMsh477/sh477
RIPA
Lysis
Reporter
250
150
100
75
50
37

Figure 3.4 Optimisation of novel zATM antibodies for detection of full-length endogenous ATM with suitable lysis buffer and antibody concentration. Whole adult zebrafish lysates were lysed in 3 buffers, RIPA, General Lysis Buffer (Lysis) and Reporter Lysis Buffer from Promega (Reporter), and were analysed by western blot (7.5% agarose gel/PVDF membrane) and probed with both zATM raised antibodies (zATM1 and zATM2) at a range of concentrations. **a.** Zebrafish lysates probed with zATM1. **b.** Zebrafish lysates probed with zATM2. **i)** antibody diluted to 1:1000 **ii)** antibody diluted to 1:500 **iii)** antibody diluted to 1:100.

It was not known whether the antibodies were capable of detecting the zebrafish protein, or if the concentration of endogenous ATM protein was below the limit of detection. For that reason, in order to determine if the antibodies were capable of detecting the truncated form of ATM, and at what limit of detection, 30 ng of the GST tagged ATM (aa 1-120) peptide that had been used to inoculate the rabbits, was serially diluted (1/3) and probed with zATM1. The predicted size of the recombinant protein is ~39 KDa (aa 1-20 of zebrafish ATM =13.8 KDa, GST tag= ~26 KDa) **(see appendix 3.2)**. The zATM1 antibody was able to detect a strong band just above 37 KDa **(figure 3.5 a),** which is likely the recombinant protein as it is similar to quality control tests carried out by Proteintech™, who also detected a band at the same molecular weight when probing with a GST antibody after protein induction in transformed bacterial lysates **(see appendix 3.2 page 4 of proteintech™ data sheet)**. The zATM1 antibody was able to detect 1.1ng of recombinant protein using a longer exposure (data not shown). There is also a lower band present at 25 KDa. This may represent a cleaved version of the GST tagged peptide purified from the bacterial cells, and can also be detected by a GST antibody **(see appendix 3.2 page 4 of Proteintech™ data sheet)**.

In order to determine whether there is a truncated protein produced in ATM$^{sh477/sh477}$ zebrafish, lysates from three ATM$^{+/+}$ and three ATM$^{sh477/sh477}$ male zebrafish (12 months) were separated on a 4-20% gradient agarose gel to allow maximum separation and visualisation of both low and high molecular weight proteins, as the truncated protein is predicted to be 31 KDa. After transferring to PVDF membrane, lysates were probed with zATM1 **(figure 3.5 b)**. Again, nothing was detected above 250 KDa in either genotype, indicating that the full-length protein was not detected. However, three bands were detected between 20-37 KDa that appeared to be much more prominent in homozygous fish compared to wild type **(figure 3.5 b green arrows)**. Although not conclusive, this result is consistent with the generation of truncated ATM protein in ATM $^{sh477/sh477}$ zebrafish, and in keeping with our inability to find evidence of nonsense mediated degradation of *ATM* mRNA.

As there is evidence suggesting that the recombinant peptide and truncated ATM protein might be detected by zATM1 **(figure 3.5 a and b)** it was hoped that the full-length protein may also be detectable, but the endogenous concentration was below the limit of detection of the antibody. Therefore, we attempted to increase its concentration by carrying out an immunoprecipitation assay (IP). The IP was optimised by lysing wild type fish in RIPA buffer as described above, and incubating 1.5 mg of whole zebrafish lysates with either zATM1, zATM2 or a control Rabbit IgG (2 µg antibody/500 µg lysate). Immunoprecipitated proteins were size separated using a 4-20% gradient PAGE, transferred to PVDF, and then incubated with the above antibodies. Both zATM antibodies detected a band well above 250 KDa **(figure 3.5 c)**; however, the same band was detected in the rabbit IgG control, so it is non-specific. The sample immunoprecipitated by zATM1 and then probed by zATM1 shows a higher molecular weight band **(figure 3.5 c, yellow arrow)**. It is possible that this was ATM as it was estimated to be an appropriate size. However, without a molecular marker beyond 250 KDa it was difficult to determine if this was a positive detection of ATM or an artefact of protein stuck either at bottom of the wells, or at the stacking/resolving gel. Therefore, another IP was attempted with lysates from three ATM$^{+/+}$ and three ATM$^{sh477/sh477}$ male zebrafish (12 months), which were both immunoprecipitated with zATM1, and the western blot probed with zATM1 **(figure 3.5 d)**. This time, landmarks of the gel such as the stacking/resolving gel interface and the bottom of the wells were marked to give context to any high molecular weight bands detected **(figure 3.5 d, asterisks)**. There was a band detected in all samples well above 250 KDa, although, this was at the stacking/resolving gel interface. Therefore, we were unable to detect zebrafish ATM full length protein using western blot. Optimisation for the ATM antibody was carried out for immunohistochemistry, and will be discussed in **chapter 4 section 4.2.2.4**. Detection of ATM peptides in ATM$^{+/+}$ and ATM$^{sh477/sh477}$ lysates, at 5 dpf by mass spectrometry was also attempted. However, ATM could not be detected in either sample (data not shown).

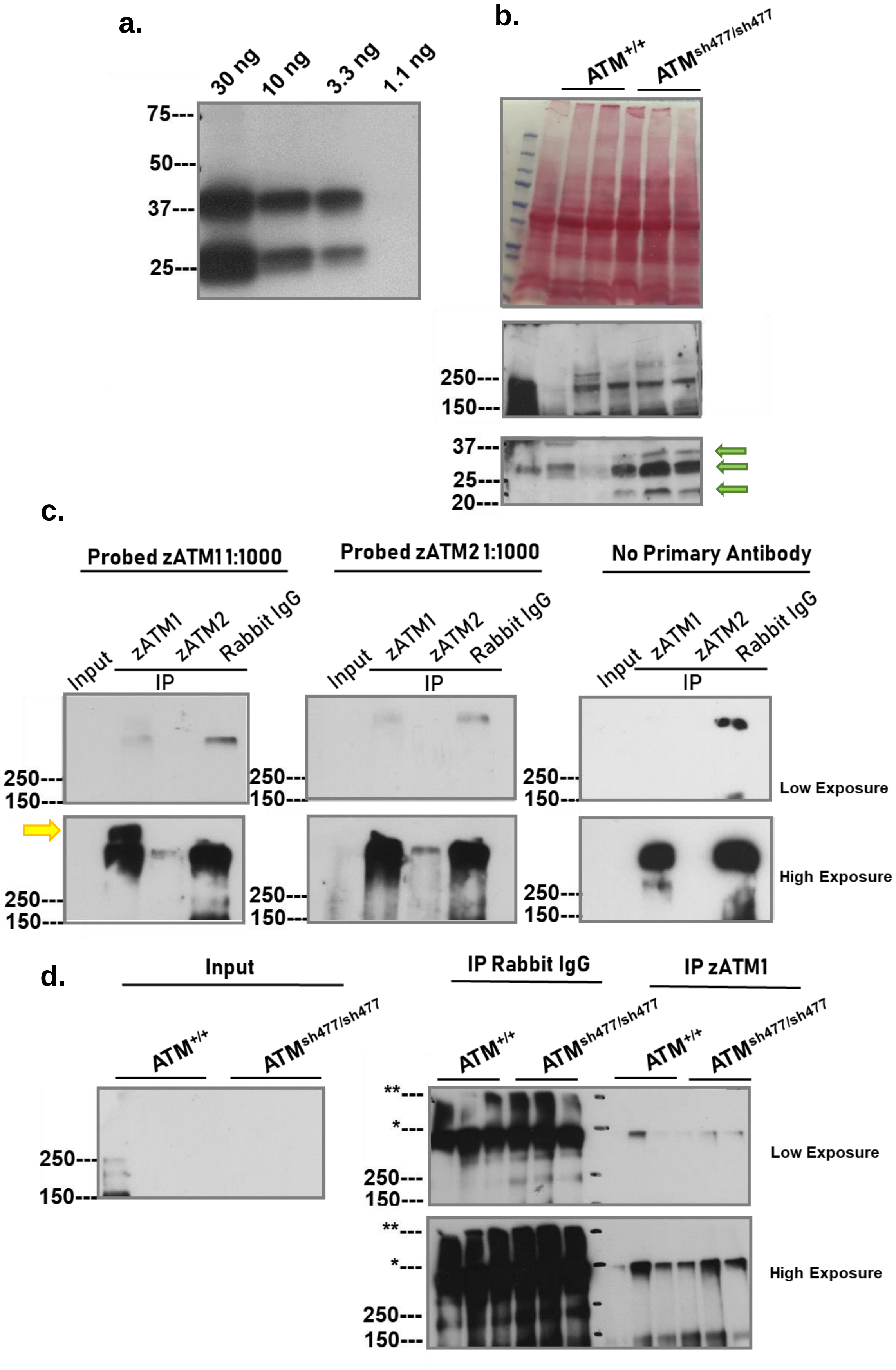
a.
30 ng
10 ng
3.3 ng
1.1 ng
75---
50---
37---
25---
b.
ATM+/+
ATMsh477/sh477
250---
150---
37---
25---
20---
c.
Probed zATM1 1:1000
Probed zATM2 1:1000
No Primary Antibody
Input
zATM1
zATM2
Rabbit IgG
IP
250---
150---
Low Exposure
High Exposure
d.
Input
IP Rabbit IgG
IP zATM1
ATM+/+
ATMsh477/sh477
**---
*---
250---
150---
Low Exposure
High Exposure

Figure 3.5 zATM antibodies do not detect endogenous full-length zebrafish ATM. a. Serial 1:3 dilution of recombinant zebrafish ATM peptide (amino acids 1-120) with GST tag is detected by zATM1 (1:1000). **b.** Lysates from sex matched zebrafish separated on a 4-20% gradient gel, transferred to PVDF membrane and probed with zATM1 (1:1000) show no protein detected above 250 KDa in either ATM$^{+/+}$ or ATM$^{sh477/sh477}$. It does show an ATM$^{sh477/sh477}$ specific band between 25 and 37 KDa and another at ~20 KDa (green arrows). **c.** Optimisation of immunoprecipitation of ATM. 1.5 mg of wild type zebrafish adult lysates were immunoprecipitated with either zATM1, zATM2 or control rabbit IgG (2 µg antibody/ 500 µg lysate), and along with 100 µg of input probed with either zATM1, zATM2 (1:1000) or no primary antibody. There appeared to be a zATM1 pulled/probed specific band (yellow arrow). **d.** IP of lysates (1 mg) from three sex matched ATM$^{+/+}$ and three ATM$^{sh477/sh477}$ adult zebrafish probed with zATM1 (1:1000), input (100 µg). ***** Stacking/resolving gel interface ****** bottom of loading wells**.**

3.2.2 ATM$^{sh477/sh477}$ Zebrafish Develop as Male

Domesticated zebrafish do not have sex chromosomes, and their sex determination is thought to be governed by unknown genetic components that are sensitive to environmental cues (Liew and Orbán, 2014). These unknown genetic components may be polygenic and may differ between strains of zebrafish (Liew and Orbán, 2014). During development, all zebrafish initially develop a ‘juvenile ovary’ which can either continue to grow into a mature ovary, or can degenerate and subsequently develop into testes through oocyte apoptosis between 19 and 27 dpf (Maack and Segner, 2003, Wang et al., 2007). However, this sexual development is also sensitive to environmental factors, particularly stress factors such as high temperature (Abozaid et al., 2011), high density (Abozaid et al., 2011), lack of resources (Lawrence et al., 2008), and low oxygen (Shang et al., 2006). Stress factors such as elevated temperature appear to consistently skew sex ratios in favour of more males (Liew and Orbán, 2014), however, low density and unknown factors can skew towards more females. Furthermore, ATM functions in HR, and mutations in *brca2*, *rad51,* and 12 other DDR genes in zebrafish have also caused female to male sex reversal (Ramanagoudr-Bhojappa et al., 2018, Rodríguez-Marí et al., 2011, Rodríguez-Marí et al., 2010, Shive et al., 2010, Vierstraete et al., 2017).

In our first in-cross of ATM$^{+/sh477}$ zebrafish we noticed that ATM$^{sh477/sh477}$ zebrafish were consistently phenotypically male. Given the link between KO of DNA repair genes and female to male sex reversal in zebrafish, we investigated further. We raised three clutches of 120 fish each, from multiple ATM$^{+/sh477}$ in-cross parent pairs, to sexual maturity (3 months) using standard housing density of 9.2 zebrafish/litre (60 per tank). The progeny were genotyped and independently assigned a sex based on their phenotypic characteristics (morphology and colour) by a member of the aquarium team who did not know the genotype of each fish. Zebrafish from the ATM$^{+/sh477}$ in-cross maintained close to a Mendelian frequency of ATM genotypes **(figure 3.6 a)**, and overall had a similar ratio of male to female fish within the clutch **(figure 3.6 b)**. However, all ATM$^{sh477/sh477}$ fish observed, with the exception of one fish, were phenotypically male **(figure 3.6 c)**. This preference of ATM$^{sh477/sh477}$ zebrafish for the male lineage was consistent in every clutch raised from ATM^{+sh477} in-crosses throughout the project, including when crossed to a TDP1 null background (data not shown).

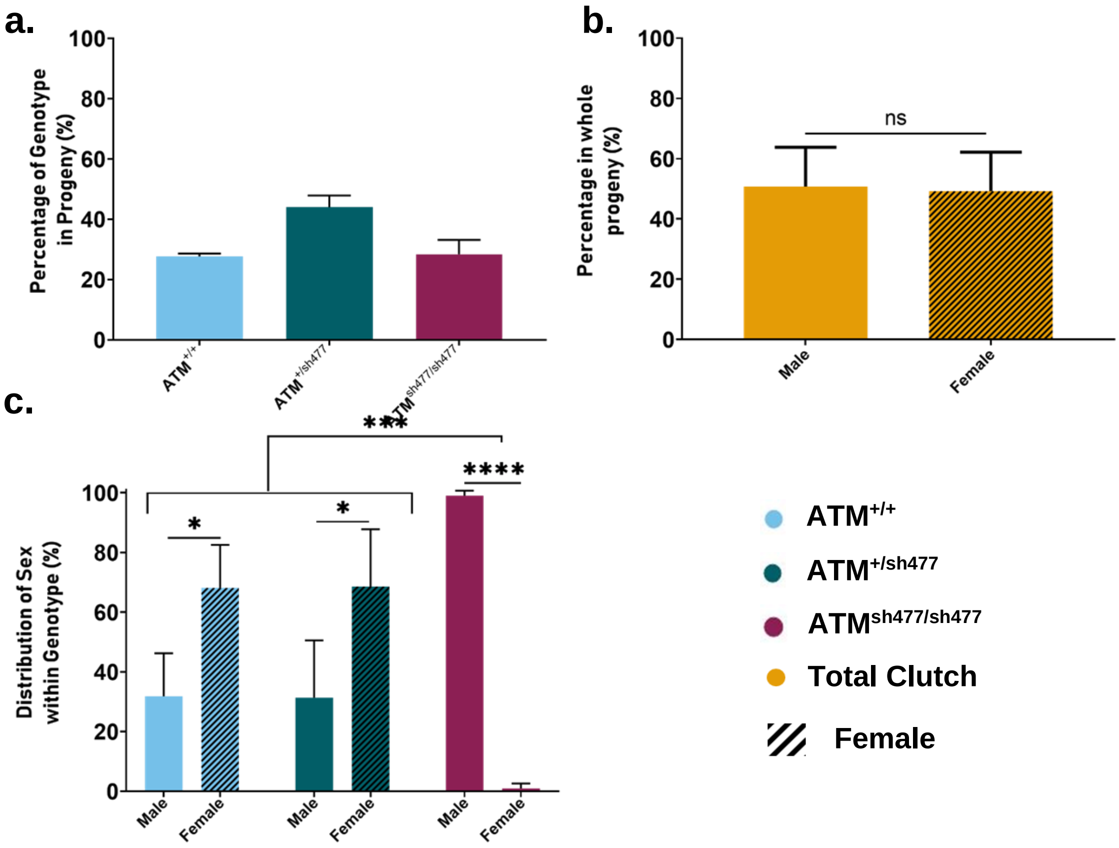

Figure 3.6 ATM$^{sh477/sh477}$ zebrafish develop as male when raised at normal densities. a. Percentage of each genotype in the progeny of 3 ATM$^{+/sh477}$ in-crosses raised at a density of 9.2 zebrafish/litre, n=315 fish. **b.** Sex distribution observed within the clutches from a. Data were analysed by unpaired t-test (p=0.8883) **c.** Sex distribution within the genotypes of the progeny from the same in-crosses. Data were analysed by a two-way ANOVA, with a *post hoc* Tukey's multiple comparisons test and Šídák's multiple comparisons test. Note: Only one ATM$^{sh477/sh477}$ female fish was observed. Error bars in all graphs represent mean +-SD. Statistical analysis can be seen in **appendix 3.4.**

3.2.3 ATM$^{sh477/sh477}$ Zebrafish Show no Increase in Radiosensitivity or Deficiency in the Somatic DNA Damage Repair Response

3.2.3.1 ATM$^{sh477/sh477}$ Zebrafish do not Exhibit any Increase in their Radiosensitivity

Radiosensitivity and deficiency in the DNA damage response is a hallmark of ATM deficient cells (Lavin and Shiloh, 1997, Kishi and Lu, 2002, Meyn, 1995). Additionally, ATM KO models in mouse and rat also exhibit radiosensitivity (Laposa et al., 2004). Furthermore, in a zebrafish ATM morpholino (MO) knockdown model, morphant embryos treated at 6 hpf with ionising radiation exhibited extreme sensitivity that presented as morphological abnormalities by 48 hpf, such as extreme curvature of the trunk and tail, developmental retardation, loss of pigment and loss of integration of the yolk sack. By 72 hpf all irradiated ATM MO-injected zebrafish had died (Imamura and Kishi, 2005). Therefore, if these morpholino effects were specific for ATM, we postulated that ATM$^{sh477/sh477}$ zebrafish should exhibit similar sensitivity to irradiation.

We have demonstrated maternal inheritance of *ATM* mRNA in early zebrafish embryos **(figure 3.2 above)**. Based on this analysis, we propose that dosing of zebrafish with ionising radiation should take place after 24 hpf, to ensure the effects of IR in ATM$^{sh477/sh477}$ larvae were not masked by maternal contribution of *ATM* mRNA.

In order to determine the effects of ionising radiation, we first established a suitable dosing range that would not be too harsh, and that would allow detection of any increase in radiosensitivity in ATM$^{sh477/sh477}$ larvae. These initial experiments used wild type zebrafish. Preliminary data suggested that zebrafish were not particularly sensitive to a single dose of IR (data not shown). Therefore, a dosing protocol for multiple serial IR treatments was optimised, using morphology as a readout. Wild type zebrafish were treated daily between 1-4 dpf with either 8, 12, or 20 Gy of ionising radiation, and imaged for morphological analysis at 5 dpf **(figure 3.7)**. Wild type zebrafish treated with serial doses of 8 Gy exhibit a small degree of sensitivity whereby gross morphology was not affected, but the eyes and head were slightly smaller, as was the swim bladder. The effects of radiation can also been seen in the development of the yolk sack; where compared to untreated controls, in 8 Gy treated zebrafish it is larger, more spherical, and retains its yellowish hue, which suggests integration of the yolk sack has been delayed (Kimmel et al., 1995). In addition, on occasion a decrease in pigmentation was observed in the wild type zebrafish treated with 8 Gy. Zebrafish treated with 12 Gy also exhibited a decrease in eye and head size that appears to be worse than that seen in 8 Gy treated fish. Similarly, 12 Gy treated zebrafish show a delay in yolk sack integration and they appear more spherical i.e. less developed. The effects of irradiation can also be seen on the swim bladder, as no properly inflated swim bladder was observed. Loss of pigmentation was also more prevalent in 12 Gy treated zebrafish. The effects of 20 Gy on zebrafish were acute, with zebrafish exhibiting gross morphological abnormalities. 20 Gy treated zebrafish are much smaller and display extreme curvature, the head and eyes are noticeably smaller, and there is little to no integration of the yolk sack. Zebrafish treated with this high dose not only showed no inflation of a swim bladder, but no structure that resembles a developing swim bladder. Loss of pigmentation was also observed, along with the presence of a yellow/green hue in the epithelium of the truck and head. All zebrafish treated with the highest dose exhibited pericardial oedema and were only able to twitch upon tactile stimulus. Therefore, the effects of serial treatment from 1-4 dpf with IR appear to be dose dependent, where treatment with 8, 12 and 20 Gy leads to an adequate range of radiosensitivity from mild effects to severe, and were therefore considered a suitable dose range to determine the radiosensitivity of ATM$^{sh477/sh477}$ zebrafish.

To determine if ATM$^{sh477/sh477}$ were any more radiosensitive than their control siblings, the progeny from an ATM$^{+/sh477}$ in-cross were treated with either 8, 12 or 20 Gy daily from 1-4 dpf ,and imaged at 5 dpf **(figure 3.8 a)**. After imaging, DNA was extracted and each fish individually genotyped. ATM$^{+/+}$ zebrafish responded similarly to the optimisation experiment. The response was again dose dependent and the severity of effects of IR on eye, head, swim bladder and yolk sack size increased in line with the IR dose **(figure 3.8 a, left panel)**. ATM$^{+/sh477}$ and ATM$^{sh477/sh477}$ zebrafish were also sensitive to the effects of IR, but the ATM$^{sh477/sh477}$ appeared no more sensitive to IR than their control siblings, as the morphological defects observed were comparable across all genotypes **(figure 3.8 a, right panel)**.

We considered the possibility that 5 dpf may not have been enough time to observe any increased radiosensitivity after treatment with IR, and that allowing the zebrafish to develop to a later age past the point of independent feeding may allow a phenotype to become apparent. Thus, the effects of IR on ATM$^{sh477/sh477}$ zebrafish were assessed at 12 dpf. As zebrafish at 12 dpf are governed by ASPA 1986, alterations to the dosing protocol had to be made to lower the overall severity limit of the experiment. As the effects of IR after 5 dpf were unknown, the dose of IR was decreased. Treatment with IR at 48 hpf induced the DDR (see below **figure 3.9** (Morsli, personal commuication), and therefore zebrafish from an ATM$^{+/sh477}$ in-cross were treated once at 48 hpf with either 2 or 8 Gy, and allowed to develop to 12 dpf. At this age the zebrafish were removed from the aquarium system, imaged and genotyped (**figure 3.8 b)**. ATM$^{+/+}$ zebrafish treated with 2 or 8 Gy IR exhibited no morphological abnormalities compared to untreated controls (**figure 3.8 b left panel)**. Eye and head size were comparable and the swim bladder was normally inflated. The yolk sack had also integrated normally into the gastrointestinal tract. Likewise, ATM$^{+/sh477}$ and ATM$^{sh477/sh477}$ IR treated zebrafish exhibited no gross abnormalities at 12 dpf and were morphologically comparable to both untreated and IR treated ATM+/+ controls **(figure 3.8 b, middle and right panel).** However, despite there being no obvious difference observed, analysis of the total length of individual fish show that 8 Gy treated zebrafish were significantly smaller **(figure 3.8 c)** than untreated zebrafish. Nevertheless, this decrease in size was to the same extent in all genotypes treated with 8 Gy, and there no differences were detected between ATM$^{+/+}$ and ATM$^{sh477/sh477}$ zebrafish. Therefore, in this assay, ATM$^{sh477/sh477}$ zebrafish exhibit no detectable increase in radiosensitivity.

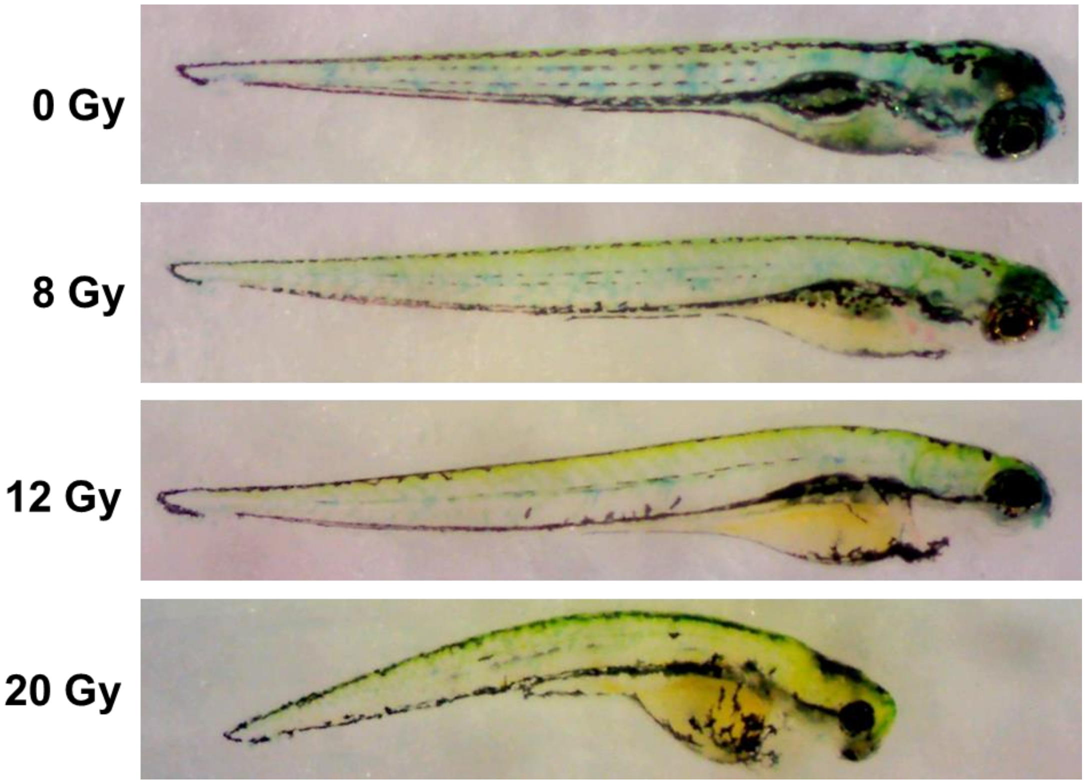

Figure 3.7 Optimisation of serial IR treatments for detection of radiosensitivity in wild type zebrafish. Zebrafish were treated daily from 1-4 dpf with the relevant dose of IR from a Caesium-137 irradiator and imaged for analysis at 5 dpf. After imaging, DNA was extracted and the zebrafish genotyped.

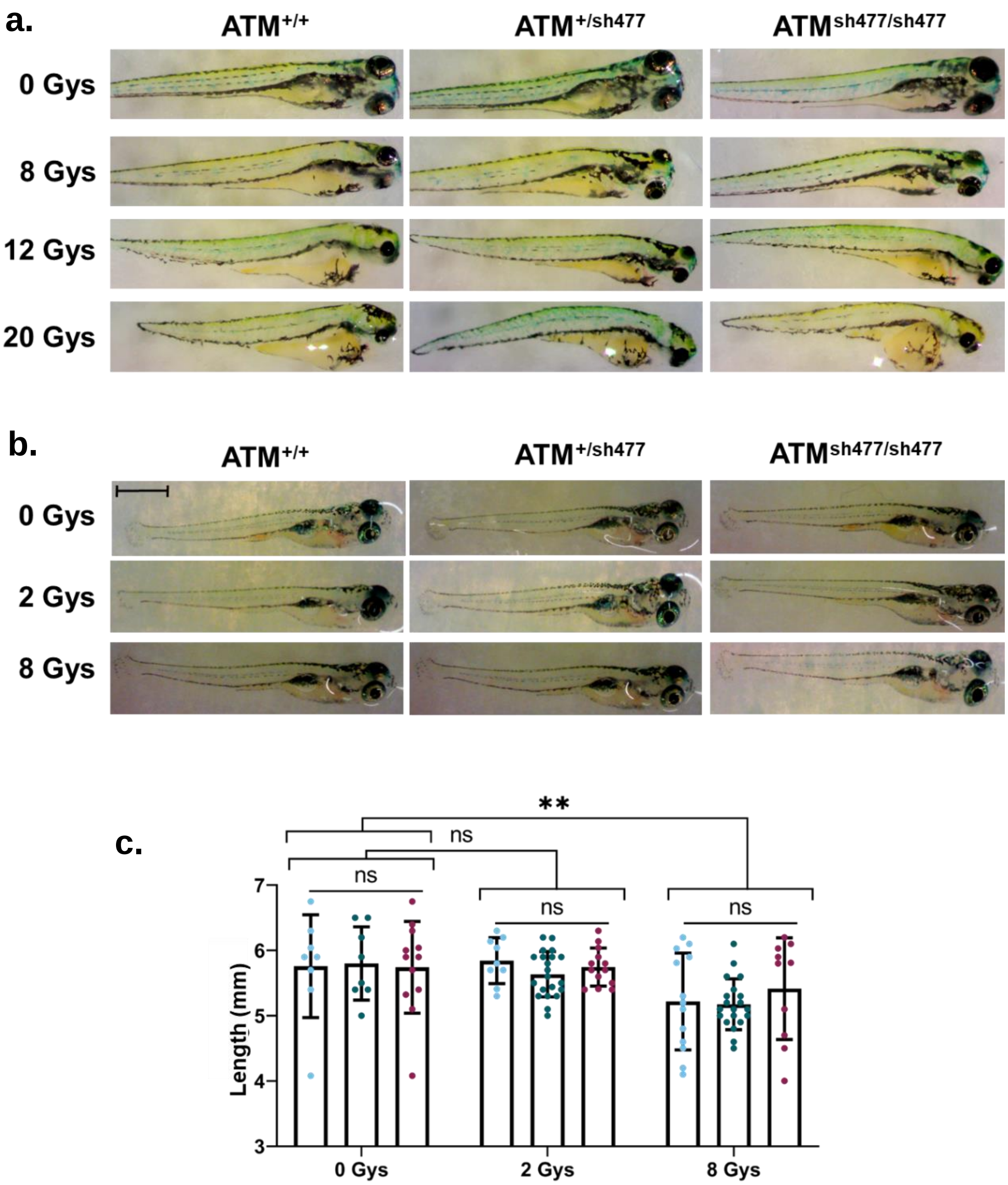
a.
ATM+/+
ATM+/sh477
ATMsh477/sh477
0 Gys
8 Gys
12 Gys
20 Gys
b.
ATM+/+
ATM+/sh477
ATMsh477/sh477
0 Gys
2 Gys
8 Gys
c.
**
ns
ns
ns
ns
Length (mm)
7
6
5
4
3
0 Gys
2 Gys
8 Gys

Figure 3.8 ATM$^{sh477/sh477}$ zebrafish morphologically exhibit no increase in their radiosensitivity compared to ATM$^{+/+}$ siblings. a. Progeny from an ATM$^{+/sh477}$ in-cross were subjected to serial doses of IR at 1-4 dpf and imaged at 5 dpf to investigate the developmental and morphological effects. n=96 fish. **b** Progeny from an ATM$^{+/sh477}$ in-cross were subjected to a single dose of IR at 48 hpf and raised to 12 dpf, when they were imaged for investigation into the developmental and morphological effects of IR. n=128. Scale bar represents 1 mm. **c**. Quantification of the length of progeny from the ATM$^{+/sh477}$ in-cross (b). Data were analysed by two-way ANOVA with a *post hoc* Tukey's multiple comparisons test. Error bars represent mean+/-SD. Statistical analysis can be seen in **appendix 3.5.**

3.2.3.2 Somatic DDR in ATM$^{sh477/sh477}$ Zebrafish.

As ATM$^{sh477/sh477}$ zebrafish did not appear to be any more radiosensitive then their ATM$^{+/+}$ siblings, we next investigated DDR directly at the molecular level. H_2AX is a member of the H2A family of histones around which DNA is wrapped, and is the most common marker used for detection of DNA damage in situ (Kopp et al., 2019). H_2AX is phosphorylated (γH_2AX) in response to DNA damage and acts as a stable platform on which repair proteins accumulate (Yan et al., 2011, Podhorecka et al., 2010). In response to ds DNA damage, H2AX is mainly activated through ATM kinase signalling, and upon activation, γH_2AX immunostaining reveals discrete nuclear puncta (Kobayashi et al., 2009, Burma et al., 2001, Yin et al., 2012, Takahashi et al., 2010, Tanaka et al., 2006b). To determine whether there was a defect at the molecular level in ATM signalling and activation of the DDR, we measured H_2AX phosphorylation in zebrafish larvae after induction of DNA damage.

Larvae from an ATM$^{+/sh477}$ in-cross were treated with 0, 8 or 12 Gy IR at 48 hpf. Larvae were fixed 1 hr post irradiation and immunostained for activated γH_2AX. The tails of individual larvae were genotyped, while the heads were mounted and imaged by confocal microscopy **(figure 3.9 a)**. To determine activation, γH_2AX foci were quantified using a custom script **(see section 2.5.2.4)** and expressed as relative area of γH_2AX foci/cell **(figure 3.9 b)**. As expected, larvae treated with IR show a significant dose dependant increase in γH_2AX foci (0 Gy v 8Gy v 12 Gy <0.0001) **(appendix 3.6) (figure 3.9 b)**. There was no difference in basal γH_2AX activation (0 Gy) between ATM$^{+/+}$ and mutant larvae (p=0.2095). When the larvae were treated with 8 Gy IR, there was a significant difference in H_2AX activation (p=0.0093), with ATM$^{sh477/sh477}$ zebrafish showing increased expression. However, when treated a higher dose of 12 Gy, no significant differences were observed between the two genotypes (p=0.0804).

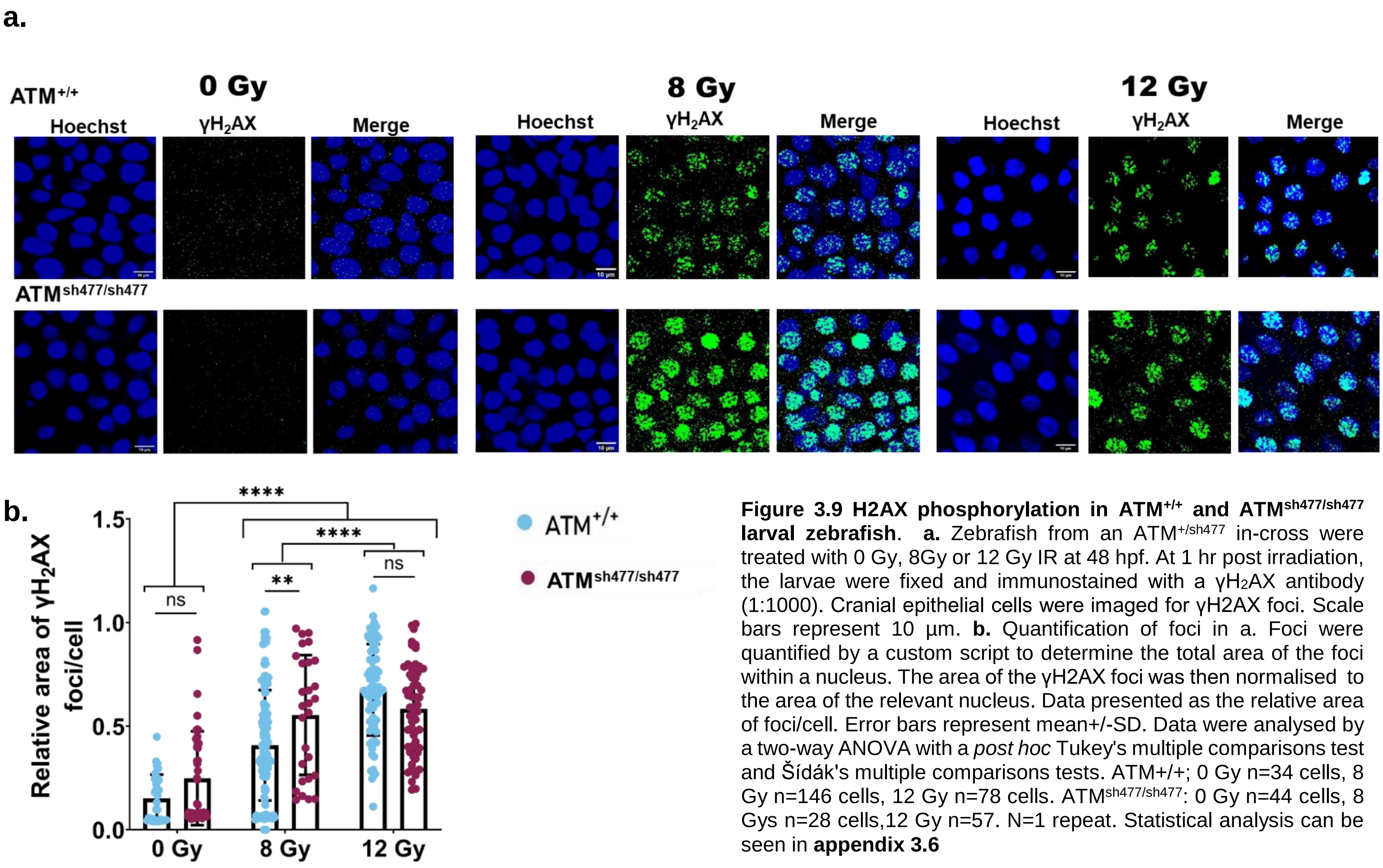
a.
ATM+/+
0 Gy
8 Gy
12 Gy
Hoechst
γH2AX
Merge
ATMsh477/sh477
b.
Relative area of γH2AX foci/cell
1.5
1.0
0.5
0.0
0 Gy
8 Gy
12 Gy
****
****
**
ns
ns
ATM+/+
ATMsh477/sh477

Figure 3.9 H2AX phosphorylation in ATM$^{+/+}$ and ATM$^{sh477/sh477}$ larval zebrafish. **a.** Zebrafish from an ATM$^{+/sh477}$ in-cross were treated with 0 Gy, 8Gy or 12 Gy IR at 48 hpf. At 1 hr post irradiation, the larvae were fixed and immunostained with a γH_2AX antibody (1:1000). Cranial epithelial cells were imaged for γH2AX foci. Scale bars represent 10 µm. **b.** Quantification of foci in a. Foci were quantified by a custom script to determine the total area of the foci within a nucleus. The area of the γH2AX foci was then normalised to the area of the relevant nucleus. Data presented as the relative area of foci/cell. Error bars represent mean+/-SD. Data were analysed by a two-way ANOVA with a *post hoc* Tukey's multiple comparisons test and Šídák's multiple comparisons tests. ATM+/+; 0 Gy n=34 cells, 8 Gy n=146 cells, 12 Gy n=78 cells. ATM$^{sh477/sh477}$: 0 Gy n=44 cells, 8 Gys n=28 cells,12 Gy n=57. N=1 repeat. Statistical analysis can be seen in **appendix 3.6**

As outlined in detail in **chapter 1, section 1.2.4.1**, AT patients suffer severe immunodeficiency as a result of the inability of an ATM deficient system to repair endogenous DNA breaks due to V(D)J and CSR events during antibody production. For this reason, AT patients have lower overall circulating levels of antibodies. Despite having the CSR initiator activation-induced cytidine deaminase (AID) that has the ability to regulate CSR, zebrafish heavy chain loci do not undergo CSR (Wakae et al., 2006). However, they do undergo V(D)J recombination (Weinstein et al., 2009, Jiang et al., 2011, Danilova and Steiner, 2002, Zimmerman et al., 2011), a process that in humans has been shown to utilise ATM (Perkins et al., 2002, Dujka et al., 2010, Bredemeyer et al., 2006b). Therefore, we hypothesised that ATM$^{sh477/sh477}$ may also have lower levels of immunoglobulins due to the inability to repair these dsDNA breaks.

Zebrafish possess three antibody classes; IgM and IgD which are homologous to IgM and IgD in mice and humans, and a third isotype that has so far only been detected in bony fish, IgZ/T (IgZ) (Zimmerman et al., 2011, Danilova et al., 2000, Danilova et al., 2005, Hansen et al., 2005, Gambón-Deza et al., 2010, Ryo et al., 2010). In order to determine whetherATM$^{sh477/sh477}$ could have lower levels of immunoglobulins, RNA was extracted from whole ATM$^{+/+}$ and ATM$^{sh477/sh477}$ zebrafish siblings at 3 months old, and the level of each immunoglobulin heavy chain mRNA was determined by RT-qPCR **(figure 3.10).** There were no significant differences observed in the expression of any immunoglobulin heavy chains between ATM$^{+/+}$ and ATM$^{sh477/sh477}$.

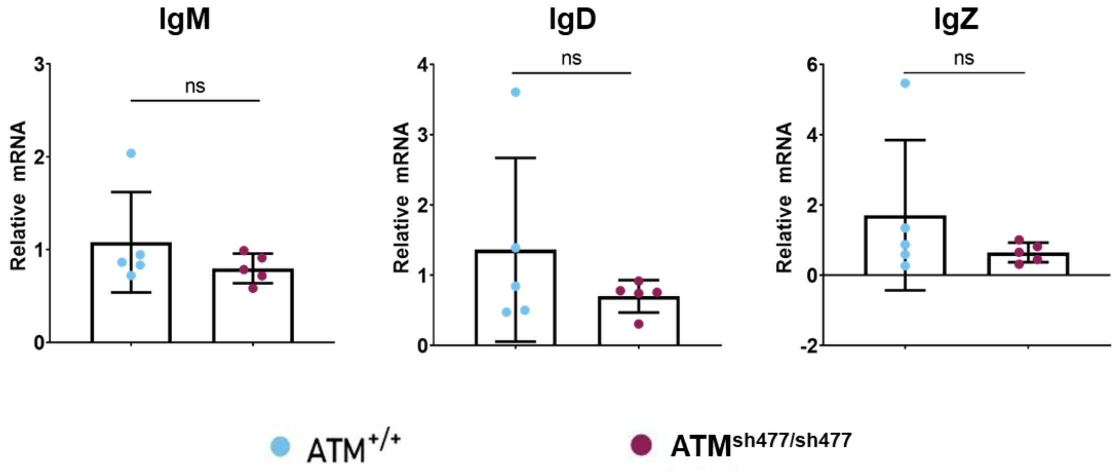

Figure 3.10 ATM$^{sh477/sh477}$ show no inability to produce immunoglobulins. RNA was extracted from 5 ATM$^{+/+}$ and 5 ATM$^{sh477/sh477}$ zebrafish at 3 months old, and relative levels of immunoglobulin heavy chains were assessed by RT-qPCR. Data were analysed by Mann Whitney test. Error bars represent mean +/- SD. Data were analysed by a Mann Whitney test and statistical analysis can be seen in **appendix 3.7.**

3.2.3.3 ATM$^{sh477/sh477}$ Zebrafish do not Exhibit an Increase in Senescence

Cellular senescence is characterised by a prolonged and irreversible cessation of the cell cycle, activation of tumour suppressor genes, alterations to cellular metabolism, and changes in cellular secretions (senescence-associated secretory phenotype (SASP)) (Hayflick and Moorhead, 1961, Gorgoulis et al., 2019). It functions in many healthy biological processes, such as pregnancy (Rajagopalan and Long, 2012), embryogenesis (Muñoz-Espín et al., 2013, Storer et al., 2013, Biran and Krizhanovsky, 2015), and tissue repair (Jun and Lau, 2010, Nishizawa et al., 2016). However, it is mainly associated with aging (van Deursen, 2014) and is protective against the oncogenic transformation of cells (Campisi, 2013, Loaiza and Demaria, 2016). Senescence that is not associated with a developmental process is largely induced by cellular stressors such as DNA damage, elevated ROS, aberrant oncogenic expression, hypoxia, mitochondrial dysfunction, telomere shortening, and impairment of autophagy, all of which also activate ATM (Wei and Ji, 2018, Gorgoulis et al., 2019) **(see chapter 1, sections 1.2.2, 1.2.3 and 1.2.4)**. ATM has been shown to play a number of roles in senescence, however, whether it positively or negatively regulates it is still not clear, and it is likely to be cell type and context dependent (Yosef et al., 2017, Zhao et al., 2020a, Aird and Zhang, 2015, Strzyz, 2017, Sunderland et al., 2020, Qian et al., 2018, Efeyan et al., 2009, Qian et al., 2017, Li et al., 2020). Nevertheless, loss of ATM in humans is associated with accelerated ageing of AT patients, and increased cellular senescence acquired from endogenous DNA damage **(see chapter 1, section 1.2.4.7).** Therefore, we postulated that ATM$^{sh477/sh477}$ zebrafish could exhibit an endogenous DNA damage senescence associated phenotype.

Six genes that are considered markers of senescence were chosen for mRNA expression analysis. These were markers of cell cycle arrest, *CCNG1* (Cyclin-g1), *p53, p21* and *p16,* and the proinflammatory markers *IL-1β* and *IL-6* (Gorgoulis et al., 2019). RNA was extracted from 5 adult ATM$^{+/+}$ and 5 ATM$^{sh477/sh477}$ zebrafish (3 months) for RT-qPCR analysis. No significant differences were observed in any senescence marker genes between ATM$^{+/+}$ and ATM$^{sh477/sh477}$ zebrafish **(figure 3.11).**

It was considered that zebrafish in an aquarium environment would not experience enough endogenous DNA damage by 3 months of age to cause a difference in senescence. Therefore, we sought to induce DNA damage with the hypothesis that after a large DNA damage insult an ATM deficient system would struggle to repair it as effectively, leading to an increase in senescent cells. Previous unpublished research (Morsli, personal communication) showed that after induction of DNA damage by ionising radiation at 48 hpf, senescence markers persisted to 12 dpf. Therefore, progeny from an ATM$^{+/sh477}$ in-cross were treated with either 2 or 8 Gy at 48 hpf and allowed to develop to 12 dpf. At 12 dpf, zebrafish were tail clipped, bodies flash frozen and tails genotyped. Once genotyped, 4 ATM$^{+/+}$ and 4 ATM$^{sh477/sh477}$ zebrafish were pooled for RNA extraction and subsequent RT-qPCR **(figure 3.12)**. Time constraints due to Covid-19 only allowed two repeats to be carried out; as such, no statistical analysis could be performed. However, based on the data collected there does appear to be an irradiation dose dependent increase in the expression of cell cycle arrest genes (*CCNG1, p21*, *p16 and p53)* and pro inflammatory genes (*IL-1β and IL-6)* in ATM$^{sh477/sh477}$ zebrafish compared to the ATM$^{+/+}$ siblings. This tentatively suggests that ATM$^{sh477/sh477}$ fish may show increased cellular senescence after DNA damage induction.

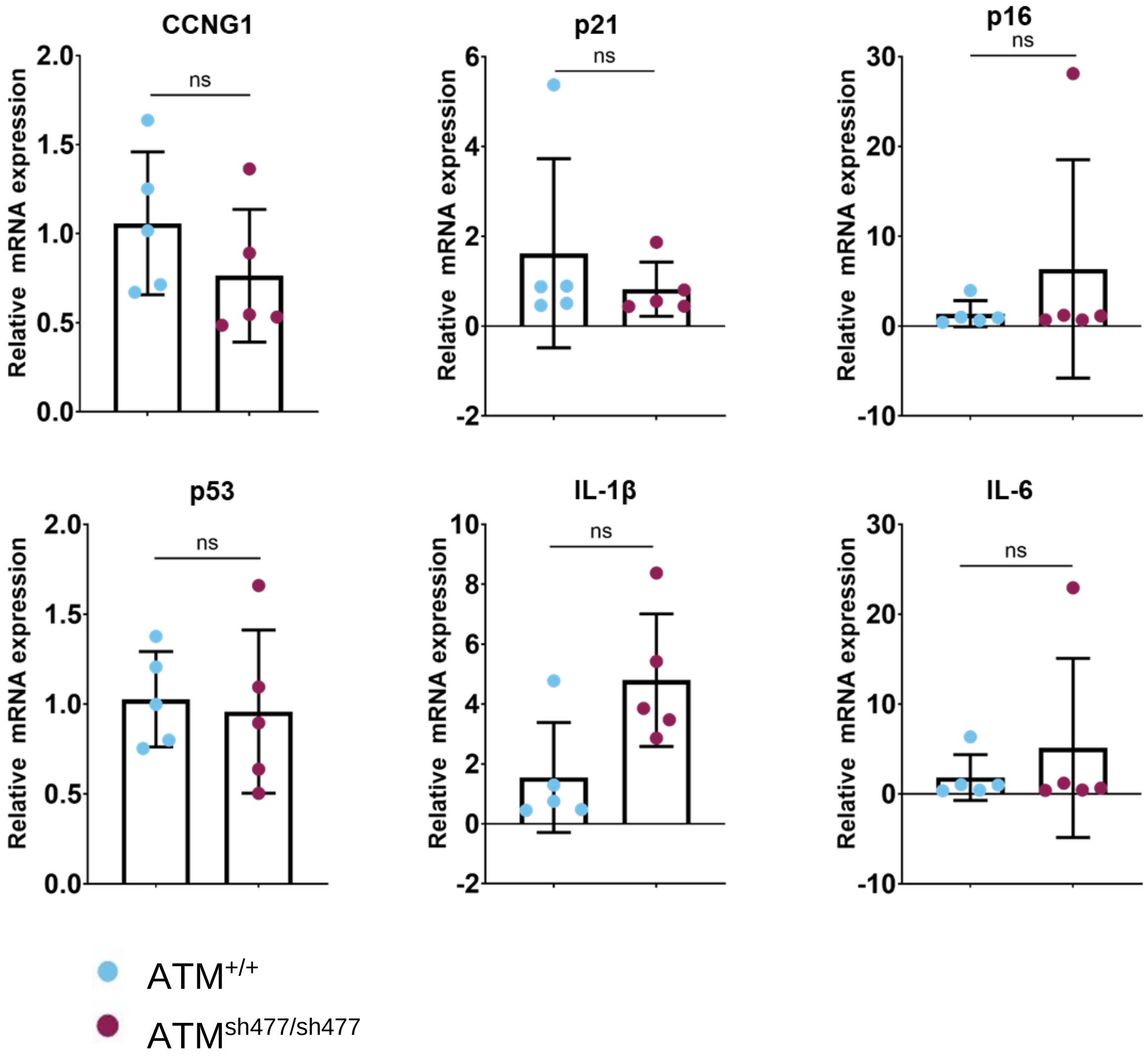

Figure 3.11 mRNA expression of senescence markers in adult zebrafish. RNA was extracted from 5 ATM$^{+/+}$ and 5 ATM$^{sh477/sh477}$ adult zebrafish (3 months) and expression of senescence markers mRNA analysed by RT-qPCR. Data were normalised to expression of β-actin as a control. Error bars represent mean+/- SD. Statistical analysis can be seen in **appendix 3.8.**

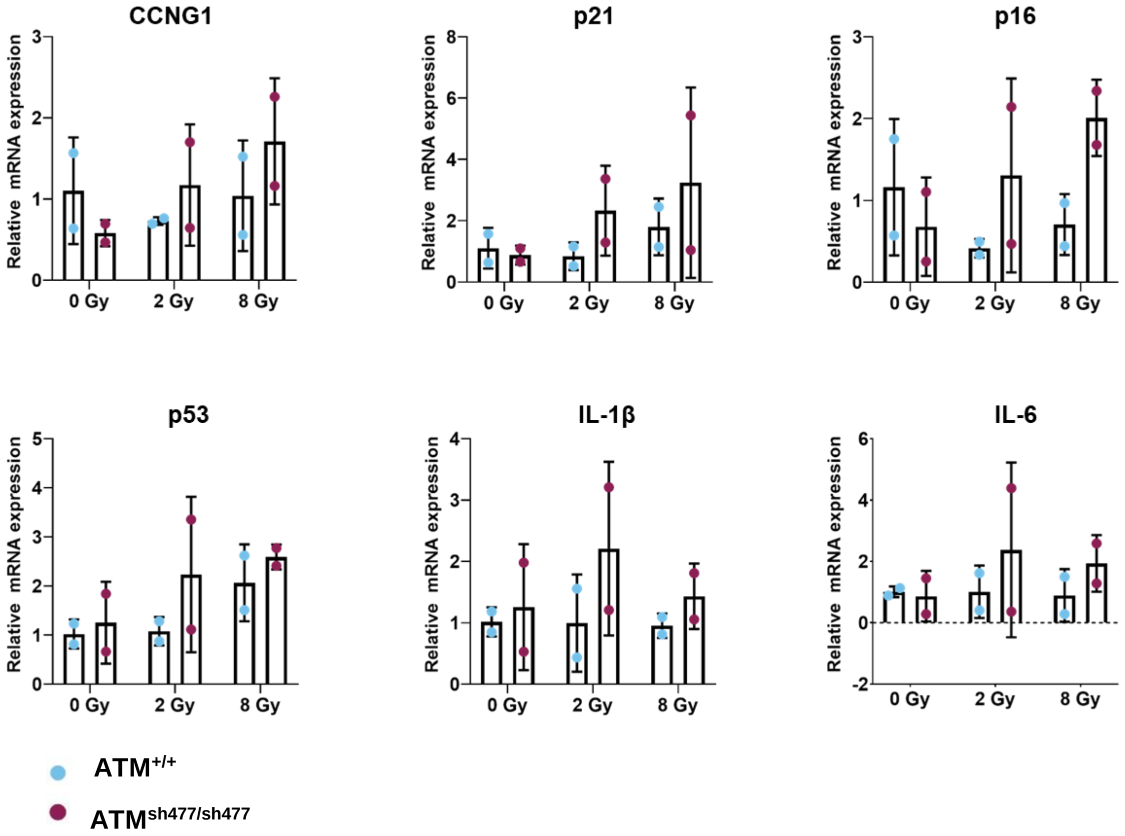

Figure 3.12 mRNA expression of senescence markers in 12 dpf zebrafish after induction of DNA damage. Zebrafish were treated with either 0, 2, or 8 Gy of IR at 48 hpf. At 12 dpf 4 fish of each genotype were pooled and RNA extracted for analysis by RT-qPCR. Data were normalised to expression of β-actin as a control. Error bars represent mean+/- SD. N= 2

3.2.4 Investigations into the Possibility of Genetic Compensation by ATR

The evidence above, that ATM$^{sh477/sh477}$ zebrafish do not exhibit any increase in radiosensitivity or in deficiency in activating the DDR, is surprising. Recently there has been much debate over the reliability of morpholino (MO) knockdown (KD) (morphants) compared with stable KO. In the former, phenotypic observations have *post hoc* been attributed to off target effects of the MO, and in the latter, the lack of an observable phenotype has often been attributed to genetic compensation (GC) by upregulated expression of homologues or genes from the same family as the mutated gene (Peng, 2019, El-Brolosy et al., 2019). Therefore, we considered that the lack of an expected phenotype in ATM$^{sh477/sh477}$ zebrafish might also be attributed to GC. Recent studies have reported that for GC to occur requires the NMD of a mutant mRNA transcript carrying a premature stop codon, and that GC is dependent on the mutant transcript and not the lack of a functional protein (El-Brolosy et al., 2019, Ma et al., 2019). While the ATM$^{sh477/sh477}$ mutant transcript does contain a premature stop codon, it appears that it does not undergo NMD, as no difference in the expression of *ATM* mRNA is observed between ATM$^{+/+}$ and ATM$^{sh477/sh477}$ zebrafish **(figure 3.2).** However, given that there is evidence to suggest that GC may be differentially regulated in a number of contexts (Ma et al., 2019), and that our understanding of how GC occurs is still potentially incomplete, it was decided GC had to be considered in this context.

Upregulation of genes in GC appears to be linked to sequence similarly between the target gene and genes upregulated in its place (Ma et al., 2019). If GC were to occur in the context of the ATM$^{sh477/sh477}$ mutation, then perhaps genes containing a similar sequence to ATM would be upregulated. However, a BLASTN search with the wild type *ATM* cDNA sequence yielded no results of a zebrafish gene with a similar sequence (data not shown). As outlined in detail in **chapter 1, section 1.2.1**, ATM belongs to the large PIKK family of proteins, and it was thought members of this family could be a possible target for upregulation. However, pairwise alignments of ATM with these 5 genes showed no areas of high sequence homology (data not shown). Nevertheless, one family member, ATR, canonically functions in the DDR in response to ssDNA breaks but has also been shown to function in response to dsDNA breaks (Igoucheva et al., 2006, Duursma et al., 2013, Cimprich, 2007, Gong et al., 2017). Therefore we performed some preliminary investigations into whether ATR could be responsible for GC in ATM$^{sh477/sh477}$ zebrafish and could explain their robustness to DNA damage.

In common with ATM, ATR is phosphorylated upon activation. However, we lacked a zebrafish specific phospho-antibody that would enable us to detect any increased activation of ATR in ATM$^{sh477/sh477}$ zebrafish, along with a zebrafish specific antibody that would allow us to detect overall endogenous protein expression. Therefore, we chose to determine if gene expression was upregulated in ATM$^{sh477/sh477}$ zebrafish by RT-qPCR.

Initially we investigated basal levels in adult fish, assuming that if GC were to occur, the endogenous DNA damage over time could be enough to induce an increase in expression. RNA was extracted from adult (3 months) zebrafish and analysed by RT-qPCR **(figure 3.13)**. Again we found no evidence that mutant *ATM* undergoes NMD, as comparable levels are expressed in both ATM$^{+/+}$ and ATM$^{sh477/sh477}$ zebrafish. There was also no significant difference in the expression of ATR between genotypes.

It was questioned whether massive DNA damage would need to be induced in order to see an increase in expression, and that perhaps prolonged DNA damage could induce an upregulation in expression. Therefore, progeny from an ATM$^{+/sh477}$ in-cross were subjected to serial treatments of IR from 1-4 dpf, and RNA extracted for analysis at 5dpf **(figure 3.14)**. No significant difference was observed in expression of ATM or ATR between genotypes either with or without IR. Interestingly, treatment with IR did not significantly increase expression of either gene at this time point. These results suggest that ATR expression is not upregulated in ATM$^{sh477/sh477}$ zebrafish.

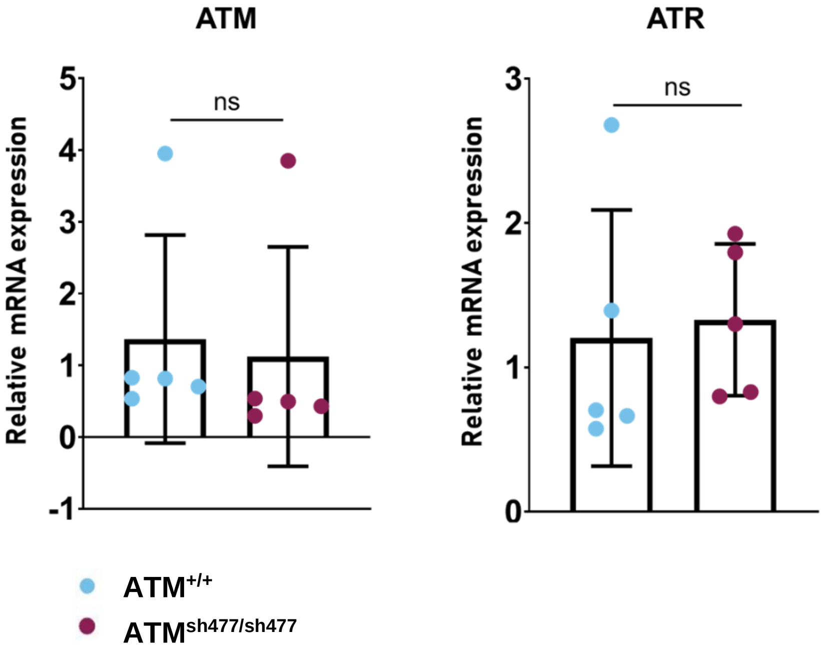

Figure 3.13 Expression of ATR mRNA is not upregulated in ATM$^{sh477/sh477}$ zebrafish. RNA from 5 ATM$^{+/+}$ and 5 ATM$^{sh477/sh477}$ sexed matched siblings was extracted and expression of *ATM* and *ATR* mRNA was analysed by RT-qPCR. Error bars represent mean+/- SD. Statistical analysis can be found in **appendix 3.9**.

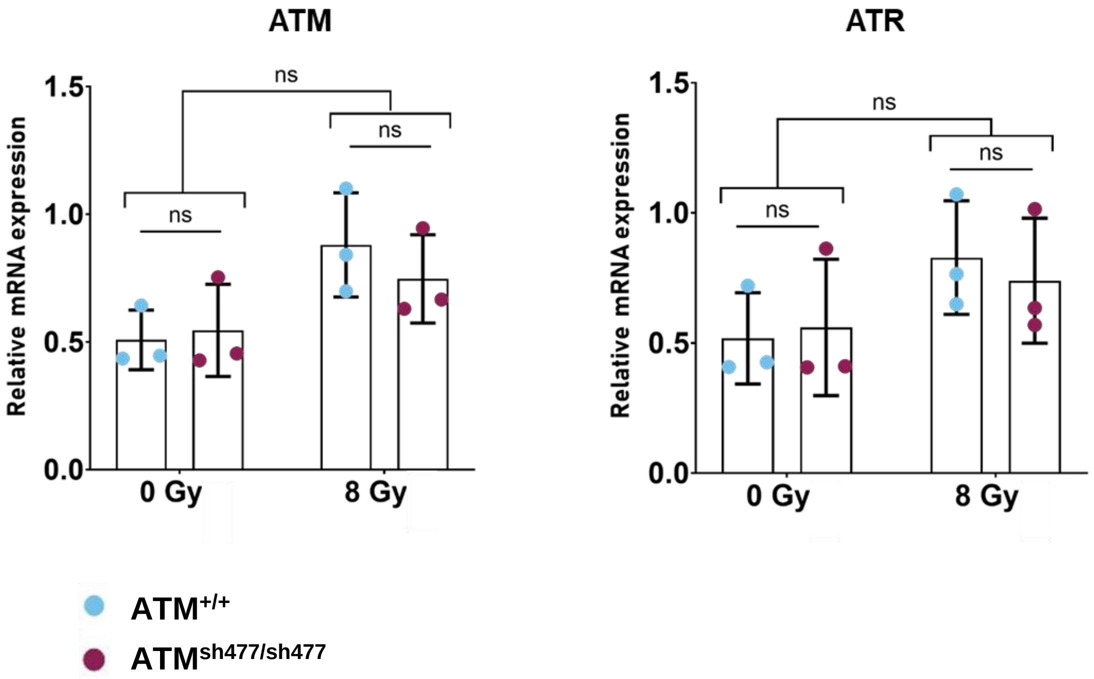

Figure 3.14 Expression of ATR mRNA is not upregulated in ATM$^{sh477/sh477}$ zebrafish after induction of DNA damage. Progeny from an ATM$^{+/sh477}$ in-cross was serially treated from 1-4 dpf with 8 Gy IR, and RNA extracted at 5 dpf for RT-qPCR analysis. Data were analysed by a two-way ANOVA with a *post hoc* Šídák's multiple comparisons test. Error bars represent mean +- SD. Statistical analysis can be seen in **appendix 3.10.**

3.3 Discussion

3.3.1 ATM$^{sh477/sh477}$ Zebrafish have Phenotypes that are Consistent with Knockout of ATM Signalling

Classical AT patients generally have null mutations, leading to complete ablation of expression of the ATM protein (Gilad et al., 1996). Other cases of classical AT may have very low ATM protein expression, however, in these cases it is evident that the ATM DNA damage response signalling pathway is defective (Stankovic et al., 1998, Micol et al., 2011a, Concannon and Gatti, 1997, Li and Swift, 2000, Fievet et al., 2019). Therefore, to ensure the ATM$^{sh477/sh477}$ zebrafish model is a KO model, and is molecularly an accurate recapitulation of the AT disease, expression of ATM in these zebrafish was characterised.

The ATM^{sh477} allele was found to consist of a 6 bp deletion in exon 6, leading to a frameshift mutation, resulting in a downstream premature stop codon **(figure 3.1)**. This type of truncating mutation is frequently found in AT patients (Mitui et al., 2005, Concannon and Gatti, 1997, Li and Swift, 2000, Gilad et al., 1996, Micol et al., 2011b, Stray-Pedersen et al., 2004, Sandoval et al., 1999, Stankovic et al., 1998). This mutation was predicted to cause ablation of ATM signalling in one of two ways; either the mutant mRNA would undergo NMD (Hug et al., 2016), or a truncated protein would be produced. This truncated protein would be expected to be non-functional, as it would lack the essential kinase domain, as well as most protein-protein binding sites **(chapter 1, section 1.2)**.

3.3.1.1 Nonsense Mediated Decay of the ATM^{sh477} Transcript

Our data indicate that the *ATM^{sh477}* mRNA transcript does not undergo NMD **(figure 3.2)**. SMG1, another member of the PIKK family, plays a fundamental a role in NMD (Causier et al., 2017). Given that PIKK family members have significant cross over in functionality **(see section 3.3.2.2 below)**, that the key role of ATM seems to be as a master regulator of cellular homeostasis **(chapter 1, section 1.2.2 and 1.2.3)**, and that ATM and SMG1 share substrate specificity (Brumbaugh et al., 2004), it is conceivable that ATM itself may play a role in NMD, particularly as there appears to be redundancy in the NMD pathway in zebrafish after loss of SMG1 (Lloyd and Davies, 2013, Wittkopp et al., 2009). Furthermore, after DNA damage, ATM has been shown to activate UPF1, an initiator of the NMD pathway (Causier et al., 2017).

Therefore, loss of signalling of ATM may cause perturbations in the NMD pathway, and as a result, the ATM mutant transcript itself may not be degraded. However, given that NMD not only functions in clearance of mutants transcripts, but also functions in homeostatic gene expression (Nickless et al., 2017), and the NMD pathway is essential for zebrafish embryonic development and survival (Wittkopp et al., 2009), it is unlikely that this pathway is drastically perturbed in ATM$^{sh477/sh477}$ zebrafish, as they do not have a corresponding phenotype.

For NMD decay to work effectively, normal stop codons and deleterious premature stop codons need to be distinguishable. Canonically, mRNA transcripts that contain a premature stop codon upstream of an exon-exon junction are marked by an exon junction protein complex (EJC), and are readily degraded. In this mechanism, transcripts with a premature stop codon 50-55 bp upstream of the exon-exon junction are most efficiently degraded (Nagy and Maquat, 1998, Thermann et al., 1998, Zhang et al., 1998, Hug et al., 2016, Le Hir et al., 2001, Nicholson et al., 2010, Lindeboom et al., 2016). Although in the *ATM^{sh477}* transcript, the predicted premature stop codon occurs upstream of an exon-exon junction, it occurs 75 bp upstream and therefore may not be as readily degraded.

Interestingly, NMD has been found to be less efficient, and significantly decreased if there isa large distance between the premature stop codon and the normal translation termination site (Lindeboom et al., 2016). ATM is an exceptionally large protein, and the *ATM* zebrafish mRNA transcript consists of 62 exons and is ~ 9.2 Kb in length (Ensembl-November 2020). The *ATM^{sh477}* transcript has ~8.4 Kb between the predicted premature stop codon and the normal translation termination site. Additionally, certain RNA-binding protein motifs in the mRNA found +/- 100 nucleotides either side of the premature stop codon have been shown to alter the efficiency of NMD (Lindeboom et al., 2016, Ray et al., 2013). The ATM transcript has one of these RNA binding motifs directly after the predicted premature stop codon **(appendix 3.11)**, and this may also alter the NMD of the mutant transcript.

3.3.1.2 Detection of the ATM Protein in Zebrafish by Western Blot

Detection of the protein was attempted by western blot with antibodies raised to the amino acids 1-120 of zebrafish ATM, upstream of the CRISPR induced mutation **(figure 3.3)**. It was predicted that the full-length protein would be detected in ATM$^{+/+}$

and not in ATM$^{sh477/sh477}$ zebrafish. Furthermore, it was plausible that by raising the antibodies to this antigen, any truncated protein might also be detected. Endogenous full-length ATM was not detected in ATM$^{+/+}$ zebrafish **(figure 3.4 and 3.5 c)**. Nevertheless, the zATM1 antibody is capable of detecting the recombinant peptide that it was raised to **(figure 3.5 a)**.

Both antibodies raised against zebrafish ATM have significant cross reactivity with other components of zebrafish lysates, as can be seen from multiple bands on the blots. There is some evidence of the occurrence of alternative transcripts of ATM (Menotta et al., 2012, Pozzi et al., 2020, Rogatcheva et al., 2007, Menotta et al., 2017, Kralovicova et al., 2016), however, if and when these are produced is controversial. Nonetheless, if present, reactivity of the antibodies with these smaller transcripts may account for the banding patterns observed. However, the possibility of an alternative functional transcript that does not contain the mutant exon 6 is unlikely. First, exon 6 is not a cassette exon; therefore skipping of only this exon would still introduce a frameshift mutation and a subsequent premature stop codon. Second, it is also unlikely that an alternative but functional transcript of the ATM protein is expressed in ATM mutants, as ATM$^{sh477/sh477}$ zebrafish exhibit a phenotype that is consistent with ablation of ATM signalling **(see section 3.3.2 above and chapter 4)**. It is much more likely that the antibodies are reacting to other similar protein sequences within the lysates. However, before production of the antibodies to the 120 amino acid immunogen, a protein blast search indicated a small probability of there being similar amino acid sequences in the zebrafish proteome.

In AT patients carrying truncating mutations throughout the length of the ATM gene, the mutant mRNA transcript does not undergo NMD as patients have normal *ATM* mRNA expression levels. However, the majority of truncating mutations show no expression of ATM at the protein level (Becker-Catania et al., 2000). This indicates that the mutant protein rather than the mutant mRNA is unstable, and is quickly degraded. Mounting evidence suggests that there is compensation for loss of the ATM at the protein level, but this compensation is not able to take place in the presence of a full-length ATM protein that is non-functional, to the detriment of the organism **(see section 3.3.2.2)**. Consequently, although the *ATM^{sh477}* transcript carrying a truncating mutation may not undergo NMD, the ATM signalling pathway is expected to be perturbed in these fish, as the mutant protein is either likely degraded, or remains but is truncated, and is therefore non-functional. Two bands, approximately the same size that the truncated protein was predicted to be, were strongly detected in ATM$^{sh477/sh477}$ lysates **(figure 3.5 b)**. However, these bands were also observed in ATM$^{+/+}$ lysates, albeit at very low levels. Therefore, while the bands observed in ATM$^{sh477/sh477}$ lysates may be truncated ATM, it would be improbable that an ATM transcript would also be detected in ATM$^{+/+}$ without the corresponding mutation. Moreover, due to a testicular pathology **(see chapter 4)**, the ATM$^{sh477/sh477}$ mutants are likely to have a different tissue contribution to the whole fish lysates that were used. Therefore, we cannot rule out that the bands in question are not a tissue specific contribution from ATM$^{sh477/sh477}$ zebrafish. Future experiments carried out to detect ATM via western blot from ATM$^{sh477/sh477}$ zebrafish should aim to use protein extracts from discrete tissues, such as muscle, brain, or eye, to ensure the results are due to expression levels in the relevant genotypes, and not contributions of specific tissues.

3.3.1.3 ATM$^{sh477/sh477}$ Zebrafish are All Males, Consistent with Loss of the HR Pathway in Zebrafish

ATM$^{sh477/sh477}$ zebrafish develop as male **(figure 3.6)**. This phenotype is consistent with loss of the DDR pathway in zebrafish, as many zebrafish models that are KOs for HR repair proteins also exhibit this female to male sex reversal (Botthof et al., 2017, Ramanagoudr-Bhojappa et al., 2018, Rodriguez-Mari et al., 2010, Rodríguez-Marí et al., 2011, Shive et al., 2010, Cayuela et al., 2019). Zebrafish sex determination is multifactorial and tends to stem from polygenic and environmental factors, although, the exact mechanisms are still relatively poorly understood (Liew and Orbán, 2014). Zebrafish initially develop as hermaphrodites, but with an immature juvenile ovary. In ~50% of zebrafish the ovary continues to develop through oogenesis, whereas in the other ~50% the ovary degenerates and they develop male gonads (Liew and Orbán, 2014, Uchida et al., 2002, Maack and Segner, 2003, Wang et al., 2007). In DDR deficient zebrafish mutants, the female to male sex reversal is attributed to increased p53 mediated apoptosis in germ cells in the juvenile ovary. Subsequently, this increase in apoptosis compromises the developing ovary, leading to masculinisation of the gonads (Rodriguez-Mari et al., 2010).

The relation of ATM to meiotic recombination and germ cell apoptosis will be discussed in more detail in **chapter 4**. It should be noted that loss of primordial germ cells has also been associated with female to male sex reversal in zebrafish

(Siegfried and Nüsslein-Volhard, 2008, Tzung et al., 2015), and this will also be discussed further in the context of results presented in **chapter 4**. While we could not show through ablation of ATM expression, or expression of a truncated protein that the ATM$^{sh477/sh477}$ zebrafish are KO for ATM, given that they display the same female to male sex reversal observed in other zebrafish DDR mutants, it strongly indicates that at least in the gonads this model has lost ATM signalling, and as such is an ATM KO model.

The data in **figure 3.6** shows that while there is a very clear female to male sex reversal in ATM$^{sh477/sh477}$ zebrafish, the remaining ATM$^{+/+}$ and ATM$^{+/sh477}$ zebrafish are strongly skewed towards female. The consequences of this were that very few age and sexed matched ATM$^{+/+}$ siblings were available for experimentation, particularly in adult behavioural analysis **(see chapter 5, section 5.2.3)**, resulting in a decrease in the numbers of fish assayed. The cause of this skew is not understood but it may be due to random chance, some unknown environmental factor or it may be due to compensation within to cutch to offset ATM$^{sh477/sh477}$ female to male sex reversal. However, there is no experimental evidence to support this and further investigation would be required.

3.3.2 Radiosensitivity and the DDR in ATM$^{sh477/sh477}$ Zebrafish

3.3.2.1 Measuring the DDR in ATM Mutant Zebrafish

In the experiments presented in this chapter, ATM$^{sh477/sh477}$ zebrafish are no more radiosensitive than wild type larvae. This was unexpected, as most other models of AT and AT patients do exhibit an increase. NHEJ appears to be the favoured mechanism of DNA repair in zebrafish (Liu et al., 2012a, Vierstraete et al., 2017); therefore, as ATM is predominantly thought to function in HR, there may be very little difference in the repair of genotoxic insults between mutant wild type zebrafish. This is supported by evidence that in the morphological studies detailed above **(figure 3.8)**, ATM$^{sh477/sh477}$ mutants appeared to have the same developmental and gross anatomical response to treatment with IR as ATM$^{+/+}$ zebrafish.

In order to understand further the capacity for ATM deficient zebrafish to repair DNA damage, we looked at their ability to activate an ATM downstream target and molecular biomarker of DNA damage, γH_2AX **(figure 3.9)**. Interestingly, ATM mutant larvae exhibited no deficiency in their ability to activate H_2AX. In **figure 3.9 c**, ATM$^{sh477/sh477}$ zebrafish larvae treated with 8 Gy IR show significantly more activated H_2AX than ATM$^{+/+}$ zebrafish treated with the same dose. However, it is not clear if the mutant cells were more efficient at activating H_2AX, resulting in an increased in foci, or if they were less efficient at repairing the DNA breaks, leading to a decrease in foci in ATM$^{+/+}$ where the damage had already been repaired. Nonetheless, this difference in γH_2AX foci is lost when the larvae are treated with a higher dose of 12 Gy IR. These differences may reflect variance in the response to higher doses of IR (Vierstraete et al., 2017), however, they likely also reflect the fact that this experiment was only done once. As a result of time constraints and significant disruption due to Covid-19, only one repeat of the experiment was performed. However, the data were included as a minimum of three fish had been analysed for all experimental conditions (with the exception of ATMs$^{h477/sh477}$ treated with 8 Gy, where only two fish where analysed) (**see appendix 3.6 for numbers of fish analysed)**.

While H_2AX is thought to be primarily activated by ATM, it can also be activated by other elements of the DDR pathway such as ATR and DNA-PKcs (Mukherjee et al., 2006, Ward and Chen, 2001, Baritaud et al., 2012). Furthermore, ionising radiation creates a number of different types of DNA lesions, and H_2AX is activated in response to many of them (Feng et al., 2017, Kopp et al., 2019, Vierstraete et al., 2017, Liu et al., 2012a). Therefore, γH_2AX may not be the most accurate measure of ATM activity. Other avenues for assessing the DDR in these mutant zebrafish are explored further in **section 3.3.3.1** below. Interestingly, brac2 deficient zebrafish are also capable of inducing H2AX activation to a similar degree as wild type controls but do exhibit deficiencies in HR (Vierstraete et al., 2017).

We next looked at the outcome of somatic recombination in mutant ATM zebrafish **(figure 3.10)**. The diversity of immunoglobulin variable regions is a result of somatic recombination events in immune cells (Chi et al., 2020). These sustained recombination events are mediated by ATM (Perkins et al., 2002, Dujka et al., 2010, Callen et al., 2007a, Bredemeyer et al., 2006b, Liao and Van Dyke, 1999, Callen et al., 2007b, Zha et al., 2009), and as such AT patients have decreased levels of circulating immunoglobulins **(chapter 1, section 1.2.4.1)**. However, ATM$^{+/+}$ and ATM$^{sh477/sh477}$ show no statistical differences in the levels of immunoglobulin heavy chain mRNA, allowing the tentative suggestion that there is no insufficiency in the repair of these V(D)J breaks. Despite the evidence that in humans, repair of these breaks requires ATM, and ATM is primarily thought to function in HR, repair of V(D)J associated breaks is exclusively done through the classical NHEJ pathway (Zha et al., 2009). In this pathway, ATM serves to stabilise RAG-mediated DNA ds break complexes, and not directly in the repair of these breaks (Bredemeyer et al., 2006a). Furthermore, both DNA-PKcs and XRCC4-like factor (XLF) have been shown to have functionally overlapping roles with ATM in this context (Kumar et al., 2014, Zha et al., 2011a, Zha et al., 2009, Zha et al., 2011b, Lee et al., 2013, Gapud and Sleckman, 2011, Gapud et al., 2011). Therefore, it is suggested that the major role of ATM in V(D)J recombination is not the direct repair of the DNA breaks, but the safeguarding genomic stability, as it is responsible for directing cells towards apoptosis, in which V(D)J recombination has gone awry (Callen et al., 2007a).

Despite the functional redundancies in ATM, XLF and DNA-PKcs in the classical NHEJ repair of V(D)J linked DNA breaks, the fact that loss of ATM in humans causes some deficiencies in V(D)J recombination, and preliminary data suggests that it appears not to in zebrafish, is interesting. It may denote fundamental differences in DNA repair in general between teleosts and humans. This is supported by the fact that zebrafish do not have an orthologue for BRCA1, a gene in humans which is essential for DNA repair and repair signalling in a number of pathways reviewed (Zhao et al., 2019). Additionally, zebrafish have an orthologue of the CSR gene *AID* but do not undergo CSR (Wakae et al., 2006).

3.3.2.2 Compensation in the DDR

Preliminary data suggests that there is likely no genetic compensation for loss of the ATM protein in the DDR, as expression of *ATR* mRNA was not upregulated after DNA damage in ATM$^{sh477/sh477}$ zebrafish **(figure 3.12 and 3.13)**. It should be noted that upregulation of expression of DNA-PKcs mRNA was not investigated, and could be considered in future work (see **section 3.3.3.1** to follow). However, due to limited current knowledge of GC, it appears to require the NMD of the mutant transcript (Peng, 2019), which does not happen in the case of the *ATM*^{sh477} transcript, therefore it is unlikely to occur. There is evidence in the literature to suggest there is likely some compensation for loss of ATM, but that it occurs at the protein level by activation of ATR and DNA-PKcs, as outlined below.

As already described in **section 3.3.2.1** above, there is functional redundancy between ATM, DNA-PKcs and XLF in DNA repair of V(D)J recombination breaks (Kumar et al., 2014, Zha et al., 2011b, Zha et al., 2009, Zha et al., 2011a, Lee et al., 2013, Gapud et al., 2011, Gapud and Sleckman, 2011). ATM, ATR and DNA-PKcs all phosphorylate the same S/T-Q motif (Kim et al., 1999), and exhibit a high degree of overlap in their downstream target pool (Yue et al., 2020). Additionally, they all exhibit capabilities of activating each other, suggesting that they use each other to amplify the DDR, and while canonically ATM and DNA-PKcs are both activated in response to ds DNA breaks and ATR in response to ss DNA breaks, it has now been shown that ATR is activated in response to ds breaks too (Adams et al., 2006, Jazayeri et al., 2006, Myers and Cortez, 2006, Tomimatsu et al., 2009). Therefore, it is conceivable that in the absence of ATM there are alternative means of activating the DDR cascade. In *in vitro* studies in ATM deficient cells treated with ionising radiation, the DDR signalling cascade was still activated, albeit to a lower level than in cells with ATM. In these ATM$^{-/-}$ cells, ATR was found to regulate cell check point proteins, while DNA-PKcs was found to regulate proteins that function in the repair of DNA (Tomimatsu et al., 2009). This has been corroborated by Schlam-Babayov (2020), as they also revealed that ATR and DNA-PK partially compensate for ATM's absence in AT cells (Schlam-Babayov et al., 2020). Further emphasising the overlap in functionality of the PIKK kinases, *ATM$^{-/-}$ dnapkcs$^{-/-}$* double mutant mice exhibit embryonic lethality (Gurley and Kemp, 2001, Sekiguchi et al., 2001, Gladdy et al., 2006). The data outlined thus far strongly suggests that while ATM is an important regulator of the DDR in response to genotoxic insults, its loss may be compensated for. Given that DNA damage poses one of the greatest intrinsic risks to maintaining cell homeostasis and viability in eukaryotic cells, protein compensation or functional redundancy amongst proteins in the DDR is not unusual (Kolb et al., 2017, Lam et al., 2008, Parsons and Elder, 2003, Lin et al., 2015).

In recent years, a number of kinase dead (KinD) mouse models of AT have been generated (Yamamoto et al., 2016, Daniel et al., 2012, Tal et al., 2018). These mice express the full-length ATM protein but have mutations that ablate the kinase activity. Mice with kinase dead mutations have a far more severe phenotype compared to ATM$^{-/-}$ mice and exhibit embryonic lethality. Furthermore, ATMT$^{KinD/-}$cells are far more sensitive to DNA damaging agents and exhibit increased deficiency in somatic HR compared to ATM$^{-/-}$ cells (Yamamoto et al., 2016, Chen et al., 2017, Rass et al., 2013). This indicates a dominant negative affect of kinase dead ATM, which has been observed in many cancers caused by somatic mutations in ATM (Scott et al., 2002, Yamamoto et al., 2012b, Yamamoto et al., 2016). This dominant negative affect is most likely caused by a steric hindrance of sorts, whereby the kinase dead ATM is unable to participate in the DDR phosphorylation cascade, and its presence prevents access of machinery that is able to compensate for its loss as it does in ATM$^{-/-}$ cells.

3.3.2.3 Radiosensitivity in the ATM$^{sh477/sh477}$ KO Model versus the ATM MO Induced KD Model

The finding that developing larval ATM$^{sh477/sh477}$ zebrafish did not exhibit any increased radiosensitivity was surprising, as zebrafish with MO induced KD of ATM exhibit extreme radiosensitivity, and even lethality without IR around 72 hpf (Imamura and Kishi, 2005). This raises questions as to why the sensitivity to IR and severity in phenotype is so different between the two models. It should be noted that MO KD models might not always recapitulate the molecular phenotype that they aim for, with phenotypic observations being more severe in MO KD compared to KO models (Peng, 2019, Kok et al., 2015). This has raised questions about their suitability as disease models. The reasons why the ATM KD radiosensitive phenotype is more severe than the KO are many and varied. First, KD with MOs are known to cause off target effects (Summerton, 2007, Amoyel et al., 2005, Gerety and Wilkinson, 2011). The ATM MO sequence targeted the kinase domain (Imamura and Kishi, 2005), and therefore could conceivably also target similar kinase domains in other DNA repair proteins. Secondly, injection of MOs upregulates p53-mediated apoptosis (Ekker and Larson, 2001, Pickart et al., 2006, Robu et al., 2007, Gerety and Wilkinson, 2011). Given that, ATM morphants all died by 72 hpf, without exogenous damage of DNA, and when the majority of the basal DNA damage is repaired by NHEJ, an argument could be made that the severity of the phenotype may be attributed to unchecked p53 mediated apoptosis, similar to gonads in other HR KO zebrafish models outlined above **(section 3.3.1.3)**. Furthermore, as ATM is a primary regulator of apoptosis through the p53-meditated pathway, loss of ATM in this context could have compounding effects. Investigators could have attempted to ameliorate this upregulation of p53 by co-injecting zebrafish larvae with a p53 morpholino.

Finally, there is convincing evidence that the published MO induced KD ATM morphant zebrafish are not conventionally KD of ATM protein expression, but may more accurately represent kinase dead morphants. The morpholino used by Imamura and Kishi (2005) targets the exon–intron junction at the 5′ side of exon 56. This causes an in frame skipping of 267 bp, corresponding to exons 56 and 57. This in frame deletion corresponds to loss of the beginning of the kinase domain. In the data presented in this chapter and seen in patients, ATM mRNA does not readily undergo NMD. Additionally, the study carried out by Imamura and Kishi (2005) does not provide any evidence of the resultant ATM protein expression, although evidence suggests that in frame exon skipping in ATM does produce a stable protein (Menotta et al., 2012, Pozzi et al., 2020, Rogatcheva et al., 2007, Menotta et al., 2017, Kralovicova et al., 2016). Therefore, the resultant protein in ATM morphants could conceivably be analogous to a kinase dead ATM. The kinase dead ATM protein has been shown to have a much more severe outcome than ablation of ATM, and in mice results in embryonic lethality (Yamamoto et al., 2012a, Daniel et al., 2012), similar to the embryoic lethality observed in zebrafish ATM morphants.

3.3.3 Future Work in the General Characterisation of the ATM$^{sh477/sh477}$ Model

3.3.3.1 Further Characterising the DDR in ATM Deficient Zebrafish

DNA damage repair is a dynamic process and employs different pathways depending on the cell type and the point of the cell cycle during which repair is required (Hakem, 2008). H_2AX phosphorylation acts as a marker of DNA damage, but does not indicate which pathway is responsible for the repair. In the results presented above, H_2AX phosphorylation was quantified 1 hr post irradiation - a single time point. As activation of the DDR was shown to occur in ATM$^{-/-}$ cells but at a slower pace (Schlam-Babayov et al., 2020), it would be important to conduct a time course experiment to determine if the rate of repair, and therefore decreased signalling of γH_2AX, changes over time between wild type and ATM$^{sh477/sh477}$ zebrafish. To complement this, a comet assay where extracted DNA migration through an agaroses gel is monitored, and the amount of lagging DNA which represent ssDNA is quantified as a measure for unrepaired DNA damage, could be performed at the corresponding time points to quantify actual DNA damage (Martins and Costa, 2020).

As outlined above **(section 3.3.2.1)**, quantification of activation of γH_2AX only denotes DNA damage repair in general, and may be a marker for multiple repair mechanisms. Most ds DNA damage is repaired through the quicker NHEJ repair pathway, which will also present with γH_2AX foci, while only a subset is repaired through the more laborious HR pathway (Jeggo et al., 2011, Liu et al., 2012a). This will largely depend on what stage during the cell cycle the repair takes place. As ATM primarily functions in the DDR as a coordinator of HR, investigating the repair of DNA through this pathway should be considered. Protocols have been developed for measuring HR in zebrafish through immunofluorescence quantification of Rad 51 foci (Vierstraete et al., 2017) – an essential protein for HR in zebrafish that functions downstream of the ATM/BRCA2 pathway (Liu et al., 2012a). Furthermore, it may be useful to compare what type of DNA repair is occurring in ATM$^{+/+}$ verses ATM$^{sh477/sh477}$ zebrafish, and whether the loss of ATM affects this in any way. A protocol for discerning between HR, NHEJ and single-strand annealing (SSA) pathways in zebrafish larvae using fluorescent reporter zebrafish has been developed (Liu et al., 2012a).

3.3.3.2 Investigating Compensation in the Model

The apparent lack of radiosensitivity and deficiency inactivating the DDR in ATM$^{sh477/sh477}$ may be due to protein-level compensation and redundancies in the DDR. Therefore, it would be interesting to understand the nature of the predicted compensation in ATM$^{sh477/sh477}$ zebrafish. The increased radiosensitivity exhibited by the MO KD model may be in part due to the presence of a kinase dead ATM protein**,** however, as confronted in this project, quantification of ATM protein levels in zebrafish is difficult. Consequently, it cannot be confirmed whether the ATM morphants have ATM protein expression. Furthermore, off target effects such as p53 activation compounding the phenotype cannot be ruled out. Therefore, there may be merits in creating a CRISPR knock in, kinase dead zebrafish mutant. An ATM kinase dead zebrafish may have many advantages in investigating the effects of complete disruption to ATM signalling compared to the kinase dead mouse model, since zebrafish KOs of essential genes are often viable for the first few days of embryonic development. Furthermore, while stable kinase-dead homozygous mutants will most likely also succumb to embryonic lethality, heterozygous mutants would be predicted to exhibit the same dominant negative effect seen in cells (Scott et al., 2002, Yamamoto et al., 2012a, Yamamoto et al., 2016). This may prove to be a valuable *in vivo* resource in chemotherapeutic development for cancers with *de novo* somatic ATM mutations. Exploratory data could be gathered into the merits of modelling loss of kinase activity with the use of ATM inhibitors. Some preliminary data and discussion on this will be presented in **chapter 5**.

In order to further scrutinise whether there is protein-level compensation in the model, it would be interesting to study the relative contribution of ATR and DNA-PKcs. Attempts have been made to transiently decrease ATR expression in ATM$^{sh477/sh477}$ zebrafish using CRISPRi (data not shown). However, no decrease in ATR mRNA was achieved, most likely because CRISPR methods activate the DDR (Haapaniemi et al., 2018, Ihry et al., 2018, Enache et al., 2020), which could have overridden the steric silencing of a DNA damage gene. Therefore, the transient ablation of ATR or DNA-PKcs expression through genetic means may not be ideal in this context. However, investigation into the contribution of compensation could be achieved using ATR and DNA-PKcs inhibitors in conjunction with ATM$^{sh477/sh477}$ zebrafish.

Chapter 4

ATM$^{sh477/sh477}$ Zebrafish Exhibit Infertility and Testicular Neoplasms

4.1 Introduction

One of the hallmarks of classical AT is infertility **(see chapter 1, section 1.2.4.6)**. This phenotype is also recapitulated in rodent and porcine models **(see chapter 1, 1.3)**, indicating that the function of ATM is highly conserved in gamete formation. During prophase I of meiosis, controlled SPO11 mediated ds breaks are introduced into developing gametes to facilitate an exchange of genetic information between sister chromatids in homologs recombination, and ATM is required for the repair of these ds breaks and for gamete formation to progress (Cooper et al., 2014, Brick et al., 2020). In vertebrate AT models, gamete formation is stalled in prophase I of meiosis at the point where these breaks should be repaired (**see table 4.1 below**), resulting in the infertility observed (Barlow et al., 1996, Quek et al., 2017a). As reported in **chapter 3**, all ATM$^{sh477/sh477}$ zebrafish develop as male. Therefore, investigations of infertility and gametogenesis of ATM$^{sh477/sh477}$ zebrafish reported in this chapter will only discuss fertility in relation to spermatogenesis.

Spermatogenesis in zebrafish occurs similarly to how it does in mammals and the key steps in this process are outlined in **figure 1.4**. , Spermatogenesis begins with a large progenitor stem cell called undifferentiated Spermatogonia A cells. These stem cells divide by mitosis and differentiate into Spermatogonia A cells which further divide into Spermatogonia B cells. These then further divide into primary spermatocytes which further divide by meiosis where homologous recombination takes places resulting in haploid secondary spermatocytes. Secondary spermatocytes then quickly develop into spermatids, and finally undergo morphologically changes where they mature into spermatozoa. (Schulz et al., 2010b, Leal et al., 2009, Xie et al., 2020). From the point of late spermatogonia B cells, each successive division increases the number of cells but decrease the size of the cells. Furthermore, as the sperm develops the nucleus undergoes progressive chromosomal condensation, further deceasing the size and changing the morphology of the cells. These changes such as the number of cells, the nuclear size and the nuclear morphology and colour (under H&E and Putt's carbol fuchsin staining) can be used to identify the cells type and stage of development (van der Van and Wester).

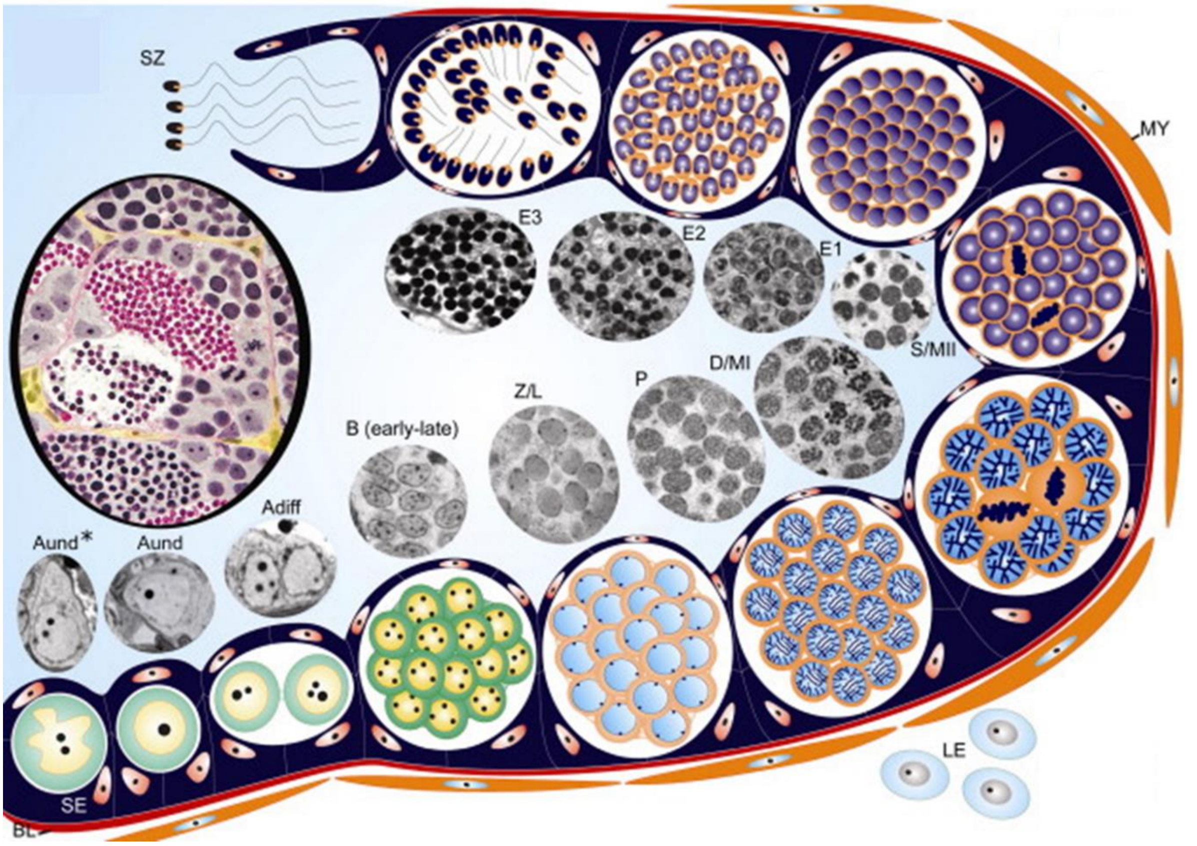

Figure 4.1 Zebrafish Spermatogenesis. The germinal epithelium delineated by a basal lamina (BL) and peritubular myoid cells (MY), From the point of late spermatogonia B cells, each successive division increases the number of cells but decrease the size of the cells. Furthermore, as the sperm develops the nucleus undergoes progressive chromosomal condensation, further deceasing the size and changing the morphology of the cells. These changes such as the number of cells, the nucler size and the nuclear morphology (and colour under H&E staining can be used to indentify the cells type and stage of sevelopment .Outside the cystic epithelium are the interstitial Leydig cells (LE). Type A undifferentiated∗ spermatogonia (Aund∗) which are the progenitor stem cell; type A undifferentiated spermatogonia (Aund); type A differentiated spermatogonia (Adiff); spermatogonia type B [B (early–late)]; leptotenic/zygotenic primary spermatocytes (L/Z); pachytenic primary spermatocytes (P); diplotenic spermatocytes/metaphase I (D/MI); secondary spermatocytes/metaphase II (S/MII); early (E1), intermediate (E2) and final spermatids (E3); spermatozoa (SZ). Figure reproduced with permissions (Schulz et al., 2010b).

4.2 Results

4.2.1 ATM$^{sh477/sh477}$ Zebrafish do not Produce Progeny

To determine if ATM$^{sh477/sh477}$ zebrafish exhibit the same infertility as other AT models, male ATM$^{+/+}$ and ATM$^{sh477/sh477}$ zebrafish were pair mated with wild type female fish that had previously produced robust clutches of embryos. Each experimental fish was paired once. Three hours after pairing, we recorded whether the wild type female laid any eggs, and after a further 3 hours, determined the number of fertilised and unfertilised eggs within the clutch. Mutant ATM zebrafish failed to induce egg laying in females in 92% of pair matings **(figure 4.2 a)**. On the one occasion where an ATM$^{sh477/sh477}$ fish did induce egg laying in the female, there were no fertilised embryos **(figure 4.2 b)**. This indicates that ATM$^{sh477/sh477}$ zebrafish recapitulate the infertility seen in other models of AT. The nature of the infertility will be detailed further in **sections 4.2.2.2 and 4.2.2.3** below.

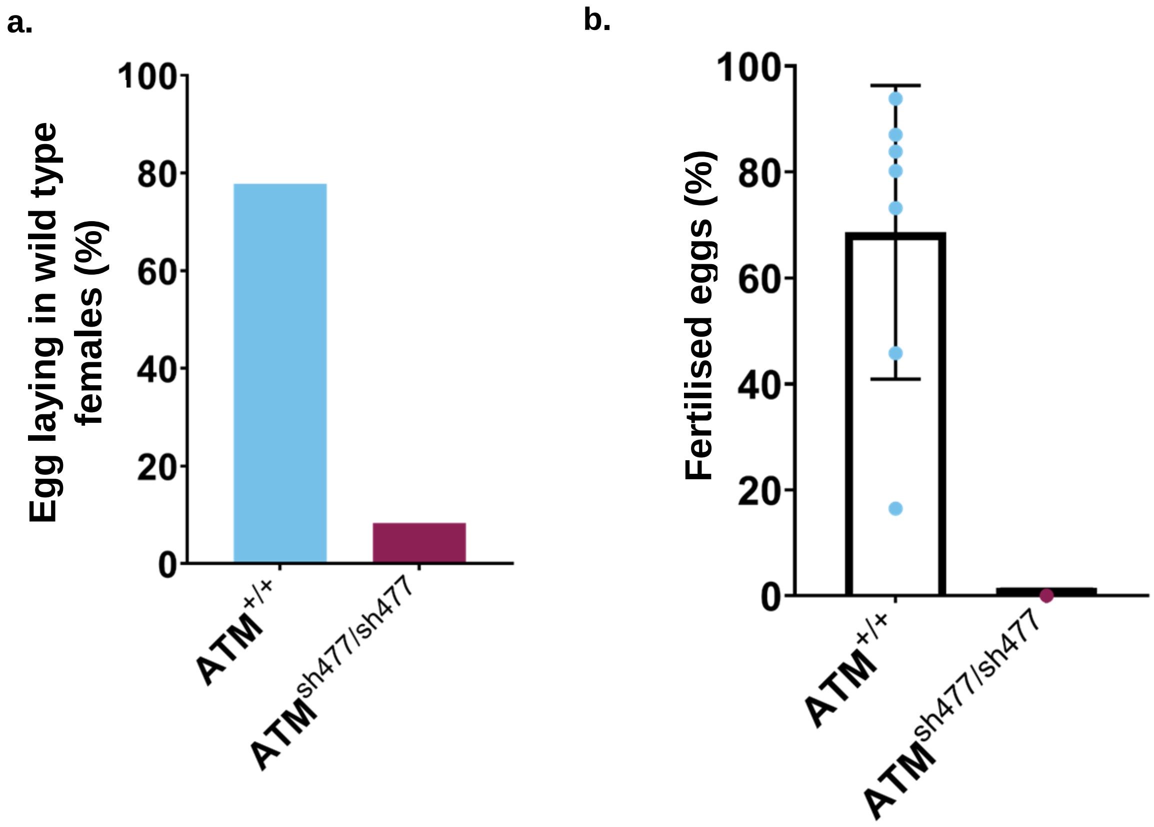

Figure 4.2 ATM$^{sh477/sh477}$ Zebrafish are infertile. Male ATM$^{+/+}$ and ATM$^{sh477/sh477}$ siblings were outcrossed by pair mating to wild type female zebrafish that had previously produced robust embryos. **a.** the percentage of outcrosses that resulted in egg laying by the wild type females. **b.** the percentage of fertilised eggs produced from individual crosses when egg laying was induced. Each data point represents a single pair mating. Error bars represent mean +-/ SD. Note only one ATM$^{sh477/sh477}$ outcross resulted in egg laying in the females. From those eggs, none were fertilised. ATM$^{+/+}$ n=9, ATM$^{sh477/sh477}$ n=12, data represents pairings carried out on 3 separate days.

4.2.2 Investigations into ATM$^{sh477/sh477}$ Testes

4.2.2.1 ATM$^{sh477/sh477}$ Zebrafish have Neoplastic Testes

It was observed over the course of the project that all ATM$^{sh477/sh477}$ zebrafish exhibited progressive swelling and distention of the abdomen **(figure 4.3 a)**. Under close inspection during development, this unusual abdominal morphology could first be detected at around 7 months, became obvious by 9 months, and became a humane end point by 18 months, as abdomens became so large that tearing of the skin could be observed around the anal fin. Upon dissection, the abdominal morphology was found to be the result of a multilobular, soft, cream coloured mass within the caudal abdominal cavity **(figure 4.3 b)**. Histological examination from one fish determined this mass to be testicular tissue (data not shown). Therefore, the testes of ATM$^{sh477/sh477}$ zebrafish were further investigated to understand the nature of the growth.

Groups of four ATM$^{+/+}$, ATM$^{+/sh477}$ and ATM$^{sh477/sh477}$ male siblings were sacrificed at 12 months of age, and prepared for formalin fixed paraffin embedded (FFPE) tissue sectioning of the abdominal cavity. Tissue sections were then stained with haematoxylin and eosin (H&E) for visualisation of the testicular structures. Testes in ATM$^{sh477/sh477}$ zebrafish were consistently larger than in their control siblings. The testicular mass fills most of the abdominal cavity, with one testis displacing the other so they sit on top of each other (as opposed to being parallel to each other) **(figure 4.4 a)**. As can be seen from **figure 4.4 b**, wild type and heterozygous zebrafish testes have an organised structural architecture that has been lost in mutant zebrafish. The irregularities in ATM$^{sh477/sh477}$ structure appear to be from neoplastic growth of polygonal cells with variably distinct cell borders, and contain a small to moderate amount of eosinophilic cytoplasm. The nuclei of these cells are variable in size and these cells form clusters of sheets that are interspersed with different cell populations **(figure 4.4 c)**. In consultation with two pathologists, Dr Clare Muir (Department of Infection, Immunity & Cardiovascular Disease) and Dr Jonathan Griffin (Department of Molecular Biology and Biotechnology), these neoplastic cells were identified as Sertoli cells.

Sertoli cells form part of the testicular epithelium and function as support cells for developing sperm (França et al., 2016, França et al., 2015). The disruption caused by Sertoli cell neoplasia to the organisation of ATM$^{sh477/sh477}$ testes is characterised in more detail in **figure 4.5**. In control testes, an epithelial barrier **(A)** surrounds each cystic tubule **(yellow dotted line)**, and progression of spermatogenesis takes place within the cystic lumen **(B)**. Spermatogenic support cells, Leydig cells **(C)** and Sertoli cells **(D)** are found on the periphery of the cyst by the epithelial barrier (Xie et al., 2020). Spermatogenesis begins with large, solitary, immortal primary germ cells called spermatogonia A **(E)**, which give rise to clusters of 4-16 spermatogonia B cells **(F)**. These cells further divide into spermatocytes **(G)** which form spermatocysts **(red dotted line)**. The spermatocyst is formed by cytoplasmic extensions of Sertoli cells, and supports expansion of the developing germ cells (Schulz et al., 2015) . Cells in spermatocysts further develop into spermatids **(H)**, which progress into mature sperm through spermiogenesis **(I)**. In ATM$^{sh477/sh477}$ zebrafish, the neoplastic Sertoli cells make up most of the testicular mass, and other cells types are difficult to discern. The relative contribution of Sertoli cells and Leydig cells to the cellular makeup of the testes between ATM$^{+/+}$ and ATM$^{sh477/sh477}$ zebrafish are quantified in **figure 4.6**. ATM$^{+/+}$ testes had an average of 4.3 +/- 2.8 Sertoli cells per mm^2, while ATM$^{sh477/sh477}$ testes had an average of 31.84 +/- 17.3 Sertoli cells per mm^2, resulting in a ~7 fold increase in Sertoli cells in ATM$^{sh477/sh477}$ testes. There was no significant difference in Leydig cell numbers between the two genotypes. The neoplastic Sertoli cells appear to be benign, as their growth was restricted to the testes and no infiltration to surrounding organs was observed (data not shown).

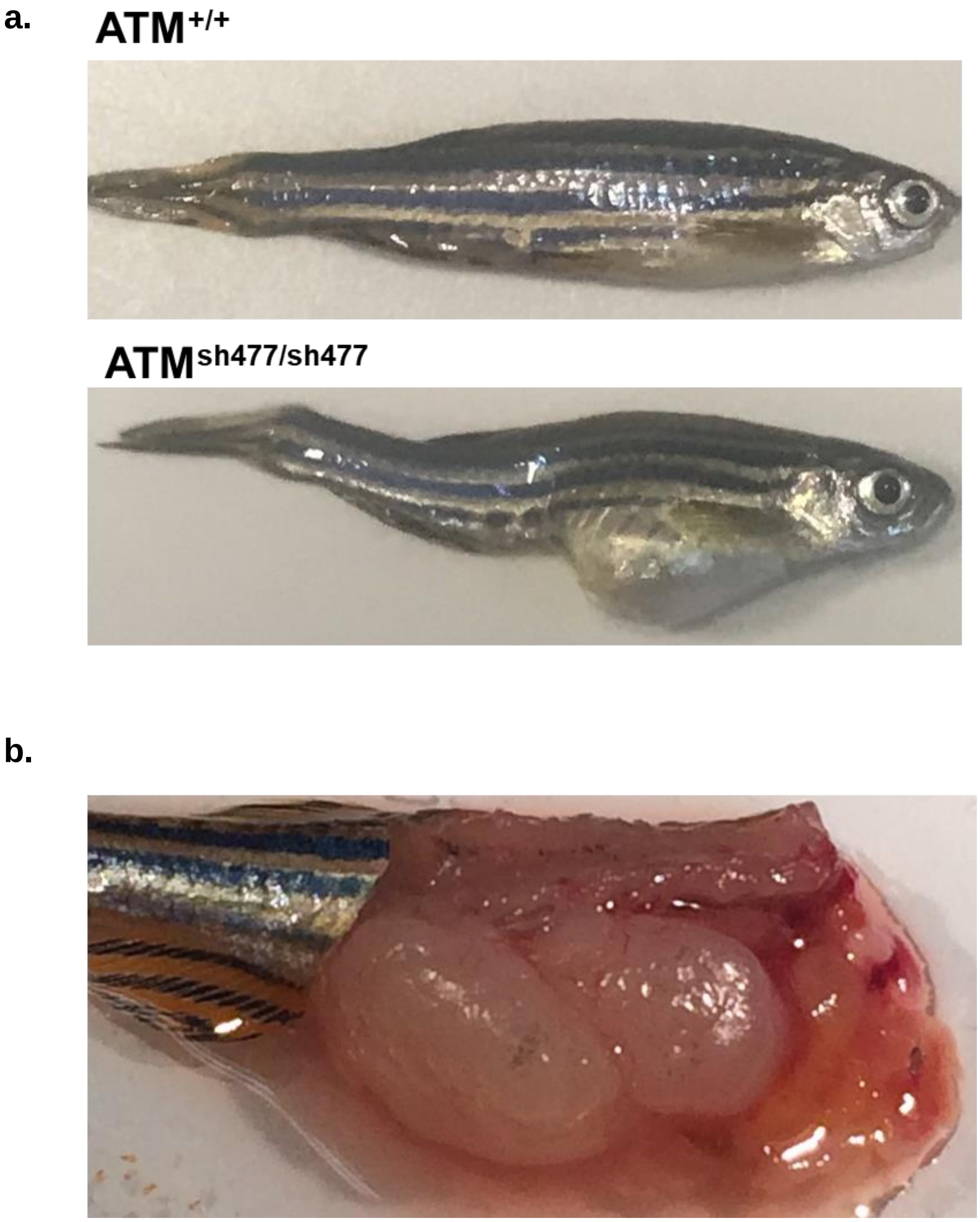

Figure 4.3 ATM$^{sh477/sh477}$ zebrafish exhibit abnormal gross abdominal morphology. a. ATM$^{sh477/sh477}$ vs ATM$^{+/+}$ male zebrafish (15 months). **b.** Abdominal dissection of ATM$^{sh477/sh477}$ (TDP null) zebrafish (18 months).

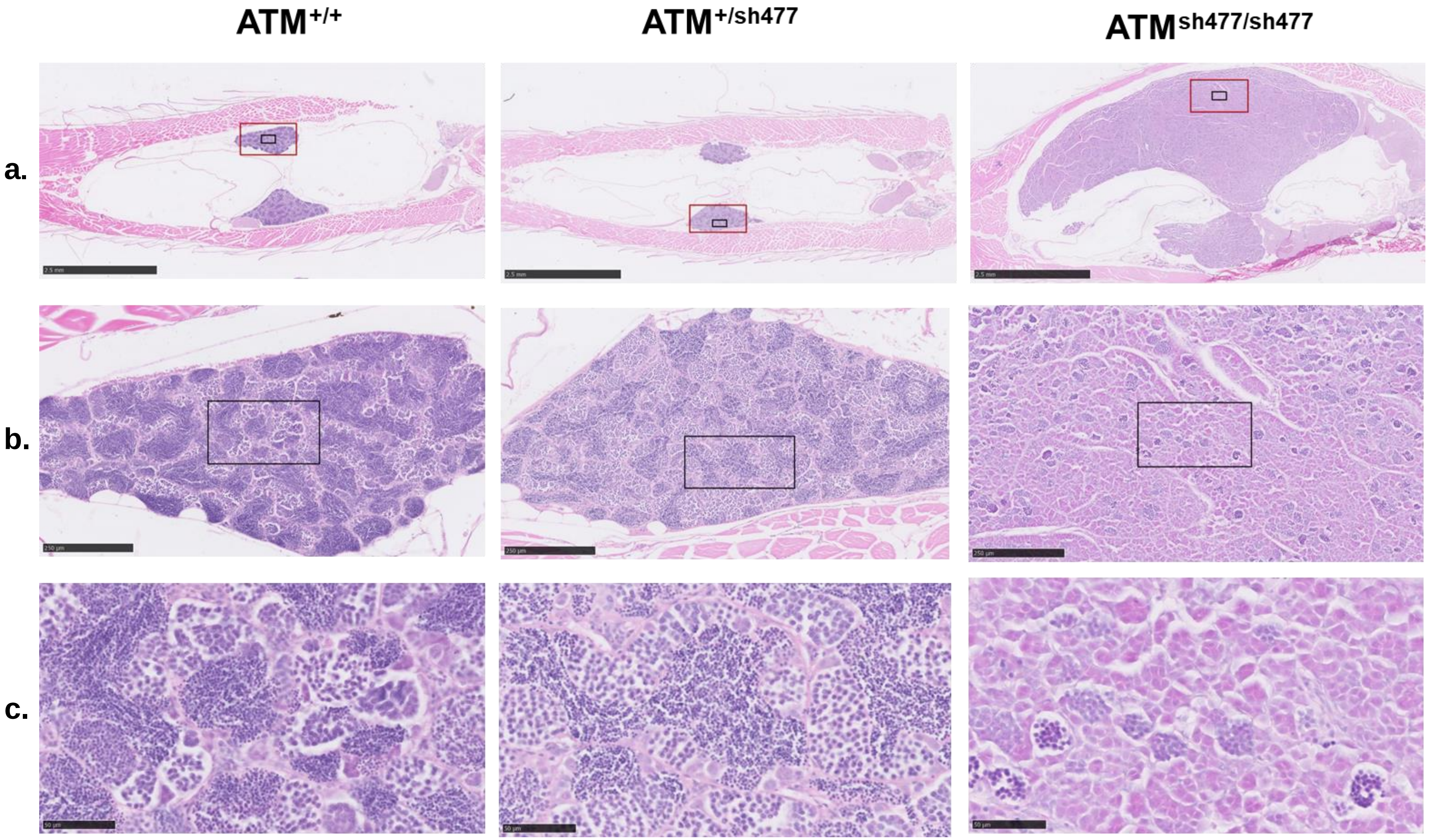
ATM$^{+/+}$
ATM$^{+/sh477}$
ATM$^{sh477/sh477}$
a.
b.
c.
2.5 mm
2.5 mm
2.5 mm
250 µm
250 µm
250 µm
50 µm
50 µm
50 µm

Figure 4.4 ATM$^{sh477/sh477}$ zebrafish testes at 12 months old exhibit neoplastic Sertoli cell growth. H&E stained horizontal sections (5 µm) of ATM$^{+/+}$ (left panel), ATM$^{+/sh477}$ (middle panel) and ATM$^{sh477/sh477}$ (right panel) testes. **a**, **b** and **c** are magnified images of the same testis where **a**. scale bar represents 2.5 mm. **b**. scale bar represents 250 µm. **c**. scale bar represents 50 µm.

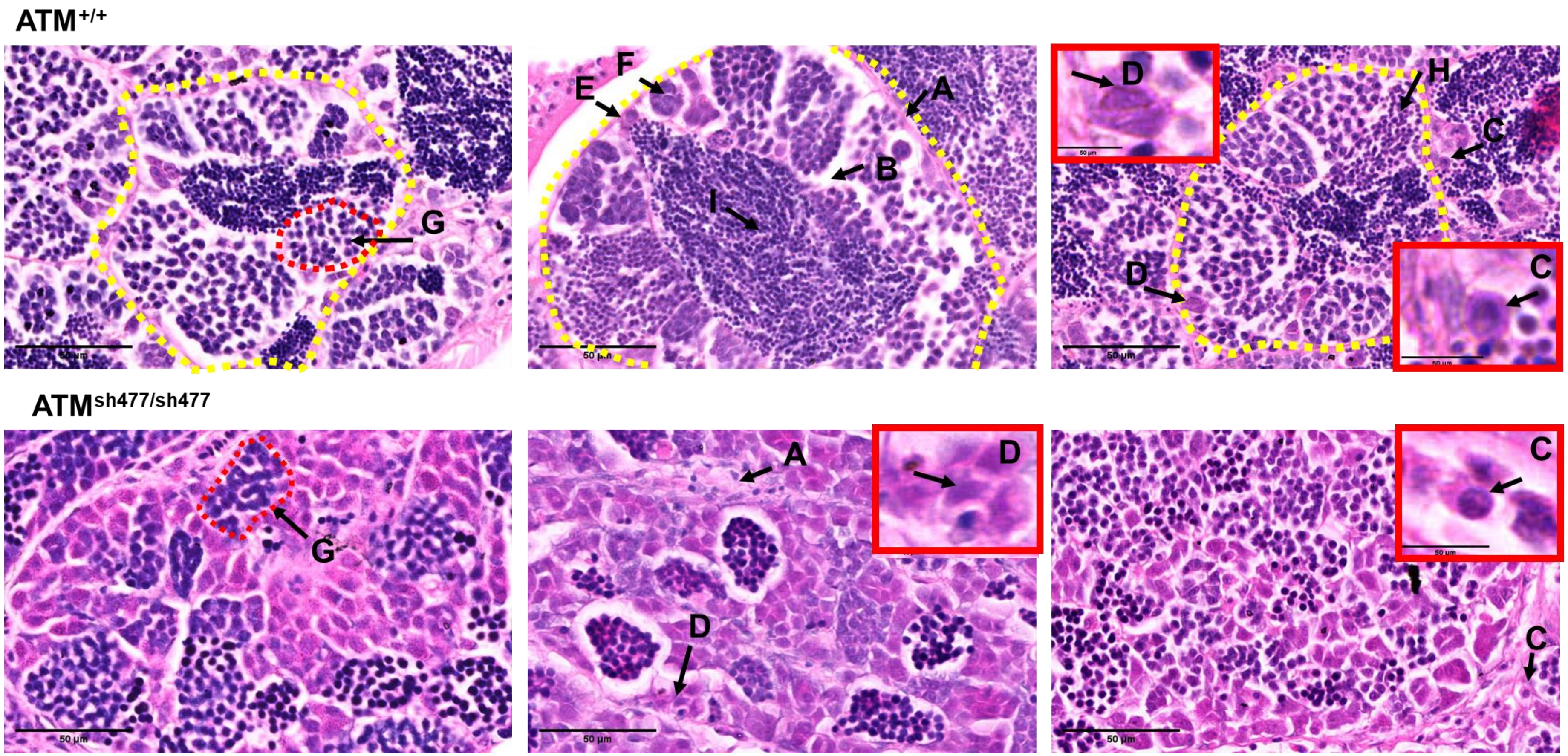

Figure 4.5 Neoplastic Sertoli cell growth disrupts the organisational structure of ATM$^{sh477/sh477}$ testes. Cystic organisational structure of 3 ATM$^{+/+}$ and 3 ATM$^{sh477/sh477}$ zebrafish at 3 months. Cyst boundary **(yellow dotted line)** comprised of interstitial connective tissue **(A)**, cystic luminal space **(B)**, Leydig cells **(C)**, Sertoli cells **(D)**, spermatogonia A **(E)**, spermatogonia B cells **(F)**, spermatocytes **(G)**, spermatocysts **(red dotted line)**, spermatids **(H)**, and mature sperm **(I)**. Scale bars represent 50 µm

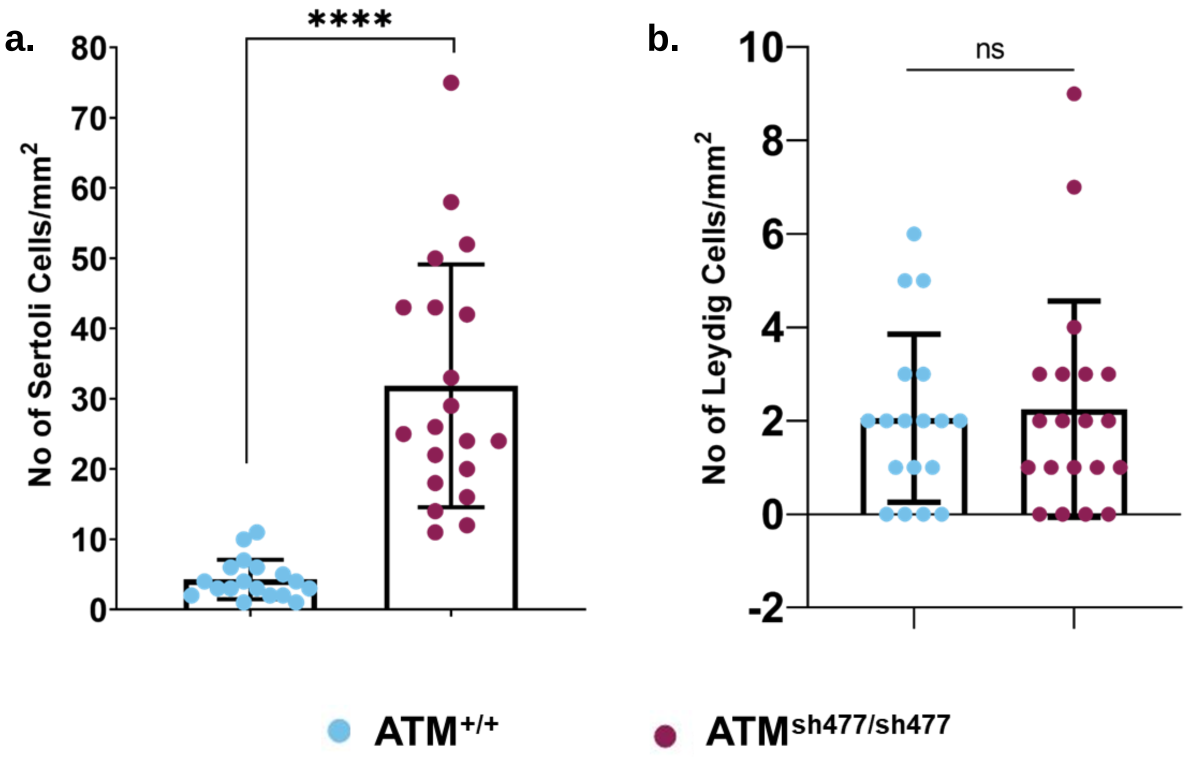

Figure 4.6 Contribution of Sertoli and Leydig cells to the makeup of 12 month old ATM$^{+/+}$ and ATM$^{sh477/sh477}$ testes. **a.** Sertoli cell contribution to testicular makeup. Data were analysed by an unpaired t test with Welch's correction (<0.0001). **b.** Leydig cell contribution to testicular makeup. Data were analysed by a Mann Whitney test (p=0.9485). Each data point represents the number of named cells in a field of view with an area of 1.1 mm^2, with 5 randomly selected fields of view analysed for each fish. ATM$^{+/+}$n=4 fish, and ATM$^{sh477/sh477}$n=4 fish. Error bars represent mean+/- the SD. Statistical analysis can be seen in **appendix 4.1.**

4.2.2.2 ATM$^{sh477/sh477}$ Zebrafish do not Develop Mature Spermatozoa

To understand the nature of the infertility exhibited by ATM$^{sh477/sh477}$ zebrafish in **figure 4.2** we further investigated the testes. However, due to the overwhelming growth of the Sertoli cells, identification of spermatogenic and other support cells was cumbersome in 12-month testes. Therefore, for ease of analysis we chose to investigate development of primary germ cells to mature sperm in testes from 3-month-old zebrafish. As they do not show any gross abdominal swelling, we postulated that there would not yet be overwhelming Sertoli cell growth, and the testicular architecture and cellular makeup of ATM$^{sh477/sh477}$ zebrafish would be more easily discernible.

Low power images of the testes **(figure 4.7)** confirm that at 3 months of age the structural architecture has been slightly disrupted; however, it has not yet completely obscured the testicular organisation. As outlined above in **figure 4.5**, zebrafish spermatogenesis occurs in cysts, and the maturational direction of developing sperm occurs from the periphery towards the centre, with mature sperm filling the central anastomosing luminal space. However, low power images of ATM$^{sh477/sh477}$ testes show the central seminiferous lumen to be largely empty **(figure 4.7, arrows)**.

Medium power images of testes **(figure 4.8 a)** show in detail how the cysts in ATM$^{sh477/sh477}$ zebrafish have become disorganised, and how it is difficult to distinguish groups of cells at different stages of spermatogenesis from each other. In ATM$^{+/+}$ testes, the central luminal spaces are filled with hyperchromatic haematoxylin stained cells, that are consistently circular in shape, with no discernible cytoplasm. These are mature sperm that have been released into the anastomotic lumen once spermatogenesis has been completed (spermiation). ATM$^{sh477/sh477}$ testes do not appear to undergo spermiation, as no mature spermatozoa are observed. However, there are cells similar in appearance to spermatozoa that are small and hyperchromatic, but these are generally clumped together as is seen in developing spermatocytes as they progress though spermatogenesis. Thus, it appears that the reason why ATM$^{sh477/sh477}$ zebrafish are infertile is because they do not produce mature spermatozoa due to incomplete spermatogenesis.

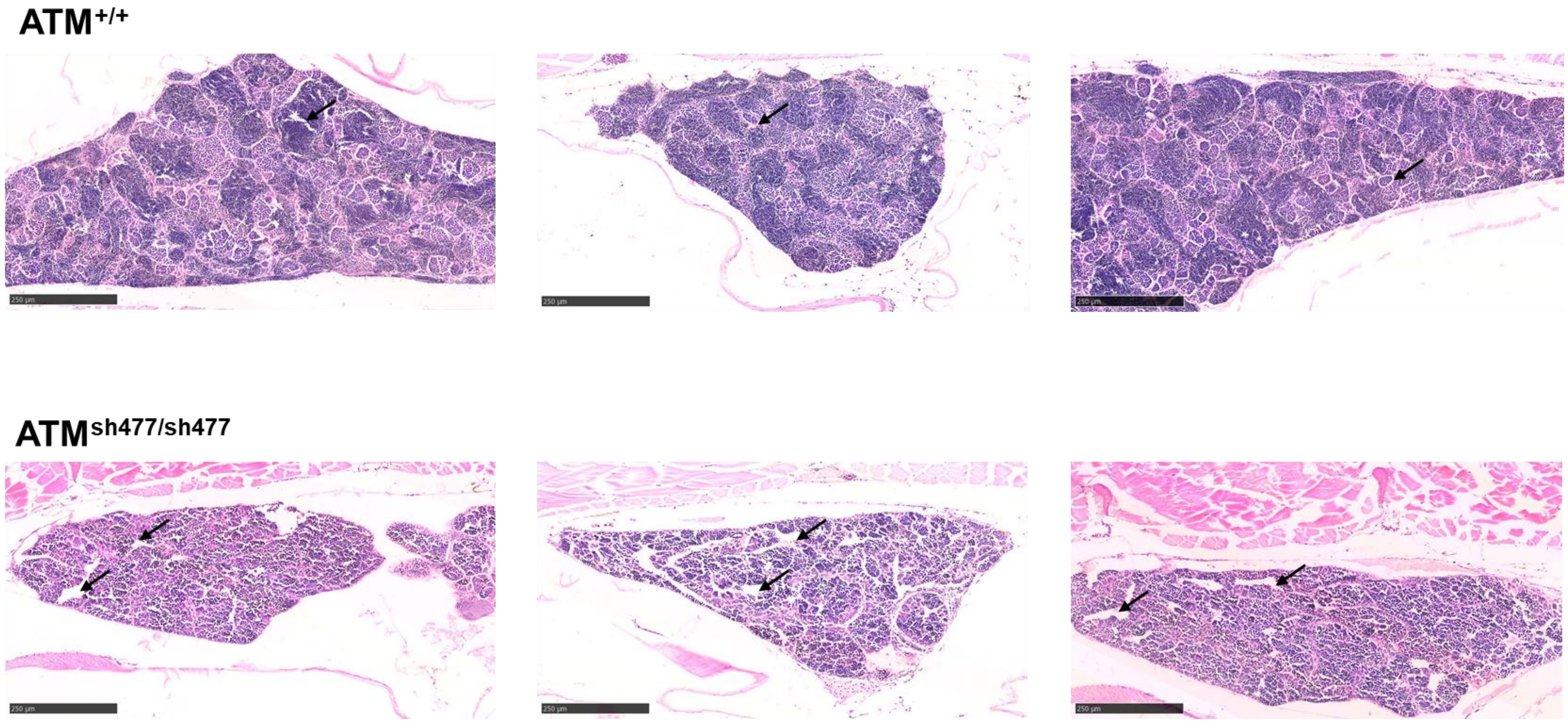
ATM$^{+/+}$
250 µm
250 µm
250 µm
ATM$^{sh477/sh477}$
250 µm
250 µm
250 µm

Figure 4.7 ATM$^{sh477/sh477}$ testes exhibit large empty seminiferous tubule lumens. Low power image of ATM$^{+/+}$ (top panel) and ATM$^{sh477/sh477}$ (bottom panel) testes at 3 months. Arrowheads denote empty seminiferous tubules. Scale bar represent 250 µm.

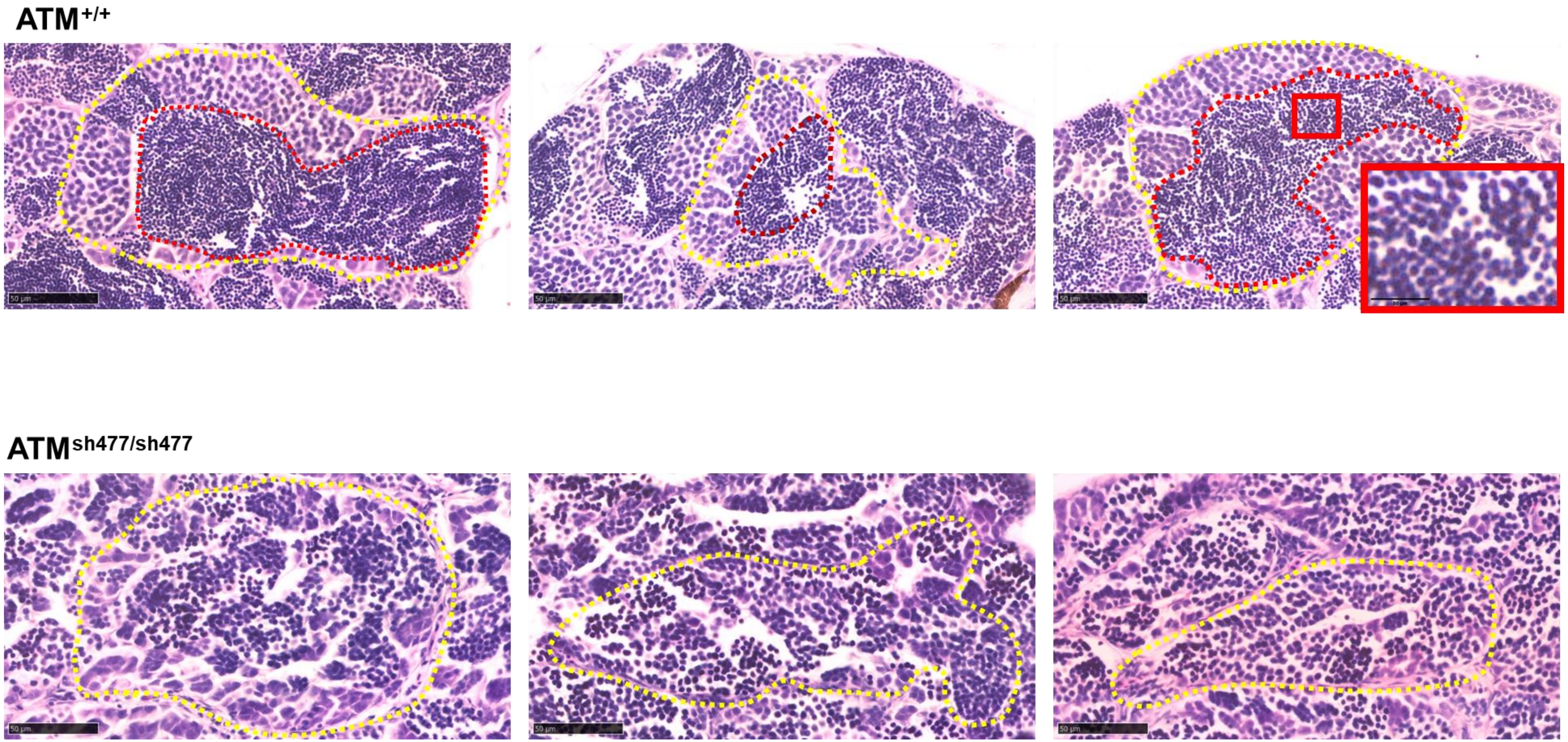

Figure 4.8 $ATM^{sh477/sh477}$ zebrafish testes do not contain mature sperm. a. Medium power images of testes from 3 $ATM^{+/+}$ (top panel) and 3 $ATM^{sh477/sh477}$ (bottom panel) zebrafish at 3 months. The dashed yellow line indicates the cyst boundary and the dashed red line indicates mature spermatozoa in the luminal space. Red inset shows magnified red box containing mature spermatozoa. Scale bars represent 50 µm**.**

4.2.2.3 ATM$^{sh477/sh477}$ Zebrafish Exhibit Stalled Spermatogenesis

Infertility in other animal models of AT stems from failure to repair the dsDNA breaks created during meiotic recombination. As shown in the above section, ATM$^{sh477/sh477}$ zebrafish appear to have stalled spermatogenesis, and we hypothesise that this failure ofspermatic development to progress beyond a certain stage could also be related to a meiotic defect. Therefore, we compared spermatogenesis between ATM$^{+/+}$ and ATM$^{sh477/sh477}$ zebrafish with regards to cell type and the expected stage of meiosis.

Figure 4.9 compares H&E images of the different stages of spermatic development. As cells develop through spermatogenesis they become progressively smaller, with an increasingly smalland more compact nucleus. Therefore, measurement of the cell size relative to other developing cells can help determine their stage of development. To quantify the size of different cell types, the area of the nucleus was measured **(figure 4.10)**. Automated analysis of cell area was attempted, however due to the large number of overlapping cells in the sections it was not possible to differentiate between individual cells **(appendix 4.2, left panel)**. Therefore, the area of different cell types was measured manually, by drawing around the perimeter of the hyperchromatic haematoxylin stained region of the cell **(see appendix 4.2, right panel)**. Spermatogenesis begins with a primary immortal germ cell called spermatogonia A (**figure 4.9 a)**. The nucleus of these cells do not stain well with haematoxylin and only lightly with eosin, and as such, these cells appear hypochromatic. They are found as a large single cell at the periphery of the cyst and are mitotically active. Spermatogonia A cells were present in both ATM$^{+/+}$ and ATM$^{sh477/sh477}$ testes. Mitotic division of these cells gives rise to early spermatogonia B **(figure 4.9 b)**. These cells are morphologically identically to spermatogonia A, are mitotically active, and are found in clusters of 2-4 cells. Again, these cells were observed in both genotypes. Through further mitotic divisions, early spermatogonia B cells develop into late spermatogonia B cells **(figure 4.9 c)**. These cells are found in clusters of 4-16 cells, are highly mitotically active, and are present in both mutant and ATM$^{+/+}$ testes. Spermatogonia B cells further develop into spermatocytes **(figure 4.9 d)**, and these cells are found grouped together in clusters called spermatocysts **(figure 4.9 d, dotted line)**. Spermatocytes are the point in spermatogenesis in which meiosis occurs. Different stages of spermatocyte development can sometimes be determined morphologically. However, differences in morphology can be difficult to characterise without visualisation of chromosomes, and therefore, only early stage primary spermatocytes were characterised in **figure 4.10**. Clusters of primary spermatocytes were found in both ATM$^{sh477/sh477}$ and ATM$^{+/+}$ testes and were of comparable size ($p>0.9999$). Primary spermatocytes undergo the first stage of meiosis and in Prophase I when cells are tetraploid, homologous recombination occurs. After the first meiotic division, cells develop into secondary spermatocytes and undergo the second meiotic division to create haploid cells. The second mitotic division is quick and as such, secondary spermatocytes are rarely seen in histological sections of testes, and on analysis of ATM$^{+/+}$ testes no cells that could be considered secondary spermatocytes were observed. In normal spermatogenesis in ATM$^{+/+}$ testes, spermatocytes divide into haploid spermatids **(figure 4.9 e)**, and then further develop into mature spermatozoa **(figure 4.9 f)**. However, in ATM$^{sh477/sh477}$ testes, no spermatids or spermatozoa were observed.

The most fully developed spermatic cells observed in ATM$^{sh477/sh477}$ testes were hyperchromatic with condensed nuclei, similar to mature spermatozoa, but were localised in small groups similar to spermatocytes and had not been released into the lumen **(figure 4.9 g).** Furthermore, when the area of these cells was compared to other developing spermatogenic cells **(figure 4.10)**, they were 1.8 times smaller than ATM$^{+/+}$ and ATM$^{sh477/sh477}$ primary spermatocytes ($p<0.0001$), and 1.9 and 3.6 times larger than ATM$^{+/+}$ spermatids ($p=0.0004$) and mature spermatozoa ($p<0.0001$), respectively in ATM$^{+/+}$ testes. Therefore, these ambiguous cells present in ATM$^{sh477/sh477}$ testes had an intermediate size between that of primary spermatocytes and spermatids. This indicates that they are at a point of development between these two cells types. However, as no secondary spermatocytes were found in ATM$^{+/+}$ testes for comparison, and as it is difficult to stage primary spermatocyte development without visualisation of the chromosomes, it was not known if these cells are primary spermatocytes that are in the late stages of the first meiotic division, or if they are secondary spermatocytes. Therefore, here we have designated them late spermatocytes, as their exact point in development between primary spermatocyte and spermatid is not known. Thus, ATM$^{sh477/sh477}$ spermatogenesis is stalled and does not progress beyond the stage of meiosis.

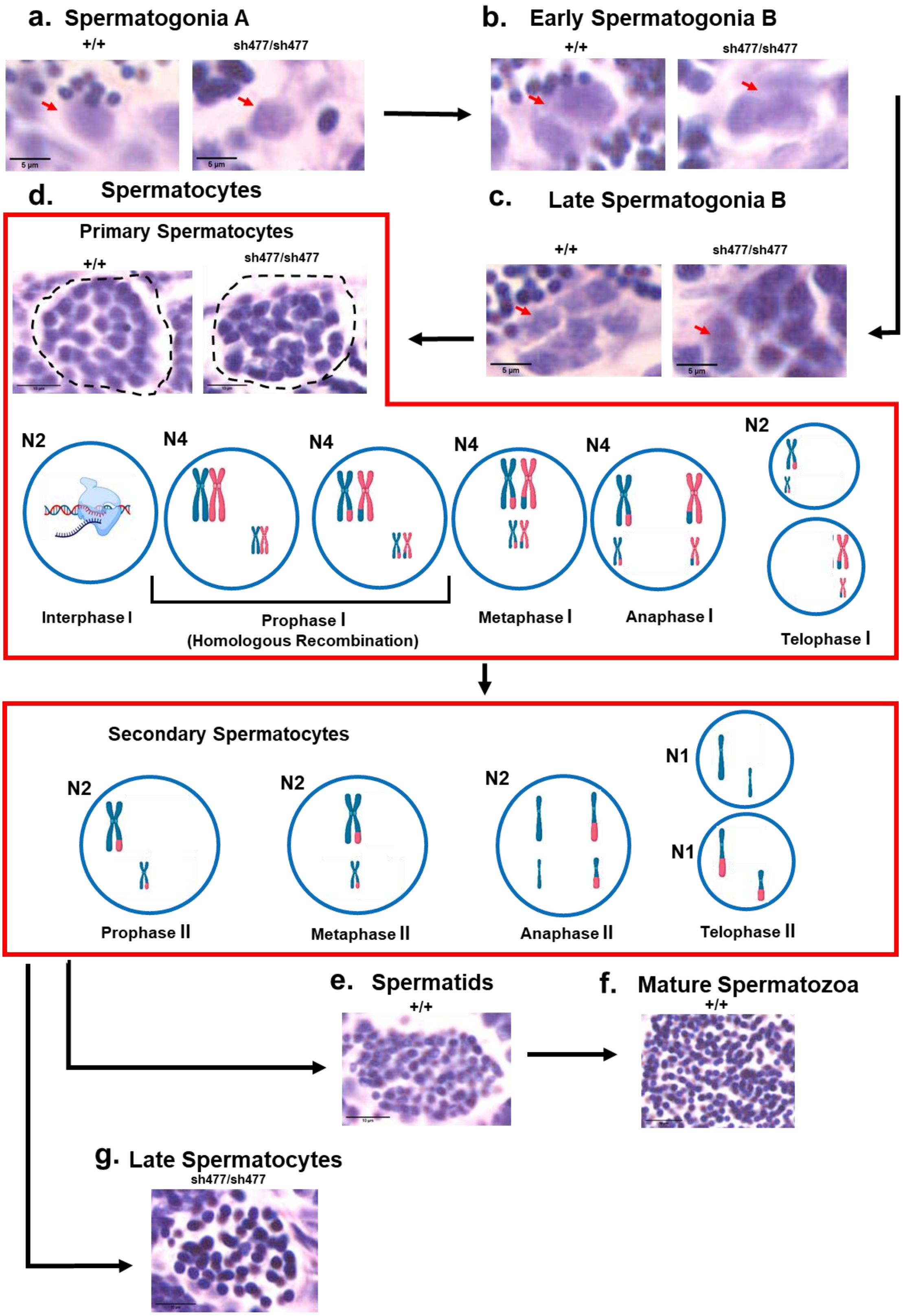
a. Spermatogonia A
+/+
sh477/sh477
5 µm
5 µm
b. Early Spermatogonia B
+/+
sh477/sh477
c. Late Spermatogonia B
+/+
sh477/sh477
5 µm
5 µm
d. Spermatocytes
Primary Spermatocytes
+/+
sh477/sh477
N2
N4
N4
N4
N4
N2
Interphase I
Prophase I
(Homologous Recombination)
Metaphase I
Anaphase I
Telophase I
Secondary Spermatocytes
N2
N2
N2
N1
N1
Prophase II
Metaphase II
Anaphase II
Telophase II
e. Spermatids
+/+
f. Mature Spermatozoa
+/+
g. Late Spermatocytes
sh477/sh477

Figure 4.9 Histological comparison of spermatogenesis between ATM$^{+/+}$ and ATM$^{sh477/sh477}$ zebrafish at 3 months. a. H&E images indicating cell stage and morphology as primary germ cells progress through spermatogenesis. **a.** Spermatogonia A, scale bar represents 5 µm. **b.** Early spermatogonia B, scale bar represents 5 µm. **c.** Late spermatogonia B cells, scale bar represents 5 µm. **d.** Spermatocytes, scale bar represents 10 µm. **e.** Spermatids, scale bar represents 10 µm. **f.** Mature spermatozoa, scale bar represents 10 µm. **g.** Presumptive late spermatocytes, scale bar represents 10 µm. Identification of cell types and stages of spermatogenesis was aided by histological sections of testes on ZFIN (van der Van and Wester).

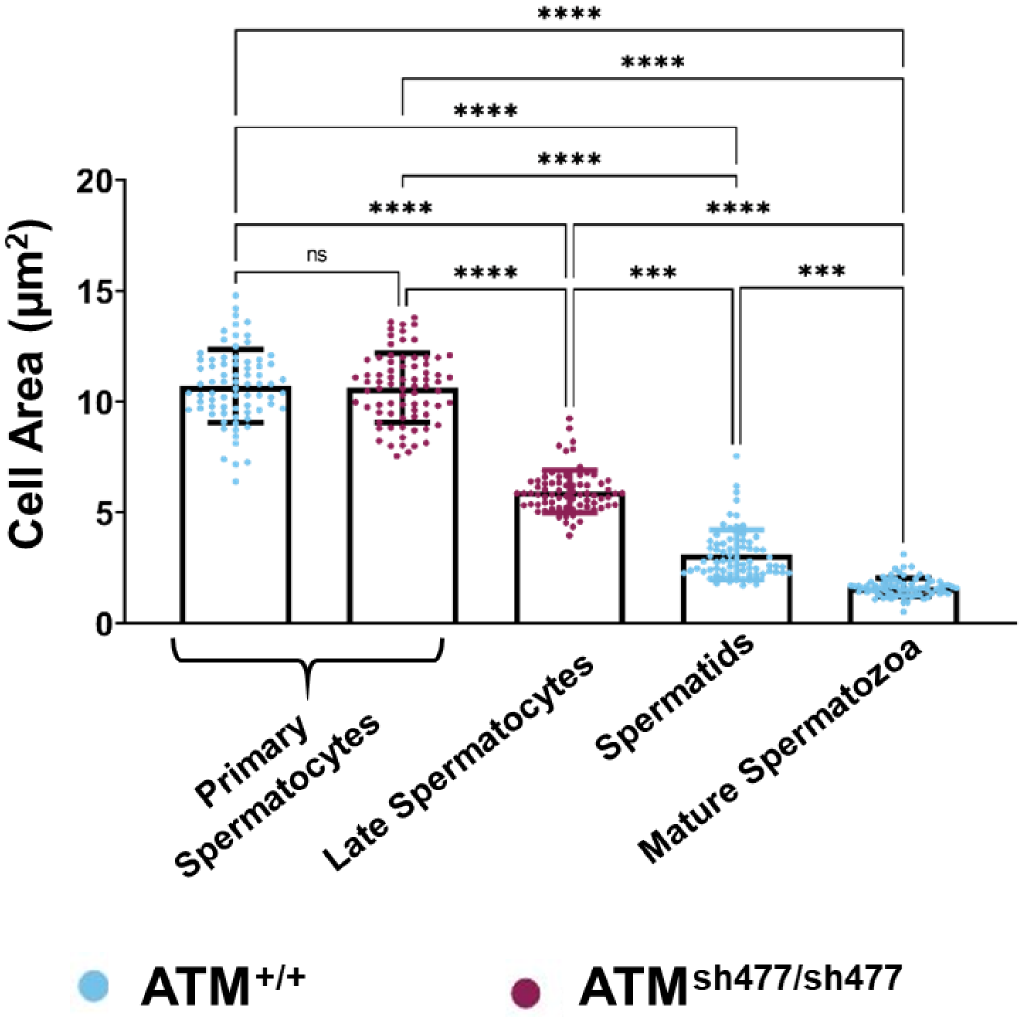

Figure 4.10 Comparison of spermatogenic cell size in ATM$^{+/+}$ and ATM$^{sh477/sh477}$ testes as a means of define cell type. The area of haematoxylin stained nucleus in cells in each of the developmental stages of spermatogenesis. Each data point represents the area of an individual cell (µm^{2}). Serological analysis was performed by measuring the haematoxylin stained area of 5 cells within a spermatocyst or seminiferous lumen, with 5 different spermatocysts or seminiferous lumens being analysed per fish. Data were analysed by Kruskal-Wallis test, with a *post hoc* Dunn's multiple comparisons test. ATM$^{+/+}$ N=3 fish, ATM$^{sh477/sh477}$ N=3 fish. Error bars represent mean +/- SD. Statistical Analysis can been seen in **appendix 4.3**.

4.2.2.4 The ATM Protein is Highly Expressed in Most Cell Types in the Zebrafish Testes

ATM$^{sh477/sh477}$ testes appear to have two distinct phenotypes, Sertoli cell hyperplasia and incomplete spermatogenesis. The reasons why loss of ATM in the testes causes dysregulated Sertoli cell growth, and the point at which spermatogenesis fails, were not known. To understand these two issues further we wanted to determine which cell types express ATM. Therefore, immunohistochemistry (IHC) for ATM was carried out on FFPE testes sections. The antibody used for IHC was the zATM1 antibody that is outlined in detail in **chapter 3 section 3.2.1.2**. In short, this antibody is a zebrafish specific polyclonal antibody, raised against amino acids 1-120 of the zebrafish ATM protein, upstream of the predicted premature stop codon introduced by the *sh477* mutation. Therefore, it should be noted that it might be capable of detecting both full-length ATM and a truncated ATM protein, if it exists in the mutant zebrafish.

a. Optimisation of the zATM1 Antibody for Immunohistochemistry

The zATM1 antibody required optimisation for IHC. As the makeup the testicular tissue was so different between ATM$^{+/+}$ and ATM$^{sh477/sh477}$ zebrafish, optimisations were carried out on both genotypes. Optimisation was performed for antigen retrieval of the antibody epitope and for antibody concentration (Shi et al., 2011).

Antigen retrieval was performed on FFPE slides of ATM$^{+/+}$ and ATM$^{sh477/sh477}$ zebrafish testes by heating the slides in buffer at either pH 6 or pH 9 to 125° C, at 300 psi, for 30 seconds in a pressure cooker. Slides were then stained with a Vectastain Elite ABC-HRP kit as per the protocol with either zATM1 (1:100), Rabbit immunoglobulin (RIgG), or no primary antibody. Antibody staining was then visualised by 3, 3'-diaminobenzidine (DAB) **(figure 4.11)**. Antibody staining was observed in both ATM$^{+/+}$ and ATM$^{sh477/sh477}$ zebrafish testes after antigen retrieval at both pH 6 and pH 9, but not in RIgG or no primary antibody samples. As a signal was detected in both ATM$^{+/+}$ and ATM$^{sh477/sh477}$ zebrafish, it suggests that either the staining is nonspecific, or a truncated mutant transcript may be expressed in the ATM mutants. However, the expression of a truncated protein in ATM$^{sh477/sh477}$ zebrafish is consistent with results observed from western blot analysis of zebrafish lysates in **chapter 3, section 3.2.1.2**. After antigen retrieval at pH 9, there appears to be much stronger detection of ATM throughout the sample, particularly in the basal membrane of the testicular cysts **(figure 4.11, ATM$^{+/+}$, right panel)** in comparison to the ATM$^{+/+}$ sample where antigen retrieval was performed at pH 6. Furthermore, staining at pH 9 appeared homogenous for all cell types in ATM$^{+/+}$ (with the exception of mature spermatozoa), which made distinguishing different cell types from each other more difficult. Interestingly, primary spermatocytes in ATM$^{+/+}$ and ATM$^{sh477/sh477}$ exhibit differential ATM expression after antigen retrieval at pH 9, with ATM$^{+/+}$ primary spermatocytes showing homogenous expression with other spermatic cells in the tissue and ATM$^{sh477/sh477}$ primary spermatocytes showing no ATM expression at all. Therefore, given that ATM was expressed in both genotypes but showed discrepancies between expression with pH 9 antigen retrieval, and the difficulty in discerning cell types with the higher pH, antigen retrieval was continued with pH 6.

ATM IHC on zebrafish testes was further optimised for antibody concentration. Following antigen retrieval at pH 6 as previously discussed, ATM$^{+/+}$ and ATM$^{sh477/sh477}$ FFPE tissue sections were probed with the zATM1 antibody at concentrations of 1:100, 1:200, 1:400, 1:800 and 1:1600, alongside a no primary antibody control **(figure 4.12)**. ATM expression was visualised with DAB as before. Staining of the tissue with zATM1 at a concentration of 1:400 appeared to give adequate signal, and therefore was chosen for continuing work.

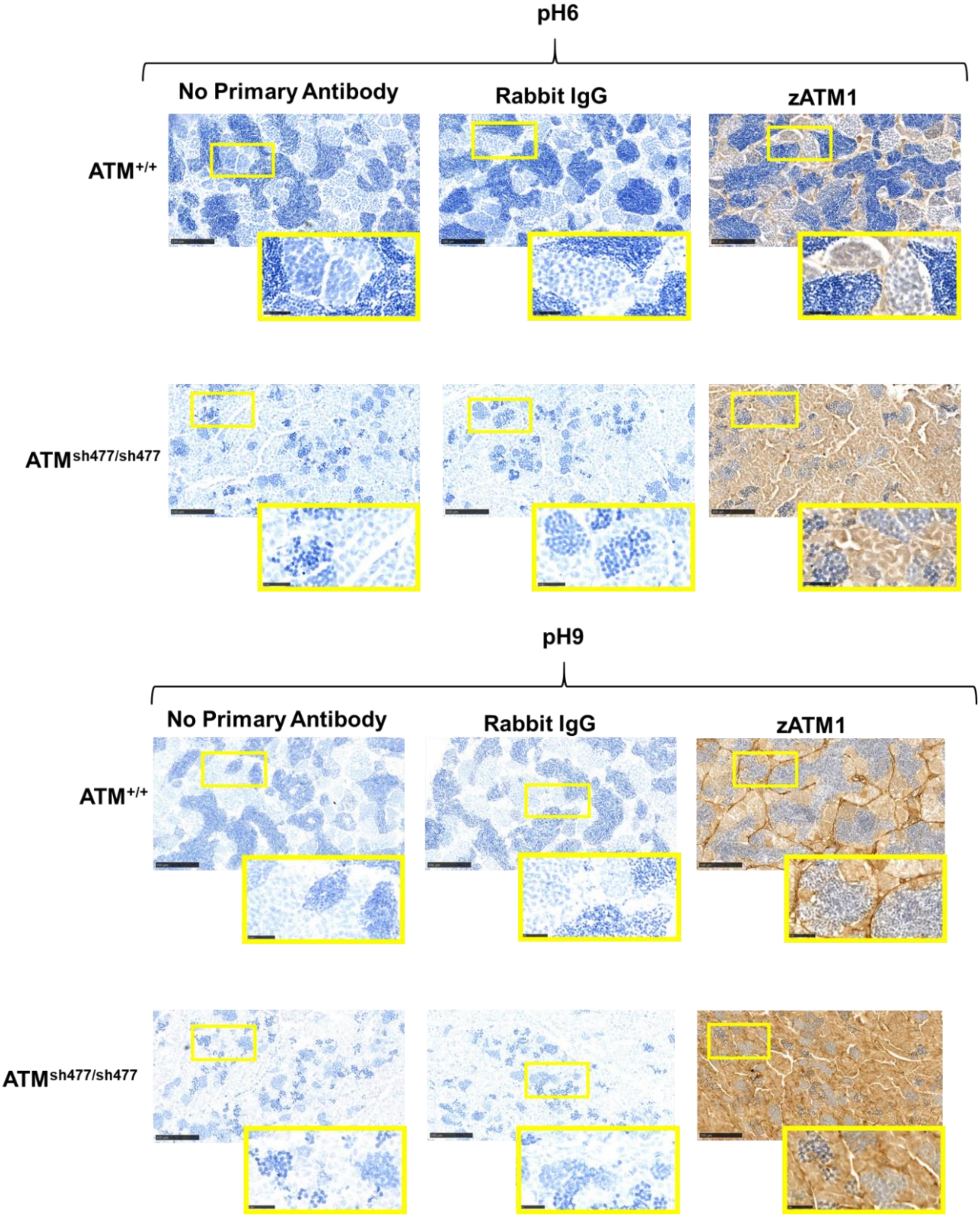
pH6
No Primary Antibody
Rabbit IgG
zATM1
ATM+/+
ATMsh477/sh477
pH9
No Primary Antibody
Rabbit IgG
zATM1
ATM+/+
ATMsh477/sh477

Figure 4.11 Optimisation of antigen retrieval for zATM1 IHC. FFPE sections of testes 5 µm of 12 month ATM$^{+/+}$ and ATM$^{sh477/sh477}$ were optimised for antigen retrieval at pH6 and pH9 by incubating them in the relevant buffer in a pressure at 125° C, at 300 psi for 30 seconds. The slides were then probed with zATM1 at 1:100 or RIgG and a no antibody control. Scale bars on larger images represents 100 µm, yellow box indicates the magnified region shown in the yellow outset, while scale bars on yellow outsets represent 25 µm.

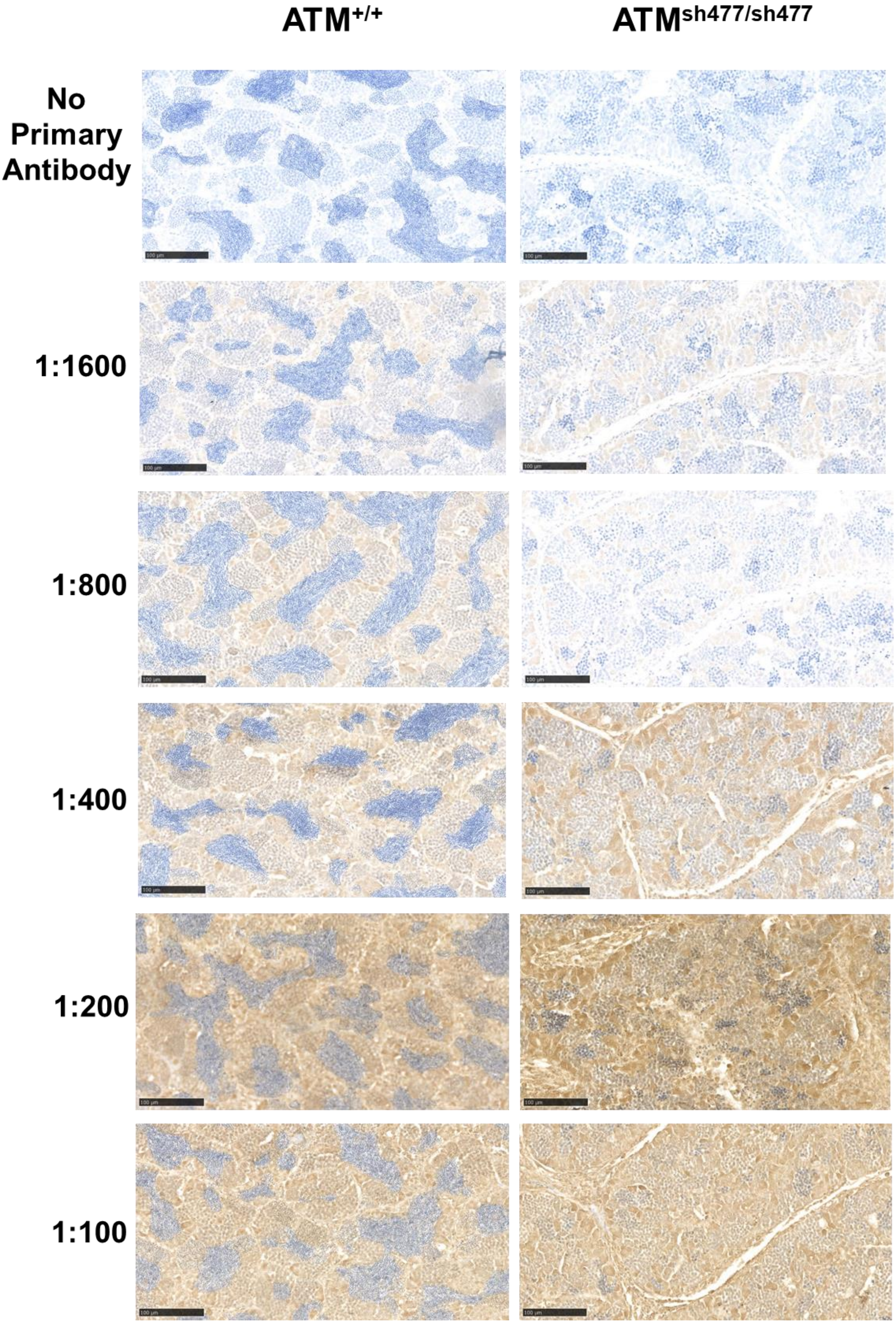
ATM+/+
ATMsh477/sh477
No Primary Antibody
1:1600
1:800
1:400
1:200
1:100

Figure 4.12 Optimisation of zATM1 for IHC on zebrafish FFPE testes sections. Zebrafish FFPE sections (5 µm) were prepared for antibody staining by antigen retrieval at pH 6, as optimised in figure 4.9. Antibody was diluted to 1:100, 1:200, 1:400, 1:800 and 1:1600 with a no primary antibody control. Scale bars represent 100 µm.

b. Immunohistochemistry of ATM in $ATM^{+/+}$ and $ATM^{sh47/sh477}$ Testes

Testes from both $ATM^{+/+}$ and $ATM^{sh477/sh477}$ zebrafish exhibit strong ATM staining throughout the testicular tissue **(figure 4.13)**, and most cell types in testes showed distinct ATM staining. Spermatogonium A and spermatogonium B cells **(figure 4.14 a, b and c)** in both genotypes exhibited robust ATM staining in both the nucleus and cytoplasm. The nuclear envelope had particularly dense staining, along with heavily stained spots in the nucleus. ATM staining in primary spermatocytes **(figure 4.14 d)** becomes less pronounced, and is mainly localised to the nucleus, where it appears granular, perhaps indicating its localisation at specific points along chromosomes. In $ATM^{+/+}$ testes, ATM is expressed in developing germ cells right up until the spermatid stage of development, where it appears to be localised to heavily stained areas within the nucleus **(figure 4.14 f)**. Once cells have developed into mature spermatozoa, ATM expression appears to have been lost **(figure 4.14 g)**. Interestingly in $ATM^{sh477/sh477}$ testes, presumptive late spermatocytes **(figure 4.14 e)**, which are predicted to be at a stage of development between primary spermatocytes and spermatids, have lost their ATM expression. This may indicate that ATM is not required for this stage of development, or that these cells do not actually represent a stage of spermatogenic development, and that their condensed morphology and lack of ATM may be due to them dying and being cleared. ATM was also expressed diffusely throughout Sertoli cells **(figure 4.14 h)**, and in Leydig cell cytoplasm **(figure 4.14 i)** in both genotypes.

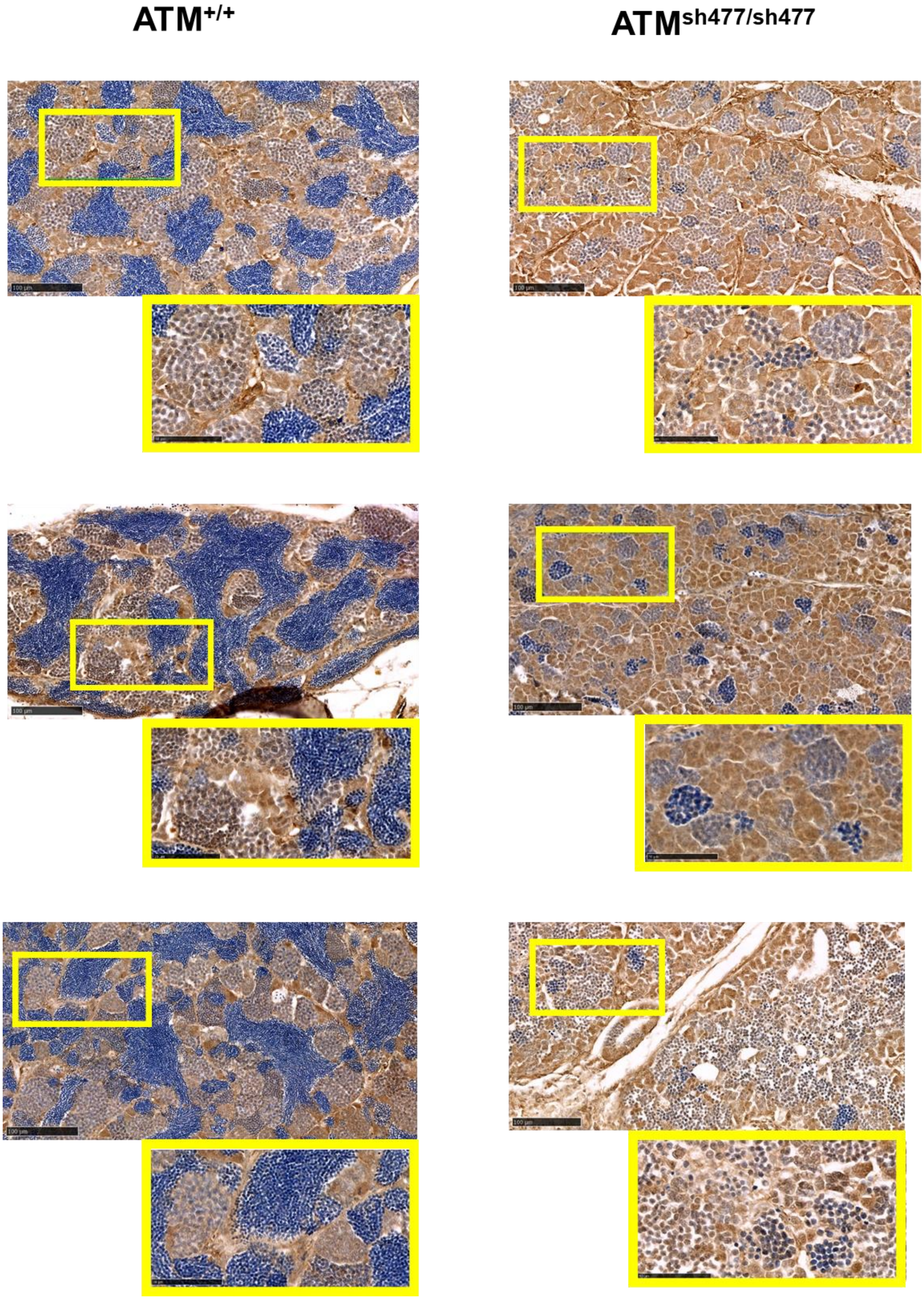

Figure 4.13 Immunohistochemistry staining with the zATM1 antibody on ATM$^{+/+}$ and ATM$^{sh477/sh477}$ testes. FFPE tissue sections (5 µm) from 12-month zebrafish were stained with the zATM1 antibody overnight at 4° C at a concentration of 1:400. Antibody staining was visualised by DAB. ATM$^{+/+}$ (left panel) N=3 fish, ATM$^{sh477/sh477}$ (right panel) N=3 fish. Scale bars represent 100 µm. Yellow box indicates the magnified region shown in the yellow outsets. Scale bars represent 50 µm.

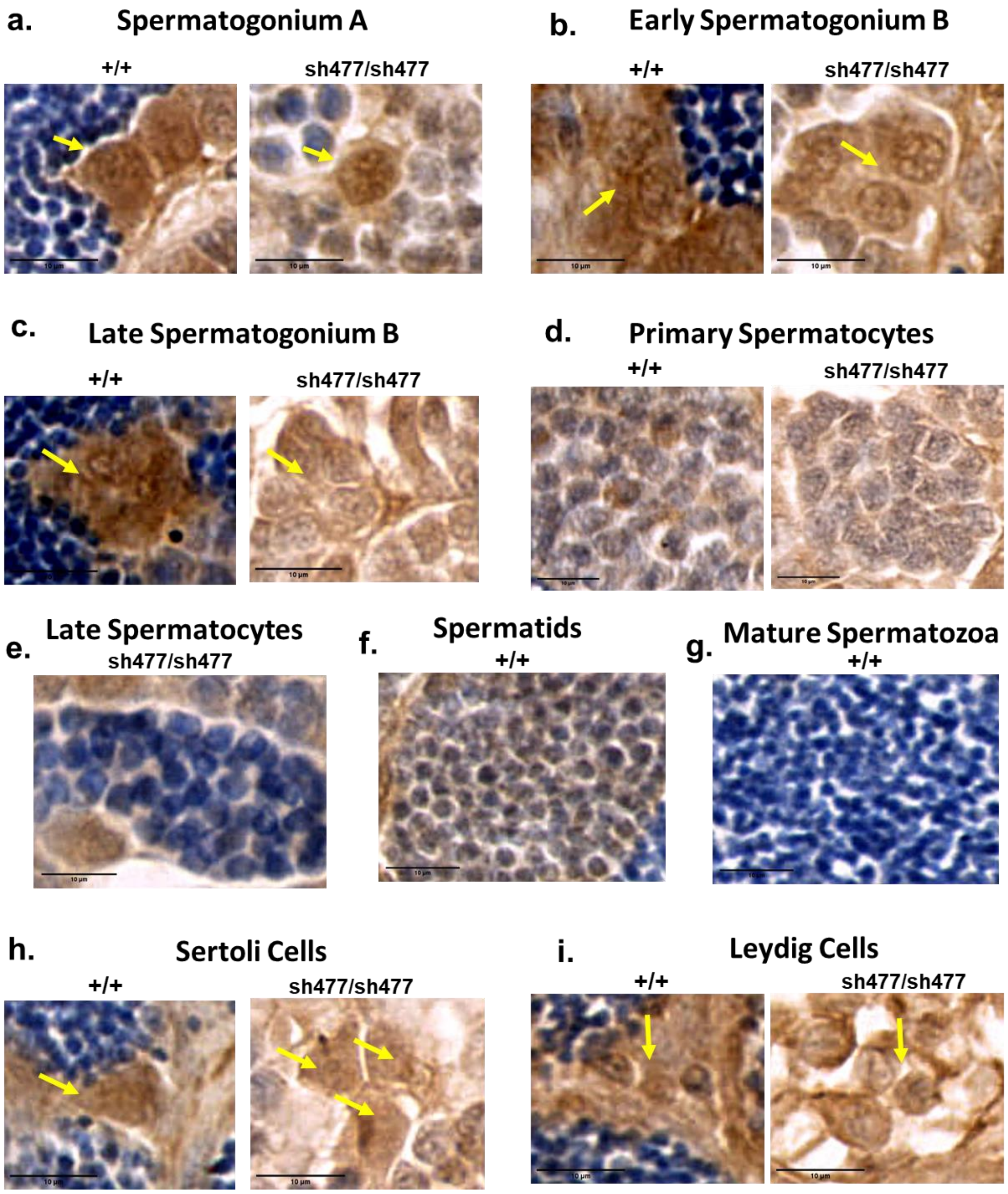
a.
Spermatogonium A
+/+
sh477/sh477
b.
Early Spermatogonium B
+/+
sh477/sh477
c.
Late Spermatogonium B
+/+
sh477/sh477
d.
Primary Spermatocytes
+/+
sh477/sh477
e.
Late Spermatocytes
sh477/sh477
f.
Spermatids
+/+
g.
Mature Spermatozoa
+/+
h.
Sertoli Cells
+/+
sh477/sh477
i.
Leydig Cells
+/+
sh477/sh477
10 µm

Figure 4.14 Cell specific staining of ATM. Magnified images of specific cells from figure 4.11 above **a.** Spermatogonium A **b.** Early spermatogonium B **c.** Late spermatogonium B **d.** Primary spermatocytes **e.** ATM$^{sh477/sh477}$ late spermatocytes **f.** ATM$^{+/+}$ spermatids **g.** ATM$^{+/+}$ mature spermatozoa. **h.** Sertoli Cells. **i.** Leydig cells. Scale bar in all images represents 10 µm.

4.3 Discussion

The results presented in this chapter indicate that ATM$^{sh477/sh477}$ zebrafish undergo incomplete spermatogenesis similar to AT patients and other vertebrate models of AT. This incomplete spermatogenesis is also observed in other zebrafish that are deficient in HR proteins. Interestingly, ATM$^{sh477/sh477}$ zebrafish also exhibit Sertoli cell neoplasia in the testes, which has not been reported in other AT models, nor have there been any case reports of this occurring in AT patients. This has however been previously reported in brca2 deficient zebrafish.

4.3.1 Loss of ATM Recapitulates Phenotypes Observed in Other Zebrafish KO Models of DNA damage Repair Genes

4.3.1.1 Loss of HR Genes in Zebrafish Results in Incomplete Spermatogenesis due to Failure to Complete Meiosis

Results presented in this chapter show that spermatogenesis in ATM$^{sh477/sh477}$ zebrafish is stalled. Given the relative size of the most developed spermatogenic cells in ATM mutants compared to other developing spermatogenic cells in both mutants and wild type testes **(figure 4.9 and 4.10)**, this suggests that spermatic development in these fish may halt as they are undergoing meiosis. Meiosis is an evolutionary conserved mechanism of cell division in sexually reproducing species that produces haploid gametes from diploid cells. A key element of meiosis is homologous recombination, which occurs when genetic information is swapped between homologous chromatids. This swapping of genetic information facilitates genetic variation between progeny. HR takes place in prophase I of meiosis, which is the longest phase in meiosis and can take days to weeks in mammals (Cohen et al., 2006). Prophase I can be subsequently be split into five sub stages. The sub stages, along with known functions of ATM during each of the sub stages, are presented in detail in **table 4.1**.

Table 4.1 Stages of Prophase I

Prophase I stages	Functional Events	Cytological Appearance
Leptotene Stage (leptonema)	Diffuse tetraploid chromatin condenses and homologue pairing starts. The synaptonemal complex (a large multi-protein complex) begins to assemble along the homologous pairs and by the end of the leptotene stage it forms a backbone along each chromosome around which the chromatids are tightly condensed. Spo11 forms excessive ds breaks in specific DNA 'hot spots', which is regulated by ATM locally at the site of the damage in a negative feedback mechanism which is not yet wholly understood. ATM also directs repair of most of these SPO11 mediated breaks by activating the DDR, particularly RAD51 and DMC1, before allowing the cell to enter the next stage of prophase I, where generally only ds breaks for one crossover event per chromosomal tetrad remains. In addition to activating the DDR locally at the point of ds DNA breaks, the presences of ATM at these sites is thought to confer some type of steric hindrance to stop too many breaks occurring close together. Chromosomes become tethered to the nuclear membrane through their telomeres, a process which is mediated by ATM. This tethering of the chromosomes to the nuclear matrix allows movement of the chromosome ends through the cytoskeleton, to aid in homologues pairing, and later separating of homologous chromosomes and sister chromatids during cell division. The capping of telomeres by ATM also prevents end to end joining of chromatids. ATM prevents cell cycle progression mediated by p53 and p21 activation if too many ds breaks persist.	The condensed chromatin forms thread like structures.
Zygotene Stage	Homologous chromosomes continue to align and are tethered together by the synaptonemal complex (synapsis). This tethering proceeds in a zipper like fashion so that at the end of the Zygotene stage homologous chromosomes are synapsed along their entire length down to matching base pairs.	Chromosomes form a bouquet where the centrosome of the chromosome is in the middle of the cell and the chromosome ends spread out along the nuclear envelope. Gives the impression of petals fanning out from the central part of the flower. This progresses to an umbrella conformation where the central part of the chromosome moves to a nuclear pole.
Pachytene Stage	Crossover of homologous chromatids occurs, after which all dsDNA breaks are repaired.	Chromatin continues to condense so the nucleus becomes highly compacted.
Diplotene Stage	The chromatids condense further and the synaptonemal complex beings to disintegrate, with homologous chromosomes beginning to repel each other. However, they are still held together at the points of recombination by chiasmata to keep the chromosome together until Anaphase I.	Chromosomes condense further
Diakinesis Stage	Loss of the nuclear membrane and formation of meiotic spindles.	Chromosomes again condense further and the tetraploid stands and points of cross over may be visible.

(Cohen et al., 2006, Cohen and Pollard, 2001, Bolcun-Filas and Handel, 2018, Keeney et al., 2014)

Three definitive prophase I mutant zebrafish models, *its, imo* and *isa,* which were identified from an ENU mutagenesis screen, have been characterised and demonstrate stalled spermatogenic development in prophase I of meiosis. The *its* mutant, which was later determined to be caused by mutation to the *sycp2* gene, whose protein product comprises an integral part of the synaptonemal complex, fails to progress into leptonema, while spermatogenesis in the *imo* and *isa* mutants fail to progress beyond the zygotene stage (Saito et al., 2011, Takemoto et al., 2020). These mutants exhibit histological similarities to the ATM$^{sh477/sh477}$ mutant where spermatogonia and primary spermatocytes are visible but they do not contain spermatids or mature spermatozoa (Saito et al., 2011). The most advanced developmental stage of spermatic development in these mutants are cells smaller than primary spermatocytes with small condensed nuclei, similar to what is observed here in ATM$^{sh477/sh477}$ testes. While these mutants are not HR mutants, they do serve to further indicated the morphology of zebrafish spermatogenic development that has stalled at prophase I.

However, a number of other zebrafish with mutations in DDR genes, particularly HR genes, have been characterised, and their testicular phenotypes are strikingly similar to the *its*, *imo* and *isa* mutants, and to ATM$^{sh477/sh477}$ zebrafish described here. The best described of these HR mutants are *Rad51* and *brca2* KO zebrafish (Botthof et al., 2017, Rodríguez-Marí et al., 2011, Shive et al., 2010). These two proteins function in the same signalling pathway downstream of ATM to repair SPO11 mediated ds breaks during HR. In this pathway, ATM, acting locally at the site of dsDNA breaks, recruits BRCA2 through PALB2 to the 3'ss overhang of the ds break. Activated BRAC2 stabilises Rad51 monomers, and shuttles them to the point of the 3' overhang reviewed (Sun et al., 2020, Woo et al., 2021). Both *Rad51* and *brca2* KO mutants exhibit almost identical defects in spermatogenic development to ATM$^{sh477/sh477}$ mutants, where their luminal space is devoid of mature spermatozoa and there are no spermatids present. Furthermore, they both exhibit clusters of primary spermatocytes in spermatocysts comparable to ATM$^{sh477/sh477}$ zebrafish and most critically, the most developed spermatic cells exhibited by these fish are small round hyperchromatic cells with condensed nuclei that are indistinguishable from the cells we have termed late spermatocytes in ATM$^{sh477/sh477}$ testes (Botthof et al., 2017, Rodríguez-Marí et al., 2011, Shive et al., 2010). Investigations of these hyperchromatic cells in the *brca2* mutants have shown them to be pyknotic cells undergoing apoptosis by caspase 3 and TUNEL staining (Rodríguez-Marí et al., 2011, Shive et al., 2010). As ATM, Rad51 and BRCA2 activation are all sequential steps in the same functional pathway, it is likely that these condensed hyperchromatic cells in Rad51 and ATM mutants are also pyknotic cells undergoing apoptosis, and do not represent any typical morphology of cells undergoing normal spermatogenesis. The similarly hyperchromatic and condensed cells in the *its* and *isa* prophase I mutants were also caspase 3 and TUNEL positive (Saito et al., 2011).

We have not experimentally investigated the exact point in meiosis in which spermatogenesis fails in ATM$^{sh477/sh477}$ zebrafish. However, the similarities between prophase I mutant testes and ATM$^{sh477/sh477}$ testes strongly indicate that spermatogenic failure in these is likely to be in prophase I. Furthermore, given the near identical spermatic histology between ATM, brca2 and Rad51 mutant testes, and that their shared functional pathway occurs primarily during the leptotene stage of prophase I **(table 4.1)**, it is likely that anomalies in the mutant testes occur at this stage. However, brca2$^{-/-}$ spermatogenesis was shown to continue past leptonema and fail at the pachytene stages of prophase I (Rodríguez-Marí et al., 2011). Therefore, while the aberrations may occur at leptonema, halting of the cell cycle and mitigation of the potential damage may not occur until the pachytene checkpoint, which is a critical checkpoint that appraises proper homolog-synapsis and dsDNA repair, and is primarily mediated by ATR (Cooper et al., 2014). However, further characterisation of spermatogenesis in these mutants in required to confirm this.

4.3.1.2 Disruption of Sertoli Cell Homeostatic Proliferation is a Feature of Loss of HR Genes in Zebrafish

Sertoli cells are nurse cells present in the testes that provide structural, nutrient and molecular support for developing spermatic cells. Here we describe a progressive and aggressive Sertoli cell neoplasia in ATM deficient testes

(section 4.2.2.1). It is not clear if these Sertoli cell proliferations are because of the failed spermatogenesis, or if it is the result of an entirely different and unrelated somatic cell pathology. Testicular organisation and Sertoli cell proliferation and regulation is quite different in teleosts compared to mammals. In mammals, Sertoli cells proliferate until the onset of puberty, where there is then a defined number of post mitotic Sertoli cells resident in the testes that will regulate spermatogenesis for life (França et al., 2016). However, in zebrafish, Sertoli cells remain mitotically active throughout the lifespan, and an individual Sertoli cell is transient rather than resident. Two pathways mediate Sertoli cell proliferation in fish. The first is the proliferation and differentiation of a new Sertoli cell from a Sertoli progenitor. The new Sertoli cell's cytoplasmic projections surround an undifferentiated spermatogonium A cell to create a new spermatocyst or niche for the developing sperm cells. The differentiation of an undifferentiated spermatogonium A cell to a mitotically active one, and the differentiation of a new Sertoli cell niche, occur together.

The second means of Sertoli cell proliferation is in conjunction with the developing spermatocyst, in which new Sertoli cells arise from the mitotic division of Sertoli cells already in place to meet the needs of the expanding niche. The number of Sertoli cells associated with a specific cyst steadily increases from spermatogonium cells up until pachytene stage in primary spermatocytes (França et al., 2016, Schulz et al., 2015, França et al., 2015, Schulz et al., 2005). The germ cell niche comprises developing spermatic cells and somatic Sertoli cells. The developing gametes rely on Sertoli cells for nutrients and to secrete signals that regulate spermatogenesis, and similarly Sertoli cell homeostasis relies on signals from the developing germ cells as they only reach terminal differentiation and become post mitotic once meiosis has taken place (Leal et al., 2009, Schulz et al., 2015, Schulz et al., 2005). After meiosis and once spermiogenesis commences, the number of Sertoli cells associated with a specific cyst decreases, until finally the spermatocyst opens to allow mature spermatozoa into the luminal space (França et al., 2015, Leal et al., 2009, Schulz et al., 2005).

A similar neoplasia to that we describe in ATM mutants was also reported in *brca2* mutant zebrafish (Shive et al., 2010, Rodríguez-Marí et al., 2011). Neoplasia in *brca2*$^{-/-}$ testes were found to be comprised of Sertoli cells and proliferating spermatogonia. While we have determined the neoplasia in ATM$^{sh477/sh477}$ zebrafish to be primarily comprised of Sertoli cells, it may be possible that spermatogonia cells also contribute, but were not readily discernible in the overgrown testicular tissue at 12 months. Work to investigate this further is outlined below in **section 4.3.4.2**. Investigations of the testes of Rad51 mutants were carried out at 4 months and no testicular neoplasia was reported (Botthof et al., 2017). However, this may have been too early to detect neoplasia, as we failed to observe increased Sertoli cells at 3 months in ATM mutant zebrafish. The paper describing the effects of Rad51 KO in zebrafish provides only limited testicular histology, however after examination of what is reported, we tentatively believe Sertoli cell proliferation may also be present in the Rad51 model, as there appears to be growth of irregularly shaped, eosinophilic cells from the basal membrane towards the luminal space, that are not present in the wild type sample.

It is plausible that the proliferation of Sertoli cells in both ATM$^{sh477/sh477}$ and brca2$^{-/-}$ zebrafish occurs as a secondary event, with the failure of spermatogenesis being the primary event. As outlined above, in fish Sertoli cells proliferate within the developing cyst and only become post mitotic after meiosis has occurred in the spermatogenic cells (Schulz et al., 2015, Schulz et al., 2005, Leal et al., 2009). As primary spermatocytes in ATM$^{sh477/sh477}$ and Brca2$^{-/-}$ zebrafish do not complete meiosis, Sertoli cell proliferation may continue unchecked. *Dead end (dnd)* is a gene which is essential for primordial germ cell development in mice and zebrafish. Ablation of *dnd* expression by injection of a *dnd* morpholino at the embryonic stage produces sterile male adults (Slanchev et al., 2005). In common with Brac2 and ATM mutants, *dnd* KD morphants also exhibit Sertoli cell overgrowth, indicating that it is the absence of mature spermatozoa that causes proliferation of the Sertoli cells, and that it is not a direct result of loss of ATM (Rodríguez-Marí et al., 2011). However, the *its*, *ims* and *isa* mutants do not report any neoplasia (Zhou et al., 2018, Saito et al., 2011).

While the literature suggests that lack of mature sperm are the result of Sertoli cell proliferation seen in ATM$^{sh477/sh477}$ testes, it should be considered that it may also be directly due to loss of ATM. Evidence in support of this is that ATM is highly expressed in zebrafish Sertoli cells **(figure 4.14 h)**. It is also highly expressed in Sertoli cells of mouse and humans, along with other DNA repair proteins, and these are not expressed in other somatic cell types in the testes (Ahmed et al., 2009, Scherthan et al., 2000). As Sertoli cells in zebrafish are highly mitotic and ATM is a key regulator of mitosis, particularly at cell cycle checkpoints (Bihani and Hinds, 2011, Boohaker et al., 2016, Yang et al., 2011a), loss of ATM may cause dysregulated proliferation of these cells. However, as almost all cells in the zebrafish undergo mitosis during the embryonic stage, it is likely that if loss of ATM had an effect on the mitosis of somatic cells in zebrafish it would manifest with defects in many tissues. Furthermore, Sertoli cells in mice and humans are not mitotic. However, while ATM and other DNA repair proteins such as PARP1 and XRCC1 were expressed in mouse Sertoli cells, other proteins crucial for the repair of damaged DNA, such as Rad51 and H2AX, are not present, although, based on comet assays they are capable of DNA repair (Ahmed et al., 2009). Therefore, at present the function of ATM in Sertoli cells is unknown, as is the exact mechanism of DNA repair that occurs in the cells. Furthermore, given the differences in mouse and zebrafish Sertoli cells, the function of ATM in this cell type between these two species may be different.

4.3.2 ATM$^{sh477/sh477}$ Zebrafish May Express a Truncated ATM Protein but Exhibit Phenotypes that are Consistent with loss of ATM Activity

In the previous chapter, we have shown that ATM$^{sh477/sh477}$ zebrafish have a 5 bp deletion mutation in exon 6, which was predicted to cause a downstream premature stop codon **(chapter 3, section 3.2.1.1, figure 3.1)**. We have also shown that this premature stop codon does not cause mutant ATM mRNA to undergo NMD **(chapter 3, section 3.2.1.1, figure 3.2)**. Therefore, it was expected that the mutant mRNA would undergo translation to generate a truncated protein that would be misfolded and degraded, or a truncated non-functional ATM protein lacking both protein-protein binding domains and the essential kinase domain **(see chapter 1, section 1.2.2)**. Attempts had been made to show that ATM$^{sh477/sh477}$ zebrafish were knockouts for the ATM protein through western blot analysis, using a zebrafish specific ATM antibody that we had raised to the first 120 amino acids of the protein upstream of the predicted stop codon in the mutants **(chapter 3, section 3.2.1.2, figure 3.3**. The aim was to show the absence of full-length ATM in mutant zebrafish, with expression of the protein in wild type controls. Alternatively, we may have detected the truncated protein in ATM$^{sh477/sh477}$ zebrafish lysates **(chapter 3, section 3.2.1.2, figure 3.5 b)**. Detection of full length ATM by western blot was not possible, however low molecular weight immunoreactive bands were identified.

In this chapter, we attempted to optimise IHC for detection of ATM expression, and ATM expression was detected in both ATM$^{+/+}$ and ATM$^{sh477/sh477}$ zebrafish testes. While this is by no means definitive, it does support the generation of a truncated ATM protein in ATM mutants and is consistent with results from western blot analysis. Alternatively, the staining observed in both genotypes could be non-specific staining. However, given that there is stage specific staining in the wild type testes, where there is signal in developing spermatogenic cells up to the last known point of ATM function in primary spermatocytes, but the signal progressively decreases as spermatids develop, and is absent in mature spermatozoa, strongly indicates that the antibody is specific for ATM detection by IHC. A key difference in immunological protein detection between western blot and IHC is that the SDS-PAGE gels used in western blot analysis are denaturing to the protein. The antigen to which the antibody was raised is relatively large and is likely to have both secondary and tertiary structure in its native form **(chapter 1, section 3.2.1.2, figure 3.3)**; therefore, the denaturing nature of an SDS-PAGE gel may cause the epitope to be lost. An advantage of IHC is that it does not cause denaturisation of the protein and keeps the tertiary structure of the proteins intact. Therefore, while there was probable ATM specific staining in ATM$^{sh477/sh477}$ zebrafish testis, they are likely KO for ATM activity as they exhibit phenotypes consistent with loss of ATM, such as stalled spermatogenesis, which is recapitulated in all vertebrate AT models **(chapter 1 section 1.3)**. Furthermore, they also exhibit phenotypes consistent with disrupted HR in zebrafish, such as sex reversal **(chapter 3, section 3.2.2)**, stalled spermatogenesis, and testicular neoplasms (Mamrak et al., 2017, Ramanagoudr-Bhojappa et al., 2018, Rodríguez-Marí et al., 2011, Botthof et al., 2017, Liu et al., 2003).

4.3.3 ATM is an Essential Component of Meiosis and Loss of ATM Causes Infertility in Animal Models of AT

Infertility due to failed gametogenesis is a feature of AT and is recapitulated in rodent models of AT **(see chapter 1 section 1.3)**. It is not known exactly at what point spermatogenesis is stalled in the rat model of AT, as in-depth analysis was not performed. Still, they report similar findings to those presented in this chapter, that ATM-deficient testes have developing germ cells up to spermatocytes, but exhibit no spermatids or mature spermatozoa (Quek et al., 2017a, Quek et al., 2017b).

Spermatogenesis defects in ATM deficient mice have been well characterised. ATM is highly expressed in mouse testes. Its expression is largely localised to Sertoli cells in agreement with the expression observed in zebrafish Sertoli cells. In mice, granular expression of ATM was also found in primary spermatocytes and localised to early spermatids, but not late spermatids or mature spermatozoa, again supporting what was observed in ATM staining of zebrafish testes **(figure 4.13 and 4.14)** (Scherthan et al., 2000).

In mouse models of AT, spermatogenesis is stalled at leptonema with only a few spermatocytes (2%) progressing as far as the zygotene stage. These stalled spermatocytes showed reduced expression and mislocalisation of ATR and downstream ATM targets involved in DNA repair, such as DMC1 and RAD51 (Barlow et al., 1998, Pandita et al., 1999, Barlow et al., 1997). SPO11 induces many ds breaks per chromosome during leptonema **(see table 4.1)**, however not all these breaks are required and usually only one crossover event is required per chromosome tetrad, therefore these excessive ds breaks need to be repaired before spermatogenesis can progress (Cooper et al., 2014). The reduced expression and mislocalisation of HR specific DNA repair proteins in ATM deficient mice indicates that cell cycle progression may be halted in leptonema due to these excessive SPO11 induced unrepaired DNA breaks. Stalling of spermatogenesis at this stage is due to halting of the cell cycle, and is supported by the evidence that there is increased expression of the cell cycle proteins p53 and p21in ATM$^{-/-}$ mouse testes, and that double knockout of p53/ATM and p21/ATM partially restores spermatogenesis and allows it to progress to the pachytene stage (Barlow et al., 1997). In addition to managing the repair of DNA breaks in spermatogenesis, ATM may also be involved in telomere tethering to the nuclear matrix and envelope. During meiosis chromosomes are tethered to the nuclear matrix through their telomeres, which move along the nuclear envelope as a means of aligning chromosomes to correctly synapse with each other. ATM$^{-/-}$ mice exhibited abnormal telomere clustering as well as chromosomal rearrangements (Pandita et al., 1999), which are thought to be contributing factors to the aberrant spermatogenesis. From the results presented in this chapter it is not yet clear at which point in ATM$^{sh477/sh477}$ zebrafish testes spermatogenesis is stalled, however, this could be resolved by utilising immunofluorescence confocal microscopy to examine expression and localisation of meiotic associated proteins during spermatogenesis in these fish. Possible investigations that could be undertaken are discussed below in **section 4.3.4.1**.

4.3.4 Future Work to Further Characterise the Testicular Phenotype in ATM$^{sh477/sh477}$ Zebrafish

4.3.4.1 Determination of When Spermatogenesis Fails in ATM$^{sh477/sh477}$ Zebrafish

Although results presented in this chapter indicate that spermatogenesis is stalled in meiosis in ATM$^{sh477/sh477}$, and these results strongly align with the stalling of spermatogenesis in brac2 and Rad51 KO zebrafish, we have not shown experimentally that this is the case, or when in meiosis spermatogenesis is stalled. The localisation of Sycp3, a key component of the synaptonemal complex, has a predictable localisation and multimeric structure as it moves though the phases of meiosis and has been effectively used to characterise the progression of prophase I in zebrafish previously (Saito et al., 2011). Staining of zebrafish testes with Sycp3 in conjunction with monitoring the resolution of Rad51 foci (Vierstraete et al., 2017) in spermatocytes, particularly with the use of confocal microscopy, could accurately define when in prophase I meiosis has gone awry in ATM$^{sh477/sh477}$ zebrafish.

Furthermore, the literature suggests that the cells we have termed late spermatocytes in ATM$^{sh477/sh477}$ testes are cells with highly condensed nuclei undergoing apoptosis (Rodríguez-Marí et al., 2011, Shive et al., 2010). Similar to experiments carried out in the brca2 and prophase I mutants, caspase 3 and TUNEL staining could be undertaken to determine if the same is true of the cells observed here (Shive et al., 2010, Rodríguez-Marí et al., 2011, Saito et al., 2011).

4.3.4.2 Further Investigations into the Testicular Neoplasia

The testicular neoplasms found in Brca2$^{-/-}$ testes were shown to be a mixture of spermatogonia and Sertoli cells (Shive et al., 2010, Rodríguez-Marí et al., 2011), while we have determined the neoplasms in ATM$^{sh477/sh477}$ testes to be primarily due to Sertoli cell proliferation. Our characterisation was carried out at 3 months, when aberrant proliferation was only beginning, and at 12 months where distinguishing between different cell types was more challenging, while characterisation of Brca2$^{-/-}$ testes was carried out at primarily at 6 months (Rodríguez-Marí et al., 2011). The difference in ages, or areas of testes examined, may account for the different profile of the neoplasia. Furthermore, no infiltration of the neoplasia to surrounding tissue was observed at 6 months in the Brca2 mutants or *dnd* KD morphants, nor was it observed at 12 months in the ATM mutants. However, when the *dnd* KD morphants were analysed at 18 months, infiltration of the surrounding tissue was observed. Investigators of the Brca2 mutants suggest that the analysis of the Brca2 mutant at the later stage of 18 months may also exhibit this tissue infiltration (Rodríguez-Marí et al., 2011), and we agree that this could also be the case with ATM$^{sh477/sh477}$ zebrafish. Therefore, further histological investigations of ATM$^{sh477/sh477}$ testes could be carried out at 6 months to determine if there is a spermatogonium cell contribution to the neoplasms, and at 18 months to determine if there is infiltration of the neoplasm to the surrounding tissue. Furthermore, vasa is a germ cell specific molecular marker (Yoon et al., 1997), and its expression and localisation in testicular tissue may be able to provide some clarity on whether there is spermatogonium contribution to the neoplasm in ATM$^{sh477/sh477}$ testes.

It is not yet clear whether the neoplasms are a direct result of loss of ATM or if they are secondary to the cessation of meiosis. The determination of which pathway of Sertoli cell proliferation has become dysregulated may shed some light on this. In zebrafish, differentiation of new Sertoli cells in conjunction with spermatogonia A to create new spermatocysts is governed by triiodothyronine (T3) and IGF-3 signalling (Wang et al., 2008, Morais et al., 2013). Laser capture microdissection of sectioned FFPE tissue, followed by gene expression analysis for these and other genes, may identify which pathway has become dysregulated.

Chapter 5

Behavioural Analysis of ATM$^{sh477/sh477}$ Zebrafish

5.1 Introduction

One of the biggest barriers to quality of life in AT patients is progressive ataxia caused by cerebellar degeneration. In addition to affecting quality of life, it also has an impact on disease mortality, as at the late stages of disease progression, difficulties in chewing and swallowing food leads to aspirations into the lungs, and an increase in respiratory infections. Therefore, understanding the mechanisms by which cerebellar degeneration occurs is of vital importance in developing therapeutic interventions for AT patients. Despite this importance, there is still no model system that accurately recapitulates the human neurodegenerative phenotype **(see chapter 1, section 1.3),** leaving an epistemic gap in our understanding of these disease mechanisms **(see chapter 1, section 1.2.4.5)**.

To determine whether the zebrafish ATM$^{sh477/sh477}$ model is a useful tool in AT research, it is important to determine if it can recapitulate any neurological phenotype. Zebrafish behaviour is increasingly being used to study neurodevelopmental and neurodegenerative phenotypes, and their behaviour patterns are being used as high throughput readouts in drug discovery (Norton and Bally-Cuif, 2010, Kokel and Peterson, 2008). Hence, we investigated whether ATM$^{sh477/sh477}$ zebrafish exhibited any behavioural abnormalities that would suggest cerebellar dysfunction. Analysis of zebrafish swimming behaviour can also serve as a useful indicator of other phenotypes (Borges et al., 2016, Miller et al., 2019, Deakin et al., 2019) that may be caused by loss of ATM. Furthermore, histological examination of adult zebrafish cerebella was undertaken to investigate whether there may be abnormalities that do not present with a behavioural phenotype.

5.2 Results

5.2.1 ATM$^{sh477/sh477}$ Zebrafish Show no Gross Defects in Larval Swimming

5.2.1.1 ATM$^{sh477/sh477}$ Larvae Exhibit no Swimming Abnormalities at 5 dpf

AT typically presents with onset of ataxia at approximately 3 years old (Boder and Sedgewick, 1958, Shaikh et al., 2013); therefore, we investigated whether the ATM$^{sh477/sh477}$ fish also exhibit an early behavioural phenotype. As development of zebrafish embryos is external from the mother and occurs at a much faster rate than found it mammals, it is difficult to comparatively stage zebrafish development to humans in the way that can be done in mouse studies (McMenamin et al., 2016, Parichy et al., 2009). Therefore, initially the effects of genotype on swimming capability were investigated at 5 dpf, and this time point was chosen for a number of reasons. First, maternal mRNA contribution resulting from an ATM$^{+/sh477}$ in-cross has likely been lost by 5 dpf **(see chapter 3 figure 3.2)**, and the molecular effects of loss of ATM may therefore have had time to present at a phenotypic level. Second, zebrafish at 5 dpf are still small enough to analyse in a 96 well format, increasing the throughput of the experiment. Third, zebrafish at 5 dpf are not considered animals under ASPA, 1986, and therefore large amounts of data can be gathered by increasing the power of the experiment while still keeping in line with the principles of the 3Rs (Replacement, Reduction and Refinement). Finally, zebrafish larvae at 5 dpf have started to develop significant cerebellar structures (Hamling et al., 2015), and exhibit behavioural changes in response to stimuli, particularly visual stimuli. It has been observed that zebrafish at this age exposed to high intensity light, which is then suddenly removed, show a significant increase in swimming activity (Easter and Nicola, 1996, Emran et al., 2008, Gao et al., 2014, Burgess and Granato, 2007). This type of response to light/dark stimuli was exploited to measure differences in the swimming between genotypes.

To measure swimming, the zebrafish larvae were analysed using a ZebraBox tracking system (ViewPoint, France). Zebrafish motility is measured in a temperature controlled, soundproof, sealed box, with a controlled cold light source. The evening before analysis, the larvae were arrayed in a 96 well plate in E3 and left to acclimatise to their new environment overnight. The following morning, the zebrafish were placed in the ZebraBox with 100% light intensity, and again left to acclimatise for 30 min. The larvae were then subjected to 6 cycles of alternating 0% light intensity /100% light intensity (dark/light), each phase lasting 5 min for a total of 30 min, while the swimming activity of each fish was tracked using an infrared camera. Where required, the larvae were then genotyped and the swimming data for each fish analysed. Larval movement was classified as follows: a swimming speed < 2 mm/sec was classed as inactive or no swimming, and a swimming speed of > 2mm/sec was considered active swimming.

To determine if ATM$^{sh477/sh477}$ zebrafish larvae exhibited any behavioural differences at 5 dpf, larvae from ATM$^{+/sh477}$ in-crosses were subjected to the above swimming analysis **(figure 5.1).** ATM$^{sh477/sh477}$ zebrafish larvae exhibited a typical response to the onset of darkness by increasing both the distance swum and consequently the duration of their active swimming in the dark phase. ATM$^{sh477/sh477}$ larvae do not exhibit any defects in swimming ability at 5dpf, as they swam comparable distances to their wild type and heterozygote siblings in both the induced swimming (dark) and basal swimming (light) phases **(figure 5.1 a and b).** Additionally, the duration of when they were active (moving >2mm/s) was similar between homozygous, heterozygous and wild type siblings **(figure 5.1 c and d).** Therefore, ATM$^{sh477/sh477}$ zebrafish larvae do not exhibit any abnormalities in their swimming behaviour in response to light/dark stimuli at 5 dpf.

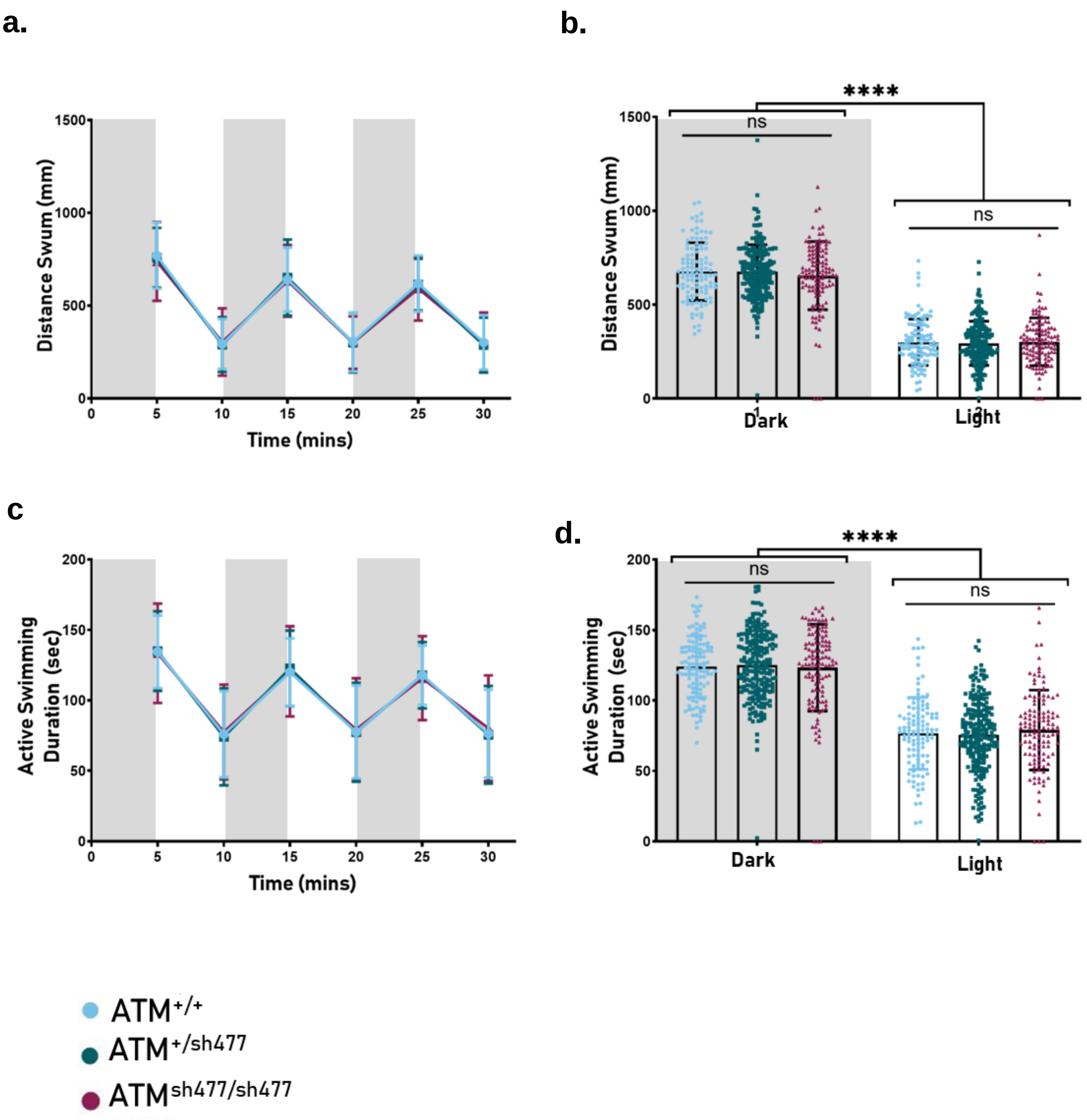

Figure 5.1 ATM$^{sh477/sh477}$ zebrafish larvae do not exhibit any detectable swimming abnormalities at 5dpf. Zebrafish larvae from ATM$^{+/sh477}$ in-crosses were arrayed on 96 well plates at 4.3 dpf. At 5 dpf they were subjected to swimming analysis by alternating dark and light cycles (light driving phases) of 5 mins each for a total of 30 mins, during which their swimming was tracked. **Note: Grey panels in the graph represent dark cycles. a.** Average distance travelled by each genotype in each of the light driving phases. **b**. Average distance travelled in dark and light phases; individual data points represent the mean value per embryo of distance travelled across the 3 dark and 3 light phases. **c**. Average duration spent in active swimming by each genotype in each of the light driving phases. **d**. Average duration of active swimming spent in dark and light phases; individual data points represent the mean value per embryo of active duration across the 3 dark and 3 light driving phases. Data were analysed by two-way ANOVA with repeated measures, with *post hoc* Tukey's and Sidak's multiple comparisons tests. Error bars represent SD. Statistical analysis can be found in **appendix 5.1**. ATM$^{+/+}$ n=110 ATM$^{+/SH477}$ n=212 ATM$^{SH477/SH477}$ n=118. Data shown is combined from N=5 replicate experiments using different ATM$^{+/sh477}$ in-crosses.

5.2.1.2 ATM$^{sh477/sh477}$ Larvae Exhibit no Swimming Abnormalities at 5 dpf After Treatments to Induce DNA Damage

ATM plays an intrinsic role in the DDR, and as deficiencies in the DDR due to loss of ATM lead to unrepaired DNA damage, it is thought to be a major contributor to neuronal cell death in AT. It was considered that at 5 dpf, in the context of an ATM$^{+/sh477}$ in-cross where there is likely to be some early maternal contribution of ATM, there may not have been enough time to reach a detrimental threshold of DNA damage in ATM$^{sh477/sh477}$ zebrafish **(see Chapter 1, section 1.2.4.5 b).** In order to test the hypothesis that induction of excessive DNA damage has a behavioural effect, we induced DNA damage through genetic, chemical, and physical approaches, and measured the swimming capability of ATM$^{sh477/sh477}$ zebrafish at 5 dpf. Moreover, we hypothesised that regardless of whether induction of DNA damage would lead to neuronal cell death in ATM$^{sh477/sh477}$ zebrafish, excessive unrepaired global DNA damage would have an impact on overall health of the zebrafish and impair swimming ability, thus leading to reduced motility in response to light/dark stimuli.

a. Genetic Approach to Induce DNA Damage.

We first sought to increase endogenous DNA damage by mutation of the *TDP1* gene. TDP1 is another DNA damage repair protein where mutation results in a hereditary ataxia; Spinocerebellar Ataxia with Axonal Neuropathy (SCAN1) (Pouliot et al., 1999, Interthal et al., 2001, Takashima et al., 2002, El-Khamisy et al., 2005). During DNA replication, Topoisomerase 1 (TOP1) binds to DNA and creates a single strand break to allow access of the replication machinery. The composite of the TOP1 bound to DNA creates a Topoisomerase cleavage complex (TOPcc), which is generally transient and resolved by hydrolysis of the shared 3’ phosphodiester bond by TDP1, allowing re-ligation of the DNA backbone. However, a loss of function mutation in *TDP1* causes TOPcc to become permanent, thus causing an unrepaired protein bound DNA single strand break (Koster et al., 2005, Humbert et al., 2009, Pouliot et al., 1999, Interthal et al., 2001, Takashima et al., 2002). These TOPcc have been shown to activate ATM, with ATM being needed for their repair (Humbert et al., 2009, Sordet et al., 2009), and ATM deficient cells show a decrease in their ability to resolve these DNA breaks (Alagoz et al., 2013, Katyal et al., 2014). Zebrafish that are homozygous for a *TDP1* loss of function mutation (TDP1$^{sh475/sh475}$) do not exhibit any detectable behavioural abnormalities at 5 dpf when compared to heterozygous controls, nor do they exhibit an increase in TOPcc or DNA damage signalling (Zaksauskaite et al., 2021). However, it was hoped that the combination of loss of both *ATM* and *TDP1* would act synergistically to impair the DNA damage response, leading to a detectable early behavioural phenotype.

Larvae from an ATM$^{+/sh477}$ TDP$^{sh475/sh475}$ in-cross were subjected to the same swimming assay as previously outlined in **figure 5.1**. ATM$^{sh477/sh477}$ larvae on a TDP1 null background exhibit no differences in their ability to swim **(figure 5.2 a and b)** nor in their response to darkness compared to their ATM$^{+/+}$TDP1$^{sh475/sh475}$ and ATM$^{+/-}$TDP1$^{sh475/sh475}$ siblings **(figure 5.2 c and d)**.

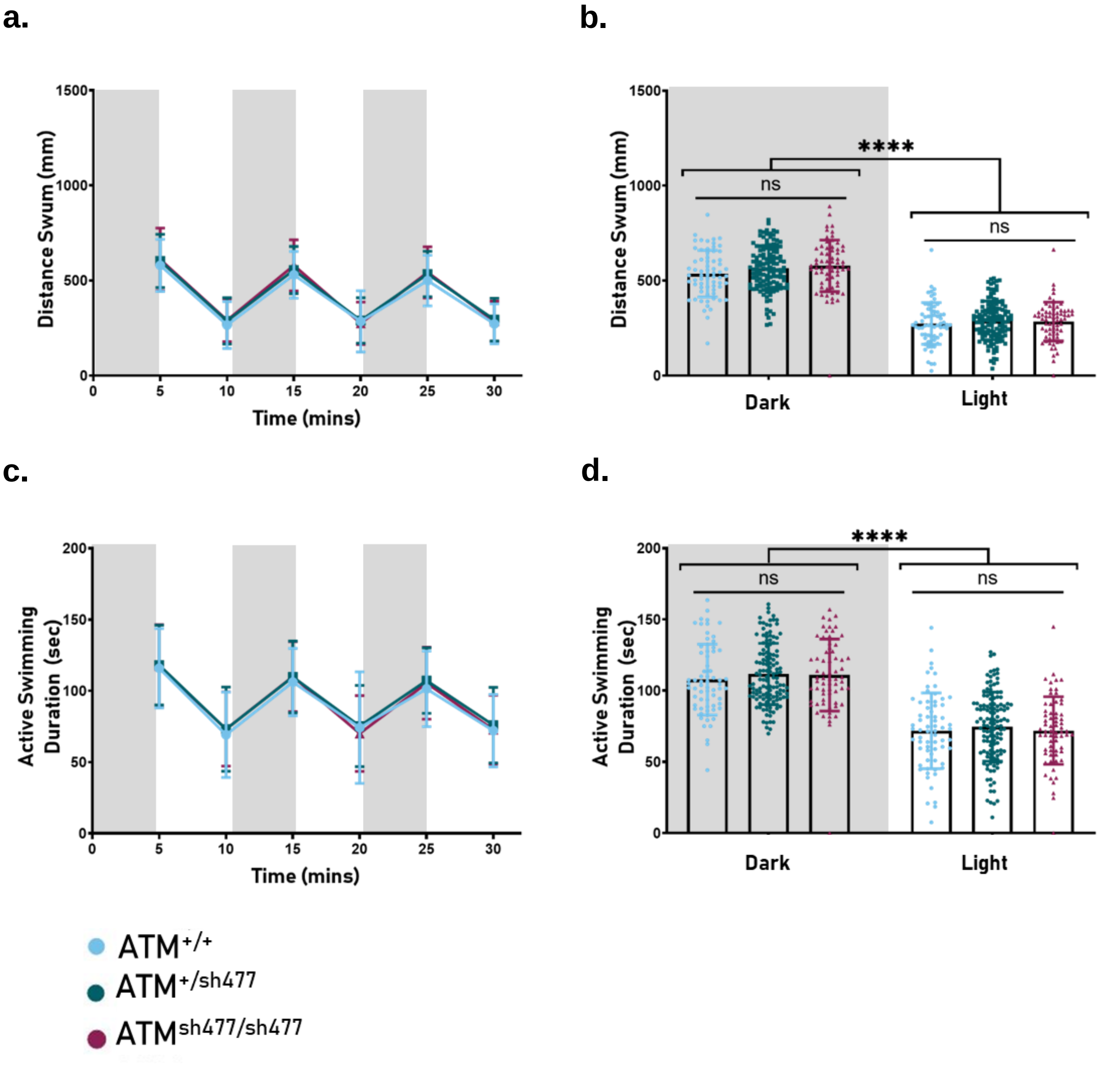

Figure 5.2 ATM$^{sh477/sh477}$ zebrafish larvae on a TDP1$^{sh475/sh475}$ (null) background do not exhibit any detectable swimming abnormalities at 5 dpf. Zebrafish larvae from ATM$^{+/sh477}$TDP1$^{SH475.SH475}$ in-crosses were arrayed on 96 well plates at 4.3 dpf. At 5 dpf they were subjected to alternating dark and light cycles (light driving phases) of 5 mins each for a total of 30 mins, during which their swimming was tracked at 5dpf. **Note: Grey panels in the graph represent dark cycles. a.** Average distance travelled by each genotype in each of the light driving phases. **b**. Average distance travelled in dark and light phases; individual data points represent the mean value per embryo of distance travelled across the 3 dark and 3 light phases. **c**. Average duration spent in active swimming by each genotype in each of the light driving phases. **d**. Average duration of active swimming spent in dark and light phases; individual data points represent the mean value per embryo of active duration across the 3 dark and 3 light driving phases. Data were analysed by two-way ANOVA with repeated measures, with *post hoc* Tukey's and Sidak's multiple comparisons tests. Error bars represent SD. Statistical analysis can be found in **appendix 5.2**. ATM$^{+/+}$ TDP1$^{sh475/sh475}$ = 67 ATM$^{+/sh477}$TDP1$^{sh475/sh475}$ = 129 ATM$^{sh477/sh477}$ TDP1$^{sh475/sh475}$ = 66 Data shown is combined from N=3 replicate experiments using different ATM$^{+/sh477}$TDP1$^{sh475/sh475}$ in-crosses.

b. Treatment with Camptothecin

Camptothecin (CPT) is a chemotherapeutic agent that binds TOPcc and prevents their hydrolysis and DNA re-ligation, effectively mimicking the SCAN1 molecular phenotype (Hsiang et al., 1985). CPT has regularly been used to induce DNA damage *in vitro* (Wan et al., 1999, Sakasai et al., 2010), and treatment of larval zebrafish with CPT decreases their ability to swim and induces DNA-protein linked DNA breaks and a DNA damage response (Zaksauskaite et al., 2021). Thus, it was reasoned that treatment of an ATM$^{+/sh477}$ in-cross with CPT would result in DNA damage that ATM$^{sh477/sh477}$ zebrafish would be unable to resolve as efficiently as wild types, and this would result in a more severe behavioural phenotype compared to control siblings.

There was little indication of the duration of CPT treatment required, or the most appropriate dose and age to induce maximal DDR without loss of viability. It was also reasoned that an appropriate dose would need to significantly decrease wild type swimming, first to show the treatment of CPT had worked as predicted, and second to allow any possible further decrease in swimming in ATM$^{sh477/sh477}$ larvae to still be detected. Therefore, a treatment protocol was optimised in LWT zebrafish. Effects of CPT and its ability to induce swimming defects were analysed by measuring the darkness-evoked swimming response as above. Viability and survival of the treated larvae were also measured, by presence/absence of a heartbeat. Furthermore, observed decreases in swimming should occur from molecular abnormalities secondary to excessive DNA damage, and should not be due to any gross morphological/developmental irregularities that would impact the ability of the larvae to swim. Consequently, zebrafish treated with CPT were monitored daily for morphological abnormalities.

i. Optimisation of DMSO Concentration

Dimethyl sulfoxide (DMSO) - $(CH_3)_2SO$, is a commonly used aprotic solvent in molecular biology, and is regularly used in the drug treatment of zebrafish to improve drug solubility (Hutchinson et al., 2006, Rammler and Zaffaroni, 1967, Kais et al., 2013a). The toxicity of the solvent has been studied in depth in zebrafish. Zebrafish larvae and embryos can withstand up to 2% without lethality

(Chen et al., 2011), and concentrations of 1-2% are routinely used in our lab to study the molecular effects of drug treatments on zebrafish. Therefore, when embryos/larvae were treated with CPT, they were also treated with DMSO. Initially during CPT optimisation, zebrafish treated with CPT were co treated with 1% DMSO **(see table 5.1)**. However, treatment with 1% DMSO resulted in a significant decrease in swimming distance compared to untreated embryos (data not shown). Consequently, optimisation of DMSO treatment concentration for behavioural assays was also required.

To optimise DMSO concentrations, embryos (6 hpf) were arrayed on a 96 well plate and at 48 hpf treated with 1%, 0.1% or 0.01% DMSO. At 5 dpf, zebrafish larvae were subjected to the darkness evoked swimming response, and data analysed **(figure 5.3)**. Zebrafish treated with 1% DMSO exhibited significant deficiencies in the distance swum in the dark **(figure 5.3 a and b)**, and consequently in the duration of time they spent in active swimming in the dark compared to untreated zebrafish **(figure 5.3 c and d)**. Zebrafish treated with 0.1% and 0.01% DMSO show no difference in the distance swum or time spent in active swimming in the dark compared to untreated siblings. As such, optimisation of CPT concentration was continued with a co-treatment of 0.1% DMSO final concentration.

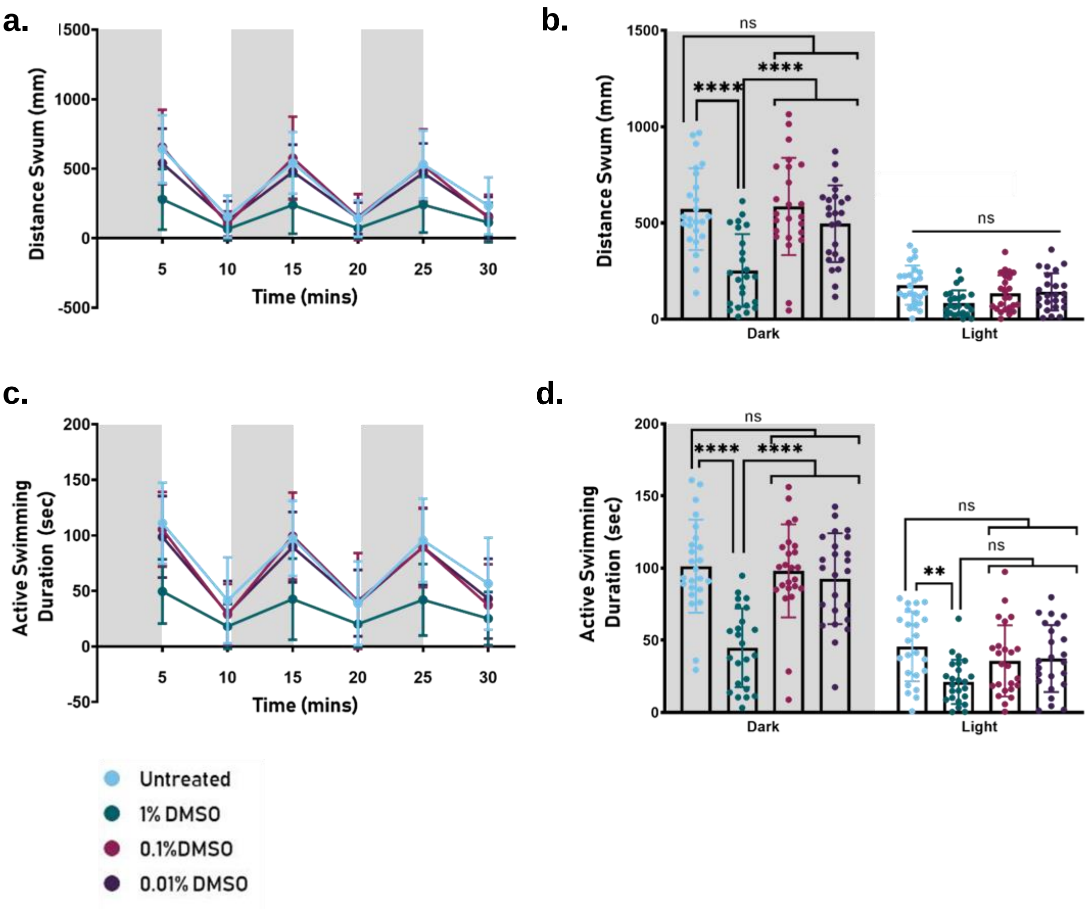

Figure 5.3 Optimisation of DMSO treatment at 48 hpf in a 96 well plate for swimming analysis at 5dpf. Wild type (LWT strain) zebrafish larvae were untreated or treated with decreasing doses of DMSO (1%, 0.1% and 0.01%) in E3 at 48 hpf in 96 well plates. At 5dpf, zebrafish were assayed by being subjected to alternating dark and light cycles (light driving phases) of 5 mins each for a total of 30 mins, during which their swimming was tracked. **Note: Grey panels in graph represent dark cycles. a.** Average distance travelled by each genotype in each of the light driving phases. **b**. Average distance travelled in dark and light phases; individual data points represent the mean value per embryo of distance travelled across the 3 dark and 3 light phases. **c**. Average duration spent in active swimming by each genotype in each of the light driving phases. **d**. Average duration of active swimming spent in dark and light phases; individual data points represent the mean value per embryo of active duration across the 3 dark and 3 light driving phases. Data were analysed by two-way ANOVA with repeated measures with a *post hoc* Tukey's multiple comparisons test. Error bars represent SD. Statistical analysis can be found in **appendix 5.3.** Untreated n=24, 1% DMSO treated n=24, 0.1% DMSO treated n=24, 0.01% treated n=24. N=1 replicate.

ii. Optimisation of Treatment Time and Dose of CPT

It was hypothesised that older zebrafish would be more resistant to the effects of CPT, therefore in order to optimise CPT dose and duration of treatment, zebrafish were treated with a broad range of doses that increased with age. A full list of all doses used for optimisation according to the time point they were used at can be found in **table 5.1**. For optimisations, zebrafish embryos at 6 hpf were arrayed on a 96 well plate in E3 media and subsequently treated with CPT/DMSO in E3 at the appropriate time point. At 5 dpf zebrafish larvae were subjected to swimming analysis as previously. The aim of optimisation was to achieve a significant change in induced swimming to ensure treatment with CPT was causing an effect, but not so large an effect that it would cause the presumed more sensitive ATM$^{sh477/sh477}$ zebrafish to completely stop or have undetectable swimming.

Table 5.1 Optimisation of Treatment Time and Dose of CPT

Age of treatment	***Doses of CPT (nM)***				
	1% DMSO		*0.1% DMSO*		
	Optimisation 1 *(Data Not shown)*	*Optimisation 2* *(Data Not shown)*	*Optimisation 3* *(appendix 5.5.1, 5.5.2, 5.5.3, 5.5.4 and 5.5.5)*	*Optimisation 4* *(figure 5.4)*	*Optimisation 5* *(figure 5.5)*
8 hpf	*2.5, 5, 10, 20*	*2, 2,5, 3, 3.5*	*1, 1.5, 2, 2.5*	-	-
24 hpf	*2.5, 5, 10, 20*	*2, 2,5, 3, 3.5*	*2, 2,5, 3, 3.5*	-	-
48 hpf	*25, 50, 100, 200*	*12.5, 25, 50, 100*	*12.5, 25, 50, 100*	*0.1, 1, 12.5, 25, 50*	*1, 10*
72 hpf	*250, 500, 600, 700*	*50, 100, 200, 400*	*50, 100, 200, 400*	-	
96 hpf	*250, 500, 600, 700*	*400, 500, 600, 700*	*400, 500, 600, 700*	-	-

Initial optimisations (optimisation 3) with 0.1% DMSO showed embryonic zebrafish treated at 8 and 24 hpf were extremely sensitive to CPT where treatment with 2 nM and 3.5 nM, respectively, were enough to significantly decrease their darkness-evoked response **(appendices 5.4.1 and 5.4.3 a and b)**. Zebrafish treated at 48 and 72 hpf showed a relatively moderate sensitivity to

CPT, where doses of 12.5 nM and 25 nM respectively, exhibited a significant decrease in their motility **(appendices 5.4.1 and 5.4.3 c and d)**. However, zebrafish treated at 48 hpf with 100 nM of CPT appear curled and atrophied upon inspection and had died by 5 dpf, so were therefore not included in swimming analysis. Larval zebrafish at 96 hpf appear comparatively robust to CPT treatment, as doses between 400-700 nM significantly decrease their darkness-evoked response to a similar level **(appendices 5.4.1 and 5.4.3 e)**. However, while zebrafish treated in this dose range swam similar distances, zebrafish treated with, 600 nM and 700 nM CPT were atrophied and curled upon inspection. It was also observed that while these fish were alive (maintained a heartbeat) **(appendix 5.4.3 a)**, their basal activity was vastly decreased compared to untreated controls, and the larvae appeared unable to move or only twitch upon tactile stimulus. These results of decreased swimming in the dark after CPT treatment are mirrored in the duration spent in active swimming in these fish **(appendix 5.4.3)**. Interestingly, treatment at 48 hpf whereby the dose was doubled for each treatment from 12.5 to 25 to 50 nM shows an approximately 50% decrease in swimming distance and swimming duration in the dark with each doubling of the dose **(appendices 5.4.1 c and 5.4.3c)**. This is also seen when treated at 72 hpf where the dose was double each time from 25, 50, and 100 nM, and again both the swimming distance and swimming duration decreased by approximately half with each dose **(appendices 5.4.1 d and 5.4.3 d).** These data confirm the hypothesis that the resistance to CPT is age dependent, and that treatment with CPT can hinder the motility of zebrafish in a dose dependent manner. Treatment with relatively moderate doses of CPT at either 48 or 72 hpf produces the desired results of a dose dependent effect on swimming with no obvious morphological defects. Optimisations were continued at 48 hpf to ensure the period of DNA damage was as prolonged as possible.

To ensure reproducibility of a dose dependent reduction in swimming, and to determine a more refined range of CPT doses, treatment with CPT at 48 hpf was optimised again **(table 5.1, optimisation 4)**. Zebrafish were treated within a relatively small dose range of CPT (0.1 nM – 50 nM) **(figure 5.4)** and their swimming analysed. Treatment with low doses of 0.1 and 1 nM CPT had no effect on swimming. Treatment with 12.5-50 nM CPT caused significant impairment in the average distance travelled and average active duration in the dark, but only the highest dose caused a decrease in motility without light-driving (**figure 5.4 b and d).** At these doses, no obvious morphological abnormalities were witnessed. Treatment with 12.5 nM CPT reduced the total distance swum by approximately half, from 1000 mm to 500 mm. However, since we hoped to detect increased sensitivity of ATM$^{sh477/sh477}$ to CPT, we felt this effect may be too strong.

Consequently, the dose was optimised one final time **(table 5.1 optimisation 5)**. Zebrafish were treated as before at 48 hpf with either 1 nM or 10 nM CPT **(figure 5.5)**. Zebrafish treated with 1 nM CPT again show no significant decrease in their swimming, however, 10 nM CPT treated fish show a ~15% decrease in the average distance travelled in induced swimming (dark phase), with an average of 156.6 mm in the 0.1% DMSO treated to 130 mm in the 10 nM CPT treated larvae **(figure 5.5 b)**. There was no significant difference observed in the duration of active swimming in the dark phases between DMSO only, control, or CPT treated zebrafish **(figure 5.5 d)**, yet there was a decrease in duration of active basal swimming (light phases) of 1 nM treatment. As 10 nM CPT treatment at 48 hpf caused a slight but significant decrease in induced swimming, it was thought to be optimum for treatment of the progeny of an ATM$^{+/sh477}$ in-cross to allow for the presumed increase sensitivity of ATM$^{sh477/sh477}$.

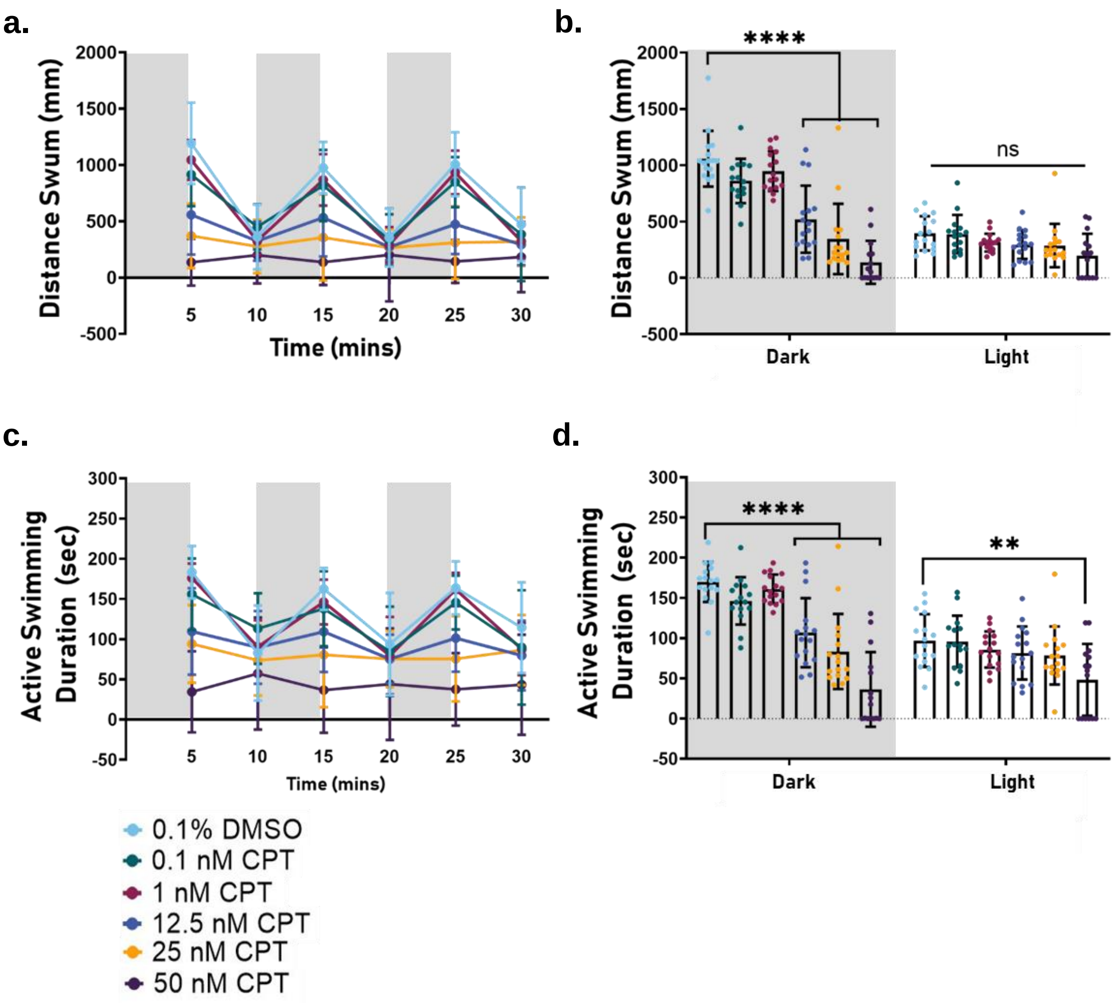

Figure 5.4 Optimisation 4 of CPT treatment on wild type (LWT) zebrafish embryos at 48 hpf in a 96 well plate for swimming analysis at 5dpf. Zebrafish larvae were treated with 0.1% DMSO or 0.1% DMSO and CPT in E3 at 48 hpf in a 96 well plate. At 5dpf, zebrafish were assayed by being subjected to alternating dark and light cycles (light driving phases) of 5 mins each for a total of 30 mins, during which their swimming was tracked. **Note: Grey panels in the graph represent dark cycles**. **a.** Average distance travelled by each genotype in each of the light driving phases. **b**. Average distance travelled in dark and light phases; individual data points represent the mean value per embryo of distance travelled across the 3 dark and 3 light phases. **c**. Average duration spent in active swimming by each genotype in each of the light driving phases. **d**. Average duration of active swimming spent in dark and light phases; individual data points represent the mean value per embryo of active duration across the 3 dark and 3 light driving phases. Data were analysed by to-way ANOVA with RM with a *post hoc* Tukey's multiple comparisons test. Error bars represent mean+/- SD. Statistical analysis can be found in **appendix 5.5.** 0.1% DMSO treated n=16, 0.1 nM CPT treated n=15, 1nM CPT treated n=16, 12.5 nM CPT treated n=16, 25 nM CPT treated n=16, 50 nM CPT treated n=15, N=1 Replicate.

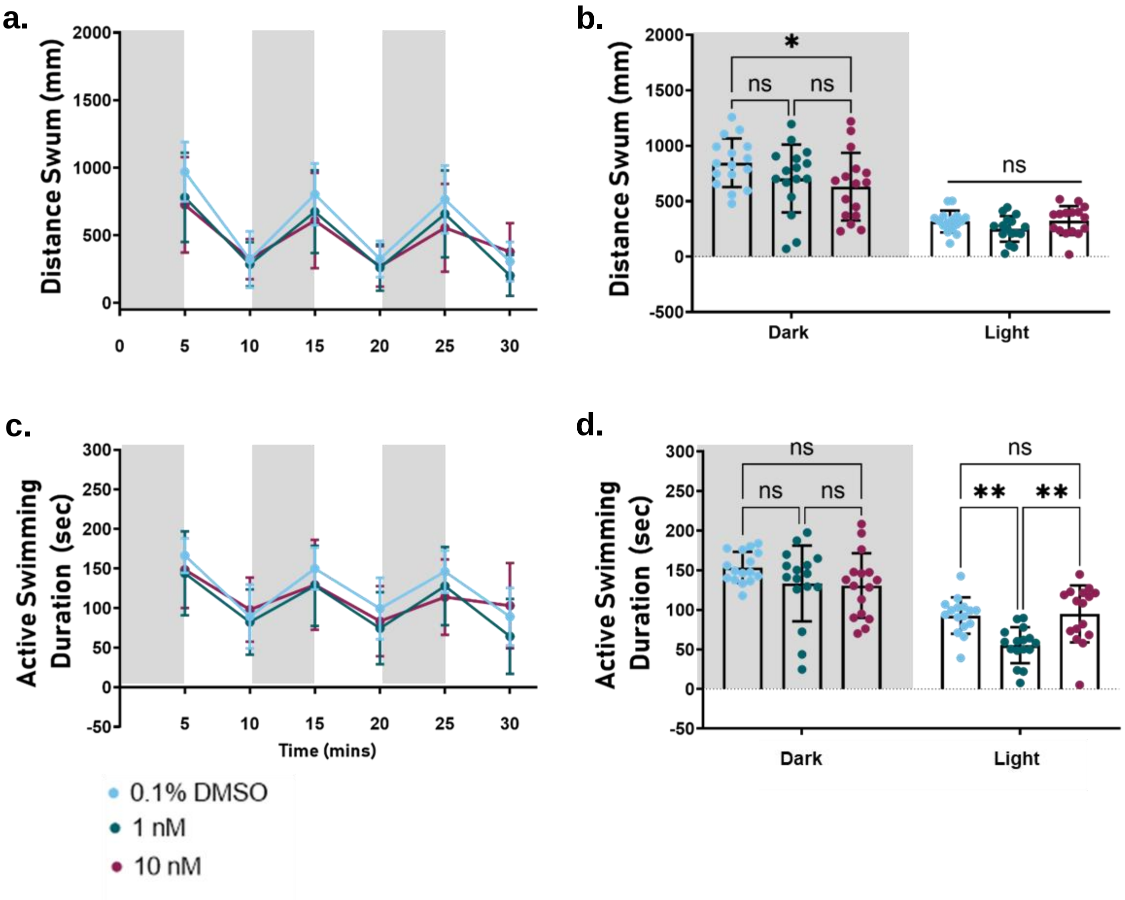

Figure 5.5 Optimisation 5 of CPT treatment on wild type (LWT) zebrafish embryos at 48 hpf in a 96 well plate for swimming analysis at 5dpf. Zebrafish larvae were untreated, treated with 0.1% DMSO or 0.1% DMSO and CPT in E3 at 48 hpf in a 96 well plate. At 5dpf, zebrafish were assayed by being subjected to alternating dark and light cycles (light driving phases) of 5 mins each for a total of 30 mins, during which their swimming was tracked. **Note: Grey panels in graph represent the dark cycles**. **a.** Average distance travelled by each genotype in each of the light driving phases. **b**. Average distance travelled in dark and light phases; individual data points represent the mean value per embryo of distance travelled across the 3 dark and 3 light phases. **c**. Average duration spent in active swimming by each genotype in each of the light driving phases. **d**. Average duration of active swimming spent in dark and light phases; individual data points represent the mean value per embryo of active duration across the 3 dark and 3 light driving phases. Data were analysed by two-way ANOVA with RM with a *post hoc* Tukey's multiple comparisons or Šídák's multiple comparisons test. Error bars represent SD. Statistical analysis can be found in **appendix 5.6.** 0.1% DMSO treated n=15, 1 nM CPT treated n=16, 10 nM CPT treated n=16, N=1 Replicate.

iii. ATM$^{sh447/sh447}$ Zebrafish do not Show Increased Sensitivity to 10 nM CPT

Larvae from an ATM$^{+/sh477}$ in-cross were treated at 48 hpf with 10 nM CPT/0.1% DMSO as previously described, and compared to 0.1% DMSO treated as control **(figure 5.6)**. Unexpectedly, ATM$^{+/+}$ zebrafish treated with 10 nM CPT showed no decrease in the average distance swum in the dark phases **(figure 5.6. b)** as previous wild type had done. ATM$^{sh477/sh477}$ mutants treated with 10 nM CPT did not show any changes in their motility and had comparable behaviour to ATM$^{+/+}$ zebrafish treated with 10 nM CPT. It remains possible that higher doses would be required to identify any increased sensitivity in ATM$^{sh477/sh477}$.

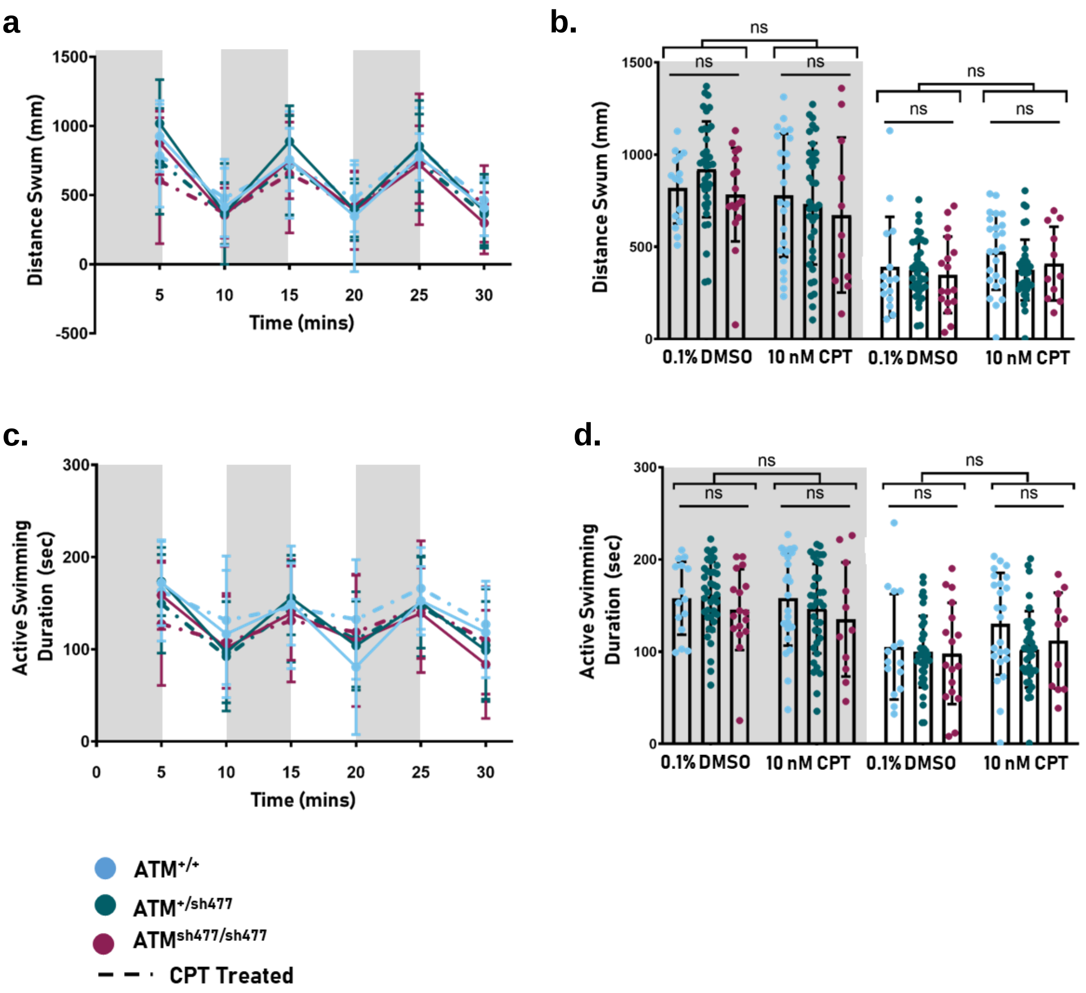

Figure 5.6 ATM$^{sh477/sh477}$ zebrafish larvae exhibit no behavioural abnormalities in response to DNA damaging agent CPT compared to their control siblings. Zebrafish larvae were treated with 0.1% DMSO or 10 nM CPT at 48 hpf in a 96 well plate. At 5dpf, zebrafish were assayed by being subjected to alternating dark and light cycles (light driving phases) of 5 mins each for a total of 30 mins, during which their swimming was tracked. **Note: Grey panels in graph represent the dark cycles. a.** Average distance travelled by each genotype in each of the light driving phases. **b**. Average distance travelled in dark and light phases; individual data points represent the mean value per embryo of distance travelled across the 3 dark and 3 light phases. **c**. Average duration spent in active swimming by each genotype in each of the light driving phases. **d**. Average duration of active swimming spent in dark and light phases; individual data points represent the mean value per embryo of active duration across the 3 dark and 3 light driving phases. Data were analysed by an ordinary two-way ANOVA with a *post hoc* Tukey's multiple comparisons test. Error bars represent SD. Statistical analysis can be found in **appendix 5.7.** N=2. 0.1% DMSO treated: ATM$^{+/+}$ n=15, ATM$^{+/sh477}$ n=38, ATM$^{sh477/sh477}$ n=17. 10 nM CPT treated: ATM$^{+/+}$ n=24, ATM$^{+/sh477}$ n=36, ATM$^{sh477/sh477}$ n=11.

c. ATM$^{sh447/sh447}$ Zebrafish do not show Increased Sensitivity to Ionising Radiation

As ATM$^{sh477/sh477}$ embryos and larvae showed no detectable increased sensitivity to treatment with moderate doses of CPT, other means of inducing DNA damage were sought. Zebrafish embryos from an ATM$^{+/sh477}$ in-cross were serially treated with a moderate dose of 8 Gy of IR, with a Caesium 137 radiation source (γ rays), daily between 1 and 4 dpf. Larvae were treated serially in this way to ensure a consistent level of DNA damage through development and to attempt to mitigate any DNA damage repair that occurred in ATM$^{sh477/sh477}$ larvae by alternative pathways. The larvae were then subjected to swimming analysis as before **(figure 5.7).** Zebrafish larvae do appear highly sensitive to IR, and while all zebrafish did exhibit a typical darkness-evoked swimming response **(figure 5.7 a and d)**, swimming distance and duration were significantly decreased in IR treated larvae **(figure 5.7 b and d)**. Nevertheless, even though there was sensitivity to IR exhibited by ATM$^{sh477/sh477}$ larvae, this was to the same extent as their wild type siblings, as no significant differences were observed in their ability to swim, or their darkness-evoked swimming response in either the dark or light cycles **(figure 5.7 b and d)**.

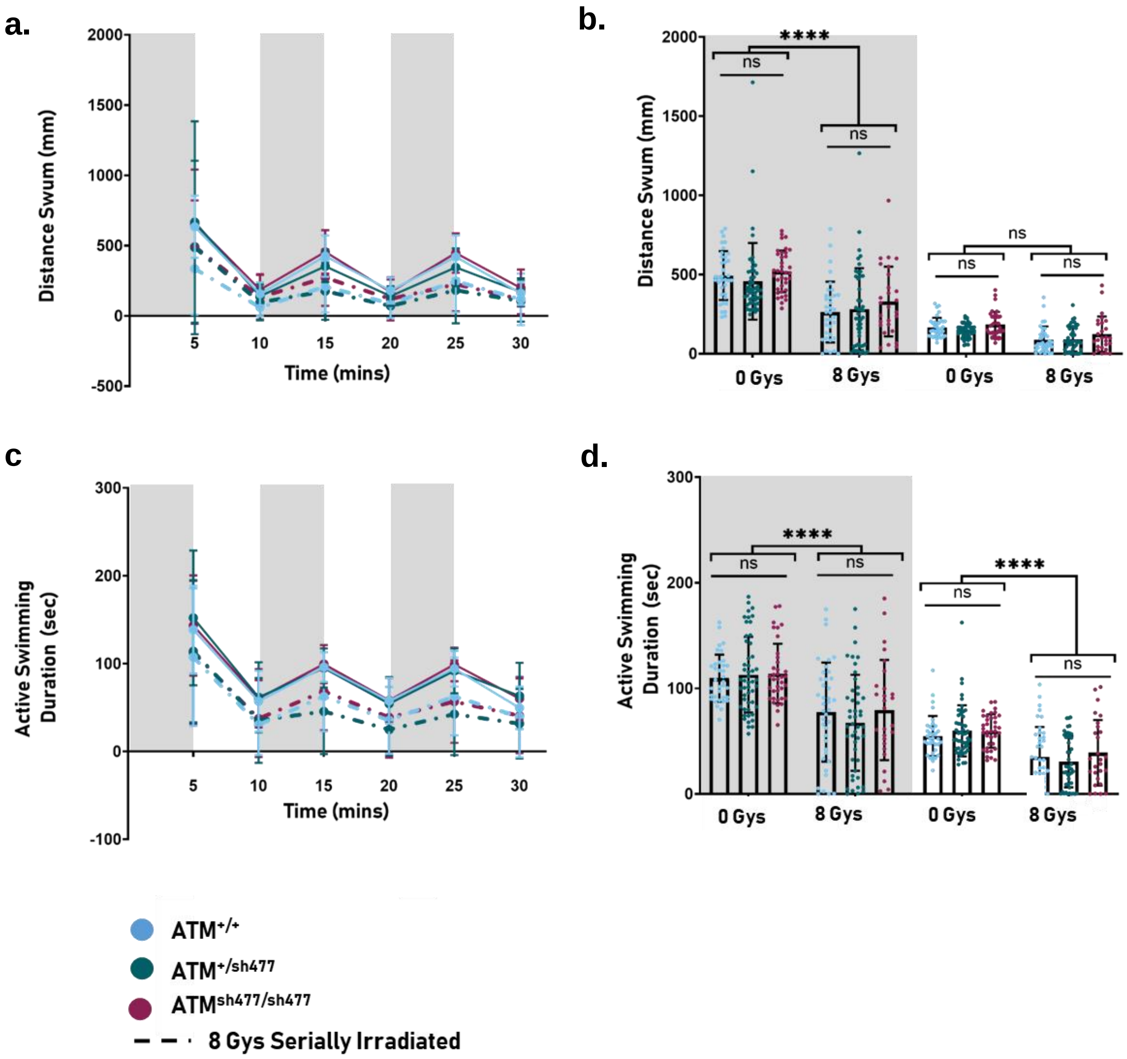

Figure 5.7 ATM$^{sh477/sh477}$ zebrafish larvae exhibit no swimming defects in response to exogenous DNA damage induced by IR compared to their control siblings. Zebrafish were treated at 1, 2, 3 and 4 dpf with 8 Gy IR. At 4.5 dpf zebrafish larvae were then arrayed on a 96 well plate and at 5dpf were subjected to alternating dark and light cycles (light driving phases) of 5 mins each for a total of 30 mins, during which their swimming was tracked. **Note: Grey panels in graph represent the dark cycles. a.** Average distance travelled by each genotype in each of the light driving phases. **b**. Average distance travelled in dark and light phases; individual data points represent the mean value per embryo of distance travelled across the 3 dark and 3 light phases. **c**. Average duration spent in active swimming by each genotype in each of the light driving phases. **d**. Average duration of active swimming spent in dark and light phases; individual data points represent the mean value per embryo of active duration across the 3 dark and 3 light driving phases. Data were analysed by ordinary two-way ANOVA with a *post hoc* Tukey's multiple comparisons test. Error bars represent SD. Statistical analysis can be found in **appendix 5.8.** Number of fish analysed: ATM$^{+/+}$=35 ATM$^{+/SH477}$=50 ATM$^{SH477/SH477}$=36, N=3 Replicates.

5.2.1.3 Treatment of Wild Type and ATM$^{sh477/sh477}$ Zebrafish Larvae with an ATM Inhibitor to Investigate Compensatory Mechanisms

Previously we have shown that ATM$^{sh477/sh477}$ zebrafish do not appear to be any more sensitive to ionising radiation than their wild type siblings, nor are there differences in their DNA damage response at the larval stage **(see chapter 3, section 3.2.3)**. In this chapter, we have shown that these mutant larvae show no difference in behaviour either before or after treatment with DNA damaging agents. In short, investigations undertaken suggest that ATM$^{sh477/sh477}$ zebrafish have no phenotypes consistent with defective somatic DNA damage repair. As previously outlined in **chapter 3, section 3.3.2.2** , it is possible that in the context of somatic DNA insult and injury in zebrafish, there is protein redundancy, and loss of ATM signalling is compensated by other aspects of the DDR. While preliminary investigations do not suggest genetic compensation by upregulation of a similar gene **(chapter 3, section 3.2.4),** it is possible that there is compensation at the protein level by activation of another protein that functions in the DDR .

The literature suggests that the compensatory mechanism acts through two other PIKK proteins, ATR and DNA-PKcs (Kumar et al., 2014, Zha et al., 2011b, Lee et al., 2013, Gapud et al., 2011, Gapud and Sleckman, 2011, Yue et al., 2020, Adams et al., 2006, Tomimatsu et al., 2009, Schlam-Babayov et al., 2020, Gurley and Kemp, 2001, Sekiguchi et al., 2001, Gladdy et al., 2006). Furthermore, mouse models that globally express ATM, but do not have a functional kinase domain (kinase dead- KinD) are embryonic lethal, and in conditional neuronal knockouts for a kinase dead ATM there is a greater amount of unrepaired DNA damage in the brain (Yamamoto et al., 2012b, Daniel et al., 2012, Yamamoto et al., 2016, Tal et al., 2018). Despite the wide range of mutations reported in the ATM gene, there have been no kinase dead mutations reported in patients, suggesting that this does not result in a viable pregnancy in humans. Similar instances of compensation have been reported after loss of ATR (Menolfi et al., 2018). Therefore, if the phenotype of a system with a non-functional ATM protein is more severe than a system without the presence of ATM, then it suggests that there is a secondary pathway that can be upregulated in the absence of ATM, and that this ameliorates at least some of the effects of its loss. Therefore, it suggests that this compensation does not happen in the presence of a non-functional ATM protein. We hypothesised that chemical inhibition of ATM kinase activity in wild type larvae would be damaging, and may induce a molecular phenotype similar to a KinD mutant, as the compensatory mechanism would not be upregulated. Conversely, in ATM$^{sh477/sh477}$ zebrafish, as there is predicted to be no ATM to inhibit, the compensatory mechanism would therefore not be affected. This is outlined in more detail in **figure 5.8**.

Consequently, we treated offspring from an ATM$^{+/sh477}$ in-cross with the ATM kinase inhibitor KU-55933 (ATMi), and used the behavioural assay outlined in the sections above as a readout to determine the 'health' of the relevant fish. While KU-55933 does have a high specificity for inhibition of ATM (IC$_{50}$ in cell free assays is 13 nM), it can inhibit ATR and DNA-PKcs at higher doses, therefore the treatment dose administered to the ATM$^{+/sh477}$ in-cross needed to be considered. Treatment of zebrafish embryos with concentrations above 3nM with KU-55933 have been shown to be high enough to affect in zebrafish embryos and concentrations of 12 nM have been shown not to induce any morphological abnormalities (Kumaran and Fazry, 2018). Therefore, zebrafish at 24 hpf were treated with 10 nM KU-55933 (ATMi). At 48 hpf, DNA damage was induced by a single dose of 12 Gy IR, and the ATMi was washed out of the media 6 hours post IR treatment and zebrafish left to develop as usual. At 5 dpf, zebrafish were subjected to the behavioural assay **(figure 5.9)**. Wild type and mutant zebrafish treated with 10 nM AMTi showed no differences in their ability to swim **(figure 5.9 a),** and both maintained their darkness-evoked response **(figure 5.9 a and c)**. However, when DNA damage was induced by treatment with 12 Gy IR, wild type larvae treated with 10 nM ATMi exhibited a decrease in their ability to swim in the dark phase, while ATM$^{sh477/sh477}$ larvae treated in the same manner did not show the same decrease, and swam at comparable levels to both DMSO only treated and 10 nM ATMi un-irradiated larvae **(figure 5.9 b and d)**. This effect could possibly be due to compensation in the DDR pathway in ATM$^{sh477/sh477}$ larvae.

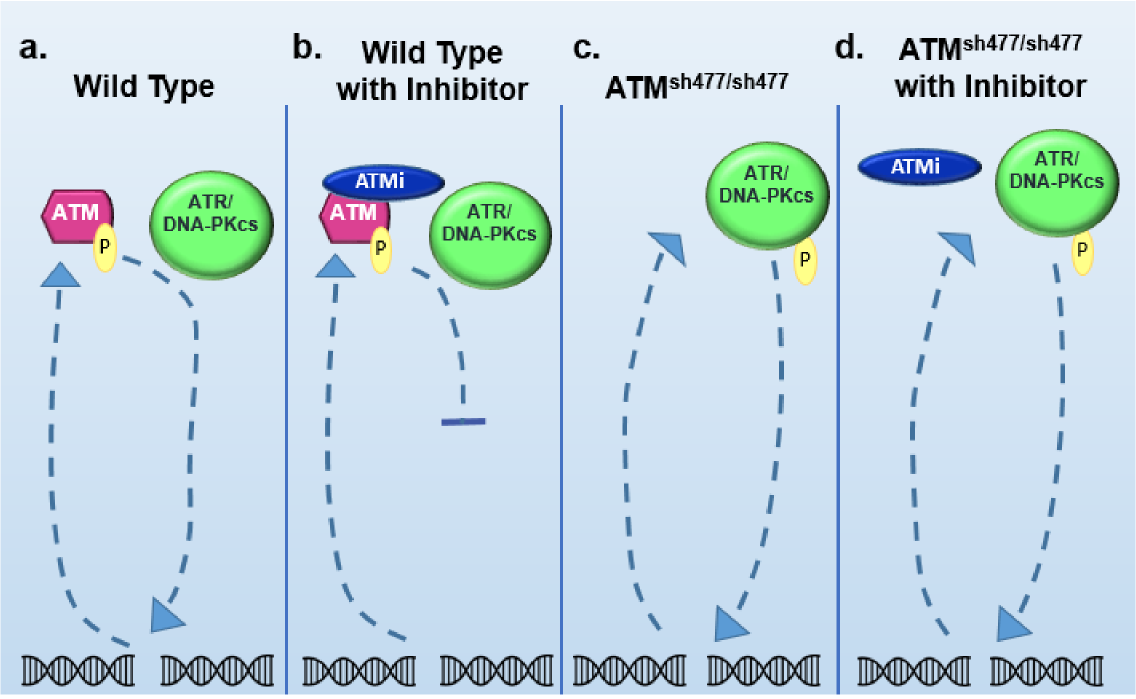
a.
Wild Type
ATM
P
ATR/
DNA-PKcs
b.
Wild Type
with Inhibitor
ATMi
ATM
P
ATR/
DNA-PKcs
c.
ATMsh477/sh477
ATR/
DNA-PKcs
P
d.
ATMsh477/sh477
with Inhibitor
ATMi
ATR/
DNA-PKcs
P

Figure 5.8. Model for the effect of ATMi on DDR in ATM$^{sh477/sh477}$ zebrafish. a. Canonically, DNA damage activates ATM, and in turn ATM activates a number of interdependent pathways to repair the damage. **b.** Functional ATM, in the presence of an ATM inhibitor, is activated by DNA damage, but is unable to activate the downstream pathway and repair the damage leading to genotoxic effects **c.** In the absence of the ATM protein, DNA damage activates other components of the DDR response and there is compensation for loss of ATM, leading to repair of DNA damage **d.** In an ATM deficient system, the ATM inhibitor has no target, therefore the compensatory mechanism leading to DNA repair is activated.

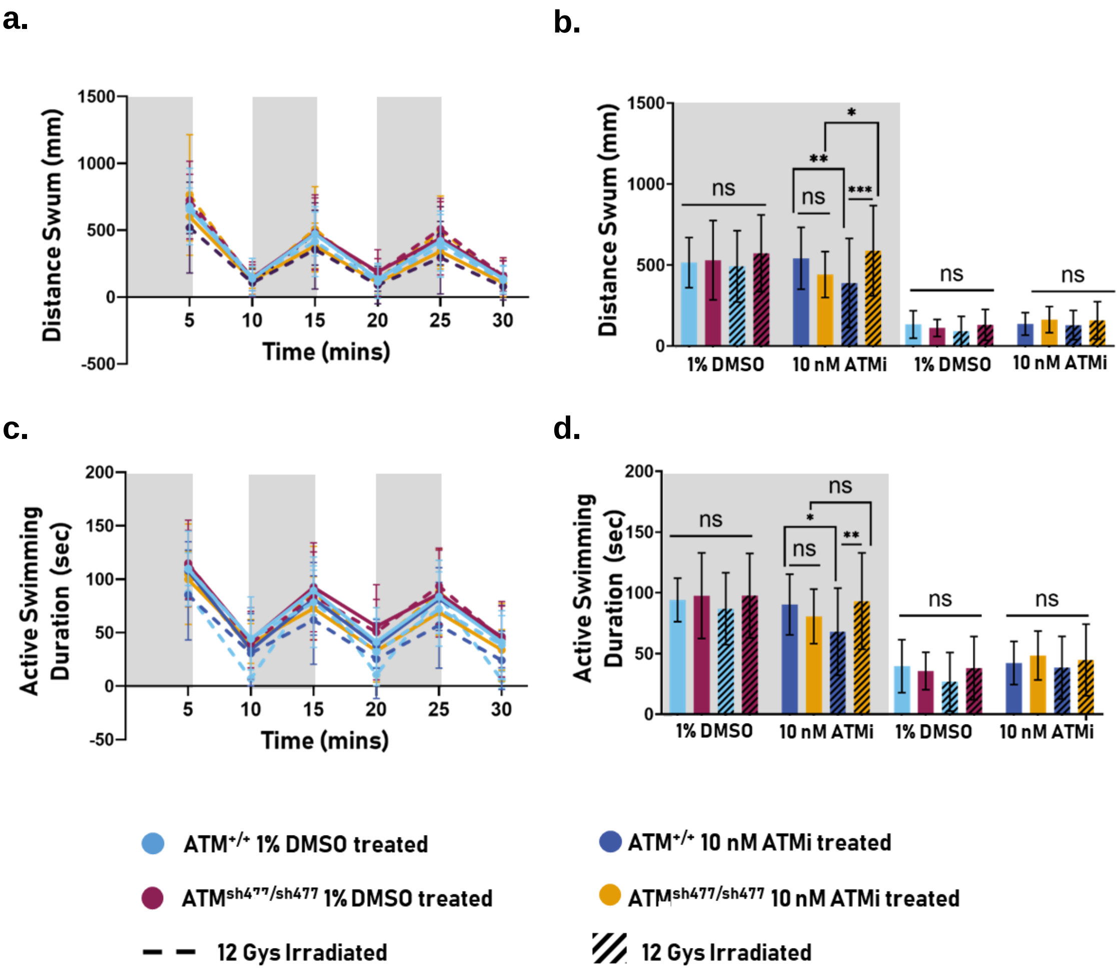

Figure 5.9 ATM$^{sh477/sh477}$ zebrafish do not exhibit sensitivity to an ATM inhibitor. Zebrafish from an ATM$^{+/sh477}$ in-cross were treated at 24 hpf with 1% DMSO/10 nM ATMi in a 6 well plate. At 48 hpf zebrafish were then treated with a single dose of 12 Gy IR and the ATMi washed out of the media 6 hours post IR treatment. At 4.5 dpf zebrafish larvae were then arrayed on a 96 well plate and at 5dpf were subjected to alternating dark and light cycles (light driving phases) of 5 mins each for a total of 30 mins, during which their swimming was tracked. **Note: Grey panels in graph represent the dark cycles. a.** Average distance travelled by each genotype in each of the light driving phases. **b**. Average distance travelled in dark and light phases; individual data points represent the mean value per embryo of distance travelled across the 3 dark and 3 light phases. **c**. Average duration spent in active swimming by each genotype in each of the light driving phases. **d**. Average duration of active swimming spent in dark and light phases; individual data points represent the mean value per embryo of active duration across the 3 dark and 3 light driving phases. Data were analysed by two-way ANOVA with a *post hoc* Tukey's multiple comparisons test. Error bars represent SD. Statistical analysis can be found in **appendix 5.9.1.** Number of fish analysed per condition can be found in **appendix 5.9.2**.

5.2.2 Investigations into ATM$^{sh477/sh477}$ Juvenile Zebrafish Swimming with and without Induction of Exogenous DNA Damage

It was considered for a number of reasons that 5 dpf may be too early to detect behavioural changes due to the loss of ATM. First, the DNA damage threshold theory **(see chapter 1, section 1.2.4.5 b)** suggests that endogenous DNA damage occurs accumulatively over time, and therefore 5 dpf may not be sufficient for this to happen, despite treatment with DNA damaging agents. This may be particularly relevant during the first few hours of development in ATM$^{sh477/sh477}$ zebrafish, as they are likely to still have ATM protein translated from maternally contributed mRNA. Therefore, a longer period of development without ATM activity might allow deleterious changes to occur. This has been observed with other neurodegenerative KO zebrafish models produced from a heterozygous in-cross in our lab (Doubi and Grierson, unpublished data). Secondly, the zebrafish cerebellum is still at an early phase of development at 5 dpf (Hamling et al., 2015), and as such many of the relevant cells are not yet fully mature. Thus, zebrafish PCs at 5 dpf may not have the same sensitivity to DNA damage as they would later in development. Finally, it is unclear whether the possible compensation investigated above in **section 5.2.1.3** is still evident later in development. However, the likely failure of meiotic recombination in adult males **(chapter 4, section 4.2.2.3)** supports the idea that some biological processes cannot be rescued by a compensatory pathway. Therefore, zebrafish from an ATM$^{+/sh477}$ in-cross were analysed for their swimming and darkness-evoked response at 12 dpf.

Zebrafish were raised in 10 cm plates in an incubator at 28 °C until 5 dpf, at which point the 5 dpf zebrafish larvae were moved to the aquarium system. At 12 dpf, zebrafish larvae were removed from the aquarium system and arrayed in 12 well plates. From this point on, zebrafish were treated as before by allowing them to acclimatise to 100% light intensity in the light box for 30 min, followed by the swimming analysis assay.

Compared to 5 dpf, at 12 dpf ATM$^{+/+}$ zebrafish show a reduced darkness-evoked swimming response, whereby they increase their swimming in the 3 dark phases from an average of 1851.12 mm in 100% light intensity, to an average of 2130.71 mm in the dark phases (p=0.0282) **(figure 5.10 a and c)**. ATM$^{+/sh477}$ and

ATM$^{sh477/sh477}$ zebrafish appear to have lost their darkness-evoked motor response. However, loss of a darkness-evoked response has been observed in other zebrafish models and their controls at 12 dpf in our lab (Doubi and Grierson, unpublished data), and this is not thought to be linked to a neurodegenerative phenotype. Despite the difference in the darkness-evoked swimming observed between ATM$^{+/+}$ zebrafish and ATM$^{+/sh477}$/ATM$^{sh477/sh477}$ zebrafish, there is no statistical difference in the average distance swum or the average duration of active swimming of each genotype in either the dark or light phases **(figure 5.10 b and d)**.

As no swimming defects were observed in 12 dpf zebrafish, larvae were treated with a single dose of either 2 Gy or 8 Gy IR at 48 hpf to induce DNA damage. In previous experiments where swimming analysis was performed at 5 dpf after treatment with IR, embryos were treated daily to ensure maximum levels of DNA damage. Here however, as the zebrafish are over 5.2 dpf, they are governed by the Animals (Scientific Procedures) Act 1986 (ASPA), which requires minimisation of adverse effects of regulated procedures performed under the project license. As can be seen from **chapter 3, figures 3.7 and 3.8,** serial treatment of zebrafish from 1-4 dpf has significant adverse effects on zebrafish morphology and consequently on their health. Therefore, it was decided that to ensure zebrafish over 5.2 dpf treated with IR remained in line with ASPA 1986, zebrafish received a single dose of IR. Zebrafish were treated at 48hpf, as treatment with IR at this age induces a DNA damage response **(see chapter 3 figure 3.10)** and cellular changes from these genotoxic insults are still detectable at 12 dpf (Morsli, unpublished data). Therefore, it was hoped that a strong induction of DNA damage early in development, coupled with the longer time of development from 5 to 12 dpf, would allow molecular changes to translate to behavioural changes and a detectable swimming defect.

Zebrafish from an ATM$^{+/sh477}$ in-cross were treated with either 0, 2, or 8 Gy IR at 48 hpf and then transferred to the aquarium system at 5 dpf. During development, zebrafish larvae were monitored daily for adverse effects of IR and viability, but none were found. At 12 dpf, zebrafish were arrayed on 12 well plates, and subjected to swimming analysis as before **(figure 5.11)**. Irradiated zebrafish still maintained their darkness-evoked response **(figure 5.11 a and c),** and there was no significant difference in the average distance swum in the dark phases, or in the duration of active swimming between untreated controls and irradiated fish **(figure 5.11 b and d)**. However, there was a difference in the average distance swum in the dark phases between 2 Gy and 8 Gy treated (p=0.0091) **(figure 5.11 b)**. In basal swimming (light phases) there was a significant increase in average swimming distance between 0 Gy and 2 Gy (p=0.0266), but no difference observed between 0 Gy and 8 Gy treated fish. Similarly to the dark phase, zebrafish treated with 2 Gy and 8 Gy show a significant difference in the average distance swum (p=0.0002), and consequently in the duration spent in active swimming (p=0.0132) **(figure 5.11 b and d)**. However, despite treatment with IR at 48 hpf having an effect on zebrafish swimming at 12 dpf, there were no differences observed between IR treated genotypes, with ATM$^{sh477/sh477}$ zebrafish appearing to exhibit the same sensitivity to IR as ATM$^{+/+}$ zebrafish.

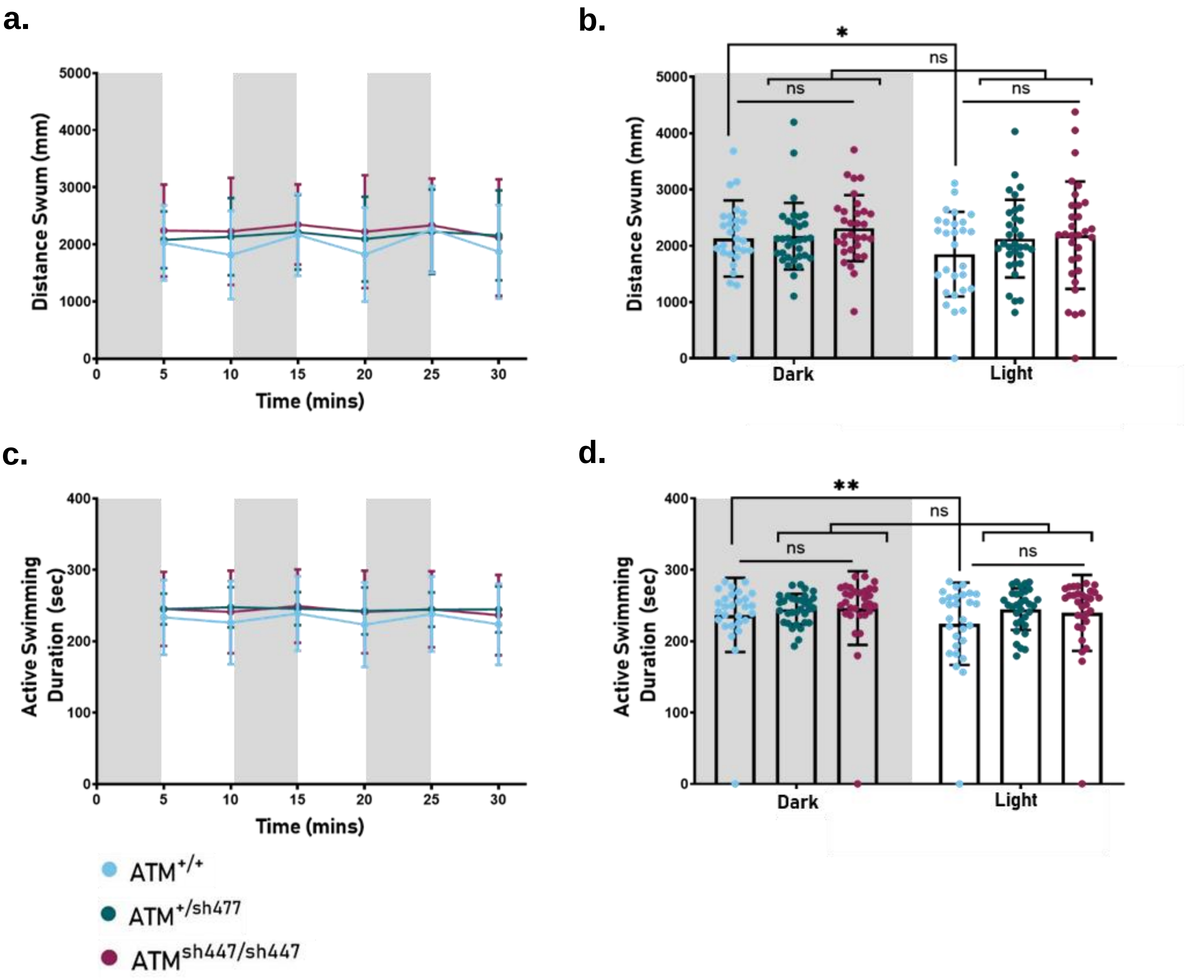

Figure 5.10 ATM$^{sh477/sh477}$ zebrafish larvae exhibit no swimming defects at 12 dpf. Zebrafish larvae were arrayed on a 12 well plates and subjected to alternating dark and light cycles (light driving phases) of 5 mins each for a total of 30 mins, during which their swimming was tracked. **Note: Grey panels in graph represent dark cycles. a.** Average distance travelled by each genotype in each of the light driving phases. **b**. Average distance travelled in dark and light phases; individual data points represent the mean value per embryo of distance travelled across the 3 dark and 3 light phases. **c**. Average duration spent in active swimming by each genotype in each of the light driving phases. **d**. Average duration of active swimming spent in dark and light phases; individual data points represent the mean value per embryo of active duration across the 3 dark and 3 light driving phases. Data were analysed by two-way ANOVA with RM, with *post hoc* Tukey's and Sidak's multiple comparisons tests. Error bars represent SD. Statistical analysis can be found in **appendix 5.10.** Number of fish analysed: ATM$^{+/+}$=28 ATM$^{+/SH477}$=32 ATM$^{SH477/SH477}$=31. N=3 Replicates.

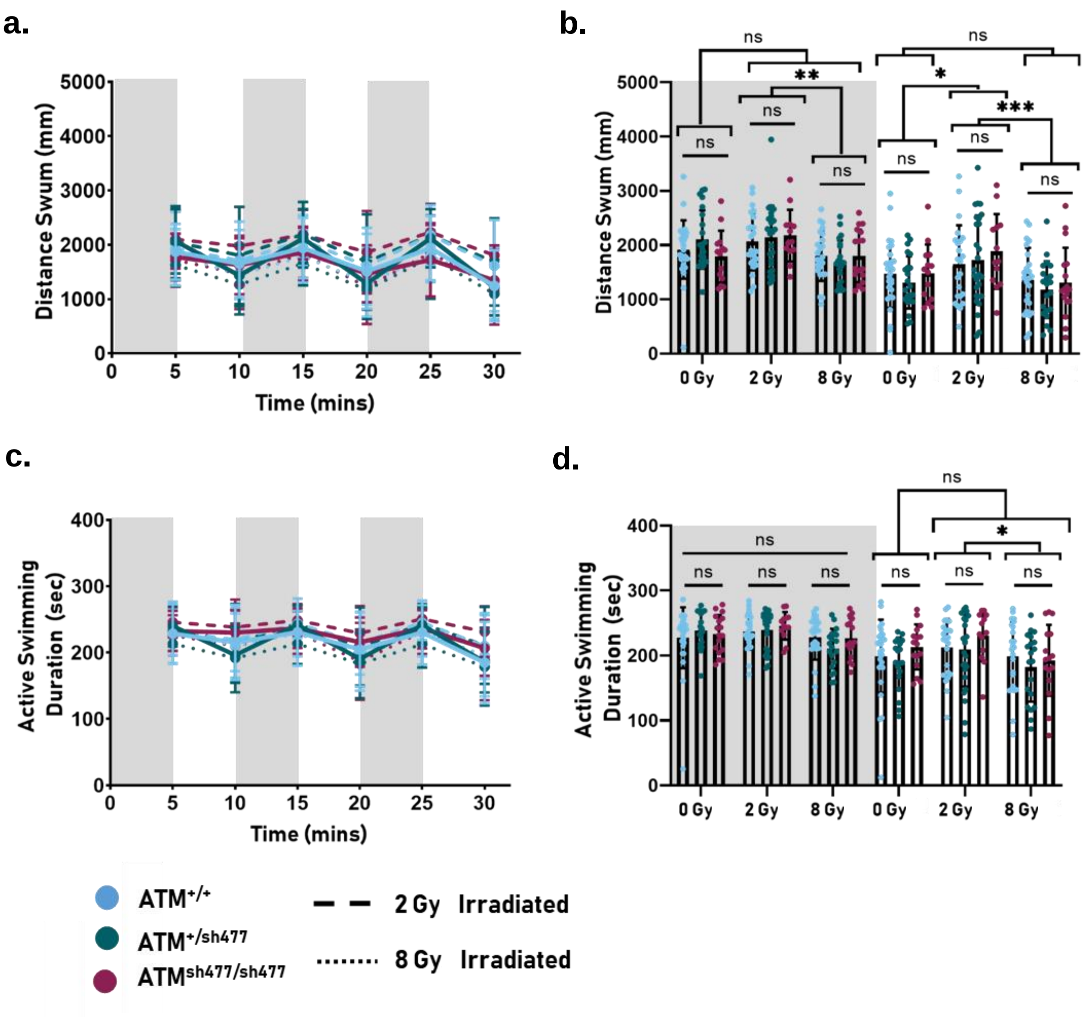

Figure 5.11 ATM$^{sh477/sh477}$ zebrafish larvae exhibit no swimming defects at 12 dpf after treatment at 48 hpf with ionising radiation. Zebrafish larvae were arrayed on a 12 well plates and subjected to alternating dark and light cycles (light driving phases) of 5 mins each for a total of 30 mins, during which their swimming was tracked. **Note: Grey panels in graph represent dark cycles. a.** Average distance travelled by each genotype in each of the light driving phases. **b**. Average distance travelled in dark and light phases; individual data points represent the mean value per embryo of distance travelled across the 3 dark and 3 light phases. **c**. Average duration spent in active swimming by each genotype in each of the light driving phases. **d**. Average duration of active swimming spent in dark and light phases; individual data points represent the mean value per embryo of active duration across the 3 dark and 3 light driving phases. Data were analysed by two-way ANOVA, with *post hoc* Tukey's multiple comparisons tests. Error bars represent mean +/- SD. Statistical analysis can be found in **appendix 5.11.1.** N=3 Replicates, n numbers for each condition can be found in **appendix 5.11.2**.

5.2.3 Investigations into Adult ATM$^{sh477/sh477}$ Zebrafish Swimming Behaviour

As the neurological symptoms of AT are progressive and usually not completely debilitating until the second decade of life (van Os et al., 2017b, Micol et al., 2011a), symptoms in an animal model of the disease may only be detectable in adult stages. Additionally, adult TDP1 null zebrafish show increased sensitivity to DNA damaging agents that result in a behavioural phenotype, whereas TDP1 null larvae do not (Zaksauskaite et al., 2021). Furthermore, if the neurological phenotype is caused by a threshold of DNA damage being reached over time, then a behavioural phenotype may not present until much later in the life of a zebrafish. Therefore, we speculated that adult ATM$^{sh477/sh477}$ zebrafish may have increased DNA damage that would present as a behavioural phenotype. As ATM$^{sh477/sh477}$ develop as males **(chapter 3, section 3.2.2),** we investigated the swimming of adult male ATM$^{sh477/sh477}$ zebrafish compared to sex-matched wild type siblings.

To investigate motor function, endurance and balance, zebrafish at 7 months were tested in the swim tunnel, a narrow tube through which the water flow rate can be controlled. The flow rate of water was increased from 6.57 cm/s to 45.5 cm/s by increments of 6.57 cm/s every 5 mins for a total of 35 mins or until the fish reached exhaustion, and the time was recorded. This data was used to calculate the critical swimming velocity (U_{crit}), which is the maximum velocity of swimming a fish can sustain for a given period of time (Brett, 1964, Plaut, 2000). The U_{crit} in zebrafish is thought to be analogous to the gait transition speed in mammals (Gilbert et al., 2014, Tierney, 2011, Peake and Farrell, 2006), and changes in gait speed can greatly affect patients suffering from ataxia (Schniepp et al., 2017, Schniepp et al., 2012).

The mean U_{crit} was lower in ATM$^{sh477/sh477}$ zebrafish (30.99 cm/s) than in ATM$^{+/+}$ siblings (34.83 cm/s), but this difference was not significant **(figure 5.12 a)**. However, several factors, including the weight and length of a fish, can affect zebrafish performance in this assay, so these were also recorded and used to normalise the U_{crit} to control for any effect these may have on swimming. No significant differences were observed in the length of ATM$^{+/+}$ and ATM$^{sh477/sh477}$ zebrafish **(figure 5.12 b),** or in their weight **(figure 5.12 c)**. Despite this, when the U_{crit} data were normalised to length **(figure 5.12 d),** the swimming ability of

ATM$^{sh477/sh477}$ zebrafish was significantly decreased from a mean of 10.86 in ATM$^{+/+}$, to a mean of 9.308 in ATM$^{sh477/sh477}$ (p= 0.0470), which is a ~15% decrease. Similarly, when the U$_{crit}$ data was normalised to weight **(figure 5.12 e)**, the swimming ability of ATM$^{sh477/sh477}$ zebrafish was also significantly decreased, from a mean of 115.3 in ATM$^{+/+}$ to a mean of 89.10 in ATM$^{sh477/sh477}$ (p= 0.0098), a decrease of ~22%. Therefore, it appears that 7-month-old ATM$^{sh477/sh477}$ have a small but significant reduction in swimming ability.

To determine whether ATM mutation also affects basal swimming, total motility was investigated by tracking unhindered movement over a 3 hour period. Zebrafish were placed in a 0.8 L tank, and swimming tracked from a side view with an infrared camera. Active swimming was categorised as movement >25 mm/sec. ATM$^{sh477/sh477}$ zebrafish show a ~24% decrease in the average distance travelled over the course of 3 hours **(figure 5.13 a and b)**, although, this decrease was not significant (p=0.2685). The duration of active swimming was also decreased in ATM$^{sh477/sh477}$ zebrafish compared to controls (~33%) **(figure 5.13 c and d)**, but again was not significant (p= 0.0685).

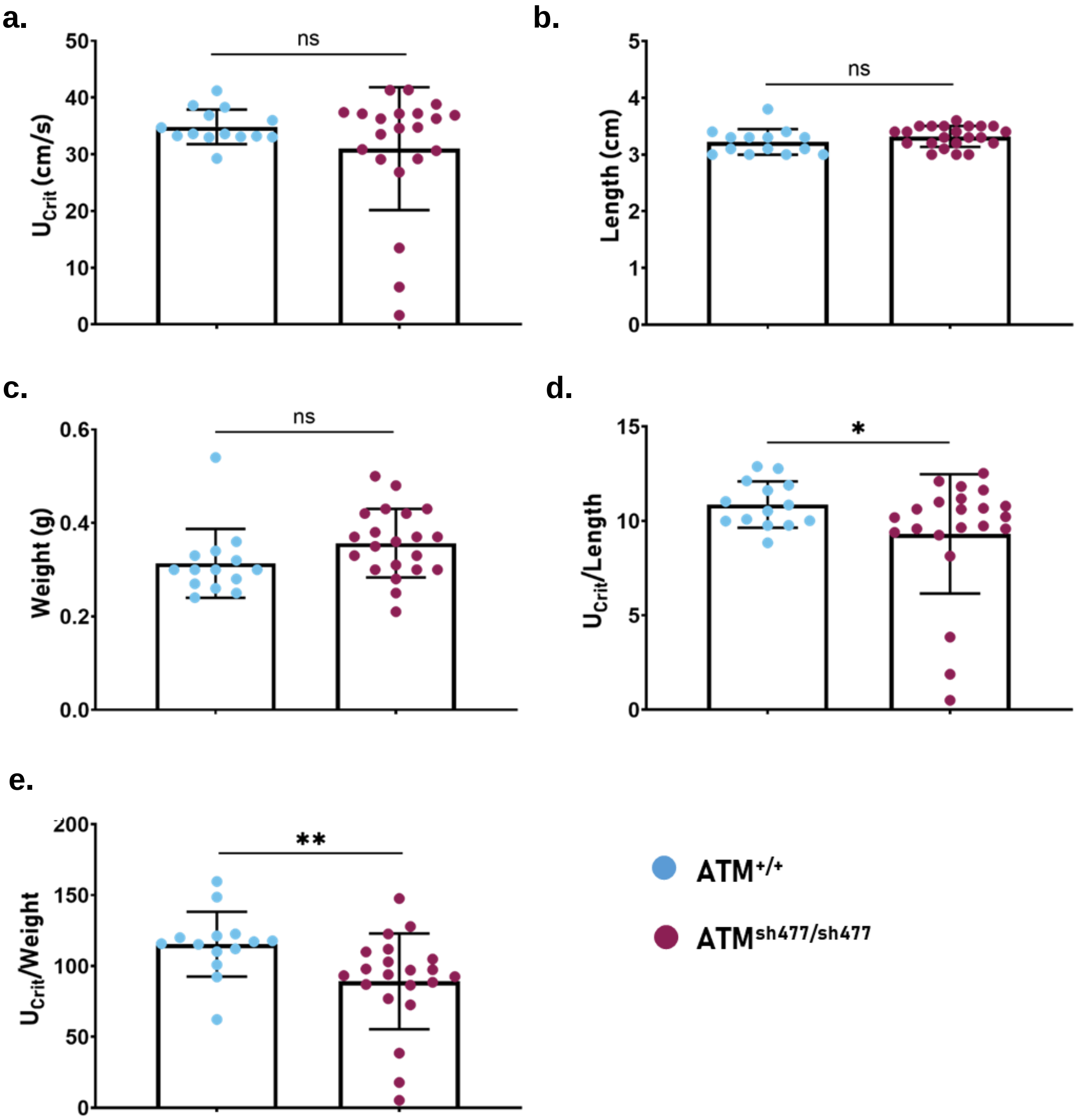

Figure 5.12 Adult male ATM$^{sh477/sh477}$ zebrafish show significant differences in their swimming endurance at 7 months of age compared to wild type siblings. Swimming endurance was determined by measuring the Critical Swimming Velocity (U_{Crit}) of sex matched fish (males) by placing each fish in a narrow tube that allowed a variable flow rate of water to pass through. The flow rate was increased in increments every 5 mins up to 35 mins or until the time the fish became exhausted. This time point was recorded and used to calculate the U_{crit}. **a.** U_{Crit} of 7 month old zebrafish. **b**. length of the fish immediately after the endurance test **c**. weight of the fish immediately after the endurance test. **d.** U_{Crit} normalised to length of fish **e.** U_{Crit} normalised to weight of fish. All data were analysed using an unpaired t-test with Welch's correction, and full statistical analysis can be found in **appendix 5.12** ATM$^{+/+}$ n=14, ATM$^{sh477/sh477}$ n= 21.

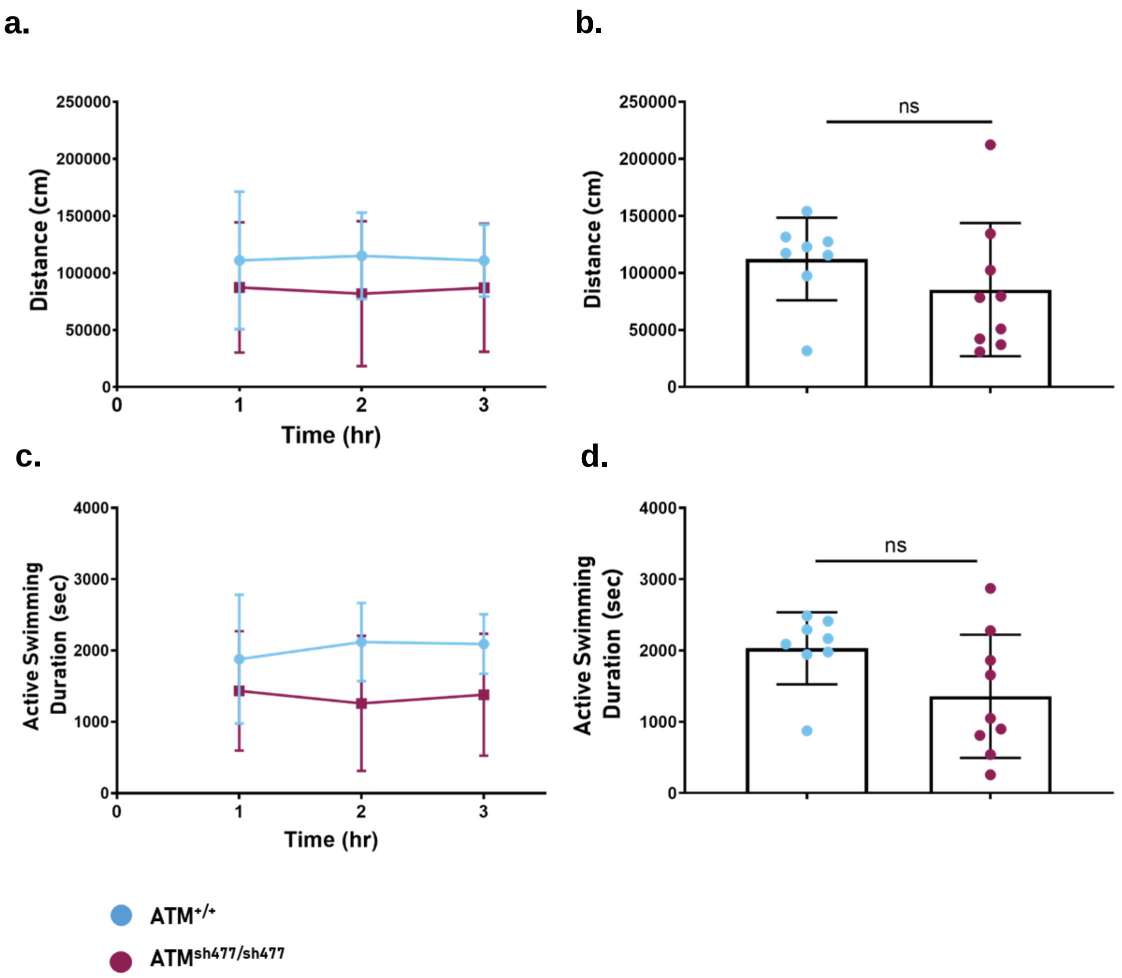

Figure 5.13 Investigations into Total Motility of ATM$^{sh477/sh477}$ zebrafish. Sex matched zebrafish (males) at 10 months were placed in individual tanks and left to acclimatise for 1 hr, after which their swimming was tracked over 3 hrs. **a**. Average distance travelled by ATM$^{+/+}$ and ATM$^{sh477/sh477}$ fish each hour. **b**. Average distance travelled by ATM$^{+/+}$ and ATM$^{sh477/sh477}$ zebrafish/hour. **c.** Average duration that each genotype spent in active swimming each hour. **d**. Average duration that each fish spent in active swimming. Data were analysed using an unpaired t-test with Welch's correction, and statistical analysis can be found in **appendix 5.13.** ATM$^{+/+}$ n=8, ATM$^{sh477/sh477}$ n=9.

5.2.4 Histological Examinations of Adult ATM$^{sh477/sh477}$ Cerebella

The reduced swimming ability in ATM$^{sh477/sh477}$ zebrafish, outlined above, indicated that there was the possibility of pathological changes in the cerebellum. Therefore, preliminary investigations of cerebellar pathology were carried out. ATM$^{sh477/sh477}$ and ATM$^{+/+}$ siblings at 12 months were formalin fixed and paraffin embedded for sectioning. Sections of 5 µm thickness were cut and stained with H&E. ATM$^{sh477/sh477}$ zebrafish had normal gross morphology and cerebellar organisation, with the granule cell layer, Purkinje cell layer and molecular layer all visible **(figure 5.14 and 5.15)**.

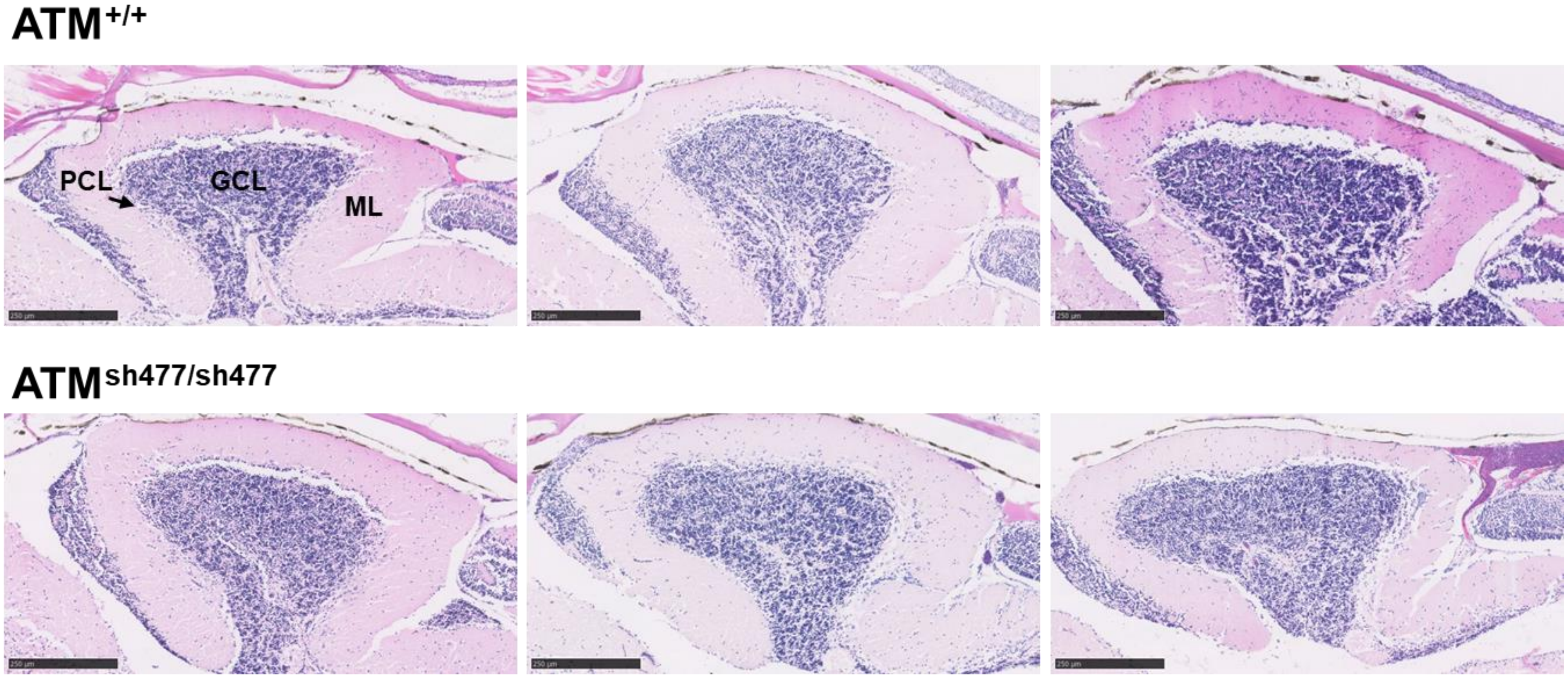
ATM+/+
PCL
GCL
ML
250 µm
ATMsh477/sh477

Figure 5.14 H&E Stained Sagittal Sections of ATM$^{+/+}$ and ATM$^{sh477/sh477}$ cerebella at 12 months. Top panel, ATM$^{+/+}$ zebrafish, bottom panel ATM$^{sh477/sh477}$ zebrafish. Arrowheads pointing to the Purkinje cell layer (PCL), granule cell layer (GCL) and molecular layer (ML) are also labelled. Scale bar represents 250 µm.

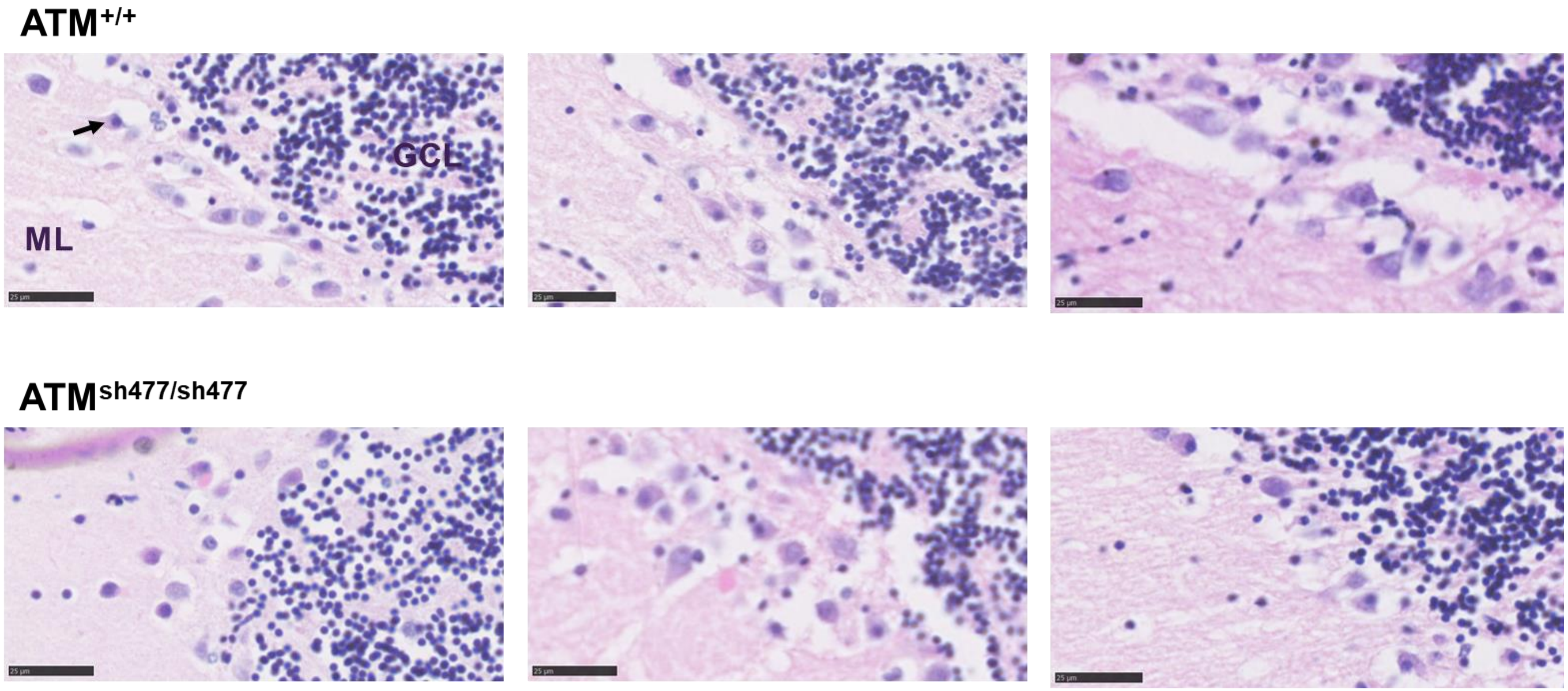

Figure 5.15 H&E Stained sagittal sections of ATM$^{+/+}$ and ATM$^{sh477/sh477}$ cerebella at 12 months (higher power). Top panel, ATM$^{+/+}$ zebrafish, bottom panel ATM$^{sh477/sh477}$ zebrafish. The Purkinje cell layer lies at the interface of the granular cell layer and the molecular layer. Purkinje cell body (arrow) with dendritic arbours extending into the molecular layer. Scale bars represent 25 µm.

5.3 Discussion

Following on from chapters 3 and 4 where the molecular and morphological effects of ATM KO in zebrafish were discussed, this chapter describes how we characterised the effects on behaviour and cerebellar morphology. As outlined in detail in **chapter 1 section 1.3,** no extant AT model accurately replicates all the neurological and behavioural characteristics seen in AT patients. This has caused a plateau in our understanding of the pathogenic mechanisms that cause neurodegeneration, and in our ability to identify new therapies. Therefore, the goals of the investigations in this chapter were twofold; first, to determine if ATM$^{sh477/sh477}$ zebrafish exhibit any signs of neurodegeneration, and second, if they do, whether these abnormalities can be feasibly exploited for drug screening.

5.3.1 ATM$^{sh477/sh477}$ Zebrafish Larvae Show no Divergence in their Behaviour from Wild Type Controls after Attempts to Induce DNA Damage

ATM$^{sh477/sh477}$ exhibited no abnormalities in behaviour at the larval stage **(figure 5.1)**. This is not surprising, as AT is thought to be a degenerative, not a developmental disorder, and the quiescent nature of the cells involved in a fully developed cerebellum is likely to be a contributing factor to neurodegeneration. At 5 dpf in zebrafish development, the cerebellum is only beginning to develop and most cells are still proliferative, and therefore may not be especially sensitive to the loss of ATM.

Results in chapter 3 indicate that that ATM$^{sh477/sh477}$ zebrafish are no more sensitive to induction of DNA damage than their wild type siblings. However, it was considered that subtle changes may exist that were not apparent in the morphological studies **(chapter 3, figure 3.8)**, and that these may be detected in the larvaes' behaviour. Furthermore, surpassing a threshold of neuronal DNA damage is a leading hypothesis for the cause of neuronal death in AT **(see chapter, 1 section 1.2.4.5 b)**. Therefore, attempts were made to induce a behavioural phenotype by induction of DNA damage, using three complementary approaches.

5.3.1.1 ATM$^{sh477/sh477}$ TDP1$^{sh475/sh475}$ Double Mutants

First we used a genetic approach to increase DNA damage. The ATM$^{+/sh477}$ line was crossed with a TDP1 KO line (TDP1$^{sh475/sh475}$), mutation of which in humans causes the hereditary ataxia SCAN1. SCAN1 is considered another DNA repair ataxia, where loss of TDP1 causes unrepaired protein linked ssDNA breaks during DNA replication (Takashima et al., 2002, El-Khamisy et al., 2005). It should be noted that although single mutation of ATM **(chapter 3, figure 3.9 and 3.10)** or TDP1 in zebrafish (Zaksauskaite et al., 2021) does not exhibit increased sensitivity to DNA damage, it is not known if double mutants of these genes do. Comparison of light/dark stimulated swimming in TDP1$^{sh475/sh475}$ mutants and ATM$^{sh477/sh477}$ TDP1$^{sh475/sh475}$ double mutant siblings under basal conditions showed no differences **(figure 5.2**), indicating that mutation of both of these genes does not result in increased DNA damage that is at least enough to pass a threshold to have deleterious effects that can be detected in swimming. Therefore, in order to determine whether ATM$^{sh477/sh477}$ TDP1$^{sh475/sh475}$ zebrafish do exhibit any increase in genotoxic insults, molecular characterisation would need to be carried out. To do this H_2AX phosphorylation with and without induction of DNA damage by IR should be considered. However, as TDP1 and ATM are both implicated in the repair of TOP1cc's during replication, then the relative expression of TOP1cc should be quantified with and without treatment with CPT in these double mutant fish.

5.3.1.2 Induction of DNA Damage by CPT

Second, attempts were made to induce DNA damage by treatment with the genotoxic agent CPT, **(figure 5.6)** (Hsiang et al., 1989, Hsiang et al., 1985, Wan et al., 1999, Sakasai et al., 2010, Zaksauskaite et al., 2021). Optimisations of CPT treatment revealed an unexpected result, whereby treatment of zebrafish with 1% DMSO led to a significant decrease in overall swimming distances and active duration **(figure 5.3)**. The reasons for this decrease in swimming were not investigated further, however, the observation that 1% DMSO treated zebrafish did not lose their darkness evoked response **(figure 5.3 a and c)** suggests that the decrease in motor function is not developmental. Previous studies have also investigated a link between DMSO concentration and motor function in zebrafish. However, these reports are conflicting, as some suggest that concentrations of 1% and below have no effect on motor function, while some report both hypo and hyper activity (Hallare et al., 2006, Sackerman et al., 2010, Chen et al., 2011, de Esch et al., 2012). However, it should be noted, that in these studies zebrafish were treated at different time points, assayed at different ages, using different assays. Therefore, the conflicting results should not be surprising. However, a recent study has been published where the effect of DMSO concentration on swimming was investigated using the same tracking system as used here, using the darkness evoked response to induce swimming, and a similar range of DMSO doses (Christou et al., 2020). In this study, DMSO concentrations of 1% and 0.55% decreased the active swimming duration, which is consistent with our observations. Furthermore, treatment with DMSO concentrations as low as 0.01% have been shown to affect the expression of genes involved in metabolism, development and heat shock (Turner et al., 2012, Hallare et al., 2006). The results presented here, and available in the literature, suggest care should be taken when treating larval zebrafish with DMSO to enhance drug solubility with behavioural analysis as the end points, and highlights the need for proper controls.

With regard to the effects of CPT, after several optimisations on wild type zebrafish **(table 5.1 and figures 5.4 and 5.5)**, 10 nM CPT treatment at 48 hpf was found to be optimum. However, not only did treatment with 10 nM CPT fail to decrease ATM$^{sh477/sh477}$ swimming compared to ATM$^{+/+}$ controls, it failed to decrease swimming overall in any genotype compared to untreated zebrafish **(figure 5.6)**. The reasons 10 nM CPT failed to elicit a decrease in motor function in ATM$^{+/+}$ zebrafish, when it had during optimisation in wild type zebrafish, may be varied and are not definitively known. Although optimisations were carried out in London Wild Type (LWT) zebrafish, and the background strain of the initial ATM$^{+/sh477}$ line was also LWT, the ATM$^{+/sh477}$ line used to create the larvae for this experiment had been outcrossed, and therefore, the genetic background consist of a number of strain differences. Not only has strain difference shown divergence in how they respond to behavioural analysis (de Esch et al., 2012, Christou et al., 2020), strain differences have also been reported in the response to DMSO, and although DMSO was used to enhance the solubility of the CPT in the media, it also enhances the permeability of the zebrafish (Christou et al., 2020, Kais et al., 2013b, Notman et al., 2006). Therefore, it is possible that differences in strain response to DMSO could affect uptake of CPT, as well as possible strain differences in response to CPT itself (de Esch et al., 2012, Pannia et al., 2014, Coe et al., 2009, Liu et al., 2014, Loucks and Carvan, 2004, Holden and Brown, 2018, Séguret et al., 2016, Audira et al., 2020). The effects of CPT on strain could be determined by repeating the above experiment with different strains housed in the aquarium facility.

5.3.1.3. Induction of DNA Damage by Treatment with Ionising Radiation

Investigations into the behaviour of ATM$^{sh477/sh477}$ 5 dpf larvae after induction of DNA damage concur with earlier results in chapter 3, in that they are no more radiosensitive than their ATM$^{+/+}$ siblings **(figure 5.7)**. It was again considered that the effects of IR on ATM mutants may have been masked by maternally contributed ATM at this age. At 12 dpf it was thought that any effects of maternally contributed ATM would have been lost. That, coupled with the fact that the cerebellum is more developed at this age (Hamling et al., 2015), suggests that a previously masked phenotype may now be apparent. However, ATM$^{sh477/sh477}$ zebrafish exhibited no differences in behaviour compared to controls with and without treatment with IR at 12 dpf **(figure 5.10 and 5.11)**. This again agrees with the data presented in **chapter 3**; that ATM$^{sh477/sh477}$ zebrafish do not exhibit an increase in radiosensitivity. For a detailed discussion on radiosensitivity in the ATM$^{sh477/sh477}$ model, see **chapter 3, section 3.3.2**.

Interestingly, treatment of all genotypes with IR did not significantly decrease the average distance travelled in the dark compared to un-irradiated controls; however, there was a significant difference between all genotypes in zebrafish treated with 2 Gy and 8 Gy **(figure 5.11 b)**. It is possible that this slight change in behaviour represents a differential response to radiation dose at the molecular level. Repair of IR induced DNA damage, particularly at relatively low doses, appears to favour repair by NHEJ as a ‘quick fix’, while higher doses of IR promote HR (Jeggo et al., 2011, Johnson and Jasin, 2001, Vierstraete et al., 2017), This is thought to be linked to the higher complexity of the damage. Therefore, zebrafish treated with 2 Gy IR may repair DNA efficiently, primarily through NHEJ, with no stopping of the cell cycle, while zebrafish treated with 8 Gy may not be able to repair the more complex DNA lesions with NHEJ and switch to HR. HR requires stalling of the cell cycle at the G2/S phase and the decreased swimming compared to 2 Gy treated zebrafish may represent a slight developmental delay as a result. Furthermore, the developmental delay may be exacerbated by possible clearing of cells where the DNA damage is too great to repair.

5.3.2 Adult ATM$^{sh477/sh477}$ Zebrafish do not Exhibit any Behavioural Defects that can be used as Therapeutic Target Readout

When the data is normalised for weight and length, 7 month old ATM$^{sh477/sh477}$ fish exhibit a slight, but significant, decrease in their swimming endurance **(figure 5.12)**. However, the exact cause of this decrease in endurance is not understood. It may be directly due to neurodegeneration, however as older ATM$^{sh477/sh477}$ zebrafish showed no statistically significant indicators of a behavioural phenotype in studies of their total motility **(figure 5.13)**, and as preliminary investigations of the cerebellum showed no gross abnormalities **(figure 5.14)**, a question remains on whether this decrease is linked to neurodegeneration. This decrease in swimming endurance in ATM$^{sh477/sh477}$ zebrafish may be more reflective of a global loss of ATM, such as a decrease in energy production due to defects in glucose transportation and insulin regulation**,** or mitochondrial dysfunction **(chapter 1, section 1.2.3, 1.2.4.4 and section 1.2.4.5 c ii)**. If the endurance decrease is caused by a metabolic defect, then this may account for the significant decrease observed in a swimming endurance assay over a total motility assay, as when investigating swimming endurance, the fish is stressed to exhaustion and would require a higher metabolic load.

Investigations into total motility of zebrafish **(figure 5.13)** were carried out at 10 months of age, and while there were no significant differences between genotypes, ATM$^{sh477/sh477}$ zebrafish did exhibit a slight decrease. It should be noted that in this experiment, the increased size of the ATM$^{sh477/sh477}$ zebrafish was not accounted for and data were not normalised to weight. Therefore, it is not known if this slight decrease is reflective of a behavioural phenotype, or if it is indicative of the increased weight. However, although the decrease in total motility observed in ATM$^{sh477/sh477}$ zebrafish is not statistically significant, it is proportionally a greater decrease than observed in the statistically significant endurance assay (U_{crit}/weight - ~22% decrease (p=0.0098), total motility - ~24% decrease in the average distance travelled over the course of 3 hours (p=0.2685), and ~33% decrease in duration of active swimming (p=0.0685). Interestingly a zebrafish model with complete ablation of Purkinje cell synaptic output exhibited a 50% decrease in distance travelled in a total motility test (Chang et al., 2020).

Based on the above adult swimming data, regardless of whether any observed differences in the behaviour of ATM$^{sh477/sh477}$ adult zebrafish represent a true behavioural phenotype, the ATM$^{sh477/sh477}$ model is not suitable for high throughput screening studies with movement analysis as a readout. This is because the variability of the data requires high numbers of adult wild type and ATM$^{sh477/sh477}$ zebrafish of the same sex, which are difficult to obtain. The experiments above were carried out using all relevant and available zebrafish raised from 3 different cohorts from an ATM$^{+/sh477}$ in-cross, each of 120 fish in total. Added to this, the requirement for male sex matching as all ATM$^{sh477/sh477}$ are male, and the resultant skewing of sex ratios in ATM$^{+/+}$, causing a decrease in expected male ATM$^{+/+}$ zebrafish within the cohort **(chapter 3, figure 3.6)**, mean that the time and cost required for further investigation become prohibitive. For the endurance assay and investigations into total motility to have 90% power, a minimum sample of size of 53 fish per group would be required **(appendix 5.12 and 5.13)**. For the endurance assay and total motility assay to have an 80% power, a more feasible sample size of 30 and 41 fish per group, respectively, would be required (data not shown). In order to be able to raise these numbers of experimental zebrafish, progeny from an ATM$^{+/sh477}$ in-cross would need to be genotyped at the larval stage, to facilitate the raising of only the genotypes of interest. This had not been done previously, as it would require the biopsy of the tail at a young age, which could differentially affect swimming. However, the facility has recently acquired a Zebrafish Embryonic Genotyper (ZEG) Unit (wFluidx), which allows extraction of genomic material from larval zebrafish while maintaining fish viability. Therefore, only the relevant ATM$^{+/+}$ and ATM$^{sh477/sh477}$ zebrafish can be raised. Furthermore, to overcome the male to female sex skewing that appears to occur in ATM$^{+/+}$ zebrafish when raised in a tank alongside the ATM$^{sh477/sh477}$ zebrafish, each genotype could now be raised separately, and the ATM$^{+/+}$ tank supplemented with the easily distinguishable nacre fish to encourage a 50/50 sex ratio.

However, due to the increased size of aged ATM$^{sh477/s477}$ zebrafish from neoplastic growth of the testes **(chapter 4)**, even when the data has been normalised to account for the increased weight, and with an adequate sample size, there is no way to control for the different morphology within the experimental design. Differences in morphology have been shown to have an effect on zebrafish locomotion, particularly in the terms of measuring their swimming endurance, with differences in the morphology between males and females accounting for over 40% of the variability observed (Conradsen et al., 2016, Conradsen and McGuigan, 2015, Leris et al., 2013). Despite zebrafish in the above experiments being sex matched, aged

ATM$^{sh477/s477}$ male zebrafish, even at 7 months, have a gross morphology more closely resembling a female at the same age. To overcome this morphological difference, zebrafish would need to be assayed at a younger age, before onset of the testicular neoplasm, at approximately 3-4 months. Nonetheless, this raises practical issues in performing the experimental assays, as zebrafish at this age can be relatively small compared to older adults, and the current swim tunnel apparatus is not suitable for very small fish. Furthermore, if the decrease in swimming is linked to an age associated neurodegenerative phenotype, it may likely not be present at a younger age.

5.3.4 Future Work and Characterisation of Neurodegeneration in the ATM$^{sh477/sh477}$ Zebrafish Model

5.3.4.1 Analysis of Larval and Juvenile Behaviour

The larval and juvenile behaviour of ATM$^{sh477/sh477}$ has been relatively well characterised in the above experiments. We also considered additional analysis of zebrafish swimming with a fast capture camera, in order to determine whether changes in movement of the tail of ATM$^{sh477/sh477}$ fish could be observed during swimming. However, this type of analysis is time consuming; using the available equipment, only 3 fish could be assayed every 2 hrs. This, coupled with the problem that the relevant genotypes to be assayed needed to be generated from an ATM$^{+/sh477}$ in-cross, meant that only 50% of the fish assayed and data collected would be relevant. We could genotype embryos at 3 dpf and then use these for larval/juvenile swimming assays. Conventionally this would involve tail biopsy, however as this might impact on the way larvae swim, it should be avoided. As mentioned above, we recently obtained a ZEG, which allows non-invasive sampling of environmental DNA from 3 dpf embryos. This approach should make high speed imaging an achievable prospect.

There is also some evidence suggesting that zebrafish may not be an appropriate system to model ataxia. A transgenic zebrafish line, with tamoxifen-induced highly specific PC cell apoptosis has been reported (Weber et al., 2016). However, communications with the author indicate that after complete ablation of cerebellar PC, no gross swimming abnormalities were observed. Therefore, it may be possible that PC are not essential for functional free swimming in zebrafish larvae, and even if ATM specific, loss of PC were to occur in the ATM$^{sh477/sh477}$ model, it may not present as a swimming abnormality. Additionally, a transgenic zebrafish model of the dominant negative HCA SCA13, where PC specific expression of the pathogenic human Kcnc3a^{R335H} gene lead to PC cell death, reported no swimming defects but did report significant behavioural abnormalities of impaired eye moment, particularly saccades (Namikawa et al., 2019b). Eye movement abnormalities have long been associated with cerebellar degeneration in AT, particularly the presence of saccades and nystagmus (Tang and Shaikh, 2019). Therefore, while ATM$^{sh477/sh477}$ zebrafish do not exhibit any swimming abnormalities, further investigations into eye movement in this model may prove fruitful.

In addition to its role in the DDR, ATM is increasingly implicated in the regulation of oxidative stress and mitochondrial function **(see chapter 1, section 1.2.4 and section 1.2.4.5 b).** Therefore, ATM KO fish may show behavioural differences when challenged with oxidative stress or mitochondrial toxins. Changes in zebrafish behaviour can serve as an indicator of increased sensitivity to treatment with oxidising agents such as hydrogen peroxide and atrazine (Blahová et al., 2013), as they have done in this chapter to determine if there was increased sensitivity to DNA damage.

5.3.4.2 Investigation into Cerebellar Degeneration

Whether ATM$^{sh477/sh477}$ zebrafish exhibit a true age-related behavioural phenotype related to neurodegeneration is not clear. Nevertheless, there may still be pathological cerebellar changes linked to loss of ATM function. Our examinations into cerebellar morphology in adult ATM$^{sh477/sh477}$ zebrafish **(figure 5.14)** showed no gross morphological abnormalities in mutant fish. However, these studies were only preliminary.

It is essential for ongoing investigations that the cerebellum, and particularly PCs of ATM$^{sh477/sh477}$ zebrafish, are accurately imaged and quantified under basal and/or stress conditions. Attempts had been made to visualise and quantify the developing cerebellum in zebrafish larvae using whole mount immunofluorescence of the protein Parvalbumin7, which is highly expressed in zebrafish PC (Bae et al., 2009). However, no cerebellar staining was observed with this antibody (data not shown). Therefore, plans were made to cross the ATM$^{+/sh477}$ line with a transgenic PC specific *Ca8* linked red fluorescent protein line (Tg(ca8:FMA-TagRFP-2A-casp8ERT2)bz11Tg), in order to visualise PC (Weber et al., 2016). However, due to a catastrophic incident in the aquarium in Germany where these transgenic fish were housed, there was a significant delay in being able to cross these two lines. The use of this RFP transgenic line over whole mount immunofluorescence has significant advantages, such as being more cost effective, time saving, and the ability to conduct live imaging. In addition to using these transgenic zebrafish to investigate cerebellar morphology, and to quantify PC number through development, this transgenic line has the ability to allow PC specific investigations after FACS analysis, for example to examine a number of parameters such as DNA damage, levels of oxidative stress, and mitochondrial number.

In this project, attempts to characterise the neuronal expression of the ATM protein in zebrafish were made using IHC and DAB staining with the zATM antibody **(chapter 3 and 4)** on FFPE tissue (data not shown). However, there was considerable background staining and therefore future work on this is required. Using fluorescence secondary antibodies with confocal microscopy may prove more fruitful in future work.

5.3.4.3 Continued Investigation into Compensation for Loss of ATM at the Protein Level

As ATM$^{sh477/sh477}$ zebrafish do not exhibit increased radiosensitivity in the experiments in this thesis, we hypothesised that there is compensation for loss of the ATM protein at the protein level **(see chapter 3, section 3.3.2.2 and section 5.2.1.3)**. Our preliminary investigations showed that ATM$^{sh477/sh477}$ zebrafish treated with an ATM kinase inhibitor appeared less sensitive to the effects of IR on behaviour compared to ATM$^{+/+}$ that had also been treated with the inhibitor **(figure 5.9)**. This suggests that there may be an alternative DDR pathway that compensates in the absence of ATM. This data is not definitive, and further investigated is warranted. For instance, the reported experiment could be repeated, this time using morphology and apoptosis as readouts of cell survival.

Similar studies could be carried out using a number of other ATM inhibitors, along with dose-response experiments. However, it should be noted that using different ATM inhibitors for these investigations might be problematic, as ATM inhibitors can also inhibit other members of the PI3-PIKK family, chiefly ATR and DNA-PKcs, which are also proteins that are expected to be involved in the putative compensation. This is particularly true when these inhibitors are used at higher doses. Therefore, care needs to be taken when inhibiting ATM, not to inhibit other PI3-PIKK members that may be upregulated in ATM$^{sh477/sh477}$ zebrafish. To further strengthen this line of investigation and to mitigate off-target effects of chemical inhibition of ATM, attempts could be made to target the kinase domain by CRISPR/Cas9 and create an ATM kinase dead line. Creating a zebrafish kinase dead ATM model has considerable advantages over a mouse model, since zebrafish develop externally and could be studied even if the fish may die at a later stage. However, given the embryonic lethality observed in ATM kinase dead mice, and in zebrafish ATM morphants that are predicted to have loss of kinase activity **(chapter 3, section 3.3.2.3)**, a stable ATM kinase dead model will also not be viable beyond the embryonic stage.

Chapter 6
Discussion

6.1 Summary of Key findings

One of the first tasks of validating ATM$^{sh477/sh477}$ zebrafish as a model of AT is determining whether it is a knockout model with loss of normal expression of a functional ATM protein, as seen in AT patients. It was hoped that the mutant *ATM*^{sh477} transcript would undergo NMD, however, this was not the case, as there was comparable expression of *ATM* mRNA in both ATM$^{+/+}$ and ATM$^{sh477/sh477}$ zebrafish at the larval, juvenile and adult stages Several attempts were made to quantify expression of the ATM protein between the two genotypes by western blot analysis, IHC and mass spectrometry. Nevertheless, detection of full-length ATM protein was not possible by western blot or mass spectrometry. IHC of ATM$^{+/+}$ testes with a new antibody, raised against the N-terminus of the zebrafish protein sequence before the predicted stop codon in mutant zebrafish, showed strong staining in cell types where ATM would be expected to be expressed. However, similar staining was also detected in ATM$^{sh477/sh477}$ zebrafish. Therefore, it is not clear if this was non-specific staining of other protein species present (as was evident by western blot), or if it was ATM specific staining of a possible truncated non-functional ATM protein in the mutant zebrafish testes. However, given that expression of the detected protein aligned with cell types where ATM would be expected to be expressed, and expression of the protein was lost in late spermatids and mature spermatozoa, as would be expected of ATM and has been observed in mouse models (Hamer et al., 2004), it is consistent with bona fide ATM expression. Furthermore, the finding that the ATM$^{sh477/sh477}$ zebrafish all develop as male, indicating they undergo the same female to male sex reversal as other DDR mutant zebrafish, and that they exhibit stalled spermatogenic development, similar to other vertebrate models of AT, and AT patients, both indicate that the ATM$^{sh477/sh477}$ model is very likely to be an ATM knockout.

One of the most surprising results of characterisation of the ATM$^{sh477/sh477}$ model is that they do not appear to exhibit any increase in radiosensitivity. However, further investigation is required to fully understand whether there are any deficiencies in the somatic DDR. Preliminary data suggests that there may not be, as there was no difference in expression in immunoglobulin mRNA transcripts between the genotypes, the production of which relies on the repair of ds breaks. Direct quantification of induction of the DDR by quantification of activation of γH_2AX after treatment with ionising radiation gave inadequate insight, and it is difficult to form a definitive conclusion from the experiment as it could only be repeated once in the time available.

While the data are currently unclear for somatic DNA repair, our data strongly indicate that there are deficiencies in DDR repair in germ cells. As indicated above, adult male $ATM^{sh477/sh477}$ zebrafish have stalled spermatogenesis, and based on their testicular histology, similarities in other DDR zebrafish models that function in the same pathway, and rodent models of AT, this stalling of spermatogenesis is most probably due to a meiotic defect. The literature strongly suggests that this meiotic defect is due to failure to repair HR linked ds DNA breaks in the developing sperm cells. Furthermore, this spermatogenic failure appears to be the root cause of two other testicular phenotypes exhibited by $ATM^{sh477/sh477}$ zebrafish. The first of these is a strong female to male sex reversal. In other zebrafish DDR models this sex reversal has been attributed to failure of meiotic recombination in the developing ovary, resulting in p53 mediated cell death of the developing oocytes, and masculinisation of the gonads (Ye and Chen, 2020). The other secondary phenotype resulting from failed meiosis is the unchecked proliferation of Sertoli cells in maturing spermatocytes in the zebrafish testes, resulting in testicular neoplasia.

Analysis of larval and juvenile zebrafish behaviour showed no abnormalities in $ATM^{sh477/sh477}$ zebrafish, suggesting that loss of ATM in zebrafish may not cause a neurological phenotype. Additionally, the same analysis after treatment with IR supported our findings that they do not exhibit any increase in their radiosensitivity. Analysis of adult swimming is not definitive, as the data indicated that there might be changes in $ATM^{sh477/sh477}$ swimming, particularly in endurance assays. However, this may not be linked to a neurological phenotype, as the changes in the fish morphology due to the testicular neoplasms cannot be ruled out as a cause of the behavioural abnormalities. Furthermore, preliminary investigations into cerebellar morphology in adult fish also indicate that there are no gross abnormalities.

Figure 6.1 summarises the key findings in the characterisation of the ATM$^{sh477/sh477}$ model, and **table 6.1** compares the key findings and phenotypes to other vertebrate models of AT.

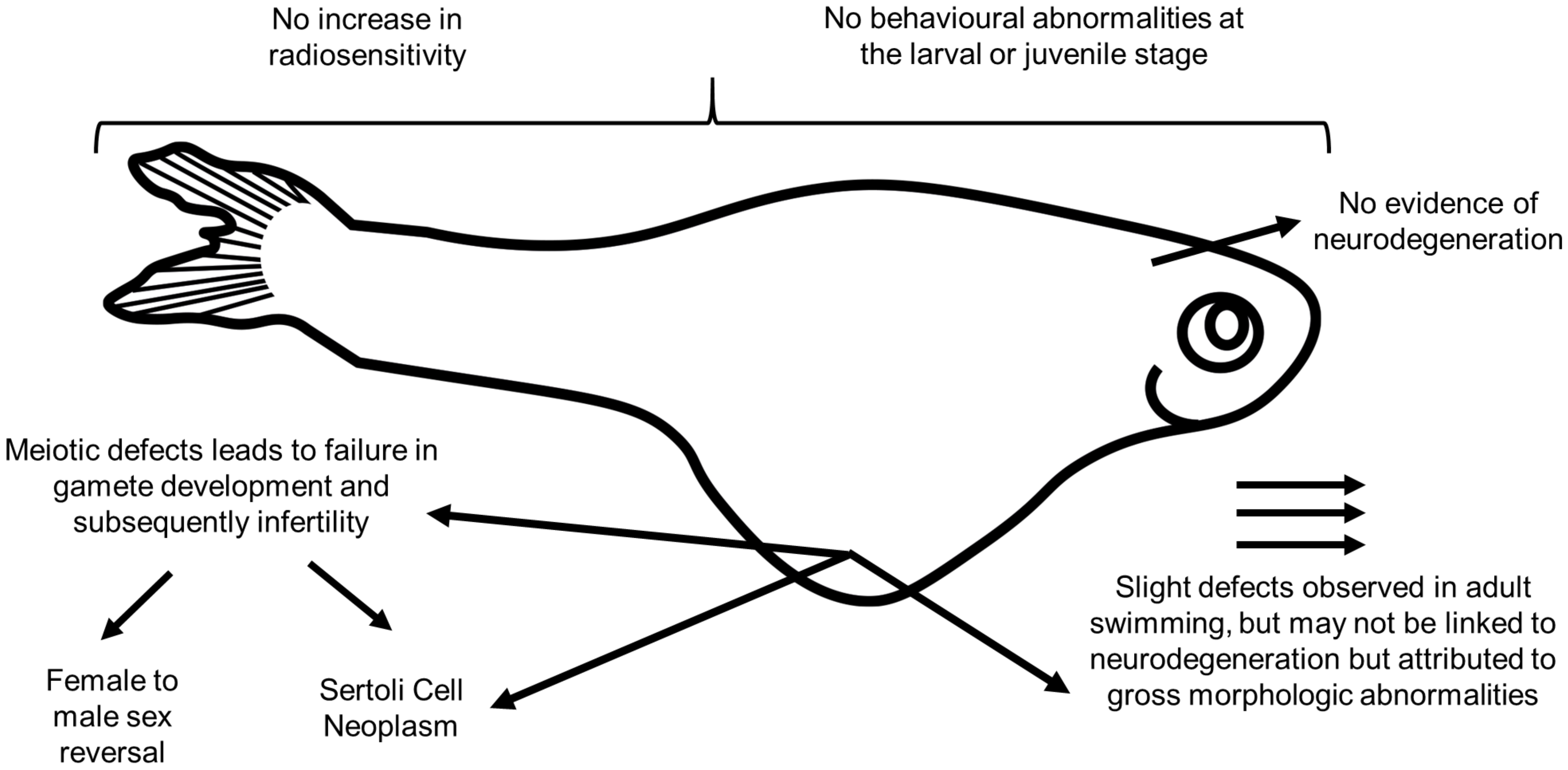
No increase in radiosensitivity
No behavioural abnormalities at the larval or juvenile stage
No evidence of neurodegeneration
Meiotic defects leads to failure in gamete development and subsequently infertility
Female to male sex reversal
Sertoli Cell Neoplasm
Slight defects observed in adult swimming, but may not be linked to neurodegeneration but attributed to gross morphologic abnormalities

Figure 6.1 Summary of key findings in the characterisation of the ATM$^{sh477/sh477}$ model. ATM$^{sh477/sh477}$ zebrafish exhibit no radiosensitivity, behavioural abnormalities at the larval or juvenile stages of development, or signs of neurodegeneration. They do, ,however, exhibit defects in germ cell development, which leads to a female to male sex reversal, and Sertoli cell neoplasm in the resultant adult males. Finally, ATM$^{sh477/sh477}$ zebrafish exhibit slight deficiencies in adult swimming, however, this is most likely a result of changes in gross morphology due to the testicular neoplasms.

Table 6.1 Comparison of key findings of the zebrafish ATM$^{sh477/sh477}$ model and other vertebrate models of AT

	Pig	*Rat*	*Mouse*	*Zebrafish*	*Notes/Further information*
Radiosensitivity	✓	✓	✓	✗	*Radiosensitivity analysis was not conducted on whole organism in pigs but in ATM deficient pig primary fibroblasts.*
Deficiencies in activating the DDR	✓	✓	✓	*IC*	*Further study is required but in our limited investigations no obvious deficiency was observed in ATM mutant zebrafish*
Senescence/Premature Ageing	*NR*	*NR*	✓	*IC*	*There was no increase in basal senescence observed in ATM$^{sh477/sh477}$ zebrafish. Differences were observed in juvenile zebrafish after induction of IR, however, more repeats are required to determine if the differences are statistically significant.*
Infertility	✓	✓	✓	✓	*Compete infertility was only observed in female pigs but male AT deficient pigs did exhibit reduced fertility and some spermatozoa defects.*
Malignancies	✓	✓	✓	✗	*Analysis by a veterinary pathologist revealed no malignancies in the liver or kidneys in histological sections of 12 month ATM mutant zebrafish.*
Neuroinflammation	*NR*	✓	✓	*NI*	
Systemic Inflammation	*NR*	✓	✓	✗	*Investigations of senescence characterised expression of proinflammatory genes IL1-β and IL6 in whole adult and juvenile zebrafish lysates under basal conditions, and no increase in expression was observed.*
Major cerebellar defects	✓	✗	✗	✗	*Preliminary investigations into cerebellar morphology showed no gross morphological defects. However, further study is required for full characterisation*
Ocular Abnormalities	*NR*	✓	*NR*	*NI*	
Liver Defects	*NR*			*NI*	
Sensitivity to Oxidative Stress	*NR*	✓	✓	*NI*	
Telangiectasias	*NR*	✓	*NR*	✗	
Neurodegeneration	✓	✓	✗	✗	
Peripheral Neuron degeneration	*NR*	✓	✗	*NI*	
Locomotor Phenotype	✓	✓	✗	*See notes*	*A small locomotor defect was observed in zebrafish, however it cannot be attributed to neurodegeneration.*
Chromosomal Instability	*NR*	*NR*	✓	*NI*	
Immunological defects	✓	✓	✓	✗	
Growth Retardation	✓	✓	✓	✗	

NR- Not reported, NI-Not investigated, IC- Inconclusive (Beraldi et al., 2017, Beraldi et al., 2015, Quek et al., 2017a, Quek et al., 2017b, Barlow et al., 1996, Elson et al., 1996, Xu et al., 1996, Hartlova et al., 2015, McDonald et al., 2011).

6.2 Contribution of the ATM$^{sh477/sh477}$ model

6.2.1 Limitations in the Characterisation of ATM$^{sh477/sh477}$ Zebrafish

6.2.1.1 It has not been experimentally shown that ATM$^{sh477/sh477}$ zebrafish are a KO model

Despite many attempts, clear experimental evidence that the ATM$^{sh477/sh477}$ zebrafish are KO for the ATM protein was not achieved. Although much of the experimental data presented here strongly indicate that it is deficient for the ATM protein, the inability to definitely determine the status of the ATM protein in these zebrafish is one of the biggest weaknesses in our characterisation of the model. Nevertheless, if time had allowed, further avenues of investigation may have been carried out to mitigate this. These could include raising another antibody, this time to a smaller epitope at the N-terminal, a few amino acids long, where the denaturing nature of an SDS PAGE gel may not have as much an effect on antibody recognition. This may allow for detection of both a full-length protein and a truncated version if present, similar to what we have already attempted. Alternatively, a new antibody could also be raised to the ATM C-terminal in the hopes of detection of a full-length protein in ATM$^{+/+}$ zebrafish lysates, and of observing no expression in mutant lysates. Interestingly, in the investigations already carried out, there was some evidence of a truncated protein species being present in mutant lysates, as three bands were detected between 20-37 KDa by western blot **(figure 3.5)**. In the future, purification and analysis of these bands by mass spectrometry may help determine if they represent truncated ATM protein.

6.2.1.2 Characterisation of the DDR at the Whole Larval/Adult Level

For the most part, characterisation of the DDR in the ATM$^{sh477/sh477}$ model has been conducted in whole larvae or whole adult zebrafish. However, this may obscure cell specific effects. We have already seen this be the case in adult tissue where loss of ATM does not appear to have an effect on somatic cells but has an acute effect on developing gametes. The resultant neoplasia in the testes also contributes an uneven tissue/cell contribution to samples that were generated from whole adult zebrafish. This may be compounded when analysing extracts from larval zebrafish, as not only may cell specific effects be missed, but also, in order to generate enough sample for analysis, larvae need to be pooled. This pooling of larvae may obscure any larvae that are outliers. Most adult tissue should provide enough sample for RNA or protein analysis. In future, discrete tissues should first be isolated before analysis. While not much can be done to mitigate the need to pool larvae to ensure enough sample is gathered, for RT-qPCR or western blot analyses, microscopy approaches such as *in situ* hybridisation and immunofluorescence could be utilised.

6.2.1.3 Radiosensitivity and the DDR has not been Investigated in Adult Zebrafish

While we characterised the radiosensitivity of larval zebrafish and began to define their response to IR, we have not done so in adult zebrafish. This is important, as fully differentiated tissues may have differing responses and mechanisms of DDR. However, due to the parameters of the project licence and the licencing of procedure rooms for schedule 1 of zebrafish under ASPA 1986, the irradiation of adult zebrafish was prohibited. The project licence has now been amended, and as the relevant rooms in the facility are now authorised for schedule 1 culling, experiments of this nature can proceed in the future.

6.2.1.4 Female to Male Sex Reversal in ATM$^{sh477/sh477}$ Zebrafish Limits the Numbers of Fish Available for Experimentation

The female to male sex skew observed in ATM mutants was quite problematic for experimental design. As all ATM$^{sh477/sh477}$ zebrafish were male, it was necessary that all control ATM$^{+/+}$ zebrafish also be male. However, the ATM$^{+/+}$ and ATM$^{+/sh477}$ zebrafish raised in the same tank as the mutants appeared to exhibit sex skewing towards female. It is not known whether this skewing is due to chance, a preference in the strain used, or if it occurs due to compensation for the all-male mutants. Although this female to male sex reversal is also exhibited by Brca2 mutant zebrafish produced from a heterozygous in-cross, and in 12 Fanconi Anaemia associated genes, wild type and heterozygous progeny do not experience female sex skewing as describe here (Rodríguez-Marí et al., 2011, Shive et al., 2010, Ramanagoudr-Bhojappa et al., 2018). There is no data available on sex ratios of other genotypes from a Rad51 heterozygous incross (Botthof et al., 2017). This has drastically reduced the numbers of control fish available, reducing the power of experiments. However, we have recently acquired a

Zebrafish Embryonic Genotyper ZEG (Lambert et al., 2018), which will allow genotyping of larval zebrafish while maintaining viability. Therefore, ATM$^{+/+}$ and ATM$^{sh477/sh477}$ zebrafish can now be raised separately, which in theory should prevent the sex skewing of ATM$^{+/+}$ fish, and permit generation of greater numbers of wild type males as ATM$^{+/sh477}$ zebrafish need not be raised alongside them.

6.2.1.5 Gross Morphological Changes in ATM$^{sh477/sh477}$ Zebrafish Make Characterisation of their Adult Swimming Ambiguous

While ATM$^{sh477/sh477}$ larval and juvenile swimming has been well characterised under basal and stress conditions (treatment with IR), it was not formally investigated in adult stages. So the results leave some ambiguity as to whether there is a behavioural phenotype or not, and if there is a behavioural defect, whether it is linked to neurodegeneration. The reasons for lack of analysis are twofold. First, we had difficulty in generating adequate numbers of male ATM$^{+/+}$ control zebrafish due to the sex reversal as outlined in the section above. Second, we were unable to mitigate for the Sertoli cell neoplasia in adult mutant fish. Further analysis of behaviour in these fish would have likely proved futile, as any discrepancies observed in ATM$^{sh477/h477}$ swimming compared to ATM$^{+/+}$ could be attributed to gross morphological differences in the adult fish. There were a number of outliers in the ATM$^{sh477/sh477}$ cohort during analysis of critical swimming velocity **(figure 5.12).** It was considered that the Sertoli neoplasia had become so pronounced in this fish that it caused more difficulty in continued swimming or perhaps the fish was in pain. However, although the relative size of the neoplasia were not measured in these fish, there was no major differences in their weight (data not shown) and thus the reason for their poor performance is unexplained. To circumvent the challenges in adult behavioural analysis caused by the increase testes size, analysis could be performed at a much younger age, before the testicular neoplasms grow to the extent that the gross morphology of fish is significantly changed. However, as neurodegeneration and a locomotor phenotype in AT is age related, analysis at a younger age may miss any abnormalities caused by neurodegeneration.

It was not possible to accurately control for the increased size, weight and altered morphology in ATM$^{sh477/sh477}$ zebrafish during the adult behavioural analysis outlined in **chapter 5**. However, this may be possible in future by inducing transient ablation of *dnd* by MO KD. The *dnd* gene regulates primordial germ cell development in zebrafish. Transient KD of this gene by injection of a *dnd* MO in early embryogenesis has been shown to completely ablate germ cells, and cause female to male sex reversal and atrophied testes in the adult fish at 6 months (Kobayashi et al., 2017, Slanchev et al., 2005, Siegfried and Nüsslein-Volhard, 2008). Therefore, if the Sertoli cell proliferation observed in ATM$^{sh477/sh477}$ zebrafish is a secondary phenotype caused by the Sertoli cells' response to incomplete spermatogenesis, then following the ablation of germ cells by *dnd* KD in the progeny from an ATM$^{+/sh477}$ in-cross, ATM$^{+/+}$ and ATM$^{sh477/sh477}$ zebrafish would be expected to have a comparable testicular phenotype. Furthermore, injection of wild type fish with the *dnd* morpholino should result in a similar female to male sex reversal to that which is observed in the mutants, leaving all ATM$^{+/+}$ male and available for sex matched experiments. However, there is a caveat to the use of a *dnd* morpholino in this way. While *dnd* injected zebrafish exhibit atrophied testes at 6 months (Slanchev et al., 2005), at 18 months they exhibit similar neoplastic growth as ATM and Brca2 mutants (Rodríguez-Marí et al., 2011) **(see chapter 4**. However, fish with testicular neoplasm should still be eligible for behavioural analysis, as after *dnd* KD, both ATM$^{+/+}$ and ATM$^{sh477/sh477}$ zebrafish would be expected to exhibit them to the same extent and therefore, aged matched fish would still be comparable. Conversely, a germ cell transplant could be performed on the ATM$^{sh477/sh477}$ at an appropriate point in development, and while the other systems in the fish will remain ATM deficient, the testis germ cells should develop as normal without the sex reversal and without the Sertoli cell neoplasia.

6.2.1.6 The Response of ATM$^{sh477/sh477}$ Zebrafish to Oxidative Stress has not een Characterised

As ATM is primarily considered a master regulator of the DDR **(see chapter 1, section 1.2.2)**, investigations contained within this thesis mainly focus on the loss of ATM signalling in the context of the DDR. However, emerging evidence in the last 10 years suggests that ATM is a regulator of oxidative stress as much as it regulates the DDR **(see chapter 1, section 1.2.3)**. Therefore, before the model can be considered to be exhaustively characterised, the effects of oxidative stress on ATM$^{sh477/sh477}$ zebrafish should be investigated. There had been the intention to perform mitochondrial complex assays on zebrafish lysates; however, these required the use of cyanide, the use of which needed training and authorisation by the central University Health and Safety committee. Due to the disruptions caused by the COVID19 pandemic, this was not possible.

6.2.2 The Sex Reversal Exhibited by ATM$^{sh477/sh477}$ Zebrafish has the Potential to be Exploited as an Assay to Determine Approaches to Restore ATM Activity

One of the aims of the project was to determine whether the ATM$^{sh477/sh477}$ model could be utilised in the screening of therapeutic targets for the return of the ATM pathway. The sex reversal exhibited by ATM$^{sh477/sh477}$ zebrafish may present an avenue for this. Brca2$^{-/-}$ zebrafish exhibit this female to male sex reversal, however, they have the potential to develop as female when p53 expression has been ablated, following which brca2-/- zebrafish subsequently develop as 50% male, 50% female. Therefore, in theory ATM$^{sh477/sh477}$ zebrafish may exhibit the same potential. A prospective assay could involve raising ATM$^{+/+}$ and ATM$^{sh477/sh477}$ zebrafish while treating them with potential therapies. After 40 dpf, when gonad determination is cemented (Ye and Chen, 2020), zebrafish could be analysed by RT-qPCR for expression of ovary associated genes such as *cyp19a1a* (Wang and Orban, 2007, Yin et al., 2017), *foxl2* (Yin et al., 2017, Yang et al., 2017), and *nanos2* and *nanos3* (Beer and Draper, 2013, Cao et al., 2019), as well as testes associated genes such as *sox9a* (Jørgensen et al., 2008), *dmrt1* (Webster et al., 2017) and *amh* (Lin et al., 2017). Validation of resultant sex ratios could also be confirmed by histological analysis on a subset of the treated fish. Furthermore, if investigated and confirmed that p53 ablation can rescue the sex reversal in ATM mutant zebrafish, similarly to the way it does in brca2-/- fish, crossing of the ATM$^{+/sh477}$ line to p53 mutants could provide a valuable positive control.

6.2.3 Validity of Modelling DDR Disorders in Zebrafish

6.2.3.1 Comparison of Zebrafish DDR Mutants

The results that ATM$^{sh477/sh477}$ zebrafish do not exhibit any increase in radiosensitivity raises the question of whether zebrafish are an adequate model for DDR disorders, or whether the repair mechanism between them and mammals have diverged too much. Other zebrafish KO models of DDR genes do exhibit phenotypes consistent with loss of that gene. For example, Brca2 deficient zebrafish exhibit chromosomal instability and sensitivity to DNA damaging agents, with a slower growth rate due to an increase in apoptotic cells (Rodríguez-Marí et al., 2011). Rad51 KO zebrafish, in which Fanconi Anaemia was modelled, similarly exhibit chromosomal instability and sensitivity to DNA damaging agents, with a drastically increased sensitivity to IR. They also recapitulate many of the features of Fanconi Anaemia, such as growth retardation, microphthalmia, kidney hypocellularity and a decrease in hematopoiesis (Botthof et al., 2017). Furthermore, KO of 11 other Fanconi Anaemia associated genes in zebrafish *(ancd1, fancd2, fanci, fancj, fancn, fancp, fanct*, *fancb, fanco, fanca and fancq)* also exhibit sensitivity to DNA damaging agents. These findings support the idea that zebrafish are a valid model for modelling DDR associated disorders. However, KO zebrafish for *tdp1*, which was created to model the DDR associated ataxia SCAN1, do not exhibit any increase in DNA damage sensitivity, nor is the protein required for Top1CC repair in zebrafish, as it is in humans (Zaksauskaite et al., 2021). This and the lack of radiosensitivity and apparently normal DDR in ATM zebrafish presented here, indicates that not all DDR associated disorders may be suitable for modelling in zebrafish. A comparison of all phenotypes presented by zebrafish DDR mutants is detailed in **table.6.2**.

Table 6.2 Comparison of phenotypes of all DDR mutant zebrafish	**Radiosensitivity or Sensitivity to DNA damaging agents**	**F>M Sex Skew**	**Stalled gametogensises or other Infertility**	**Testicular Neoplasia**	**Growth Retardation**	**Reduced Survival**	**Behavioural Defects**	**Other**
atm	X	✓	✓	✓	X	X	X	
tdp1	Increased sensitivity in adults	X	X	X	X	X	Mild Adult defects	
brca2/fancd1	✓	✓	✓	✓	X	X	NR	
rad51/fanco	✓	✓	✓	*See Note	✓	X	NR	Microphthalmia kidney hypocellularity defective heamatopoises Increased Inflammation
fanca	✓	X	X	X	X	X	NR	
fancb	UT	X	X	X	X	X	NR	
fancc	UT	✓	X	X	X	X	NR	
fancd2	✓	✓	X	X	X	X	NR	
fance	UT	✓	X	X	X	X	NR	
fancf	UT	✓	X	X	X	X	NR	
fancg	UT	✓	X	X	X	X	NR	
fanci	✓	✓	X	X	X	X	NR	
fancj/brip1	UT	✓	✓	X	X	X	NR	

fancl	UT	✓	X	X	X	X	NR
fancm	UT	✓	X	X	X	X	NR
fancn/palb2	✓	✓	X	X	X	X	NR
fancp/slx4	✓	✓	X	X	✓	✓	NR
fancq/ercc4	UT		X	X	✓	✓	NR
fanct/ube2t	✓	✓	X	X	✓	✓	NR
faap100	UT		X	X	✓	✓	NR
faap24	UT		X	X	✓	✓	NR

6.2.3.2 Conservation on DDR genes in Zebrafish

One of the key factors in determining whether zebrafish is a suitable model for a DDR associated disorder may be whether the gene in question has a highly conserved sequence identity between zebrafish and humans, as a divergence in sequence may indicate a divergence in function. For example, complete ablation of rad51 protein expression in zebrafish appears to recapitulate the phenotype of rad51 associated Fanconi Anaemia patients well (Botthof et al., 2017), and from a protein-protein blast sequence alignment (Altschul et al., 1997), the zebrafish rad51 protein shares a total sequence identity of 84% with the human protein **(appendix 6.1 a)**, which rises to a 96% sequence identity **(appendix 6.1 b)** in the core functional domain, which is essential for rad51 activity (Buchhop et al., 1997). This is similar for brca2 mutants, in that they also exhibit phenotypes consistent with loss of brca2 activity and the functional domains between human and zebrafish brac2 are well conserved (Rodríguez-Marí et al., 2011).

In contrast, zebrafish ATM merely shares 54% sequence identity with the human protein **(appendix 6.2 a)**, which only rises to 64% in the TAN domain **(appendix 6.2 b)**. Additionally, in the HEAT repeats where most protein-protein interactions occur **(chapter 1, section 1.2.2)**, the sequence identity drops as low as 46% **(appendix 6.2 c)**. However, the kinase and FATC domains between zebrafish and human ATM share 84% and 94% sequence identity, respectively **(appendix 6.2 e and f)**, indicating that the functions of these domains are highly conserved. Similarly to ATM$^{sh477/sh477}$ mutants, zebrafish TDP1 mutants do not recapitulate the SCAN1 phenotype well (Zaksauskaite et al., 2021). The zebrafish TDP1 protein shares a total sequence identity of 55% with the human protein **(appendix 6.3 a)**. Essential residues for DNA binding are conserved between the two orthologues **(appendix 6.3 a, green)**, as well as the active site residues **(appendix 6.3 a, yellow and pink)**, however the N-terminal regulatory domain which is essential for localisations to the nucleus, as well as protein-protein binding, only shares 30% sequence identity **(appendix 6.3 b)** (Kawale and Povirk, 2018). Therefore, there may be a correlation between how well the protein sequence of a particular DDR gene is conserved in zebrafish and humans respectively, and how well zebrafish will recapitulate loss of this gene.

As there is suggestion that ATR and DNA-PKcs can compensate for loss of ATM in cellular and mouse models of AT **(see chapter 3 section 3.3.2.2)**, and as we propose that this may also be the case in the Zebrafish model, it is important to consider whether these proteins are also well conserved in zebrafish in both sequence and function. The Zebrafish and human ATR proteins share a relatively high level of sequence identity (65%), particularly at the N-terminal **(appendix 6.4)**. There is not much known about the function of ATR in zebrafish, as there has only been one report of a MO KD model. Mutations in this gene in humans cause the genetic disorder Seckel syndrome 1, patients exhibit growth retardation, microcephaly, mental incapacitation and bird like features {O'Driscoll, 2003, A splicing mutation affecting expression of ataxia-telangiectasia and Rad3-related protein (ATR) results in Seckel syndrome}. Interestingly, the ATR MO KD did exhibit decrease head and eye size, along with a reduction of anterior neural structures and overall growth retardation (Stiff et al., 2016), suggesting that the function of ATR may be well conserved between humans and zebrafish. While zebrafish do have a DNA-PKcs homolog, no studies of its function in zebrafish has so far been carried out. However, a protein-protein blast alignment of the human and zebrafish sequences shows that they share a 58% sequence identity **(appendix 6.5)**.

6.2.3.3 Considerations When Creating Zebrafish Models of DDR Disorders

Another aspect of modelling DDR associated disorders in zebrafish is the type of mutation introduced to the gene of interest. As already discussed in **chapter 3 section 3.3.2.2** a mouse model of AT that expresses a full-length but kinase dead ATM protein has a much more severe phenotype than a KO model of the disease (Yamamoto et al., 2012b, Daniel et al., 2012). This has been attributed to a dominant negative effect of the kinase dead protein that prevents any compensatory pathways from being activated. We have observed similarities in the zebrafish model of AT. Our stable presumed KO of the ATM protein exhibits a far milder phenotype compared to the morpholino KD that is predicted to act as a kinase dead morphant (**see chapter 3, section 3.3.2.3 for full discussion)**. This may also explain why the brca2$^{-/-}$ zebrafish exhibits radiosensitivity and the ATM$^{sh477/sh477}$ does not, as the brac2 mutant zebrafish have an in frame deletion of exon 11 which disrupts key functional domains in the protein but is still predicted to produce a near full length protein (Rodríguez-Marí et al., 2011). Therefore, there is the possibility that the severity of the phenotype exhibited by these fish may also be attributed to a dominant negative effect of a present but non-functional brca2 protein. Consequently, when making a DDR mutant zebrafish to model a particular disease, the type of mutation introduced into the gene of interest should be carefully considered. For example, while the literature suggests that a kinase dead ATM mutant zebrafish may have a more severe phenotype compared to a KO, it does not recapitulate what happens in the human disease, as there have been no homozygous kinase dead mutations reported in patients. Therefore, studying a zebrafish kinase dead mutant as a model of AT in patients may not exhibit the same phenotype at the molecular level, and may obscure pathways that are at play in the human disease.

6.2.4 Validity of Modelling Hereditary Cerebellar Ataxia Disorders in Zebrafish

With the exception of the pig, no AT model has thus far has been able to recapitulate the neurodegenerative or locomotor phenotype of AT patients. Therefore, it was hoped that this could be achieved in the zebrafish model. However, due to the obvious differences in movement on land versus aquatic vertebrates, it was unclear if ataxia could be modelled in fish. As hereditary cerebellar ataxias can arise as a result of disruption of many different genes **(see appendix 1.1)** in both shared and divergent pathways **(see table 1.2)**, the suitability of zebrafish as a model for hereditary ataxias will depend on the pathway that is disrupted.

Exactly what ataxia would look like in zebrafish is unclear, and the behavioural analyses carried out in this thesis are based on behavioural assays already in use in our facility. Therefore, they may not be optimum for detection of ataxia if it is present. Despite divergent genes and pathways, all hereditary cerebellar ataxias share loss of cerebellar PCs. Recently a tamoxifen inducible loss of PC transgenic line (Weber et al., 2016), as well as an inducible PC synaptic transmission silencer line (Chang et al., 2020) have been reported. While no behavioural data have been reported on the tamoxifen inducible loss of PC cell line, silencing of PC synaptic transmission has shown abnormal swimming with episodes of decreased speeds compared to controls (Chang et al., 2020). This indicates that PC dysfunction gives a quantifiable swimming phenotype in zebrafish, and behavioural analysis could potentially be used as a readout of severity. Comprehensive behavioural analysis of these two published models could provide both a road map for appropriate behavioural assays to be carried out in future models of cerebellar ataxia in zebrafish and a valuable positive control for comparison.

6.2.5 Other Uses for the ATM$^{sh477/sh477}$ Zebrafish Model

While the ATM$^{sh477/sh477}$ zebrafish model may not recapitulate key aspects of AT pathology, it still may to be used in other areas of study. The testicular neoplasms exhibited by ATM mutant zebrafish due to the over proliferation of Sertoli cells has the potential to be used as a model for Sertoli cell tumours in human testes. However, it should be noted that Sertoli cell tumours in humans are exceedingly rare, with only a handful of cases being reported (Chang et al., 2020, Anderson, 1995, Ishida et al., 2013, Giglio et al., 2003, Esber et al., 2012, Brunocilla et al., 2012, Gourgari et al., 2012).

6.3 Future work

Additional work may be required to facilitate publication of the results in this thesis. First, further characterisation of the DDR in ATM$^{sh477/sh477}$ is needed. This should entail a time course experiment of H_2AX activation and foci resolution, along with Rad51 foci, after induction of IR at a number of doses, by confocal microscopy. Second, based on our data and the literature, we have inferred that ATM$^{sh477/sh477}$ spermatogenesis is stalled in meiosis. However, we have not experimentally shown it. Spy3 is an integral member of the synaptonemal complex, and immunostaining of this protein and characterisation of its localisation in developing spermatocytes can help stage meiosis. Therefore, ATM$^{sh477/sh477}$ testes should be immunostained with an antibody to the protein and again analysed by confocal microscopy to confirm that there is a meiotic defect. Finally, while there has been considerable analysis of ATM mutant zebrafish behaviour, the actual status of PCs in these fish has not been investigated. We had intended to investigate this using a RFP PC specific reporter line imported from Germany. However, due a catastrophic event in their home aquarium, receipt of these fish was delayed by nearly two years, and experiments with them were further hampered by the COVID-19 pandemic. However, analysis and quantification of PC development in ATM$^{sh477/sh477}$ at the same ages that the behavioural analysis was carried out would provide valuable complimentary data to support the observation that the larvae swam normally.

Bibliography

ABOZAID, H., WESSELS, S. & HÖRSTGEN-SCHWARK, G. 2011. Effect of rearing temperatures during embryonic development on the phenotypic sex in zebrafish (Danio rerio). *Sex Dev,* 5**,** 259-65.

ABRAHAM, R. T. 1996. Phosphatidylinositol 3-kinase related kinases. *Curr Opin Immunol,* 8**,** 412-8.

ADAMS, K. E., MEDHURST, A. L., DART, D. A. & LAKIN, N. D. 2006. Recruitment of ATR to sites of ionising radiation-induced DNA damage requires ATM and components of the MRN protein complex. *Oncogene,* 25**,** 3894-3904.

AGBAGA, M. P., BRUSH, R. S., MANDAL, M. N., HENRY, K., ELLIOTT, M. H. & ANDERSON, R. E. 2008. Role of Stargardt-3 macular dystrophy protein (ELOVL4) in the biosynthesis of very long chain fatty acids. *Proc Natl Acad Sci U S A,* 105**,** 12843-8.

AHMED, E. A., RIJBROEK, A. D. B.-V., KAL, H. B., SADRI-ARDEKANI, H., MIZRAK, S. C., PELT, A. M. M. V. & ROOIJ, D. G. D. 2009. Proliferative Activity In Vitro and DNA Repair Indicate that Adult Mouse and Human Sertoli Cells Are Not Terminally Differentiated, Quiescent Cells1. *Biology of Reproduction,* 80**,** 1084-1091.

AIRD, K. M. & ZHANG, R. 2015. ATM in senescence. *Oncotarget,* 6**,** 14729-14730.

AIROLDI, G., GUIDARELLI, A., CANTONI, O., PANZERI, C., VANTAGGIATO, C., BONATO, S., GRAZIA D'ANGELO, M., FALCONE, S., DE PALMA, C., TONELLI, A., CRIMELLA, C., BONDIONI, S., BRESOLIN, N., CLEMENTI, E. & BASSI, M. T. 2010. Characterization of two novel SETX mutations in AOA2 patients reveals aspects of the pathophysiological role of senataxin. *Neurogenetics,* 11**,** 91-100.

AKIZU, N., CANTAGREL, V., ZAKI, M. S., AL-GAZALI, L., WANG, X., ROSTI, R. O., DIKOGLU, E., GELOT, A. B., ROSTI, B., VAUX, K. K., SCOTT, E. M., SILHAVY, J. L., SCHROTH, J., COPELAND, B., SCHAFFER, A. E., GORDTS, P. L., ESKO, J. D., BUSCHMAN, M. D., FIELD, S. J., NAPOLITANO, G., ABDEL-SALAM, G. M., OZGUL, R. K., SAGIROGLU, M. S., AZAM, M., ISMAIL, S., AGLAN, M., SELIM, L., MAHMOUD, I. G., ABDEL-HADI, S., BADAWY, A. E., SADEK, A. A., MOJAHEDI, F., KAYSERILI, H., MASRI, A., BASTAKI, L., TEMTAMY, S., MULLER, U., DESGUERRE, I., CASANOVA, J. L., DURSUN, A., GUNEL, M., GABRIEL, S. B., DE LONLAY, P. & GLEESON, J. G. 2015. Biallelic mutations in SNX14 cause a syndromic form of cerebellar atrophy and lysosome-autophagosome dysfunction. *Nat Genet,* 47**,** 528-34.

AL TASSAN, N., KHALIL, D., SHINWARI, J., AL SHARIF, L., BAVI, P., ABDULJALEEL, Z., ABU DHAIM, N., MAGRASHI, A., BOBIS, S., AHMED, H., ALAHMED, S. & BOHLEGA, S. 2012. A missense mutation in PIK3R5 gene in a family with ataxia and oculomotor apraxia. *Hum Mutat,* 33**,** 351-4.

ALAGOZ, M., CHIANG, S. C., SHARMA, A. & EL-KHAMISY, S. F. 2013. ATM deficiency results in accumulation of DNA-topoisomerase I covalent intermediates in neural cells. *PLoS One,* 8**,** e58239.

ALEXANDER, A., CAI, S. L., KIM, J., NANEZ, A., SAHIN, M., MACLEAN, K. H., INOKI, K., GUAN, K. L., SHEN, J., PERSON, M. D., KUSEWITT, D., MILLS, G. B., KASTAN, M. B. & WALKER, C. L. 2010. ATM signals to TSC2 in the cytoplasm to regulate mTORC1 in response to ROS. *Proc Natl Acad Sci U S A,* 107**,** 4153-8.

ALONSO, I., JARDIM, L. B., ARTIGALAS, O., SARAIVA-PEREIRA, M. L., MATSUURA, T., ASHIZAWA, T., SEQUEIROS, J. & SILVEIRA, I. 2006. Reduced penetrance of intermediate size alleles in spinocerebellar ataxia type 10. *Neurology,* 66**,** 1602-4.

ALTSCHUL, S. F., MADDEN, T. L., SCHÄFFER, A. A., ZHANG, J., ZHANG, Z., MILLER, W. & LIPMAN, D. J. 1997. Gapped BLAST and PSI-BLAST: a new generation of protein database search programs. *Nucleic Acids Res,* 25**,** 3389-402.

AMBROSE, M., GOLDSTINE, J. V. & GATTI, R. A. 2007. Intrinsic mitochondrial dysfunction in ATM-deficient lymphoblastoid cells. *Hum Mol Genet,* 16**,** 2154-64.

AMINO, T., ISHIKAWA, K., TORU, S., ISHIGURO, T., SATO, N., TSUNEMI, T., MURATA, M., KOBAYASHI, K., INAZAWA, J., TODA, T. & MIZUSAWA, H. 2007. Redefining the disease locus of 16q22.1-linked autosomal dominant cerebellar ataxia. *J Hum Genet,* 52**,** 643-9.

AMIRIFAR, P., MOZDARANI, H., YAZDANI, R., KIAEI, F., MOEINI SHAD, T., SHAHKARAMI, S., ABOLHASSANI, H., DELAVARI, S., SOHANI, M., REZAEI, A., HASSANPOUR, G., AKRAMI, S. M. & AGHAMOHAMMADI, A. 2020. Effect of Class Switch Recombination Defect on the Phenotype of Ataxia-Telangiectasia Patients. *Immunol Invest***,** 1-15.

AMMANN, A. J., DUQUESNOY, R. J. & GOOD, R. A. 1970. Endocrinological studies in ataxiatelangiectasia and other immunological deficiency diseases. *Clin Exp Immunol,* 6**,** 587-95.

AMORES, A., FORCE, A., YAN, Y.-L., JOLY, L., AMEMIYA, C., FRITZ, A., HO, R. K., LANGELAND, J., PRINCE, V., WANG, Y.-L., WESTERFIELD, M., EKKER, M. & POSTLETHWAIT, J. H. 1998. Zebrafish hox Clusters and Vertebrate Genome Evolution. *Science,* 282**,** 1711.

AMOYEL, M., CHENG, Y.-C., JIANG, Y.-J. & WILKINSON, D. G. 2005. Wnt1 regulates neurogenesis and mediates lateral inhibition of boundary cell specification in the zebrafish hindbrain. *Development,* 132**,** 775.

ANDEGEKO, Y., MOYAL, L., MITTELMAN, L., TSARFATY, I., SHILOH, Y. & ROTMAN, G. 2001. Nuclear retention of ATM at sites of DNA double strand breaks. *J Biol Chem,* 276**,** 38224-30.

ANDERSON, G. A. 1995. Sclerosing Sertoli cell tumor of the testis: a distinct histological subtype. *J Urol,* 154**,** 1756-8.

ANDRADE, M. A. & BORK, P. 1995. HEAT repeats in the Huntington's disease protein. *Nat Genet,* 11**,** 115-6.

ANDREWS, A. D., BARRETT, S. F. & ROBBINS, J. H. 1978. Xeroderma pigmentosum neurological abnormalities correlate with colony-forming ability after ultraviolet radiation. *Proc Natl Acad Sci U S A,* 75**,** 1984-8.

ANDRISSE, S., PATEL, G. D., CHEN, J. E., WEBBER, A. M., SPEARS, L. D., KOEHLER, R. M., ROBINSON-HILL, R. M., CHING, J. K., JEONG, I. & FISHER, J. S. 2013. ATM and GLUT1-S490 phosphorylation regulate GLUT1 mediated transport in skeletal muscle. *PLoS One,* 8**,** e66027.

ANGELOVA, P. R. & ABRAMOV, A. Y. 2018. Role of mitochondrial ROS in the brain: from physiology to neurodegeneration. *FEBS Lett,* 592**,** 692-702.

ANHEIM, M., FLEURY, M., MONGA, B., LAUGEL, V., CHAIGNE, D., RODIER, G., GINGLINGER, E., BOULAY, C., COURTOIS, S., DROUOT, N., FRITSCH, M., DELAUNOY, J. P., STOPPA-LYONNET, D., TRANCHANT, C. & KOENIG, M. 2010. Epidemiological, clinical, paraclinical and molecular study of a cohort of 102 patients affected with autosomal recessive progressive cerebellar ataxia from Alsace, Eastern France: implications for clinical management. *Neurogenetics,* 11**,** 1-12.

ANHEIM, M., MONGA, B., FLEURY, M., CHARLES, P., BARBOT, C., SALIH, M., DELAUNOY, J. P., FRITSCH, M., ARNING, L., SYNOFZIK, M., SCHÖLS, L., SEQUEIROS, J., GOIZET, C., MARELLI, C., LE BER, I., KOHT, J., GAZULLA, J., DE BLEECKER, J., MUKHTAR, M., DROUOT, N., ALI-PACHA, L., BENHASSINE, T., CHBICHEB, M., M'ZAHEM, A., HAMRI, A., CHABROL, B., POUGET, J., MURPHY, R., WATANABE, M., COUTINHO, P., TAZIR, M., DURR, A., BRICE, A., TRANCHANT, C. & KOENIG, M. 2009. Ataxia with oculomotor apraxia type 2: clinical, biological and genotype/phenotype correlation study of a cohort of 90 patients. *Brain,* 132**,** 2688-98.

ANTONIOU, A. C., CUNNINGHAM, A. P., PETO, J., EVANS, D. G., LALLOO, F., NAROD, S. A., RISCH, H. A., EYFJORD, J. E., HOPPER, J. L., SOUTHEY, M. C., OLSSON, H., JOHANNSSON, O., BORG, A., PASINI, B., RADICE, P., MANOUKIAN, S., ECCLES, D. M., TANG, N., OLAH, E., ANTON-CULVER, H., WARNER, E., LUBINSKI, J., GRONWALD, J., GORSKI, B., TRYGGVADOTTIR, L., SYRJAKOSKI, K., KALLIONIEMI, O. P., EEROLA, H., NEVANLINNA, H., PHAROAH, P. D. & EASTON, D. F. 2008.

The BOADICEA model of genetic susceptibility to breast and ovarian cancers: updates and extensions. *Br J Cancer,* 98**,** 1457-66.

ANTTONEN, A. K., MAHJNEH, I., HAMALAINEN, R. H., LAGIER-TOURENNE, C., KOPRA, O., WARIS, L., ANTTONEN, M., JOENSUU, T., KALIMO, H., PAETAU, A., TRANEBJAERG, L., CHAIGNE, D., KOENIG, M., EEG-OLOFSSON, O., UDD, B., SOMER, M., SOMER, H. & LEHESJOKI, A. E. 2005. The gene disrupted in Marinesco-Sjogren syndrome encodes SIL1, an HSPA5 cochaperone. *Nat Genet,* 37**,** 1309-11.

AQEILAN, R. I., TRAPASSO, F., HUSSAIN, S., COSTINEAN, S., MARSHALL, D., PEKARSKY, Y., HAGAN, J. P., ZANESI, N., KAOU, M., STEIN, G. S., LIAN, J. B. & CROCE, C. M. 2007. Targeted deletion of Wwox reveals a tumor suppressor function. *Proc Natl Acad Sci U S A,* 104**,** 3949-54.

ARAUJO, J., BREUER, P., DIERINGER, S., KRAUSS, S., DORN, S., ZIMMERMANN, K., PFEIFER, A., KLOCKGETHER, T., WUELLNER, U. & EVERT, B. O. 2011. FOXO4-dependent upregulation of superoxide dismutase-2 in response to oxidative stress is impaired in spinocerebellar ataxia type 3. *Hum Mol Genet,* 20**,** 2928-41.

ARMSTRONG, G. A., LIAO, M., YOU, Z., LISSOUBA, A., CHEN, B. E. & DRAPEAU, P. 2016. Homology Directed Knockin of Point Mutations in the Zebrafish tardbp and fus Genes in ALS Using the CRISPR/Cas9 System. *PLoS One,* 11**,** e0150188.

ASAI, H., HIRANO, M., SHIMADA, K., KIRIYAMA, T., FURIYA, Y., IKEDA, M., IWAMOTO, T., MORI, T., NISHINAKA, K., KONISHI, N., UDAKA, F. & UENO, S. 2009. Protein kinase C gamma, a protein causative for dominant ataxia, negatively regulates nuclear import of recessive-ataxia-related aprataxin. *Hum Mol Genet,* 18**,** 3533-43.

ASSOUM, M., SALIH, M. A., DROUOT, N., H'MIDA-BEN BRAHIM, D., LAGIER-TOURENNE, C., ALDREES, A., ELMALIK, S. A., AHMED, T. S., SEIDAHMED, M. Z., KABIRAJ, M. M. & KOENIG, M. 2010. Rundataxin, a novel protein with RUN and diacylglycerol binding domains, is mutant in a new recessive ataxia. *Brain,* 133**,** 2439-47.

ASSOUM, M., SALIH, M. A., DROUOT, N., HNIA, K., MARTELLI, A. & KOENIG, M. 2013. The Salih ataxia mutation impairs Rubicon endosomal localization. *Cerebellum,* 12**,** 835-40.

AUDIRA, G., SIREGAR, P., STRUNGARU, S.-A., HUANG, J.-C. & HSIAO, C.-D. 2020. Which Zebrafish Strains Are More Suitable to Perform Behavioral Studies? A Comprehensive Comparison by Phenomic Approach. *Biology,* 9**,** 200.

AURE, K., BENOIST, J. F., OGIER DE BAULNY, H., ROMERO, N. B., RIGAL, O. & LOMBES, A. 2004. Progression despite replacement of a myopathic form of coenzyme Q10 defect. *Neurology,* 63**,** 727-9.

AURIAS, A., CROQUETTE, M. F., NUYTS, J. P., GRISCELLI, C. & DUTRILLAUX, B. 1986. New data on clonal anomalies of chromosome 14 in ataxia telangiectasia: tct(14;14) and inv(14). *Hum Genet,* 72**,** 22-4.

AURIAS, A. & DUTRILLAUX, B. 1986. A possible new type of chromosome rearrangement: telomere-centromere translocation (tct) followed by double duplication. *Hum Genet,* 72**,** 25-6.

AURIAS, A., DUTRILLAUX, B., BURIOT, D. & LEJEUNE, J. 1980. High frequencies of inversions and translocations of chromosomes 7 and 14 in ataxia telangiectasia. *Mutat Res,* 69**,** 369-74.

AYGÜN, F. D., NEPESOV, S., ÇOKUĞRAŞ, H. & CAMCIOĞLU, Y. 2015. Bladder Wall Telangiectasia in a Patient with Ataxia-Telangiectasia and How to Manage? *Case Rep Pediatr,* 2015**,** 615368.

BABOVIC-VUKSANOVIC, D., SNOW, K., PATTERSON, M. C. & MICHELS, V. V. 1998. Spinocerebellar ataxia type 2 (SCA 2) in an infant with extreme CAG repeat expansion. *Am J Med Genet,* 79**,** 383-7.

BAE, Y. K., KANI, S., SHIMIZU, T., TANABE, K., NOJIMA, H., KIMURA, Y., HIGASHIJIMA, S. & HIBI, M. 2009. Anatomy of zebrafish cerebellum and screen for mutations affecting its development. *Dev Biol,* 330**,** 406-26.

BAETS, J., DECONINCK, T., SMETS, K., GOOSSENS, D., VAN DEN BERGH, P., DAHAN, K., SCHMEDDING, E., SANTENS, P., RASIC, V. M., VAN DAMME, P., ROBBERECHT, W., DE MEIRLEIR, L., MICHIELSENS, B., DEL-FAVERO, J., JORDANOVA, A. & DE JONGHE, P. 2010. Mutations in SACS cause atypical and late-onset forms of ARSACS. *Neurology,* 75**,** 1181-8.

BAGLEY, J., SINGH, G. & IACOMINI, J. 2007. Regulation of oxidative stress responses by ataxia-telangiectasia mutated is required for T cell proliferation. *J Immunol,* 178**,** 4757-63.

BAHL, S., VIRDI, K., MITTAL, U., SACHDEVA, M. P., KALLA, A. K., HOLMES, S. E., O'HEARN, E., MARGOLIS, R. L., JAIN, S., SRIVASTAVA, A. K. & MUKERJI, M. 2005. Evidence of a common founder for SCA12 in the Indian population. *Ann Hum Genet,* 69**,** 528-34.

BAKALKIN, G., WATANABE, H., JEZIERSKA, J., DEPOORTER, C., VERSCHUUREN-BEMELMANS, C., BAZOV, I., ARTEMENKO, K. A., YAKOVLEVA, T., DOOIJES, D., VAN DE WARRENBURG, B. P., ZUBAREV, R. A., KREMER, B., KNAPP, P. E., HAUSER, K. F., WIJMENGA, C., NYBERG, F., SINKE, R. J. & VERBEEK, D. S. 2010. Prodynorphin mutations cause the neurodegenerative disorder spinocerebellar ataxia type 23. *Am J Hum Genet,* 87**,** 593-603.

BAKER, B. S., BOYD, J. B., CARPENTER, A. T., GREEN, M. M., NGUYEN, T. D., RIPOLL, P. & SMITH, P. D. 1976. Genetic controls of meiotic recombination and somatic DNA metabolism in Drosophila melanogaster. *Proc Natl Acad Sci U S A,* 73**,** 4140-4.

BAKKENIST, C. J. & KASTAN, M. B. 2003. DNA damage activates ATM through intermolecular autophosphorylation and dimer dissociation. *Nature,* 421**,** 499-506.

BALLINGER, C. A., CONNELL, P., WU, Y., HU, Z., THOMPSON, L. J., YIN, L. Y. & PATTERSON, C. 1999. Identification of CHIP, a novel tetratricopeptide repeat-containing protein that interacts with heat shock proteins and negatively regulates chaperone functions. *Mol Cell Biol,* 19**,** 4535-45.

BALREIRA, A., BOCZONADI, V., BARCA, E., PYLE, A., BANSAGI, B., APPLETON, M., GRAHAM, C., HARGREAVES, I. P., RASIC, V. M., LOCHMULLER, H., GRIFFIN, H., TAYLOR, R. W., NAINI, A., CHINNERY, P. F., HIRANO, M., QUINZII, C. M. & HORVATH, R. 2014. ANO10 mutations cause ataxia and coenzyme Q(1)(0) deficiency. *J Neurol,* 261**,** 2192-8.

BALTA, G., PATIROGLU, T. & GUMRUK, F. 2019. Fanconi Anemia and Ataxia Telangiectasia in Siblings who Inherited Unique Combinations of Novel FANCA and ATM Null Mutations. *Journal of Pediatric Hematology Oncology,* 41**,** 243-246.

BANFI, S., BASSI, M. T., ANDOLFI, G., MARCHITIELLO, A., ZANOTTA, S., BALLABIO, A., CASARI, G. & FRANCO, B. 1999. Identification and characterization of AFG3L2, a novel paraplegin-related gene. *Genomics,* 59**,** 51-8.

BANFI, S., SERVADIO, A., CHUNG, M. Y., KWIATKOWSKI, T. J., JR., MCCALL, A. E., DUVICK, L. A., SHEN, Y., ROTH, E. J., ORR, H. T. & ZOGHBI, H. Y. 1994. Identification and characterization of the gene causing type 1 spinocerebellar ataxia. *Nat Genet,* 7**,** 513-20.

BANGA, S. S., SHENKAR, R. & BOYD, J. B. 1986. Hypersensitivity of Drosophila mei-41 mutants to hydroxyurea is associated with reduced mitotic chromosome stability. *Mutat Res,* 163**,** 157-65.

BANIN, S., MOYAL, L., SHIEH, S., TAYA, Y., ANDERSON, C. W., CHESSA, L., SMORODINSKY, N. I., PRIVES, C., REISS, Y., SHILOH, Y. & ZIV, Y. 1998. Enhanced phosphorylation of p53 by ATM in response to DNA damage. *Science,* 281**,** 1674-7.

BAR, R. S., LEVIS, W. R., RECHLER, M. M., HARRISON, L. C., SIEBERT, C., PODSKALNY, J., ROTH, J. & MUGGEO, M. 1978. Extreme insulin resistance in ataxia telangiectasia: defect in affinity of insulin receptors. *N Engl J Med,* 298**,** 1164-71.

BARBI, G., SCHERES, J. M., SCHINDLER, D., TAALMAN, R. D., RODENS, K., MEHNERT, K., MÜLLER, M. & SEYSCHAB, H. 1991. Chromosome instability and X-ray hypersensitivity in a microcephalic and growth-retarded child. *Am J Med Genet,* 40**,** 44-50.

BARBOT, C., COUTINHO, P., CHORAO, R., FERREIRA, C., BARROS, J., FINEZA, I., DIAS, K., MONTEIRO, J., GUIMARAES, A., MENDONCA, P., DO CEU MOREIRA, M. & SEQUEIROS, J. 2001. Recessive ataxia with ocular apraxia: review of 22 Portuguese patients. *Arch Neurol,* 58**,** 201-5.

BARETIĆ, D., POLLARD, H. K., FISHER, D. I., JOHNSON, C. M., SANTHANAM, B., TRUMAN, C. M., KOUBA, T., FERSHT, A. R., PHILLIPS, C. & WILLIAMS, R. L. 2017. Structures of closed and open conformations of dimeric human ATM. *Sci Adv,* 3**,** e1700933.

BARITAUD, M., CABON, L., DELAVALLEE, L., GALAN-MALO, P., GILLES, M. E., BRUNELLE-NAVAS, M. N. & SUSIN, S. A. 2012. AIF-mediated caspase-independent necroptosis requires ATM and DNA-PK-induced histone H2AX Ser139 phosphorylation. *Cell Death & Disease,* 3.

BARLOW, C., HIROTSUNE, S., PAYLOR, R., LIYANAGE, M., ECKHAUS, M., COLLINS, F., SHILOH, Y., CRAWLEY, J. N., RIED, T., TAGLE, D. & WYNSHAW-BORIS, A. 1996. Atm-deficient mice: a paradigm of ataxia telangiectasia. *Cell,* 86**,** 159-71.

BARLOW, C., LIYANAGE, M., MOENS, P. B., DENG, C.-X., RIED, T. & WYNSHAW-BORIS, A. 1997. Partial rescue of the prophase I defects of Atm-deficient mice by p53 and p21 null alleles. *Nature Genetics,* 17**,** 462-466.

BARLOW, C., LIYANAGE, M., MOENS, P. B., TARSOUNAS, M., NAGASHIMA, K., BROWN, K., ROTTINGHAUS, S., JACKSON, S. P., TAGLE, D., RIED, T. & WYNSHAW-BORIS, A. 1998. Atm deficiency results in severe meiotic disruption as early as leptonema of prophase I. *Development,* 125**,** 4007-17.

BARLOW, C., RIBAUT-BARASSIN, C., ZWINGMAN, T. A., POPE, A. J., BROWN, K. D., OWENS, J. W., LARSON, D., HARRINGTON, E. A., HAEBERLE, A. M., MARIANI, J., ECKHAUS, M., HERRUP, K., BAILLY, Y. & WYNSHAW-BORIS, A. 2000. ATM is a cytoplasmic protein in mouse brain required to prevent lysosomal accumulation. *Proc Natl Acad Sci U S A,* 97**,** 871-6.

BARONE, G., GROOM, A., REIMAN, A., SRINIVASAN, V., BYRD, P. J. & TAYLOR, A. M. 2009. Modeling ATM mutant proteins from missense changes confirms retained kinase activity. *Hum Mutat,* 30**,** 1222-30.

BARZILAI, A., BITON, S. & SHILOH, Y. 2008. The role of the DNA damage response in neuronal development, organization and maintenance. *DNA Repair (Amst),* 7**,** 1010-27.

BASNET, R. M., ZIZIOLI, D., TAWEEDET, S., FINAZZI, D. & MEMO, M. 2019. Zebrafish Larvae as a Behavioral Model in Neuropharmacology. *Biomedicines,* 7**,** 23.

BAYAT, V., THIFFAULT, I., JAISWAL, M., TETREAULT, M., DONTI, T., SASARMAN, F., BERNARD, G., DEMERS-LAMARCHE, J., DICAIRE, M. J., MATHIEU, J., VANASSE, M., BOUCHARD, J. P., RIOUX, M. F., LOURENCO, C. M., LI, Z., HAUETER, C., SHOUBRIDGE, E. A., GRAHAM, B. H., BRAIS, B. & BELLEN, H. J. 2012. Mutations in the mitochondrial methionyl-tRNA synthetase cause a neurodegenerative phenotype in flies and a recessive ataxia (ARSAL) in humans. *PLoS Biol,* 10**,** e1001288.

BECKER, T., WULLIMANN, M. F., BECKER, C. G., BERNHARDT, R. R. & SCHACHNER, M. 1997. Axonal regrowth after spinal cord transection in adult zebrafish. *J Comp Neurol,* 377**,** 577-95.

BECKER-CATANIA, S. G., CHEN, G., HWANG, M. J., WANG, Z., SUN, X., SANAL, O., BERNATOWSKA-MATUSZKIEWICZ, E., CHESSA, L., LEE, E. Y. & GATTI, R. A. 2000. Ataxia-telangiectasia: phenotype/genotype studies of ATM protein expression, mutations, and radiosensitivity. *Mol Genet Metab,* 70**,** 122-33.

BEDNAREK, A. K., LAFLIN, K. J., DANIEL, R. L., LIAO, Q., HAWKINS, K. A. & ALDAZ, C. M. 2000. WWOX, a novel WW domain-containing protein mapping to human chromosome 16q23.3-24.1, a region frequently affected in breast cancer. *Cancer Res,* 60**,** 2140-5.

BEER, R. L. & DRAPER, B. W. 2013. nanos3 maintains germline stem cells and expression of the conserved germline stem cell gene nanos2 in the zebrafish ovary. *Developmental Biology,* 374**,** 308-318.

BEGAM, N., JAMIL, K. & RAJU, S. G. 2017. Promoter Hypermethylation of the ATM Gene as a Novel Biomarker for Breast Cancer. *Asian Pacific journal of cancer prevention : APJCP,* 18**,** 3003-3009.

BENCOKOVA, Z., KAUFMANN, M. R., PIRES, I. M., LECANE, P. S., GIACCIA, A. J. & HAMMOND, E. M. 2009. ATM activation and signaling under hypoxic conditions. *Mol Cell Biol,* 29**,** 526-37.

BENOMAR, A., KROLS, L., STEVANIN, G., CANCEL, G., LEGUERN, E., DAVID, G., OUHABI, H., MARTIN, J. J., DURR, A., ZAIM, A. & ET AL. 1995. The gene for autosomal dominant cerebellar ataxia with pigmentary macular dystrophy maps to chromosome 3p12-p21.1. *Nat Genet,* 10**,** 84-8.

BERALDI, R., CHAN, C. H., ROGERS, C. S., KOVACS, A. D., MEYERHOLZ, D. K., TRANTZAS, C., LAMBERTZ, A. M., DARBRO, B. W., WEBER, K. L., WHITE, K. A. M., RHEEDEN, R. V., KRUER, M. C., DACKEN, B. A., WANG, X. J., DAVIS, B. T., ROHRET, J. A., STRUZYNSKI, J. T., ROHRET, F. A., WEIMER, J. M. & PEARCE, D. A. 2015. A novel porcine model of ataxia telangiectasia reproduces neurological features and motor deficits of human disease. *Human Molecular Genetics,* 24**,** 6473-6484.

BERALDI, R., MEYERHOLZ, D. K., SAVINOV, A., KOVACS, A. D., WEIMER, J. M., DYKSTRA, J. A., GERAETS, R. D. & PEARCE, D. A. 2017. Genetic ataxia telangiectasia porcine model phenocopies the multisystemic features of the human disease. *Biochimica Et Biophysica Acta-Molecular Basis of Disease,* 1863**,** 2862-2870.

BERGENHEM, N. C., SAIT, S. S., EDDY, R. L., SHOWS, T. B. & TASHIAN, R. E. 1995. Assignment of the gene for human carbonic anhydrase VIII(CA8) to chromosome 8q11-->q12. *Cytogenet Cell Genet,* 71**,** 299-300.

BERGSTRAND, C. G. & CZAR, B. 1956. Demonstration of a new protein fraction in serum from the human fetus. *Scand J Clin Lab Invest,* 8**,** 174.

BERTHEL, E., FERLAZZO, M. L., DEVIC, C., BOURGUIGNON, M. & FORAY, N. 2019a. What Does the History of Research on the Repair of DNA Double-Strand Breaks Tell Us?-A Comprehensive Review of Human Radiosensitivity. *Int J Mol Sci,* 20.

BERTHEL, E., FORAY, N. & FERLAZZO, M. L. 2019b. The Nucleoshuttling of the ATM Protein: A Unified Model to Describe the Individual Response to High- and Low-Dose of Radiation? *Cancers (Basel),* 11.

BIHANI, T. & HINDS, P. W. 2011. Mitosis Hit with an ATM Transaction Fee: Aurora B-Mediated Activation of ATM during Mitosis. *Molecular Cell,* 44**,** 513-514.

BIRAN, A. & KRIZHANOVSKY, V. 2015. Senescent cells talk frankly with their neighbors. *Cell cycle (Georgetown, Tex.),* 14**,** 2181-2182.

BISOGNO, T., HOWELL, F., WILLIAMS, G., MINASSI, A., CASCIO, M. G., LIGRESTI, A., MATIAS, I., SCHIANO-MORIELLO, A., PAUL, P., WILLIAMS, E. J., GANGADHARAN, U., HOBBS, C., DI MARZO, V. & DOHERTY, P. 2003. Cloning of the first sn1-DAG lipases points to the spatial and temporal regulation of endocannabinoid signaling in the brain. *J Cell Biol,* 163**,** 463-8.

BITON, S., DAR, I., MITTELMAN, L., PEREG, Y., BARZILAI, A. & SHILOH, Y. 2006. Nuclear ataxia-telangiectasia mutated (ATM) mediates the cellular response to DNA double strand breaks in human neuron-like cells. *J Biol Chem,* 281**,** 17482-91.

BLAHOVÁ, J., PLHALOVÁ, L., HOSTOVSKÝ, M., DIVIŠOVÁ, L., DOBŠÍKOVÁ, R., MIKULÍKOVÁ, I., ŠTĚPÁNOVÁ, S. & SVOBODOVÁ, Z. 2013. Oxidative stress responses in zebrafish Danio rerio after subchronic exposure to atrazine. *Food and Chemical Toxicology,* 61**,** 82-85.

BOAKYE, M., MOREHOUSE, J., ETHRIDGE, J., BURKE, D. A., KHATTAR, N. K., KUMAR, C., MANOUCHEHRI, N., STREIJGER, F., REED, R., MAGNUSON, D. S. K., SHERWOOD, L., KWON, B. K. & HOWLAND, D. R. 2020. Treadmill-Based Gait Kinematics in the Yucatan Mini Pig. *Journal of Neurotrauma,* 37**,** 2277-2291.

BODENSTEINER, J. B., GOLDBLUM, R. M. & GOLDMAN, A. S. 1980. Progressive dystonia masking ataxia in ataxia-telangiectasia. *Arch Neurol,* 37**,** 464-5.

BODER, E. & SEDGEWICK, R. 1958. ATAXIA-TELANGIECTASIA - A FAMILIAL SYNDROME OF PROGRESSIVE CEREBELLAR ATAXIA, OCULOCUTANEOUS TELANGIECTASIA, AND FREQUENT PULMONARY INFECTION. *Archives of Dermatology,* 78**,** 402-405.

BODER, E. & SEDGWICK, R. P. 1958. Ataxia-telangiectasia; a familial syndrome of progressive cerebellar ataxia, oculocutaneous telangiectasia and frequent pulmonary infection. *Pediatrics,* 21**,** 526-54.

BODGI, L. & FORAY, N. 2016. The nucleo-shuttling of the ATM protein as a basis for a novel theory of radiation response: resolution of the linear-quadratic model*. *International Journal of Radiation Biology,* 92**,** 117-131.

BOEHRS, J. K., HE, J., HALABY, M. J. & YANG, D. Q. 2007. Constitutive expression and cytoplasmic compartmentalization of ATM protein in differentiated human neuron-like SH-SY5Y cells. *J Neurochem,* 100**,** 337-45.

BOLCUN-FILAS, E. & HANDEL, M. A. 2018. Meiosis: the chromosomal foundation of reproduction. *Biology of Reproduction,* 99**,** 112-126.

BOLT, J., VO, Q. N., KIM, W. J., MCWHORTER, A. J., THOMSON, J., HAGENSEE, M. E., FRIEDLANDER, P., BROWN, K. D. & GILBERT, J. 2005. The ATM/p53 pathway is commonly targeted for inactivation in squamous cell carcinoma of the head and neck (SCCHN) by multiple molecular mechanisms. *Oral Oncol,* 41**,** 1013-20.

BOMONT, P., WATANABE, M., GERSHONI-BARUSH, R., SHIZUKA, M., TANAKA, M., SUGANO, J., GUIRAUD-CHAUMEIL, C. & KOENIG, M. 2000. Homozygosity mapping of spinocerebellar ataxia with cerebellar atrophy and peripheral neuropathy to 9q33-34, and with hearing impairment and optic atrophy to 6p21-23. *Eur J Hum Genet,* 8**,** 986-90.

BOOHAKER, R. J., ZENG, Q. H. & XU, B. 2016. Identification and characterization of ATM substrates in mitosis. *Cancer Research,* 76.

BORGES, A. C., PEREIRA, N., FRANCO, M., VALE, L., PEREIRA, M., CUNHA, M. V., AMARO, A., ALBUQUERQUE, T. & REBELO, M. 2016. Implementation of a Zebrafish Health Program in a Research Facility: A 4-Year Retrospective Study. *Zebrafish,* 13 Suppl 1**,** S115-S126.

BORGHESANI, P. R., ALT, F. W., BOTTARO, A., DAVIDSON, L., AKSOY, S., RATHBUN, G. A., ROBERTS, T. M., SWAT, W., SEGAL, R. A. & GU, Y. 2000. Abnormal development of Purkinje cells and lymphocytes in Atm mutant mice. *Proc Natl Acad Sci U S A,* 97**,** 3336-41.

BOSE, A. & BEAL, M. F. 2016. Mitochondrial dysfunction in Parkinson's disease. *J Neurochem,* 139 Suppl 1**,** 216-231.

BOSOTTI, R., ISACCHI, A. & SONNHAMMER, E. L. 2000. FAT: a novel domain in PIK-related kinases. *Trends Biochem Sci,* 25**,** 225-7.

BOSSY-WETZEL, E., PETRILLI, A. & KNOTT, A. B. 2008. Mutant huntingtin and mitochondrial dysfunction. *Trends Neurosci,* 31**,** 609-16.

BOTT, L., LEBRETON, J., THUMERELLE, C., CUVELLIER, J., DESCHILDRE, A. & SARDET, A. 2007. Lung disease in ataxia-telangiectasia. *Acta Paediatr,* 96**,** 1021-4.

BOTTHOF, J. G., BIELCZYK-MACZYŃSKA, E., FERREIRA, L. & CVEJIC, A. 2017. Loss of the homologous recombination gene rad51 leads to Fanconi anemia-like symptoms in zebrafish. *Proceedings of the National Academy of Sciences,* 114**,** E4452.

BOUCHARD, J., BEDARD, P. & BOUCHARD, R. 1980. Study of a family with progressive ataxia, tremor and severe distal amyotrophy. *Can J Neurol Sci,* 7**,** 345-9.

BOUCHARD, J. P., BARBEAU, A., BOUCHARD, R. & BOUCHARD, R. W. 1978. Autosomal recessive spastic ataxia of Charlevoix-Saguenay. *Can J Neurol Sci,* 5**,** 61-9.

BOURASSA, C. V., MEIJER, I. A., MERNER, N. D., GREWAL, K. K., STEFANELLI, M. G., HODGKINSON, K., IVES, E. J., PRYSE-PHILLIPS, W., JOG, M., BOYCOTT, K., GRIMES, D. A., GOOBIE, S., LECKEY, R., DION, P. A. & ROULEAU, G. A. 2012. VAMP1 mutation causes dominant hereditary spastic ataxia in Newfoundland families. *Am J Hum Genet,* 91**,** 548-52.

BOUSLAM, N., BOUHOUCHE, A., BENOMAR, A., HANEIN, S., KLEBE, S., AZZEDINE, H., DI GIANDOMENICO, S., BOLAND-AUGE, A., SANTORELLI, F. M., DURR, A., BRICE, A., YAHYAOUI, M. & STEVANIN, G. 2007. A novel locus for autosomal recessive spastic ataxia on chromosome 17p. *Hum Genet,* 121**,** 413-20.

BOYCOTT, K. M., FLAVELLE, S., BUREAU, A., GLASS, H. C., FUJIWARA, T. M., WIRRELL, E., DAVEY, K., CHUDLEY, A. E., SCOTT, J. N., MCLEOD, D. R. & PARBOOSINGH, J. S. 2005. Homozygous deletion of the very low density lipoprotein receptor gene causes autosomal recessive cerebellar hypoplasia with cerebral gyral simplification. *Am J Hum Genet,* 77**,** 477-83.

BRAND, M., YAMAMOTO, K., STAUB, A. & TORA, L. 1999. Identification of TATA-binding protein-free TAFII-containing complex subunits suggests a role in nucleosome acetylation and signal transduction. *The Journal of biological chemistry,* 274**,** 18285-18289.

BRAS, J., ALONSO, I., BARBOT, C., COSTA, M. M., DARWENT, L., ORME, T., SEQUEIROS, J., HARDY, J., COUTINHO, P. & GUERREIRO, R. 2015. Mutations in PNKP cause recessive ataxia with oculomotor apraxia type 4. *Am J Hum Genet,* 96**,** 474-9.

BREDEMEYER, A. L., SHARMA, G. G., HUANG, C.-Y., HELMINK, B. A., WALKER, L. M., KHOR, K. C., NUSKEY, B., SULLIVAN, K. E., PANDITA, T. K., BASSING, C. H. & SLECKMAN, B. P. 2006a. ATM stabilizes DNA double-strand-break complexes during V(D)J recombination. *Nature,* 442**,** 466-470.

BREDEMEYER, A. L., SHARMA, G. G., HUANG, C. Y., HELMINK, B. A., WALKER, L. M., KHOR, K. C., NUSKEY, B., SULLIVAN, K. E., PANDITA, T. K., BASSING, C. H. & SLECKMAN, B. P. 2006b. ATM stabilizes DNA double-strand-break complexes during V(D)J recombination. *Nature,* 442**,** 466-470.

BREEDVELD, G. J., VAN WETTEN, B., TE RAA, G. D., BRUSSE, E., VAN SWIETEN, J. C., OOSTRA, B. A. & MAAT-KIEVIT, J. A. 2004. A new locus for a childhood onset, slowly progressive autosomal recessive spinocerebellar ataxia maps to chromosome 11p15. *J Med Genet.* England.

BRETT, J. R. 1964. The Respiratory Metabolism and Swimming Performance of Young Sockeye Salmon. *Journal of the Fisheries Research Board of Canada,* 21**,** 1183-1226.

BRICK, K., PRATTO, F. & CAMERINI-OTERO, R. D. 2020. After the break: DSB end processing in mouse meiosis. *Genes & Development,* 34**,** 731-732.

BRITEL, M., BOURGUIGNON, M. & FORAY, N. 2018. The use of the term ‘radiosensitivity’ through history of radiation: from clarity to confusion. *International Journal of Radiation Biology,* 94**,** 503-512.

BRKANAC, Z., BYLENOK, L., FERNANDEZ, M., MATSUSHITA, M., LIPE, H., WOLFF, J., NOCHLIN, D., RASKIND, W. H. & BIRD, T. D. 2002. A new dominant spinocerebellar ataxia linked to chromosome 19q13.4-qter. *Arch Neurol,* 59**,** 1291-5.

BROCK, C., SCHAEFER, M., REUSCH, H. P., CZUPALLA, C., MICHALKE, M., SPICHER, K., SCHULTZ, G. & NURNBERG, B. 2003. Roles of G beta gamma in membrane recruitment and activation of p110 gamma/p101 phosphoinositide 3-kinase gamma. *J Cell Biol,* 160**,** 89-99.

BROOKS, P. J., CHENG, T.-F. & COOPER, L. 2008. Do all of the neurologic diseases in patients with DNA repair gene mutations result from the accumulation of DNA damage? *DNA Repair,* 7**,** 834-848.

BROWN, K. D., BARLOW, C., DENG, C. X., TAGLE, D. A. & WYNSHAWBORIS, A. 1997a. ATM selectivity regulates distinct downstream p53-dependent pathways of cell cycle progression and apoptosis in vivo. *Molecular Biology of the Cell,* 8**,** 95-95.

BROWN, K. D., ZIV, Y., SADANANDAN, S. N., CHESSA, L., COLLINS, F. S., SHILOH, Y. & TAGLE, D. A. 1997b. The ataxia-telangiectasia gene product, a constitutively expressed nuclear protein that is not up-regulated following genome damage. *Proc Natl Acad Sci U S A,* 94**,** 1840-5.

BROWNE, D. L., GANCHER, S. T., NUTT, J. G., BRUNT, E. R., SMITH, E. A., KRAMER, P. & LITT, M. 1994. Episodic ataxia/myokymia syndrome is associated with point mutations in the human potassium channel gene, KCNA1. *Nat Genet,* 8**,** 136-40.

BROWNE, S. E., ROBERTS, L. J., 2ND, DENNERY, P. A., DOCTROW, S. R., BEAL, M. F., BARLOW, C. & LEVINE, R. L. 2004. Treatment with a catalytic antioxidant corrects the neurobehavioral defect in ataxia-telangiectasia mice. *Free Radic Biol Med,* 36**,** 938-42.

BRUMBAUGH, K. M., OTTERNESS, D. M., GEISEN, C., OLIVEIRA, V., BROGNARD, J., LI, X., LEJEUNE, F., TIBBETTS, R. S., MAQUAT, L. E. & ABRAHAM, R. T. 2004. The mRNA Surveillance Protein hSMG-1 Functions in Genotoxic Stress Response Pathways in Mammalian Cells. *Molecular Cell,* 14**,** 585-598.

BRUNOCILLA, E., PULTRONE, C. V., SCHIAVINA, R., ROCCA, C., PASSARETTI, G., CORTI, B. & MARTORANA, G. 2012. Testicular sclerosing Sertoli cell tumor: an additional case and review of the literature. *Anticancer Res,* 32**,** 5127-30.

BUBIEN, V., BONNET, F., DUPIOT-CHIRON, J., BAROUK-SIMONET, E., JONES, N., DE REYNIES, A., MACGROGAN, G., SEVENET, N., LETOUZE, E. & LONGY, M. 2017. Combined tumor genomic profiling and exome sequencing in a breast cancer family implicates ATM in tumorigenesis: A proof of principle study. *Genes Chromosomes & Cancer,* 56**,** 788-799.

BUCHHOP, S., GIBSON, M. K., WANG, X. W., WAGNER, P., STÜRZBECHER, H. W. & HARRIS, C. C. 1997. Interaction of p53 with the human Rad51 protein. *Nucleic Acids Res,* 25**,** 3868-74.

BUCKLEY, R. H. 2004. Pulmonary complications of primary immunodeficiencies. *Paediatr Respir Rev,* 5 Suppl A**,** S225-33.

BUDANOV, A. V. & KARIN, M. 2008. p53 target genes sestrin1 and sestrin2 connect genotoxic stress and mTOR signaling. *Cell,* 134**,** 451-60.

BURGESS, H. A. & GRANATO, M. 2007. Modulation of locomotor activity in larval zebrafish during light adaptation. *J Exp Biol,* 210**,** 2526-39.

BURK, K., ZUHLKE, C., KONIG, I. R., ZIEGLER, A., SCHWINGER, E., GLOBAS, C., DICHGANS, J. & HELLENBROICH, Y. 2004. Spinocerebellar ataxia type 5: clinical and molecular genetic features of a German kindred. *Neurology,* 62**,** 327-9.

BURKE, J. R., WINGFIELD, M. S., LEWIS, K. E., ROSES, A. D., LEE, J. E., HULETTE, C., PERICAK-VANCE, M. A. & VANCE, J. M. 1994. The Haw River syndrome: dentatorubropallidoluysian atrophy (DRPLA) in an African-American family. *Nat Genet,* 7**,** 521-4.

BURMA, S., CHEN, B. P., MURPHY, M., KURIMASA, A. & CHEN, D. J. 2001. ATM phosphorylates histone H2AX in response to DNA double-strand breaks. *J Biol Chem,* 276**,** 42462-7.

BURNS, R., MAJCZENKO, K., XU, J., PENG, W., YAPICI, Z., DOWLING, J. J., LI, J. Z. & BURMEISTER, M. 2014. Homozygous splice mutation in CWF19L1 in a Turkish family with recessive ataxia syndrome. *Neurology,* 83**,** 2175-82.

BUTTNER, N., GESCHWIND, D., JEN, J. C., PERLMAN, S., PULST, S. M. & BALOH, R. W. 1998. Oculomotor phenotypes in autosomal dominant ataxias. *Arch Neurol,* 55**,** 1353-7.

CABALLERO, T., CABA-MOLINA, M., SALMERÓN, J. & GÓMEZ-MORALES, M. 2014. Nonalcoholic steatohepatitis in a patient with ataxia-telangiectasia. *Case Reports Hepatol,* 2014**,** 761250.

CABANA, M. D., CRAWFORD, T. O., WINKELSTEIN, J. A., CHRISTENSEN, J. R. & LEDERMAN, H. M. 1998. Consequences of the delayed diagnosis of ataxia-telangiectasia. *Pediatrics,* 102**,** 98-100.

CADIEUX-DION, M., TURCOTTE-GAUTHIER, M., NOREAU, A., MARTIN, C., MELOCHE, C., GRAVEL, M., DROUIN, C. A., ROULEAU, G. A., NGUYEN, D. K. & COSSETTE, P. 2014. Expanding the clinical phenotype associated with ELOVL4 mutation: study of a large French-Canadian family with autosomal dominant spinocerebellar ataxia and erythrokeratodermia. *JAMA Neurol,* 71**,** 470-5.

CAGNOLI, C., MARIOTTI, C., TARONI, F., SERI, M., BRUSSINO, A., MICHIELOTTO, C., GRISOLI, M., DI BELLA, D., MIGONE, N., GELLERA, C., DI DONATO, S. & BRUSCO, A. 2006. SCA28, a novel form of autosomal dominant cerebellar ataxia on chromosome 18p11.22-q11.2. *Brain,* 129**,** 235-42.

CAGNOLI, C., STEVANIN, G., BRUSSINO, A., BARBERIS, M., MANCINI, C., MARGOLIS, R. L., HOLMES, S. E., NOBILI, M., FORLANI, S., PADOVAN, S., PAPPI, P., ZAROS, C., LEBER, I., RIBAI, P., PUGLIESE, L., ASSALTO, C., BRICE, A., MIGONE, N., DURR, A. & BRUSCO, A. 2010. Missense mutations in the AFG3L2 proteolytic domain account for approximately 1.5% of European autosomal dominant cerebellar ataxias. *Hum Mutat,* 31**,** 1117-24.

CALLEN, E., JANKOVIC, M., DIFILIPPANTONIO, S., DANIEL, J. A., CHEN, H. T., CELESTE, A., PELLEGRINI, M., MCBRIDE, K., WANGSA, D., BREDEMEYER, A. L., SLECKMAN, B. P., RIED, T., NUSSENZWEIG, M. & NUSSENZWEIG, A. 2007a. ATM prevents the persistence and propagation of chromosome breaks in lymphocytes. *Cell,* 130**,** 63-75.

CALLEN, E., NUSSENZWEIG, M. C. & NUSSENZWEIG, A. 2007b. Breaking down cell cycle checkpoints and DNA repair during antigen receptor gene assembly. *Oncogene,* 26**,** 7759-7764.

CAM, H., EASTON, J. B., HIGH, A. & HOUGHTON, P. J. 2010. mTORC1 signaling under hypoxic conditions is controlled by ATM-dependent phosphorylation of HIF-1α. *Mol Cell,* 40**,** 509-20.

CAMPBELL, A., KRUPP, B., BUSHMAN, J., NOBLE, M., PROSCHEL, C. & MAYER-PROSCHEL, M. 2015. A novel mouse model for ataxia-telangiectasia with a N-terminal mutation displays a behavioral defect and a low incidence of lymphoma but no increased oxidative burden. *Hum Mol Genet,* 24**,** 6331-49.

CAMPBELL, C., MITUI, M., ENG, L., COUTINHO, G., THORSTENSON, Y. & GATTI, R. A. 2003. ATM mutations on distinct SNP and STR haplotypes in ataxia-telangiectasia patients of differing ethnicities reveal ancestral founder effects. *Human Mutation,* 21**,** 80-85.

CAMPISI, J. 2013. Aging, cellular senescence, and cancer. *Annual review of physiology,* 75**,** 685-705.

CAMPUZANO, V., MONTERMINI, L., MOLTO, M. D., PIANESE, L., COSSEE, M., CAVALCANTI, F., MONROS, E., RODIUS, F., DUCLOS, F., MONTICELLI, A., ZARA, F., CANIZARES, J., KOUTNIKOVA, H., BIDICHANDANI, S. I., GELLERA, C., BRICE, A., TROUILLAS, P., DE MICHELE, G., FILLA, A., DE FRUTOS, R., PALAU, F., PATEL, P. I., DI DONATO, S., MANDEL, J. L., COCOZZA, S., KOENIG, M. & PANDOLFO, M. 1996. Friedreich's ataxia: autosomal recessive disease caused by an intronic GAA triplet repeat expansion. *Science,* 271**,** 1423-7.

CANCEL, G., DUYCKAERTS, C., HOLMBERG, M., ZANDER, C., YVERT, G., LEBRE, A. S., RUBERG, M., FAUCHEUX, B., AGID, Y., HIRSCH, E. & BRICE, A. 2000. Distribution of ataxin-7 in normal human brain and retina. *Brain,* 123 Pt 12**,** 2519-30.

CANMAN, C. E., LIM, D. S., CIMPRICH, K. A., TAYA, Y., TAMAI, K., SAKAGUCHI, K., APPELLA, E., KASTAN, M. B. & SILICIANO, J. D. 1998. Activation of the ATM kinase by ionizing radiation and phosphorylation of p53. *Science,* 281**,** 1677-9.

CAO, Z., MAO, X. & LUO, L. 2019. Germline Stem Cells Drive Ovary Regeneration in Zebrafish. *Cell Reports,* 26**,** 1709-1717.e3.

CARDIFF, I. O. M. G. I. 2017. *The Human Gene Mutation Database* [Online]. [Accessed 22.01.18 2018].

CARROLL, P., RENONCOURT, Y., GAYET, O., DE BOVIS, B. & ALONSO, S. 2001. Sorting nexin-14, a gene expressed in motoneurons trapped by an in vitro preselection method. *Dev Dyn,* 221**,** 431-42.

CASTELLOTTI, B., MARIOTTI, C., RIMOLDI, M., FANCELLU, R., PLUMARI, M., CAIMI, S., UZIEL, G., NARDOCCI, N., MORONI, I., ZORZI, G., PAREYSON, D., DI BELLA, D., DI DONATO, S., TARONI, F. & GELLERA, C. 2011. Ataxia with oculomotor apraxia type1 (AOA1): novel and recurrent aprataxin mutations, coenzyme Q10 analyses, and clinical findings in Italian patients. *Neurogenetics,* 12**,** 193-201.

CAUSIER, B., LI, Z., DE SMET, R., LLOYD, J. P. B., VAN DE PEER, Y. & DAVIES, B. 2017. Conservation of Nonsense-Mediated mRNA Decay Complex Components Throughout Eukaryotic Evolution. *Scientific Reports,* 7**,** 16692.

CAYUELA, M. L., CLAES, K. B. M., FERREIRA, M. G., HENRIQUES, C. M., VAN EEDEN, F., VARGA, M., VIERSTRAETE, J. & MIONE, M. C. 2019. The Zebrafish as an Emerging Model to Study DNA Damage in Aging, Cancer and Other Diseases. *Frontiers in cell and developmental biology,* 6**,** 178-178.

CHAI, Y., SHAO, J., MILLER, V. M., WILLIAMS, A. & PAULSON, H. L. 2002. Live-cell imaging reveals divergent intracellular dynamics of polyglutamine disease proteins and supports a sequestration model of pathogenesis. *Proc Natl Acad Sci U S A,* 99**,** 9310-5.

CHAMBERLAIN, S., SHAW, J., ROWLAND, A., WALLIS, J., SOUTH, S., NAKAMURA, Y., VON GABAIN, A., FARRALL, M. & WILLIAMSON, R. 1988. Mapping of mutation causing Friedreich's ataxia to human chromosome 9. *Nature,* 334**,** 248-50.

CHANG, N., SUN, C., GAO, L., ZHU, D., XU, X., ZHU, X., XIONG, J.-W. & XI, J. J. 2013. Genome editing with RNA-guided Cas9 nuclease in Zebrafish embryos. *Cell Research,* 23**,** 465.

CHANG, N. S., DOHERTY, J. & ENSIGN, A. 2003. JNK1 physically interacts with WW domain-containing oxidoreductase (WOX1) and inhibits WOX1-mediated apoptosis. *J Biol Chem,* 278**,** 9195-202.

CHANG, W., PEDRONI, A., HOHENDORF, V., GIACOMELLO, S., HIBI, M., KÖSTER, R. W. & AMPATZIS, K. 2020. Functionally distinct Purkinje cell types show temporal precision in encoding locomotion. *Proceedings of the National Academy of Sciences,* 117**,** 17330.

CHARLESWORTH, G., MOHIRE, M. D., SCHNEIDER, S. A., STAMELOU, M., WOOD, N. W. & BHATIA, K. P. 2013. Ataxia telangiectasia presenting as dopa-responsive cervical dystonia. *Neurology,* 81**,** 1148-51.

CHEN, C. C., KASS, E. M., YEN, W. F., LUDWIG, T., MOYNAHAN, M. E., CHAUDHURI, J. & JASIN, M. 2017. ATM loss leads to synthetic lethality in BRCA1 BRCT mutant mice associated with exacerbated defects in homology-directed repair. *Proc Natl Acad Sci U S A,* 114**,** 7665-7670.

CHEN, D. H., BRKANAC, Z., VERLINDE, C. L., TAN, X. J., BYLENOK, L., NOCHLIN, D., MATSUSHITA, M., LIPE, H., WOLFF, J., FERNANDEZ, M., CIMINO, P. J., BIRD, T. D. & RASKIND, W. H. 2003a. Missense mutations in the regulatory domain of PKC gamma: a new mechanism for dominant nonepisodic cerebellar ataxia. *Am J Hum Genet,* 72**,** 839-49.

CHEN, P., PENG, C., LUFF, J., SPRING, K., WATTERS, D., BOTTLE, S., FURUYA, S. & LAVIN, M. F. 2003b. Oxidative stress is responsible for deficient survival and dendritogenesis in purkinje neurons from ataxia-telangiectasia mutated mutant mice. *J Neurosci,* 23**,** 11453-60.

CHEN, P. C., LAVIN, M. F., KIDSON, C. & MOSS, D. 1978. Identification of ataxia telangiectasia heterozygotes, a cancer prone population. *Nature,* 274**,** 484-6.

CHEN, T., DONG, B., LU, Z., TIAN, B., ZHANG, J., ZHOU, J., WU, H., ZHANG, Y., WU, J., LIN, P., XU, H. & MO, X. 2010. A functional single nucleotide polymorphism in promoter of ATM is associated with longevity. *Mech Ageing Dev,* 131**,** 636-40.

CHEN, T. H., WANG, Y. H. & WU, Y. H. 2011. Developmental exposures to ethanol or dimethylsulfoxide at low concentrations alter locomotor activity in larval zebrafish: implications for behavioral toxicity bioassays. *Aquat Toxicol,* 102**,** 162-6.

CHEN, Y. W., ALLEN, M. D., VEPRINTSEV, D. B., LOWE, J. & BYCROFT, M. 2004. The structure of the AXH domain of spinocerebellar ataxin-1. *J Biol Chem,* 279**,** 3758-65.

CHENG, Q. & CHEN, J. 2010. Mechanism of p53 stabilization by ATM after DNA damage. *Cell cycle (Georgetown, Tex.),* 9**,** 472-478.

CHESSA, L., PETRINELLI, P., ANTONELLI, A., FIORILLI, M., ELLI, R., MARCUCCI, L., FEDERICO, A. & GANDINI, E. 1992. Heterogeneity in ataxia-telangiectasia: classical phenotype associated with intermediate cellular radiosensitivity. *Am J Med Genet,* 42**,** 741-6.

CHI, X. Y., LI, Y. & QIU, X. Y. 2020. V(D)J recombination, somatic hypermutation and class switch recombination of immunoglobulins: mechanism and regulation. *Immunology,* 160**,** 233-247.

CHILDS, B. G., DURIK, M., BAKER, D. J. & VAN DEURSEN, J. M. 2015. Cellular senescence in aging and age-related disease: from mechanisms to therapy. *Nature medicine,* 21**,** 1424-1435.

CHING, J. K., LUEBBERT, S. H., COLLINS, R. L. T., ZHANG, Z., MARUPUDI, N., BANERJEE, S., HURD, R. D., RALSTON, L. & FISHER, J. S. 2013. Ataxia telangiectasia mutated impacts insulin-like growth factor 1 signalling in skeletal muscle. *Exp Physiol,* 98**,** 526-35.

CHOI, M., KIPPS, T. & KURZROCK, R. 2016. ATM Mutations in Cancer: Therapeutic Implications. *Molecular Cancer Therapeutics,* 15**,** 1781-1791.

CHOI, S., GAMPER, A. M., WHITE, J. S. & BAKKENIST, C. J. 2010. Inhibition of ATM kinase activity does not phenocopy ATM protein disruption: implications for the clinical utility of ATM kinase inhibitors. *Cell Cycle,* 9**,** 4052-7.

CHRISTMANN, M., HEITKAMP, S., LAMBRECHT, E., DOERRIES, K., SCHUBERT, R. & ZIELEN, S. 2009. Haemorrhagic cystitis and polyomavirus JC infection in ataxia telangiectasia. *J Pediatr Urol,* 5**,** 324-6.

CHRISTOFFELS, A., KOH, E. G., CHIA, J. M., BRENNER, S., APARICIO, S. & VENKATESH, B. 2004. Fugu genome analysis provides evidence for a whole-genome duplication early during the evolution of ray-finned fishes. *Mol Biol Evol,* 21**,** 1146-51.

CHRISTOU, M., KAVALIAUSKIS, A., ROPSTAD, E. & FRASER, T. W. K. 2020. DMSO effects larval zebrafish (Danio rerio) behavior, with additive and interaction effects when combined with positive controls. *Science of The Total Environment,* 709**,** 134490.

CHUNG, K. T., SHEN, Y. & HENDERSHOT, L. M. 2002. BAP, a mammalian BiP-associated protein, is a nucleotide exchange factor that regulates the ATPase activity of BiP. *J Biol Chem,* 277**,** 47557-63.

CHUNG, M. Y., LU, Y. C., CHENG, N. C. & SOONG, B. W. 2003. A novel autosomal dominant spinocerebellar ataxia (SCA22) linked to chromosome 1p21-q23. *Brain,* 126**,** 1293-9.

CHURCHYARD, A., STELL, R. & MASTAGLIA, F. L. 1991. Ataxia telangiectasia presenting as an extrapyramidal movement disorder and ocular motor apraxia without overt telangiectasia. *Clin Exp Neurol,* 28**,** 90-6.

CIMPRICH, K. A. 2007. Probing ATR activation with model DNA templates. *Cell Cycle,* 6**,** 2348-2354.

CIURA, S., LATTANTE, S., LE BER, I., LATOUCHE, M., TOSTIVINT, H., BRICE, A. & KABASHI, E. 2013. Loss of function of C9orf72 causes motor deficits in a zebrafish model of amyotrophic lateral sclerosis. *Ann Neurol,* 74**,** 180-7.

CLARKSON, Y. L., PERKINS, E. M., CAIRNCROSS, C. J., LYNDON, A. R., SKEHEL, P. A. & JACKSON, M. 2014. beta-III spectrin underpins ankyrin R function in Purkinje cell dendritic trees: protein complex critical for sodium channel activity is impaired by SCA5-associated mutations. *Hum Mol Genet,* 23**,** 3875-82.

COE, T. S., HAMILTON, P. B., GRIFFITHS, A. M., HODGSON, D. J., WAHAB, M. A. & TYLER, C. R. 2009. Genetic variation in strains of zebrafish (Danio rerio) and the implications for ecotoxicology studies. *Ecotoxicology,* 18**,** 144-50.

COHEN, J. M., CUCKOW, P. & DAVIES, E. G. 2008. Bladder wall telangiectasis causing life-threatening haematuria in ataxia-telangiectasia: a new observation. *Acta Paediatr,* 97**,** 667-9.

COHEN, M. M., SHAHAM, M., DAGAN, J., SHMUELI, E. & KOHN, G. 1975. Cytogenetic investigations in families with ataxia-telangiectasia. *Cytogenet Cell Genet,* 15**,** 338-56.

COHEN, P. E., POLLACK, S. E. & POLLARD, J. W. 2006. Genetic Analysis of Chromosome Pairing, Recombination, and Cell Cycle Control during First Meiotic Prophase in Mammals. *Endocrine Reviews,* 27**,** 398-426.

COHEN, P. E. & POLLARD, J. W. 2001. Regulation of meiotic recombination and prophase I progression in mammals. *Bioessays,* 23**,** 996-1009.

COHEN, S., PUGET, N., LIN, Y. L., CLOUAIRE, T., AGUIRREBENGOA, M., ROCHER, V., PASERO, P., CANITROT, Y. & LEGUBE, G. 2018. Senataxin resolves RNA:DNA hybrids forming at DNA double-strand breaks to prevent translocations. *Nat Commun,* 9**,** 533.

COLE, J., ARLETT, C. F., GREEN, M. H., HARCOURT, S. A., PRIESTLEY, A., HENDERSON, L., COLE, H., JAMES, S. E. & RICHMOND, F. 1988. Comparative human cellular radiosensitivity: II. The survival following gamma-irradiation of unstimulated (G0) T-lymphocytes, T-lymphocyte lines, lymphoblastoid cell lines and fibroblasts from normal donors, from ataxia-telangiectasia patients and from ataxia-telangiectasia heterozygotes. *Int J Radiat Biol,* 54**,** 929-43.

CONCANNON, P. & GATTI, R. A. 1997. Diversity of ATM gene mutations detected in patients with ataxia-telangiectasia. *Hum Mutat,* 10**,** 100-7.

CONG, L., RAN, F. A., COX, D., LIN, S., BARRETTO, R., HABIB, N., HSU, P. D., WU, X., JIANG, W., MARRAFFINI, L. A. & ZHANG, F. 2013. Multiplex genome engineering using CRISPR/Cas systems. *Science,* 339**,** 819-23.

CONNELLY, P. J., SMITH, N., CHADWICK, R., EXLEY, A. R., SHNEERSON, J. M. & PEARSON, E. R. 2016. Recessive mutations in the cancer gene Ataxia Telangiectasia Mutated (ATM), at a locus previously associated with metformin response, cause dysglycaemia and insulin resistance. *Diabetic Medicine,* 33**,** 371-375.

CONRADSEN, C. & MCGUIGAN, K. 2015. Sexually dimorphic morphology and swimming performance relationships in wild-type zebrafish Danio rerio. *J Fish Biol,* 87**,** 1219-33.

CONRADSEN, C., WALKER, J. A., PERNA, C. & MCGUIGAN, K. 2016. Repeatability of locomotor performance and morphology-locomotor performance relationships. *J Exp Biol,* 219**,** 2888-2897.

COOPER, T. J., WARDELL, K., GARCIA, V. & NEALE, M. J. 2014. Homeostatic regulation of meiotic DSB formation by ATM/ATR. *Experimental Cell Research,* 329**,** 124-131.

CORNET, C., DI DONATO, V. & TERRIENTE, J. 2018. Combining Zebrafish and CRISPR/Cas9: Toward a More Efficient Drug Discovery Pipeline. *Frontiers in Pharmacology,* 9**,** 11.

COSENTINO, C., GRIECO, D. & COSTANZO, V. 2011. ATM activates the pentose phosphate pathway promoting anti-oxidant defence and DNA repair. *Embo j,* 30**,** 546-55.

COUTELIER, M., BLESNEAC, I., MONTEIL, A., MONIN, M. L., ANDO, K., MUNDWILLER, E., BRUSCO, A., LE BER, I., ANHEIM, M., CASTRIOTO, A., DUYCKAERTS, C., BRICE, A., DURR, A., LORY, P. & STEVANIN, G. 2015. A Recurrent Mutation in CACNA1G Alters Cav3.1 T-Type Calcium-Channel Conduction and Causes Autosomal-Dominant Cerebellar Ataxia. *Am J Hum Genet,* 97**,** 726-37.

CRAWFORD, T. O. 1998. Ataxia telangiectasia. *Semin Pediatr Neurol,* 5**,** 287-94.

CRAWFORD, T. O., SKOLASKY, R. L., FERNANDEZ, R., ROSQUIST, K. J. & LEDERMAN, H. M. 2006. Survival probability in ataxia telangiectasia. *Arch Dis Child,* 91**,** 610-1.

CRISCUOLO, C., MANCINI, P., SACCA, F., DE MICHELE, G., MONTICELLI, A., SANTORO, L., SCARANO, V., BANFI, S. & FILLA, A. 2004. Ataxia with oculomotor apraxia type 1 in Southern Italy: late onset and variable phenotype. *Neurology,* 63**,** 2173-5.

CROSBY, A. H., PATEL, H., CHIOZA, B. A., PROUKAKIS, C., GURTZ, K., PATTON, M. A., SHARIFI, R., HARLALKA, G., SIMPSON, M. A., DICK, K., REED, J. A., AL-MEMAR, A., CHRZANOWSKA-LIGHTOWLERS, Z. M., CROSS, H. E. & LIGHTOWLERS, R. N. 2010. Defective mitochondrial mRNA maturation is associated with spastic ataxia. *Am J Hum Genet,* 87**,** 655-60.

CUMMINS, G., JAWAD, T., TAYLOR, M. & LYNCH, T. 2013. Myoclonic head jerks and extensor axial dystonia in the variant form of ataxia telangiectasia. *Parkinsonism & Related Disorders,* 19**,** 1173-1174.

D'ALMEIDA, A. K., CAVACIUTI, E., DONDON, M. G., LAUGE, A., JANIN, N., STOPPA-LYONNET, D. & ANDRIEU, N. 2005. Increased risk of breast cancer among female relatives of patients with ataxia-telangiectasia: a causal relationship? *British Journal of Cancer,* 93**,** 730-732.

DALSKI, A., ATICI, J., KREUZ, F. R., HELLENBROICH, Y., SCHWINGER, E. & ZUHLKE, C. 2005. Mutation analysis in the fibroblast growth factor 14 gene: frameshift mutation and polymorphisms in patients with inherited ataxias. *Eur J Hum Genet,* 13**,** 118-20.

DANIEL, J. A., PELLEGRINI, M., LEE, B. S., GUO, Z., FILSUF, D., BELKINA, N. V., YOU, Z., PAULL, T. T., SLECKMAN, B. P., FEIGENBAUM, L. & NUSSENZWEIG, A. 2012. Loss of ATM kinase activity leads to embryonic lethality in mice. *J Cell Biol,* 198**,** 295-304.

DANILOVA, N., BUSSMANN, J., JEKOSCH, K. & STEINER, L. A. 2005. The immunoglobulin heavy-chain locus in zebrafish: identification and expression of a previously unknown isotype, immunoglobulin Z. *Nat Immunol,* 6**,** 295-302.

DANILOVA, N., HOHMAN, V. S., KIM, E. H. & STEINER, L. A. 2000. Immunoglobulin variable-region diversity in the zebrafish. *Immunogenetics,* 52**,** 81-91.

DANILOVA, N. & STEINER, L. A. 2002. B cells develop in the zebrafish pancreas. *Proceedings of the National Academy of Sciences,* 99**,** 13711.

DAS, B. B., ANTONY, S., GUPTA, S., DEXHEIMER, T. S., REDON, C. E., GARFIELD, S., SHILOH, Y. & POMMIER, Y. 2009. Optimal function of the DNA repair enzyme TDP1 requires its phosphorylation by ATM and/or DNA-PK. *Embo j,* 28**,** 3667-80.

DATE, H., ONODERA, O., TANAKA, H., IWABUCHI, K., UEKAWA, K., IGARASHI, S., KOIKE, R., HIROI, T., YUASA, T., AWAYA, Y., SAKAI, T., TAKAHASHI, T., NAGATOMO, H., SEKIJIMA, Y., KAWACHI, I., TAKIYAMA, Y., NISHIZAWA, M., FUKUHARA, N., SAITO, K., SUGANO, S. & TSUJI, S. 2001. Early-onset ataxia with ocular motor apraxia and hypoalbuminemia is caused by mutations in a new HIT superfamily gene. *Nat Genet,* 29**,** 184-8.

DAUGHERITY, E. K., BALMUS, G., AL SAEI, A., MOORE, E. S., ABI ABDALLAH, D., ROGERS, A. B., WEISS, R. S. & MAURER, K. J. 2012. The DNA damage checkpoint protein ATM promotes hepatocellular apoptosis and fibrosis in a mouse model of non-alcoholic fatty liver disease. *Cell Cycle,* 11**,** 1918-28.

DAUGHTERS, R. S., TUTTLE, D. L., GAO, W., IKEDA, Y., MOSELEY, M. L., EBNER, T. J., SWANSON, M. S. & RANUM, L. P. 2009. RNA gain-of-function in spinocerebellar ataxia type 8. *PLoS Genet,* 5**,** e1000600.

DAVID, G., ABBAS, N., COULLIN, P., STEVANIN, G., HORTA, W., GEMMILL, R., WEISSENBACH, J., WOOD, N., CUNHA, S., DRABKIN, H., HARDING, A. E., AGID, Y. & BRICE, A. 1996. The gene for autosomal dominant cerebellar ataxia type II is located in a 5-cM region in 3p12-p13: Genetic and physical mapping of the SCA7 locus. *American Journal of Human Genetics,* 59**,** 1328-1336.

DAVID, G., ABBAS, N., STEVANIN, G., DURR, A., YVERT, G., CANCEL, G., WEBER, C., IMBERT, G., SAUDOU, F., ANTONIOU, E., DRABKIN, H., GEMMILL, R., GIUNTI, P., BENOMAR, A., WOOD, N., RUBERG, M., AGID, Y., MANDEL, J. L. & BRICE, A. 1997. Cloning of the SCA7 gene reveals a highly unstable CAG repeat expansion. *Nat Genet,* 17**,** 65-70.

DAWSON, A. J., MARLES, S., TOMIUK, M., RIORDAN, D. & GATTI, R. A. 2015. Ataxia-telangiectasia with female fertility. *Am J Med Genet A,* 167a**,** 1937-9.

DE CHIARA, C., GIANNINI, C., ADINOLFI, S., DE BOER, J., GUIDA, S., RAMOS, A., JODICE, C., KIOUSSIS, D. & PASTORE, A. 2003. The AXH module: an independently folded domain common to ataxin-1 and HBP1. *FEBS Lett,* 551**,** 107-12.

DE CHIARA, C., MENON, R. P., STROM, M., GIBSON, T. J. & PASTORE, A. 2009. Phosphorylation of S776 and 14-3-3 binding modulate ataxin-1 interaction with splicing factors. *PLoS One,* 4**,** e8372.

DE ESCH, C., VAN DER LINDE, H., SLIEKER, R., WILLEMSEN, R., WOLTERBEEK, A., WOUTERSEN, R. & DE GROOT, D. 2012. Locomotor activity assay in zebrafish larvae: influence of age, strain and ethanol. *Neurotoxicol Teratol,* 34**,** 425-33.

DE VILLARTAY, J. P. 2002. V(D)J recombination and DNA repair: lessons from human immune deficiencies and other animal models. *Current Opinion in Allergy and Clinical Immunology,* 2**,** 473-479.

DE VRIES, B., MAMSA, H., STAM, A. H., WAN, J., BAKKER, S. L., VANMOLKOT, K. R., HAAN, J., TERWINDT, G. M., BOON, E. M., HOWARD, B. D., FRANTS, R. R., BALOH, R. W., FERRARI, M. D., JEN, J. C. & VAN DEN MAAGDENBERG, A. M. 2009. Episodic ataxia associated with EAAT1 mutation C186S affecting glutamate reuptake. *Arch Neurol,* 66**,** 97-101.

DEAKIN, A. G., BUCKLEY, J., ALZU'BI, H. S., COSSINS, A. R., SPENCER, J. W., AL'NUAIMY, W., YOUNG, I. S., THOMSON, J. S. & SNEDDON, L. U. 2019. Automated monitoring of behaviour in zebrafish after invasive procedures. *Scientific Reports,* 9**,** 9042.

DELATYCKI, M. B., KNIGHT, M., KOENIG, M., COSSEE, M., WILLIAMSON, R. & FORREST, S. M. 1999. G130V, a common FRDA point mutation, appears to have arisen from a common founder. *Hum Genet,* 105**,** 343-6.

DELIA, D., PIANE, M., BUSCEMI, G., SAVIO, C., PALMERI, S., LULLI, P., CARLESSI, L., FONTANELLA, E. & CHESSA, L. 2004. MRE11 mutations and impaired ATM-dependent responses in an Italian family with ataxia-telangiectasia-like disorder. *Hum Mol Genet,* 13**,** 2155-63.

DELPLANQUE, J., DEVOS, D., HUIN, V., GENET, A., SAND, O., MOREAU, C., GOIZET, C., CHARLES, P., ANHEIM, M., MONIN, M. L., BUEE, L., DESTEE, A., GROLEZ, G., DELMAIRE, C., DUJARDIN, K., DELLACHERIE, D., BRICE, A., STEVANIN, G., STRUBI-VUILLAUME, I., DURR, A. & SABLONNIERE, B. 2014. TMEM240 mutations cause spinocerebellar ataxia 21 with mental retardation and severe cognitive impairment. *Brain,* 137**,** 2657-63.

DENKER, S. P., HUANG, D. C., ORLOWSKI, J., FURTHMAYR, H. & BARBER, D. L. 2000. Direct binding of the Na--H exchanger NHE1 to ERM proteins regulates the cortical cytoskeleton and cell shape independently of H(+) translocation. *Mol Cell,* 6**,** 1425-36.

DESCHAVANNE, P. J. & FERTIL, B. 1996. A review of human cell radiosensitivity in vitro. *Int J Radiat Oncol Biol Phys,* 34**,** 251-66.

DEVEAU, A. P., BENTLEY, V. L. & BERMAN, J. N. 2017. Using zebrafish models of leukemia to streamline drug screening and discovery. *Experimental Hematology,* 45**,** 1-9.

DEVOS, D., SCHRAEN-MASCHKE, S., VUILLAUME, I., DUJARDIN, K., NAZE, P., WILLOTEAUX, C., DESTEE, A. & SABLONNIERE, B. 2001. Clinical features and genetic analysis of a new form of spinocerebellar ataxia. *Neurology,* 56**,** 234-8.

DI BELLA, D., LAZZARO, F., BRUSCO, A., PLUMARI, M., BATTAGLIA, G., PASTORE, A., FINARDI, A., CAGNOLI, C., TEMPIA, F., FRONTALI, M., VENEZIANO, L., SACCO, T., BODA, E., BRUSSINO, A., BONN, F., CASTELLOTTI, B., BARATTA, S., MARIOTTI, C., GELLERA, C., FRACASSO, V., MAGRI, S., LANGER, T., PLEVANI, P., DI DONATO, S., MUZI-FALCONI, M. & TARONI, F. 2010. Mutations in the mitochondrial protease gene AFG3L2 cause dominant hereditary ataxia SCA28. *Nat Genet,* 42**,** 313-21.

DI NARDO, A., WERTZ, M. H., KWIATKOWSKI, E., TSAI, P. T., LEECH, J. D., GREENE-COLOZZI, E., GOTO, J., DILSIZ, P., TALOS, D. M., CLISH, C. B., KWIATKOWSKI, D. J. & SAHIN, M. 2014. Neuronal Tsc1/2 complex controls autophagy through AMPK-dependent regulation of ULK1. *Hum Mol Genet,* 23**,** 3865-74.

DI SIENA, S., CAMPOLO, F., GIMMELLI, R., DI PIETRO, C., MARAZZITI, D., DOLCI, S., LENZI, A., NUSSENZWEIG, A. & PELLEGRINI, M. 2018. Atm reactivation reverses ataxia telangiectasia phenotypes in vivo. *Cell Death Dis,* 9**,** 314.

DIBBLE, C. C., ELIS, W., MENON, S., QIN, W., KLEKOTA, J., ASARA, J. M., FINAN, P. M., KWIATKOWSKI, D. J., MURPHY, L. O. & MANNING, B. D. 2012. TBC1D7 is a third subunit of the TSC1-TSC2 complex upstream of mTORC1. *Mol Cell,* 47**,** 535-46.

DIRIONG, S., LORY, P., WILLIAMS, M. E., ELLIS, S. B., HARPOLD, M. M. & TAVIAUX, S. 1995. Chromosomal localization of the human genes for alpha 1A, alpha 1B, and alpha 1E voltage-dependent Ca2+ channel subunits. *Genomics,* 30**,** 605-9.

DIXON, J. E., SHI, W., WANG, H. S., MCDONALD, C., YU, H., WYMORE, R. S., COHEN, I. S. & MCKINNON, D. 1996. Role of the Kv4.3 K+ channel in ventricular muscle. A molecular correlate for the transient outward current. *Circ Res,* 79**,** 659-68.

DODSON, M. W. & GUO, M. 2007. Pink1, Parkin, DJ-1 and mitochondrial dysfunction in Parkinson's disease. *Curr Opin Neurobiol,* 17**,** 331-7.

DOHLINGER, S., HAUSER, T. K., BORKERT, J., LUFT, A. R. & SCHULZ, J. B. 2008. Magnetic resonance imaging in spinocerebellar ataxias. *Cerebellum,* 7**,** 204-214.

DOI, H., YOSHIDA, K., YASUDA, T., FUKUDA, M., FUKUDA, Y., MORITA, H., IKEDA, S., KATO, R., TSURUSAKI, Y., MIYAKE, N., SAITSU, H., SAKAI, H., MIYATAKE, S., SHIINA, M., NUKINA, N., KOYANO, S., TSUJI, S., KUROIWA, Y. & MATSUMOTO, N. 2011. Exome sequencing reveals a homozygous SYT14 mutation in adult-onset, autosomal-recessive spinocerebellar ataxia with psychomotor retardation. *Am J Hum Genet,* 89**,** 320-7.

DONATH, H., WOELKE, S., THEIS, M., HEß, U., KNOP, V., HERRMANN, E., KRAUSKOPF, D., KIESLICH, M., SCHUBERT, R. & ZIELEN, S. 2019. Progressive Liver Disease in Patients With Ataxia Telangiectasia. *Front Pediatr,* 7**,** 458.

DOR, T., CINNAMON, Y., RAYMOND, L., SHAAG, A., BOUSLAM, N., BOUHOUCHE, A., GAUSSEN, M., MEYER, V., DURR, A., BRICE, A., BENOMAR, A., STEVANIN, G., SCHUELKE, M. & EDVARDSON,

S. 2014. KIF1C mutations in two families with hereditary spastic paraparesis and cerebellar dysfunction. *J Med Genet,* 51**,** 137-42.

DORNER, C., CIOSSEK, T., MULLER, S., MOLLER, P. H., ULLRICH, A. & LAMMERS, R. 1998. Characterization of KIF1C, a new kinesin-like protein involved in vesicle transport from the Golgi apparatus to the endoplasmic reticulum. *J Biol Chem,* 273**,** 20267-75.

DOU, T., GU, S., LIU, J., CHEN, F., ZENG, L., GUO, L., XIE, Y. & MAO, Y. 2005. Isolation and characterization of ubiquitin-activating enzyme E1-domain containing 1, UBE1DC1. *Mol Biol Rep,* 32**,** 265-71.

DRIESSEN, G. J., IJSPEERT, H., WEEMAES, C. M., HARALDSSON, Á., TRIP, M., WARRIS, A., VAN DER FLIER, M., WULFFRAAT, N., VERHAGEN, M. M., TAYLOR, M. A., VAN ZELM, M. C., VAN DONGEN, J. J., VAN DEUREN, M. & VAN DER BURG, M. 2013. Antibody deficiency in patients with ataxia telangiectasia is caused by disturbed B- and T-cell homeostasis and reduced immune repertoire diversity. *J Allergy Clin Immunol,* 131**,** 1367-75.e9.

DU, F. X., ZHANG, M. J., LI, X. H., YANG, C. Y., MENG, H., WANG, D., CHANG, S., XU, Y., PRICE, B. & SUN, Y. L. 2014. Dimer monomer transition and dimer re-formation play important role for ATM cellular function during DNA repair. *Biochemical and Biophysical Research Communications,* 452**,** 1034-1039.

DUAN, R., SHI, Y., YU, L., ZHANG, G., LI, J., LIN, Y., GUO, J., WANG, J., SHEN, L., JIANG, H., WANG, G. & TANG, B. 2016. UBA5 Mutations Cause a New Form of Autosomal Recessive Cerebellar Ataxia. *PLoS One,* 11**,** e0149039.

DUARRI, A., JEZIERSKA, J., FOKKENS, M., MEIJER, M., SCHELHAAS, H. J., DEN DUNNEN, W. F., VAN DIJK, F., VERSCHUUREN-BEMELMANS, C., HAGEMAN, G., VAN DE VLIES, P., KUSTERS, B., VAN DE WARRENBURG, B. P., KREMER, B., WIJMENGA, C., SINKE, R. J., SWERTZ, M. A., KAMPINGA, H. H., BODDEKE, E. & VERBEEK, D. S. 2012. Mutations in potassium channel kcnd3 cause spinocerebellar ataxia type 19. *Ann Neurol,* 72**,** 870-80.

DUJKA, M. E., PUEBLA-OSORIO, N., TAVANA, O., SANG, M. & ZHU, C. 2010. ATM and p53 are essential in the cell-cycle containment of DNA breaks during V(D)J recombination in vivo. *Oncogene,* 29**,** 957-65.

DUNPHY, G., FLANNERY, S. M., ALMINE, J. F., CONNOLLY, D. J., PAULUS, C., JØNSSON, K. L., JAKOBSEN, M. R., NEVELS, M. M., BOWIE, A. G. & UNTERHOLZNER, L. 2018. Non-canonical Activation of the DNA Sensing Adaptor STING by ATM and IFI16 Mediates NF-κB Signaling after Nuclear DNA Damage. *Mol Cell,* 71**,** 745-760.e5.

DUPRE, N., GROS-LOUIS, F., CHRESTIAN, N., VERREAULT, S., BRUNET, D., DE VERTEUIL, D., BRAIS, B., BOUCHARD, J. P. & ROULEAU, G. A. 2007. Clinical and genetic study of autosomal recessive cerebellar ataxia type 1. *Ann Neurol,* 62**,** 93-8.

DUPRÉ, A., BOYER-CHATENET, L. & GAUTIER, J. 2006. Two-step activation of ATM by DNA and the Mre11-Rad50-Nbs1 complex. *Nat Struct Mol Biol,* 13**,** 451-7.

DUQUETTE, A., RODDIER, K., MCNABB-BALTAR, J., GOSSELIN, I., ST-DENIS, A., DICAIRE, M. J., LOISEL, L., LABUDA, D., MARCHAND, L., MATHIEU, J., BOUCHARD, J. P. & BRAIS, B. 2005. Mutations in senataxin responsible for Quebec cluster of ataxia with neuropathy. *Ann Neurol,* 57**,** 408-14.

DUURSMA, A. M., DRISCOLL, R., ELIAS, J. E. & CIMPRICH, K. A. 2013. A Role for the MRN Complex in ATR Activation via TOPBP1 Recruitment. *Molecular Cell,* 50**,** 116-122.

DY, M. E., SIMS, K. B. & FRIEDMAN, J. 2015. TPP1 deficiency: Rare cause of isolated childhood-onset progressive ataxia. *Neurology,* 85**,** 1259-61.

EASTER, S. S., JR. & NICOLA, G. N. 1996. The development of vision in the zebrafish (Danio rerio). *Dev Biol,* 180**,** 646-63.

EATON, J. S., LIN, Z. P., SARTORELLI, A. C., BONAWITZ, N. D. & SHADEL, G. S. 2007. Ataxia-telangiectasia mutated kinase regulates ribonucleotide reductase and mitochondrial homeostasis. *J Clin Invest,* 117**,** 2723-34.

EFEYAN, A., MURGA, M., MARTINEZ-PASTOR, B., ORTEGA-MOLINA, A., SORIA, R., COLLADO, M., FERNANDEZ-CAPETILLO, O. & SERRANO, M. 2009. Limited role of murine ATM in oncogene-induced senescence and p53-dependent tumor suppression. *PloS one,* 4**,** e5475-e5475.

EKKER, S. C. & LARSON, J. D. 2001. Morphant technology in model developmental systems. *Genesis,* 30**,** 89-93.

EL-BROLOSY, M. A., KONTARAKIS, Z., ROSSI, A., KUENNE, C., GÜNTHER, S., FUKUDA, N., KIKHI, K., BOEZIO, G. L. M., TAKACS, C. M., LAI, S.-L., FUKUDA, R., GERRI, C., GIRALDEZ, A. J. & STAINIER, D. Y. R. 2019. Genetic compensation triggered by mutant mRNA degradation. *Nature,* 568**,** 193-197.

EL-KHAMISY, S. F., SAIFI, G. M., WEINFELD, M., JOHANSSON, F., HELLEDAY, T., LUPSKI, J. R. & CALDECOTT, K. W. 2005. Defective DNA single-strand break repair in spinocerebellar ataxia with axonal neuropathy-1. *Nature,* 434**,** 108-13.

ELSAYED, S. M., HELLER, R., THOENES, M., ZAKI, M. S., SWAN, D., ELSOBKY, E., ZUHLKE, C., EBERMANN, I., NURNBERG, G., NURNBERG, P. & BOLZ, H. J. 2014. Autosomal dominant SCA5 and autosomal recessive infantile SCA are allelic conditions resulting from SPTBN2 mutations. *Eur J Hum Genet,* 22**,** 286-8.

ELSON, A., WANG, Y., DAUGHERTY, C. J., MORTON, C. C., ZHOU, F., CAMPOS-TORRES, J. & LEDER, P. 1996. Pleiotropic defects in ataxia-telangiectasia protein-deficient mice. *Proc Natl Acad Sci U S A,* 93**,** 13084-9.

EMELYANOV, A., GAO, Y., NAQVI, N. I. & PARINOV, S. 2006. Trans-kingdom transposition of the maize dissociation element. *Genetics,* 174**,** 1095-1104.

EMRAN, F., RIHEL, J. & DOWLING, J. E. 2008. A behavioral assay to measure responsiveness of zebrafish to changes in light intensities. *J Vis Exp*.

ENACHE, O. M., RENDO, V., ABDUSAMAD, M., LAM, D., DAVISON, D., PAL, S., CURRIMJEE, N., HESS, J., PANTEL, S., NAG, A., THORNER, A. R., DOENCH, J. G., VAZQUEZ, F., BEROUKHIM, R., GOLUB, T. R. & BEN-DAVID, U. 2020. Cas9 activates the p53 pathway and selects for p53-inactivating mutations. *Nature Genetics,* 52**,** 662-668.

ENSEMBLE. 2017. *ENST00000278616.8* [Online]. Available: http://uswest.ensembl.org/Homo_sapiens/Transcript/Exons?db=core [Accessed].

ERICHSEN, A. K., KOHT, J., STRAY-PEDERSEN, A., ABDELNOOR, M. & TALLAKSEN, C. M. 2009. Prevalence of hereditary ataxia and spastic paraplegia in southeast Norway: a population-based study. *Brain,* 132**,** 1577-88.

ESBER, C. M., SHABSIGH, A. & ZYNGER, D. L. 2012. Sclerosing Sertoli cell tumor without expression of typical sex cord stromal tumor markers: case report and literature review. *Pathol Res Pract,* 208**,** 121-5.

ESCAYG, A., DE WAARD, M., LEE, D. D., BICHET, D., WOLF, P., MAYER, T., JOHNSTON, J., BALOH, R., SANDER, T. & MEISLER, M. H. 2000. Coding and noncoding variation of the human calcium-channel beta4-subunit gene CACNB4 in patients with idiopathic generalized epilepsy and episodic ataxia. *Am J Hum Genet,* 66**,** 1531-9.

ESCAYG, A., JONES, J. M., KEARNEY, J. A., HITCHCOCK, P. F. & MEISLER, M. H. 1998. Calcium channel beta 4 (CACNB4): human ortholog of the mouse epilepsy gene lethargic. *Genomics,* 50**,** 14-22.

ETO, K., SUMI, S. M., BIRD, T. D., MCEVOY-BUSH, T., BOEHNKE, M. & SCHELLENBERG, G. 1990. Family with dominantly inherited ataxia, amyotrophy, and peripheral sensory loss. Spinopontine atrophy or Machado-Joseph Azorean disease in another non-Portuguese family? *Arch Neurol,* 47**,** 968-74.

EUNSON, L. H., REA, R., ZUBERI, S. M., YOUROUKOS, S., PANAYIOTOPOULOS, C. P., LIGUORI, R., AVONI, P., MCWILLIAM, R. C., STEPHENSON, J. B., HANNA, M. G., KULLMANN, D. M. & SPAUSCHUS, A. 2000. Clinical, genetic, and expression studies of mutations in the potassium channel gene KCNA1 reveal new phenotypic variability. *Ann Neurol,* 48**,** 647-56.

EVERS, C., KAUFMANN, L., SEITZ, A., PARAMASIVAM, N., GRANZOW, M., KARCH, S., FISCHER, C., HINDERHOFER, K., GDYNIA, G., ELSASSER, M., PINKERT, S., SCHLESNER, M., BARTRAM, C. R. & MOOG, U. 2016. Exome sequencing reveals a novel CWF19L1 mutation associated with intellectual disability and cerebellar atrophy. *Am J Med Genet A,* 170**,** 1502-9.

EVERT, B. O., ARAUJO, J., VIEIRA-SAECKER, A. M., DE VOS, R. A., HARENDZA, S., KLOCKGETHER, T. & WULLNER, U. 2006a. Ataxin-3 represses transcription via chromatin binding, interaction with histone deacetylase 3, and histone deacetylation. *J Neurosci,* 26**,** 11474-86.

EVERT, B. O., ARAUJO, J., VIEIRA-SAECKER, A. M., DE VOS, R. A. I., HARENDZA, S., KLOCKGETHER, T. & WULLNER, U. 2006b. Ataxin-3 represses transcription via chromatin binding, interaction with histone deacetylase 3, and histone deacetylation. *Journal of Neuroscience,* 26**,** 11474-11486.

EVERT, B. O., VOGT, I. R., VIEIRA-SAECKER, A. M., OZIMEK, L., DE VOS, R. A. I., BRUNT, E. R. P., KLOCKGETHER, T. & WULLNER, U. 2003. Gene expression profiling in ataxin-3 expressing cell lines reveals distinct effects of normal and mutant ataxin-3. *Journal of Neuropathology and Experimental Neurology,* 62**,** 1006-1018.

FAN, L., MOON, J., CRODIAN, J. & COLLODI, P. 2006. Homologous recombination in zebrafish ES cells. *Transgenic Res,* 15**,** 21-30.

FANG, E. F. & BOHR, V. A. 2017. NAD(+): The convergence of DNA repair and mitophagy. *Autophagy,* 13**,** 442-443.

FANG, E. F., KASSAHUN, H., CROTEAU, D. L., SCHEIBYE-KNUDSEN, M., MAROSI, K., LU, H., SHAMANNA, R. A., KALYANASUNDARAM, S., BOLLINENI, R. C., WILSON, M. A., ISER, W. B., WOLLMAN, B. N., MOREVATI, M., LI, J., KERR, J. S., LU, Q., WALTZ, T. B., TIAN, J., SINCLAIR, D. A., MATTSON, M. P., NILSEN, H. & BOHR, V. A. 2016. NAD(+) Replenishment Improves Lifespan and Healthspan in Ataxia Telangiectasia Models via Mitophagy and DNA Repair. *Cell Metab,* 24**,** 566-581.

FENG, Y. L., XIANG, J. F., LIU, S. C., GUO, T., YAN, G. F., FENG, Y., KONG, N., LI, H. D., HUANG, Y., LIN, H., CAI, X. J. & XIE, A. Y. 2017. H2AX facilitates classical non-homologous end joining at the expense of limited nucleotide loss at repair junctions. *Nucleic Acids Research,* 45**,** 10614-10633.

FERGUSON, F. R. & CRITCHLEY, M. 1929. A CLINICAL STUDY OF AN HEREDO-FAMILIAL DISEASE RESEMBLING DISSEMINATED SCLEROSIS. *Brain,* 52**,** 203-225.

FERNANDEZ, J. 2019. *Ataxia-Telangiectasia* [Online]. MSD Manual. Available: https://www.msdmanuals.com/home/immune-disorders/immunodeficiency-disorders/ataxia-telangiectasia [Accessed 02.04.20 2020].

FERNET, M., GRIBAA, M., SALIH, M. A., SEIDAHMED, M. Z., HALL, J. & KOENIG, M. 2005. Identification and functional consequences of a novel MRE11 mutation affecting 10 Saudi Arabian patients with the ataxia telangiectasia-like disorder. *Hum Mol Genet,* 14**,** 307-18.

FERNET, M., MOULLAN, N., LAUGE, A., STOPPA-LYONNET, D. & HALL, J. 2004. Cellular responses to ionising radiation of AT heterozygotes: differences between missense and truncating mutation carriers. *Br J Cancer,* 90**,** 866-73.

FETT, M. E., PILSL, A., PAQUET, D., VAN BEBBER, F., HAASS, C., TATZELT, J., SCHMID, B. & WINKLHOFER, K. F. 2010. Parkin is protective against proteotoxic stress in a transgenic zebrafish model. *PLoS One,* 5**,** e11783.

FIEVET, A., BELLANGER, D., RIEUNIER, G., D'ENGHIEN, C. D., SOPHIE, J., CALVAS, P., CARRIERE, J. P., ANHEIM, M., CASTRIOTO, A., FLABEAU, O., DEGOS, B., EWENCZYK, C., MAHLAOUI, N., TOUZOT, F., SUAREZ, F., HULLY, M., ROUBERTIE, A., ALADJIDI, N., TISON, F., ANTOINE-POIREL, H., DAHAN, K., DOUMMAR, D., NOUGUES, M. C., IOOS, C., ROUGEOT, C., MASUREL, A., BOURJAULT, C., GINGLINGER, E., PRIEUR, F., SIRI, A., BORDIGONI, P., NGUYEN, K., PHILIPPE, N., BELLESME, C., DEMEOCQ, F., ALTUZARRA, C., MATHIEU-DRAMARD, M., COUDERC, F., DORK, T., AUGER, N., PARFAIT, B., ABIDALLAH, K., MONCOUTIER, V., COLLET, A., STOPPA-

LYONNET, D. & STERN, M. H. 2019. Functional classification of ATM variants in ataxia-telangiectasia patients. *Human Mutation,* 40**,** 1713-1730.

FIGUEROA, K. P., MINASSIAN, N. A., STEVANIN, G., WATERS, M., GARIBYAN, V., FORLANI, S., STRZELCZYK, A., BURK, K., BRICE, A., DURR, A., PAPAZIAN, D. M. & PULST, S. M. 2010. KCNC3: phenotype, mutations, channel biophysics-a study of 260 familial ataxia patients. *Hum Mutat,* 31**,** 191-6.

FIGUEROA, K. P., WATERS, M. F., GARIBYAN, V., BIRD, T. D., GOMEZ, C. M., RANUM, L. P., MINASSIAN, N. A., PAPAZIAN, D. M. & PULST, S. M. 2011. Frequency of KCNC3 DNA variants as causes of spinocerebellar ataxia 13 (SCA13). *PLoS One,* 6**,** e17811.

FIÉVET, A., BELLANGER, D., VALENCE, S., MOBUCHON, L., AFENJAR, A., GIULIANO, F., DUBOIS D'ENGHIEN, C., PARFAIT, B., PEDESPAN, J. M., AUGER, N., RIEUNIER, G., COLLET, A., BURGLEN, L., STOPPA-LYONNET, D. & STERN, M. H. 2019. Three new cases of ataxia-telangiectasia-like disorder: No impairment of the ATM pathway, but S-phase checkpoint defect. *Hum Mutat,* 40**,** 1690-1699.

FLYNN, A. & PROUD, C. G. 1996. The role of eIF4 in cell proliferation. *Cancer Surv,* 27**,** 293-310.

FORAY, N., PRIESTLEY, A., ALSBEIH, G., BADIE, C., CAPULAS, E. P., ARLETT, C. F. & MALAISE, E. P. 1997. Hypersensitivity of ataxia telangiectasia fibroblasts to ionizing radiation is associated with a repair deficiency of DNA double-strand breaks. *Int J Radiat Biol,* 72**,** 271-83.

FORCE, A., LYNCH, M., PICKETT, F. B., AMORES, A., YAN, Y. L. & POSTLETHWAIT, J. 1999. Preservation of duplicate genes by complementary, degenerative mutations. *Genetics,* 151**,** 1531-1545.

FRANCHI, A., PERUCCA-LOSTANLEN, D. & POUYSSEGUR, J. 1986. Functional expression of a human Na+/H+ antiporter gene transfected into antiporter-deficient mouse L cells. *Proc Natl Acad Sci U S A,* 83**,** 9388-92.

FRANÇA, L. R., HESS, R. A., DUFOUR, J. M., HOFMANN, M. C. & GRISWOLD, M. D. 2016. The Sertoli cell: one hundred fifty years of beauty and plasticity. *Andrology,* 4**,** 189-212.

FRANÇA, L. R., NÓBREGA, R. H., MORAIS, R. D. V. S., DE CASTRO ASSIS, L. H. & SCHULZ, R. W. 2015. 13 - Sertoli cell structure and function in anamniote vertebrates. *In:* GRISWOLD, M. D. (ed.) *Sertoli Cell Biology (Second Edition).* Oxford: Academic Press.

FUJITA, R., AGID, Y., TROUILLAS, P., SECK, A., TOMMASI-DAVENAS, C., DRIESEL, A. J., OLEK, K., GRZESCHIK, K. H., NAKAMURA, Y., MANDEL, J. L. & HANAUER, A. 1989. Confirmation of linkage of Friedreich ataxia to chromosome 9 and identification of a new closely linked marker. *Genomics,* 4**,** 110-1.

FUKUDA, M. 2003. Molecular cloning, expression, and characterization of a novel class of synaptotagmin (Syt XIV) conserved from Drosophila to humans. *J Biochem,* 133**,** 641-9.

GAMBÓN-DEZA, F., SÁNCHEZ-ESPINEL, C. & MAGADÁN-MOMPÓ, S. 2010. Presence of an unique IgT on the IGH locus in three-spined stickleback fish (Gasterosteus aculeatus) and the very recent generation of a repertoire of VH genes. *Dev Comp Immunol,* 34**,** 114-22.

GANCHER, S. T. & NUTT, J. G. 1986. Autosomal dominant episodic ataxia: a heterogeneous syndrome. *Mov Disord,* 1**,** 239-53.

GANDHI, J., ANTONELLI, A. C., AFRIDI, A., VATSIA, S., JOSHI, G., ROMANOV, V., MURRAY, I. V. J. & KHAN, S. A. 2019. Protein misfolding and aggregation in neurodegenerative diseases: a review of pathogeneses, novel detection strategies, and potential therapeutics. *Rev Neurosci,* 30**,** 339-358.

GAO, Y., CHAN, R. H., CHOW, T. W., ZHANG, L., BONILLA, S., PANG, C. P., ZHANG, M. & LEUNG, Y. F. 2014. A High-Throughput Zebrafish Screening Method for Visual Mutants by Light-Induced Locomotor Response. *IEEE/ACM Trans Comput Biol Bioinform,* 11**,** 693-701.

GAO, Y., SUN, Y., FRANK, K. M., DIKKES, P., FUJIWARA, Y., SEIDL, K. J., SEKIGUCHI, J. M., RATHBUN, G. A., SWAT, W., WANG, J., BRONSON, R. T., MALYNN, B. A., BRYANS, M., ZHU, C., CHAUDHURI, J., DAVIDSON, L., FERRINI, R., STAMATO, T., ORKIN, S. H., GREENBERG, M. E. & ALT, F. W.

1998. A critical role for DNA end-joining proteins in both lymphogenesis and neurogenesis. *Cell,* 95**,** 891-902.

GAPUD, E. J., DORSETT, Y., YIN, B., CALLEN, E., BREDEMEYER, A., MAHOWALD, G. K., OMI, K. Q., WALKER, L. M., BEDNARSKI, J. J., MCKINNON, P. J., BASSING, C. H., NUSSENZWEIG, A. & SLECKMAN, B. P. 2011. Ataxia telangiectasia mutated (Atm) and DNA-PKcs kinases have overlapping activities during chromosomal signal joint formation. *Proc Natl Acad Sci U S A,* 108**,** 2022-7.

GAPUD, E. J. & SLECKMAN, B. P. 2011. Unique and redundant functions of ATM and DNA-PKcs during V(D)J recombination. *Cell cycle (Georgetown, Tex.),* 10**,** 1928-1935.

GARCIA-MURIAS, M., QUINTANS, B., ARIAS, M., SEIXAS, A. I., CACHEIRO, P., TARRIO, R., PARDO, J., MILLAN, M. J., ARIAS-RIVAS, S., BLANCO-ARIAS, P., DAPENA, D., MOREIRA, R., RODRIGUEZ-TRELLES, F., SEQUEIROS, J., CARRACEDO, A., SILVEIRA, I. & SOBRIDO, M. J. 2012. 'Costa da Morte' ataxia is spinocerebellar ataxia 36: clinical and genetic characterization. *Brain,* 135**,** 1423-35.

GATTI, R. A., BERKEL, I., BODER, E., BRAEDT, G., CHARMLEY, P., CONCANNON, P., ERSOY, F., FOROUD, T., JASPERS, N. G., LANGE, K. & ET AL. 1988. Localization of an ataxia-telangiectasia gene to chromosome 11q22-23. *Nature,* 336**,** 577-80.

GATTI, R. A., TWARD, A. & CONCANNON, P. 1999. Cancer risk in ATM heterozygotes: a model of phenotypic and mechanistic differences between missense and truncating mutations. *Mol Genet Metab,* 68**,** 419-23.

GATTI, R. A. & VINTERS, H. V. 1985. Cerebellar pathology in ataxia-telangiectasia: the significance of basket cells. *Kroc Found Ser,* 19**,** 225-32.

GAUTIER, T., BERGES, T., TOLLERVEY, D. & HURT, E. 1997. Nucleolar KKE/D repeat proteins Nop56p and Nop58p interact with Nop1p and are required for ribosome biogenesis. *Mol Cell Biol,* 17**,** 7088-98.

GERETY, S. S. & WILKINSON, D. G. 2011. Morpholino artifacts provide pitfalls and reveal a novel role for pro-apoptotic genes in hindbrain boundary development. *Dev Biol,* 350**,** 279-89.

GHANSHANI, S., PAK, M., MCPHERSON, J. D., STRONG, M., DETHLEFS, B., WASMUTH, J. J., SALKOFF, L., GUTMAN, G. A. & CHANDY, K. G. 1992. Genomic organization, nucleotide sequence, and cellular distribution of a Shaw-related potassium channel gene, Kv3.3, and mapping of Kv3.3 and Kv3.4 to human chromosomes 19 and 1. *Genomics,* 12**,** 190-6.

GIGLIO, M., MEDICA, M., DE ROSE, A. F., GERMINALE, F., RAVETTI, J. L. & CARMIGNANI, G. 2003. Testicular sertoli cell tumours and relative sub-types. Analysis of clinical and prognostic features. *Urol Int,* 70**,** 205-10.

GILAD, S., CHESSA, L., KHOSRAVI, R., RUSSELL, P., GALANTY, Y., PIANE, M., GATTI, R. A., JORGENSEN, T. J., SHILOH, Y. & BAR-SHIRA, A. 1998. Genotype-phenotype relationships in ataxia-telangiectasia and variants. *Am J Hum Genet,* 62**,** 551-61.

GILAD, S., KHOSRAVI, R., SHKEDY, D., UZIEL, T., ZIV, Y., SAVITSKY, K., ROTMAN, G., SMITH, S., CHESSA, L., JORGENSEN, T. J., HARNIK, R., FRYDMAN, M., SANAL, O., PORTNOI, S., GOLDWICZ, Z., JASPERS, N. G. J., GATTI, R. A., LENOIR, G., LAVIN, M. F., TATSUMI, K., WEGNER, R. D., SHILOH, Y. & BAR-SHIRA, A. 1996. Predominance of Null Mutations in Ataxia-Telangiectasia. *Human Molecular Genetics,* 5**,** 433-439.

GILBERT, M. J. H., ZERULLA, T. C. & TIERNEY, K. B. 2014. Zebrafish (Danio rerio) as a model for the study of aging and exercise: Physical ability and trainability decrease with age. *Experimental Gerontology,* 50**,** 106-113.

GIOVANNETTI, A., MAZZETTA, F., CAPRINI, E., AIUTI, A., MARZIALI, M., PIERDOMINICI, M., COSSARIZZA, A., CHESSA, L., SCALA, E., QUINTI, I., RUSSO, G. & FIORILLI, M. 2002. Skewed T-cell receptor repertoire, decreased thymic output, and predominance of terminally differentiated T cells in ataxia telangiectasia. *Blood,* 100**,** 4082-9.

GLADDY, R. A., NUTTER, L. M., KUNATH, T., DANSKA, J. S. & GUIDOS, C. J. 2006. p53-Independent apoptosis disrupts early organogenesis in embryos lacking both ataxia-telangiectasia mutated and Prkdc. *Mol Cancer Res,* 4**,** 311-8.

GLASS, H. C., BOYCOTT, K. M., ADAMS, C., BARLOW, K., SCOTT, J. N., CHUDLEY, A. E., FUJIWARA, T. M., MORGAN, K., WIRRELL, E. & MCLEOD, D. R. 2005. Autosomal recessive cerebellar hypoplasia in the Hutterite population. *Dev Med Child Neurol,* 47**,** 691-5.

GLAUDEMANS, B., VAN DER WIJST, J., SCOLA, R. H., LORENZONI, P. J., HEISTER, A., VAN DER KEMP, A. W., KNOERS, N. V., HOENDEROP, J. G. & BINDELS, R. J. 2009. A missense mutation in the Kv1.1 voltage-gated potassium channel-encoding gene KCNA1 is linked to human autosomal dominant hypomagnesemia. *J Clin Invest,* 119**,** 936-42.

GOLDOWITZ, D. & HAMRE, K. 1998. The cells and molecules that make a cerebellum. *Trends Neurosci,* 21**,** 375-82.

GOMEZ, C. M., THOMPSON, R. M., GAMMACK, J. T., PERLMAN, S. L., DOBYNS, W. B., TRUWIT, C. L., ZEE, D. S., CLARK, H. B. & ANDERSON, J. H. 1997. Spinocerebellar ataxia type 6: gaze-evoked and vertical nystagmus, Purkinje cell degeneration, and variable age of onset. *Ann Neurol,* 42**,** 933-50.

GOMEZ-HERREROS, F., SCHUURS-HOEIJMAKERS, J. H., MCCORMACK, M., GREALLY, M. T., RULTEN, S., ROMERO-GRANADOS, R., COUNIHAN, T. J., CHAILA, E., CONROY, J., ENNIS, S., DELANTY, N., CORTES-LEDESMA, F., DE BROUWER, A. P., CAVALLERI, G. L., EL-KHAMISY, S. F., DE VRIES, B. B. & CALDECOTT, K. W. 2014. TDP2 protects transcription from abortive topoisomerase activity and is required for normal neural function. *Nat Genet,* 46**,** 516-21.

GONG, Y., HANDA, N., KOWALCZYKOWSKI, S. C. & DE LANGE, T. 2017. PHF11 promotes DSB resection, ATR signaling, and HR. *Genes & Development,* 31**,** 46-58.

GOODARZI, M. O., DUMESIC, D. A., CHAZENBALK, G. & AZZIZ, R. 2011. Polycystic ovary syndrome: etiology, pathogenesis and diagnosis. *Nature Reviews Endocrinology,* 7**,** 219-231.

GOOLD, R., HUBANK, M., HUNT, A., HOLTON, J., MENON, R. P., REVESZ, T., PANDOLFO, M. & MATILLA-DUENAS, A. 2007. Down-regulation of the dopamine receptor D2 in mice lacking ataxin 1. *Hum Mol Genet,* 16**,** 2122-34.

GORGOULIS, V., ADAMS, P. D., ALIMONTI, A., BENNETT, D. C., BISCHOF, O., BISHOP, C., CAMPISI, J., COLLADO, M., EVANGELOU, K., FERBEYRE, G., GIL, J., HARA, E., KRIZHANOVSKY, V., JURK, D., MAIER, A. B., NARITA, M., NIEDERNHOFER, L., PASSOS, J. F., ROBBINS, P. D., SCHMITT, C. A., SEDIVY, J., VOUGAS, K., VON ZGLINICKI, T., ZHOU, D., SERRANO, M. & DEMARIA, M. 2019. Cellular Senescence: Defining a Path Forward. *Cell,* 179**,** 813-827.

GORODETSKY, E., CALKINS, S., AHN, J. & BROOKS, P. J. 2007. ATM, the Mre11/Rad50/Nbs1 complex, and topoisomerase I are concentrated in the nucleus of Purkinje neurons in the juvenile human brain. *DNA Repair (Amst),* 6**,** 1698-707.

GOURGARI, E., SALOUSTROS, E. & STRATAKIS, C. A. 2012. Large-cell calcifying Sertoli cell tumors of the testes in pediatrics. *Current opinion in pediatrics,* 24**,** 518-522.

GRANZOTTO, A., BENADJAOUD, M. A., VOGIN, G., DEVIC, C., FERLAZZO, M. L., BODGI, L., PEREIRA, S., SONZOGNI, L., FORCHERON, F., VIAU, M., ETAIX, A., MALEK, K., MENGUE-BINDJEME, L., ESCOFFIER, C., ROUVET, I., ZABOT, M. T., JOUBERT, A., VINCENT, A., DALLA VENEZIA, N., BOURGUIGNON, M., CANAT, E. P., D'HOMBRES, A., THÉBAUD, E., ORBACH, D., STOPPA-LYONNET, D., RADJI, A., DORÉ, E., POINTREAU, Y., BOURGIER, C., LEBLOND, P., DEFACHELLES, A. S., LERVAT, C., GUEY, S., FEUVRET, L., GILSOUL, F., BERGER, C., MONCHARMONT, C., DE LAROCHE, G., MOREAU-CLAEYS, M. V., CHAVAUDRA, N., COMBEMALE, P., BISTON, M. C., MALET, C., MARTEL-LAFAY, I., LAUDE, C., HAU-DESBAT, N. H., ZIOUÉCHE, A., TANGUY, R., SUNYACH, M. P., RACADOT, S., POMMIER, P., CLAUDE, L., BALEYDIER, F., FLEURY, B., DE CREVOISIER, R., SIMON, J. M., VERRELLE, P., PEIFFERT, D., BELKACEMI, Y., BOURHIS, J., LARTIGAU, E., CARRIE, C., DE VATHAIRE, F., ESCHWEGE, F., PUISIEUX, A., LAGRANGE, J. L., BALOSSO, J. & FORAY, N. 2016. Influence of Nucleoshuttling of the ATM Protein in the

Healthy Tissues Response to Radiation Therapy: Toward a Molecular Classification of Human Radiosensitivity. *Int J Radiat Oncol Biol Phys,* 94**,** 450-60.

GRAVES, T. D., RAJAKULENDRAN, S., ZUBERI, S. M., MORRIS, H. R., SCHORGE, S., HANNA, M. G. & KULLMANN, D. M. 2010. Nongenetic factors influence severity of episodic ataxia type 1 in monozygotic twins. *Neurology,* 75**,** 367-72.

GREAVES, M. F. & WIEMELS, J. 2003. Origins of chromosome translocations in childhood leukaemia. *Nat Rev Cancer,* 3**,** 639-49.

GREENBERGER, S., BERKUN, Y., BEN-ZEEV, B., LEVI, Y. B., BARZILIAI, A. & NISSENKORN, A. 2013. Dermatologic manifestations of ataxia-telangiectasia syndrome. *J Am Acad Dermatol,* 68**,** 932-6.

GREWAL, K. K., STEFANELLI, M. G., MEIJER, I. A., HAND, C. K., ROULEAU, G. A. & IVES, E. J. 2004. A founder effect in three large Newfoundland families with a novel clinically variable spastic ataxia and supranuclear gaze palsy. *Am J Med Genet A,* 131**,** 249-54.

GREWAL, R. P., TAYAG, E., FIGUEROA, K. P., ZU, L., DURAZO, A., NUNEZ, C. & PULST, S. M. 1998. Clinical and genetic analysis of a distinct autosomal dominant spinocerebellar ataxia. *Neurology,* 51**,** 1423-6.

GRIBAA, M., SALIH, M., ANHEIM, M., LAGIER-TOURENNE, C., H'MIDA, D., DROUOT, N., MOHAMED, A., ELMALIK, S., KABIRAJ, M., AL-RAYESS, M., ALMUBARAK, M., BETARD, C., GOEBEL, H. & KOENIG, M. 2007. A new form of childhood onset, autosomal recessive spinocerebellar ataxia and epilepsy is localized at 16q21-q23. *Brain,* 130**,** 1921-8.

GROS-LOUIS, F., DUPRE, N., DION, P., FOX, M. A., LAURENT, S., VERREAULT, S., SANES, J. R., BOUCHARD, J. P. & ROULEAU, G. A. 2007. Mutations in SYNE1 lead to a newly discovered form of autosomal recessive cerebellar ataxia. *Nat Genet,* 39**,** 80-5.

GRUNSEICH, C., WANG, I. X., WATTS, J. A., BURDICK, J. T., GUBER, R. D., ZHU, Z., BRUZEL, A., LANMAN, T., CHEN, K., SCHINDLER, A. B., EDWARDS, N., RAY-CHAUDHURY, A., YAO, J., LEHKY, T., PISZCZEK, G., CRAIN, B., FISCHBECK, K. H. & CHEUNG, V. G. 2018. Senataxin Mutation Reveals How R-Loops Promote Transcription by Blocking DNA Methylation at Gene Promoters. *Mol Cell,* 69**,** 426-437.e7.

GU, X., QI, Y., FENG, Z., MA, L., GAO, K. & ZHANG, Y. 2018. Lead (Pb) induced ATM-dependent mitophagy via PINK1/Parkin pathway. *Toxicol Lett,* 291**,** 92-100.

GUEVEN, N., LUFF, J., PENG, C., HOSOKAWA, K., BOTTLE, S. E. & LAVIN, M. F. 2006. Dramatic extension of tumor latency and correction of neurobehavioral phenotype in Atm-mutant mice with a nitroxide antioxidant. *Free Radic Biol Med,* 41**,** 992-1000.

GUISSART, C., LI, X., LEHEUP, B., DROUOT, N., MONTAUT-VERIENT, B., RAFFO, E., JONVEAUX, P., ROUX, A. F., CLAUSTRES, M., FLIEGEL, L. & KOENIG, M. 2015. Mutation of SLC9A1, encoding the major Na(+)/H(+) exchanger, causes ataxia-deafness Lichtenstein-Knorr syndrome. *Hum Mol Genet,* 24**,** 463-70.

GULSUNER, S., TEKINAY, A. B., DOERSCHNER, K., BOYACI, H., BILGUVAR, K., UNAL, H., ORS, A., ONAT, O. E., ATALAR, E., BASAK, A. N., TOPALOGLU, H., KANSU, T., TAN, M., TAN, U., GUNEL, M. & OZCELIK, T. 2011. Homozygosity mapping and targeted genomic sequencing reveal the gene responsible for cerebellar hypoplasia and quadrupedal locomotion in a consanguineous kindred. *Genome Res,* 21**,** 1995-2003.

GUMY-PAUSE, F., WACKER, P. & SAPPINO, A. P. 2004. ATM gene and lymphoid malignancies. *Leukemia,* 18**,** 238-242.

GUO, Q. Q., WANG, S. S., ZHANG, S. S., XU, H. D., LI, X. M., GUAN, Y., YI, F., ZHOU, T. T., JIANG, B., BAI, N., MA, M. T., WANG, Z., FENG, Y. L., GUO, W. D., WU, X., ZHAO, G. F., FAN, G. J., ZHANG, S. P., WANG, C. G., CAO, L. Y., O'ROURKE, B. P., LIU, S. H., WANG, P. Y., HAN, S., SONG, X. Y. & CAO, L. ATM-CHK2-Beclin 1 axis promotes autophagy to maintain ROS homeostasis under oxidative stress. *Embo Journal***,** 17.

GUO, Q. Q., WANG, S. S., ZHANG, S. S., XU, H. D., LI, X. M., GUAN, Y., YI, F., ZHOU, T. T., JIANG, B., BAI, N., MA, M. T., WANG, Z., FENG, Y. L., GUO, W. D., WU, X., ZHAO, G. F., FAN, G. J., ZHANG, S. P., WANG, C. G., CAO, L. Y., O'ROURKE, B. P., LIU, S. H., WANG, P. Y., HAN, S., SONG, X. Y. & CAO, L. 2020. ATM-CHK2-Beclin 1 axis promotes autophagy to maintain ROS homeostasis under oxidative stress. *Embo j*, e103111.

GUO, Y. C., LIN, J. J., LIAO, Y. C., TSAI, P. C., LEE, Y. C. & SOONG, B. W. 2014. Spinocerebellar ataxia 35: novel mutations in TGM6 with clinical and genetic characterization. *Neurology,* 83**,** 1554-61.

GUO, Z., DESHPANDE, R. & PAULL, T. T. 2010a. ATM activation in the presence of oxidative stress. *Cell Cycle,* 9**,** 4805-11.

GUO, Z., KOZLOV, S., LAVIN, M. F., PERSON, M. D. & PAULL, T. T. 2010b. ATM activation by oxidative stress. *Science,* 330**,** 517-21.

GURLEY, K. E. & KEMP, C. J. 2001. Synthetic lethality between mutation in Atm and DNA-PK(cs) during murine embryogenesis. *Curr Biol,* 11**,** 191-4.

HAAPANIEMI, E., BOTLA, S., PERSSON, J., SCHMIERER, B. & TAIPALE, J. 2018. CRISPR–Cas9 genome editing induces a p53-mediated DNA damage response. *Nature Medicine,* 24**,** 927-930.

HAAS, M., WARD, D. C., LEE, J., ROSES, A. D., CLARKE, V., D'EUSTACHIO, P., LAU, D., VEGA-SAENZ DE MIERA, E. & RUDY, B. 1993. Localization of Shaw-related K+ channel genes on mouse and human chromosomes. *Mammalian Genome,* 4**,** 711-715.

HADIAN, K. & KRAPPMANN, D. 2011. Signals from the nucleus: activation of NF-kappaB by cytosolic ATM in the DNA damage response. *Sci Signal,* 4**,** pe2.

HADJIVASSILIOU, M., AESCHLIMANN, P., STRIGUN, A., SANDERS, D. S., WOODROOFE, N. & AESCHLIMANN, D. 2008. Autoantibodies in gluten ataxia recognize a novel neuronal transglutaminase. *Ann Neurol,* 64**,** 332-43.

HAKEM, R. 2008. DNA-damage repair; the good, the bad, and the ugly. *Embo Journal,* 27**,** 589-605.

HALABY, M. J., HIBMA, J. C., HE, J. & YANG, D. Q. 2008. ATM protein kinase mediates full activation of Akt and regulates glucose transporter 4 translocation by insulin in muscle cells. *Cell Signal,* 20**,** 1555-63.

HALLARE, A., NAGEL, K., KÖHLER, H. R. & TRIEBSKORN, R. 2006. Comparative embryotoxicity and proteotoxicity of three carrier solvents to zebrafish (Danio rerio) embryos. *Ecotoxicol Environ Saf,* 63**,** 378-88.

HALLEN, L., KLEIN, H., STOSCHEK, C., WEHRMEYER, S., NONHOFF, U., RALSER, M., WILDE, J., ROHR, C., SCHWEIGER, M. R., ZATLOUKAL, K., VINGRON, M., LEHRACH, H., KONTHUR, Z. & KROBITSCH, S. 2011. The KRAB-containing zinc-finger transcriptional regulator ZBRK1 activates SCA2 gene transcription through direct interaction with its gene product, ataxin-2. *Hum Mol Genet,* 20**,** 104-14.

HALLIWELL, B. 2006. Oxidative stress and neurodegeneration: where are we now? *J Neurochem,* 97**,** 1634-58.

HAMER, G., KAL, H. B., WESTPHAL, C. H., ASHLEY, T. & DE ROOIJ, D. G. 2004. Ataxia telangiectasia mutated expression and activation in the testis. *Biol Reprod,* 70**,** 1206-12.

HAMLING, K. R., TOBIAS, Z. J. & WEISSMAN, T. A. 2015. Mapping the development of cerebellar Purkinje cells in zebrafish. *Dev Neurobiol,* 75**,** 1174-88.

HANSEN, J. D., LANDIS, E. D. & PHILLIPS, R. B. 2005. Discovery of a unique Ig heavy-chain isotype (IgT) in rainbow trout: Implications for a distinctive B cell developmental pathway in teleost fish. *Proceedings of the National Academy of Sciences of the United States of America,* 102**,** 6919.

HARA, K., FUKUSHIMA, T., SUZUKI, T., SHIMOHATA, T., OYAKE, M., ISHIGURO, H., HIROTA, K., MIYASHITA, A., KUWANO, R., KURISAKI, H., YOMONO, H., GOTO, J., KANAZAWA, I. & TSUJI, S. 2004. Japanese SCA families with an unusual phenotype linked to a locus overlapping with SCA15 locus. *Neurology,* 62**,** 648-51.

HARA, K., SHIGA, A., NOZAKI, H., MITSUI, J., TAKAHASHI, Y., ISHIGURO, H., YOMONO, H., KURISAKI, H., GOTO, J., IKEUCHI, T., TSUJI, S., NISHIZAWA, M. & ONODERA, O. 2008. Total deletion and a missense mutation of ITPR1 in Japanese SCA15 families. *Neurology,* 71**,** 547-51.

HARDING, A. E. 1982. The clinical features and classification of the late onset autosomal dominant cerebellar ataxias. A study of 11 families, including descendants of the 'the Drew family of Walworth'. *Brain,* 105**,** 1-28.

HARTLOVA, A., ERTTMANN, S. F., RAFFI, F. A., SCHMALZ, A. M., RESCH, U., ANUGULA, S., LIENENKLAUS, S., NILSSON, L. M., KROGER, A., NILSSON, J. A., EK, T., WEISS, S. & GEKARA, N. O. 2015. DNA damage primes the type I interferon system via the cytosolic DNA sensor STING to promote anti-microbial innate immunity. *Immunity,* 42**,** 332-43.

HAWLEY, R. S. & FRIEND, S. H. 1996. Strange bedfellows in even stranger places: the role of ATM in meiotic cells, lymphocytes, tumors, and its functional links to p53. *Genes Dev,* 10**,** 2383-8.

HAYFLICK, L. & MOORHEAD, P. S. 1961. The serial cultivation of human diploid cell strains. *Experimental Cell Research,* 25**,** 585-621.

HEKMAN, K. E., YU, G. Y., BROWN, C. D., ZHU, H., DU, X., GERVIN, K., UNDLIEN, D. E., PETERSON, A., STEVANIN, G., CLARK, H. B., PULST, S. M., BIRD, T. D., WHITE, K. P. & GOMEZ, C. M. 2012. A conserved eEF2 coding variant in SCA26 leads to loss of translational fidelity and increased susceptibility to proteostatic insult. *Hum Mol Genet,* 21**,** 5472-83.

HENSHALL, T. L., TUCKER, B., LUMSDEN, A. L., NORNES, S., LARDELLI, M. T. & RICHARDS, R. I. 2009. Selective neuronal requirement for huntingtin in the developing zebrafish. *Hum Mol Genet,* 18**,** 4830-42.

HERMAN-BERT, A., STEVANIN, G., NETTER, J. C., RASCOL, O., BRASSAT, D., CALVAS, P., CAMUZAT, A., YUAN, Q., SCHALLING, M., DURR, A. & BRICE, A. 2000. Mapping of spinocerebellar ataxia 13 to chromosome 19q13.3-q13.4 in a family with autosomal dominant cerebellar ataxia and mental retardation. *Am J Hum Genet,* 67**,** 229-35.

HERNANDEZ, D., MCCONVILLE, C. M., STACEY, M., WOODS, C. G., BROWN, M. M., SHUTT, P., RYSIECKI, G. & TAYLOR, A. M. 1993. A family showing no evidence of linkage between the ataxia telangiectasia gene and chromosome 11q22-23. *J Med Genet,* 30**,** 135-40.

HERRERO-TURRION, M. J., FUKUDA, M. & MOLLINEDO, F. 2006. Cloning and genomic characterization of sytdep, a new synaptotagmin XIV-related gene. *Biochem Biophys Res Commun,* 340**,** 386-94.

HERZOG, K. H., CHONG, M. J., KAPSETAKI, M., MORGAN, J. I. & MCKINNON, P. J. 1998. Requirement for Atm in ionizing radiation-induced cell death in the developing central nervous system. *Science,* 280**,** 1089-91.

HEWITT, S. L., YIN, B., JI, Y., CHAUMEIL, J., MARSZALEK, K., TENTHOREY, J., SALVAGIOTTO, G., STEINEL, N., RAMSEY, L. B., GHYSDAEL, J., FARRAR, M. A., SLECKMAN, B. P., SCHATZ, D. G., BUSSLINGER, M., BASSING, C. H. & SKOK, J. A. 2009. RAG-1 and ATM coordinate monoallelic recombination and nuclear positioning of immunoglobulin loci. *Nat Immunol,* 10**,** 655-64.

HIEL, J. A., VAN ENGELEN, B. G., WEEMAES, C. M., BROEKS, A., VERRIPS, A., TER LAAK, H., VINGERHOETS, H. M., VAN DEN HEUVEL, L. P., LAMMENS, M., GABREELS, F. J., LAST, J. I. & TAYLOR, A. M. 2006. Distal spinal muscular atrophy as a major feature in adult-onset ataxia telangiectasia. *Neurology,* 67**,** 346-9.

HILLS, L. B., MASRI, A., KONNO, K., KAKEGAWA, W., LAM, A. T., LIM-MELIA, E., CHANDY, N., HILL, R. S., PARTLOW, J. N., AL-SAFFAR, M., NASIR, R., STOLER, J. M., BARKOVICH, A. J., WATANABE, M., YUZAKI, M. & MOCHIDA, G. H. 2013. Deletions in GRID2 lead to a recessive syndrome of cerebellar ataxia and tonic upgaze in humans. *Neurology,* 81**,** 1378-86.

HIROTA, J., ANDO, H., HAMADA, K. & MIKOSHIBA, K. 2003. Carbonic anhydrase-related protein is a novel binding protein for inositol 1,4,5-trisphosphate receptor type 1. *Biochem J,* 372**,** 435-41.

HOCHE, F., SEIDEL, K., THEIS, M., VLAHO, S., SCHUBERT, R., ZIELEN, S. & KIESLICH, M. 2012. Neurodegeneration in ataxia telangiectasia: what is new? What is evident? *Neuropediatrics,* 43**,** 119-29.

HOLDEN, L. A. & BROWN, K. H. 2018. Baseline mRNA expression differs widely between common laboratory strains of zebrafish. *Scientific Reports,* 8**,** 4780.

HOLMES, S. E., O'HEARN, E. E., MCINNIS, M. G., GORELICK-FELDMAN, D. A., KLEIDERLEIN, J. J., CALLAHAN, C., KWAK, N. G., INGERSOLL-ASHWORTH, R. G., SHERR, M., SUMNER, A. J., SHARP, A. H., ANANTH, U., SELTZER, W. K., BOSS, M. A., VIERIA-SAECKER, A. M., EPPLEN, J. T., RIESS, O., ROSS, C. A. & MARGOLIS, R. L. 1999. Expansion of a novel CAG trinucleotide repeat in the 5' region of PPP2R2B is associated with SCA12. *Nat Genet,* 23**,** 391-2.

HORIKAWA, S., TAKAI, T., TOYOSATO, M., TAKAHASHI, H., NODA, M., KAKIDANI, H., KUBO, T., HIROSE, T., INAYAMA, S., HAYASHIDA, H. & ET AL. 1983. Isolation and structural organization of the human preproenkephalin B gene. *Nature,* 306**,** 611-4.

HOULDEN, H., JOHNSON, J., GARDNER-THORPE, C., LASHLEY, T., HERNANDEZ, D., WORTH, P., SINGLETON, A. B., HILTON, D. A., HOLTON, J., REVESZ, T., DAVIS, M. B., GIUNTI, P. & WOOD, N. W. 2007. Mutations in TTBK2, encoding a kinase implicated in tau phosphorylation, segregate with spinocerebellar ataxia type 11. *Nat Genet,* 39**,** 1434-6.

HOWE, K., CLARK, M. D., TORROJA, C. F., TORRANCE, J., BERTHELOT, C., MUFFATO, M., COLLINS, J. E., HUMPHRAY, S., MCLAREN, K., MATTHEWS, L., MCLAREN, S., SEALY, I., CACCAMO, M., CHURCHER, C., SCOTT, C., BARRETT, J. C., KOCH, R., RAUCH, G. J., WHITE, S., CHOW, W., KILIAN, B., QUINTAIS, L. T., GUERRA-ASSUNCAO, J. A., ZHOU, Y., GU, Y., YEN, J., VOGEL, J. H., EYRE, T., REDMOND, S., BANERJEE, R., CHI, J., FU, B., LANGLEY, E., MAGUIRE, S. F., LAIRD, G. K., LLOYD, D., KENYON, E., DONALDSON, S., SEHRA, H., ALMEIDA-KING, J., LOVELAND, J., TREVANION, S., JONES, M., QUAIL, M., WILLEY, D., HUNT, A., BURTON, J., SIMS, S., MCLAY, K., PLUMB, B., DAVIS, J., CLEE, C., OLIVER, K., CLARK, R., RIDDLE, C., ELLIOT, D., THREADGOLD, G., HARDEN, G., WARE, D., BEGUM, S., MORTIMORE, B., KERRY, G., HEATH, P., PHILLIMORE, B., TRACEY, A., CORBY, N., DUNN, M., JOHNSON, C., WOOD, J., CLARK, S., PELAN, S., GRIFFITHS, G., SMITH, M., GLITHERO, R., HOWDEN, P., BARKER, N., LLOYD, C., STEVENS, C., HARLEY, J., HOLT, K., PANAGIOTIDIS, G., LOVELL, J., BEASLEY, H., HENDERSON, C., GORDON, D., AUGER, K., WRIGHT, D., COLLINS, J., RAISEN, C., DYER, L., LEUNG, K., ROBERTSON, L., AMBRIDGE, K., LEONGAMORNLERT, D., MCGUIRE, S., GILDERTHORP, R., GRIFFITHS, C., MANTHRAVADI, D., NICHOL, S., BARKER, G., et al. 2013. The zebrafish reference genome sequence and its relationship to the human genome. *Nature,* 496**,** 498-503.

HSIANG, Y. H., HERTZBERG, R., HECHT, S. & LIU, L. F. 1985. Camptothecin induces protein-linked DNA breaks via mammalian DNA topoisomerase I. *J Biol Chem,* 260**,** 14873-8.

HSIANG, Y. H., LIHOU, M. G. & LIU, L. F. 1989. Arrest of replication forks by drug-stabilized topoisomerase I-DNA cleavable complexes as a mechanism of cell killing by camptothecin. *Cancer Res,* 49**,** 5077-82.

HUANG, C.-Y., SHARMA, G. G., WALKER, L. M., BASSING, C. H., PANDITA, T. K. & SLECKMAN, B. P. 2007. Defects in coding joint formation in vivo in developing ATM-deficient B and T lymphocytes. *The Journal of experimental medicine,* 204**,** 1371-1381.

HUEN, M. S., GRANT, R., MANKE, I., MINN, K., YU, X., YAFFE, M. B. & CHEN, J. 2007. RNF8 transduces the DNA-damage signal via histone ubiquitylation and checkpoint protein assembly. *Cell,* 131**,** 901-14.

HUG, N., LONGMAN, D. & CÁCERES, J. F. 2016. Mechanism and regulation of the nonsense-mediated decay pathway. *Nucleic acids research,* 44**,** 1483-1495.

HUMBERT, N., MARTIEN, S., AUGERT, A., DA COSTA, M., MAUEN, S., ABBADIE, C., DE LAUNOIT, Y., GIL, J. & BERNARD, D. 2009. A genetic screen identifies topoisomerase 1 as a regulator of senescence. *Cancer Res,* 69**,** 4101-6.

HUTCHINSON, T. H., SHILLABEER, N., WINTER, M. J. & PICKFORD, D. B. 2006. Acute and chronic effects of carrier solvents in aquatic organisms: A critical review. *Aquatic Toxicology,* 76**,** 69-92.

HWANG, W. Y., FU, Y., REYON, D., MAEDER, M. L., TSAI, S. Q., SANDER, J. D., PETERSON, R. T., YEH, J. R. & JOUNG, J. K. 2013. Efficient genome editing in zebrafish using a CRISPR-Cas system. *Nat Biotechnol,* 31**,** 227-9.

HÜBNER, G. M., LARSEN, J. N., GUERRA, B., NIEFIND, K., VRECL, M. & ISSINGER, O. G. 2014. Evidence for aggregation of protein kinase CK2 in the cell: a novel strategy for studying CK2 holoenzyme interaction by BRET(2). *Mol Cell Biochem,* 397**,** 285-93.

IGOUCHEVA, O., ALEXEEV, V. & YOON, K. 2006. Differential cellular responses to exogenous DNA in mammalian cells and its effect on oligonucleotide-directed gene modification. *Gene Therapy,* 13**,** 266-275.

IHRY, R. J., WORRINGER, K. A., SALICK, M. R., FRIAS, E., HO, D., THERIAULT, K., KOMMINENI, S., CHEN, J., SONDEY, M., YE, C., RANDHAWA, R., KULKARNI, T., YANG, Z., MCALLISTER, G., RUSS, C., REECE-HOYES, J., FORRESTER, W., HOFFMAN, G. R., DOLMETSCH, R. & KAYKAS, A. 2018. p53 inhibits CRISPR–Cas9 engineering in human pluripotent stem cells. *Nature Medicine,* 24**,** 939-946.

IIIZUMI, M., ARAKAWA, H., MORI, T., ANDO, A. & NAKAMURA, Y. 2002. Isolation of a novel gene, CABC1, encoding a mitochondrial protein that is highly homologous to yeast activity of bc1 complex. *Cancer Res,* 62**,** 1246-50.

IKEDA, Y., DICK, K. A., WEATHERSPOON, M. R., GINCEL, D., ARMBRUST, K. R., DALTON, J. C., STEVANIN, G., DURR, A., ZUHLKE, C., BURK, K., CLARK, H. B., BRICE, A., ROTHSTEIN, J. D., SCHUT, L. J., DAY, J. W. & RANUM, L. P. 2006. Spectrin mutations cause spinocerebellar ataxia type 5. *Nat Genet,* 38**,** 184-90.

IKEDA, Y., SHIZUKA, M., WATANABE, M., OKAMOTO, K. & SHOJI, M. 2000. Molecular and clinical analyses of spinocerebellar ataxia type 8 in Japan. *Neurology,* 54**,** 950-5.

IMAMURA, S. & KISHI, S. 2005. Molecular cloning and functional characterization of zebrafish ATM. *The International Journal of Biochemistry & Cell Biology,* 37**,** 1105-1116.

IMSENG, S., AYLETT, C. H. & MAIER, T. 2018. Architecture and activation of phosphatidylinositol 3-kinase related kinases. *Curr Opin Struct Biol,* 49**,** 177-189.

INTERTHAL, H., POULIOT, J. J. & CHAMPOUX, J. J. 2001. The tyrosyl-DNA phosphodiesterase Tdp1 is a member of the phospholipase D superfamily. *Proc Natl Acad Sci U S A,* 98**,** 12009-14.

IOUROV, I. Y., VORSANOVA, S. G., LIEHR, T., KOLOTII, A. D. & YUROV, Y. B. 2009a. Increased chromosome instability dramatically disrupts neural genome integrity and mediates cerebellar degeneration in the ataxia-telangiectasia brain. *Hum Mol Genet,* 18**,** 2656-69.

IOUROV, I. Y., VORSANOVA, S. G., LIEHR, T. & YUROV, Y. B. 2009b. Aneuploidy in the normal, Alzheimer's disease and ataxia-telangiectasia brain: differential expression and pathological meaning. *Neurobiol Dis,* 34**,** 212-20.

ISBRANDT, D., LEICHER, T., WALDSCHUTZ, R., ZHU, X., LUHMANN, U., MICHEL, U., SAUTER, K. & PONGS, O. 2000. Gene structures and expression profiles of three human KCND (Kv4) potassium channels mediating A-type currents I(TO) and I(SA). *Genomics,* 64**,** 144-54.

ISHIDA, M., FUJIWARA, R., TOMITA, K., YOSHIDA, T., IWAI, M., YOSHIDA, K., KAGOTANI, A., KAWAUCHI, A. & OKABE, H. 2013. Sclerosing Sertoli cell tumor of the testis: a case report with review of the literature. *International journal of clinical and experimental pathology,* 6**,** 2640-2643.

ISHIKAWA, K., NAGASE, T., SUYAMA, M., MIYAJIMA, N., TANAKA, A., KOTANI, H., NOMURA, N. & OHARA, O. 1998. Prediction of the coding sequences of unidentified human genes. X. The complete sequences of 100 new cDNA clones from brain which can code for large proteins in vitro. *DNA Res,* 5**,** 169-76.

ISHIKAWA, K., TANAKA, H., SAITO, M., OHKOSHI, N., FUJITA, T., YOSHIZAWA, K., IKEUCHI, T., WATANABE, M., HAYASHI, A., TAKIYAMA, Y., NISHIZAWA, M., NAKANO, I., MATSUBAYASHI, K., MIWA, M., SHOJI, S., KANAZAWA, I., TSUJI, S. & MIZUSAWA, H. 1997. Japanese families with autosomal dominant pure cerebellar ataxia map to chromosome 19p13.1-p13.2 and are strongly associated with mild CAG expansions in the spinocerebellar ataxia type 6 gene in chromosome 19p13.1. *Am J Hum Genet,* 61**,** 336-46.

ITO, H., KAWAKAMI, H., WATE, R., MATSUMOTO, S., IMAI, T., HIRANO, A. & KUSAKA, H. 2006. Clinicopathologic investigation of a family with expanded SCA8 CTA/CTG repeats. *Neurology,* 67**,** 1479-81.

IWAKI, A., KAWANO, Y., MIURA, S., SHIBATA, H., MATSUSE, D., LI, W., FURUYA, H., OHYAGI, Y., TANIWAKI, T., KIRA, J. & FUKUMAKI, Y. 2008. Heterozygous deletion of ITPR1, but not SUMF1, in spinocerebellar ataxia type 16. *J Med Genet,* 45**,** 32-5.

IZUMI, Y., MIYAMOTO, R., MORINO, H., YOSHIZAWA, A., NISHINAKA, K., UDAKA, F., KAMEYAMA, M., MARUYAMA, H. & KAWAKAMI, H. 2013. Cerebellar ataxia with SYNE1 mutation accompanying motor neuron disease. *Neurology,* 80**,** 600-1.

JACKSON, M., SONG, W., LIU, M.-Y., JIN, L., DYKES-HOBERG, M., LIN, C.-L. G., BOWERS, W. J., FEDEROFF, H. J., STERNWEIS, P. C. & ROTHSTEIN, J. D. 2001. Modulation of the neuronal glutamate transporter EAAT4 by two interacting proteins. *Nature,* 410**,** 89-93.

JACOB, F. D., HO, E. S., MARTINEZ-OJEDA, M., DARRAS, B. T. & KHWAJA, O. S. 2013. Case of infantile onset spinocerebellar ataxia type 5. *J Child Neurol,* 28**,** 1292-5.

JACQUEMIN, V., RIEUNIER, G., JACOB, S., BELLANGER, D., D'ENGHIEN, C. D., LAUGÉ, A., STOPPA-LYONNET, D. & STERN, M. H. 2012. Underexpression and abnormal localization of ATM products in ataxia telangiectasia patients bearing ATM missense mutations. *Eur J Hum Genet,* 20**,** 305-12.

JAGANNATHAN, S., PUNT, E. L., GU, Y., ARNOULT, C., SAKKAS, D., BARRATT, C. L. & PUBLICOVER, S. J. 2002. Identification and localization of T-type voltage-operated calcium channel subunits in human male germ cells. Expression of multiple isoforms. *J Biol Chem,* 277**,** 8449-56.

JANG, E. R., CHOI, J. D., PARK, M. A., JEONG, G., CHO, H. & LEE, J. S. 2010. ATM modulates transcription in response to histone deacetylase inhibition as part of its DNA damage response. *Experimental and Molecular Medicine,* 42**,** 195-204.

JAYADEV, S. & BIRD, T. D. 2013. Hereditary ataxias: overview. *Genetics in Medicine,* 15**,** 673-683.

JAZAYERI, A., FALCK, J., LUKAS, C., BARTEK, J., SMITH, G. C., LUKAS, J. & JACKSON, S. P. 2006. ATM- and cell cycle-dependent regulation of ATR in response to DNA double-strand breaks. *Nat Cell Biol,* 8**,** 37-45.

JEGGO, P. A., GEUTING, V. & LÖBRICH, M. 2011. The role of homologous recombination in radiation-induced double-strand break repair. *Radiother Oncol,* 101**,** 7-12.

JEN, J. C., WAN, J., PALOS, T. P., HOWARD, B. D. & BALOH, R. W. 2005. Mutation in the glutamate transporter EAAT1 causes episodic ataxia, hemiplegia, and seizures. *Neurology,* 65**,** 529-34.

JEONG, I., PATEL, A. Y., ZHANG, Z., PATIL, P. B., NADELLA, S. T., NAIR, S., RALSTON, L., HOORMANN, J. K. & FISHER, J. S. 2010. Role of ataxia telangiectasia mutated in insulin signalling of muscle-derived cell lines and mouse soleus. *Acta Physiol (Oxf),* 198**,** 465-75.

JEPPESEN, D. K., BOHR, V. A. & STEVNSNER, T. 2011. DNA repair deficiency in neurodegeneration. *Progress in Neurobiology,* 94**,** 166-200.

JIANG, H., ZHU, H. P. & GOMEZ, C. M. 2010. SCA32: An autosomal dominant cerebellar ataxia with azoospermia maps to chromosome 7q32-q33. *Movement Disorders,* 25**,** S192-S192.

JIANG, N., WEINSTEIN, J. A., PENLAND, L., WHITE, R. A., FISHER, D. S. & QUAKE, S. R. 2011. Determinism and stochasticity during maturation of the zebrafish antibody repertoire. *Proceedings of the National Academy of Sciences,* 108**,** 5348.

JILANI, A., RAMOTAR, D., SLACK, C., ONG, C., YANG, X. M., SCHERER, S. W. & LASKO, D. D. 1999. Molecular cloning of the human gene, PNKP, encoding a polynucleotide kinase 3'-

phosphatase and evidence for its role in repair of DNA strand breaks caused by oxidative damage. *J Biol Chem,* 274**,** 24176-86.

JOBLING, R. K., ASSOUM, M., GAKH, O., BLASER, S., RAIMAN, J. A., MIGNOT, C., ROZE, E., DURR, A., BRICE, A., LEVY, N., PRASAD, C., PATON, T., PATERSON, A. D., ROSLIN, N. M., MARSHALL, C. R., DESVIGNES, J. P., ROECKEL-TREVISIOL, N., SCHERER, S. W., ROULEAU, G. A., MEGARBANE, A., ISAYA, G., DELAGUE, V. & YOON, G. 2015. PMPCA mutations cause abnormal mitochondrial protein processing in patients with non-progressive cerebellar ataxia. *Brain,* 138**,** 1505-17.

JOHNSON, K. J., JONES, P. J., SPURR, N., NIMMO, E., DAVIES, J., CREED, H., WEISS, M. & WILLIAMSON, R. 1988. Linkage relationships of the protein kinase C gamma gene which exclude it as a candidate for myotonic dystrophy. *Cytogenet Cell Genet,* 48**,** 13-5.

JOHNSON, R. D. & JASIN, M. 2001. Double-strand-break-induced homologous recombination in mammalian cells. *Biochem Soc Trans,* 29**,** 196-201.

JOUBERT, A., ZIMMERMAN, K. M., BENCOKOVA, Z., GASTALDO, J., CHAVAUDRA, N., FAVAUDON, V., ARLETT, C. F. & FORAY, N. 2008. DNA double-strand break repair defects in syndromes associated with acute radiation response: at least two different assays to predict intrinsic radiosensitivity? *Int J Radiat Biol,* 84**,** 107-25.

JUN, J. I. & LAU, L. F. 2010. The matricellular protein CCN1 induces fibroblast senescence and restricts fibrosis in cutaneous wound healing. *Nat Cell Biol,* 12**,** 676-85.

JUNGMICHEL, S., CLAPPERTON, J. A., LLOYD, J., HARI, F. J., SPYCHER, C., PAVIC, L., LI, J., HAIRE, L. F., BONALLI, M., LARSEN, D. H., LUKAS, C., LUKAS, J., MACMILLAN, D., NIELSEN, M. L., STUCKI, M. & SMERDON, S. J. 2012. The molecular basis of ATM-dependent dimerization of the Mdc1 DNA damage checkpoint mediator. *Nucleic Acids Res,* 40**,** 3913-28.

JØRGENSEN, A., MORTHORST, J. E., ANDERSEN, O., RASMUSSEN, L. J. & BJERREGAARD, P. 2008. Expression profiles for six zebrafish genes during gonadal sex differentiation. *Reproductive Biology and Endocrinology,* 6**,** 25.

KABASHI, E., LIN, L., TRADEWELL, M. L., DION, P. A., BERCIER, V., BOURGOUIN, P., ROCHEFORT, D., BEL HADJ, S., DURHAM, H. D., VANDE VELDE, C., ROULEAU, G. A. & DRAPEAU, P. 2010. Gain and loss of function of ALS-related mutations of TARDBP (TDP-43) cause motor deficits in vivo. *Hum Mol Genet,* 19**,** 671-83.

KAIS, B., SCHNEIDER, K. E., KEITER, S., HENN, K., ACKERMANN, C. & BRAUNBECK, T. 2013a. DMSO modifies the permeability of the zebrafish (Danio rerio) chorion-Implications for the fish embryo test (FET). *Aquatic Toxicology,* 140-141**,** 229-238.

KAIS, B., SCHNEIDER, K. E., KEITER, S., HENN, K., ACKERMANN, C. & BRAUNBECK, T. 2013b. DMSO modifies the permeability of the zebrafish (Danio rerio) chorion-implications for the fish embryo test (FET). *Aquat Toxicol,* 140-141**,** 229-38.

KAMSLER, A., DAILY, D., HOCHMAN, A., STERN, N., SHILOH, Y., ROTMAN, G. & BARZILAI, A. 2001. Increased oxidative stress in ataxia telangiectasia evidenced by alterations in redox state of brains from Atm-deficient mice. *Cancer Res,* 61**,** 1849-54.

KANEDA, Y., HAYES, H., UCHIDA, T., YOSHIDA, M. C. & OKADA, Y. 1987. Regional assignment of five genes on human chromosome 19. *Chromosoma,* 95**,** 8-12.

KARLSSON, H. K., ZIERATH, J. R., KANE, S., KROOK, A., LIENHARD, G. E. & WALLBERG-HENRIKSSON, H. 2005. Insulin-stimulated phosphorylation of the Akt substrate AS160 is impaired in skeletal muscle of type 2 diabetic subjects. *Diabetes,* 54**,** 1692-7.

KATO, K. 1990. Sequence of a novel carbonic anhydrase-related polypeptide and its exclusive presence in Purkinje cells. *FEBS Lett,* 271**,** 137-40.

KATO, M., YANO, K., MOROTOMI-YANO, K., SAITO, H. & MIKI, Y. 2002. Identification and characterization of the human protein kinase-like gene NTKL: mitosis-specific centrosomal localization of an alternatively spliced isoform. *Genomics,* 79**,** 760-7.

KATYAL, S., LEE, Y., NITISS, K. C., DOWNING, S. M., LI, Y., SHIMADA, M., ZHAO, J., RUSSELL, H. R., PETRINI, J. H., NITISS, J. L. & MCKINNON, P. J. 2014. Aberrant topoisomerase-1 DNA lesions are pathogenic in neurodegenerative genome instability syndromes. *Nat Neurosci,* 17**,** 813-21.

KAWAHARA, G. & HAYASHI, Y. K. 2016. Characterization of Zebrafish Models of Marinesco-Sjogren Syndrome. *Plos One,* 11**,** 12.

KAWALE, A. S. & POVIRK, L. F. 2018. Tyrosyl-DNA phosphodiesterases: rescuing the genome from the risks of relaxation. *Nucleic Acids Res,* 46**,** 520-537.

KAWARAI, T., TAJIMA, A., KURODA, Y., SAJI, N., ORLACCHIO, A., TERASAWA, H., SHIMIZU, H., KITA, Y., IZUMI, Y., MITSUI, T., IMOTO, I. & KAJI, R. 2016. A homozygous mutation of VWA3B causes cerebellar ataxia with intellectual disability. *J Neurol Neurosurg Psychiatry,* 87**,** 656-62.

KAYMAZ, N. E., KÜPELI, S., YALÇIN, B. & BÜYÜKPAMUKÇU, M. 2009. Hemorrhagic cystitis in a child with Hodgkin lymphoma and ataxia-telangiectasia after cyclophosphamide. *Pediatr Blood Cancer,* 53**,** 516.

KEENEY, S., LANGE, J. & MOHIBULLAH, N. 2014. Self-organization of meiotic recombination initiation: general principles and molecular pathways. *Annu Rev Genet,* 48**,** 187-214.

KETTLEBOROUGH, R. N., BUSCH-NENTWICH, E. M., HARVEY, S. A., DOOLEY, C. M., DE BRUIJN, E., VAN EEDEN, F., SEALY, I., WHITE, R. J., HERD, C., NIJMAN, I. J., FENYES, F., MEHROKE, S., SCAHILL, C., GIBBONS, R., WALI, N., CARRUTHERS, S., HALL, A., YEN, J., CUPPEN, E. & STEMPLE, D. L. 2013. A systematic genome-wide analysis of zebrafish protein-coding gene function. *Nature,* 496**,** 494-7.

KHAYAT, Z. A., TONG, P., YAWORSKY, K., BLOCH, R. J. & KLIP, A. 2000. Insulin-induced actin filament remodeling colocalizes actin with phosphatidylinositol 3-kinase and GLUT4 in L6 myotubes. *J Cell Sci,* 113 Pt 2**,** 279-90.

KIM, H., SAKA, B., KNIGHT, S., BORGES, M., CHILDS, E., KLEIN, A., WOLFGANG, C., HERMAN, J., ADSAY, V. N., HRUBAN, R. H. & GOGGINS, M. 2014a. Having pancreatic cancer with tumoral loss of ATM and normal TP53 protein expression is associated with a poorer prognosis. *Clinical cancer research : an official journal of the American Association for Cancer Research,* 20**,** 1865-1872.

KIM, H., SONG, K. D., KIM, H. J., PARK, W., KIM, J., LEE, T., SHIN, D. H., KWAK, W., KWON, Y. J., SUNG, S., MOON, S., LEE, K. T., KIM, N., HONG, J. K., EO, K. Y., SEO, K. S., KIM, G., PARK, S., YUN, C. H., CHOI, K., LEE, W. K., KIM, D. K., OH, J. D., KIM, E. S., CH, S., LEE, H. K. & KIM, T. H. 2015. Exploring the Genetic Signature of Body Size in Yucatan Miniature Pig. *Plos One,* 10**,** 16.

KIM, H. S., KIM, M. A., HODGSON, D., HARBRON, C., WELLINGS, R., O'CONNOR, M. J., WOMACK, C., YIN, X., BANG, Y. J., IM, S. A., LEE, B. L. & KIM, W. H. 2013. Concordance of ATM (ataxia telangiectasia mutated) immunohistochemistry between biopsy or metastatic tumor samples and primary tumors in gastric cancer patients. *Pathobiology,* 80**,** 127-37.

KIM, J., KUNDU, M., VIOLLET, B. & GUAN, K. L. 2011. AMPK and mTOR regulate autophagy through direct phosphorylation of Ulk1. *Nat Cell Biol,* 13**,** 132-41.

KIM, J. W., IM, S. A., KIM, M. A., CHO, H. J., LEE, D. W., LEE, K. H., KIM, T. Y., HAN, S. W., OH, D. Y., LEE, H. J., YANG, H. K., KIM, W. H. & BANG, Y. J. 2014b. Ataxia-telangiectasia-mutated protein expression with microsatellite instability in gastric cancer as prognostic marker. *Int J Cancer,* 134**,** 72-80.

KIM, S. T., LIM, D. S., CANMAN, C. E. & KASTAN, M. B. 1999. Substrate specificities and identification of putative substrates of ATM kinase family members. *J Biol Chem,* 274**,** 37538-43.

KIM, S. T., XU, B. & KASTAN, M. B. 2002. Involvement of the cohesin protein, Smc1, in Atm-dependent and independent responses to DNA damage. *Genes Dev,* 16**,** 560-70.

KIM, T. S., KAWAGUCHI, M., SUZUKI, M., JUNG, C. G., ASAI, K., SHIBAMOTO, Y., LAVIN, M. F., KHANNA, K. K. & MIURA, Y. 2010. The ZFHX3 (ATBF1) transcription factor induces PDGFRB, which activates ATM in the cytoplasm to protect cerebellar neurons from oxidative stress. *Dis Model Mech,* 3**,** 752-62.

KIMMEL, C. B., BALLARD, W. W., KIMMEL, S. R., ULLMANN, B. & SCHILLING, T. F. 1995. Stages of embryonic development of the zebrafish. *Dev Dyn,* 203**,** 253-310.

KIRSCH, I. R., MORTON, C. C., NAKAHARA, K. & LEDER, P. 1982. Human immunoglobulin heavy chain genes map to a region of translocations in malignant B lymphocytes. *Science,* 216**,** 301-3.

KIRSCHNER, M. A., ARRIZA, J. L., COPELAND, N. G., GILBERT, D. J., JENKINS, N. A., MAGENIS, E. & AMARA, S. G. 1994. The mouse and human excitatory amino acid transporter gene (EAAT1) maps to mouse chromosome 15 and a region of syntenic homology on human chromosome 5. *Genomics,* 22**,** 631-3.

KISHI, S. & LU, K. P. 2002. A critical role for Pin2/TRF1 in ATM-dependent regulation. Inhibition of Pin2/TRF1 function complements telomere shortening, radiosensitivity, and the G(2)/M checkpoint defect of ataxia-telangiectasia cells. *J Biol Chem,* 277**,** 7420-9.

KIZIL, C., KASLIN, J., KROEHNE, V. & BRAND, M. 2012. Adult neurogenesis and brain regeneration in zebrafish. *Dev Neurobiol,* 72**,** 429-61.

KLEIN, C., WENNING, G. K., QUINN, N. P. & MARSDEN, C. D. 1996. Ataxia without telangiectasia masquerading as benign hereditary chorea. *Mov Disord,* 11**,** 217-20.

KNIGHT, M. A., GARDNER, R. J., BAHLO, M., MATSUURA, T., DIXON, J. A., FORREST, S. M. & STOREY, E. 2004. Dominantly inherited ataxia and dysphonia with dentate calcification: spinocerebellar ataxia type 20. *Brain,* 127**,** 1172-81.

KNIGHT, M. A., HERNANDEZ, D., DIEDE, S. J., DAUWERSE, H. G., RAFFERTY, I., VAN DE LEEMPUT, J., FORREST, S. M., GARDNER, R. J., STOREY, E., VAN OMMEN, G. J., TAPSCOTT, S. J., FISCHBECK, K. H. & SINGLETON, A. B. 2008. A duplication at chromosome 11q12.2-11q12.3 is associated with spinocerebellar ataxia type 20. *Hum Mol Genet,* 17**,** 3847-53.

KNIGHT, M. A., KENNERSON, M. L., ANNEY, R. J., MATSUURA, T., NICHOLSON, G. A., SALIMI-TARI, P., GARDNER, R. J., STOREY, E. & FORREST, S. M. 2003. Spinocerebellar ataxia type 15 (sca15) maps to 3p24.2-3pter: exclusion of the ITPR1 gene, the human orthologue of an ataxic mouse mutant. *Neurobiol Dis,* 13**,** 147-57.

KOBAYASHI, H., ABE, K., MATSUURA, T., IKEDA, Y., HITOMI, T., AKECHI, Y., HABU, T., LIU, W., OKUDA, H. & KOIZUMI, A. 2011. Expansion of intronic GGCCTG hexanucleotide repeat in NOP56 causes SCA36, a type of spinocerebellar ataxia accompanied by motor neuron involvement. *Am J Hum Genet,* 89**,** 121-30.

KOBAYASHI, J., TAUCHI, H., CHEN, B., BRUMA, S., TASHIRO, S., MATSUURA, S., TANIMOTO, K., CHEN, D. J. & KOMATSU, K. 2009. Histone H2AX participates the DNA damage-induced ATM activation through interaction with NBS1. *Biochemical and Biophysical Research Communications,* 380**,** 752-757.

KOBAYASHI, M., TANI-MATSUHANA, S., OHKAWA, Y., SAKAMOTO, H. & INOUE, K. 2017. DND protein functions as a translation repressor during zebrafish embryogenesis. *Biochemical and Biophysical Research Communications,* 484**,** 235-240.

KOCHER, S. & DAHM-DAPHI, J. 2010. HOMOLOGOUS RECOMBINATION IS DIFFERENTIALLY AFFECTED BY ATM AND ARTEMIS. *Radiotherapy and Oncology,* 96**,** S50-S50.

KOIDE, R., KOBAYASHI, S., SHIMOHATA, T., IKEUCHI, T., MARUYAMA, M., SAITO, M., YAMADA, M., TAKAHASHI, H. & TSUJI, S. 1999. A neurological disease caused by an expanded CAG trinucleotide repeat in the TATA-binding protein gene: a new polyglutamine disease? *Hum Mol Genet,* 8**,** 2047-53.

KOJIS, T. L., GATTI, R. A. & SPARKES, R. S. 1991. The cytogenetics of ataxia telangiectasia. *Cancer Genet Cytogenet,* 56**,** 143-56.

KOJIS, T. L., SCHRECK, R. R., GATTI, R. A. & SPARKES, R. S. 1989. Tissue specificity of chromosomal rearrangements in ataxia-telangiectasia. *Human Genetics,* 83**,** 347-352.

KOK, F. O., SHIN, M., NI, C. W., GUPTA, A., GROSSE, A. S., VAN IMPEL, A., KIRCHMAIER, B. C., PETERSON-MADURO, J., KOURKOULIS, G., MALE, I., DESANTIS, D. F., SHEPPARD-TINDELL, S., EBARASI, L., BETSHOLTZ, C., SCHULTE-MERKER, S., WOLFE, S. A. & LAWSON, N. D. 2015. Reverse genetic screening reveals poor correlation between morpholino-induced and mutant phenotypes in zebrafish. *Developmental cell,* 32**,** 97-108.

KOKEL, D. & PETERSON, R. T. 2008. Chemobehavioural phenomics and behaviour-based psychiatric drug discovery in the zebrafish. *Brief Funct Genomic Proteomic,* 7**,** 483-90.

KOLAS, N. K., CHAPMAN, J. R., NAKADA, S., YLANKO, J., CHAHWAN, R., SWEENEY, F. D., PANIER, S., MENDEZ, M., WILDENHAIN, J., THOMSON, T. M., PELLETIER, L., JACKSON, S. P. & DUROCHER, D. 2007. Orchestration of the DNA-damage response by the RNF8 ubiquitin ligase. *Science,* 318**,** 1637-40.

KOLB, A.-L., GUNN, A. R. & LAKIN, N. D. 2017. Redundancy between nucleases required for homologous recombination promotes PARP inhibitor resistance in the eukaryotic model organism Dictyostelium. *Nucleic Acids Research,* 45**,** 10056-10067.

KOMATSU, M., CHIBA, T., TATSUMI, K., IEMURA, S., TANIDA, I., OKAZAKI, N., UENO, T., KOMINAMI, E., NATSUME, T. & TANAKA, K. 2004. A novel protein-conjugating system for Ufm1, a ubiquitin-fold modifier. *Embo j,* 23**,** 1977-86.

KONG, W., PO, S., YAMAGISHI, T., ASHEN, M. D., STETTEN, G. & TOMASELLI, G. F. 1998. Isolation and characterization of the human gene encoding Ito: further diversity by alternative mRNA splicing. *Am J Physiol,* 275**,** H1963-70.

KOOB, M. D., MOSELEY, M. L., SCHUT, L. J., BENZOW, K. A., BIRD, T. D., DAY, J. W. & RANUM, L. P. 1999. An untranslated CTG expansion causes a novel form of spinocerebellar ataxia (SCA8). *Nat Genet,* 21**,** 379-84.

KOPP, B., KHOURY, L. & AUDEBERT, M. 2019. Validation of the γH2AX biomarker for genotoxicity assessment: a review. *Archives of Toxicology,* 93**,** 2103-2114.

KOPPEN, M., METODIEV, M. D., CASARI, G., RUGARLI, E. I. & LANGER, T. 2007. Variable and tissue-specific subunit composition of mitochondrial m-AAA protease complexes linked to hereditary spastic paraplegia. *Mol Cell Biol,* 27**,** 758-67.

KORDASIEWICZ, H. B., THOMPSON, R. M., CLARK, H. B. & GOMEZ, C. M. 2006. C-termini of P/Q-type Ca2+ channel alpha1A subunits translocate to nuclei and promote polyglutamine-mediated toxicity. *Hum Mol Genet,* 15**,** 1587-99.

KOSTER, D. A., CROQUETTE, V., DEKKER, C., SHUMAN, S. & DEKKER, N. H. 2005. Friction and torque govern the relaxation of DNA supercoils by eukaryotic topoisomerase IB. *Nature,* 434**,** 671-4.

KOZLOV, S., GUEVEN, N., KEATING, K., RAMSAY, J. & LAVIN, M. F. 2003. ATP activates ataxia-telangiectasia mutated (ATM) in vitro - Importance of autophosphorylation. *Journal of Biological Chemistry,* 278**,** 9309-9317.

KOZLOV, S. V., GRAHAM, M. E., JAKOB, B., TOBIAS, F., KIJAS, A. W., TANUJI, M., CHEN, P., ROBINSON, P. J., TAUCHER-SCHOLZ, G., SUZUKI, K., SO, S., CHEN, D. & LAVIN, M. F. 2011. Autophosphorylation and ATM activation: additional sites add to the complexity. *J Biol Chem,* 286**,** 9107-19.

KOZLOV, S. V., GRAHAM, M. E., PENG, C., CHEN, P., ROBINSON, P. J. & LAVIN, M. F. 2006. Involvement of novel autophosphorylation sites in ATM activation. *Embo Journal,* 25**,** 3504-3514.

KOZLOV, S. V., WAARDENBERG, A. J., ENGHOLM-KELLER, K., ARTHUR, J. W., GRAHAM, M. E. & LAVIN, M. 2016. Reactive Oxygen Species (ROS)-Activated ATM-Dependent Phosphorylation of Cytoplasmic Substrates Identified by Large-Scale Phosphoproteomics Screen. *Mol Cell Proteomics,* 15**,** 1032-47.

KRACKER, S. & DURANDY, A. 2011. Insights into the B cell specific process of immunoglobulin class switch recombination. *Immunol Lett,* 138**,** 97-103.

KRALOVICOVA, J., KNUT, M., CROSS, N. C. P. & VORECHOVSKY, I. 2016. Exon-centric regulation of ATM expression is population-dependent and amenable to antisense modification by pseudoexon targeting. *Scientific Reports,* 6**,** 18741.

KUBOTA, S., ISHIBASHI, K., YUKI, R. & YAMAGUCHI, N. 2014. Cell-cycle arrest at the G1-S phase boundary through mimosine-induced ATM activation. *Febs Journal,* 281**,** 67-67.

KUHM, C., GALLENMÜLLER, C., DÖRK, T., MENZEL, M., BISKUP, S. & KLOPSTOCK, T. 2015. Novel ATM mutation in a German patient presenting as generalized dystonia without classical signs of ataxia-telangiectasia. *J Neurol,* 262**,** 768-70.

KUK, M. U., KIM, J. W., LEE, Y. S., CHO, K. A., PARK, J. T. & PARK, S. C. 2019. Alleviation of Senescence via ATM Inhibition in Accelerated Aging Models. *Molecules and Cells,* 42**,** 210-217.

KULINSKI, J. M., LEONARDO, S. M., MOUNCE, B. C., MALHERBE, L., GAULD, S. B. & TARAKANOVA, V. L. 2012. Ataxia telangiectasia mutated kinase controls chronic gammaherpesvirus infection. *J Virol,* 86**,** 12826-37.

KULJIS, R. O., XU, Y., AGUILA, M. C. & BALTIMORE, D. 1997. Degeneration of neurons, synapses, and neuropil and glial activation in a murine Atm knockout model of ataxia-telangiectasia. *Proc Natl Acad Sci U S A,* 94**,** 12688-93.

KUMAR, V., ALT, F. W. & OKSENYCH, V. 2014. Functional overlaps between XLF and the ATM-dependent DNA double strand break response. *DNA repair,* 16**,** 11-22.

KUMARAN, M. & FAZRY, S. 2018. The effect of MRN complex and ATM kinase inhibitors on Zebrafish embryonic development. *AIP Conference Proceedings,* 1940**,** 020074.

KUWANO, A., MORIMOTO, Y., NAGAI, T., FUKUSHIMA, Y., OHASHI, H., HASEGAWA, T. & KONDO, I. 1996. Precise chromosomal locations of the genes for dentatorubral-pallidoluysian atrophy (DRPLA), von Willebrand factor (F8vWF) and parathyroid hormone-like hormone (PTHLH) in human chromosome 12p by deletion mapping. *Hum Genet,* 97**,** 95-8.

KWAST, O. & IGNATOWICZ, R. 1990. Progressive peripheral neuron degeneration in ataxia-telangiectasia: an electrophysiological study in children. *Dev Med Child Neurol,* 32**,** 800-7.

LAGIER-TOURENNE, C., TRANEBAERG, L., CHAIGNE, D., GRIBAA, M., DOLLFUS, H., SILVESTRI, G., BETARD, C., WARTER, J. M. & KOENIG, M. 2003. Homozygosity mapping of Marinesco-Sjogren syndrome to 5q31. *Eur J Hum Genet,* 11**,** 770-8.

LALOUETTE, A., GUENET, J. L. & VRIZ, S. 1998. Hotfoot mouse mutations affect the delta 2 glutamate receptor gene and are allelic to lurcher. *Genomics,* 50**,** 9-13.

LAM, A. F., KROGH, B. O. & SYMINGTON, L. S. 2008. Unique and overlapping functions of the Exo1, Mre11 and Pso2 nucleases in DNA repair. *DNA Repair,* 7**,** 655-662.

LAMBERT, C. J., FRESHNER, B. C., CHUNG, A., STEVENSON, T. J., BOWLES, D. M., SAMUEL, R., GALE, B. K. & BONKOWSKY, J. L. 2018. An automated system for rapid cellular extraction from live zebrafish embryos and larvae: Development and application to genotyping. *PLoS One,* 13**,** e0193180.

LANGE, J., PAN, J., COLE, F., THELEN, M. P., JASIN, M. & KEENEY, S. 2011. ATM controls meiotic double-strand-break formation. *Nature,* 479**,** 237-40.

LAPKOUSKI, M. & HALLBERG, B. M. 2015. Structure of mitochondrial poly(A) RNA polymerase reveals the structural basis for dimerization, ATP selectivity and the SPAX4 disease phenotype. *Nucleic Acids Research,* 43**,** 9065-9075.

LAPOSA, R. R., HENDERSON, J. T., XU, E. & WELLS, P. G. 2004. Atm-null mice exhibit enhanced radiation-induced birth defects and a hybrid form of embryonic programmed cell death indicating a teratological suppressor function for ATM. *Faseb j,* 18**,** 896-8.

LAU, W. C., LI, Y., LIU, Z., GAO, Y., ZHANG, Q. & HUEN, M. S. 2016. Structure of the human dimeric ATM kinase. *Cell Cycle,* 15**,** 1117-24.

LAVIN, M. F. & SHILOH, Y. 1997. The genetic defect in ataxia-telangiectasia. *Annu Rev Immunol,* 15**,** 177-202.

LAWRENCE, C., EBERSOLE, J. P. & KESSELI, R. V. 2008. Rapid growth and out-crossing promote female development in zebrafish (Danio rerio). *Environmental Biology of Fishes,* 81**,** 239-246.

LE BER, I., BOUSLAM, N., RIVAUD-PÉCHOUX, S., GUIMARÃES, J., BENOMAR, A., CHAMAYOU, C., GOIZET, C., MOREIRA, M. C., KLUR, S., YAHYAOUI, M., AGID, Y., KOENIG, M., STEVANIN, G., BRICE, A. & DÜRR, A. 2004. Frequency and phenotypic spectrum of ataxia with oculomotor apraxia 2: a clinical and genetic study in 18 patients. *Brain,* 127**,** 759-67.

LE HIR, H., GATFIELD, D., IZAURRALDE, E. & MOORE, M. J. 2001. The exon-exon junction complex provides a binding platform for factors involved in mRNA export and nonsense-mediated mRNA decay. *The EMBO journal,* 20**,** 4987-4997.

LEAL, M. C., CARDOSO, E. R., NÓBREGA, R. H., BATLOUNI, S. R., BOGERD, J., FRANÇA, L. R. & SCHULZ, R. W. 2009. Histological and stereological evaluation of zebrafish (Danio rerio) spermatogenesis with an emphasis on spermatogonial generations. *Biol Reprod,* 81**,** 177-87.

LEDESMA, F. C., EL KHAMISY, S. F., ZUMA, M. C., OSBORN, K. & CALDECOTT, K. W. 2009. A human 5[prime]-tyrosyl DNA phosphodiesterase that repairs topoisomerase-mediated DNA damage. *Nature,* 461**,** 674-678.

LEE, B. S., GAPUD, E. J., ZHANG, S., DORSETT, Y., BREDEMEYER, A., GEORGE, R., CALLEN, E., DANIEL, J. A., OSIPOVICH, O., OLTZ, E. M., BASSING, C. H., NUSSENZWEIG, A., LEES-MILLER, S., HAMMEL, M., CHEN, B. P. & SLECKMAN, B. P. 2013. Functional intersection of ATM and DNA-dependent protein kinase catalytic subunit in coding end joining during V(D)J recombination. *Mol Cell Biol,* 33**,** 3568-79.

LEE, J. H., MAND, M. R., KAO, C. H., ZHOU, Y., RYU, S. W., RICHARDS, A. L., COON, J. J. & PAULL, T. T. 2018. ATM directs DNA damage responses and proteostasis via genetically separable pathways. *Sci Signal,* 11.

LEE, J. H. & PAULL, T. T. 2004. Direct activation of the ATM protein kinase by the Mre11/Rad50/Nbs1 complex. *Science,* 304**,** 93-96.

LEE, J. H. & PAULL, T. T. 2005. ATM activation by DNA double-strand breaks through the Mre11-Rad50-Nbs1 complex. *Science,* 308**,** 551-4.

LEE, Y., CHONG, M. J. & MCKINNON, P. J. 2001. Ataxia telangiectasia mutated-dependent apoptosis after genotoxic stress in the developing nervous system is determined by cellular differentiation status. *J Neurosci,* 21**,** 6687-93.

LEE, Y. C., DURR, A., MAJCZENKO, K., HUANG, Y. H., LIU, Y. C., LIEN, C. C., TSAI, P. C., ICHIKAWA, Y., GOTO, J., MONIN, M. L., LI, J. Z., CHUNG, M. Y., MUNDWILLER, E., SHAKKOTTAI, V., LIU, T. T., TESSON, C., LU, Y. C., BRICE, A., TSUJI, S., BURMEISTER, M., STEVANIN, G. & SOONG, B. W. 2012. Mutations in KCND3 cause spinocerebellar ataxia type 22. *Ann Neurol,* 72**,** 859-69.

LEMPIÄINEN, H. & HALAZONETIS, T. D. 2009. Emerging common themes in regulation of PIKKs and PI3Ks. *The EMBO Journal,* 28**,** 3067.

LERIS, I., SFAKIANAKIS, D. G. & KENTOURI, M. 2013. Are zebrafish Danio rerio males better swimmers than females? *J Fish Biol,* 83**,** 1381-6.

LEWIS, R. F. & CRAWFORD, T. O. 1998. Ocular motor abnormalities in ataxia telangiectasia. *Neurology,* 50**,** A10-A10.

LI, A. & SWIFT, M. 2000. Mutations at the ataxia-telangiectasia locus and clinical phenotypes of A–T patients. *American Journal of Medical Genetics,* 92**,** 170-177.

LI, L., SAEGUSA, H. & TANABE, T. 2009. Deficit of heat shock transcription factor 1-heat shock 70 kDa protein 1A axis determines the cell death vulnerability in a model of spinocerebellar ataxia type 6. *Genes Cells,* 14**,** 1253-69.

LI, M., ISHIKAWA, K., TORU, S., TOMIMITSU, H., TAKASHIMA, M., GOTO, J., TAKIYAMA, Y., SASAKI, H., IMOTO, I., INAZAWA, J., TODA, T., KANAZAWA, I. & MIZUSAWA, H. 2003. Physical map and haplotype analysis of 16q-linked autosomal dominant cerebellar ataxia (ADCA) type III in Japan. *J Hum Genet,* 48**,** 111-8.

LI, M., PANG, S. Y., SONG, Y., KUNG, M. H., HO, S. L. & SHAM, P. C. 2013. Whole exome sequencing identifies a novel mutation in the transglutaminase 6 gene for spinocerebellar ataxia in a Chinese family. *Clin Genet,* 83**,** 269-73.

LI, Z., KIM, J. H., KIM, J., LYU, J. I., ZHANG, Y., GUO, H., NAM, H. G. & WOO, H. R. 2020. ATM suppresses leaf senescence triggered by DNA double-strand break through epigenetic control of senescence-associated genes in Arabidopsis. *New Phytologist,* 227**,** 473-484.

LIAO, M. J. & VAN DYKE, T. 1999. Critical role for Atm in suppressing V(D)J recombination-driven thymic lymphoma. *Genes & Development,* 13**,** 1246-1250.

LIEW, W. C. & ORBÁN, L. 2014. Zebrafish sex: a complicated affair. *Brief Funct Genomics,* 13**,** 172-87.

LIM, D. S., KIRSCH, D. G., CANMAN, C. E., AHN, J. H., ZIV, Y., NEWMAN, L. S., DARNELL, R. B., SHILOH, Y. & KASTAN, M. B. 1998. ATM binds to beta-adaptin in cytoplasmic vesicles. *Proc Natl Acad Sci U S A,* 95**,** 10146-51.

LIM, J., CRESPO-BARRETO, J., JAFAR-NEJAD, P., BOWMAN, A. B., RICHMAN, R., HILL, D. E., ORR, H. T. & ZOGHBI, H. Y. 2008. Opposing effects of polyglutamine expansion on native protein complexes contribute to SCA1. *Nature,* 452**,** 713-8.

LIN, C. H., CHEN, C. M., HOU, Y. T., WU, Y. R., HSIEH-LI, H. M., SU, M. T. & LEE-CHEN, G. J. 2010. The CAG repeat in SCA12 functions as a cis element to up-regulate PPP2R2B expression. *Hum Genet,* 128**,** 205-12.

LIN, C. P., BAN, Y., LYU, Y. L., DESAI, S. D. & LIU, L. F. 2008. A ubiquitin-proteasome pathway for the repair of topoisomerase I-DNA covalent complexes. *J Biol Chem,* 283**,** 21074-83.

LIN, H., HA, K., LU, G., FANG, X., CHENG, R., ZUO, Q. & ZHANG, P. 2015. Cdc14A and Cdc14B Redundantly Regulate DNA Double-Strand Break Repair. *Molecular and Cellular Biology,* 35**,** 3657.

LIN, M. T. & BEAL, M. F. 2006. Mitochondrial dysfunction and oxidative stress in neurodegenerative diseases. *Nature,* 443**,** 787-95.

LIN, Q., MEI, J., LI, Z., ZHANG, X., ZHOU, L. & GUI, J. F. 2017. Distinct and Cooperative Roles of amh and dmrt1 in Self-Renewal and Differentiation of Male Germ Cells in Zebrafish. *Genetics,* 207**,** 1007-1022.

LIN, S., GAIANO, N., CULP, P., BURNS, J. C., FRIEDMANN, T., YEE, J. K. & HOPKINS, N. 1994. Integration and germ-line transmission of a pseudotyped retroviral vector in zebrafish. *Science,* 265**,** 666-9.

LIN, Y., CAI, X., WANG, G., OUYANG, G. & CAO, H. 2018. Model construction of Niemann-Pick type C disease in zebrafish. *Biol Chem,* 399**,** 903-910.

LINDBLAD, K., SAVONTAUS, M. L., STEVANIN, G., HOLMBERG, M., DIGRE, K., ZANDER, C., EHRSSON, H., DAVID, G., BENOMAR, A., NIKOSKELAINEN, E., TROTTIER, Y., HOLMGREN, G., PTACEK, L. J., ANTTINEN, A., BRICE, A. & SCHALLING, M. 1996. An expanded CAG repeat sequence in spinocerebellar ataxia type 7. *Genome Res,* 6**,** 965-71.

LINDEBOOM, R. G. H., SUPEK, F. & LEHNER, B. 2016. The rules and impact of nonsense-mediated mRNA decay in human cancers. *Nature Genetics,* 48**,** 1112-1118.

LINDENBERG, K. S., YVERT, G., MULLER, K. & LANDWEHRMEYER, G. B. 2000. Expression analysis of ataxin-7 mRNA and protein in human brain: evidence for a widespread distribution and focal protein accumulation. *Brain Pathol,* 10**,** 385-94.

LISE, S., CLARKSON, Y., PERKINS, E., KWASNIEWSKA, A., SADIGHI AKHA, E., SCHNEKENBERG, R. P., SUMINAITE, D., HOPE, J., BAKER, I., GREGORY, L., GREEN, A., ALLAN, C., LAMBLE, S., JAYAWANT, S., QUAGHEBEUR, G., CADER, M. Z., HUGHES, S., ARMSTRONG, R. J., KANAPIN, A., RIMMER, A., LUNTER, G., MATHIESON, I., CAZIER, J. B., BUCK, D., TAYLOR, J. C., BENTLEY, D., MCVEAN, G., DONNELLY, P., KNIGHT, S. J., JACKSON, M., RAGOUSSIS, J. & NEMETH, A. H. 2012. Recessive mutations in SPTBN2 implicate beta-III spectrin in both cognitive and motor development. *PLoS Genet,* 8**,** e1003074.

LITT, M., BUROKER, N. E., KONDOLEON, S., DOUGLASS, J., LISTON, D., SHEEHY, R. & MAGENIS, R. E. 1988. Chromosomal localization of the human proenkephalin and prodynorphin genes. *Am J Hum Genet,* 42**,** 327-34.

LITT, M., KRAMER, P., BROWNE, D., GANCHER, S., BRUNT, E. R., ROOT, D., PHROMCHOTIKUL, T., DUBAY, C. J. & NUTT, J. 1994. A gene for episodic ataxia/myokymia maps to chromosome 12p13. *Am J Hum Genet,* 55**,** 702-9.

LIU, B. H., WANG, Z. M., GHOSH, S. & ZHOU, Z. J. 2013. Defective ATM-Kap-1-mediated chromatin remodeling impairs DNA repair and accelerates senescence in progeria mouse model. *Aging Cell,* 12**,** 316-318.

LIU, H., CHEN, S., HUANG, K., KIM, J., MO, H., IOVINE, R., GENDRE, J., PASCAL, P., LI, Q., SUN, Y., DONG, Z., ARKIN, M., GUO, S. & HUANG, B. 2016a. A High-Content Larval Zebrafish Brain Imaging Method for Small Molecule Drug Discovery. *PLoS One,* 11**,** e0164645.

LIU, J., GONG, L., CHANG, C., LIU, C., PENG, J. & CHEN, J. 2012a. Development of novel visual-plus quantitative analysis systems for studying DNA double-strand break repairs in zebrafish. *J Genet Genomics,* 39**,** 489-502.

LIU, J., LUO, S., ZHAO, H., LIAO, J., LI, J., YANG, C., XU, B., STERN, D. F., XU, X. & YE, K. 2012b. Structural mechanism of the phosphorylation-dependent dimerization of the MDC1 forkhead-associated domain. *Nucleic Acids Res,* 40**,** 3898-912.

LIU, K., JIAN, Y., SUN, X., YANG, C., GAO, Z., ZHANG, Z., LIU, X., LI, Y., XU, J., JING, Y., MITANI, S. & HE, S. 2016b. Negative regulation of phosphatidylinositol 3-phosphate levels in early-to-late endosome conversion. *J Cell Biol,* 212**,** 181-98.

LIU, S. C., LANE, W. S. & LIENHARD, G. E. 2000. Cloning and preliminary characterization of a 105 kDa protein with an N-terminal kinase-like domain. *Biochim Biophys Acta,* 1517**,** 148-52.

LIU, T. X., HOWLETT, N. G., DENG, M., LANGENAU, D. M., HSU, K., RHODES, J., KANKI, J. P., D'ANDREA, A. D. & LOOK, A. T. 2003. Knockdown of Zebrafish Fancd2 Causes Developmental Abnormalities via p53-Dependent Apoptosis. *Developmental Cell,* 5**,** 903-914.

LIU, X., GUO, N., LIN, J., ZHANG, Y., CHEN, X. Q., LI, S., HE, L. & LI, Q. 2014. Strain-dependent differential behavioral responses of zebrafish larvae to acute MK-801 treatment. *Pharmacology Biochemistry and Behavior,* 127**,** 82-89.

LIU, Y. & LIU, Q. H. 2011. ATM Signals miRNA Biogenesis through KSRP. *Molecular Cell,* 41**,** 367-368.

LLOYD, J. P. B. & DAVIES, B. 2013. SMG1 is an ancient nonsense-mediated mRNA decay effector. *The Plant Journal,* 76**,** 800-810.

LOAIZA, N. & DEMARIA, M. 2016. Cellular senescence and tumor promotion: Is aging the key? *Biochimica et Biophysica Acta (BBA) - Reviews on Cancer,* 1865**,** 155-167.

LOBBE, A. M., KANG, J. S., HILKER, R., HACKSTEIN, H., MULLER, U. & NOLTE, D. 2014. A Novel Missense Mutation in AFG3L2 Associated with Late Onset and Slow Progression of Spinocerebellar Ataxia Type 28. *Journal of Molecular Neuroscience,* 52**,** 493-496.

LOLLI, G., PINNA, L. A. & BATTISTUTTA, R. 2012. Structural determinants of protein kinase CK2 regulation by autoinhibitory polymerization. *ACS Chem Biol,* 7**,** 1158-63.

LORENZO, D. N., FORREST, S. M., IKEDA, Y., DICK, K. A., RANUM, L. P. & KNIGHT, M. A. 2006. Spinocerebellar ataxia type 20 is genetically distinct from spinocerebellar ataxia type 5. *Neurology,* 67**,** 2084-5.

LOU, Z., MINTER-DYKHOUSE, K., FRANCO, S., GOSTISSA, M., RIVERA, M. A., CELESTE, A., MANIS, J. P., VAN DEURSEN, J., NUSSENZWEIG, A., PAULL, T. T., ALT, F. W. & CHEN, J. 2006. MDC1 maintains genomic stability by participating in the amplification of ATM-dependent DNA damage signals. *Mol Cell,* 21**,** 187-200.

LOUCKS, E. & CARVAN, M. J., 3RD 2004. Strain-dependent effects of developmental ethanol exposure in zebrafish. *Neurotoxicol Teratol,* 26**,** 745-55.

LOVEJOY, C. A. & CORTEZ, D. 2009. Common mechanisms of PIKK regulation. *DNA Repair (Amst),* 8**,** 1004-8.

LUMSDEN, A. L., HENSHALL, T. L., DAYAN, S., LARDELLI, M. T. & RICHARDS, R. I. 2007. Huntingtin-deficient zebrafish exhibit defects in iron utilization and development. *Hum Mol Genet,* 16**,** 1905-20.

LUMSDEN, J. M., MCCARTY, T., PETINIOT, L. K., SHEN, R., BARLOW, C., WYNN, T. A., MORSE, H. C., 3RD, GEARHART, P. J., WYNSHAW-BORIS, A., MAX, E. E. & HODES, R. J. 2004. Immunoglobulin class switch recombination is impaired in Atm-deficient mice. *J Exp Med,* 200**,** 1111-21.

LUO, K., YUAN, J. & LOU, Z. 2011. Oligomerization of MDC1 protein is important for proper DNA damage response. *J Biol Chem,* 286**,** 28192-9.

LUO, X. Q., SUZUKI, M., GHANDHI, S. A., AMUNDSON, S. A. & BOOTHMAN, D. A. 2014. ATM Regulates Insulin-Like Growth Factor 1-Secretory Clusterin (IGF-1-sCLU) Expression that Protects Cells against Senescence. *Plos One,* 9.

MA, Y. C., SHI, X. J., KE, Y., ZI, X. L., DAI, M. Y., ZHAO, W. & LIU, H. M. 2013. ATM-mediated Chk1/2 and Cdc2 phosphorylation is involved in Jaridonin-induced cell cycle arrest in human esophageal cancer cells. *Acta Pharmacologica Sinica,* 34**,** 11-12.

MA, Z., ZHU, P., SHI, H., GUO, L., ZHANG, Q., CHEN, Y., CHEN, S., ZHANG, Z., PENG, J. & CHEN, J. 2019. PTC-bearing mRNA elicits a genetic compensation response via Upf3a and COMPASS components. *Nature,* 568**,** 259-263.

MAACK, G. & SEGNER, H. 2003. Morphological development of the gonads in zebrafish. *Journal of Fish Biology,* 62**,** 895-906.

MAHMOOD, F., FU, S., COOKE, J., WILSON, S. W., COOPER, J. D. & RUSSELL, C. 2013. A zebrafish model of CLN2 disease is deficient in tripeptidyl peptidase 1 and displays progressive neurodegeneration accompanied by a reduction in proliferation. *Brain,* 136**,** 1488-1507.

MAILAND, N., BEKKER-JENSEN, S., FAUSTRUP, H., MELANDER, F., BARTEK, J., LUKAS, C. & LUKAS, J. 2007. RNF8 ubiquitylates histones at DNA double-strand breaks and promotes assembly of repair proteins. *Cell,* 131**,** 887-900.

MAILLET, P., BONNEFOI, H., VAUDAN-VUTSKITS, G., PAJK, B., CUFER, T., FOULKES, W. D., CHAPPUIS, P. O. & SAPPINO, A. P. 2002. Constitutional alterations of the ATM gene in early onset sporadic breast cancer. *Journal of Medical Genetics,* 39**,** 751-753.

MALI, P., YANG, L., ESVELT, K. M., AACH, J., GUELL, M., DICARLO, J. E., NORVILLE, J. E. & CHURCH, G. M. 2013. RNA-guided human genome engineering via Cas9. *Science,* 339**,** 823-6.

MALLARET, M., SYNOFZIK, M., LEE, J., SAGUM, C. A., MAHAJNAH, M., SHARKIA, R., DROUOT, N., RENAUD, M., KLEIN, F. A., ANHEIM, M., TRANCHANT, C., MIGNOT, C., MANDEL, J. L., BEDFORD, M., BAUER, P., SALIH, M. A., SCHULE, R., SCHOLS, L., ALDAZ, C. M. & KOENIG, M. 2014. The tumour suppressor gene WWOX is mutated in autosomal recessive cerebellar ataxia with epilepsy and mental retardation. *Brain,* 137**,** 411-9.

MALLETTE, F. A., GAUMONT-LECLERC, M. F. & FERBEYRE, G. 2007. The DNA damage signaling pathway is a critical mediator of oncogene-induced senescence. *Genes & Development,* 21**,** 43-48.

MALTECCA, F., BASEGGIO, E., CONSOLATO, F., MAZZA, D., PODINI, P., YOUNG, S. M., DRAGO, I., BAHR, B. A., PULITI, A., CODAZZI, F., QUATTRINI, A. & CASARI, G. 2015. Purkinje neuron Ca2+ influx reduction rescues ataxia in SCA28 model. *Journal of Clinical Investigation,* 125**,** 263-274.

MAMRAK, N. E., SHIMAMURA, A. & HOWLETT, N. G. 2017. Recent discoveries in the molecular pathogenesis of the inherited bone marrow failure syndrome Fanconi anemia. *Blood Rev,* 31**,** 93-99.

MARABITTI, V., LILLO, G., MALACARIA, E., PALERMO, V., SANCHEZ, M., PICHIERRI, P. & FRANCHITTO, A. 2019. ATM pathway activation limits R-loop-associated genomic instability in Werner syndrome cells. *Nucleic Acids Res,* 47**,** 3485-3502.

MARTINEZ, E., KUNDU, T. K., FU, J. & ROEDER, R. G. 1998. A human SPT3-TAFII31-GCN5-L acetylase complex distinct from transcription factor IID. *J Biol Chem,* 273**,** 23781-5.

MARTINS, C. & COSTA, P. M. 2020. Technical Updates to the Comet Assay In Vivo for Assessing DNA Damage in Zebrafish Embryos from Fresh and Frozen Cell Suspensions. *Zebrafish*.

MATILLA, A., KOSHY, B. T., CUMMINGS, C. J., ISOBE, T., ORR, H. T. & ZOGHBI, H. Y. 1997. The cerebellar leucine-rich acidic nuclear protein interacts with ataxin-1. *Nature,* 389**,** 974-8.

MATSUDA, Y., IMAI, T., SHIOMI, J., SAITO, T., YAMAUCHI, M., FUKAO, T., AKAO, Y., SEKI, N., ITO, H. & HORI, T. 1996. Comparative genome mapping of the ataxia-telangiectasia region in mouse, rat, and Syrian hamster. *Genomics,* 34**,** 347-352.

MATSUMOTO, M., NAKAGAWA, T., INOUE, T., NAGATA, E., TANAKA, K., TAKANO, H., MINOWA, O., KUNO, J., SAKAKIBARA, S., YAMADA, M., YONESHIMA, H., MIYAWAKI, A., FUKUUCHI, Y., FURUICHI, T., OKANO, H., MIKOSHIBA, K. & NODA, T. 1996. Ataxia and epileptic seizures in mice lacking type 1 inositol 1,4,5-trisphosphate receptor. *Nature,* 379**,** 168-71.

MATSUNAGA, K., SAITOH, T., TABATA, K., OMORI, H., SATOH, T., KUROTORI, N., MAEJIMA, I., SHIRAHAMA-NODA, K., ICHIMURA, T., ISOBE, T., AKIRA, S., NODA, T. & YOSHIMORI, T. 2009. Two Beclin 1-binding proteins, Atg14L and Rubicon, reciprocally regulate autophagy at different stages. *Nat Cell Biol,* 11**,** 385-96.

MATSUOKA, S., BALLIF, B. A., SMOGORZEWSKA, A., MCDONALD, E. R., 3RD, HUROV, K. E., LUO, J., BAKALARSKI, C. E., ZHAO, Z., SOLIMINI, N., LERENTHAL, Y., SHILOH, Y., GYGI, S. P. & ELLEDGE, S. J. 2007. ATM and ATR substrate analysis reveals extensive protein networks responsive to DNA damage. *Science,* 316**,** 1160-6.

MATSUURA, T., ACHARI, M., KHAJAVI, M., BACHINSKI, L. L., ZOGHBI, H. Y. & ASHIZAWA, T. 1999. Mapping of the gene for a novel spinocerebellar ataxia with pure cerebellar signs and epilepsy. *Ann Neurol,* 45**,** 407-11.

MATTEI, M. G., SARDET, C., FRANCHI, A. & POUYSSEGUR, J. 1988. The human amiloride-sensitive Na+/H+ antiporter: localization to chromosome 1 by in situ hybridization. *Cytogenet Cell Genet,* 48**,** 6-8.

MAYER, R. E., HENDRIX, P., CRON, P., MATTHIES, R., STONE, S. R., GORIS, J., MERLEVEDE, W., HOFSTEENGE, J. & HEMMINGS, B. A. 1991. Structure of the 55-kDa regulatory subunit of protein phosphatase 2A: evidence for a neuronal-specific isoform. *Biochemistry,* 30**,** 3589-97.

MCCAMPBELL, A., TAYLOR, J. P., TAYE, A. A., ROBITSCHEK, J., LI, M., WALCOTT, J., MERRY, D., CHAI, Y., PAULSON, H., SOBUE, G. & FISCHBECK, K. H. 2000. CREB-binding protein sequestration by expanded polyglutamine. *Hum Mol Genet,* 9**,** 2197-202.

MCCAW, B. K., HECHT, F., HARNDEN, D. G. & TEPLITZ, R. L. 1975. Somatic rearrangement of chromosome 14 in human lymphocytes. *Proc Natl Acad Sci U S A,* 72**,** 2071-5.

MCCOOL, K. W. & MIYAMOTO, S. 2012. DNA damage-dependent NF-κB activation: NEMO turns nuclear signaling inside out. *Immunol Rev,* 246**,** 311-26.

MCDONALD, C. J., OSTINI, L., WALLACE, D. F., JOHN, A. N., WATTERS, D. J. & SUBRAMANIAM, V. N. 2011. Iron loading and oxidative stress in the Atm(-/-) mouse liver. *American Journal of Physiology-Gastrointestinal and Liver Physiology,* 300**,** G554-G560.

MCKINNON, P. J. 2009. DNA repair deficiency and neurological disease. *Nat Rev Neurosci,* 10**,** 100-12.

MCMENAMIN, S. K., CHANDLESS, M. N. & PARICHY, D. M. 2016. Working with zebrafish at postembryonic stages. *Methods in cell biology,* 134**,** 587-607.

MEEK, K., XU, Y., BAILIE, C., YU, K. & NEAL, J. A. 2016. The ATM Kinase Restrains Joining of Both VDJ Signal and Coding Ends. *J Immunol,* 197**,** 3165-3174.

MEGARBANE, A., DELAGUE, V., SALEM, N. & LOISELET, J. 1999. Autosomal recessive congenital cerebellar hypoplasia and short stature in a large inbred family. *Am J Med Genet.* United States.

MEHDIPOUR, P., KARAMI, F., JAVAN, F. & MEHRAZIN, M. 2015. Linking ATM Promoter Methylation to Cell Cycle Protein Expression in Brain Tumor Patients: Cellular Molecular Triangle Correlation in ATM Territory. *Mol Neurobiol,* 52**,** 293-302.

MEIJER, I. A., HAND, C. K., GREWAL, K. K., STEFANELLI, M. G., IVES, E. J. & ROULEAU, G. A. 2002. A locus for autosomal dominant hereditary spastic ataxia, SAX1, maps to chromosome 12p13. *Am J Hum Genet,* 70**,** 763-9.

MELBERG, A., HETTA, J., DAHL, N., NENNESMO, I., BENGTSSON, M., WIBOM, R., GRANT, C., GUSTAVSON, K. H. & LUNDBERG, P. O. 1995. Autosomal dominant cerebellar ataxia deafness and narcolepsy. *J Neurol Sci,* 134**,** 119-29.

MENG, X. B., DONG, Y. & SUN, Z. X. 1999. ATM acts in DNA damage signal transduction by catalyzing protein phosphorylation. *Chinese Science Bulletin,* 44**,** 1790-1794.

MENOLFI, D., JIANG, W., LEE, B. J., MOISEEVA, T., SHAO, Z., ESTES, V., FRATTINI, M. G., BAKKENIST, C. J. & ZHA, S. 2018. Kinase-dead ATR differs from ATR loss by limiting the dynamic exchange of ATR and RPA. *Nature Communications,* 9**,** 5351.

MENOTTA, M., BIAGIOTTI, S., BIANCHI, M., CHESSA, L. & MAGNANI, M. 2012. Dexamethasone partially rescues ataxia telangiectasia-mutated (ATM) deficiency in ataxia telangiectasia by promoting a shortened protein variant retaining kinase activity. *J Biol Chem,* 287**,** 41352-63.

MENOTTA, M., BIAGIOTTI, S., SPAPPERI, C., ORAZI, S., ROSSI, L., CHESSA, L., LEUZZI, V., D'AGNANO, D., SORESINA, A., MICHELI, R. & MAGNANI, M. 2017. ATM splicing variants as biomarkers for low dose dexamethasone treatment of A-T. *Orphanet journal of rare diseases,* 12**,** 126-126.

MEYER, A. & VAN DE PEER, Y. 2005. From 2R to 3R: evidence for a fish-specific genome duplication (FSGD). *Bioessays,* 27**,** 937-45.

MEYN, M. S. 1995. Ataxia-telangiectasia and cellular responses to DNA damage. *Cancer Res,* 55**,** 5991-6001.

MEYN, M. S. 1999. Ataxia-telangiectasia, cancer and the pathobiology of the ATM gene. *Clin Genet,* 55**,** 289-304.

MICOL, R., BEN SLAMA, L., SUAREZ, F., LE MIGNOT, L., BEAUTÉ, J., MAHLAOUI, N., DUBOIS D'ENGHIEN, C., LAUGÉ, A., HALL, J., COUTURIER, J., VALLÉE, L., DELOBEL, B., RIVIER, F., NGUYEN, K., BILLETTE DE VILLEMEUR, T., STEPHAN, J. L., BORDIGONI, P., BERTRAND, Y., ALADJIDI, N., PEDESPAN, J. M., THOMAS, C., PELLIER, I., KOENIG, M., HERMINE, O., PICARD, C., MOSHOUS, D., NEVEN, B., LANTERNIER, F., BLANCHE, S., TARDIEU, M., DEBRÉ, M., FISCHER, A. & STOPPA-LYONNET, D. 2011a. Morbidity and mortality from ataxia-telangiectasia are associated with ATM genotype. *J Allergy Clin Immunol,* 128**,** 382-9.e1.

MICOL, R., BEN SLAMA, L., SUAREZ, F., LE MIGNOT, L., BEAUTÉ, J., MAHLAOUI, N., DUBOIS D’ENGHIEN, C., LAUGÉ, A., HALL, J., COUTURIER, J., VALLÉE, L., DELOBEL, B., RIVIER, F., NGUYEN, K., BILLETTE DE VILLEMEUR, T., STEPHAN, J.-L., BORDIGONI, P., BERTRAND, Y., ALADJIDI, N., PEDESPAN, J.-M., THOMAS, C., PELLIER, I., KOENIG, M., HERMINE, O., PICARD, C., MOSHOUS, D., NEVEN, B., LANTERNIER, F., BLANCHE, S., TARDIEU, M., DEBRÉ, M., FISCHER, A. & STOPPA-LYONNET, D. 2011b. Morbidity and mortality from ataxia-telangiectasia are associated with ATM genotype. *Journal of Allergy and Clinical Immunology,* 128**,** 382-389.e1.

MILLER, M., SABRAUTZKI, S., BEYERLEIN, A. & BRIELMEIER, M. 2019. Combining fish and environmental PCR for diagnostics of diseased laboratory zebrafish in recirculating systems. *PLoS One,* 14**,** e0222360.

MIN, J. N., WHALEY, R. A., SHARPLESS, N. E., LOCKYER, P., PORTBURY, A. L. & PATTERSON, C. 2008. CHIP deficiency decreases longevity, with accelerated aging phenotypes accompanied by altered protein quality control. *Mol Cell Biol,* 28**,** 4018-25.

MITUI, M., BERNATOWSKA, E., PIETRUCHA, B., PIOTROWSKA-JASTRZEBSKA, J., ENG, L., NAHAS, S., TERAOKA, S., SHOLTY, G., PURAYIDOM, A., CONCANNON, P. & GATTI, R. A. 2005. ATM gene founder haplotypes and associated mutations in Polish families with ataxia-telangiectasia. *Ann Hum Genet,* 69**,** 657-64.

MITUI, M., CAMPBELL, C., COUTINHO, G., SUN, X., LAI, C. H., THORSTENSON, Y., CASTELLVI-BEL, S., FERNANDEZ, L., MONROS, E., CARVALHO, B. T., PORRAS, O., FONTAN, G. & GATTI, R. A. 2003.

Independent mutational events are rare in the ATM gene: haplotype prescreening enhances mutation detection rate. *Hum Mutat,* 22**,** 43-50.

MIYAMOTO, R., MORINO, H., YOSHIZAWA, A., MIYAZAKI, Y., MARUYAMA, H., MURAKAMI, N., FUKADA, K., IZUMI, Y., MATSUURA, S., KAJI, R. & KAWAKAMI, H. 2014. Exome sequencing reveals a novel MRE11 mutation in a patient with progressive myoclonic ataxia. *J Neurol Sci,* 337**,** 219-23.

MOCHAN, T. A., VENERE, M., DITULLIO, R. A., JR. & HALAZONETIS, T. D. 2003. 53BP1 and NFBD1/MDC1-Nbs1 function in parallel interacting pathways activating ataxia-telangiectasia mutated (ATM) in response to DNA damage. *Cancer Res,* 63**,** 8586-91.

MOLLET, J., DELAHODDE, A., SERRE, V., CHRETIEN, D., SCHLEMMER, D., LOMBES, A., BODDAERT, N., DESGUERRE, I., DE LONLAY, P., DE BAULNY, H. O., MUNNICH, A. & ROTIG, A. 2008. CABC1 gene mutations cause ubiquinone deficiency with cerebellar ataxia and seizures. *Am J Hum Genet,* 82**,** 623-30.

MORAIS, R. D. V. S., NÓBREGA, R. H., GÓMEZ-GONZÁLEZ, N. E., SCHMIDT, R., BOGERD, J., FRANÇA, L. R. & SCHULZ, R. W. 2013. Thyroid Hormone Stimulates the Proliferation of Sertoli Cells and Single Type A Spermatogonia in Adult Zebrafish (Danio rerio) Testis. *Endocrinology,* 154**,** 4365-4376.

MOREIRA, M. C., BARBOT, C., TACHI, N., KOZUKA, N., MENDONCA, P., BARROS, J., COUTINHO, P., SEQUEIROS, J. & KOENIG, M. 2001. Homozygosity mapping of Portuguese and Japanese forms of ataxia-oculomotor apraxia to 9p13, and evidence for genetic heterogeneity. *Am J Hum Genet,* 68**,** 501-8.

MOREIRA, M. C., KLUR, S., WATANABE, M., NEMETH, A. H., LE BER, I., MONIZ, J. C., TRANCHANT, C., AUBOURG, P., TAZIR, M., SCHOLS, L., PANDOLFO, M., SCHULZ, J. B., POUGET, J., CALVAS, P., SHIZUKA-IKEDA, M., SHOJI, M., TANAKA, M., IZATT, L., SHAW, C. E., M'ZAHEM, A., DUNNE, E., BOMONT, P., BENHASSINE, T., BOUSLAM, N., STEVANIN, G., BRICE, A., GUIMARAES, J., MENDONCA, P., BARBOT, C., COUTINHO, P., SEQUEIROS, J., DURR, A., WARTER, J. M. & KOENIG, M. 2004. Senataxin, the ortholog of a yeast RNA helicase, is mutant in ataxia-ocular apraxia 2. *Nat Genet,* 36**,** 225-7.

MORI, K., WENG, S. M., ARZBERGER, T., MAY, S., RENTZSCH, K., KREMMER, E., SCHMID, B., KRETZSCHMAR, H. A., CRUTS, M., VAN BROECKHOVEN, C., HAASS, C. & EDBAUER, D. 2013. The C9orf72 GGGGCC repeat is translated into aggregating dipeptide-repeat proteins in FTLD/ALS. *Science,* 339**,** 1335-8.

MORINAGA, T., YASUDA, H., HASHIMOTO, T., HIGASHIO, K. & TAMAOKI, T. 1991. A human alpha-fetoprotein enhancer-binding protein, ATBF1, contains four homeodomains and seventeen zinc fingers. *Mol Cell Biol,* 11**,** 6041-9.

MORINO, H., MATSUDA, Y., MUGURUMA, K., MIYAMOTO, R., OHSAWA, R., OHTAKE, T., OTOBE, R., WATANABE, M., MARUYAMA, H., HASHIMOTO, K. & KAWAKAMI, H. 2015. A mutation in the low voltage-gated calcium channel CACNA1G alters the physiological properties of the channel, causing spinocerebellar ataxia. *Mol Brain,* 8**,** 89.

MORITA, A., TANIMOTO, K., MURAKAMI, T., MORINAGA, T. & HOSOI, Y. 2014. Mitochondria are required for ATM activation by extranuclear oxidative stress in cultured human hepatoblastoma cell line Hep G2 cells. *Biochem Biophys Res Commun,* 443**,** 1286-90.

MORITA, H., YOSHIDA, K., SUZUKI, K. & IKEDA, S. 2006. A Japanese case of SCA14 with the Gly128Asp mutation. *J Hum Genet,* 51**,** 1118-21.

MORRELL, D., CHASE, C. L. & SWIFT, M. 1990. Cancers in 44 families with ataxia-telangiectasia. *Cancer Genet Cytogenet,* 50**,** 119-23.

MOU, J., HU, T., WANG, Z., CHEN, W., WANG, Y. & ZHANG, W. 2020. ATM gene polymorphisms are associated with poor prognosis of non-small cell lung cancer receiving radiation therapy. *Aging (Albany NY),* 12.

MU, J. J., WANG, Y., LUO, H., LENG, M., ZHANG, J., YANG, T., BESUSSO, D., JUNG, S. Y. & QIN, J. 2007. A proteomic analysis of ataxia telangiectasia-mutated (ATM)/ATM-Rad3-related (ATR) substrates identifies the ubiquitin-proteasome system as a regulator for DNA damage checkpoints. *J Biol Chem,* 282**,** 17330-4.

MUKHERJEE, B., KESSINGER, C., KOBAYASHI, J., CHEN, B. P., CHEN, D. J., CHATTERJEE, A. & BURMA, S. 2006. DNA-PK phosphorylates histone H2AX during apoptotic DNA fragmentation in mammalian cells. *DNA Repair (Amst),* 5**,** 575-90.

MUONA, M., BERKOVIC, S. F., DIBBENS, L. M., OLIVER, K. L., MALJEVIC, S., BAYLY, M. A., JOENSUU, T., CANAFOGLIA, L., FRANCESCHETTI, S., MICHELUCCI, R., MARKKINEN, S., HERON, S. E., HILDEBRAND, M. S., ANDERMANN, E., ANDERMANN, F., GAMBARDELLA, A., TINUPER, P., LICCHETTA, L., SCHEFFER, I. E., CRISCUOLO, C., FILLA, A., FERLAZZO, E., AHMAD, J., AHMAD, A., BAYKAN, B., SAID, E., TOPCU, M., RIGUZZI, P., KING, M. D., OZKARA, C., ANDRADE, D. M., ENGELSEN, B. A., CRESPEL, A., LINDENAU, M., LOHMANN, E., SALETTI, V., MASSANO, J., PRIVITERA, M., ESPAY, A. J., KAUFFMANN, B., DUCHOWNY, M., MOLLER, R. S., STRAUSSBERG, R., AFAWI, Z., BEN-ZEEV, B., SAMOCHA, K. E., DALY, M. J., PETROU, S., LERCHE, H., PALOTIE, A. & LEHESJOKI, A. E. 2015. A recurrent de novo mutation in KCNC1 causes progressive myoclonus epilepsy. *Nat Genet,* 47**,** 39-46.

MUÑOZ-ESPÍN, D., CAÑAMERO, M., MARAVER, A., GÓMEZ-LÓPEZ, G., CONTRERAS, J., MURILLO-CUESTA, S., RODRÍGUEZ-BAEZA, A., VARELA-NIETO, I., RUBERTE, J., COLLADO, M. & SERRANO, M. 2013. Programmed cell senescence during mammalian embryonic development. *Cell,* 155**,** 1104-18.

MYERS, J. S. & CORTEZ, D. 2006. Rapid activation of ATR by ionizing radiation requires ATM and Mre11. *J Biol Chem,* 281**,** 9346-50.

MÜLLER, W. G., WALKER, D., HAGER, G. L. & MCNALLY, J. G. 2001. Large-scale chromatin decondensation and recondensation regulated by transcription from a natural promoter. *J Cell Biol,* 154**,** 33-48.

NAGAFUCHI, S., YANAGISAWA, H., SATO, K., SHIRAYAMA, T., OHSAKI, E., BUNDO, M., TAKEDA, T., TADOKORO, K., KONDO, I., MURAYAMA, N. & ET AL. 1994. Dentatorubral and pallidoluysian atrophy expansion of an unstable CAG trinucleotide on chromosome 12p. *Nat Genet,* 6**,** 14-8.

NAGAOKA, U., TAKASHIMA, M., ISHIKAWA, K., YOSHIZAWA, K., YOSHIZAWA, T., ISHIKAWA, M., YAMAWAKI, T., SHOJI, S. & MIZUSAWA, H. 2000. A gene on SCA4 locus causes dominantly inherited pure cerebellar ataxia. *Neurology,* 54**,** 1971-5.

NAGASE, T., KIKUNO, R., ISHIKAWA, K., HIROSAWA, M. & OHARA, O. 2000. Prediction of the coding sequences of unidentified human genes. XVII. The complete sequences of 100 new cDNA clones from brain which code for large proteins in vitro. *DNA Res,* 7**,** 143-50.

NAGASE, T., SEKI, N., ISHIKAWA, K., OHIRA, M., KAWARABAYASI, Y., OHARA, O., TANAKA, A., KOTANI, H., MIYAJIMA, N. & NOMURA, N. 1996. Prediction of the coding sequences of unidentified human genes. VI. The coding sequences of 80 new genes (KIAA0201-KIAA0280) deduced by analysis of cDNA clones from cell line KG-1 and brain. *DNA Res,* 3**,** 321-9, 341-54.

NAGY, E. & MAQUAT, L. E. 1998. A rule for termination-codon position within intron-containing genes: when nonsense affects RNA abundance. *Trends in Biochemical Sciences,* 23**,** 198-199.

NAIR, R. R., BAGHERI, M. & SAINI, D. K. 2015. Temporally distinct roles of ATM and ROS in genotoxic-stress-dependent induction and maintenance of cellular senescence. *Journal of Cell Science,* 128**,** 342-353.

NAJMABADI, H., HU, H., GARSHASBI, M., ZEMOJTEL, T., ABEDINI, S. S., CHEN, W., HOSSEINI, M., BEHJATI, F., HAAS, S., JAMALI, P., ZECHA, A., MOHSENI, M., PUTTMANN, L., VAHID, L. N., JENSEN, C., MOHEB, L. A., BIENEK, M., LARTI, F., MUELLER, I., WEISSMANN, R., DARVISH, H., WROGEMANN, K., HADAVI, V., LIPKOWITZ, B., ESMAEELI-NIEH, S., WIECZOREK, D., KARIMINEJAD, R., FIROUZABADI, S. G., COHEN, M., FATTAHI, Z., ROST, I., MOJAHEDI, F., HERTZBERG, C., DEHGHAN, A., RAJAB, A., BANAVANDI, M. J., HOFFER, J., FALAH, M., MUSANTE, L., KALSCHEUER, V., ULLMANN, R., KUSS, A. W., TZSCHACH, A., KAHRIZI, K. & ROPERS, H. H. 2011. Deep sequencing reveals 50 novel genes for recessive cognitive disorders. *Nature,* 478**,** 57-63.

NAKAMURA, K., JEONG, S. Y., UCHIHARA, T., ANNO, M., NAGASHIMA, K., NAGASHIMA, T., IKEDA, S., TSUJI, S. & KANAZAWA, I. 2001. SCA17, a novel autosomal dominant cerebellar ataxia caused by an expanded polyglutamine in TATA-binding protein. *Hum Mol Genet,* 10**,** 1441-8.

NAKAMURA, Y., TAGAWA, K., OKA, T., SASABE, T., ITO, H., SHIWAKU, H., LA SPADA, A. R. & OKAZAWA, H. 2012. Ataxin-7 associates with microtubules and stabilizes the cytoskeletal network. *Hum Mol Genet,* 21**,** 1099-110.

NAKAYAMA, T., SATO, Y., UEMATSU, M., TAKAGI, M., HASEGAWA, S., KUMADA, S., KIKUCHI, A., HINO-FUKUYO, N., SASAHARA, Y., HAGINOYA, K. & KURE, S. 2015. Myoclonic axial jerks for diagnosing atypical evolution of ataxia telangiectasia. *Brain Dev,* 37**,** 362-5.

NAMIKAWA, K., DORIGO, A. & KOSTER, R. W. 2019a. Neurological Disease Modelling for Spinocerebellar Ataxia Using Zebrafish. *Journal of Experimental Neuroscience,* 13**,** 5.

NAMIKAWA, K., DORIGO, A., ZAGREBELSKY, M., RUSSO, G., KIRMANN, T., FAHR, W., DUBEL, S., KORTE, M. & KOSTER, R. W. 2019b. Modeling Neurodegenerative Spinocerebellar Ataxia Type 13 in Zebrafish Using a Purkinje Neuron Specific Tunable Coexpression System. *Journal of Neuroscience,* 39**,** 3948-3969.

NAVRATIL, M., DURANOVIC, V., NOGALO, B., SVIGIR, A., DUMBOVIC DUBRAVCIC, I. & TURKALJ, M. 2015. Ataxia-Telangiectasia Presenting as Cerebral Palsy and Recurrent Wheezing: A Case Report. *Am J Case Rep,* 16**,** 631-6.

NEMETH, A. H., BOCHUKOVA, E., DUNNE, E., HUSON, S. M., ELSTON, J., HANNAN, M. A., JACKSON, M., CHAPMAN, C. J. & TAYLOR, A. M. 2000. Autosomal recessive cerebellar ataxia with oculomotor apraxia (ataxia-telangiectasia-like syndrome) is linked to chromosome 9q34. *Am J Hum Genet,* 67**,** 1320-6.

NEUBAUER, S., ARUTYUNYAN, R., STUMM, M., DÖRK, T., BENDIX, R., BREMER, M., VARON, R., SAUER, R. & GEBHART, E. 2002. Radiosensitivity of ataxia telangiectasia and Nijmegen breakage syndrome homozygotes and heterozygotes as determined by three-color FISH chromosome painting. *Radiat Res,* 157**,** 312-21.

NGUYEN, M., BOESTEN, I., HELLEBREKERS, D. M., VANOEVELEN, J., KAMPS, R., DE KONING, B., DE COO, I. F., GERARDS, M. & SMEETS, H. J. 2016. Pathogenic CWF19L1 variants as a novel cause of autosomal recessive cerebellar ataxia and atrophy. *Eur J Hum Genet,* 24**,** 619-22.

NICHOLSON, P., YEPISKOPOSYAN, H., METZE, S., ZAMUDIO OROZCO, R., KLEINSCHMIDT, N. & MÜHLEMANN, O. 2010. Nonsense-mediated mRNA decay in human cells: mechanistic insights, functions beyond quality control and the double-life of NMD factors. *Cell Mol Life Sci,* 67**,** 677-700.

NICKLESS, A., BAILIS, J. M. & YOU, Z. 2017. Control of gene expression through the nonsense-mediated RNA decay pathway. *Cell & Bioscience,* 7**,** 26.

NIEFIND, K. & ISSINGER, O. G. 2005. Primary and secondary interactions between CK2alpha and CK2beta lead to ring-like structures in the crystals of the CK2 holoenzyme. *Mol Cell Biochem,* 274**,** 3-14.

NISHIZAWA, H., IGUCHI, G., FUKUOKA, H., TAKAHASHI, M., SUDA, K., BANDO, H., MATSUMOTO, R., YOSHIDA, K., ODAKE, Y., OGAWA, W. & TAKAHASHI, Y. 2016. IGF-I induces senescence of hepatic stellate cells and limits fibrosis in a p53-dependent manner. *Scientific Reports,* 6**,** 34605.

NISSANKA, N. & MORAES, C. T. 2018. Mitochondrial DNA damage and reactive oxygen species in neurodegenerative disease. *FEBS Lett,* 592**,** 728-742.

NISSENKORN, A., LEVY-SHRAGA, Y., BANET-LEVI, Y., LAHAD, A., SAROUK, I. & MODAN-MOSES, D. 2016. Endocrine abnormalities in ataxia telangiectasia: findings from a national cohort. *Pediatr Res,* 79**,** 889-94.

NOORDZIJ, J. G., WULFFRAAT, N. M., HARALDSSON, A., MEYTS, I., VAN'T VEER, L. J., HOGERVORST, F. B., WARRIS, A. & WEEMAES, C. M. 2009. Ataxia-telangiectasia patients presenting with hyper-IgM syndrome. *Arch Dis Child,* 94**,** 448-9.

NORMAN, R. M. 1940. PRIMARY DEGENERATION OF THE GRANULAR LAYER OF THE CEREBELLUM: AN UNUSUAL FORM OF FAMILIAL CEREBELLAR ATROPHY OCCURRING IN EARLY LIFE. *Brain,* 63**,** 365-379.

NORTON, W. & BALLY-CUIF, L. 2010. Adult zebrafish as a model organism for behavioural genetics. *BMC Neurosci,* 11**,** 90.

NOTMAN, R., NORO, M., O'MALLEY, B. & ANWAR, J. 2006. Molecular basis for dimethylsulfoxide (DMSO) action on lipid membranes. *J Am Chem Soc,* 128**,** 13982-3.

NOVARINO, G., FENSTERMAKER, A. G., ZAKI, M. S., HOFREE, M., SILHAVY, J. L., HEIBERG, A. D., ABDELLATEEF, M., ROSTI, B., SCOTT, E., MANSOUR, L., MASRI, A., KAYSERILI, H., AL-AAMA, J. Y., ABDEL-SALAM, G. M., KARMINEJAD, A., KARA, M., KARA, B., BOZORGMEHRI, B., BEN-OMRAN, T., MOJAHEDI, F., MAHMOUD, I. G., BOUSLAM, N., BOUHOUCHE, A., BENOMAR, A., HANEIN, S., RAYMOND, L., FORLANI, S., MASCARO, M., SELIM, L., SHEHATA, N., AL-ALLAWI, N., BINDU, P. S., AZAM, M., GUNEL, M., CAGLAYAN, A., BILGUVAR, K., TOLUN, A., ISSA, M. Y., SCHROTH, J., SPENCER, E. G., ROSTI, R. O., AKIZU, N., VAUX, K. K., JOHANSEN, A., KOH, A. A., MEGAHED, H., DURR, A., BRICE, A., STEVANIN, G., GABRIEL, S. B., IDEKER, T. & GLEESON, J. G. 2014. Exome sequencing links corticospinal motor neuron disease to common neurodegenerative disorders. *Science,* 343**,** 506-11.

NOWAK-WEGRZYN, A., CRAWFORD, T. O., WINKELSTEIN, J. A., CARSON, K. A. & LEDERMAN, H. M. 2004. Immunodeficiency and infections in ataxia-telangiectasia. *J Pediatr,* 144**,** 505-11.

NUCIFORA, F. C., JR., LI, S. H., DANOFF, S., ULLRICH, A. & ROSS, C. A. 1995. Molecular cloning of a cDNA for the human inositol 1,4,5-trisphosphate receptor type 1, and the identification of a third alternatively spliced variant. *Brain Res Mol Brain Res,* 32**,** 291-6.

OGRYZKO, V. V., KOTANI, T., ZHANG, X., SCHILTZ, R. L., HOWARD, T., YANG, X.-J., HOWARD, B. H., QIN, J. & NAKATANI, Y. 1998. Histone-like TAFs within the PCAF Histone Acetylase Complex. *Cell,* 94**,** 35-44.

OHATA, T., YOSHIDA, K., SAKAI, H., HAMANOUE, H., MIZUGUCHI, T., SHIMIZU, Y., OKANO, T., TAKADA, F., ISHIKAWA, K., MIZUSAWA, H., YOSHIURA, K., FUKUSHIMA, Y., IKEDA, S. & MATSUMOTO, N. 2006. A -16C>T substitution in the 5' UTR of the puratrophin-1 gene is prevalent in autosomal dominant cerebellar ataxia in Nagano. *J Hum Genet,* 51**,** 461-6.

OKA, A. & TAKASHIMA, S. 1998. Expression of the ataxia-telangiectasia gene (ATM) product in human cerebellar neurons during development. *Neurosci Lett,* 252**,** 195-8.

OKANO, M., SAKIYAMA, Y., MATSUMOTO, S., MIZUNO, F. & OSATO, T. 1993. HIGH IRRADIATION SENSITIVITY OF EPSTEIN-BARR-VIRUS (EBV) IN LYMPHOBLASTOID-CELLS FROM PATIENTS WITH ATAXIA-TELANGIECTASIA AND EBV GENOME-POSITIVE BURKITTS-LYMPHOMA. *International Journal of Oncology,* 2**,** 1023-1026.

OKUNO, Y., NAKAMURA-ISHIZU, A., OTSU, K., SUDA, T. & KUBOTA, Y. 2012. Pathological neoangiogenesis depends on oxidative stress regulation by ATM. *Nat Med,* 18**,** 1208-16.

OLCINA, M. M., FOSKOLOU, I. P., ANBALAGAN, S., SENRA, J. M., PIRES, I. M., JIANG, Y., RYAN, A. J. & HAMMOND, E. M. 2013. Replication stress and chromatin context link ATM activation to a role in DNA replication. *Mol Cell,* 52**,** 758-66.

OLESON, B. J., TARAKANOVA, V. L. & CORBETT, J. A. 2014. ATM-dependent gamma H2AX Formation Is Associated with Apoptosis in Cytokine-treated beta-Cells. *Diabetes,* 63**,** A559-A559.

ONAT, O. E., GULSUNER, S., BILGUVAR, K., NAZLI BASAK, A., TOPALOGLU, H., TAN, M., TAN, U., GUNEL, M. & OZCELIK, T. 2013. Missense mutation in the ATPase, aminophospholipid transporter protein ATP8A2 is associated with cerebellar atrophy and quadrupedal locomotion. *Eur J Hum Genet,* 21**,** 281-5.

OPHOFF, R. A., TERWINDT, G. M., VERGOUWE, M. N., VAN EIJK, R., OEFNER, P. J., HOFFMAN, S. M., LAMERDIN, J. E., MOHRENWEISER, H. W., BULMAN, D. E., FERRARI, M., HAAN, J., LINDHOUT, D., VAN OMMEN, G. J., HOFKER, M. H., FERRARI, M. D. & FRANTS, R. R. 1996. Familial hemiplegic migraine and episodic ataxia type-2 are caused by mutations in the Ca2+ channel gene CACNL1A4. *Cell,* 87**,** 543-52.

ORNIK, V. & FERK, P. 2013. Variability in pharmacological response to metformin treatment. *Zdravniski Vestnik-Slovenian Medical Journal,* 82**,** 487-496.

ORR, H. T., CHUNG, M. Y., BANFI, S., KWIATKOWSKI, T. J., JR., SERVADIO, A., BEAUDET, A. L., MCCALL, A. E., DUVICK, L. A., RANUM, L. P. & ZOGHBI, H. Y. 1993. Expansion of an unstable trinucleotide CAG repeat in spinocerebellar ataxia type 1. *Nat Genet,* 4**,** 221-6.

OSHITA, A., KISHIDA, S., KOBAYASHI, H., MICHIUE, T., ASAHARA, T., ASASHIMA, M. & KIKUCHI, A. 2003. Identification and characterization of a novel Dvl-binding protein that suppresses Wnt signalling pathway. *Genes Cells,* 8**,** 1005-17.

OUSSET, M., BOUQUET, F., FALLONE, F., BIARD, D., DRAY, C., VALET, P., SALLES, B. & MULLER, C. 2010. Loss of ATM positively regulates the expression of hypoxia inducible factor 1 (HIF-1) through oxidative stress: Role in the physiopathology of the disease. *Cell Cycle,* 9**,** 2814-22.

OWADA, K., ISHIKAWA, K., TORU, S., ISHIDA, G., GOMYODA, M., TAO, O., NOGUCHI, Y., KITAMURA, K., KONDO, I., NOGUCHI, E., ARINAMI, T. & MIZUSAWA, H. 2005. A clinical, genetic, and neuropathologic study in a family with 16q-linked ADCA type III. *Neurology,* 65**,** 629-32.

OXFORD, J. M., HARNDEN, D. G., PARRINGTON, J. M. & DELHANTY, J. D. 1975. Specific chromosome aberrations in ataxia telangiectasia. *J Med Genet,* 12**,** 251-62.

OZCELIK, T., AKARSU, N., UZ, E., CAGLAYAN, S., GULSUNER, S., ONAT, O. E., TAN, M. & TAN, U. 2008. Mutations in the very low-density lipoprotein receptor VLDLR cause cerebellar hypoplasia and quadrupedal locomotion in humans. *Proc Natl Acad Sci U S A,* 105**,** 4232-6.

PAGANO, G., KORKINA, L. G., BRUNK, U. T., CHESSA, L., DEGAN, P., DEL PRINCIPE, D., KELLY, F. J., MALORNI, W., PALLARDÓ, F., PASQUIER, C., SCOVASSI, I., ZATTERALE, A. & FRANCESCHI, C. 1998. Congenital disorders sharing oxidative stress and cancer proneness as phenotypic hallmarks: prospects for joint research in pharmacology. *Med Hypotheses,* 51**,** 253-66.

PAIANO, J., WU, W., YAMADA, S., SCIASCIA, N., CALLEN, E., PAOLA COTRIM, A., DESHPANDE, R. A., MAMAN, Y., DAY, A., PAULL, T. T. & NUSSENZWEIG, A. 2020. ATM and PRDM9 regulate SPO11-bound recombination intermediates during meiosis. *Nat Commun,* 11**,** 857.

PALMERI, S., RUFA, A., PUCCI, B., SANTARNECCHI, E., MALANDRINI, A., STROMILLO, M. L., MANDALÀ, M., ROSINI, F., DE STEFANO, N. & FEDERICO, A. 2013. Clinical course of two Italian siblings with ataxia-telangiectasia-like disorder. *Cerebellum,* 12**,** 596-9.

PAN, Q., PETIT-FRÉRE, C., LÄHDESMÄKI, A., GREGOREK, H., CHRZANOWSKA, K. H. & HAMMARSTRÖM, L. 2002. Alternative end joining during switch recombination in patients with ataxia-telangiectasia. *Eur J Immunol,* 32**,** 1300-8.

PAN-HAMMARSTRÖM, Q., DAI, S., ZHAO, Y., VAN DIJK-HÄRD, I. F., GATTI, R. A., BØRRESEN-DALE, A. L. & HAMMARSTRÖM, L. 2003. ATM is not required in somatic hypermutation of VH, but is involved in the introduction of mutations in the switch mu region. *J Immunol,* 170**,** 3707-16.

PANDITA, T. K., WESTPHAL, C. H., ANGER, M., SAWANT, S. G., GEARD, C. R., PANDITA, R. K. & SCHERTHAN, H. 1999. Atm inactivation results in aberrant telomere clustering during meiotic prophase. *Molecular and cellular biology,* 19**,** 5096-5105.

PANEPINTO, L. M., PHILLIPS, R. W., WESTMORELAND, N. & LUMB, W. V. 1982. THE YUCATAN MINIATURE PIG - BIOMEDICAL-RESEARCH MODEL. *Zeitschrift Fur Versuchstierkunde,* 24**,** 54-54.

PANNIA, E., TRAN, S., RAMPERSAD, M. & GERLAI, R. 2014. Acute ethanol exposure induces behavioural differences in two zebrafish (Danio rerio) strains: a time course analysis. *Behav Brain Res,* 259**,** 174-85.

PARFITT, D. A., MICHAEL, G. J., VERMEULEN, E. G., PRODROMOU, N. V., WEBB, T. R., GALLO, J. M., CHEETHAM, M. E., NICOLL, W. S., BLATCH, G. L. & CHAPPLE, J. P. 2009. The ataxia protein sacsin is a functional co-chaperone that protects against polyglutamine-expanded ataxin-1. *Hum Mol Genet,* 18**,** 1556-65.

PARICHY, D. M., ELIZONDO, M. R., MILLS, M. G., GORDON, T. N. & ENGESZER, R. E. 2009. Normal table of postembryonic zebrafish development: staging by externally visible anatomy of the living fish. *Developmental dynamics : an official publication of the American Association of Anatomists,* 238**,** 2975-3015.

PAROLIN SCHNEKENBERG, R., PERKINS, E. M., MILLER, J. W., DAVIES, W. I., D'ADAMO, M. C., PESSIA, M., FAWCETT, K. A., SIMS, D., GILLARD, E., HUDSPITH, K., SKEHEL, P., WILLIAMS, J., O'REGAN, M., JAYAWANT, S., JEFFERSON, R., HUGHES, S., LUSTENBERGER, A., RAGOUSSIS, J., JACKSON, M., TUCKER, S. J. & NEMETH, A. H. 2015. De novo point mutations in patients diagnosed with ataxic cerebral palsy. *Brain,* 138**,** 1817-32.

PARSONS, J. L. & ELDER, R. H. 2003. DNA N-glycosylase deficient mice: a tale of redundancy. *Mutation Research/Fundamental and Molecular Mechanisms of Mutagenesis,* 531**,** 165-175.

PAUCAR, M., SCHECHTMANN, G., TAYLOR, A. M. & SVENNINGSSON, P. 2019. Variant ataxia-telangiectasia with prominent camptocormia. *Parkinsonism Relat Disord,* 62**,** 253-255.

PAULINO, T. L., RAFAEL, M. N., HIX, S., AJZEN, S. A., DE SOUZA, F. I. S., KOCHI, C., SILVA, R., CARVALHO, B. T. C. & SARNI, R. O. S. 2015. Risk of Atherosclerosis and Diabetes in Patients with Ataxia Telangiectasia. *Journal of Clinical Immunology,* 35**,** S28-S28.

PAULINO, T. L., RAFAEL, M. N., HIX, S., SHIGUEOKA, D. C., AJZEN, S. A., KOCHI, C., SUANO-SOUZA, F. I., DA SILVA, R., COSTA-CARVALHO, B. T. & SARNI, R. O. S. 2017. Is age a risk factor for liver disease and metabolic alterations in ataxia Telangiectasia patients? *Orphanet J Rare Dis,* 12**,** 136.

PAULL, T. T. & GELLERT, M. 1998. The 3' to 5' exonuclease activity of Mre 11 facilitates repair of DNA double-strand breaks. *Mol Cell,* 1**,** 969-79.

PAULL, T. T. & LEE, J. H. 2005. The Mre11/Rad50/Nbs1 complex and its role as a DNA double-strand break sensor for ATM. *Cell Cycle,* 4**,** 737-40.

PEAKE, S. J. & FARRELL, A. P. 2006. Fatigue is a behavioural response in respirometer-confined smallmouth bass. *Journal of Fish Biology,* 68**,** 1742-1755.

PEARSON, T. S. 2016. More Than Ataxia: Hyperkinetic Movement Disorders in Childhood Autosomal Recessive Ataxia Syndromes. *Tremor Other Hyperkinet Mov (N Y),* 6**,** 368.

PEDERSEN, M., TIONG, S. & CAMPBELL, S. D. 2010. Molecular genetic characterization of Drosophila ATM conserved functional domains. *Genome,* 53**,** 778-86.

PEI, D.-S. & STRAUSS, P. R. 2013. Zebrafish as a model system to study DNA damage and repair. *Mutation Research/Fundamental and Molecular Mechanisms of Mutagenesis,* 743-744**,** 151-159.

PENG, J. 2019. Gene redundancy and gene compensation: An updated view. *Journal of Genetics and Genomics,* 46**,** 329-333.

PERETZ, S., JENSEN, R., BASERGA, R. & GLAZER, P. M. 2001. ATM-dependent expression of the insulin-like growth factor-I receptor in a pathway regulating radiation response. *Proc Natl Acad Sci U S A,* 98**,** 1676-81.

PEREZ-REYES, E., CRIBBS, L. L., DAUD, A., LACERDA, A. E., BARCLAY, J., WILLIAMSON, M. P., FOX, M., REES, M. & LEE, J. H. 1998. Molecular characterization of a neuronal low-voltage-activated T-type calcium channel. *Nature,* 391**,** 896-900.

PERKINS, E. J., NAIR, A., COWLEY, D. O., VAN DYKE, T., CHANG, Y. & RAMSDEN, D. A. 2002. Sensing of intermediates in V(D)J recombination by ATM. *Genes Dev,* 16**,** 159-64.

PERNIN, D., BAY, J. O., UHRHAMMER, N. & BIGNON, Y. J. 1999. ATM heterozygote cells exhibit intermediate levels of apoptosis in response to streptonigrin and etoposide. *Eur J Cancer,* 35**,** 1130-5.

PERRY, J. & KLECKNER, N. 2003. The ATRs, ATMs, and TORs are giant HEAT repeat proteins. *Cell.* United States.

PETERSEN, A. J., KATZENBERGER, R. J. & WASSARMAN, D. A. 2013. The innate immune response transcription factor relish is necessary for neurodegeneration in a Drosophila model of ataxia-telangiectasia. *Genetics,* 194**,** 133-42.

PETERSEN, A. J., RIMKUS, S. A. & WASSARMAN, D. A. 2012. ATM kinase inhibition in glial cells activates the innate immune response and causes neurodegeneration in Drosophila. *Proc Natl Acad Sci U S A,* 109**,** E656-64.

PETERSON, R. D., KELLY, W. D. & GOOD, R. A. 1964. ATAXIA-TELANGIECTASIA. ITS ASSOCIATION WITH A DEFECTIVE THYMUS, IMMUNOLOGICAL-DEFICIENCY DISEASE, AND MALIGNANCY. *Lancet,* 1**,** 1189-93.

PI, Y., HE, K. Z., ZHANG, W. Q., DONG, Z. Q., JIANG, F. G., JIANG, K. J. & GUO, S. 2020. Complexity of Detecting CRISPR/Cas9-Mediated Homologous Recombination in Zebrafish. *Molecular Biology,* 54**,** 382-390.

PIACERI, I., BAGNOLI, S., TEDDE, A., SORBI, S. & NACMIAS, B. 2013. Ataxia-telangiectasia mutated (ATM) genetic variant in Italian centenarians. *Neurol Sci,* 34**,** 573-5.

PICKART, M. A., KLEE, E. W., NIELSEN, A. L., SIVASUBBU, S., MENDENHALL, E. M., BILL, B. R., CHEN, E., ECKFELDT, C. E., KNOWLTON, M., ROBU, M. E., LARSON, J. D., DENG, Y., SCHIMMENTI, L. A., ELLIS, L. B., VERFAILLIE, C. M., HAMMERSCHMIDT, M., FARBER, S. A. & EKKER, S. C. 2006. Genome-wide reverse genetics framework to identify novel functions of the vertebrate secretome. *PLoS One,* 1**,** e104.

PIERSON, T. M., ADAMS, D., BONN, F., MARTINELLI, P., CHERUKURI, P. F., TEER, J. K., HANSEN, N. F., CRUZ, P., MULLIKIN FOR THE NISC COMPARATIVE SEQUENCING PROGRAM, J. C., BLAKESLEY, R. W., GOLAS, G., KWAN, J., SANDLER, A., FUENTES FAJARDO, K., MARKELLO, T., TIFFT, C., BLACKSTONE, C., RUGARLI, E. I., LANGER, T., GAHL, W. A. & TORO, C. 2011. Whole-exome sequencing identifies homozygous AFG3L2 mutations in a spastic ataxia-neuropathy syndrome linked to mitochondrial m-AAA proteases. *PLoS Genet,* 7**,** e1002325.

PILLSBURY, L. H., PETERS, S. M., WIENTZEN, R. L., PHILLIPS, T., PAPADOPOULOU, Z. L. & BELLANTI, J. A. 1985. Ataxia telangiectasia: immunologically mediated renal and hepatic failure. *Ann Allergy,* 55**,** 539-40, 593-8.

PIZARRO, J. G., FOLCH, J., VERDAGUER, E., JUNYENT, F. & PALLAS, M. 2009. ATM is involved in cell cycle control through the regulation of retinoblastoma protein phosphorylation in rat dopaminergic B65 cells. *Journal of Neurochemistry,* 110**,** 22-22.

PLAUT, I. 2000. Effects of fin size on swimming performance, swimming behaviour and routine activity of zebrafish Danio rerio. *J Exp Biol,* 203**,** 813-20.

PODHORECKA, M., SKLADANOWSKI, A. & BOZKO, P. 2010. H2AX Phosphorylation: Its Role in DNA Damage Response and Cancer Therapy. *Journal of nucleic acids,* 2010**,** 920161.

POLETTO, M., YANG, D., FLETCHER, S. C., VENDRELL, I., FISCHER, R., LEGRAND, A. J. & DIANOV, G. L. 2017. Modulation of proteostasis counteracts oxidative stress and affects DNA base excision repair capacity in ATM-deficient cells. *Nucleic acids research,* 45**,** 10042-10055.

PONOMAREVA, O. Y., ELICEIRI, K. W. & HALLORAN, M. C. 2016. Charcot-Marie-Tooth 2b associated Rab7 mutations cause axon growth and guidance defects during vertebrate sensory neuron development. *Neural Development,* 11**,** 14.

POSTLETHWAIT, J. H. 2006. The zebrafish genome: a review and msx gene case study. *Genome Dyn,* 2**,** 183-197.

POSTMA, A. V., BEZZINA, C. R., DE VRIES, J. F., WILDE, A. A., MOORMAN, A. F. & MANNENS, M. M. 2000. Genomic organisation and chromosomal localisation of two members of the KCND ion channel family, KCND2 and KCND3. *Hum Genet,* 106**,** 614-9.

POULIOT, J. J., YAO, K. C., ROBERTSON, C. A. & NASH, H. A. 1999. Yeast gene for a Tyr-DNA phosphodiesterase that repairs topoisomerase I complexes. *Science,* 286**,** 552-5.

POZZI, E., GIORGIO, E., MANCINI, C., LO BUONO, N., AUGERI, S., FERRERO, M., DI GREGORIO, E., RIBERI, E., VINCIGUERRA, M., NANETTI, L., BIANCHI, F. T., SASSI, M. P., COSTANZO, V., MARIOTTI, C., FUNARO, A., CAVALIERI, S. & BRUSCO, A. 2020. In vitro dexamethasone treatment does not induce alternative ATM transcripts in cells from Ataxia–Telangiectasia patients. *Scientific Reports,* 10**,** 20182.

PRYKHOZHIJ, S. V., FULLER, C., STEELE, S. L., VEINOTTE, C. J., RAZAGHI, B., ROBITAILLE, J. M., MCMASTER, C. R., SHLIEN, A., MALKIN, D. & BERMAN, J. N. 2018. Optimized knock-in of point mutations in zebrafish using CRISPR/Cas9. *Nucleic Acids Res,* 46**,** e102.

PUCKELWARTZ, M. J., KESSLER, E., ZHANG, Y., HODZIC, D., RANDLES, K. N., MORRIS, G., EARLEY, J. U., HADHAZY, M., HOLASKA, J. M., MEWBORN, S. K., PYTEL, P. & MCNALLY, E. M. 2009. Disruption of nesprin-1 produces an Emery Dreifuss muscular dystrophy-like phenotype in mice. *Hum Mol Genet,* 18**,** 607-20.

PYLE, A., SMERTENKO, T., BARGIELA, D., GRIFFIN, H., DUFF, J., APPLETON, M., DOUROUDIS, K., PFEFFER, G., SANTIBANEZ-KOREF, M., EGLON, G., YU-WAI-MAN, P., RAMESH, V., HORVATH, R. & CHINNERY, P. F. 2015. Exome sequencing in undiagnosed inherited and sporadic ataxias. *Brain,* 138**,** 276-83.

PYPE, S., DECLERCQ, W., IBRAHIMI, A., MICHIELS, C., VAN RIETSCHOTEN, J. G., DEWULF, N., DE BOER, M., VANDENABEELE, P., HUYLEBROECK, D. & REMACLE, J. E. 2000. TTRAP, a novel protein that associates with CD40, tumor necrosis factor (TNF) receptor-75 and TNF receptor-associated factors (TRAFs), and that inhibits nuclear factor-kappa B activation. *J Biol Chem,* 275**,** 18586-93.

QI, Y., QIU, Q., GU, X., TIAN, Y. & ZHANG, Y. 2016. ATM mediates spermidine-induced mitophagy via PINK1 and Parkin regulation in human fibroblasts. *Sci Rep,* 6**,** 24700.

QIAN, M., LIU, Z., PENG, L., MENG, F., TANG, X., AO, Y., SHI, L., ZHOU, M., WANG, M., QIN, B., CAO, X., WANG, Z., ZHOU, Z. & LIU, B. 2017. Boosting ATM Activity Promotes Longevity in Nematodes and Mice. *bioRxiv***,** 240606.

QIAN, M., LIU, Z., PENG, L., TANG, X., MENG, F., AO, Y., ZHOU, M., WANG, M., CAO, X., QIN, B., WANG, Z., ZHOU, Z., WANG, G., GAO, Z., XU, J. & LIU, B. 2018. Boosting ATM activity alleviates aging and extends lifespan in a mouse model of progeria. *Elife,* 7.

QUEK, H., LUFF, J., CHEUNG, K., KOZLOV, S., GATEI, M., LEE, C. S., BELLINGHAM, M., NOAKES, P., LIM, Y. C., BARNETT, N., DINGWALL, S., WOLVETANG, E., MASHIMO, T., ROBERTS, T. & LAVIN, M. 2016. Neuroinflammation drives the neuronal degenerative phenotype in a rat model of Ataxia-telangiectasia. *European Journal of Immunology,* 46**,** 1041-1042.

QUEK, H., LUFF, J., CHEUNG, K., KOZLOV, S., GATEI, M., LEE, C. S., BELLINGHAM, M. C., NOAKES, P. G., LIM, Y. C., BARNETT, N. L., DINGWALL, S., WOLVETANG, E., MASHIMO, T., ROBERTS, T. L. & LAVIN, M. F. 2017a. A rat model of ataxia-telangiectasia: evidence for a neurodegenerative phenotype. *Human Molecular Genetics,* 26**,** 109-123.

QUEK, H., LUFF, J., CHEUNG, K., KOZLOV, S., GATEI, M., LEE, C. S., BELLINGHAM, M. C., NOAKES, P. G., LIM, Y. C., BARNETT, N. L., DINGWALL, S., WOLVETANG, E., MASHIMO, T., ROBERTS, T. L. & LAVIN, M. F. 2017b. Rats with a missense mutation in Atm display neuroinflammation and neurodegeneration subsequent to accumulation of cytosolic DNA following unrepaired DNA damage. *J Leukoc Biol,* 101**,** 927-947.

QUINTERO-RIVERA, F., CHAN, A., DONOVAN, D. J., GUSELLA, J. F. & LIGON, A. H. 2007. Disruption of a synaptotagmin (SYT14) associated with neurodevelopmental abnormalities. *Am J Med Genet A,* 143a**,** 558-63.

RAGAMIN, A., YIGIT, G., BOUSSET, K., BELEGGIA, F., VERHEIJEN, F. W., DE WIT, M. Y., STROM, T. M., DÖRK, T., WOLLNIK, B. & MANCINI, G. M. S. 2020. Human RAD50 deficiency: Confirmation of a distinctive phenotype. *Am J Med Genet A,* 182**,** 1378-1386.

RAJAGOPALAN, S. & LONG, E. O. 2012. Cellular senescence induced by CD158d reprograms natural killer cells to promote vascular remodeling. *Proc Natl Acad Sci U S A,* 109**,** 20596-601.

RALSER, M., ALBRECHT, M., NONHOFF, U., LENGAUER, T., LEHRACH, H. & KROBITSCH, S. 2005. An integrative approach to gain insights into the cellular function of human ataxin-2. *J Mol Biol,* 346**,** 203-14.

RAMANAGOUDR-BHOJAPPA, R., CARRINGTON, B., RAMASWAMI, M., BISHOP, K., ROBBINS, G. M., JONES, M., HARPER, U., FREDERICKSON, S. C., KIMBLE, D. C., SOOD, R. & CHANDRASEKHARAPPA, S. C. 2018. Multiplexed CRISPR/Cas9-mediated knockout of 19 Fanconi anemia pathway genes in zebrafish revealed their roles in growth, sexual development and fertility. *PLoS Genet,* 14**,** e1007821.

RAMESH, T., LYON, A. N., PINEDA, R. H., WANG, C., JANSSEN, P. M., CANAN, B. D., BURGHES, A. H. & BEATTIE, C. E. 2010. A genetic model of amyotrophic lateral sclerosis in zebrafish displays phenotypic hallmarks of motoneuron disease. *Dis Model Mech,* 3**,** 652-62.

RAMMLER, D. H. & ZAFFARONI, A. 1967. Biological implications of DMSO based on a review of its chemical properties. *Ann N Y Acad Sci,* 141**,** 13-23.

RANUM, L. P., SCHUT, L. J., LUNDGREN, J. K., ORR, H. T. & LIVINGSTON, D. M. 1994. Spinocerebellar ataxia type 5 in a family descended from the grandparents of President Lincoln maps to chromosome 11. *Nat Genet,* 8**,** 280-4.

RASHI-ELKELES, S., ELKON, R., SHAVIT, S., LERENTHAL, Y., LINHART, C., KUPERSHTEIN, A., AMARIGLIO, N., RECHAVI, G., SHAMIR, R. & SHILOH, Y. 2011. Transcriptional modulation induced by ionizing radiation: p53 remains a central player. *Mol Oncol,* 5**,** 336-48.

RASHI-ELKELES, S., ELKON, R., WEIZMAN, N., LINHART, C., AMARIGLIO, N., STERNBERG, G., RECHAVI, G., BARZILAI, A., SHAMIR, R. & SHILOH, Y. 2006. Parallel induction of ATM-dependent pro- and antiapoptotic signals in response to ionizing radiation in murine lymphoid tissue. *Oncogene,* 25**,** 1584-92.

RASS, E., CHANDRAMOULY, G., ZHA, S., ALT, F. W. & XIE, A. 2013. Ataxia telangiectasia mutated (ATM) is dispensable for endonuclease I-SceI-induced homologous recombination in mouse embryonic stem cells. *J Biol Chem,* 288**,** 7086-95.

RAY, D., KAZAN, H., COOK, K. B., WEIRAUCH, M. T., NAJAFABADI, H. S., LI, X., GUEROUSSOV, S., ALBU, M., ZHENG, H., YANG, A., NA, H., IRIMIA, M., MATZAT, L. H., DALE, R. K., SMITH, S. A., YAROSH, C. A., KELLY, S. M., NABET, B., MECENAS, D., LI, W., LAISHRAM, R. S., QIAO, M., LIPSHITZ, H. D., PIANO, F., CORBETT, A. H., CARSTENS, R. P., FREY, B. J., ANDERSON, R. A., LYNCH, K. W., PENALVA, L. O. F., LEI, E. P., FRASER, A. G., BLENCOWE, B. J., MORRIS, Q. D. & HUGHES, T. R. 2013. A compendium of RNA-binding motifs for decoding gene regulation. *Nature,* 499**,** 172-177.

RCSB. 2017. *ATM Closed Conformation- 5NP0* [Online]. Available: http://www.rcsb.org/structure/5NP0 [Accessed 26/03.2020 2020].

REED, W. B., EPSTEIN, W. L., BODER, E. & SEDGWICK, R. 1966. Cutaneous manifestations of ataxia - telangiectasia. *JAMA,* 195**,** 746-753.

REIMAN, A., SRINIVASAN, V., BARONE, G., LAST, J. I., WOOTTON, L. L., DAVIES, E. G., VERHAGEN, M. M., WILLEMSEN, M. A., WEEMAES, C. M., BYRD, P. J., IZATT, L., EASTON, D. F., THOMPSON, D. J. & TAYLOR, A. M. 2011. Lymphoid tumours and breast cancer in ataxia telangiectasia; substantial protective effect of residual ATM kinase activity against childhood tumours. *Br J Cancer,* 105**,** 586-91.

REINA-SAN-MARTIN, B., CHEN, H. T., NUSSENZWEIG, A. & NUSSENZWEIG, M. C. 2004a. ATM is required for efficient recombination between immunoglobulin switch regions. *Journal of Experimental Medicine,* 200**,** 1103-1110.

REINA-SAN-MARTIN, B., CHEN, H. T., NUSSENZWEIG, A. & NUSSENZWEIG, M. C. 2004b. ATM is required for efficient recombination between immunoglobulin switch regions. *J Exp Med,* 200**,** 1103-10.

REISZ, J. A., BANSAL, N., QIAN, J., ZHAO, W. & FURDUI, C. M. 2014. Effects of ionizing radiation on biological molecules--mechanisms of damage and emerging methods of detection. *Antioxidants & redox signaling,* 21, 260-292.

RELIENE, R., FLEMING, S. M., CHESSELET, M. F. & SCHIESTL, R. H. 2008. Effects of antioxidants on cancer prevention and neuromotor performance in Atm deficient mice. *Food Chem Toxicol,* 46, 1371-7.

RICHTER, A., RIOUX, J. D., BOUCHARD, J. P., MERCIER, J., MATHIEU, J., GE, B., POIRIER, J., JULIEN, D., GYAPAY, G., WEISSENBACH, J., HUDSON, T. J., MELANCON, S. B. & MORGAN, K. 1999. Location score and haplotype analyses of the locus for autosomal recessive spastic ataxia of Charlevoix-Saguenay, in chromosome region 13q11. *Am J Hum Genet,* 64, 768-75.

RIMKUS, S. A., KATZENBERGER, R. J., TRINH, A. T., DODSON, G. E., TIBBETTS, R. S. & WASSARMAN, D. A. 2008. Mutations in String/CDC25 inhibit cell cycle re-entry and neurodegeneration in a Drosophila model of Ataxia telangiectasia. *Genes & development,* 22, 1205-1220.

RIMKUS, S. A., PETERSEN, A. J., KATZENBERGER, R. J. & WASSARMAN, D. A. 2010. The effect of ATM knockdown on ionizing radiation-induced neuronal cell cycle reentry in Drosophila. *Cell cycle (Georgetown, Tex.),* 9, 2686-2687.

ROBITAILLE, Y., SCHUT, L. & KISH, S. J. 1995. Structural and immunocytochemical features of olivopontocerebellar atrophy caused by the spinocerebellar ataxia type 1 (SCA-1) mutation define a unique phenotype. *Acta Neuropathol,* 90, 572-81.

ROBU, M. E., LARSON, J. D., NASEVICIUS, A., BEIRAGHI, S., BRENNER, C., FARBER, S. A. & EKKER, S. C. 2007. p53 activation by knockdown technologies. *PLoS Genet,* 3, e78.

RODRIGUEZ-MARI, A., CANESTRO, C., BREMILLER, R. A., NGUYEN-JOHNSON, A., ASAKAWA, K., KAWAKAMI, K. & POSTLETHWAIT, J. H. 2010. Sex reversal in zebrafish fancl mutants is caused by Tp53-mediated germ cell apoptosis. *PLoS Genet,* 6, e1001034.

RODRÍGUEZ-MARÍ, A., CAÑESTRO, C., BREMILLER, R. A., NGUYEN-JOHNSON, A., ASAKAWA, K., KAWAKAMI, K. & POSTLETHWAIT, J. H. 2010. Sex reversal in zebrafish fancl mutants is caused by Tp53-mediated germ cell apoptosis. *PLoS Genet,* 6, e1001034.

RODRÍGUEZ-MARÍ, A., WILSON, C., TITUS, T. A., CAÑESTRO, C., BREMILLER, R. A., YAN, Y. L., NANDA, I., JOHNSTON, A., KANKI, J. P., GRAY, E. M., HE, X., SPITSBERGEN, J., SCHINDLER, D. & POSTLETHWAIT, J. H. 2011. Roles of brca2 (fancd1) in oocyte nuclear architecture, gametogenesis, gonad tumors, and genome stability in zebrafish. *PLoS Genet,* 7, e1001357.

ROGATCHEVA, M. B., FRITZ, K. L., RUND, L. A., POLLOCK, C. B., BEEVER, J. E., COUNTER, C. M. & SCHOOK, L. B. 2007. Characterization of the porcine ATM gene: Towards the generation of a novel non-murine animal model for Ataxia-Telangiectasia. *Gene,* 405, 27-35.

ROTH, D. B. 2014. V(D)J Recombination: Mechanism, Errors, and Fidelity. *Microbiol Spectr,* 2.

ROTHBLUM-OVIATT, C., WRIGHT, J., LEFTON-GREIF, M. A., MCGRATH-MORROW, S. A., CRAWFORD, T. O. & LEDERMAN, H. M. 2016. Ataxia telangiectasia: a review. *Orphanet J Rare Dis,* 11, 159.

RUBINSTEIN, J. D., BURNS, K., ABSALON, M., LUTZKO, C., LEEMHUIS, T., CHANDRA, S., HANLEY, P. J., KELLER, M. D., DAVIES, S. M., NELSON, A. & GRIMLEY, M. 2020. EBV-directed viral-specific T-lymphocyte therapy for the treatment of EBV-driven lymphoma in two patients with primary immunodeficiency and DNA repair defects. *Pediatric Blood & Cancer,* 67, 6.

RYO, S., WIJDEVEN, R. H., TYAGI, A., HERMSEN, T., KONO, T., KARUNASAGAR, I., ROMBOUT, J. H., SAKAI, M., VERBURG-VAN KEMENADE, B. M. & SAVAN, R. 2010. Common carp have two subclasses of bonyfish specific antibody IgZ showing differential expression in response to infection. *Dev Comp Immunol,* 34, 1183-90.

RYTER, S. W., KIM, H. P., HOETZEL, A., PARK, J. W., NAKAHIRA, K., WANG, X. & CHOI, A. M. 2007. Mechanisms of cell death in oxidative stress. *Antioxid Redox Signal,* 9, 49-89.

SAAR, K., CHRZANOWSKA, K. H., STUMM, M., JUNG, M., NÜRNBERG, G., WIENKER, T. F., SEEMANOVÁ, E., WEGNER, R. D., REIS, A. & SPERLING, K. 1997. The gene for the ataxia-telangiectasia variant, Nijmegen breakage syndrome, maps to a 1-cM interval on chromosome 8q21. *Am J Hum Genet,* 60**,** 605-10.

SACKERMAN, J., DONEGAN, J. J., CUNNINGHAM, C. S., NGUYEN, N. N., LAWLESS, K., LONG, A., BENNO, R. H. & GOULD, G. G. 2010. Zebrafish Behavior in Novel Environments: Effects of Acute Exposure to Anxiolytic Compounds and Choice of Danio rerio Line. *International journal of comparative psychology / ISCP ; sponsored by the International Society for Comparative Psychology and the University of Calabria,* 23**,** 43-61.

SAFAR, A. M., SPENCER, H., 3RD, SU, X., COFFEY, M., COONEY, C. A., RATNASINGHE, L. D., HUTCHINS, L. F. & FAN, C. Y. 2005. Methylation profiling of archived non-small cell lung cancer: a promising prognostic system. *Clin Cancer Res,* 11**,** 4400-5.

SAITO, K., SIEGFRIED, K. R., NUSSLEIN-VOLHARD, C. & SAKAI, N. 2011. Isolation and Cytogenetic Characterization of Zebrafish Meiotic Prophase I Mutants. *Developmental Dynamics,* 240**,** 1779-1792.

SAKASAI, R., TERAOKA, H., TAKAGI, M. & TIBBETTS, R. S. 2010. Transcription-dependent Activation of Ataxia Telangiectasia Mutated Prevents DNA-dependent Protein Kinase-mediated Cell Death in Response to Topoisomerase I Poison. *Journal of Biological Chemistry,* 285**,** 15201-15208.

SALLMYR, A. & TOMKINSON, A. E. 2018. Repair of DNA double-strand breaks by mammalian alternative end-joining pathways. *The Journal of biological chemistry,* 293**,** 10536-10546.

SALMAN, M. S., LEE, E. J., TJAHJADI, A. & CHODIRKER, B. N. 2013. The epidemiology of intermittent and chronic ataxia in children in Manitoba, Canada. *Developmental Medicine and Child Neurology,* 55**,** 341-347.

SANAL, O., ERSOY, F., YEL, L., TEZCAN, I., METIN, A., OZYÜREK, H., GARIBOGLU, S., FIKRIG, S., BERKEL, A. I., RIJKERS, G. T. & ZEGERS, B. J. 1999. Impaired IgG antibody production to pneumococcal polysaccharides in patients with ataxia-telangiectasia. *J Clin Immunol,* 19**,** 326-34.

SANAL, O., WEI, S., FOROUD, T., MALHOTRA, U., CONCANNON, P., CHARMLEY, P., SALSER, W., LANGE, K. & GATTI, R. A. 1990. Further mapping of an ataxia-telangiectasia locus to the chromosome 11q23 region. *Am J Hum Genet,* 47**,** 860-6.

SANDOVAL, N., PLATZER, M., ROSENTHAL, A., DÖRK, T., BENDIX, R., SKAWRAN, B., STUHRMANN, M., WEGNER, R.-D., SPERLING, K., BANIN, S., SHILOH, Y., BAUMER, A., BERNTHALER, U., SENNEFELDER, H., BROHM, M., WEBER, B. H. F. & SCHINDLER, D. 1999. Characterization of ATM Gene Mutations in 66 Ataxia Telangiectasia Families. *Human Molecular Genetics,* 8**,** 69-79.

SANO, H., KANE, S., SANO, E., MÎINEA, C. P., ASARA, J. M., LANE, W. S., GARNER, C. W. & LIENHARD, G. E. 2003. Insulin-stimulated phosphorylation of a Rab GTPase-activating protein regulates GLUT4 translocation. *J Biol Chem,* 278**,** 14599-602.

SANO, Y., DATE, H., IGARASHI, S., ONODERA, O., OYAKE, M., TAKAHASHI, T., HAYASHI, S., MORIMATSU, M., TAKAHASHI, H., MAKIFUCHI, T., FUKUHARA, N. & TSUJI, S. 2004. Aprataxin, the causative protein for EAOH is a nuclear protein with a potential role as a DNA repair protein. *Ann Neurol,* 55**,** 241-9.

SARBASSOV, D. D., ALI, S. M. & SABATINI, D. M. 2005. Growing roles for the mTOR pathway. *Curr Opin Cell Biol,* 17**,** 596-603.

SASAKI, M., IKEDA, H., SATO, Y. & NAKANUMA, Y. 2008. Proinflammatory cytokine-induced cellular senescence of biliary epithelial cells is mediated via oxidative stress and activation of ATM pathway: A culture study. *Free Radical Research,* 42**,** 625-632.

SATO, N., AMINO, T., KOBAYASHI, K., ASAKAWA, S., ISHIGURO, T., TSUNEMI, T., TAKAHASHI, M., MATSUURA, T., FLANIGAN, K. M., IWASAKI, S., ISHINO, F., SAITO, Y., MURAYAMA, S., YOSHIDA, M., HASHIZUME, Y., TAKAHASHI, Y., TSUJI, S., SHIMIZU, N., TODA, T., ISHIKAWA, K. & MIZUSAWA, H. 2009. Spinocerebellar ataxia type 31 is associated with "inserted" penta-nucleotide repeats containing (TGGAA)n. *Am J Hum Genet,* 85**,** 544-57.

SATTERFIELD, T. F. & PALLANCK, L. J. 2006. Ataxin-2 and its Drosophila homolog, ATX2, physically assemble with polyribosomes. *Hum Mol Genet,* 15**,** 2523-32.

SAUNDERS-PULLMAN, R., RAYMOND, D., STOESSL, A. J., HOBSON, D., NAKAMURA, K., PULLMAN, S., LEFTON, D., OKUN, M. S., UITTI, R., SACHDEV, R., STANLEY, K., SAN LUCIANO, M., HAGENAH, J., GATTI, R., OZELIUS, L. J. & BRESSMAN, S. B. 2012. Variant ataxia-telangiectasia presenting as primary-appearing dystonia in Canadian Mennonites. *Neurology,* 78**,** 649-57.

SAVIC, V., YIN, B., MAAS, N. L., BREDEMEYER, A. L., CARPENTER, A. C., HELMINK, B. A., YANG-IOTT, K. S., SLECKMAN, B. P. & BASSING, C. H. 2009. Formation of dynamic gamma-H2AX domains along broken DNA strands is distinctly regulated by ATM and MDC1 and dependent upon H2AX densities in chromatin. *Mol Cell,* 34**,** 298-310.

SAVIOZZI, S., SALUTO, A., TAYLOR, A. M., LAST, J. I., TREBINI, F., PARADISO, M. C., GROSSO, E., FUNARO, A., PONZIO, G., MIGONE, N. & BRUSCO, A. 2002. A late onset variant of ataxia-telangiectasia with a compound heterozygous genotype, A8030G/7481insA. *J Med Genet,* 39**,** 57-61.

SAVITSKY, K., BAR-SHIRA, A., GILAD, S., ROTMAN, G., ZIV, Y., VANAGAITE, L., TAGLE, D. A., SMITH, S., UZIEL, T., SFEZ, S., ASHKENAZI, M., PECKER, I., FRYDMAN, M., HARNIK, R., PATANJALI, S. R., SIMMONS, A., CLINES, G. A., SARTIEL, A., GATTI, R. A., CHESSA, L., SANAL, O., LAVIN, M. F., JASPERS, N. G., TAYLOR, A. M., ARLETT, C. F., MIKI, T., WEISSMAN, S. M., LOVETT, M., COLLINS, F. S. & SHILOH, Y. 1995. A single ataxia telangiectasia gene with a product similar to PI-3 kinase. *Science,* 268**,** 1749-53.

SCHALCH, D. S., MCFARLIN, D. E. & BARLOW, M. H. 1970. An unusual form of diabetes mellitus in ataxia telangiectasia. *N Engl J Med,* 282**,** 1396-402.

SCHELHAAS, H. J., VERBEEK, D. S., VAN DE WARRENBURG, B. P. & SINKE, R. J. 2004. SCA19 and SCA22: evidence for one locus with a worldwide distribution. *Brain.* England.

SCHERTHAN, H., JERRATSCH, M., DHAR, S., WANG, Y. A., GOFF, S. P. & PANDITA, T. K. 2000. Meiotic telomere distribution and Sertoli cell nuclear architecture are altered in Atm- and Atm-p53-deficient mice. *Molecular and cellular biology,* 20**,** 7773-7783.

SCHLAM-BABAYOV, S., BENSIMON, A., HAREL, M., GEIGER, T., AEBERSOLD, R., ZIV, Y. & SHILOH, Y. 2020. Phosphoproteomics reveals novel modes of function and inter-relationships among PIKKs in response to genotoxic stress. *The EMBO Journal,* n/a**,** e104400.

SCHMID, B., HRUSCHA, A., HOGL, S., BANZHAF-STRATHMANN, J., STRECKER, K., VAN DER ZEE, J., TEUCKE, M., EIMER, S., HEGERMANN, J., KITTELMANN, M., KREMMER, E., CRUTS, M., SOLCHENBERGER, B., HASENKAMP, L., VAN BEBBER, F., VAN BROECKHOVEN, C., EDBAUER, D., LICHTENTHALER, S. F. & HAASS, C. 2013. Loss of ALS-associated TDP-43 in zebrafish causes muscle degeneration, vascular dysfunction, and reduced motor neuron axon outgrowth. *Proc Natl Acad Sci U S A,* 110**,** 4986-91.

SCHMIDT, W. M., RUTLEDGE, S. L., SCHULE, R., MAYERHOFER, B., ZUCHNER, S., BOLTSHAUSER, E. & BITTNER, R. E. 2015. Disruptive SCYL1 Mutations Underlie a Syndrome Characterized by Recurrent Episodes of Liver Failure, Peripheral Neuropathy, Cerebellar Atrophy, and Ataxia. *Am J Hum Genet,* 97**,** 855-61.

SCHMUCKER, S., ARGENTINI, M., CARELLE-CALMELS, N., MARTELLI, A. & PUCCIO, H. 2008. The in vivo mitochondrial two-step maturation of human frataxin. *Hum Mol Genet,* 17**,** 3521-31.

SCHNEIDER, J. G., FINCK, B. N., REN, J., STANDLEY, K. N., TAKAGI, M., MACLEAN, K. H., BERNAL-MIZRACHI, C., MUSLIN, A. J., KASTAN, M. B. & SEMENKOVICH, C. F. 2006. ATM-dependent suppression of stress signaling reduces vascular disease in metabolic syndrome. *Cell Metab,* 4**,** 377-89.

SCHNIEPP, R., MÖHWALD, K. & WUEHR, M. 2017. Gait ataxia in humans: vestibular and cerebellar control of dynamic stability. *Journal of Neurology,* 264**,** 87-92.

SCHNIEPP, R., WUEHR, M., NEUHAEUSSER, M., KAMENOVA, M., DIMITRIADIS, K., KLOPSTOCK, T., STRUPP, M., BRANDT, T. & JAHN, K. 2012. Locomotion speed determines gait variability in cerebellar ataxia and vestibular failure. *Mov Disord,* 27**,** 125-31.

SCHOENAKER, M. H. D., VAN OS, N. J. H., VAN DER FLIER, M., VAN DEUREN, M., SEYGER, M. M., TAYLOR, A. M. R., WEEMAES, C. M. R. & WILLEMSEN, M. 2018. Telangiectasias in Ataxia Telangiectasia: Clinical significance, role of ATM deficiency and potential pathophysiological mechanisms. *Eur J Med Genet,* 61**,** 284-287.

SCHOLS, L., SZYMANSKI, S., PETERS, S., PRZUNTEK, H., EPPLEN, J. T., HARDT, C. & RIESS, O. 2000. Genetic background of apparently idiopathic sporadic cerebellar ataxia. *Hum Genet,* 107**,** 132-7.

SCHOLS, L., VIEIRA-SAECKER, A. M., SCHOLS, S., PRZUNTEK, H., EPPLEN, J. T. & RIESS, O. 1995. Trinucleotide expansion within the MJD1 gene presents clinically as spinocerebellar ataxia and occurs most frequently in German SCA patients. *Hum Mol Genet,* 4**,** 1001-5.

SCHUBERT, R., ERKER, L., BARLOW, C., YAKUSHIJI, H., LARSON, D., RUSSO, A., MITCHELL, J. B. & WYNSHAW-BORIS, A. 2004. Cancer chemoprevention by the antioxidant tempol in Atm-deficient mice. *Hum Mol Genet,* 13**,** 1793-802.

SCHUBERT, R., REICHENBACH, J. & ZIELEN, S. 2002. Deficiencies in CD4+ and CD8+ T cell subsets in ataxia telangiectasia. *Clin Exp Immunol,* 129**,** 125-32.

SCHULZ, J. B., BORKERT, J., WOLF, S., SCHMITZ-HUBSCH, T., RAKOWICZ, M., MARIOTTI, C., SCHOELS, L., TIMMANN, D., VAN DE WARRENBURG, B., DURR, A., PANDOLFO, M., KANG, J. S., MANDLY, A. G., NAGELE, T., GRISOLI, M., BOGUSLAWSKA, R., BAUER, P., KLOCKGETHER, T. & HAUSER, T. K. 2010a. Visualization, quantification and correlation of brain atrophy with clinical symptoms in spinocerebellar ataxia types 1, 3 and 6. *Neuroimage,* 49**,** 158-168.

SCHULZ, R. D. W., MENTING, S., BOGERD, J., FRANÇA, L. R., VILELA, D. A. R. & GODINHO, H. P. 2005. Sertoli Cell Proliferation in the Adult Testis—Evidence from Two Fish Species Belonging to Different Orders1. *Biology of Reproduction,* 73**,** 891-898.

SCHULZ, R. W., DE FRANÇA, L. R., LAREYRE, J.-J., LEGAC, F., CHIARINI-GARCIA, H., NOBREGA, R. H. & MIURA, T. 2010b. Spermatogenesis in fish. *General and Comparative Endocrinology,* 165**,** 390-411.

SCHULZ, R. W., NOBREGA, R. H., MORAIS, R., DE WAAL, P. P., FRANCA, L. R. & BOGERD, J. 2015. Endocrine and paracrine regulation of zebrafish spermatogenesis: the Sertoli cell perspective. *Animal Reproduction,* 12**,** 81-87.

SCHURIG, V., ORMAN, A. V. & BOWEN, P. 1981. Nonprogressive cerebellar disorder with mental retardation and autosomal recessive inheritance in Hutterites. *Am J Med Genet,* 9**,** 43-53.

SCHWEIGHOFER, N., LERCHBAUM, E., TRUMMER, O., SCHWETZ, V., PIEBER, T. & OBERMAYER-PIETSCH, B. 2014. Metformin resistance alleles in polycystic ovary syndrome: pattern and association with glucose metabolism. *Pharmacogenomics,* 15**,** 305-317.

SCHWEIKL, H., PETZEL, C., BOLAY, C., HILLER, K. A., BUCHALLA, W. & KRIFKA, S. 2014. Signaling through ATM and p53 mediates HEMA-induced apoptosis. *Naunyn-Schmiedebergs Archives of Pharmacology,* 387**,** S91-S91.

SCOTT, S. P., BENDIX, R., CHEN, P., CLARK, R., DORK, T. & LAVIN, M. F. 2002. Missense mutations but not allelic variants alter the function of ATM by dominant interference in patients with breast cancer. *Proc Natl Acad Sci U S A,* 99**,** 925-30.

SEEMANOVÁ, E., PASSARGE, E., BENESKOVA, D., HOUSTĚK, J., KASAL, P. & SEVCÍKOVÁ, M. 1985. Familial microcephaly with normal intelligence, immunodeficiency, and risk for lymphoreticular malignancies: a new autosomal recessive disorder. *Am J Med Genet,* 20**,** 639-48.

SEIDEL, J. J., ANDERSON, C. M. & BLACKBURN, E. H. 2008. A novel Tel1/ATM N-terminal motif, TAN, is essential for telomere length maintenance and a DNA damage response. *Mol Cell Biol,* 28**,** 5736-46.

SEKIGUCHI, J., FERGUSON, D. O., CHEN, H. T., YANG, E. M., EARLE, J., FRANK, K., WHITLOW, S., GU, Y., XU, Y., NUSSENZWEIG, A. & ALT, F. W. 2001. Genetic interactions between ATM and the nonhomologous end-joining factors in genomic stability and development. *Proceedings of the National Academy of Sciences,* 98**,** 3243.

SENDEREK, J., KRIEGER, M., STENDEL, C., BERGMANN, C., MOSER, M., BREITBACH-FALLER, N., RUDNIK-SCHONEBORN, S., BLASCHEK, A., WOLF, N. I., HARTING, I., NORTH, K., SMITH, J., MUNTONI, F., BROCKINGTON, M., QUIJANO-ROY, S., RENAULT, F., HERRMANN, R., HENDERSHOT, L. M., SCHRODER, J. M., LOCHMULLER, H., TOPALOGLU, H., VOIT, T., WEIS, J., EBINGER, F. & ZERRES, K. 2005. Mutations in SIL1 cause Marinesco-Sjogren syndrome, a cerebellar ataxia with cataract and myopathy. *Nat Genet,* 37**,** 1312-4.

SERVADIO, A., KOSHY, B., ARMSTRONG, D., ANTALFFY, B., ORR, H. T. & ZOGHBI, H. Y. 1995. Expression analysis of the ataxin-1 protein in tissues from normal and spinocerebellar ataxia type 1 individuals. *Nat Genet,* 10**,** 94-8.

SHAIKH, A. G., MARTI, S., TARNUTZER, A. A., PALLA, A., CRAWFORD, T. O., STRAUMANN, D., TAYLOR, A. M. & ZEE, D. S. 2009. Gaze fixation deficits and their implication in ataxia-telangiectasia. *J Neurol Neurosurg Psychiatry,* 80**,** 858-64.

SHAIKH, A. G., ZEE, D. S., MANDIR, A. S., LEDERMAN, H. M. & CRAWFORD, T. O. 2013. Disorders of Upper Limb Movements in Ataxia-Telangiectasia. *PLoS One,* 8**,** e67042.

SHANBHAG, N. M., RAFALSKA-METCALF, I. U., BALANE-BOLIVAR, C., JANICKI, S. M. & GREENBERG, R. A. 2010. ATM-dependent chromatin changes silence transcription in cis to DNA double-strand breaks. *Cell,* 141**,** 970-81.

SHANG, E. H., YU, R. M. & WU, R. S. 2006. Hypoxia affects sex differentiation and development, leading to a male-dominated population in zebrafish (Danio rerio). *Environ Sci Technol,* 40**,** 3118-22.

SHARMA, N. K., LEBEDEVA, M., THOMAS, T., KOVALENKO, O. A., STUMPF, J. D., SHADEL, G. S. & SANTOS, J. H. 2014. Intrinsic mitochondrial DNA repair defects in Ataxia Telangiectasia. *DNA Repair (Amst),* 13**,** 22-31.

SHEN, Y., LEE, G., CHOE, Y., ZOLTEWICZ, J. S. & PETERSON, A. S. 2007. Functional architecture of atrophins. *J Biol Chem,* 282**,** 5037-44.

SHENG, D., QU, D., KWOK, K. H., NG, S. S., LIM, A. Y., AW, S. S., LEE, C. W., SUNG, W. K., TAN, E. K., LUFKIN, T., JESUTHASAN, S., SINNAKARUPPAN, M. & LIU, J. 2010. Deletion of the WD40 domain of LRRK2 in Zebrafish causes Parkinsonism-like loss of neurons and locomotive defect. *PLoS Genet,* 6**,** e1000914.

SHI, C. H., SCHISLER, J. C., RUBEL, C. E., TAN, S., SONG, B., MCDONOUGH, H., XU, L., PORTBURY, A. L., MAO, C. Y., TRUE, C., WANG, R. H., WANG, Q. Z., SUN, S. L., SEMINARA, S. B., PATTERSON, C. & XU, Y. M. 2014. Ataxia and hypogonadism caused by the loss of ubiquitin ligase activity of the U box protein CHIP. *Hum Mol Genet,* 23**,** 1013-24.

SHI, S.-R., SHI, Y. & TAYLOR, C. R. 2011. Antigen retrieval immunohistochemistry: review and future prospects in research and diagnosis over two decades. *The journal of histochemistry and cytochemistry : official journal of the Histochemistry Society,* 59**,** 13-32.

SHI, Y., WANG, J., LI, J. D., REN, H., GUAN, W., HE, M., YAN, W., ZHOU, Y., HU, Z., ZHANG, J., XIAO, J., SU, Z., DAI, M., JIANG, H., GUO, J., ZHANG, F., LI, N., DU, J., XU, Q., HU, Y., PAN, Q., SHEN, L., WANG, G., XIA, K., ZHANG, Z. & TANG, B. 2013. Identification of CHIP as a novel causative gene for autosomal recessive cerebellar ataxia. *PLoS One,* 8**,** e81884.

SHILOH, Y., TABOR, E. & BECKER, Y. 1982. Colony-forming ability of ataxia-telangiectasia skin fibroblasts is an indicator of their early senescence and increased demand for growth factors. *Exp Cell Res,* 140**,** 191-9.

SHILOH, Y. & ZIV, Y. 2013. The ATM protein kinase: regulating the cellular response to genotoxic stress, and more. *Nat Rev Mol Cell Biol,* 14**,** 197-210.

SHIMAZAKI, H., KOBAYASHI, J., SUGAYA, R., NAKANO, I. & FUJIMOTO, S. 2020. Late-onset autosomal recessive cerebellar ataxia and neuropathy with a novel splicing mutation in the ATM gene. *J Integr Neurosci,* 19**,** 125-129.

SHIMOHATA, T., NAKAJIMA, T., YAMADA, M., UCHIDA, C., ONODERA, O., NARUSE, S., KIMURA, T., KOIDE, R., NOZAKI, K., SANO, Y., ISHIGURO, H., SAKOE, K., OOSHIMA, T., SATO, A., IKEUCHI, T., OYAKE, M., SATO, T., AOYAGI, Y., HOZUMI, I., NAGATSU, T., TAKIYAMA, Y., NISHIZAWA, M., GOTO, J., KANAZAWA, I., DAVIDSON, I., TANESE, N., TAKAHASHI, H. & TSUJI, S. 2000. Expanded polyglutamine stretches interact with TAFII130, interfering with CREB-dependent transcription. *Nat Genet,* 26**,** 29-36.

SHIVE, H. R., WEST, R. R., EMBREE, L. J., AZUMA, M., SOOD, R., LIU, P. & HICKSTEIN, D. D. 2010. brca2 in zebrafish ovarian development, spermatogenesis, and tumorigenesis. *Proc Natl Acad Sci U S A,* 107**,** 19350-5.

SHUKLA, A., UPADHYAI, P., SHAH, J., NEETHUKRISHNA, K., BIELAS, S. & GIRISHA, K. M. 2017. Autosomal recessive spinocerebellar ataxia 20: Report of a new patient and review of literature. *European Journal of Medical Genetics,* 60**,** 118-123.

SIEGFRIED, K. R. & NÜSSLEIN-VOLHARD, C. 2008. Germ line control of female sex determination in zebrafish. *Dev Biol,* 324**,** 277-87.

SILICIANO, J. D., CANMAN, C. E., TAYA, Y., SAKAGUCHI, K., APPELLA, E. & KASTAN, M. B. 1997. DNA damage induces phosphorylation of the amino terminus of p53. *Genes Dev,* 11**,** 3471-81.

SILVA, E., TIONG, S., PEDERSEN, M., HOMOLA, E., ROYOU, A., FASULO, B., SIRIACO, G. & CAMPBELL, S. D. 2004. ATM is required for telomere maintenance and chromosome stability during Drosophila development. *Curr Biol,* 14**,** 1341-7.

SLANCHEV, K., STEBLER, J., DE LA CUEVA-MÉNDEZ, G. & RAZ, E. 2005. Development without germ cells: The role of the germ line in zebrafish sex differentiation. *Proceedings of the National Academy of Sciences of the United States of America,* 102**,** 4074.

SMALLWOOD, P. M., MUNOZ-SANJUAN, I., TONG, P., MACKE, J. P., HENDRY, S. H., GILBERT, D. J., COPELAND, N. G., JENKINS, N. A. & NATHANS, J. 1996. Fibroblast growth factor (FGF) homologous factors: new members of the FGF family implicated in nervous system development. *Proc Natl Acad Sci U S A,* 93**,** 9850-7.

SO, S., DAVIS, A. J. & CHEN, D. J. 2010. Autophosphorylation at serine 1981 stabilizes ATM at DNA damage sites (vol 7, pg 977, 2009). *Journal of Cell Biology,* 188**,** 443-443.

SONG, Y. H., MIREY, G., BETSON, M., HABER, D. A. & SETTLEMAN, J. 2004. The Drosophila ATM ortholog, dATM, mediates the response to ionizing radiation and to spontaneous DNA damage during development. *Curr Biol,* 14**,** 1354-9.

SORDET, O., NAKAMURA, A. J., REDON, C. E. & POMMIER, Y. 2010. DNA double-strand breaks and ATM activation by transcription-blocking DNA lesions. *Cell Cycle,* 9**,** 274-278.

SORDET, O., REDON, C. E., GUIROUILH-BARBAT, J., SMITH, S., SOLIER, S., DOUARRE, C., CONTI, C., NAKAMURA, A. J., DAS, B. B., NICOLAS, E., KOHN, K. W., BONNER, W. M. & POMMIER, Y. 2009. Ataxia telangiectasia mutated activation by transcription- and topoisomerase I-induced DNA double-strand breaks. *EMBO Rep,* 10**,** 887-93.

SOUSA, S. B., RAMOS, F., GARCIA, P., PAIS, R. P., PAIVA, C., BEALES, P. L., MOORE, G. E., SARAIVA, J. M. & HENNEKAM, R. C. 2014. Intellectual disability, coarse face, relative macrocephaly, and cerebellar hypotrophy in two sisters. *Am J Med Genet A,* 164a**,** 10-4.

SOUTOGLOU, E. & MISTELI, T. 2008. Activation of the cellular DNA damage response in the absence of DNA lesions. *Science,* 320**,** 1507-10.

SPENCER, A. C., HECK, A., TAKEUCHI, N., WATANABE, K. & SPREMULLI, L. L. 2004. Characterization of the human mitochondrial methionyl-tRNA synthetase. *Biochemistry,* 43**,** 9743-54.

SPOENDLIN, H. 1974. Optic cochleovestibular degenerations in hereditary ataxias. II. Temporal bone pathology in two cases of Friedreich's ataxia with vestibulo-cochlear disorders. *Brain,* 97**,** 41-8.

SPRING, K., CROSS, S., LI, C., WATTERS, D., BEN-SENIOR, L., WARING, P., AHANGARI, F., LU, S. L., CHEN, P., MISKO, I., PATERSON, C., KAY, G., SMORODINSKY, N. I., SHILOH, Y. & LAVIN, M. F. 2001. Atm knock-in mice harboring an in-frame deletion corresponding to the human ATM 7636del9 common mutation exhibit a variant phenotype. *Cancer Research,* 61**,** 4561-4568.

ST GEORGE-HYSLOP, P., ROGAEVA, E., HUTERER, J., TSUDA, T., SANTOS, J., HAINES, J. L., SCHLUMPF, K., ROGAEV, E. I., LIANG, Y., MCLACHLAN, D. R. & ET AL. 1994. Machado-Joseph disease in pedigrees of Azorean descent is linked to chromosome 14. *Am J Hum Genet,* 55**,** 120-5.

STANKEWICH, M. C., TSE, W. T., PETERS, L. L., CH'NG, Y., JOHN, K. M., STABACH, P. R., DEVARAJAN, P., MORROW, J. S. & LUX, S. E. 1998. A widely expressed betaIII spectrin associated with Golgi and cytoplasmic vesicles. *Proc Natl Acad Sci U S A,* 95**,** 14158-63.

STANKOVIC, T., KIDD, A. M., SUTCLIFFE, A., MCGUIRE, G. M., ROBINSON, P., WEBER, P., BEDENHAM, T., BRADWELL, A. R., EASTON, D. F., LENNOX, G. G., HAITES, N., BYRD, P. J. & TAYLOR, A. M. 1998. ATM mutations and phenotypes in ataxia-telangiectasia families in the British Isles: expression of mutant ATM and the risk of leukemia, lymphoma, and breast cancer. *American journal of human genetics,* 62**,** 334-345.

STAPLES, E. R., MCDERMOTT, E. M., REIMAN, A., BYRD, P. J., RITCHIE, S., TAYLOR, A. M. & DAVIES, E. G. 2008. Immunodeficiency in ataxia telangiectasia is correlated strongly with the presence of two null mutations in the ataxia telangiectasia mutated gene. *Clin Exp Immunol,* 153**,** 214-20.

STERN, N., HOCHMAN, A., ZEMACH, N., WEIZMAN, N., HAMMEL, I., SHILOH, Y., ROTMAN, G. & BARZILAI, A. 2002. Accumulation of DNA damage and reduced levels of nicotine adenine dinucleotide in the brains of Atm-deficient mice. *J Biol Chem,* 277**,** 602-8.

STEWART, G. S., MASER, R. S., STANKOVIC, T., BRESSAN, D. A., KAPLAN, M. I., JASPERS, N. G., RAAMS, A., BYRD, P. J., PETRINI, J. H. & TAYLOR, A. M. 1999. The DNA double-strand break repair gene hMRE11 is mutated in individuals with an ataxia-telangiectasia-like disorder. *Cell,* 99**,** 577-87.

STIFF, T., CASAR TENA, T., O'DRISCOLL, M., JEGGO, P. A. & PHILIPP, M. 2016. ATR promotes cilia signalling: links to developmental impacts. *Human molecular genetics,* 25**,** 1574-1587.

STORER, M., MAS, A., ROBERT-MORENO, A., PECORARO, M., ORTELLS, M. C., DI GIACOMO, V., YOSEF, R., PILPEL, N., KRIZHANOVSKY, V., SHARPE, J. & KEYES, W. M. 2013. Senescence is a developmental mechanism that contributes to embryonic growth and patterning. *Cell,* 155**,** 1119-30.

STOREY, E., BAHLO, M., FAHEY, M., SISSON, O., LUECK, C. J. & GARDNER, R. J. 2009. A new dominantly inherited pure cerebellar ataxia, SCA 30. *J Neurol Neurosurg Psychiatry,* 80**,** 408-11.

STOREY, E., GARDNER, R. J., KNIGHT, M. A., KENNERSON, M. L., TUCK, R. R., FORREST, S. M. & NICHOLSON, G. A. 2001. A new autosomal dominant pure cerebellar ataxia. *Neurology,* 57**,** 1913-5.

STRACKER, T. H., ROIG, I., KNOBEL, P. A. & MARJANOVIĆ, M. 2013. The ATM signaling network in development and disease. *Front Genet,* 4**,** 37.

STRAY-PEDERSEN, A., AABERGE, I. S., FRÜH, A. & ABRAHAMSEN, T. G. 2005. Pneumococcal conjugate vaccine followed by pneumococcal polysaccharide vaccine; immunogenicity in patients with ataxia-telangiectasia. *Clin Exp Immunol,* 140**,** 507-16.

STRAY-PEDERSEN, A., BORRESEN-DALE, A. L., PAUS, E., LINDMAN, C. R., BURGERS, T. & ABRAHAMSEN, T. G. 2007. Alpha fetoprotein is increasing with age in ataxia-telangiectasia. *Eur J Paediatr Neurol,* 11**,** 375-80.

STRAY-PEDERSEN, A., JÓNSSON, T., HEIBERG, A., LINDMAN, C. R., WIDING, E., AABERGE, I. S., BORRESEN-DALE, A. L. & ABRAHAMSEN, T. G. 2004. The impact of an early truncating founder ATM mutation on immunoglobulins, specific antibodies and lymphocyte populations in ataxia-telangiectasia patients and their parents. *Clinical and experimental immunology,* 137**,** 179-186.

STRICH, S. J. 1966. Pathological findings in three cases of ataxia-telangiectasia. *Journal of Neurology, Neurosurgery &amp; Psychiatry,* 29**,** 489.

STRZYZ, P. 2017. A new role for ATM. *Nature Reviews Molecular Cell Biology,* 18**,** 277-277.

STUCKI, M., CLAPPERTON, J. A., MOHAMMAD, D., YAFFE, M. B., SMERDON, S. J. & JACKSON, S. P. 2005. MDC1 directly binds phosphorylated histone H2AX to regulate cellular responses to DNA double-strand breaks. *Cell,* 123**,** 1213-26.

STUCKI, M. & JACKSON, S. P. 2006. gammaH2AX and MDC1: anchoring the DNA-damage-response machinery to broken chromosomes. *DNA Repair (Amst),* 5**,** 534-43.

SUAREZ, F., MAHLAOUI, N., CANIONI, D., ANDRIAMANGA, C., DUBOIS D'ENGHIEN, C., BROUSSE, N., JAIS, J. P., FISCHER, A., HERMINE, O. & STOPPA-LYONNET, D. 2015. Incidence, presentation, and prognosis of malignancies in ataxia-telangiectasia: a report from the French national registry of primary immune deficiencies. *J Clin Oncol,* 33**,** 202-8.

SUH, K. J., RYU, H. S., LEE, K. H., KIM, H., MIN, A., KIM, T. Y., YANG, Y., MOON, H. G., HAN, S. W., OH, D. Y., HAN, W., PARK, I. A., NOH, D. Y. & IM, S. A. 2016. Loss of ataxia-telangiectasia-mutated protein expression correlates with poor prognosis but benefits from anthracycline-containing adjuvant chemotherapy in breast cancer. *Breast Cancer Res Treat,* 158**,** 233-41.

SUMMERTON, J. E. 2007. Morpholino, siRNA, and S-DNA compared: impact of structure and mechanism of action on off-target effects and sequence specificity. *Curr Top Med Chem,* 7**,** 651-60.

SUN, Y., ALMOMANI, R., BREEDVELD, G. J., SANTEN, G. W., ATEN, E., LEFEBER, D. J., HOFF, J. I., BRUSSE, E., VERHEIJEN, F. W., VERDIJK, R. M., KRIEK, M., OOSTRA, B., BREUNING, M. H., LOSEKOOT, M., DEN DUNNEN, J. T., VAN DE WARRENBURG, B. P. & MAAT-KIEVIT, A. J. 2013. Autosomal recessive spinocerebellar ataxia 7 (SCAR7) is caused by variants in TPP1, the gene involved in classic late-infantile neuronal ceroid lipofuscinosis 2 disease (CLN2 disease). *Hum Mutat,* 34**,** 706-13.

SUN, Y., MCCORVIE, T. J., YATES, L. A. & ZHANG, X. 2020. Structural basis of homologous recombination. *Cellular and Molecular Life Sciences,* 77**,** 3-18.

SUNDERLAND, P., AUGUSTYNIAK, J., LENART, J., BUŻAŃSKA, L., CARLESSI, L., DELIA, D. & SIKORA, E. 2020. ATM-deficient neural precursors develop senescence phenotype with disturbances in autophagy. *Mechanisms of Ageing and Development,* 190**,** 111296.

SURAWEERA, A., LIM, Y., WOODS, R., BIRRELL, G. W., NASIM, T., BECHEREL, O. J. & LAVIN, M. F. 2009. Functional role for senataxin, defective in ataxia oculomotor apraxia type 2, in transcriptional regulation. *Hum Mol Genet,* 18**,** 3384-96.

SUZUKI, K., TSUGAWA, K., OKI, E., MORIO, T., ITO, E. & TANAKA, H. 2008. Vesical varices and telangiectasias in a patient with ataxia telangiectasia. *Pediatr Nephrol,* 23**,** 1005-8.

SVENSTRUP, K., NIELSEN, T. T., AIDT, F., ROSTGAARD, N., DUNO, M., WIBRAND, F., VINTHER-JENSEN, T., LAW, I., VISSING, J., ROOS, P., HJERMIND, L. E. & NIELSEN, J. E. 2017. SCA28: Novel Mutation in the AFG3L2 Proteolytic Domain Causes a Mild Cerebellar Syndrome with Selective Type-1 Muscle Fiber Atrophy. *Cerebellum,* 16**,** 62-67.

SWIFT, M. 2001. Public health burden of cancer in ataxia-telangiectasia heterozygotes. *Journal of the National Cancer Institute,* 93**,** 84-85.

SWIFT, M., MORRELL, D., CROMARTIE, E., CHAMBERLIN, A. R., SKOLNICK, M. H. & BISHOP, D. T. 1986. The incidence and gene frequency of ataxia-telangiectasia in the United States. *Am J Hum Genet,* 39**,** 573-83.

SYNOFZIK, M., SCHULE, R., SCHULZE, M., GBUREK-AUGUSTAT, J., SCHWEIZER, R., SCHIRMACHER, A., KRAGELOH-MANN, I., GONZALEZ, M., YOUNG, P., ZUCHNER, S., SCHOLS, L. & BAUER, P. 2014. Phenotype and frequency of STUB1 mutations: next-generation screenings in Caucasian ataxia and spastic paraplegia cohorts. *Orphanet J Rare Dis,* 9**,** 57.

SÉGURET, A., COLLIGNON, B. & HALLOY, J. 2016. Strain differences in the collective behaviour of zebrafish (Danio rerio) in heterogeneous environment. *Royal Society open science,* 3**,** 160451-160451.

TAKAHASHI, A., MORI, E., SU, X. M., NAKAGAWA, Y., OKAMOTO, N., UEMURA, H., KONDO, N., NODA, T., TOKI, A., EJIMA, Y., CHEN, D. J., OHNISHI, K. & OHNISHI, T. 2010. ATM is the Predominant Kinase Involved in the Phosphorylation of Histone H2AX after Heating. *Journal of Radiation Research,* 51**,** 417-422.

TAKAHASHI, J., TANAKA, J., ARAI, K., FUNATA, N., HATTORI, T., FUKUDA, T., FUJIGASAKI, H. & UCHIHARA, T. 2001. Recruitment of nonexpanded polyglutamine proteins to intranuclear aggregates in neuronal intranuclear hyaline inclusion disease. *J Neuropathol Exp Neurol,* 60**,** 369-76.

TAKAHATA, T., YAMADA, K., YAMADA, Y., ONO, S., KINOSHITA, A., MATSUZAKA, T., YOSHIURA, K. & KITAOKA, T. 2010. Novel mutations in the SIL1 gene in a Japanese pedigree with the Marinesco-Sjogren syndrome. *J Hum Genet,* 55**,** 142-6.

TAKAI, S., YAMADA, K., KAWAKAMI, H., TANAKA, K. & NAKAMURA, S. 1995. Localization of the gene (SLC1A3) encoding human glutamate transporter (GluT-1) to 5p13 by fluorescence in situ hybridization. *Cytogenet Cell Genet,* 69**,** 209-10.

TAKASHIMA, H., BOERKOEL, C. F., JOHN, J., SAIFI, G. M., SALIH, M. A., ARMSTRONG, D., MAO, Y., QUIOCHO, F. A., ROA, B. B., NAKAGAWA, M., STOCKTON, D. W. & LUPSKI, J. R. 2002. Mutation of TDP1, encoding a topoisomerase I-dependent DNA damage repair enzyme, in spinocerebellar ataxia with axonal neuropathy. *Nat Genet,* 32**,** 267-72.

TAKEMOTO, K., IMAI, Y., SAITO, K., KAWASAKI, T., CARLTON, P. M., ISHIGURO, K. & SAKAI, N. 2020. Sycp2 is essential for synaptonemal complex assembly, early meiotic recombination and homologous pairing in zebrafish spermatocytes. *Plos Genetics,* 16.

TAKIYAMA, Y., NISHIZAWA, M., TANAKA, H., KAWASHIMA, S., SAKAMOTO, H., KARUBE, Y., SHIMAZAKI, H., SOUTOME, M., ENDO, K., OHTA, S. & ET AL. 1993. The gene for Machado-Joseph disease maps to human chromosome 14q. *Nat Genet,* 4**,** 300-4.

TAKUBO, K., HIRAO, A., OHMURA, M., AZUMA, M., ARAI, F., NAGAMATSU, G. & SUDA, T. 2006. Premeiotic germ cell defect in seminiferous tubules of Atm-null testis. *Biochemical and Biophysical Research Communications,* 351**,** 993-998.

TAL, E., ALFO, M., ZHA, S., BARZILAI, A., DE ZEEUW, C. I., ZIV, Y. & SHILOH, Y. 2018. Inactive Atm abrogates DSB repair in mouse cerebellum more than does Atm loss, without causing a neurological phenotype. *DNA Repair,* 72**,** 10-17.

TANAKA, T., HALICKA, H. D., HUANG, X., TRAGANOS, F. & DARZYNKIEWICZ, Z. 2006a. Constitutive histone H2AX phosphorylation and ATM activation, the reporters of DNA damage by endogenous oxidants. *Cell Cycle,* 5**,** 1940-5.

TANAKA, T., KUROSE, A., HUANG, X., DAI, W. & DARZYNKIEWICZ, Z. 2006b. ATM activation and histone H2AX phosphorylation as indicators of DNA damage by DNA topoisomerase I inhibitor topotecan and during apoptosis. *Cell Proliferation,* 39**,** 49-60.

TANG, S. Y. & SHAIKH, A. G. 2019. Past and Present of Eye Movement Abnormalities in Ataxia-Telangiectasia. *Cerebellum (London, England),* 18**,** 556-564.

TAO, Y. L., MEI, Y. X., YING, R. B., CHEN, S. S. & WEI, Z. P. 2020. The ATM rs189037 G > A polymorphism is associated with the risk and prognosis of gastric cancer in Chinese individuals: A case-control study. *Gene,* 741**,** 5.

TAVANI, F., ZIMMERMAN, R. A., BERRY, G. T., SULLIVAN, K., GATTI, R. & BINGHAM, P. 2003. Ataxia-telangiectasia: the pattern of cerebellar atrophy on MRI. *Neuroradiology,* 45**,** 315-319.

TAVIAUX, S., WILLIAMS, M. E., HARPOLD, M. M., NARGEOT, J. & LORY, P. 1997. Assignment of human genes for beta 2 and beta 4 subunits of voltage-dependent Ca2+ channels to chromosomes 10p12 and 2q22-q23. *Hum Genet,* 100**,** 151-4.

TAYLOR, A. M., GROOM, A. & BYRD, P. J. 2004. Ataxia-telangiectasia-like disorder (ATLD)-its clinical presentation and molecular basis. *DNA Repair (Amst),* 3**,** 1219-25.

TAYLOR, A. M., LAM, Z., LAST, J. I. & BYRD, P. J. 2015. Ataxia telangiectasia: more variation at clinical and cellular levels. *Clin Genet,* 87**,** 199-208.

TAYLOR, A. M., METCALFE, J. A., THICK, J. & MAK, Y. F. 1996. Leukemia and lymphoma in ataxia telangiectasia. *Blood,* 87**,** 423-38.

TEIVE, H. A. G., CAMARGO, C. H. F. & MUNHOZ, R. P. 2018. More than ataxia - Movement disorders in ataxia-telangiectasia. *Parkinsonism & Related Disorders,* 46**,** 3-8.

THAKUR, V. S. & WELFORD, S. M. 2020. Generation of a conditional mutant knock-in under the control of the natural promoter using CRISPR-Cas9 and Cre-Lox systems. *Plos One,* 15.

THERMANN, R., NEU-YILIK, G., DETERS, A., FREDE, U., WEHR, K., HAGEMEIER, C., HENTZE, M. W. & KULOZIK, A. E. 1998. Binary specification of nonsense codons by splicing and cytoplasmic translation. *The EMBO journal,* 17**,** 3484-3494.

THIFFAULT, I., RIOUX, M. F., TETREAULT, M., JARRY, J., LOISELLE, L., POIRIER, J., GROS-LOUIS, F., MATHIEU, J., VANASSE, M., ROULEAU, G. A., BOUCHARD, J. P., LESAGE, J. & BRAIS, B. 2006. A new autosomal recessive spastic ataxia associated with frequent white matter changes maps to 2q33-34. *Brain,* 129**,** 2332-40.

THOMAS, A. C., WILLIAMS, H., SETO-SALVIA, N., BACCHELLI, C., JENKINS, D., O'SULLIVAN, M., MENGRELIS, K., ISHIDA, M., OCAKA, L., CHANUDET, E., JAMES, C., LESCAI, F., ANDERSON, G., MORROGH, D., RYTEN, M., DUNCAN, A. J., PAI, Y. J., SARAIVA, J. M., RAMOS, F., FARREN, B., SAUNDERS, D., VERNAY, B., GISSEN, P., STRAATMAAN-IWANOWSKA, A., BAAS, F., WOOD, N. W., HERSHESON, J., HOULDEN, H., HURST, J., SCOTT, R., BITNER-GLINDZICZ, M., MOORE, G. E., SOUSA, S. B. & STANIER, P. 2014. Mutations in SNX14 cause a distinctive autosomal-recessive cerebellar ataxia and intellectual disability syndrome. *Am J Hum Genet,* 95**,** 611-21.

THYME, S. B. & SCHIER, A. F. 2016. Polq-Mediated End Joining Is Essential for Surviving DNA Double-Strand Breaks during Early Zebrafish Development. *Cell reports,* 15**,** 707-714.

TIERNEY, K. B. 2011. Swimming performance assessment in fishes. *Journal of visualized experiments : JoVE***,** 2572.

TOMIMATSU, N., MUKHERJEE, B. & BURMA, S. 2009. Distinct roles of ATR and DNA-PKcs in triggering DNA damage responses in ATM-deficient cells. *EMBO Rep,* 10**,** 629-35.

TONG, X., GUI, H., JIN, F., HECK, B. W., LIN, P., MA, J., FONDELL, J. D. & TSAI, C. C. 2011. Ataxin-1 and Brother of ataxin-1 are components of the Notch signalling pathway. *EMBO Rep,* 12**,** 428-35.

TOYOSHIMA, M., HARA, T., ZHANG, H., YAMAMOTO, T., AKABOSHI, S., NANBA, E., OHNO, K., HORI, N., SATO, K. & TAKESHITA, K. 1998. Ataxia-telangiectasia without immunodeficiency: novel point mutations within and adjacent to the phosphatidylinositol 3-kinase-like domain. *Am J Med Genet,* 75**,** 141-4.

TRESINI, M., MARTEIJN, J. A. & VERMEULEN, W. 2016. Bidirectional coupling of splicing and ATM signaling in response to transcription-blocking DNA damage. *RNA Biol,* 13**,** 272-8.

TRIMIS, G. G., ATHANASSAKI, C. K., KANARIOU, M. M. & GIANNOULIA-KARANTANA, A. A. 2004. Unusual absence of neurologic symptoms in a six-year old girl with ataxia-telangiectasia. *J Postgrad Med,* 50**,** 270-1.

TRIPATHI, D. N., CHOWDHURY, R., TRUDEL, L. J., TEE, A. R., SLACK, R. S., WALKER, C. L. & WOGAN, G. N. 2013. Reactive nitrogen species regulate autophagy through ATM-AMPK-TSC2-mediated suppression of mTORC1. *Proc Natl Acad Sci U S A,* 110**,** E2950-7.

TRIPATHI, D. N., ZHANG, J., JING, J., DERE, R. & WALKER, C. L. 2016. A new role for ATM in selective autophagy of peroxisomes (pexophagy). *Autophagy,* 12**,** 711-2.

TRUJILLO, K. M., YUAN, S. S., LEE, E. Y. & SUNG, P. 1998. Nuclease activities in a complex of human recombination and DNA repair factors Rad50, Mre11, and p95. *J Biol Chem,* 273**,** 21447-50.

TSAI, C. C., KAO, H. Y., MITZUTANI, A., BANAYO, E., RAJAN, H., MCKEOWN, M. & EVANS, R. M. 2004. Ataxin 1, a SCA1 neurodegenerative disorder protein, is functionally linked to the silencing mediator of retinoid and thyroid hormone receptors. *Proceedings of the National Academy of Sciences of the United States of America,* 101**,** 4047-4052.

TSOI, H., YU, A. C., CHEN, Z. S., NG, N. K., CHAN, A. Y., YUEN, L. Y., ABRIGO, J. M., TSANG, S. Y., TSUI, S. K., TONG, T. M., LO, I. F., LAM, S. T., MOK, V. C., WONG, L. K., NGO, J. C., LAU, K. F., CHAN, T. F. & CHAN, H. Y. 2014. A novel missense mutation in CCDC88C activates the JNK pathway and causes a dominant form of spinocerebellar ataxia. *J Med Genet,* 51**,** 590-5.

TURKMEN, S., DEMIRHAN, O., HOFFMANN, K., DIERS, A., ZIMMER, C., SPERLING, K. & MUNDLOS, S. 2006. Cerebellar hypoplasia and quadrupedal locomotion in humans as a recessive trait mapping to chromosome 17p. *J Med Genet.* England.

TURKMEN, S., GUO, G., GARSHASBI, M., HOFFMANN, K., ALSHALAH, A. J., MISCHUNG, C., KUSS, A., HUMPHREY, N., MUNDLOS, S. & ROBINSON, P. N. 2009. CA8 mutations cause a novel syndrome characterized by ataxia and mild mental retardation with predisposition to quadrupedal gait. *PLoS Genet,* 5**,** e1000487.

TURNER, C., SAWLE, A., FENSKE, M. & COSSINS, A. 2012. Implications of the solvent vehicles dimethylformamide and dimethylsulfoxide for establishing transcriptomic endpoints in the zebrafish embryo toxicity test. *Environ Toxicol Chem,* 31**,** 593-604.

TURNER, K. J., BRACEWELL, T. G. & HAWKINS, T. A. 2014. Anatomical Dissection of Zebrafish Brain Development. *In:* SPRECHER, S. G. (ed.) *Brain Development: Methods and Protocols.* Totowa: Humana Press Inc.

TYSON, J. R. & STIRLING, C. J. 2000. LHS1 and SIL1 provide a lumenal function that is essential for protein translocation into the endoplasmic reticulum. *Embo j,* 19**,** 6440-52.

TZUNG, K. W., GOTO, R., SAJU, J. M., SREENIVASAN, R., SAITO, T., ARAI, K., YAMAHA, E., HOSSAIN, M. S., CALVERT, M. E. K. & ORBÁN, L. 2015. Early depletion of primordial germ cells in zebrafish promotes testis formation. *Stem Cell Reports,* 4**,** 61-73.

UCHIDA, D., YAMASHITA, M., KITANO, T. & IGUCHI, T. 2002. Oocyte apoptosis during the transition from ovary-like tissue to testes during sex differentiation of juvenile zebrafish. *J Exp Biol,* 205**,** 711-8.

UTINE, G. E., HALILOGLU, G., SALANCI, B., CETINKAYA, A., KIPER, P. O., ALANAY, Y., AKTAS, D., BODUROGLU, K. & ALIKASIFOGLU, M. 2013. A homozygous deletion in GRID2 causes a human phenotype with cerebellar ataxia and atrophy. *J Child Neurol,* 28**,** 926-32.

UZIEL, T., SAVITSKY, K., PLATZER, M., ZIV, Y., HELBITZ, T., NEHLS, M., BOEHM, T., ROSENTHAL, A., SHILOH, Y. & ROTMAN, G. 1996. Genomic Organization of the ATM gene. *Genomics,* 33**,** 317-20.

VACCHIO, M. S., OLARU, A., LIVAK, F. & HODES, R. J. 2007. ATM deficiency impairs thymocyte maturation because of defective resolution of T cell receptor alpha locus coding end breaks. *Proc Natl Acad Sci U S A,* 104**,** 6323-8.

VAHEDI, K., JOUTEL, A., VAN BOGAERT, P., DUCROS, A., MACIAZECK, J., BACH, J. F., BOUSSER, M. G. & TOURNIER-LASSERVE, E. 1995. A gene for hereditary paroxysmal cerebellar ataxia maps to chromosome 19p. *Ann Neurol,* 37**,** 289-93.

VALENTIN-VEGA, Y. A. & KASTAN, M. B. 2012. A new role for ATM: regulating mitochondrial function and mitophagy. *Autophagy,* 8**,** 840-1.

VALENTIN-VEGA, Y. A., MACLEAN, K. H., TAIT-MULDER, J., MILASTA, S., STEEVES, M., DORSEY, F. C., CLEVELAND, J. L., GREEN, D. R. & KASTAN, M. B. 2012. Mitochondrial dysfunction in ataxia-telangiectasia. *Blood,* 119**,** 1490-500.

VALERO, E., DE BONIS, S., FILHOL, O., WADE, R. H., LANGOWSKI, J., CHAMBAZ, E. M. & COCHET, C. 1995. Quaternary structure of casein kinase 2. Characterization of multiple oligomeric states and relation with its catalytic activity. *J Biol Chem,* 270**,** 8345-52.

VAN BOGAERT, L. & MARTIN, L. 1974. Optic and cochleovestibular degenerations in the hereditary ataxias. I. Clinico-pathological and genetic aspects. *Brain,* 97**,** 15-40.

VAN DE LEEMPUT, J., CHANDRAN, J., KNIGHT, M. A., HOLTZCLAW, L. A., SCHOLZ, S., COOKSON, M. R., HOULDEN, H., GWINN-HARDY, K., FUNG, H. C., LIN, X., HERNANDEZ, D., SIMON-SANCHEZ, J., WOOD, N. W., GIUNTI, P., RAFFERTY, I., HARDY, J., STOREY, E., GARDNER, R. J., FORREST, S. M., FISHER, E. M., RUSSELL, J. T., CAI, H. & SINGLETON, A. B. 2007. Deletion at ITPR1 underlies ataxia in mice and spinocerebellar ataxia 15 in humans. *PLoS Genet,* 3**,** e108.

VAN DE WARRENBURG, B. P., VERBEEK, D. S., PIERSMA, S. J., HENNEKAM, F. A., PEARSON, P. L., KNOERS, N. V., KREMER, H. P. & SINKE, R. J. 2003. Identification of a novel SCA14 mutation in a Dutch autosomal dominant cerebellar ataxia family. *Neurology,* 61**,** 1760-5.

VAN DER VAN, L. & WESTER, P. *<p class="MsoNormal" style="margin-top:12.0pt;text-align:justify;line-height:*

150%;tab-stops:153.35pt">Histology and Histopathology Atlas of the Zebrafish<p class="MsoNormal" style="margin-top:12.0pt;text-align:justify;line-height:

150%;tab-stops:153.35pt"> [Online]. Available: http://zfin.org/hh_atlas/tesgen.html [Accessed 01.02.2021 2021].

VAN DEURSEN, J. M. 2014. The role of senescent cells in ageing. *Nature,* 509**,** 439-446.

VAN DYKE, D. H., GRIGGS, R. C., MURPHY, M. J. & GOLDSTEIN, M. N. 1975. Hereditary myokymia and periodic ataxia. *Journal of the Neurological Sciences,* 25**,** 109-118.

VAN EGMOND, M. E., ELTING, J. W., KUIPER, A., ZUTT, R., HEINEMAN, K. R., BROUWER, O. F., SIVAL, D. A., WILLEMSEN, M. A., TIJSSEN, M. A. & DE KONING, T. J. 2015. Myoclonus in childhood-onset neurogenetic disorders: The importance of early identification and treatment. *Eur J Paediatr Neurol,* 19**,** 726-9.

VAN OS, N. J., ROELEVELD, N., WEEMAES, C. M., JONGMANS, M. C., JANSSENS, G. O., TAYLOR, A. M., HOOGERBRUGGE, N. & WILLEMSEN, M. A. 2016. Health risks for ataxia-telangiectasia mutated heterozygotes: a systematic review, meta-analysis and evidence-based guideline. *Clin Genet,* 90**,** 105-17.

VAN OS, N. J. H., HAAXMA, C. A., VAN DER FLIER, M., MERKUS, P., VAN DEUREN, M., DE GROOT, I. J. M., LOEFFEN, J., VAN DE WARRENBURG, B. P. C. & WILLEMSEN, M. 2017a. Ataxia-telangiectasia: recommendations for multidisciplinary treatment. *Dev Med Child Neurol,* 59**,** 680-689.

VAN OS, N. J. H., JANSEN, A. F. M., VAN DEUREN, M., HARALDSSON, A., VAN DRIEL, N. T. M., ETZIONI, A., VAN DER FLIER, M., HAAXMA, C. A., MORIO, T., RAWAT, A., SCHOENAKER, M. H. D., SORESINA, A., TAYLOR, A. M. R., VAN DE WARRENBURG, B. P. C., WEEMAES, C. M. R., ROELEVELD, N. & WILLEMSEN, M. 2017b. Ataxia-telangiectasia: Immunodeficiency and survival. *Clin Immunol,* 178**,** 45-55.

VAN SWIETEN, J. C., BRUSSE, E., DE GRAAF, B. M., KRIEGER, E., VAN DE GRAAF, R., DE KONING, I., MAAT-KIEVIT, A., LEEGWATER, P., DOOIJES, D., OOSTRA, B. A. & HEUTINK, P. 2003. A mutation in the fibroblast growth factor 14 gene is associated with autosomal dominant cerebellar ataxia [corrected]. *Am J Hum Genet,* 72**,** 191-9.

VARGHESE, S., SCHMIDT-ULLRICH, R. K., DRITSCHILO, A. & JUNG, M. 1999. Enhanced radiation late effects and cellular radiation sensitivity in an ATM heterozygous breast cancer patient. *Radiat Oncol Investig,* 7**,** 231-7.

VERBEEK, D. S., SCHELHAAS, J. H., IPPEL, E. F., BEEMER, F. A., PEARSON, P. L. & SINKE, R. J. 2002. Identification of a novel SCA locus (SCA19) in a Dutch autosomal dominant cerebellar ataxia family on chromosome region 1p21-q21. *Hum Genet,* 111**,** 388-93.

VERBEEK, D. S., VAN DE WARRENBURG, B. P., WESSELING, P., PEARSON, P. L., KREMER, H. P. & SINKE, R. J. 2004. Mapping of the SCA23 locus involved in autosomal dominant cerebellar ataxia to chromosome region 20p13-12.3. *Brain,* 127**,** 2551-7.

VERHAGEN, M. M., ABDO, W. F., WILLEMSEN, M. A., HOGERVORST, F. B., SMEETS, D. F., HIEL, J. A., BRUNT, E. R., VAN RIJN, M. A., MAJOOR KRAKAUER, D., OLDENBURG, R. A., BROEKS, A., LAST, J. I., VAN'T VEER, L. J., TIJSSEN, M. A., DUBOIS, A. M., KREMER, H. P., WEEMAES, C. M., TAYLOR, A. M. & VAN DEUREN, M. 2009. Clinical spectrum of ataxia-telangiectasia in adulthood. *Neurology,* 73**,** 430-7.

VERHAGEN, M. M., LAST, J. I., HOGERVORST, F. B., SMEETS, D. F., ROELEVELD, N., VERHEIJEN, F., CATSMAN-BERREVOETS, C. E., WULFFRAAT, N. M., COBBEN, J. M., HIEL, J., BRUNT, E. R., PEETERS, E. A., GOMEZ GARCIA, E. B., VAN DER KNAAP, M. S., LINCKE, C. R., LAAN, L. A., TIJSSEN, M. A., VAN RIJN, M. A., MAJOOR-KRAKAUER, D., VISSER, M., VAN 'T VEER, L. J., KLEIJER, W. J., VAN DE WARRENBURG, B. P., WARRIS, A., DE GROOT, I. J., DE GROOT, R., BROEKS, A., PREIJERS, F., KREMER, B. H., WEEMAES, C. M., TAYLOR, M. A., VAN DEUREN, M. & WILLEMSEN, M. A. 2012a. Presence of ATM protein and residual kinase activity correlates with the phenotype in ataxia-telangiectasia: a genotype-phenotype study. *Hum Mutat,* 33**,** 561-71.

VERHAGEN, M. M., MARTIN, J. J., VAN DEUREN, M., CEUTERICK-DE GROOTE, C., WEEMAES, C. M., KREMER, B. H., TAYLOR, M. A., WILLEMSEN, M. A. & LAMMENS, M. 2012b. Neuropathology in classical and variant ataxia-telangiectasia. *Neuropathology,* 32**,** 234-44.

VERMEER, S., HOISCHEN, A., MEIJER, R. P., GILISSEN, C., NEVELING, K., WIESKAMP, N., DE BROUWER, A., KOENIG, M., ANHEIM, M., ASSOUM, M., DROUOT, N., TODOROVIC, S., MILIC-RASIC, V., LOCHMULLER, H., STEVANIN, G., GOIZET, C., DAVID, A., DURR, A., BRICE, A., KREMER, B., VAN DE WARRENBURG, B. P., SCHIJVENAARS, M. M., HEISTER, A., KWINT, M., ARTS, P., VAN DER WIJST, J., VELTMAN, J., KAMSTEEG, E. J., SCHEFFER, H. & KNOERS, N. 2010. Targeted next-generation sequencing of a 12.5 Mb homozygous region reveals ANO10 mutations in patients with autosomal-recessive cerebellar ataxia. *Am J Hum Genet,* 87**,** 813-9.

VERMEULEN, W. & TRESINI, M. 2017. Non-canonical role of ATM in the R-loop dependent-DNA Damage Response. *Febs Journal,* 284**,** 10-10.

VIERSTRAETE, J., WILLAERT, A., VERMASSEN, P., COUCKE, P. J., VRAL, A. & CLAES, K. B. M. 2017. Accurate quantification of homologous recombination in zebrafish: brca2 deficiency as a paradigm. *Scientific Reports,* 7**,** 16518.

VILLARREAL, M. A., BIEDIGER, N. M., BONNER, N. A., MILLER, J. N., ZEPEDA, S. K., RICARD, B. J., GARCIA, D. M. & LEWIS, K. A. 2017. Determining Zebrafish Epitope Reactivity to Commercially Available Antibodies. *Zebrafish,* 14**,** 387-389.

VINIEGRA, J. G., MARTÍNEZ, N., MODIRASSARI, P., HERNÁNDEZ LOSA, J., PARADA COBO, C., SÁNCHEZ-ARÉVALO LOBO, V. J., ACEVES LUQUERO, C. I., ALVAREZ-VALLINA, L., RAMÓN Y CAJAL, S., ROJAS, J. M. & SÁNCHEZ-PRIETO, R. 2005. Full activation of PKB/Akt in response to insulin or ionizing radiation is mediated through ATM. *J Biol Chem,* 280**,** 4029-36.

VO, Q. N., KIM, W. J., CVITANOVIC, L., BOUDREAU, D. A., GINZINGER, D. G. & BROWN, K. D. 2004. The ATM gene is a target for epigenetic silencing in locally advanced breast cancer. *Oncogene,* 23**,** 9432-7.

VON BREDERLOW, B., HAHN, A. F., KOOPMAN, W. J., EBERS, G. C. & BULMAN, D. E. 1995. Mapping the gene for acetazolamide responsive hereditary paryoxysmal cerebellar ataxia to chromosome 19p. *Hum Mol Genet,* 4**,** 279-84.

WAKAE, K., MAGOR, B. G., SAUNDERS, H., NAGAOKA, H., KAWAMURA, A., KINOSHITA, K., HONJO, T. & MURAMATSU, M. 2006. Evolution of class switch recombination function in fish activation-induced cytidine deaminase, AID. *Int Immunol,* 18**,** 41-7.

WALDMANN, T. A. & MCINTIRE, K. R. 1972. Serum-alpha-fetoprotein levels in patients with ataxia-telangiectasia. *Lancet,* 2**,** 1112-5.

WALTES, R., KALB, R., GATEI, M., KIJAS, A. W., STUMM, M., SOBECK, A., WIELAND, B., VARON, R., LERENTHAL, Y., LAVIN, M. F., SCHINDLER, D. & DÖRK, T. 2009. Human RAD50 deficiency in a Nijmegen breakage syndrome-like disorder. *Am J Hum Genet,* 84**,** 605-16.

WAN, G. H., ZHANG, X. N., LANGLEY, R. R., LIU, Y. H., HU, X. X., HAN, C., PENG, G., ELLIS, L. M., JONES, S. N. & LU, X. B. 2013. DNA-Damage-Induced Nuclear Export of Precursor MicroRNAs Is Regulated by the ATM-AKT Pathway. *Cell Reports,* 3**,** 2100-2112.

WAN, S. H., CAPASSO, H. & WALWORTH, N. C. 1999. The topoisomerase I poison camptothecin generates a Chk1-dependent DNA damage checkpoint signal in fission yeast. *Yeast,* 15**,** 821-828.

WANG, B. & ELLEDGE, S. J. 2007. Ubc13/Rnf8 ubiquitin ligases control foci formation of the Rap80/Abraxas/Brca1/Brcc36 complex in response to DNA damage. *Proc Natl Acad Sci U S A,* 104**,** 20759-63.

WANG, D.-S., JIAO, B., HU, C., HUANG, X., LIU, Z. & CHENG, C. H. K. 2008. Discovery of a gonad-specific IGF subtype in teleost. *Biochemical and Biophysical Research Communications,* 367**,** 336-341.

WANG, G., SAWAI, N., KOTLIAROVA, S., KANAZAWA, I. & NUKINA, N. 2000. Ataxin-3, the MJD1 gene product, interacts with the two human homologs of yeast DNA repair protein RAD23, HHR23A and HHR23B. *Hum Mol Genet,* 9**,** 1795-803.

WANG, H., WANG, L., ERDJUMENT-BROMAGE, H., VIDAL, M., TEMPST, P., JONES, R. S. & ZHANG, Y. 2004. Role of histone H2A ubiquitination in Polycomb silencing. *Nature,* 431**,** 873-8.

WANG, J., WU, D., GUO, H. & LI, M. 2019. Hyperandrogenemia and insulin resistance: The chief culprit of polycystic ovary syndrome. *Life Sciences,* 236**,** 116940.

WANG, J. L., YANG, X., XIA, K., HU, Z. M., WENG, L., JIN, X., JIANG, H., ZHANG, P., SHEN, L., GUO, J. F., LI, N., LI, Y. R., LEI, L. F., ZHOU, J., DU, J., ZHOU, Y. F., PAN, Q., WANG, J., LI, R. Q. & TANG, B. S. 2010a. TGM6 identified as a novel causative gene of spinocerebellar ataxias using exome sequencing. *Brain,* 133**,** 3510-8.

WANG, K., YE, Y., XU, Z., ZHANG, X., HOU, Z., CUI, Y. & SONG, Y. 2010b. Interaction between BRCA1/BRCA2 and ATM/ATR associate with breast cancer susceptibility in a Chinese Han population. *Cancer Genet Cytogenet,* 200**,** 40-6.

WANG, L., RAJAN, H., PITMAN, J. L., MCKEOWN, M. & TSAI, C. C. 2006. Histone deacetylase-associating Atrophin proteins are nuclear receptor corepressors. *Genes Dev,* 20**,** 525-30.

WANG, Q. H., GOLDSTEIN, M., ALEXANDER, P., WAKEMAN, T. P., SUN, T., FENG, J. J., LOU, Z. K., KASTAN, M. B. & WANG, X. F. 2014. Rad17 recruits the MRE11-RAD50-NBS1 complex to regulate the cellular response to DNA double-strand breaks. *Embo Journal,* 33**,** 862-877.

WANG, X. G., BARTFAI, R., SLEPTSOVA-FREIDRICH, I. & ORBAN, L. 2007. The timing and extent of ‘juvenile ovary’ phase are highly variable during zebrafish testis differentiation. *Journal of Fish Biology,* 70**,** 33-44.

WANG, X. G. & ORBAN, L. 2007. Anti-Müllerian hormone and 11 beta-hydroxylase show reciprocal expression to that of aromatase in the transforming gonad of zebrafish males. *Dev Dyn,* 236**,** 1329-38.

WARD, I. M. & CHEN, J. 2001. Histone H2AX is phosphorylated in an ATR-dependent manner in response to replicational stress. *J Biol Chem,* 276**,** 47759-62.

WARREN, R., DOMM, W., YEE, M., CAMPBELL, A., MALONE, J., WRIGHT, T., MAYER-PRÖSCHEL, M. & O'REILLY, M. A. 2019. Ataxia-telangiectasia mutated is required for the development of protective immune memory after influenza A virus infection. *Am J Physiol Lung Cell Mol Physiol,* 317**,** L591-l601.

WATCHON, M., YUAN, K. C., MACKOVSKI, N., SVAHN, A. J., COLE, N. J., GOLDSBURY, C., RINKWITZ, S., BECKER, T. S., NICHOLSON, G. A. & LAIRD, A. S. 2017. Calpain Inhibition Is Protective in Machado-Joseph Disease Zebrafish Due to Induction of Autophagy. *Journal of Neuroscience,* 37**,** 7782-7794.

WATERS, M. F., FEE, D., FIGUEROA, K. P., NOLTE, D., MULLER, U., ADVINCULA, J., COON, H., EVIDENTE, V. G. & PULST, S. M. 2005. An autosomal dominant ataxia maps to 19q13: Allelic heterogeneity of SCA13 or novel locus? *Neurology,* 65**,** 1111-3.

WATTERS, D., KEDAR, P., SPRING, K., BJORKMAN, J., CHEN, P., GATEI, M., BIRRELL, G., GARRONE, B., SRINIVASA, P., CRANE, D. I. & LAVIN, M. F. 1999. Localization of a portion of extranuclear ATM to peroxisomes. *J Biol Chem,* 274**,** 34277-82.

WATTS, M. E., POCOCK, R. & CLAUDIANOS, C. 2018. Brain Energy and Oxygen Metabolism: Emerging Role in Normal Function and Disease. *Frontiers in molecular neuroscience,* 11**,** 216-216.

WEBER, A. M. & RYAN, A. J. 2015. ATM and ATR as therapeutic targets in cancer. *Pharmacol Ther,* 149**,** 124-38.

WEBER, T., NAMIKAWA, K., WINTER, B., MÜLLER-BROWN, K., KÜHN, R., WURST, W. & KÖSTER, R. W. 2016. Caspase-mediated apoptosis induction in zebrafish cerebellar Purkinje neurons. *Development,* 143**,** 4279-4287.

WEBSTER, K. A., SCHACH, U., ORDAZ, A., STEINFELD, J. S., DRAPER, B. W. & SIEGFRIED, K. R. 2017. Dmrt1 is necessary for male sexual development in zebrafish. *Developmental Biology,* 422**,** 33-46.

WEGNER, R. D., METZGER, M., HANEFELD, F., JASPERS, N. G., BAAN, C., MAGDORF, K., KUNZE, J. & SPERLING, K. 1988. A new chromosomal instability disorder confirmed by complementation studies. *Clin Genet,* 33**,** 20-32.

WEI, W. & JI, S. 2018. Cellular senescence: Molecular mechanisms and pathogenicity. *J Cell Physiol,* 233**,** 9121-9135.

WEINSTEIN, J. A., JIANG, N., WHITE, R. A., 3RD, FISHER, D. S. & QUAKE, S. R. 2009. High-throughput sequencing of the zebrafish antibody repertoire. *Science (New York, N.Y.),* 324**,** 807-810.

WEISS, B., KRAUTHAMMER, A., SOUDACK, M., LAHAD, A., SAROUK, I., SOMECH, R., HEIMER, G., BEN-ZEEV, B. & NISSENKORN, A. 2016. Liver Disease in Pediatric Patients With Ataxia Telangiectasia: A Novel Report. *J Pediatr Gastroenterol Nutr,* 62**,** 550-5.

WHITEHOUSE, C. J., TAYLOR, R. M., THISTLETHWAITE, A., ZHANG, H., KARIMI-BUSHERI, F., LASKO, D. D., WEINFELD, M. & CALDECOTT, K. W. 2001. XRCC1 stimulates human polynucleotide kinase activity at damaged DNA termini and accelerates DNA single-strand break repair. *Cell,* 104**,** 107-17.

WIECZOREK, E., BRAND, M., JACQ, X. & TORA, L. 1998. Function of TAF(II)-containing complex without TBP in transcription by RNA polymerase II. *Nature,* 393**,** 187-91.

WILKINSON, D. S., TSAI, W. W., SCHUMACHER, M. A. & BARTON, M. C. 2008. Chromatin-bound p53 anchors activated Smads and the mSin3A corepressor to confer transforming-growth-factor-beta-mediated transcription repression. *Mol Cell Biol,* 28**,** 1988-98.

WILLEMS, P. J., VAN ROY, B. C., KLEIJER, W. J., VAN DER KRAAN, M. & MARTIN, J. J. 1993. Atypical clinical presentation of ataxia telangiectasia. *Am J Med Genet,* 45**,** 777-82.

WILSON, W. C., HORNIG-DO, H. T., BRUNI, F., CHANG, J. H., JOURDAIN, A. A., MARTINOU, J. C., FALKENBERG, M., SPAHR, H., LARSSON, N. G., LEWIS, R. J., HEWITT, L., BASLE, A., CROSS, H. E., TONG, L., LEBEL, R. R., CROSBY, A. H., CHRZANOWSKA-LIGHTOWLERS, Z. M. & LIGHTOWLERS, R. N. 2014. A human mitochondrial poly(A) polymerase mutation reveals the complexities of post-transcriptional mitochondrial gene expression. *Hum Mol Genet,* 23**,** 6345-55.

WINKELMANN, J., LIN, L., SCHORMAIR, B., KORNUM, B. R., FARACO, J., PLAZZI, G., MELBERG, A., CORNELIO, F., URBAN, A. E., PIZZA, F., POLI, F., GRUBERT, F., WIELAND, T., GRAF, E., HALLMAYER, J., STROM, T. M. & MIGNOT, E. 2012. Mutations in DNMT1 cause autosomal dominant cerebellar ataxia, deafness and narcolepsy. *Hum Mol Genet,* 21**,** 2205-10.

WINTER, N., KOVERMANN, P. & FAHLKE, C. 2012. A point mutation associated with episodic ataxia 6 increases glutamate transporter anion currents. *Brain,* 135**,** 3416-25.

WITTKOPP, N., HUNTZINGER, E., WEILER, C., SAULIÈRE, J., SCHMIDT, S., SONAWANE, M. & IZAURRALDE, E. 2009. Nonsense-mediated mRNA decay effectors are essential for zebrafish embryonic development and survival. *Mol Cell Biol,* 29**,** 3517-28.

WOO, T.-T., CHUANG, C.-N. & WANG, T.-F. 2021. Budding yeast Rad51: a paradigm for how phosphorylation and intrinsic structural disorder regulate homologous recombination and protein homeostasis. *Current Genetics*.

WOOD, J. D., NUCIFORA, F. C., JR., DUAN, K., ZHANG, C., WANG, J., KIM, Y., SCHILLING, G., SACCHI, N., LIU, J. M. & ROSS, C. A. 2000. Atrophin-1, the dentato-rubral and pallido-luysian atrophy gene product, interacts with ETO/MTG8 in the nuclear matrix and represses transcription. *J Cell Biol,* 150**,** 939-48.

WOOD, J. L., SINGH, N., MER, G. & CHEN, J. 2007. MCPH1 functions in an H2AX-dependent but MDC1-independent pathway in response to DNA damage. *J Biol Chem,* 282**,** 35416-23.

WOOD, L. M., SANKAR, S., REED, R. E., HAAS, A. L., LIU, L. F., MCKINNON, P. & DESAI, S. D. 2011. A novel role for ATM in regulating proteasome-mediated protein degradation through suppression of the ISG15 conjugation pathway. *PLoS One,* 6**,** e16422.

WOODS, C. G. & TAYLOR, A. M. 1992. Ataxia telangiectasia in the British Isles: the clinical and laboratory features of 70 affected individuals. *Q J Med,* 82**,** 169-79.

WORTH, P. F., GIUNTI, P., GARDNER-THORPE, C., DIXON, P. H., DAVIS, M. B. & WOOD, N. W. 1999. Autosomal dominant cerebellar ataxia type III: linkage in a large British family to a 7.6-cM region on chromosome 15q14-21.3. *Am J Hum Genet,* 65**,** 420-6.

WU, Q. & MANIATIS, T. 1999. A striking organization of a large family of human neural cadherin-like cell adhesion genes. *Cell,* 97**,** 779-90.

XIE, X., NÓBREGA, R. & PŠENIČKA, M. 2020. Spermatogonial Stem Cells in Fish: Characterization, Isolation, Enrichment, and Recent Advances of In Vitro Culture Systems. *Biomolecules,* 10**,** 644.

XU, Y., ASHLEY, T., BRAINERD, E. E., BRONSON, R. T., MEYN, M. S. & BALTIMORE, D. 1996. Targeted disruption of ATM leads to growth retardation, chromosomal fragmentation during meiosis, immune defects, and thymic lymphoma. *Genes Dev,* 10**,** 2411-22.

XU, Y. & BALTIMORE, D. 1996. Dual roles of ATM in the cellular response to radiation and in cell growth control. *Genes Dev,* 10**,** 2401-10.

YAMAMOTO, K., WANG, J., SPRINZEN, L., XU, J., HADDOCK, C. J., LI, C., LEE, B. J., LOREDAN, D. G., JIANG, W., VINDIGNI, A., WANG, D., RABADAN, R. & ZHA, S. 2016. Kinase-dead ATM protein is highly oncogenic and can be preferentially targeted by Topo-isomerase I inhibitors. *Elife,* 5.

YAMAMOTO, K., WANG, Y., JIANG, W., LIU, X., DUBOIS, R. L., LIN, C.-S., LUDWIG, T., BAKKENIST, C. J. & ZHA, S. 2012a. Kinase-dead ATM protein causes genomic instability and early embryonic lethality in mice. *The Journal of cell biology,* 198**,** 305-313.

YAMAMOTO, K., WANG, Y., JIANG, W., LIU, X., DUBOIS, R. L., LIN, C. S., LUDWIG, T., BAKKENIST, C. J. & ZHA, S. 2012b. Kinase-dead ATM protein causes genomic instability and early embryonic lethality in mice. *J Cell Biol,* 198**,** 305-13.

YAMASHITA, I., SASAKI, H., YABE, I., FUKAZAWA, T., NOGOSHI, S., KOMEICHI, K., TAKADA, A., SHIRAISHI, K., TAKIYAMA, Y., NISHIZAWA, M., KANEKO, J., TANAKA, H., TSUJI, S. & TASHIRO, K. 2000. A novel locus for dominant cerebellar ataxia (SCA14) maps to a 10.2-cM interval flanked by D19S206 and D19S605 on chromosome 19q13.4-qter. *Ann Neurol,* 48**,** 156-63.

YAN, C., LU, J., ZHANG, G., GAN, T., ZENG, Q., SHAO, Z., DUERKSEN-HUGHES, P. J. & YANG, J. 2011. Benzo[a]pyrene induces complex H2AX phosphorylation patterns by multiple kinases including ATM, ATR, and DNA-PK. *Toxicol In Vitro,* 25**,** 91-9.

YANG, C. Y., TANG, X., GUO, X. J., WONG, S., FU, L. & XU, B. 2011a. ATM is activated in mitosis and required for the spindle checkpoint. *Cancer Research,* 71.

YANG, D. Q., HALABY, M. J., LI, Y., HIBMA, J. C. & BURN, P. 2011b. Cytoplasmic ATM protein kinase: an emerging therapeutic target for diabetes, cancer and neuronal degeneration. *Drug Discovery Today,* 16**,** 332-338.

YANG, D. Q. & KASTAN, M. B. 2000. Participation of ATM in insulin signalling through phosphorylation of eIF-4E-binding protein 1. *Nat Cell Biol,* 2**,** 893-8.

YANG, Y. J., WANG, Y., LI, Z., ZHOU, L. & GUI, J. F. 2017. Sequential, Divergent, and Cooperative Requirements of Foxl2a and Foxl2b in Ovary Development and Maintenance of Zebrafish. *Genetics,* 205**,** 1551-1572.

YAPICI, Z. & ERAKSOY, M. 2005. Non-progressive congenital ataxia with cerebellar hypoplasia in three families. *Acta Paediatr,* 94**,** 248-53.

YASUDA, H., MIZUNO, A., TAMAOKI, T. & MORINAGA, T. 1994. ATBF1, a multiple-homeodomain zinc finger protein, selectively down-regulates AT-rich elements of the human alpha-fetoprotein gene. *Mol Cell Biol,* 14**,** 1395-401.

YAZDI, P. T., WANG, Y., ZHAO, S., PATEL, N., LEE, E. Y. & QIN, J. 2002. SMC1 is a downstream effector in the ATM/NBS1 branch of the human S-phase checkpoint. *Genes Dev,* 16**,** 571-82.

YE, M. & CHEN, Y. 2020. Zebrafish as an emerging model to study gonad development. *Computational and structural biotechnology journal,* 18**,** 2373-2380.

YIN, B., LEE, B. S., YANG-IOTT, K. S., SLECKMAN, B. P. & BASSING, C. H. 2012. Redundant and Nonredundant Functions of ATM and H2AX in alpha beta T-Lineage Lymphocytes. *Journal of Immunology,* 189**,** 1372-1379.

YIN, Y., TANG, H., LIU, Y., CHEN, Y., LI, G., LIU, X. & LIN, H. 2017. Targeted Disruption of Aromatase Reveals Dual Functions of cyp19a1a During Sex Differentiation in Zebrafish. *Endocrinology,* 158**,** 3030-3041.

YING, K. L. & DECOTEAU, W. E. 1981. Cytogenetic anomalies in a patient with ataxia, immune deficiency, and high alpha-fetoprotein in the absence of telangiectasia. *Cancer Genet Cytogenet,* 4**,** 311-7.

YODER, J. A., YEN, R. W., VERTINO, P. M., BESTOR, T. H. & BAYLIN, S. B. 1996. New 5' regions of the murine and human genes for DNA (cytosine-5)-methyltransferase. *J Biol Chem,* 271**,** 31092-7.

YOON, C., KAWAKAMI, K. & HOPKINS, N. 1997. Zebrafish vasa homologue RNA is localized to the cleavage planes of 2- and 4-cell-stage embryos and is expressed in the primordial germ cells. *Development,* 124**,** 3157.

YOSEF, R., PILPEL, N., PAPISMADOV, N., GAL, H., OVADYA, Y., VADAI, E., MILLER, S., PORAT, Z., BEN-DOR, S. & KRIZHANOVSKY, V. 2017. p21 maintains senescent cell viability under persistent DNA damage response by restraining JNK and caspase signaling. *Embo j,* 36**,** 2280-2295.

YOU, Z., BAILIS, J. M., JOHNSON, S. A., DILWORTH, S. M. & HUNTER, T. 2007. Rapid activation of ATM on DNA flanking double-strand breaks. *Nat Cell Biol,* 9**,** 1311-8.

YOUNG, D. B., JONNALAGADDA, J., GATEI, M., JANS, D. A., MEYN, S. & KHANNA, K. K. 2005. Identification of domains of ataxia-telangiectasia mutated required for nuclear localization and chromatin association. *J Biol Chem,* 280**,** 27587-94.

YU, G. Y., HOWELL, M. J., ROLLER, M. J., XIE, T. D. & GOMEZ, C. M. 2005. Spinocerebellar ataxia type 26 maps to chromosome 19p13.3 adjacent to SCA6. *Ann Neurol,* 57**,** 349-54.

YUAN, J., ADAMSKI, R. & CHEN, J. 2010. Focus on histone variant H2AX: to be or not to be. *FEBS Lett,* 584**,** 3717-24.

YUE, S., SERRA, H. G., ZOGHBI, H. Y. & ORR, H. T. 2001. The spinocerebellar ataxia type 1 protein, ataxin-1, has RNA-binding activity that is inversely affected by the length of its polyglutamine tract. *Hum Mol Genet,* 10**,** 25-30.

YUE, X., BAI, C., XIE, D., MA, T. & ZHOU, P.-K. 2020. DNA-PKcs: A Multi-Faceted Player in DNA Damage Response. *Frontiers in Genetics,* 11**,** 1692.

YUKAWA, M., NAGATA, M. & AOKI, F. 2008. Involvement of ATM in H2AX phosphorylation during early preimplantation development in mice. *Biology of Reproduction***,** 132-132.

YUN, J., ROCIC, P., PUNG, Y. F., BELMADANI, S., CARRAO, A. C., OHANYAN, V. & CHILIAN, W. M. 2009. Redox-dependent mechanisms in coronary collateral growth: the "redox window" hypothesis. *Antioxid Redox Signal,* 11**,** 1961-74.

ZADIK, Z., LEVIN, S., PRAGER-LEWIN, R. & LARON, Z. 1978. Gonadal dysfunction in patients with ataxia telangiectasia. *Acta Paediatr Scand,* 67**,** 477-9.

ZAKSAUSKAITE, R., THOMAS, R. C., VAN EEDEN, F. & EL-KHAMISY, S. F. 2021. Tdp1 protects from topoisomerase 1-mediated chromosomal breaks in adult zebrafish but is dispensable during larval development. *Sci Adv,* 7.

ZHA, S., GUO, C., BOBOILA, C., OKSENYCH, V., CHENG, H. L., ZHANG, Y., WESEMANN, D. R., YUEN, G., PATEL, H., GOFF, P. H., DUBOIS, R. L. & ALT, F. W. 2011a. ATM damage response and XLF repair factor are functionally redundant in joining DNA breaks. *Nature,* 469**,** 250-4.

ZHA, S., JIANG, W. X., FUJIWARA, Y., PATEL, H., GOFF, P. H., BRUSH, J. W., DUBOIS, R. L. & ALT, F. W. 2011b. Ataxia telangiectasia-mutated protein and DNA-dependent protein kinase have complementary V(D)J recombination functions. *Proceedings of the National Academy of Sciences of the United States of America,* 108**,** 2028-2033.

ZHA, S., LI, G., CHENG, H. L., BRUSH, J., PATEL, H., GOFF, P. & ALT, F. 2009. ATM and XLF/Cernunnos synergize in DNA repair during V(D)J recombination. *Cancer Research,* 69.

ZHAN, H., SUZUKI, T., AIZAWA, K., MIYAGAWA, K. & NAGAI, R. 2010. Ataxia Telangiectasia Mutated (ATM)-mediated DNA Damage Response in Oxidative Stress-induced Vascular Endothelial Cell Senescence. *Journal of Biological Chemistry,* 285**,** 29662-29670.

ZHANG, J., KIM, J., ALEXANDER, A., CAI, S., TRIPATHI, D. N., DERE, R., TEE, A. R., TAIT-MULDER, J., DI NARDO, A., HAN, J. M., KWIATKOWSKI, E., DUNLOP, E. A., DODD, K. M., FOLKERTH, R. D., FAUST, P. L., KASTAN, M. B., SAHIN, M. & WALKER, C. L. 2013. A tuberous sclerosis complex signalling node at the peroxisome regulates mTORC1 and autophagy in response to ROS. *Nat Cell Biol,* 15**,** 1186-96.

ZHANG, J., SUN, X., QIAN, Y., LADUCA, J. P. & MAQUAT, L. E. 1998. At least one intron is required for the nonsense-mediated decay of triosephosphate isomerase mRNA: a possible link between nuclear splicing and cytoplasmic translation. *Mol Cell Biol,* 18**,** 5272-83.

ZHANG, J., TRIPATHI, D. N., JING, J., ALEXANDER, A., KIM, J., POWELL, R. T., DERE, R., TAIT-MULDER, J., LEE, J. H., PAULL, T. T., PANDITA, R. K., CHARAKA, V. K., PANDITA, T. K., KASTAN, M. B. & WALKER, C. L. 2015a. ATM functions at the peroxisome to induce pexophagy in response to ROS. *Nat Cell Biol,* 17**,** 1259-1269.

ZHANG, J. W., TRIPATHI, D. N., JING, J., ALEXANDER, A., KIM, J., POWELL, R. T., DERE, R., TAIT-MULDER, J., LEE, J. H., PAULL, T. T., PANDITA, R. K., CHARAKA, V. K., PANDITA, T. K., KASTAN, M. B. & WALKER, C. L. 2015b. ATM functions at the peroxisome to induce pexophagy in response to ROS. *Nature Cell Biology,* 17**,** 1259-+.

ZHANG, N., CHEN, P., KHANNA, K. K., SCOTT, S., GATEI, M., KOZLOV, S., WATTERS, D., SPRING, K., YEN, T. & LAVIN, M. F. 1997. Isolation of full-length ATM cDNA and correction of the ataxia-telangiectasia cellular phenotype. *Proc Natl Acad Sci U S A,* 94**,** 8021-6.

ZHANG, Q., GREEN, M. D., LANG, X., LAZARUS, J., PARSELS, J. D., WEI, S., PARSELS, L. A., SHI, J., RAMNATH, N., WAHL, D. R., PASCA DI MAGLIANO, M., FRANKEL, T. L., KRYCZEK, I., LEI, Y. L., LAWRENCE, T. S., ZOU, W. & MORGAN, M. A. 2019. Inhibition of ATM Increases Interferon Signaling and Sensitizes Pancreatic Cancer to Immune Checkpoint Blockade Therapy. *Cancer Res,* 79**,** 3940-3951.

ZHANG, Q., SKEPPER, J. N., YANG, F., DAVIES, J. D., HEGYI, L., ROBERTS, R. G., WEISSBERG, P. L., ELLIS, J. A. & SHANAHAN, C. M. 2001. Nesprins: a novel family of spectrin-repeat-containing proteins that localize to the nuclear membrane in multiple tissues. *J Cell Sci,* 114**,** 4485-98.

ZHANG, S., XU, L., LEE, J. & XU, T. 2002. Drosophila atrophin homolog functions as a transcriptional corepressor in multiple developmental processes. *Cell,* 108**,** 45-56.

ZHANG, X., WAN, G., BERGER, F. G., HE, X. & LU, X. 2011. The ATM kinase induces microRNA biogenesis in the DNA damage response. *Mol Cell,* 41**,** 371-83.

ZHANG, Y., HUANG, H., ZHANG, B. & LIN, S. 2016. TALEN- and CRISPR- enhanced DNA homologous recombination for gene editing in zebrafish. *Zebrafish: Genetics, Genomics, and Transcriptomics, 4th Edition,* 135**,** 107-120.

ZHANG, Y., LEE, J. H., PAULL, T. T., GEHRKE, S., D'ALESSANDRO, A., DOU, Q., GLADYSHEV, V. N., SCHROEDER, E. A., STEYL, S. K., CHRISTIAN, B. E. & SHADEL, G. S. 2018. Mitochondrial redox sensing by the kinase ATM maintains cellular antioxidant capacity. *Sci Signal,* 11.

ZHAO, D. Y., GISH, G., BRAUNSCHWEIG, U., LI, Y., NI, Z., SCHMITGES, F. W., ZHONG, G., LIU, K., LI, W., MOFFAT, J., VEDADI, M., MIN, J., PAWSON, T. J., BLENCOWE, B. J. & GREENBLATT, J. F. 2016. SMN and symmetric arginine dimethylation of RNA polymerase II C-terminal domain control termination. *Nature,* 529**,** 48-53.

ZHAO, J., ZHANG, L., LU, A. P., HAN, Y. C., COLANGELO, D., BUKATA, C., SCIBETTA, A., YOUSEFZADEH, M. J., LI, X. S., GURKAR, A. U., MCGOWAN, S. J., ANGELINI, L., O'KELLY, R., LI, H. S., CORBO, L., SANO, T., NICK, H., POLA, E., PILLA, S. P. S., LADIGES, W. C., VO, N., HUARD, J., NIEDERNHOFER, L. J. & ROBBINS, P. D. 2020a. ATM is a key driver of NF-kappa B-dependent DNA-damage-induced senescence, stem cell dysfunction and aging. *Aging-Us,* 12**,** 4688-4710.

ZHAO, K., WANG, X., XUE, X., LI, L. & HU, Y. 2020b. A long noncoding RNA sensitizes genotoxic treatment by attenuating ATM activation and homologous recombination repair in cancers. *PLoS Biol,* 18**,** e3000666.

ZHAO, W., WIESE, C., KWON, Y., HROMAS, R. & SUNG, P. 2019. The BRCA Tumor Suppressor Network in Chromosome Damage Repair by Homologous Recombination. *Annual review of biochemistry,* 88**,** 221-245.

ZHOU, L., FENG, Y., WANG, F., DONG, X., JIANG, L., LIU, C., ZHAO, Q. & LI, K. 2018. Generation of all-male-like sterile zebrafish by eliminating primordial germ cells at early development. *Scientific Reports,* 8**,** 1834.

ZHU, H. P., JIANG, H., DU, X. F., FRUTIGER, S. A., PRYOR, J. L., ROE, C. A., COX, N. J. & GOMEZ, C. 2011. Mutation of PODXL, a Cell Surface and Mitochondrial Protein, Underlies Azoospermia and Neurodegeneration in Spinocerebellar Ataxia Type 32 (SCA32). *Neurology,* 76**,** A21-A21.

ZHUCHENKO, O., BAILEY, J., BONNEN, P., ASHIZAWA, T., STOCKTON, D. W., AMOS, C., DOBYNS, W. B., SUBRAMONY, S. H., ZOGHBI, H. Y. & LEE, C. C. 1997. Autosomal dominant cerebellar ataxia (SCA6) associated with small polyglutamine expansions in the alpha 1A-voltage-dependent calcium channel. *Nat Genet,* 15**,** 62-9.

ZIMMERMAN, A. M., MOUSTAFA, F. M., ROMANOWSKI, K. E. & STEINER, L. A. 2011. Zebrafish immunoglobulin IgD: Unusual exon usage and quantitative expression profiles with IgM and IgZ/T heavy chain isotypes. *Molecular Immunology,* 48**,** 2220-2223.

ZU, L., FIGUEROA, K. P., GREWAL, R. & PULST, S. M. 1999. Mapping of a new autosomal dominant spinocerebellar ataxia to chromosome 22. *Am J Hum Genet,* 64**,** 594-9.

ZUHLKE, C., DALSKI, A., HELLENBROICH, Y., BUBEL, S., SCHWINGER, E. & BURK, K. 2002. Spinocerebellar ataxia type 1 (SCA1): phenotype-genotype correlation studies in intermediate alleles. *Eur J Hum Genet,* 10**,** 204-9.

ZÜCHNER, S., MERSIYANOVA, I. V., MUGLIA, M., BISSAR-TADMOURI, N., ROCHELLE, J., DADALI, E. L., ZAPPIA, M., NELIS, E., PATITUCCI, A., SENDEREK, J., PARMAN, Y., EVGRAFOV, O., JONGHE, P. D., TAKAHASHI, Y., TSUJI, S., PERICAK-VANCE, M. A., QUATTRONE, A., BATTALOGLU, E., POLYAKOV, A. V., TIMMERMAN, V., SCHRÖDER, J. M. & VANCE, J. M. 2004. Mutations in the mitochondrial GTPase mitofusin 2 cause Charcot-Marie-Tooth neuropathy type 2A. *Nat Genet,* 36**,** 449-51.

Appendix 1

Appendix 1.1 Summary table of hereditary ataxias

PolyQ Disorders						
Ataxia	***Genomic Locus***	***Protein***	***Protein Function***	***Threshold repeat no.***	***Neurodegenerative Pathways***	***Sources***
SCA1 (Spinocerebellar Ataxia)	*6p22.3*	*Ataxin-1*	*1. Co transcriptional activator and repressor* *2.RNA Splicing protein*	*>39*		*(Orr et al., 1993, Banfi et al., 1994, Servadio et al., 1995, Zuhlke et al., 2002, Robitaille et al., 1995, de Chiara et al., 2003, Goold et al., 2007, Chen et*

					al., 2004, Yue et al., 2001, Lim et al., 2008, de Chiara et al., 2009, Matilla et al., 1997, Tong et al., 2011, Tsai et al., 2004)
SCA2	*12q24.12*	*Ataxin-2*	*Transcriptional Regulator*	*>31* *Note there is an association of repeat length >29 with amyotrophic lateral sclerosis*	*(Eto et al., 1990, Babovic-Vuksanovic et al., 1998, Ralser et al., 2005, Satterfield and Pallanck*

						, 2006, Hallen et al., 2011)
SCA3 (Machado-Joseph Disease)	14q32.12	Ataxin-3	1. Thought to function as a transcriptional repressor by binding to proteins such as TAFII130, CBP, HDAC3 AND HADC6. 2. Ataxin-3 functions as a positive regulator of stress response proteins 3. May also function in some DNA repair pathways	>44 Note that incomplete penetrance is associated with a repeat number between 45-51	the expanded protein is thought to upregulate inflammatory reactions	(Li et al., 2009, Buttner et al., 1998, Takiyama et al., 1993, St George-Hyslop et al., 1994, Schols et al., 1995, Shimohata et al., 2000, Takahashi et al., 2001, McCampbell et al., 2000, Chai et al., 2002, Evert et

					al., 2006a, Wang et al., 2000, Evert et al., 2003, Evert et al., 2006b, Araujo et al., 2011)
SCA6	*19p13.13*	*CACNA1A*	*Subunit of voltage-dependent calcium channel*	*>18*	*(Li et al., 2009, Zhuchenko et al., 1997, Gomez et al., 1997, Ishikawa et al., 1997)*
SCA7	*3p14.1*	*Ataxin-7*	*1. Nuclear Ataxin-7 acts as a transcription factor as part of a number or complexes* *a) TATA-binding protein-free TAF complex (TFTC)* *b) acetyltransferase complex (STAGA)* *c) PCAF/GCN5 complex*	*>38*	*(Benomar et al., 1995, David et al., 1996, Lindblad et al., 1996,*

			2. Cytosolic Ataxin-7 functions as a microtubule stabilizer		*David et al., 1997, Harding, 1982, Wieczorek et al., 1998, Brand et al., 1999, Martinez et al., 1998, Ogryzko et al., 1998, Cancel et al., 2000, Lindenberg et al., 2000, Nakamura et al., 2012)*
SCA17	*6q27*	*TATA-binding protein*	*Binds to the TATA box upstream of the transcription start site*	*>44*	*(Nakamura et al., 2001, Koide et al., 1999)*

SCA8/ *ATAXIN8OS*	*13q21*	*Ataxin-8*	*Unknown*	*107-127*	*ATAXIN8OS* *(SCA8 is caused by a CAG repeat, however ATAXIN8OS is caused by the transcription of a CTG repeat in the same genomic locus on the opposite strand) (bidirectional transcription*	*(Ikeda et al., 2000, Ito et al., 2006, Koob et al., 1999, Daughters et al., 2009)*
DRPLA *(Dentatorubral-Pallidoluysian Atrophy)*	*12p13.31*	*Atrophin-1*	*Transcriptional co-repressor*	*>23*		*(Kuwano et al., 1996, Nagafuchi et al., 1994, Burke et al., 1994, Zhang et al., 2002, Wang et al., 2006, Shen et al., 2007, Wood et al., 2000)*

Intronic Repeat Ataxias

Ataxia	*Genomic Locus*	*Protein*	*Protein Function*	*Repeat Expansion*	*Neurodegenerative Pathways*	*Sources*
SCA10	*22q13.31*	*ATXN-10*	*Unknown*	***ATTCT*** *>400* *Although an affected individual with 280 repeats has been reported*		*(Alonso et al., 2006, Grewal et al., 1998, Matsuura et al., 1999, Zu et al., 1999)*
SCA12	*5q32*	*Neuronal specific subunit of the protein phosphatase PP2A*	*Serine/Theronine phosphatase that has been implicated in gene transcription and cell growth and division*	*>51* ***CAG** repeats* *Although the nucleotide sequence code for a PolyQ tract this is not regarded a PolyQ disorder as the expansion is located upstream of the transcription start site and not normally transcribed*		*(Bahl et al., 2005, Holmes et al., 1999, Mayer et al., 1991, Lin et al., 2010)*
SCA31	*16q21* *(Note that the locus is the same as SCA4 but disorders differ in their phenotype)*	*BEAN* *Note a homozygous mutation has been reported that encompasse*	*Unknown*	*Pre-sequence of **TCAC** followed by either* ***(TGGAA)n*** ***(TAGAA)n*** ***(TAAAA)n***		*(Nagaoka et al., 2000, Li et al., 2003, Owada et al.,*

		s the TK2 gene on the OS			*2005, Amino et al., 2007, Ohata et al., 2006, Sato et al., 2009)*
SCA36	*20p13*	*NOP56*	*Subunit of box C/D small nucleolar ribonucleoprotein complexes that function in RNA processing*	*650-2500* ***GGCCTG***	*(Kobayashi et al., 2011, Garcia-Murias et al., 2012, Gautier et al., 1997)*
Friedreich Ataxia	*9q21.11*	*FXN*	*Mitochondrial iron chaperone*	*GAA* *>70* *However point mutations have also been described for this gene and account for approx 2% of Friedreich Ataxias*	*(Schols et al., 2000, Mallaret et al., 2014, Chamberlain et al., 1988, Fujita et al., 1989, Delatycki et al., 1999,*

							Schmucker et al., 2008, Campuzano et al., 1996)
Dominantly Inherited Ataxias with Conventional Mutations							
Ataxia	*Genomic Locus*	*Gene*	*Mutation*	*Protein*	*Protein Function*	*Neurodegenerative Pathways*	*Sources*
SCA5 (See also SCAR14)	*11q13.2*	*SPTBN2*	*SCA5 is caused by dominant heterozygous mutations. These have been reported to be in frame deletions and missense mutations (Note repeat expansion of the same genomic locus is associated with SCAR14)* *The missense R480W mutation is associated with infantile onset*	*ß-spectrin, non-erythrocytic 2*	*Cytoplasmic membrane stabiliser*		*(Jacob et al., 2013, Parolin Schnekenberg et al., 2015, Burk et al., 2004, Ranum et al., 1994, Ikeda et al., 2006, Jackson et al., 2001, Clarkson et al., 2014)*

SCA11	*15q15.2*	*TTBK2*	*Currently two mutations have been described in this gene. Insertion of an adenosine at 1329 and a deletion of GA leading to a frameshift mutation in exon 13*	*tau tubulin kinase-2*	*Protein Kinases known to phosphorylate tau and tubulin*	*(Houlden et al., 2007, Worth et al., 1999)*
SCA13	*19q13.33*	*KCNC3*	*SCA13 is inherited in a heterozygous fashion and reported mutations result in a gain of function of or dominant negative protein product. The most common allelic variants reported are R420H, F448L, R420H, T428I*	*KCNC3*	*Voltage gated* K^+ *channel*	*(Herman-Bert et al., 2000, Waters et al., 2005, Pyle et al., 2015, Parolin Schnekenberg et al., 2015, Ghanshani et al., 1992, Haas et al., 1993, Figueroa et al., 2010, Figueroa et al., 2011)*
SCA14	*19q13.42*	*PRKCG*	*Multiple mutations associated with SCA14*	*Protein Kinase C, Gamma*	*Key isoform of protein kinase C found in PC*	*(Asai et al.,*

			locus have been reported and are generally autosomal dominant although an autosomal recessive mutations have been reported			*2009, Yamashita et al., 2000, Brkanac et al., 2002, Chen et al., 2003a, Morita et al., 2006, van de Warrenburg et al., 2003, Johnson et al., 1988)*
SCA15/ 16 *(SCA29 – also mutation in this locus and differs from SCA15 with an juvenile onset)*	*3p26.1* *Note: Mutations in this sometimes include the SUMF1 gene but these mutations were found not to be causative of SCA15*	*ITPR1*	*SCA15 appears to be caused by haploinsufficency due to large deletions in the ITPR1 gene*	*inositol 1,4,5-triphosphate (IP3) receptor*	*IP3-gated calcium channel highly expressed in PC*	*(Storey et al., 2001, Knight et al., 2003, van de Leemput et al., 2007, Hara et al., 2004, Matsumoto et*

						al., 1996, Nucifora et al., 1995, Iwaki et al., 2008, Hara et al., 2008)
SCA18 (SMNA)	*7q22-q32*	*IFRD1 (candidate gene)*	*An I172V is thought to be the causative mutation as isoleucine is well conserved. However, this is still debated as the mutated valine is also conserved across elephants, zebrafish and chicken.*	*interferon-related developmental regulator*	*histone deacetylase-dependent transcriptional coregulator*	*Brkanac et al., 2002b, Brkanac et al., 2009, Buanne et al., 1998)*
SCA19/SCA22	*1p13.2*	*KCND3*	*Most reported mutations are point mutations leading to missense proteins but deletions have also been reported. As SCA19 is dominantly inherited that these mutations are antimorphic but this has yet to be shown*	*Kv4.3*	*alpha subunit of the Shal family of A-type voltage-gated potassium channels*	*(Duarri et al., 2012, Chung et al., 2003, Verbeek et al., 2002, Schelhaas et al., 2004, Kong et al., 1998, Isbrandt et al.,*

						2000, Dixon et al., 1996, Postma et al., 2000, Lee et al., 2012)
SCA21	*1p36.33*	*TMEM240*	*The disorder is transmitted in an autosomal dominant fashion with some anticipation observed. Observed mutation are generally missense however no functional studies have yet been carried out.*	*TMEM240*	*Transmembrane protein with unknown function*	*(Devos et al., 2001, Delplanque et al., 2014)*
SCA23	*20p13*	*PDYN*	*Affected individuals are heterozygous for the mutant allele of which 4 variants have been reported, R138S, R215C, L211S, R212W*	*Prodynorphin*	*Synaptic transmission*	*(Bakalkin et al., 2010, Verbeek et al., 2004, Horikawa et al., 1983, Litt et al., 1988)*
SCA26	*19p13.3*	*EEF2*	*To date one heterozygous mutation has been reported in the gene, P596H*	*Eukaryotic translation elongation factor 2*	*Required for translocation during protein synthesis*	*(Yu et al., 2005, Hekman et al.,*

						2012, Kaneda et al., 1987)
SCA27	*13q33.1*	*FGF14*	*Reported mutations include a point mutation of F145S and 487delA resulting in a truncated protein*	*fibroblast growth factor-14*	*Growth factor in expressed during neuronal development*	*(van Swieten et al., 2003, Dalski et al., 2005, Smallwood et al., 1996)*
SCA28	*13q33.1*	*AFG3L2*	*Heterozygous mutation that have been reported to be dominant negative or loss of function leading to haploinsufficentcy* *Note that a loss of function homozygous mutations cause SPAX5*	*ATPase family gene 3-like 2*	*Catalytic subunit the mitochondrial metalloprotease which functions in degradation of miss folding proteins and RNA assembly*	*(Cagnoli et al., 2006, Cagnoli et al., 2010, Di Bella et al., 2010, Banfi et al., 1999, Koppen et al., 2007, Lobbe et al., 2014, Svenstrup et al., 2017,*

							Maltecca et al., 2015)
SCA34	*6q14.1*	*ELOVL4*	*One mutation for this disorder has been reported, a heterozygous point mutation (L168F)*	*Elongation of very long chain fatty acids-like 4*	*Synthesis of long chain fatty acid*		*(Cadieux-Dion et al., 2014, Agbaga et al., 2008)*
SCA35	*20p13*	*TGM6*	*Heterozygous mutation*	*Transglutaminase 6*	*Transglutaminases*		*(Wang et al., 2010a, Li et al., 2013, Guo et al., 2014, Hadjivassiliou et al., 2008)*
SCA40	*14q32.11-q32.12*	*CCDC88C*	*Heterozygous gain of function mutation that has been reported in one kindred R464H*	*Coiled-coil domain-containing protein 88c*	*Negative regulator of the Wnt signalling pathway*		*(Tsoi et al., 2014, Oshita et al., 2003)*
SCA42	*17q21.33*	*CACNA1G*	*Currently only one heterozygous mutation has been reported R1715H*	*Calcium chanel, voltage-dependant, t type, alpha-1g subunit*	*Voltage active* Ca^{++} *channel*		*(Coutelier et al., 2015, Morino et al., 2015, Perez-Reyes et al.,*

							1998, Jagannathan et al., 2002)
ADCADN (Cerebellar ataxia, deafness, and narcolepsy, autosomal dominant)	*19p13.2*	*DNMT1*	*Heterozygous mutation*	*DNA methyltransferase 1*	*DNA methylation*		*(Melberg et al., 1995, Winkelmann et al., 2012, Yoder et al., 1996)*
EA1 (Episodic Ataxia)	*12p13.32*	*KCNA1*	*Heterozygous mutation*	*Potassium Channel, Voltage-Gated, Shaker-Related Subfamily, Member 1*	*K^+ channel*		*(Van Dyke et al., 1975, Gancher and Nutt, 1986, Graves et al., 2010, Litt et al., 1994, Glaudemans et al., 2009,*

						Browne et al., 1994, Eunson et al., 2000)
EA2	*19p13.13*	*CACNA1A*	*Heterozygous mutation*	*Calcium Channel, Voltage-Dependent, P/Q Type*	*Ca^{++} channel*	*(von Brederlow et al., 1995, Vahedi et al., 1995, Kordasiewicz et al., 2006, Ophoff et al., 1996, Diriong et al., 1995)*
EA5	*2q23.3*	*CACNB4*	*Heterozygous mutation*	*Calcium Channel, Voltage-Dependent, Beta-4 Subunit*	*Ca^{++} channel*	*(Escayg et al., 2000, Escayg et al., 1998, Taviaux et al., 1997)*
EA6	*5p13.2*	*SLC1A3*	*Heterozygous mutation*	*Glial High Affinity Glutamate Transporter, Member 3*	*Na^{+} dependant transporter that regulated*	*(Jen et al., 2005, de Vries*

					neurotransmitter at glutamangeric synapses		*et al., 2009, Winter et al., 2012, Kirschner et al., 1994, Takai et al., 1995)*
SPAX1 (Autosomal dominant spastic ataxia)	*12p13.31*	*VAMP1*	*Heterozygous(Ferguson and Critchley, 1929) mutations thought to lead to haploinsufficiency*	*vesicle-associated membrane protein-1 (synaptobrevin-1)*	*Synaptic vesical cycle*		*(Ferguson and Critchley, 1929, Meijer et al., 2002, Grewal et al., 2004, Bourassa et al., 2012)*
SPAX7							

Recessively Inherited Ataxias with Conventional Mutations

Ataxia	**Genomic Locus**	**Gene**	**Mutation**	**Protein**	**Protein Function**	**Neurodegenerative Pathways**	**Sources**
AOA1 ataxia-oculomotor apraxia 1 (may	*9p21.1*	*APTX*	*Homozygous mutation where insertions and deletions are thought to confer a more sever phenotype while missense*	*aprataxin*	*histidine triad (HIT) superfamily that function in DNA single strand break repair*		*(Moreira et al., 2001, Barbot et al., 2001,*

also be denoted as EAOH)			*mutation phenotype tends to be milder.* *It should be noted that a compound heterozygous genotype has also been observed (W279X)*			*Criscuolo et al., 2004, Castellotti et al., 2011, Date et al., 2001, Sano et al., 2004, Whitehouse et al., 2001)*
AOA2 – also denoted as SCAR1)	*9q34.13*	*SETX* *Note a mutation in this gene is also associated with ALS*	*Homozygous or compound heterozygous mutation*	*senataxin*	*Transcriptional regulator* *DNA repair*	*(Moreira et al., 2004, Duquette et al., 2005, Bouchard et al., 1980, Nemeth et al., 2000, Bomont et al., 2000, Suraweera et al., 2009, Airoldi*

						et al., 2010)
AOA3	*17p13.1*	*PIK3R5*	*One case has been reported of a consanguineous Saudi Arabian family with a homozygous mutation P629S*	*phosphatidylinositol 3-kinase, regulatory subunit 5*	*Cell proliferation, survival and chemotaxis*	*(Al Tassan et al., 2012, Brock et al., 2003)*
AOA4	*19q13.33*	*PNKP*	*Homozygous or compound heterozygous mutation*	*polynucleotide kinase*	*DNA repair*	*(Bras et al., 2015, Jilani et al., 1999)*
CAMRQ1 cerebellar ataxia, mental retardation, and dysequilibrium syndrome 1	*9p24.2*	*VLDLR*	*Homozygous mutation*	*low density lipoprotein receptor*	*Nervous system development*	*(Schurig et al., 1981, Glass et al., 2005, Boycott et al., 2005, Ozcelik et al., 2008)*
CAMRQ2	*17p13.3*	*WDR81*	*Homozygous mutation*	*WD repeat-containing protein 81*	*Conversation of early endosome to late endosome*	*(Gulsuner et al., 2011, Turkmen et al., 2006, Ozcelik*

							et al., 2008, Liu et al., 2016b)
CAMRQ3	*8q12.1*	*CA8*	*Two homozygous mutation in a consanguineous families have been reported, S100P and R237Q*	*Carbonic Anhydrase VIII*	*zinc metalloenzymes*		*(Turkmen et al., 2009, Najmabadi et al., 2011, Kato, 1990, Bergenhem et al., 1995, Hirota et al., 2003)*
CAMRQ4	*13q12.13*	*ATP8A2*	*One reported homozygous mutation I376M from a consanguineous family*	*ATPase, Class I, Type 8a, Member 2*	*transport of aminophospholipids*		*(Onat et al., 2013)*
SCAR2	*9q34.3*	*PMPCA*	*Homozygous or compound heterozygous mutation*	*Peptidase, Mitochondrial Processing, Alpha*	*subunit of a mitochondrial protease*		*(Norman, 1940, Megarbane et al., 1999, Jobling et al., 2015)*
SCAR3	*6p23-p21*						*(van Bogaert and*

						Martin, 1974, Spoendlin, 1974, Bomont et al., 2000)
SACR7	*11p15.4*	*TPP1* *Note Biallelic mutation on this gene may also result in neuronal ceroid lipofuscinosis-2*	*Mutations tend to be compound heterozygous*	*Tripeptidyl Peptidase I*	*lysosomal exopeptidase*	*(Breedveld et al., 2004, Sun et al., 2013, Dy et al., 2015)*
SCAR8	*6q25.2*	*SYNE1*	*Homozygous mutations*	*Spectrin Repeat-Containing Nuclear Envelope Protein 1*	*Links plasma membrane to actin skeleton*	*(Gros-Louis et al., 2007, Izumi et al., 2013, Dupre et al., 2007, Zhang et al., 2001, Puckelwartz et al., 2009)*

SCAR9	*1q42.13*	*ADCK3*	*Homozygous and compound heterozygous mutation*	*Coenzyme Q8A*	*Synthesis of coenzyme Q10*	*(Puckelwartz et al., 2009, Mollet et al., 2008, Aure et al., 2004, Iizumi et al., 2002)*
SCAR10	*3p22.1-p21.3*	*ANO10*	*Homozygous and compound heterozygous mutations*	*ANOCTAMIN 10*	Ca^{++} *activated chloride channel*	*(Vermeer et al., 2010, Balreira et al., 2014)*
SCAR11	*1q32.2*	*SYT14*	*Homozygous and translocation mutation*	*Synaptotagmin 14*	*Membrane trafficking*	*(Doi et al., 2011, Fukuda, 2003, Quintero-Rivera et al., 2007, Herrero-Turrion et al., 2006)*
SCAR12	*16q23.1-q23.2*	*WWOX*	*Homozygous mutation* *Note that a biallelic mutation in this gene also causes infantile epileptic encephalopathy-28*	*WW Domain-Containing Oxidoreductase*	*Transcriptional regulator*	*(Mallaret et al., 2014, Gribaa et al.,*

						2007, Bednarek et al., 2000, Aqeilan et al., 2007, Chang et al., 2003)
SCAR14 (see also SCA5)	*11q13.2*	*SPTBN2*	*Homozygous mutation* *Note a heterozygous mutation in the SPTBN2 causes SCA5*			*(Lise et al., 2012, Elsayed et al., 2014, Jackson et al., 2001, Clarkson et al., 2014, Stankewich et al., 1998)*
SCAR15	*3q29*	*KIAA0226*	*Homozygous mutation of which one has been reported, 1 bp deletion, 2927delC*	*Run Domain- And Cysteine-Rich Domain-Containing Beclin-1-Interacting Protein*	*Maturation of endosomes and vesicular trafficking*	*(Assoum et al., 2010, Assoum et al., 2013, Matsunaga et al., 2009, Nagase*

							et al., 1996)
SCAR16	16p13.3	STUB1	*Homozygous and compound heterozygous mutations*	*Stip1 Homologous And U Box-Containing Protein 1*	*Ubiquitin ligase and chaperone that regulates protein degradation*		*(Shi et al., 2013, Shi et al., 2014, Synofzik et al., 2014, Min et al., 2008, Ballinger et al., 1999)*
SCAR17	10q24.31	CWF19L1	*Homozygous and compound heterozygous mutation*	*Cwf19-Like Protein 1*	*mRNA processing and possibly DNA repair (unconfirmed)*		*(Evers et al., 2016, Yapici and Eraksoy, 2005, Nguyen et al., 2016, Burns et al., 2014)*
SCAR18	4q22.1-q22.2	GRID2	*Homozygous deletion Two mutations have been reported*	*Glutamate Receptor, Ionotropic, Delta 2*	*Neurotransmitter receptor*		*(Hills et al., 2013, Utine et al., 2013, Lalouett*

						e et al., 1998)
SCAR19 (Lichtenstein-Knorr Syndrome)	1p36.11	SLC9A1	Homozygous mutation One mutation has been reported, G305R	Solute Carrier Family 9, Member 1	Na+/H+ antiporter involved in pH regulation and actin filament anchor	(Guissart et al., 2015, Mattei et al., 1988, Franchi et al., 1986, Denker et al., 2000)
SCAR20	6q14.3	SNX14	Homozygous mutation	Sorting Nexin 14	Endosome sorting	(Thomas et al., 2014, Sousa et al., 2014, Akizu et al., 2015, Carroll et al., 2001, Shukla et al., 2017)
SCAR21	11q13.1	SCYL1	Homozygous and compound heterozygous mutations	SCY1-like 1	intracellular transport	(Schmidt et al., 2015, Kato et al., 2002, Liu et al.,

						2000, Shukla et al., 2017)
SCAR22	2q11.2	VWA3B	Homozygous mutation One mutation has been reported, K622T	Von Willebrand Factor A Domain-Containing Protein 3B	Predicted to function in transcription, DNA repair as well as ribosomal and membrane transport	(Kawarai et al., 2016)
SCAR23	6p22.3	TDP2	Two homozygous mutations have been reported, intron 3 splice site mutation (G/A) and Ser138Ter	Tyrosyl-DNA PhosphodiesterasE 2	DNA repair	(Gomez-Herreros et al., 2014, Ledesma et al., 2009, Pype et al., 2000)
SCAR24	3q22.1	UBA5	Compound heterozygous mutation Two such mutations has been reported R246X and K310E	Ubiquitin-Like Modifier Activating Enzyme 5	ubiquitin-fold modifier 1-activating enzyme	(Duan et al., 2016, Komatsu et al., 2004, Dou et al., 2005)
Ataxia-Telangiectasia	11q22.3	ATM	Homozygous and compound heterozygous mutations	Ataxia-Telangiectasia Mutated	DNA repair, cell cycle control, telomere length regulator, epigenetic regulator, vesicular trafficking	(Sanal et al., 1990, Woods and Taylor, 1992, Savitsky et al., 1995,

							Uziel et al., 1996, Gatti et al., 1988, Hawley and Friend, 1996, Banin et al., 1998, Canman et al., 1998, Lim et al., 1998, Banga et al., 1986, Baker et al., 1976)
Ataxia-Telangiectasia-Like Disorder-1	*11q21*	*MRE11A*	*Homozygous and compound heterozygous*	*Meiotic Recombination 11, S. Cerevisiae, Homolog of A*	*DNA repair*		*(Hernandez et al., 1993, Stewart et al., 1999, Paull and Gellert, 1998, Trujillo*

						et al., 1998)
Marine sco-Sjogren Syndrome	*5q31.2*	*SIL1*	*Homozygous and compound heterozygous*	*SIL1*	*nucleotide exchange factor*	*(Lagier-Tourenne et al., 2003, Anttonen et al., 2005, Senderek et al., 2005, Chung et al., 2002, Takahata et al., 2010, Tyson and Stirling, 2000)*
SPAX2	*17p13.2*	*KIF1C*	*Homozygous mutation*	*Kinesin Family Member 1C*	*Microtubule motor protein*	*(Dor et al., 2014, Bouslam et al., 2007, Novarino et al., 2014, Dorner et al., 1998)*
SPAX3	*2q33.1*	*MARS2*	*Homozygous and compound heterozygous*	*Methionyl-tRNA Synthetase 2*	*Aminoacylation of tRNA in transcription*	*(Thiffault et al., 2006,*

			Mutations tend to be duplications			*Bayat et al., 2012, Spencer et al., 2004)*
SPAX4	*10p11.23*	*MTPAP*	*Homozygous*	*Mitochondrial Poly(A) Polymerase*	*Processing of mitochondrial mRNA*	*(Crosby et al., 2010, Wilson et al., 2014, Lapkouski and Hallberg, 2015)*
SPAX5	*18p11.21*	*AFG3L2*	*Homozygous mutation* *Note: Heterozygous mutations cause SCA28*	*ATPase Family Gene 3-Like 2*	*Catalytic subunit the mitochondrial metalloprotease which functions in degradation of miss folding proteins and RNA assembly*	*(Pierson et al., 2011, Muona et al., 2015, Koppen et al., 2007, Banfi et al., 1999)*
SPAX6 (Spastic Ataxia, Charlevoix-Saguen	*13q12.12*	*SACS*	*Homozygous and compounder heterozygous mutation*	*Sacsin*	*Ubiqination and processing of Ataxin-1*	*(Baets et al., 2010, Bouchard et al., 1978, Richter et al., 1999,*

ay Type)						Parfitt et al., 2009)
SCAN1	14q32.11	Tdp1	Homozygous mutation	tyrosyl-DNA phosphodiesterase-1	Hydrolyses the protein-DNA bond during replication DNA repair	(Takashima et al., 2002, El-Khamisy et al., 2005, Pouliot et al., 1999, Interthal et al., 2001)

Other/Unknown Mutation/ Undefined

Ataxia	Genomic Locus	Gene	Protein	Protein Function		
SCA20	11q12	Pericentromeric duplication of 12 of genes, including SPTBN2 (SCA5) and DAGLA. It was determined that SCA5 and SCA20 and distinct disease and that SCA20	DAGLA	diacylglycerol lipase that catalyses lipidation of DAG		(Knight et al., 2004, Lorenzo et al., 2006, Knight et al., 2008, Bisogno et al., 2003, Ishikawa et al., 1998)

		is caused by a copy number variation of DAGLA			
SCA30	*4q34.3-q35.1*	*ODZ3 (candidate gene)*	*Unknown*	*Teneurin transmembrane protein 3*	*(Storey et al., 2009, Nagase et al., 2000)*
SCA32	*7q32-q33*	*PODXL (candidate gene – unconfirmed)*	*Unknown*	*Unknown*	*(Jiang et al., 2010, Zhu et al., 2011)*

Appendix 1.2. Table Exhibiting Incidence of presentation/diagnosis of Genetic Ataxias discussed in section 1.1 of the text, seen at the Sheffield Ataxia Centre, UK, over a 20-year period

Ataxia	*Percentage of all Ataxias presented at the clinic*	*Percentage of Genetic Ataxias*
SCA1	*0.2*	*0.8*
SCA2	*0.7*	*2.4*
SCA3	*0.2*	*0.6*
SCA5	*0.3*	*0.9*
SCA6	*3*	*10*
SCA7	*0.4*	*1.3*
SCA8	*0.06*	*0.2*
SCA11	*0.13*	*0.44*
SCA13	*0.26*	*0.9*
SCA14	*0.3*	*1.1*
SCA15	*0.2*	*0.66*
SCA17	*0.06*	*0.2*
SCA18	*0.06*	*0.2*
SCA19	*0.2*	*0.6*
SAC27	*0.06*	*0.2*
SCA28	*0.2*	*0.6*
SCA29	*0.06*	*0.2*
SCA35	*0.3*	*1.1*
EA1	*0.13*	*0.44*
EA2	*2.8*	*9.2*
EA5	*0.13*	*0.44*
EA6	*0.13*	*0.44*
Friedreich's ataxia	*4.8*	*16*
AOA2	*0.26*	*0.9*
Ataxia Telangiectasia	*0.2*	*0.6*

Appendix 1.3 Map summarising ATM effector protein activation/inactivation in the DDR. Map was collated using SPIKE database (331). Protein families are shown in yellow, protein complexes are in green, individual proteins in grey, a microRNA in blue.

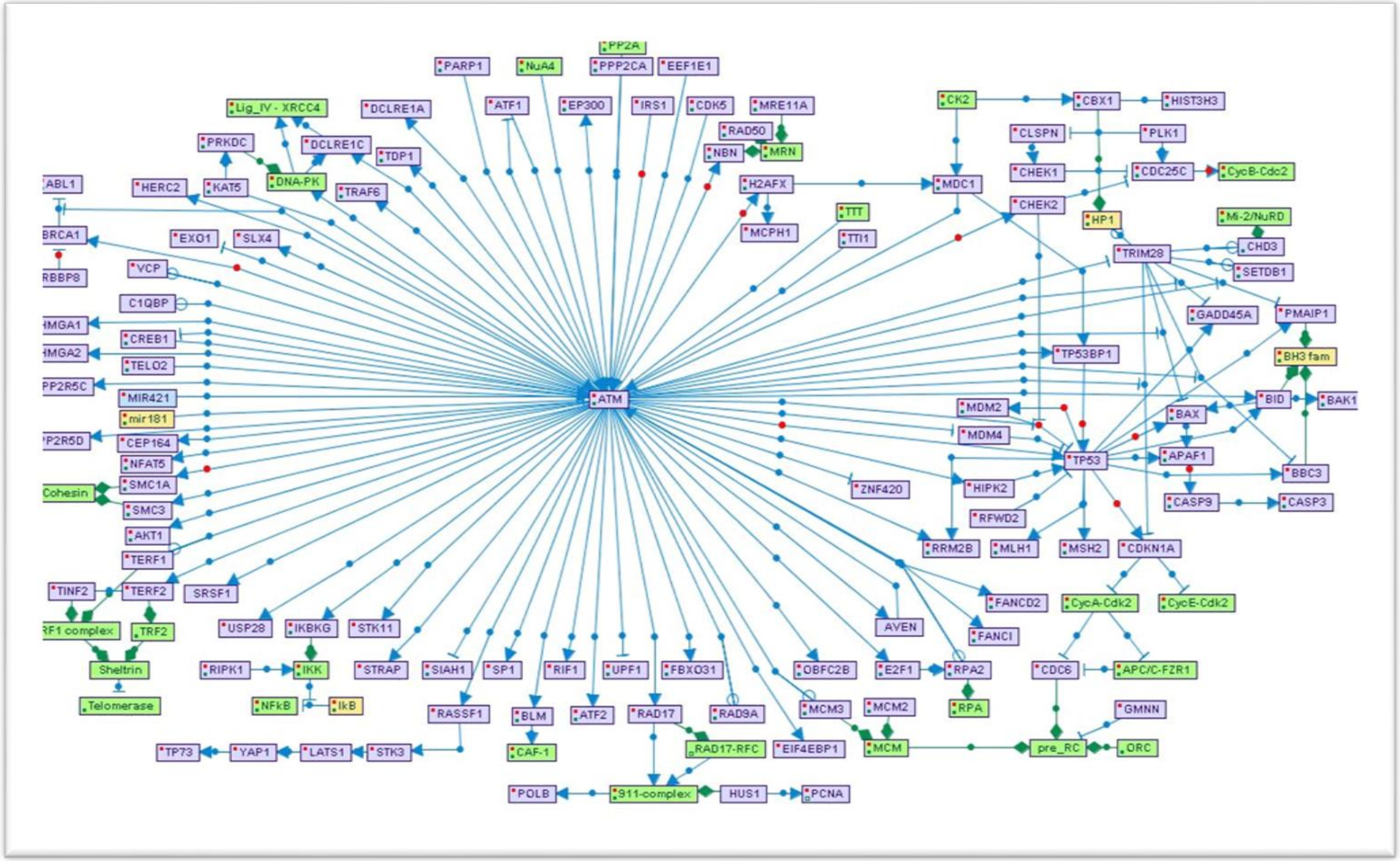
PP2A
PARP1
NuA4
PPP2CA
EEF1E1
Lig_IV - XRCC4
DCLRE1A
ATF1
EP300
IRS1
CDK5
MRE11A
CK2
CBX1
HIST3H3
PRKDC
DCLRE1C
TDP1
RAD50
NBN
MRN
CLSPN
PLK1
ABL1
HERC2
KAT5
DNA-PK
TRAF6
H2AFX
MDC1
CHEK1
CDC25C
CycB-Cdc2
CHEK2
TTT
HP1
Mi-2/NuRD
BRCA1
EXO1
SLX4
MCPH1
TTI1
TRIM28
CHD3
RBBP8
VCP
SETDB1
C1QBP
GADD45A
PMAIP1
MGA1
CREB1
MGA2
TELO2
TP53BP1
BH3 fam
PP2R5C
MIR421
ATM
BID
BAK1
mir181
MDM2
BAX
PP2R5D
CEP164
MDM4
APAF1
NFAT5
TP53
Cohesin
SMC1A
ZNF420
HIPK2
BBC3
SMC3
CASP9
CASP3
RFWD2
AKT1
RRM2B
MLH1
MSH2
CDKN1A
TERF1
TINF2
TERF2
SRSF1
FANCD2
CycA-Cdk2
CycE-Cdk2
RF1 complex
TRF2
USP28
IKBKG
STK11
AVEN
FANCI
Sheltrin
RIPK1
IKK
STRAP
SIAH1
SP1
RIF1
UPF1
FBXO31
OBFC2B
E2F1
RPA2
CDC6
APC/C-FZR1
Telomerase
NFkB
IkB
RASSF1
BLM
ATF2
RAD17
RAD9A
MCM3
MCM2
RPA
GMNN
CAF-1
RAD17-RFC
EIF4EBP1
MCM
pre_RC
ORC
TP73
YAP1
LATS1
STK3
POLB
911-complex
HUS1
PCNA

Appendix 1.4 Clustal Ω Alignment of ATM protein sequences from a selection vertebrates. *Similarly, to figure 1.3 in text, human TAN domain is denoted in orange (residues 8-165), HEAT domain in blue (residues 166- 1939), FAT domain in green (residues 1940-2566), Kinase domain in pink (residues 2712- 2962) and FATC domain in grey (3023-3056).*

```
Zebrafish      MSLALHELLVCCRGLENEKATERKKEVDRFRRLICSPDTVEELDRTSGSKGSKQLTWDAV 60
Rat            MSLALNDLLICCRQLEHDRATERRKEVDKFKRLIQDPETVQHLDRHSDSKQGKYLNWDAV 60
Mouse          MSLALNDLLICCRQLEHDRATERRKEVDKFKRLIQDPETVQHLDRHSDSKQGKYLNWDAV 60
Pig            MSLALNDLLICCRQLEHDRATERRKAVENFRHLIQDPETVQHLDQHSDSKQGKYLNWDAA 60
Rabbit         MSLALNDLLICCRHLEHDRATERRKEVEKFKRLIRDPETVQQLDRHSDSKQGKYLNWDAV 60
Human          MSLVLNDLLICCRQLEHDRATERKKEVEKFKRLIRDPETIKHLDRHSDSKQGKYLNWDAV 60
Chimp          MSLVLNDLLICCRQLEHDRATERKKEVEKFKRLIRDPETIKHLDRHSDSKQGKYLNWDAV 60
               ***.*::**:*** **:::****:* *:.*::** .*:*::.**: *.** .* *.***.

Zebrafish      FRFLQKFLKKETELLQSGKANVSASTQANRQKKMQEISSLMKFFIRCANQRGPRLKCAEL 120
Rat            FRFLQKYIQKETESLRTAKSNVSASTQTSRQKKMQEISSLVRFFIKCANKRAPRLKCQDL 120
Mouse          FRFLQKYIQKEMESLRTAKSNVSATTQSSRQKKMQEISSLVRYFIKCANKRAPRLKCQDL 120
Pig            FRFLQKYIQKETECLRTAKQNVSASTQATRQKKMQEISSLVKYFIKCANKRAPRLKCQEL 120
Rabbit         FRFLQKYIQKETECLRTAKPNVSASTQASRQKKMQEISSLVKYFIKCANKRAPRLKCQEL 120
Human          FRFLQKYIQKETECLRIAKPNVSASTQASRQKKMQEISSLVKYFIKCANRRAPRLKCQEL 120
Chimp          FRFLQKYIQKETECLRIAKPNVSASTQASRQKKMQEISSLVKYFIKCANRRAPRLKCQEL 120
               ******:::** * *: .* ****:**:.***********:::**:***:*.***** :*

Zebrafish      ISHVVEVLQSPFSCVAYGEDYSSILLKNILSVRKYWCEMSQQQWHSLLDLFCGLFNRGTR 180
Rat            LNYVMDTVKDSSNGATYGADCSNILLKDILSVRKYWCEVSQQQWLELFSLYIRLYLKPSQ 180
Mouse          LNYVMDTVKDSSNGLTYGADCSNILLKDILSVRKYWCEVSQQQWLELFSLYFRLYLKPSQ 180
Pig            LNYIMDTVRDSSNNPIYGADYSNILLKDILSVRKYWCEISQQQWRELFLIYFTLYLKPSQ 180
Rabbit         LNYIMETVKDSSNGGVYAADCSNILLKDILSVRKYWCEIPQQQWLDLFSVYLRLYLKPSQ 180
Human          LNYIMDTVKDSSNGAIYGADCSNILLKDILSVRKYWCEISQQQWLELFSVYFRLYLKPSQ 180
Chimp          LNYIMDTVKDSSSGAIYGADCSNILLKDILSVRKYWCEISQQQWLELFSVYFRLYLKPSQ 180
               :.::::.::.  .   *. * *.****:**********: **** .*: ::  *: : ::

Zebrafish      SINRVQVSRIIYTVVWGCCVQTEGLSHTLFNFFLKALSNSRAEKQLMVLENLVSAVNVFL 240
Rat            DINRVLVARIIHAVTRGCCSQTDGLPSKFLDLFSKAIQYARQEKSSPGLSHILAALNIFL 240
Mouse          DINRVLVARIIHAVTRGCCSQTDGLPSKFLDLFSKAIQYARQEKSSPGLSHILAALNIFL 240
Pig            DINRLLVARIIQAVTKGCCSQTDGLNSEFLDFFTKAIQNARQEKSSPGLNHILAAYVIFL 240
Rabbit         DINRVLVARIIHAVTKGCCLQTDGLNSKFLDFFSKAIQYARQEKSSAGLNHILAALIIFL 240
Human          DVHRVLVARIIHAVTKGCCSQTDGLNSKFLDFFSKAIQCARQEKSSSGLNHILAALTIFL 240
Chimp          DVHRVLVARIIHAVTKGCCSQTDGLNSKFLDFFSKAIQCARQEKSSSGLNHILAALTIFL 240
               .::*: *:*** :*. *** **:**   ::::* **:. :* **.   *.::::*  :**

Zebrafish      RSVLLSCRKRVCGLGEEVLSDMLCVYTGMRPSSVLKEELVKFFQIQLFVHHPKGAKTIET 300
Rat            KTLAVNFRKRVCEIGDEILPTLLYIWTQHRLNDSLKEVIIELIHLQIYIHHPQGAKAPEE 300
Mouse          KSLAVNFRKRVCEAGDEILPTLLYIWTQHRLNDSLKEVIIELIQLQIYIHHPQGARAPEE 300
Pig            KTLAANFRIRVCELGDKILPTLLYIWTQHRLNDSLKEVIVELFQLQVYMHHPKGAKTQEK 300
Rabbit         KTLAINCRIRACELGDEILPTLLYIWAQHRLNDSLKEVIIELFQLQVSIHHPKGAKTEDR 300
Human          KTLAVNFRIRVCELGDEILPTLLYIWTQHRLNDSLKEVIIELFQLQIYIHHPKGAKTQEK 300
Chimp          KTLAVNFRIRVCELGDEILPTLLYIWTQHRLNDSLKEVIIELFQLQIYIHHPKGAKTQEK 300
               :::  . * *.*  *:::*  :* :::  * .. *** :::::::*: :***:**:: :

Zebrafish      GAQAQDWVKWRSQLCTLYDALVSEISQIGSRGKYATGSRHIAVKENLIELTADVCHQLFN 360
Rat            GAY--ESMKWKRILYNLYDLLVNEISHIGSRGKYSSGSRNIAVKENLIDLMADVCYQLFN 358
Mouse          GAY--ESMKWKSILYNLYDLLVNEISHIGSRGKYSSGSRNIAVKENLIDLMADICYQLFD 358
Pig            GAY--ESAKWKSILYNLYDLLVNEISRIGSRGKYSSGSRNIAVKENLIELMADICHQVFN 358
Rabbit         GAF--KSAKWQSILYNLYDLIVNEISYIGSRGKYSSGSRNIAVKENLIELMADICHQVFN 358
Human          GAY--ESTKWRSILYNLYDLLVNEISHIGSRGKYSSGFRNIAVKENLIELMADICHQVFN 358
Chimp          GAY--ESTKWRSILYNLYDLLVNEISHIGSRGKYYSGFRNIAVKENLIELMADICHQVFN 358
               **   .  **:  * .*** :*.*** *******  :* *:********:* **:*:*:*:

Zebrafish      QSTRVQEVTSSVCRD--TQRDSPQSCKRRRVELSNWELIRSKLQPHHSDFDMIPWLQVTA 418
Rat            ADTRSVEISQSYA-TQRESTDYSVPCKRRKIDI-GWEVIKDYLQKSQNDFDLVPWLQITT 416
Mouse          ADTRSVEISQSYV-TQRESTDYSVPCKRRKIDV-GWEVIKDYLQKSQSDFDLVPWLQITT 416
Pig            EDTRSLEISQSYTTTQREFSDYNAPCKKRKIEL-GWGVIKDHLQKSQNDFDVVPWLQIAT 417
Rabbit         EDTRSLEISQSYTTTQRESSEYSTPCKRKKIEL-GWEVIKDHLQKSQNDFDLVPWLQITT 417
Human          EDTRSLEISQSYTTTQRESSDYSVPCKRKKIEL-GWEVIKDHLQKSQNDFDLVPWLQIAT 417
Chimp          EDTRSLEISQSYTTTQRESSDYSVPCKRKKIEL-GWEVIKDHLQKSQNDFDLVPWLQIAT 417
                .**  *::.*         :    **:::::: .* :*:. **  :.***::****:::
```

```
Zebrafish      ALISKYPSILLTDDVVPLLGLLCQLQGEQQRRGERAPYVLRCLKELALCHAKSSANSSAC 478
Rat            RLISKYPSSLPNCELSPLILILYQLL-PQQRRGERIPHVLRCLTEVALCQGKKSNLESSQ 475
Mouse          RLISKYPSSLPNCELSPLILILYQLL-PQQRRGERIPYVLRCLKEVALCQGKKSNLESSQ 475
Pig            QLISKYPASLPNCELSPLLMILYQLL-PQQRRGERTPYVLRCLMEVALCQGKKPNLESSH 476
Rabbit         QLISKYPASLPNHDLSSLLMILYQLL-PQQRRGERTPYVLRCLTEVALCQGKKSDLESSQ 476
Human          QLISKYPASLPNCELSPLLMILSQLL-PQQRHGERTPYVLRCLTEVALCQDKRSNLESSQ 476
Chimp          QLISKYPASLPNCELSPLLMILSQLL-PQQRHGERTPYVLRCLTEVALCQDKRSNLESSQ 476
                ******: * . ::  *: :* **   ***:*** *:***** *:***: *    .*:

Zebrafish      TAELGRLWARVWVLALRGVSSAQTGSLCLELLRIMVQESLVPVDREFWKVFSGAVCKPSL 538
Rat            KSDLLKLWIKIWSITFRGISSEQTQTENFGLLGAIIQGSLVELDREFWKLFTGSACKPSS 535
Mouse          KSDLLKLWIKIWSITFRGISSGQTQTENFGLLEAIIQGSLVELDREFWKLFTGSACKPSS 535
Pig            KSDLLKIWIKIWSITFRGISSEQIQAENFGLLGAIIQGSLVEVDREFWKLFTGSACKPSC 536
Rabbit         KSDLLKLWIKIWTMAFRGISSEQVQAENFGLLGAIIQGSLVEVDREFWKLFTGSACRPSC 536
Human          KSDLLKLWNKIWCITFRGISSEQIQAENFGLLGAIIQGSLVEVDREFWKLFTGSACRPSC 536
Chimp          KSDLLKLWNKIWCITFRGISSEQIQAENFGLLGAIIQGSLVEVDREFWKLFTGSACRPSC 536
               .::* ::* ::* :::**:** *  :  : **  ::* *** :******:*:*:.*:**

Zebrafish      VSALSLTQALLKCSVPKSVHSRDATSVVLTDAGGEPPSLRDSIISWLIMNEQNEETEENC 598
Rat            PSVRCLTLALSMCVVPDAIKMGTEQSVC---DANRSFSVKESIMRWLLFYQLEGDLEDSA 592
Mouse          PSVCCLTLALSICVVPDAIKMGTEQSVC---EANRSFSVKESIMRWLLFYQLEDDLEDST 592
Pig            PTVCCLTLALKTCVVPETVETGME-NIC---DGNRKFSLKESIMKWLLFCQLEDDFEDRI 592
Rabbit         STVYCLALAMSSCIVPETVKTGIELNIC---EVNRSFSLKELIMKWLLFYQLEDDLEDSI 593
Human          PAVCCLTLALTTSIVPGTVKMGIEQNMC---EVNRSFSLKESIMKWLLFYQLEGDLENST 593
Chimp          PAVCCLTLALTTSIVPGTVKMGIEQNMC---EVNRSFSLKESIMKWLLFYQLEGDLENST 593
                :. .*: *:  . ** ::.     .:      ..  *::: *: **:: : : : *:

Zebrafish      RPHLIISRDFPLYLIPRIVVSLTLKDSRAGLTFLMGSLKPDCFSPENSSLTETKATMDEV 658
Rat            EPPPILQSNFPHLILEKILVSLTMKNSKAAMKFFQSA--PECEQH---CEDTEEPSFSEA 647
Mouse          ELPPILQSNFPHLVVEKILVSLTMKNSKAAMKFFQSV--PECEQH---CEDKEEPSFSEV 647
Pig            ELPPILHSNFPHLALEKILVSLIMKNCKAAMNFFQSV--PECEQH---QKDTEEPSLLEV 647
Rabbit         ELPPILHSNFPHCILEKILVSLTMKNSKAAMKFFQSG--QECEHQ----KVKEEPSFSEI 647
Human          EVPPILHSNFPHLVLEKILVSLTMKNCKAAMNFFQSV--PECEHH---QKDKEELSFSEV 648
Chimp          EVPPILHSNFPHLVLEKILVSLTMKNCKAAMNFFQSV--PECEHH---QKDKEELSFSEV 648
               .   *:  :**   : :*:*** :*:.:*.:.*: .    :*           : :: *

Zebrafish      ESLFLQFSFDEAHSSAGFTVDKDSVYSEKPQFTVIQALRSKLEHSLLSIAEQLFTCYSPD 718
Rat            EELFLQTTFDKMDFLTPVKEDTVEKFQSRVGFSVHQNLKESLDHYLLGLSEQLLSNYSSE 707
Mouse          EELFLQTTFDKMDFLTTVKEYAVEKFQSSVGFSVQQNLKESLDHYLLGLSEQLLSNYSSE 707
Pig            EELFLQTTFDKMDFLTVVQECTIEKHQSSVGFSFHQNLKESLDRYLLGLSEQLLNNYLPE 707
Rabbit         EELFLQTTFDKMDFLTVVKECATEKLQSSIGFSVHQNLKESLNRYLLGLSEQLLNNYSSE 707
Human          EELFLQTTFDKMDFLTIVRECGIEKHQSSIGFSVHQNLKESLDRCLLGLSEQLLNNYSSE 708
Chimp          EELFLQTTFDKMDFLTIVRECGIEKHQSSIGFSVHQNLKESLDRCLLGLSEQLLNNYSSE 708
               *.**** :**: .  : .     .  ..   *:. * *:..*:: **.::***:. *  :

Zebrafish      STNTPHECVLRCVSLLIGVLAAYVCIGMLSEEQACLSPLFLKAKALVHEFSHYTSTAKSK 778
Rat            ITS--SETLVRCSSLLVGVLGCYCYMGVITEDEAYKSELFQKAKSLMQCAGESISLFKNK 765
Mouse          ITS--SETLVRCSSLLVGVLGCYCYMGIITEDEAHKSELFQKAKSLMQCAGESISLFKNK 765
Pig            TSD--SETLVRCSSLLVGVLGCYCYVGVIAEEEAYTSELFQKAKSLMQCAGESITLFKSK 765
Rabbit         ITN--LETLVRCSSLLVGVLGCYSSMGIIAEEEACKSELFQKAKSLMQCAGESITLFKNK 765
Human          ITN--SETLVRCSRLLVGVLGCYCYMGVIAEEEAYKSELFQKAKSLMQCAGESITLFKNK 766
Chimp          ITN--SETLVRCSRLLVGVLGCYCYMGVIAEEEAYKSELFQKAKSLMQCAGESITLFKNK 766
                :.   * ::**  **:***..*  :*:::*::*  * ** ***:*::  ..  :  *.*

Zebrafish      LAENETLASVQSVMLLCSDCICRREKGDKMSTISRTLFMKTLPVRLLNDLCDMSKQLLSN 838
Rat            TNEESRVGSLRSVIHLCTSCLCRHTKHT-LNKIASGFFLRLLTSKLMNDIADICKSLASC 824
Mouse          TNEESRIGSLRNVMHLCTSCLCIHTKHT-PNKIASGFFLRLLTSKLMNDIADICKSLASC 824
Pig            TNEESRIISLRNMMHLCTNCLYKCAKRS-PNKIASGFFLRLLTSKLMHDIADVCRSLAFI 824
Rabbit         TYEESRIGSLRNMMHICTSCLCNCTKQN-PNKITSGFFLRLLTSKLMNDIADICKSLATL 824
Human          TNEEFRIGSLRNMMQLCTRCLSNCTKKS-PNKIASGFFLRLLTSKLMNDIADICKSLASF 825
Chimp          TNEEFRIGSLRNMMQLCTRCLSNCTKKS-PNKIASGFFLRLLTSKLMNDIADICKSLASL 825
                 *:  : *::.:: :*: *:    *    ..*:  :*:: *  :*::*:.*:.:.*

Zebrafish      SGKKDTI-VIES--------EPVDMQTSRIQVDNQEEIDLFEDGDGTQHITSRPSQSNEE 889
Rat            TKKPFDYGEEHSLRDDDDDGDGGDGGESLMETQGSSSTDLFSDYSASTV------SDAND 878
Mouse          TKKPLDHGVHPG-----EDDEDGGGCDSLMEAEGPSSTGLSTAYPASSV------SDAND 873
Pig            IKKPFDCREVESMEDDT--------DKNLMEMNDQSSMSLFNDNPASSV------IDANE 870
Rabbit         IKKPFDCGEIESMEDDT--------TENLMEVEDQSSMNLFNDHSASSE------SDANE 870
Human          IKKPFDRGEVESMEDDT--------NGNLMEVEDQSSMNLFNDYPDSSV------SDANE 871
Chimp          IKKPFDRGEVESMEDDT--------NGNLMEVEDQSSMNLFNDYPDSSV------SDANE 871
```

```
                 *        .               . :: :. .. .*      :         . ::

Zebrafish      AADSKFITGTKSALSEEHLSKQDLTFLSVLGFLSLCASSELNGGFSFKPLDTQRKLLKLL 949
Rat            YGENQNAVGAANPLTADWLSRQDHLLLDMLRFLCLSVTACQSRTASFRGADIRRKLLMLL 938
Mouse          YGENQNAVGAMSPLAADYLSKQDHLLLDMLRFLGRSVTASQSHTVSFRGADIRRKLLLLL 933
Pig            SGESQITMGAMNPLAEEHLSKQDLLVLDMLRFLCMCITIAQSNTMSFRAADIRRKLLMLI 930
Rabbit         FGENQNTIGAMNPLAEEYLSKHDLLLLDMVKFLCMCVTTSQTSTVSFRAADIRRKLLMLV 930
Human          PGESQSTIGAINPLAEEYLSKQDLLFLDMLKFLCLCVTTAQTNTVSFRAADIRRKLLMLI 931
Chimp          PGESQSTIGAINPLAEEYLSKQDLLFLDMLKFLCLCVTTAQTNTVSFRAADIRRKLLMLI 931
                .:.:   *: . *: : **::*  .*.:: **  . :   .   **:  * :**** *:

Zebrafish      DLA--DFSQMLHLQMYLSLLKKLPAEVASLDPEEFNALLRPLADVCSLYRQDQEVCSAIL 1007
Rat            DPSTLDLTKSLHLHMYLVLLKDLPGKEHLLPMEDVVELLQPLSLVCSLYRRDQDVCKTIL 998
Mouse          DSSILDLMKPLHLHMYLVLLKDLPGNEHSLPMEDVVELLQPLSLVCSLHRRDQDVCKTIL 993
Pig            DSDRLDPTKSLHLHMYLVLLKELPGEEYPLPMEDVVELLKPLSSVCSLYRRDQDVCKTIL 990
Rabbit         DSSILDPTKSVHLHMYLVLLKELPRGEYPLPMEDIVELLKPLSNVCSLYRRDQDVCKTVL 990
Human          DSSTLEPTKSLHLHMYLMLLKELPGEEYPLPMEDVLELLKPLSNVCSLYRRDQDVCKTIL 991
Chimp          DSSTLDPTKSLHLHMYLMLLKELPGEEYPLPMEDVLELLKPLSNVCSLYRRDQDVCKTIL 991
               *    :  : :**:*** ***.**     *  *:.  **:**: ****:*:**:**.::*

Zebrafish      FSLLPSIRCLGLSSSGSEQEEDMADIKGSLLKVISGFCFLGKSGKCTSSVRVALRQCLLA 1067
Rat            SNVLHIVTNLGQGSVD---TESTRNAQGQFLTVMGAFWHLTKEKKCIFSVRMALVKCLQT 1055
Mouse          SNVLHIVTNLGQGSVD---MESTRIAQGHFLTVMGAFWHLTKEKKCVFSVRMALVKCLQT 1050
Pig            NHVLHIVPNLCRENVD---AESTRDAQGQFLTVIGAFWHLTKEGKCTFSVRLALVKCLKT 1047
Rabbit         NHVLPVVTNLGQGNLD---AENTRDAQGQFLTVIGAFWHLTRERKCTFSVRVALVQCLKT 1047
Human          NHVLHVVKNLGQSNMD---SENTRDAQGQFLTVIGAFWHLTKERKYIFSVRMALVNCLKT 1048
Chimp          NHVLHVVKNLGQSNMD---SENTRDAQGQFLTVIGAFWHLTKERKYIFSVRMALVNCLKT 1048
                 :*  :  *   . .    *.    :* :*.*:..* .* :. *   ***:** :** :

Zebrafish      LLEADPCCKWAVLTLREEELPVSAVLSSLLADSHQHVCMLTALSVESLFLKKALHSS--R 1125
Rat            LLEADPYSKWAILNVKGQDFPVREAFPQFLADGHHHVRMLAAGSISRLFQDMRQGDSSRS 1115
Mouse          LLEADPYSEWAILNVKGQDFPVNEAFSQFLADDHHQVRMLAAGSVNRLFQDMRQGDFSRS 1110
Pig            LLEADPYSRWAILNVMEKDFPVNEVFPQFLADNHHQVCMLAAGLINRLFQHMKQGDSSTI 1107
Rabbit         LLEADPYSKWAILNVMGKDFPVNEVFPQFLADDHHQVRMLAAESINRLFQDMKQGDCPRL 1107
Human          LLEADPYSKWAILNVMGKDFPVNEVFTQFLADNHHQVRMLAAESINRLFQDTK-GDSSRL 1107
Chimp          LLEADPYSKWAILNVMGKDFPVNEVFTQFLADNHHQVRMLAAESINRLFQDTK-GDSSRL 1107
               ****** ..**:*.:  :::**  .: .:***.*::* **:*  :. **  .    .

Zebrafish      KMMLPLKNQQTAFENIYLKAQEGIRRQKNCPS--EDLPDETFNRRATLLKSVSMVMSCSP 1183
Rat            LKALPLKFQQTSFNSAYMIAEAGIRELL-CDSQNPDLLDEIYNRKSVLLTVIAVVLHCSP 1174
Mouse          LKALPLKFQQTSFNNAYTTAEAGIRGLL-CDSQNPDLLDEIYNRKSVLLMMIAVVLHCSP 1169
Pig            MRALPLKLQQTAFENAYLKAQERIRQVKSQGGENRELLDEICNRKAVLLTMIAVVLCCSP 1167
Rabbit         WKALPLKLQQTAFDNACLKTQEGMREVS-HSAENPEILDETYNRKSVLLMMIAVVLYCSP 1166
Human          LKALPLKLQQTAFENAYLKAQEGMREMS-HSAENPETLDEIYNRKSVLLTLIAVVLSCSP 1166
Chimp          LKALPLKLQQTAFENAYLKAQEGMREMS-HSAENPEPLDEIYNRKSVLLTLIAVVLSCSP 1166
                  **** ***:*:.    ::  :*      .   :  **  **::.**  :::*: ***

Zebrafish      VCEKQALFALFQSYKENGIDEQLIKKVLRGISKSLGNRDHKSLINSHLYYLVAEWLNQKQ 1243
Rat            ICEKQALFALCKSVKENGLEPHLVKKVLEKVSESFGCRCLEDFMASHLDYLVLEWLNLQ- 1233
Mouse          VCEKQALFALCKSVKENRLEPHLVKKVLEKVSESFGCRSLEDFMISHLDYLVLEWLNLQ- 1228
Pig            VCEKQALFALCKSVKENGLEPHLIKKVLEKVSETFGYRHLEDFMASHLDYLVLEWLHLQ- 1226
Rabbit         VCEKQALFALCKSVKENGLEPHLVKKVLEKVSEAFGYRNLEDFMASHLDYLVLEWLNCQ- 1225
Human          ICEKQALFALCKSVKENGLEPHLVKKVLEKVSETFGYRRLEDFMASHLDYLVLEWLNLQ- 1225
Chimp          ICEKQALFALCKSVKENGLEPHLVKKVLEKVSETFGYRRLEDFMASHLDYLVLEWLNLQ- 1225
               :********* :* *** :: :*:****. :*:::* *  :.:: *** *** ***: :

Zebrafish      SDSSYTLQSFPYALLDCCSLEEFFRSSYHVLIPHLVFLNDFEGVKSIGDHLGQDWKQLLA 1303
Rat            -DAKYSLSSFPFTLLNYMSVEDFYRSCYKILIPHLVIRKHFDEVKSIANQIQRCWKSLLI 1292
Mouse          -DTEYSLSSFPFMLLNYTSIEDFYRSCYKILIPHLVIRSHFDEVKSIANQIQKCWKSLLV 1287
Pig            -DAEYSLSSFPFILLNYTNIEDFYRSCYKVLIPHLVMRCHFDEVKSIANQIQGDWKSLLT 1285
Rabbit         -NTEYRLSSFPYILLNYKNVEDFYRSCYKILIPHLVIRSHFDEVKAIANQIQEDWKSLLV 1284
Human          -DTEYNLSSFPFILLNYTNIEDFYRSCYKVLIPHLVIRSHFDEVKSIANQIQEDWKSLLT 1284
Chimp          -DTEYNLSSFPFILLNYTNIEDFYRSCYKVLIPHLVIRNHFDEVKSIANQIQEDWKSLLT 1284
                ::.* *.***: **:  .:*:*:**.*::******:  .*: **:*.:::   **.**

Zebrafish      KCFPKIMVNILPHFALAGQ-DTHVAQQREKAHRVYDILKNSNCLGKQQIDSLICNNLPDI 1362
Rat            DCFPKMLVHILPYFACEGTGDSSSAQKRETATEVYDTLKGEDFLGK-QIDQVFISNLPEI 1351
Mouse          DCFPKILVHILPYFAYEGTRDSYVSQKRETATKVYDTLKGEDFLGK-QIDQVFISNLPEI 1346
Pig            DCFPKILVNILPYFAYEDTGDRGMAQQRETASKVYDMLKDENLLGK-QIDQLFINNLPEI 1344
Rabbit         DCFPKILVNILPYFAYEDAKDSGMAQQREIASTVYDMLKSENLLGK-QIDHLFISNLPEI 1343
Human          DCFPKILVNILPYFAYEGTRDSGMAQQRETATKVYDMLKSENLLGK-QIDHLFISNLPEI 1343
```

```
Chimp          DCFPKILVNILPYFAYEGTGDSGMAQQRETATKVYDMLKSENLLGK-QIDHLFISNLPEI 1343
               .****::*:***:**  .  *   :*:** *  *** **..: *** *** :: .***:*

Zebrafish      VVELLMTLHETAGD--------KGDLQKFTGELDPAPNPPFFSSYVIKATLDYLSKCHSA 1414
Rat            VVELLMTLHETADSDSG----QSPDLCDFSGDLDPAPNPPYFPSHVIKATFAYISSCHKT 1407
Mouse          VVELLMTLHETADSADSDASQSATALCDFSGDLDPAPNPPYFPSHVIQATFAYISNCHKT 1406
Pig            VVELLMTLHEPATSDAS----QSTDPCDFSGDLDPPPNPPHFPSHVIKATFAYISNCHKT 1400
Rabbit         VVELLMTLHEPANSDAS----QSTDLSEFSGDLDPAPNPPHFPSHVIKATFAYISNCHKT 1399
Human          VVELLMTLHEPANSSAS----QSTDLCDFSGDLDPAPNPPHFPSHVIKATFAYISNCHKT 1399
Chimp          VVELLMTLHEPANSSAS----QSTYLYDFSGDLDPAPNPPHFPSHVIKATFAYISNCHKT 1399
               ********** * .             .*:*:*** ****.* *:**:**: *:*.**.:

Zebrafish      NHKSLVAILSKTPMSIQRILVAVCQKADETTNAYERHRILMMYHLFVSLLLKEVKDGLGG 1474
Rat            KFKSILEILSKIPDSYQKILLAICEQAAETNNVFKKHRILKIYHLFVSLLLKDIQSGLGG 1467
Mouse          KFKSILEILSKIPDSYQKILLAICEQAAETNNVFKKHRILKIYHLFVSLLLKDIQSGLGG 1466
Pig            KLKSILEVLSKSPDSYQKILLAICEQAAETNNVYKKHRILKIYHLFVSLLLKDMKSGLGG 1460
Rabbit         KLKSILEILSKSPDSYQKILLAICEQAAETNNVYRRHRILKIYHLFVSLLLKDIKSGLGG 1459
Human          KLKSILEILSKSPDSYQKILLAICEQAAETNNVYKKHRILKIYHLFVSLLLKDIKSGLGG 1459
Chimp          KLKSILEILSKSPDSYQKILLAICEQAAETNNVYKKHRILKIYHLFVSLLLKDIKSGLGG 1459
               : **:: :*** * * *:**:*:*::* **.*.:.:**** :**********:::.****

Zebrafish      AWAFVLRDIIYTLIHHINSRSSQQDEVSTRSLSLCCDLLSLVCQTAVEYCDDALESHLQV 1534
Rat            AWAFVLRDVIYTLIHYINKRSSHFTDVSLRSFSLCCDLLSRVCRTAVTHCKDALENHLHV 1527
Mouse          AWAFVLRDVIYTLIHYINKRSSHFTDVSLRSFSLCCDLLSRVCHTAVTQCKDALESHLHV 1526
Pig            AWAFVLRDVIYTLIHYINKRPSRFMDVSLRSFSLCCDLLSRVCHTAVTYSKDALESHLHV 1520
Rabbit         AWAFVLRDVIYTLIHYINKRPSRFMDVSLRSFSLCCDLLSRVCQTAVTHCKDALENHLHV 1519
Human          AWAFVLRDVIYTLIHYINQRPSCIMDVSLRSFSLCCDLLSQVCQTAVTYCKDALENHLHV 1519
Chimp          AWAFVLRDVIYTLIHYINQRPSCIMDVSLHSFSLCCDLLSQVCQTAVTYCKDALENHLHV 1519
               ********:******:**.* *   :** :*:******** **:***  ..****.**:*

Zebrafish      IVGTLTAQVTEQSAISEQVLSLLRFLVMENPENRMLRKSIPLLEPFPEQPNFAELRAAQH 1594
Rat            IVGTLIPLVDY-QEVQEQVLDLLKYLVIDNKDNKNLFVTIKLLDPFPDHVVFKDLRLTQQ 1586
Mouse          IVGTLIPLVDY-QEVQEQVLDLLKYLVIDNKDNKNLSVTIKLLDPFPDHVIFKDLRLTQQ 1585
Pig            IVGTLIPLVDGQMEVQKQVLDLLKYLVIDNKDNENLYVMIKLLDPFPDNAVFKDLRITQQ 1580
Rabbit         IVGTLIPLVHDQVEVQEQVLDLLKYLVIDNKDNENLYITIKLLDPFPDHVVFKDLRITQQ 1579
Human          IVGTLIPLVYEQVEVQKQVLDLLKYLVIDNKDNENLYITIKLLDPFPDHVVFKDLRITQQ 1579
Chimp          IVGTLIPLVYEQVEVQKQVLDLLKYLVIDNKDNENLYLTIKLLDPFPDHVVFKDLRITQQ 1579
               *****   *     :.:***.**::**::* :*. *   * **:***::  * :** :*:

Zebrafish      ALKYSSGAFTLRQEIEHFLSVASCDSLPLARLEGLKDLKRQLHSHKQQIGQLLKECHADL 1654
Rat            KIKYSGGPFTLLEEINHFLSVSAYNPLPLTRLEGLKDLRRQLEQHKDQMLDLVRASQDNP 1646
Mouse          KIKYSGGPFSLLEEINHFLSVSAYNPLPLTRLEGLKDLRRQLEQHKDQMLDLLRASQDNP 1645
Pig            EIKYSKGPFSLLEEINHFLSVSVYDALPLTRLEGLKDLRRQLAQHKDQMMDLMRASQDNP 1640
Rabbit         KIKYCRGSFSLLEEINHFLSVSIYDALPLTRLEGLKDLQRQLAKHKDQMMDLMRASQDNP 1639
Human          KIKYSRGPFSLLEEINHFLSVSVYDALPLTRLEGLKDLRRQLELHKDQMVDIMRASQDNP 1639
Chimp          KIKYSRGPFSLLEEINHFLSVSVYDALPLTRLEGLKDLRRQLELHKDQMVDIMRASQDNP 1639
                :**. * *:* :**:*****:  : ***:********:***  **:*: :::: .: :

Zebrafish      DSCILVNLVLNLLQLCKIAANHPGGGDIMKAAGRCLGELGPVDLSSIALHHGKDQLYARA 1714
Rat            QDGIVVKLVVSLLQLSKMAVNQTGEREVLEAVGRCLGEIGPLDFSTIAVQHSKDTPYTKA 1706
Mouse          QDGIVVKLVVSLLQLSKMAVNQTGEREVLEAVGRCLGEIGPLDFSTIAVQHNKDVSYTKA 1705
Pig            QDGIVVKLVVSLLQLSKMAVNHTGEREVLEAVGRCLGEVGPIDFSTIAIQHSKDMPYTKA 1700
Rabbit         KDGIMVKLVITLLHLSKTAVNHTGEREVLEAVGSCLGELGPIDFSTIAIQHNKDTSYTKA 1699
Human          QDGIMVKLVVNLLQLSKMAINHTGEKEVLEAVGSCLGEVGPIDFSTIAIQHSKDASYTKA 1699
Chimp          QDGIMVQLVVNLLQLSKMAINHTGEKEVLEAVGSCLGEVGPIDFSTIAIQHSKDASYTKA 1699
               .. *:*:**:.**:*.* * *: *  ::::*.* ****:**:*:*:**::*.**  *::*

Zebrafish      AKLFHNVPHQWIFIILNSMDNALTNHSIAVRQTAGLCIKDILATQSGIEFGEIHKSKRDP 1774
Rat            YGLPEDRELQWTLIMLTALNNTLVEDSVKIRSAAATCLKNILATKTGHIFWENHKTSADP 1766
Mouse          YGLPEDRELQWTLIMLTALNNTLVEDSVKIRSAAATCLKNILATKIGHIFWENYKTSADP 1765
Pig            LELFEDKEHHWTLMMLTYLNSTLVEDCVKVRSAAVTCLKSILATKTGHGFWEIFKTTADP 1760
Rabbit         FKLFEDKELCWTLIILTYLNNTLVEDCVRVRSAAATCLKNILATKTGHSFWEVYKMSTDP 1759
Human          LKLFEDKELQWTFIMLTYLNNTLVEDCVKVRSAAVTCLKNILATKTGHSFWEIYKMTTDP 1759
Chimp          LKLFEDKELQWTFIMLTYLNNTLVEDCVKVRSAAVTCLKNILATKTGHSFWEIYKMTTDP 1759
                 * .:    * :::*. ::.:*.:..: :*.:*  *:*.****: *  * * .* . **

Zebrafish      LLAYLNPFRSSKKREPIMAMDVTPESRDRLTSADLWLMQPDGHKDWLKNLCMALLDSGGV 1834
Rat            MLTYLQPFRASRKKFLELPQFVKEDALEGLDDVNLWVPQSESHDIWIKTLTCAFLDSGGI 1826
Mouse          MLTYLQPFRTSRKKFLEVPRSVKEDVLEGLDAVNLWVPQSESHDIWIKTLTCAFLDSGGI 1825
Pig            MLTYLLPFRTSRKKFLEVPRLNKESPLEGLDDISLWIPQSENHDIWIKTLTCALLDSGGI 1820
Rabbit         MLIYLQPFRTSRKKFLEVPRPDKESPLESLDDTSLWIPQSENHDIWIKTLTCALLDSGGI 1819
```

```
Human          MLAYLQPFRTSRKKFLEVPRFDKENPFEGLDDINLWIPLSENHDIWIKTLTCAFLDSGGT 1819
Chimp          MLAYLQPFRTSRKKFLEVPRFDKENPFEGLDDTNLWIPLSENHDIWIKTLTCAFLDSGGT 1819
               :* ** ***:*:*:   :    . .  : *   .**:   :.*. *:*.*  *:*****

Zebrafish      RNEALLLTRPLCEVKTDFCQRMLPLFVHDILLGDVDGSWRQLLSTHIQSFFSQCRRPSTP 1894
Rat            KSEILQLLKPMCEVKTDFCQMVLPYLIHDVLLQDTHESWRTLLSTHVRGFFTNCFKHSSQ 1886
Mouse          NSEILQLLKPMCEVKTDFCQMLLPYLIHDVLLQDTHESWRTLLSAHVRGFFTSCFKHSSQ 1885
Pig            NSEVLQLLKPMCEVKTDFCQTVLPYLIHDILLQDTNESWRSLLSTHIQGFFTNCFRHSSQ 1880
Rabbit         KSEILQLLKPMCEVKTDFCQTVLPYLIHDILLQDTNESWRNLLSAHIQGFFTSCFRHNSQ 1879
Human          KCEILQLLKPMCEVKTDFCQTVLPYLIHDILLQDTNESWRNLLSTHVQGFFTSCLRHFSQ 1879
Chimp          KCEILQLLKPMCEVKTDFCQTVLPYLIHDILLQDTNESWRNLLSTHVQGFFTSCLRHFSQ 1879
               . * * * :*:********* :** ::**:** *.. *** ***:*::.**:.* :  :

Zebrafish      TSRPTTPMLSDSGNTTDAANQCQIDKASLRSMLAVIDHLRQQSRPLAPGSNEYGTVCDSN 1954
Rat            ASRSATPANSDSE--SENFLRCCLDKKSQRTMLAVVDYLRRQKRPS------SGTAFEDA 1938
Mouse          ASRSATPANSDSE--SENFLRCCLDKKSQRTMLAVVDYLRRQKRPS------SGTAFDDA 1937
Pig            TSRSTTPANMDSE--SEHVFRCHLDKKSQRTMLAVVDYMRRQKRSS------SGTVFDDA 1932
Rabbit         TSRSTTPANLDSD--SEHFFRCCVDKKSQRTMLAVVDYMRRQKRPS------IGTVFDDA 1931
Human          TSRSTTPANLDSE--SEHFFRCCLDKKSQRTMLAVVDYMRRQKRPS------SGTIFNDA 1931
Chimp          TSRSTTPANLDSE--SEHFFRCCLDKKSQRTMLAVVDYMRRQKRPS------SGTIFNDA 1931
               :** :**   **   ::   :* :** * *:****:*::*:*.*         **  :.

Zebrafish      FWLDLNYLEVAGAAQMCSAHFTALLYSEIYVDKIRSNMEQNRRSQSRASRRITFEDNSQT 2014
Rat            FWLDLNYLEVAKVAQSCAAHFTALLYAEIYSDKKNMD--------EQEKRSPTFEEGSQG 1990
Mouse          FWLDLNYLEVAKVAQSCSAHFTALLYAEIYSDKKSTD--------EQEKRSPTFEEGSQG 1989
Pig            FWLELNYLEVAKVAQSCAAHFTALLYAEIYADKKNMD--------DQEKRSPTFEEGSQS 1984
Rabbit         FWLDFNYLEVAKVAQSCAAHFTALLYAEIYADKKSLD--------DQEKRSLTFEEGSQN 1983
Human          FWLDLNYLEVAKVAQSCAAHFTALLYAEIYADKKSMD--------DQEKRSLAFEEGSQS 1983
Chimp          FWLDLNYLEVAKVAQSCAAHFTALLYAEIYADKKSMD--------DQEKRSLAFEEGSQS 1983
               ***::****** .** *:********:*** **   :        .: .*  :**:.**

Zebrafish      LSVSNLNERSLEDSGFSLQDLLIEVYRCIGEPDSLYGCGGGKLTSPLTRIRTYEHEAMWE 2074
Rat            TTISSLSEKSKEETGISLQDLLLEIYRSIGEPDSLYGCGGGKVLQPLTRIRTYEHEATWE 2050
Mouse          TTISSLSEKSKEETGISLQDLLLEIYRSIGEPDSLYGCGGGKMLQPLTRIRTYEHEATWE 2049
Pig            TTISSLSEKSKEETGISLQDLLLEIYRSIGEPDSLYGCGGGKMLQPLTRLRTYEHEAMWG 2044
Rabbit         TTISSLSEKSREETGISLQDLLLEIYRSIGEPDSLYGCGGGKMLQPLTRLRTYEHEAVWD 2043
Human          TTISSLSEKSKEETGISLQDLLLEIYRSIGEPDSLYGCGGGKMLQPITRLRTYEHEAMWG 2043
Chimp          TTISSLSEKSREETGISLQDLLLEIYRSIGEPDSLYGCGGGKMLQPITRLRTYEHEAMWG 2043
                ::*.*.*:* *::*:******:*:**.**************: .*:**:******* *

Zebrafish      KALVSYDLHSNLPEVTRQIGIVEGLQNFGLCSILSTYLHGLEKDGMEWGPELRELRFQAA 2134
Rat            KALVTYDLETTISSSTRQSGIIQALQNLGLSHILSIYLKGLDHERREWCGELQELHYQAA 2110
Mouse          KALVTYDLETSISSSTRQSGIIQALQNLGLSHILSVYLKGLDYERREWCAELQELRYQAA 2109
Pig            KALVTYDLETAISSSTRQAGIIQALQNLGLCHILSVYLKGLDHENKEQCAELQELHYQVA 2104
Rabbit         KALVTYDLETAICPSTRQAGIIQALQNLGLCHILSVYLKGLDHENVECCAELQELHYQAA 2103
Human          KALVTYDLETAIPSSTRQAGIIQALQNLGLCHILSVYLKGLDYENKDWCPELEELHYQAA 2103
Chimp          KALVTYDLETAIPSSTRQAGIIQALQNLGLCHILAVYLKGLDYENKDWCPELEELHYQAA 2103
               ****:***.: :   *** **::.***:**. **: **:**: :  :   **.**::*.*

Zebrafish      WRSTQWDCDLPERNEKLKPGINESLFNALQALRDKEFSLFEQTLNYA---RGREVEELCR 2191
Rat            WRNMQWDLCTSANQELEGTSYHESLYNALQCLRNREFSTFYDSLRHA---RVKEVEELSK 2167
Mouse          WRNMQWGLCASAGQEVEGTSYHESLYNALQCLRNREFSTFYESLRYASLFRVKEVEELSK 2169
Pig            WRNMQWDSCVSVNKGMEGTSYHESLYNALQSLRDREFSTFYESLKYA---RVKEVEELCK 2161
Rabbit         WRNMQWDHCTSVNKGIEGTSYHESLYNALQSLRDREFSTFFESLKYA---RVKEVEELCK 2160
Human          WRNMQWDHCTSVSKEVEGTSYHESLYNALQSLRDREFSTFYESLKYA---RVKEVEEMCK 2160
Chimp          WRNMQWDHCTSVSKEVEGTSYHESLYNALQSLRDREFSTFYENLKYA---RVKEVEELCK 2160
               **. **.      :     . :***:****.**::*** * :.*.:*   * :****:.:

Zebrafish      GSLEAVSSLYPALCNLQRISELQSVEELFSRPVTDSSLNEVYRKWQQHSDLLTDSDFSLV 2251
Rat            GSLESVYSLYPTLSRLQAVGELENSGELFSRSVTDRERSEVYLKWQKHSQLLKDSDFSFQ 2227
Mouse          GSLESVYSLYPTLSRLQAIGELENSGELFSRSVTDRERSEAYWKWQKHSQLLKDSDFSFQ 2229
Pig            GSLESVYSLYPTLSRLQAIGELENIGELFSRSVTDRQPSEVYNKWWKHSQLLKDSDFSFQ 2221
Rabbit         GSLESVYSLYPRLSRLQAIGELENIGELVSRSVMDKQFSEVYVKWQKHSQLLKDSDFNFQ 2220
Human          RSLESVYSLYPTLSRLQAIGELESIGELFSRSVTHRQLSEVYIKWQKHSQLLKDSDFSFQ 2220
Chimp          RSLESVYSLYPTLSRLQAIGELESIGELFSRSVTHRQLSEVYIKWQKHSQLLKDSDFSFQ 2220
                ***:* **** *..** :.**:.  **.** * . . .*.* ** :**:**.****.:

Zebrafish      EPVLALRSSIQEALISSETDPDRKNYLISTYSSHLMELCRLARSAGNTQLAERAVFHMKQ 2311
Rat            EPLMALRTVILEILVQKEMENSQGGCSKDILTKHLVEFSVLARTFKNTQLPERAIFKIKQ 2287
Mouse          EPLMALRTVILETLVQKEMERSQGACSKDILTKHLVEFSVLARTFKNTQLPERAIFKIKQ 2289
Pig            EPIMALRTVILEILMEKEMENSQRECLKDILTKHLVELSLLARTFQNTQLPERAIFQIKQ 2281
```

```
Rabbit          EPIMALRTVILEILMEKEVNNSQRECFKDILTKHLTEFSILARTFKNTQLPERAVFQIKQ 2280
Human           EPIMALRTVILEILMEKEMDNSQRECIKDILTKHLVELSILARTFKNTQLPERAIFQIKQ 2280
Chimp           EPIMALRTVILEILMEKEMDNSQRECIKDILTKHLVELSILARTFKNTQLPERAIFQIKQ 2280
                **::***: * * *:..* : .:     .  :.** *:. ***:  **** ***:*::**

Zebrafish       HNLVMSGSGSSSWAWQLEEAQVFWVKKEHGLALELLKQMIHKLDDLVC---VNPAVVPVY 2368
Rat             YNPAICGI----SEWHLEEAQVFWAKKEQSLALSILKQMIKKLDSSFRE--NEAGLKGLH 2341
Mouse           YNSAICGI----SEWHLEEAQVFWAKKEQSLALSILKQMIKKLDSSFKDKENDAGLKVIY 2345
Pig             YNSANCGV----SEWQLEEAQVFWAKKEQSLALSILKQMIKKLDASCTE--NDPRLKLIH 2335
Rabbit          YNSVSHEV----SEWQLEEAQVFWAKKEQSLALSILKQMIKKLDTSCRE--NDSRLKLIH 2334
Human           YNSVSCGV----SEWQLEEAQVFWAKKEQSLALSILKQMIKKLDASCAA--NNPSLKLTY 2334
Chimp           YNSVSCGV----SEWQLEEAQVFWAKKEQSLALSILKQMIKKLDASCAA--NNPSLKLTY 2334
                :* .          *:********.***:.***.:*****:***        :  :   :

Zebrafish       SECLRLCGSWLAESCLESPAVILENYLERAVEVIEEHCGGLKSKLQSQKTQAYFSLARFS 2428
Rat             AECLRVCGNWLAETCLENPAVIMQTYLEKAVKVAGSYDGDS-RELRNGQMKAFLSLARFS 2400
Mouse           AECLRVCGSWLAETCLENPAVIMQTYLEKAVKVAGSYDGNS-RELRNGQMKAFLSLARFS 2404
Pig             IECLRVCGTWLAETCLENPAVIMQTYLEKAVELAGNYDGESNDELRNGKMKAFLSLARFS 2395
Rabbit          TECLRVCGNWLAETCLENPTVIMQTYLEKAVEVAESCDGENNDELRNGKMKAFLSLARFS 2394
Human           TECLRVCGNWLAETCLENPAVIMQTYLEKAVEVAGNYDGESSDELRNGKMKAFLSLARFS 2394
Chimp           TECLRVCGNWLAETCLENPAVIMQTYLEKAVEVAGNYDGESSDELRNGKMKAFLSLARFS 2394
                 ****:**.****:***.*:**::.***:**::  .  *    :*:. : :*::******

Zebrafish       DAQYQGIENYMKSSEFENKHALLEKAKEEVDLMRERKVNNNRYTVKVQRELELDVKALAN 2488
Rat             DTQYQRIENYMKSSEFENKQALLKRAKEEVGLIREHKIQTNRYTIKVQRELELDECALRA 2460
Mouse           DTQYQRIENYMKSSEFENKQTLLKRAKEEVGLLREHKIQTNRYTVKVQRELELDECALRA 2464
Pig             DTQYQRIENYMKSSEFENKQALLKRAKEEVGLLREHKIQTNRYTIKVQRELELDEGALRA 2455
Rabbit          DTQYQRIENYMKSSEFENKQALLKRAKEEVGLLREHKIQTNRYTVKVQRELELDECALRA 2454
Human           DTQYQRIENYMKSSEFENKQALLKRAKEEVGLLREHKIQTNRYTVKVQRELELDELALRA 2454
Chimp           DTQYQRIENYMKSSEFENKQALLKRAKEEVGLLREHKIQTNRYTVKVQRELELDELALRA 2454
                *:*** *************::**::*****.*:**:*::.****:*********  **

Zebrafish       LQADRNRFLLKAVENYIECLELGEEHDTWVFRLASLWLENADVKAVNDKMKSGVKKIPSY 2548
Rat             LKEDRKRFLCKAVENYISCLLSGEEHDLWVFRLCSLWLENSGVSEVNGMMKRDGMKISSY 2520
Mouse           LREDRKRFLCKAVENYINCLLSGEEHDLWVFRLCSLWLENSGVSEVNGMMKKDGMKISSY 2524
Pig             LKKDRKRFLCKAVENYINCLLSGEGHDMWIFRLCSLWLENSGVSEVNGMMKRDGMKIPSY 2515
Rabbit          LKEDRKRFLCKAVENYINCLLSGEEHDMWVFRLCSLWLENSGVPEVNGMMKGPGMEIPSY 2514
Human           LKEDRKRFLCKAVENYINCLLSGEEHDMWVFRLCSLWLENSGVSEVNGMMKRDGMKIPTY 2514
Chimp           LKEDRKRFLCKAVENYINCLLSGEEHDMWVFRLCSLWLENSGVSEVNGMMKRDGMKIPTY 2514
                *: **:*** *******.**  ** ** *:***.******:.*  **. **    :* :*

Zebrafish       KFLPLMYQLAARMGTKVSSSMASQDVGFHHVLNELICQSSVDHPHHTLFIILALVNANKD 2608
Rat             KFLPLMYQLAARMGTKMTG-----GLGFHEVLNNLISRISMDHPHHTLFIILALANANKD 2575
Mouse           KFLPLMYQLAARMGTKMTG-----GLGFHEVLNNLISRISLDHPHHTLFIILALANANKD 2579
Pig             KFLPLMYQLAARMGTKMMG-----GLGFHDVLNSLISRISVDHPHHTLFIILALANANKD 2570
Rabbit          KFLPLMYQLAARMGTKMMG-----GVGFHEVLNNLISRVSMDHPHHTLFIILALANANKD 2569
Human           KFLPLMYQLAARMGTKMMG-----GLGFHEVLNNLISRISMDHPHHTLFIILALANANRD 2569
Chimp           KFLPLMYQLAARMGTKMMG-----GLGFHEVLNNLISRISMDHPHHTLFIILALANANRD 2569
                ****************: .     .:***.***.**.: *:*************.***:*

Zebrafish       DSFSR------SRSSKSSARQPSPLDLERAEVARKIIDVVRKKRAKMVKDIEMLCNAYIT 2662
Rat             EFLSKPETARRGRITKNAPKESSQLDEDRAEAASRIIHTIRSARRTMVKDMEALCDAYII 2635
Mouse           EFLSKPETTRRSRITKSTSKENSHLDEDRTEAATRIIHSIRSKRCKMVKDMEALCDAYII 2639
Pig             EFLTKPEAARSSRITKNTPKESSQLDEDRTEAANKVICTLRNRRRQMVRSVEALCDAYII 2630
Rabbit          EFLTKPEAARRSRITKNAPKQSSQLDEDRMEAANNIISTIRSKRPQMVRSVEALCDAYIL 2629
Human           EFLTKPEVARRSRITKNVPKQSSQLDEDRTEAANRIICTIRSRRPQMVRSVEALCDAYII 2629
Chimp           EFLTKPEVARRSRITKNVPKQSSQLDEDRTEAANRIICTIRSRRPQMVRSVEALCDAYII 2629
                : :::      .* :*.  :: * ** :* *.* .:*  :*. *  **:.:* **:***

Zebrafish       LAYMDASRHKTEKKAIPIPAEQPLMQIKDLEDVIIPTMDIKVDPSGRYEDVVTVRSFKRH 2722
Rat             LANLDASQWRNQRKGISIPANQPITKLKNLEDVVVPTMEIKVDPTGEYEKLVTIKSFKTE 2695
Mouse           LANMDASQWRAQRKGINIPANQPITKLKNLEDVVVPTMEIKVDPTGEYENLVTIKSFKTE 2699
Pig             LANLDATQWRTQRKGIRIPADQPITKLKNLEDVVVPTMEIKVDPTGEYGNMVTIQSFKPE 2690
Rabbit          LANLDATQWKTQRKGIIIPADQPITKLKNLEAVVVPTMEIKVDPTGEYENLVTIQSFKAE 2689
Human           LANLDATQWKTQRKGINIPADQPITKLKNLEDVVVPTMEIKVDHTGEYGNLVTIQSFKAE 2689
Chimp           LANLDATQWKTQRKGINIPADQPITKLKNLEDVVVPTMEIKVDHTGEYGNLVTIQSFKAE 2689
                ** :**:: : ::*.* ***:**: ::*:** *::***:**** :*.* .:**::*** .

Zebrafish       FHLAGGVNLPKIIDCEGSDGISRRQLVKGQDDLRQDAVMQQVFHMCSTLLQRNAETRKRK 2782
Rat             FRLAGGLNLPKIIDCVGSDGKERRQLVKGRDDLRQDAVMQQVFQMCNMLLQRNTETRKRK 2755
Mouse           FRLAGGLNLPKIIDCVGSDGKERRQLVKGRDDLRQDAVMQQVFQMCNTLLQRNTETRKRK 2759
```

```
Pig             FRLAGGLNLPKIIDCVGSDGKERRQLVKGRDDLRQDAVMQQVFQMCNTLLQRNTETRKRK 2750
Rabbit          FRLAGGINLPKIIDCVGSDGRERRQLVKGRDDLRQDAVMQQVFQLCNMLLQRNTETRKRK 2749
Human           FRLAGGVNLPKIIDCVGSDGKERRQLVKGRDDLRQDAVMQQVFQMCNTLLQRNTETRKRK 2749
Chimp           FRLAGGVNLPKIIDCVGSDGKERRQLVKGRDDLRQDAVMQQVFQMCNTLLQRNTETRKRK 2749
                *:****:******** **** .*******:*************::*. *****:******

Zebrafish       LNIRRYKVVPFSQRSGVLEWCSGTVPIGEFLVDPQKGAHKRFRPQDWANMLCRKKMMEAQ 2842
Rat             LTICTYKVVPLSQRSGVLEWCTGTIPIGEYLVNNEEGAHKRYRPNDLSANQCQKKMMEVQ 2815
Mouse           LTICTYKVVPLSQRSGVLEWCTGTVPIGEYLVNSEDGAHRRYRPNDFSANQCQKKMMEVQ 2819
Pig             LTICTYKVVPLSQRSGVLEWCTGTVPIGEYLVNNDTGAHKRYRPKDFSPVQCQKKMMEAQ 2810
Rabbit          LTICTYKVVPLSQRSGVLEWCTGTIPIGEFLTDSEGGAHKRYRPTDFSSVQCQKKMIEIQ 2809
Human           LTICTYKVVPLSQRSGVLEWCTGTVPIGEFLVNNEDGAHKRYRPNDFSAFQCQKKMMEVQ 2809
Chimp           LTICTYKVVPLSQRSGVLEWCTGTVPIGEFLVNNEDGAHKRYRPNDFSAFQCQKKMMEVQ 2809
                *.*  *****:**********:**:****:*.: : ***:*:** * :   *:***:* *

Zebrafish       RMEFNDKLQAFTEVCQNFRPVFRYFCMERFLDPAIWLERRLAYTRSVATSSIVGYIVGLG 2902
Rat             KKSFEEKYETFMTICQNFEPVFRYFCMEKFLDPAVWFEKRLAYTRSVATSSIVGYILGLG 2875
Mouse           KKSFEEKYDTFMTICQNFEPVFRYFCMEKFLDPAVWFEKRLAYTRSVATSSIVGYILGLG 2879
Pig             NKSFEEKYEIFMNICQNFQPVFRYFCMEKFLDPAVWFERRLAYTQSVATSSIVGYILGLG 2870
Rabbit          KKSFEEKYKTFMNICKHFQPVFRYFCMEKFLDPAVWFEKRLAYTRSVATSSIVGYILGLG 2869
Human           KKSFEEKYEVFMDVCQNFQPVFRYFCMEKFLDPAIWFEKRLAYTRSVATSSIVGYILGLG 2869
Chimp           KKSFEEKYEVFMDVCQNFQPVFRYFCMEKFLDPAIWFEKRLAYTRSVATSSIVGYILGLG 2869
                . .*::* . *  :*::*.*********:*****:*:*:*****:***********:***

Zebrafish       DRHIQNILIDEQTSELVHIDLGVAFEQGKILPTPETVPFRLSRDIVDGMGITGVEGVFRR 2962
Rat             DRHVQNILINEQSAELVHIDLGVAFEQGKILPTPETVPFRLSRDIVDGMGITGVEGVFRR 2935
Mouse           DRHVQNILINEQSAELVHIDLGVAFEQGKILPTPETVPFRLSRDIVDGMGITGVEGVFRR 2939
Pig             DRHVQNILINEQSAELVHIDLGVAFEQGKILPTPETVPFRLTRDIVDGMGITGVEGVFRR 2930
Rabbit          DRHIQNILINEQSAELVHIDLGVAFEQGKILPTPETVPFRLTRDIVDGMGITGVEGVFRR 2929
Human           DRHVQNILINEQSAELVHIDLGVAFEQGKILPTPETVPFRLTRDIVDGMGITGVEGVFRR 2929
Chimp           DRHVQNILINEQSAELVHIDLGVAFEQGKILPTPETVPFRLTRDIVDGMGITGVEGVFRR 2929
                ***:*****:**::***************************:******************

Zebrafish       CCEKTMEVMRSSQEALLTIVEVLLYDPLFDWTMNPLKAFYLQQHDEQAELNATLNPTPGG 3022
Rat             CCEKTMEVMRSSQEALLTIVEVLLYDPLFDWTMNPLKALYLQQRPED---ETDLQSTPSA 2992
Mouse           CCEKTMEVMRSSQETLLTIVEVLLYDPLFDWTMNPLKALYLQQRPED---ESDLHSTPNA 2996
Pig             CCEKTMEVMRNSQETLLTIVEVLLYDPLFDWTMNPLKALYLQQRPED---ESELHSTPRA 2987
Rabbit          CCEKTMEVMRNSQETLLTIVEVLLYDPLFDWTMNPLKALYLQQRPED---ETEFQSTPNA 2986
Human           CCEKTMEVMRNSQETLLTIVEVLLYDPLFDWTMNPLKALYLQQRPED---ETELHPTLNA 2986
Chimp           CCEKTMEVMRNSQETLLTIVEVLLYDPLFDWTMNPLKALYLQQRPED---ETELHPTLNA 2986
                **********.***:***********************:****: *:   :: :: *  .

Zebrafish       DEIETHRKASD-SQSFNKVAERVLLRLQEKLKGVEDGTVLSVGGQVNLLIQQAMDPKNLS 3081
Rat             DDQECKRSLSDTDQSFNKVAERVLMRLQEKLKGVEEGTVLSVGGQVNLLIQQAMDPKNLS 3052
Mouse           DDQECKQSLSDTDQSFNKVAERVLMRLQEKLKGVEEGTVLSVGGQVNLLIQQAMDPKNLS 3056
Pig             DDQECKRNLSDTDQSFNKVAERVLMRLQEKLKGVEEGTVLSVGGQVNFLIQQAMDPKNLS 3047
Rabbit          DDQECKRNLSDIDQSLNKVAERVLIRLQEKLKGVEEGTVLSVSGQVNLLIQQAMDPKNLS 3046
Human           DDQECKRNLSDIDQSFNKVAERVLMRLQEKLKGVEEGTVLSVGGQVNLLIQQAIDPKNLS 3046
Chimp           DDQECKRNLSDIDQSFNKVAERVLMRLQEKLKGVEEGTVLSVGGQVNLLIQQAIDPKNLS 3046
                *: * ::. ** .**:********:**********:******.****:*****:******

Zebrafish       RLFPGWQAWV   3091
Rat             RLFPGWKAWV   3062
Mouse           RLFPGWKAWV   3066
Pig             KLFSGWKAWV   3057
Rabbit          RLFPGWKAWV   3056
Human           RLFPGWKAWV   3056
Chimp           RLFPGWKAWV   3056
                :** **:***
```

Appendix 3

Appendix 3.1 Statisitical Analysis Coresponding to figure 3.2: Expression of ATM mRNA in wild type and ATM$^{sh477/sh477}$ zebrafish

Figure b: Expression of ATM mRNA through first 7 days of development normalised to 7 dpf

Ordinary one-way ANOVA	*F Value*	*P value*	*P value summary*	*Significant diff. among means (P < 0.05)?*	*R squared*
	163.5	<0.0001	****	Yes	0.9864

Tukey's multiple comparisons test	*Mean Diff.*	*95.00% CI of diff.*	*Below threshold?*	*Summary*	*Adjusted P Value*
16 cell vs. 50% epiboly	7.750	6.806 to 8.693	Yes	****	<0.0001
16 cell vs. End of gastrulation	7.750	6.806 to 8.693	Yes	****	<0.0001
16 cell vs. 24 hpf	7.668	6.724 to 8.611	Yes	****	<0.0001
16 cell vs. 2 dpf	6.977	6.034 to 7.921	Yes	****	<0.0001
16 cell vs. 3 dpf	6.735	5.791 to 7.678	Yes	****	<0.0001
16 cell vs. 4 dpf	6.283	5.340 to 7.226	Yes	****	<0.0001
16 cell vs. 5 dpf	6.882	5.938 to 7.825	Yes	****	<0.0001
16 cell vs. 7 dpf	7.130	6.187 to 8.074	Yes	****	<0.0001
50% epiboly vs. End of gastrulation	0.000	-0.9433 to 0.9433	No	ns	>0.9999
50% epiboly vs. 24 hpf	-0.08201	-1.025 to 0.8613	No	ns	>0.9999
50% epiboly vs. 2 dpf	-0.7721	-1.715 to 0.1712	No	ns	0.1622
50% epiboly vs. 3 dpf	-1.015	-1.958 to -0.07155	Yes	*	0.0295
50% epiboly vs. 4 dpf	-1.467	-2.410 to -0.5234	Yes	***	0.0009
50% epiboly vs. 5 dpf	-0.8678	-1.811 to 0.07552	No	ns	0.0855
50% epiboly vs. 7 dpf	-0.6191	-1.562 to 0.3242	No	ns	0.3908
End of gastrulation vs. 24 hpf	-0.08201	-1.025 to 0.8613	No	ns	>0.9999
End of gastrulation vs. 2 dpf	-0.7721	-1.715 to 0.1712	No	ns	0.1622
End of gastrulation vs. 3 dpf	-1.015	-1.958 to -0.07155	Yes	*	0.0295
End of gastrulation vs. 4 dpf	-1.467	-2.410 to -0.5234	Yes	***	0.0009
End of gastrulation vs. 5 dpf	-0.8678	-1.811 to 0.07552	No	ns	0.0855
End of gastrulation vs. 7 dpf	-0.6191	-1.562 to 0.3242	No	ns	0.3908
24 hpf vs. 2 dpf	-0.6901	-1.633 to 0.2532	No	ns	0.2669

24 hpf vs. 3 dpf	-0.9329	-1.876 to 0.01046	No	ns	0.0539
24 hpf vs. 4 dpf	-1.385	-2.328 to -0.4413	Yes	**	0.0017
24 hpf vs. 5 dpf	-0.7858	-1.729 to 0.1575	No	ns	0.1485
24 hpf vs. 7 dpf	-0.5371	-1.480 to 0.4062	No	ns	0.5648
2 dpf vs. 3 dpf	-0.2428	-1.186 to 0.7006	No	ns	0.9900
2 dpf vs. 4 dpf	-0.6946	-1.638 to 0.2488	No	ns	0.2602
2 dpf vs. 5 dpf	-0.09569	-1.039 to 0.8477	No	ns	>0.9999
2 dpf vs. 7 dpf	0.1530	-0.7903 to 1.096	No	ns	0.9996
3 dpf vs. 4 dpf	-0.4518	-1.395 to 0.4915	No	ns	0.7515
3 dpf vs. 5 dpf	0.1471	-0.7963 to 1.090	No	ns	0.9997
3 dpf vs. 7 dpf	0.3958	-0.5476 to 1.339	No	ns	0.8550
4 dpf vs. 5 dpf	0.5989	-0.3445 to 1.542	No	ns	0.4313
4 dpf vs. 7 dpf	0.8476	-0.09576 to 1.791	No	ns	0.0984
5 dpf vs. 7 dpf	0.2487	-0.6946 to 1.192	No	ns	0.9883

Figure c: Expression of ATM mRNA from 7-28 dpf, normalised to 7 dpf.

Ordinary one-way ANOVA	**F Value**	**P value**	**P value summary**	**Significant diff. among means (P < 0.05)?**	**R squared**
	7.312	0.0111	*	Yes	0.7328

Tukey's multiple comparisons test	**Mean Diff.**	**95.00% CI of diff.**	**Below threshold?**	**Summary**	**Adjusted P Value**
7 dpf vs. 14 dpf	-8.504	-14.58 to -2.430	Yes	**	0.0088
7 dpf vs. 21 dpf	-2.588	-8.661 to 3.486	No	ns	0.5522
7 dpf vs. 28 dpf	-5.086	-11.16 to 0.9872	No	ns	0.1042
14 dpf vs. 21 dpf	5.916	-0.1573 to 11.99	No	ns	0.0562
14 dpf vs. 28 dpf	3.418	-2.656 to 9.491	No	ns	0.3389
21 dpf vs. 28 dpf	-2.499	-8.572 to 3.575	No	ns	0.5780

Figure d: Expression of ATM$^{+/+}$ and ATM$^{sh477/sh477}$ at 5dpf

Unpaired t test	**P value**	**P value summary**	**Significantly different (P < 0.05)?**	**One- or two-tailed P value?**	**t, df**	**Effect Size**	**Sample Size required for 90% power**	**Sample size in esperiment**
ATM$^{+/+}$ vs ATM$^{sh477/sh477}$	0.7797	ns	No	Two-tailed	t=0.2992, df=4	**0.569**	**132**	**6**

Figure e. Expression of ATM$^{+/+}$, ATM$^{+/sh477}$ and ATM$^{sh477/sh477}$ at 3 weeks old

Ordinary one-way ANOVA	F Value	P value	P value summary	Significant diff. among means (P < 0.05)?	R squared	Effect Size	Sample Size required for 90% power	Sample size in Experiment
	0.3818	0.6981	ns	No	0.1129	0.315	132	9
Tukey's multiple comparisons test	**Mean Diff.**	**95.00% CI of diff.**	**Below threshold?**	**Summary**	**Adjusted P Value**			
$ATM^{+/+}$ vs. $ATM^{+/sh477}$	-0.004468	-0.04203 to 0.03310	No	ns	0.9300			
$ATM^{+/+}$ vs. $ATM^{sh477/sh477}$	0.006185	-0.03138 to 0.04375	No	ns	0.8716			
$ATM^{+/sh477}$ vs. $ATM^{sh477/sh477}$	0.01065	-0.02691 to 0.04822	No	ns	0.6770			

Figure f. 3’ expression (exons 1-2) of ATM mRNA at 3 weeks

Ordinary one-way ANOVA	F Value	P value	P value summary	Significant diff. among means (P < 0.05)?	R squared	Effect Size	Sample Size required for 90% power	Sample size in esperiment
	1.242	0.3536	ns	No	0.2929	0.534	48	9
Tukey's multiple comparisons test	**Mean Diff.**	**95.00% CI of diff.**	**Below threshold?**	**Summary**	**Adjusted P Value**			
$ATM^{+/+}$ vs. $ATM^{+/sh477}$	0.5195	-2.999 to 4.038	No	ns	0.8949	0.821		
$ATM^{+/+}$ vs. $ATM^{sh477/sh477}$	-1.240	-4.758 to 2.279	No	ns	0.5586	0.695		
$ATM^{+/sh477}$ vs. $ATM^{sh477/sh477}$	-1.759	-5.277 to 1.759	No	ns	0.3416	0.799		

Figure g. 3’ expression (exons 4-5) of ATM mRNA at 3 weeks

Ordinary one-way ANOVA	F Value	P value	P value summary	Significant diff. among means (P < 0.05)?	R squared	Effect Size	Sample Size required for 90% power	Sample size in esperiment
	1.469	0.3025	Ns	No	0.3287	0.737887	27	9
Tukey's multiple comparisons test	**Mean Diff.**	**95.00% CI of diff.**	**Below threshold?**	**Summary**	**Adjusted P Value**			
$ATM^{+/+}$ vs. $ATM^{+/sh477}$	0.4559	-1.823 to 2.735	No	ns	0.8183			

ATM$^{+/+}$ vs. ATM$^{sh477/sh477}$	-0.8016	-3.081 to 1.478	No	ns	0.5597
ATM$^{+/sh477}$ vs. ATM$^{sh477/sh477}$	-1.257	-3.537 to 1.022	No	ns	0.2825

Figure h. ATM mRNA global expression in adult zebrafish

Unpaired t test	***P value***	***P value summary***	***Significantly different (P < 0.05)?***	***One- or two-tailed P value?***	***t, df***	***Effect Size***	***Sample Size required for 90% power***	***Sample size in esperiment***
ATM$^{+/+}$ vs ATM$^{sh477/sh477}$	*0.7576*	*ns*	*No*	*Two-tailed*	*t=0.3305, df=4*	***0.636***	***106***	***6***

Figure i. ATM mRNA expression in the brain of adult zebrafish

Unpaired t test	***P value***	***P value summary***	***Significantly different (P < 0.05)?***	***One- or two-tailed P value?***	***t, df***	***Effect Size***	***Sample Size required for 90% power***	***Sample size in esperiment***
ATM$^{+/+}$ vs ATM$^{sh477/sh477}$	0.2549	*ns*	*No*	*Two-tailed*	t=1.328, df=4	***0.778***	***72***	***6***

Appendix 3.2 Prodiction of zebrafish specific ATM antibody by Proteintech™

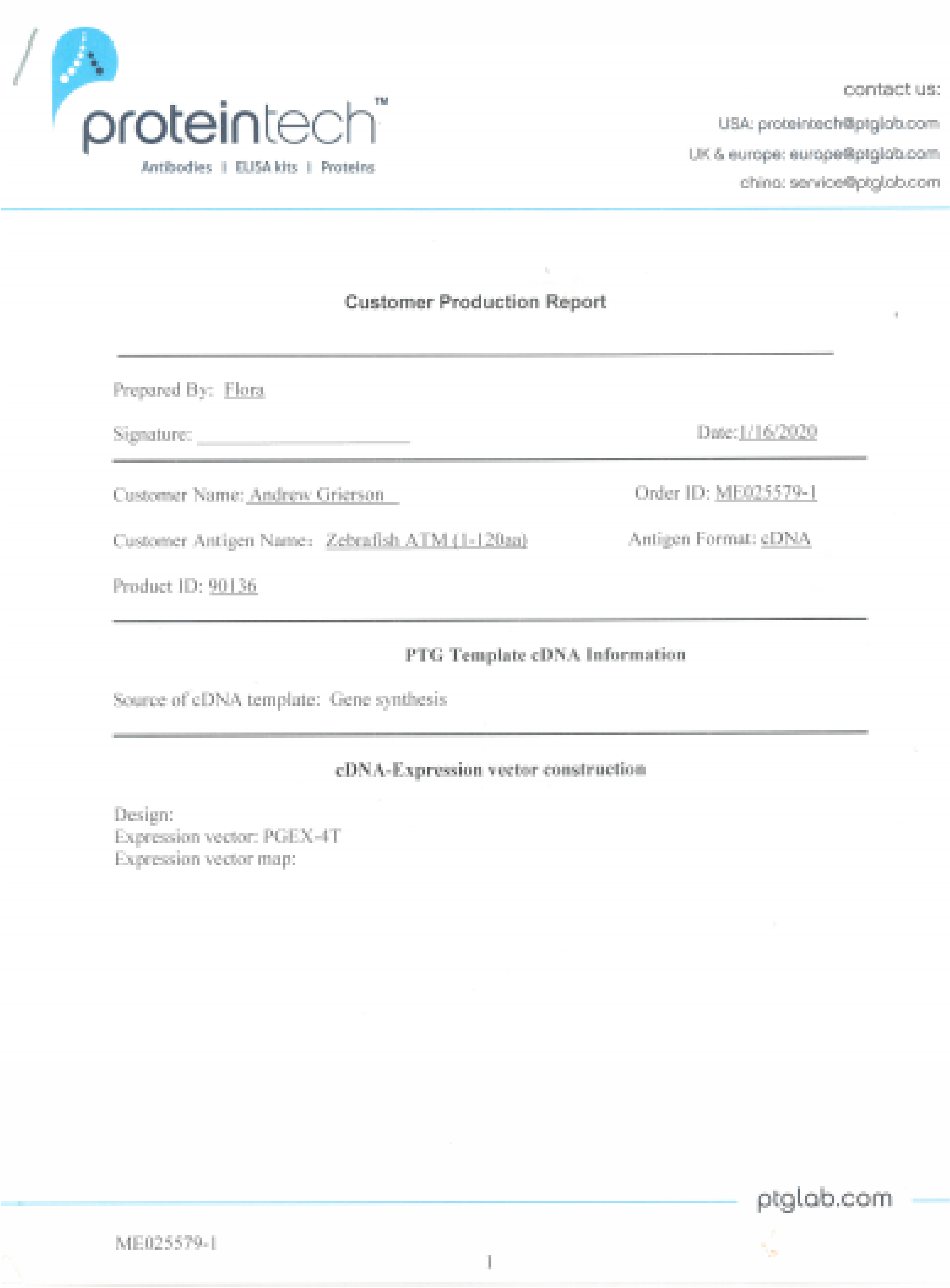

proteintech™
Antibodies | ELISA kits | Proteins

contact us:
USA: proteintech@ptglab.com
UK & europe: europe@ptglab.com
china: service@ptglab.com

Customer Production Report

Prepared By: Flora

Signature: ____________________ Date:1/16/2020

Customer Name: Andrew Grierson

Order ID: ME025579-1

Customer Antigen Name: Zebrafish ATM (1-120aa)

Antigen Format: cDNA

Product ID: 90136

PTG Template cDNA Information

Source of cDNA template: Gene synthesis

cDNA-Expression vector construction

Design:
Expression vector: PGEX-4T
Expression vector map:

ptglab.com

ME025579-1

1

proteintech™
Antibodies | ELISA kits | Proteins

contact us:
USA: proteintech@ptglab.com
UK & europe: europe@ptglab.com
china: service@ptglab.com

Customer Production Report

MCS

pGEX-4T-1 (27-4580-01)

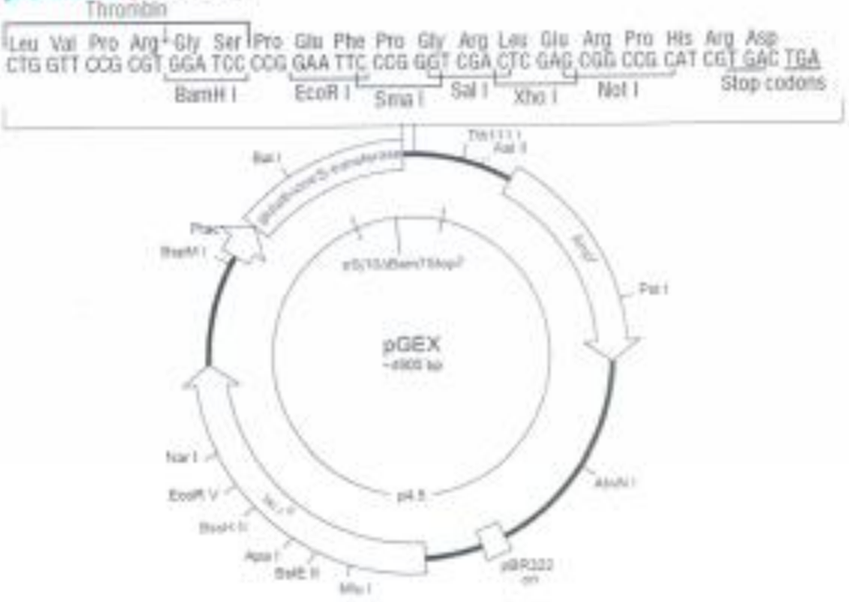
Thrombin
Leu Val Pro Arg Gly Ser Pro Glu Phe Pro Gly Arg Leu Glu Arg Pro His Arg Asp
CTG GTT CCG CGT GGA TCC CCG GAA TTC CCG GGT CGA CTC GAG CGG CCG CAT CGT GAC TGA
BamH I
EcoR I
Sma I
Sal I
Xho I
Not I
Stop codons
Bal I
Tth111 I
Aat II
Ptac
BspM I
glutathione S-transferase
pGEX
~4900 bp
Ampr
Pst I
Ava I
Nar I
EcoR V
BssH II
Apa I
BstE II
Mlu I
pBR322 ori
p4.5

Cloned cDNA region: 1-360 nt
Fusion Protein Region: 1-120 aa

Primer Pair: Sense: 5' –TTTT GGATCC ATG AGT CTG GCG CTG CAT GAA C
Antisense: 5' –TTTT CTCGAG CAG CTC CGC GCA CTT CAG ACG

Ligation Restriction sites: Upstream –BamhI
Downstream –XhoI

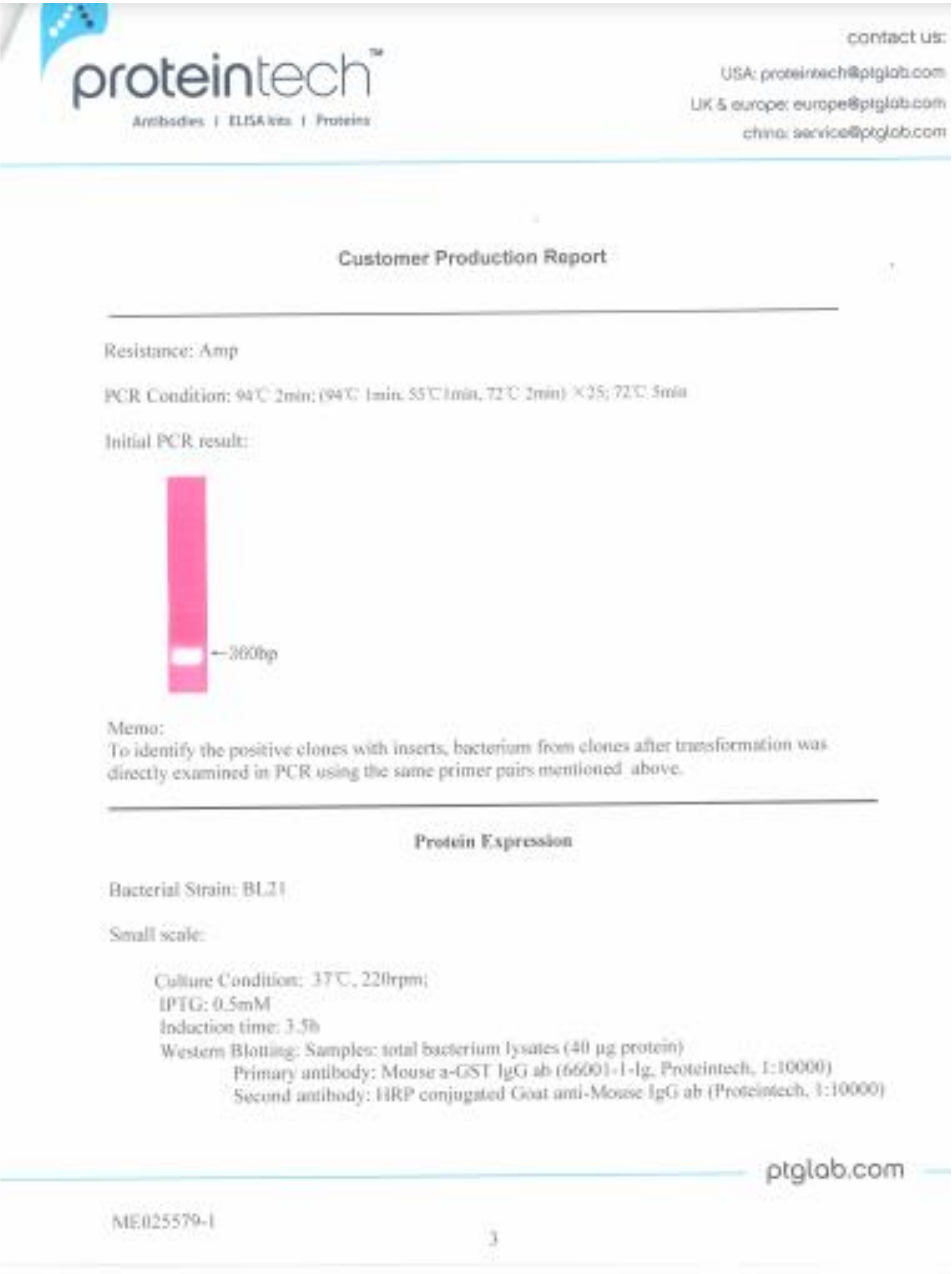

proteintech™
Antibodies | ELISA kits | Proteins

contact us:
USA: proteintech@ptglab.com
UK & europe: europe@ptglab.com
china: service@ptglab.com

Customer Production Report

Resistance: Amp

PCR Condition: 94℃ 2min; (94℃ 1min, 55℃1min, 72℃ 2min) ×25; 72℃ 5min

Initial PCR result:

Memo:
To identify the positive clones with inserts, bacterium from clones after transformation was directly examined in PCR using the same primer pairs mentioned above.

Protein Expression

Bacterial Strain: BL21

Small scale:

Culture Condition: 37℃, 220rpm;
IPTG: 0.5mM
Induction time: 3.5h
Western Blotting: Samples: total bacterium lysates (40 μg protein)
Primary antibody: Mouse a-GST IgG ab (66001-1-Ig, Proteintech, 1:10000)
Second antibody: HRP conjugated Goat anti-Mouse IgG ab (Proteintech, 1:10000)

Customer Production Report

SDS PAGE-Western Blot Data:

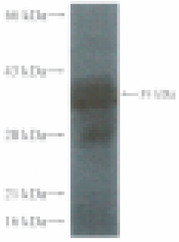
43 kDa
28 kDa

Large scale:

Culture Condition: 37℃, 220rpm
IPTG: 0.5mM
Induction time: 3.5h
SDS PAGE and CBB staining: 10% gel

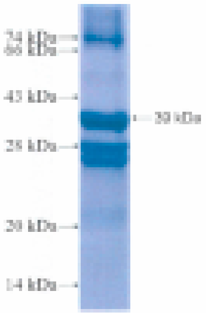
74 kDa
66 kDa
43 kDa
30 kDa
28 kDa
20 kDa
14 kDa

Total Number of Purification Runs: 1

Total Amount of Purified Protein: >2mg

Total Volume of Purified Protein: 0.6ml

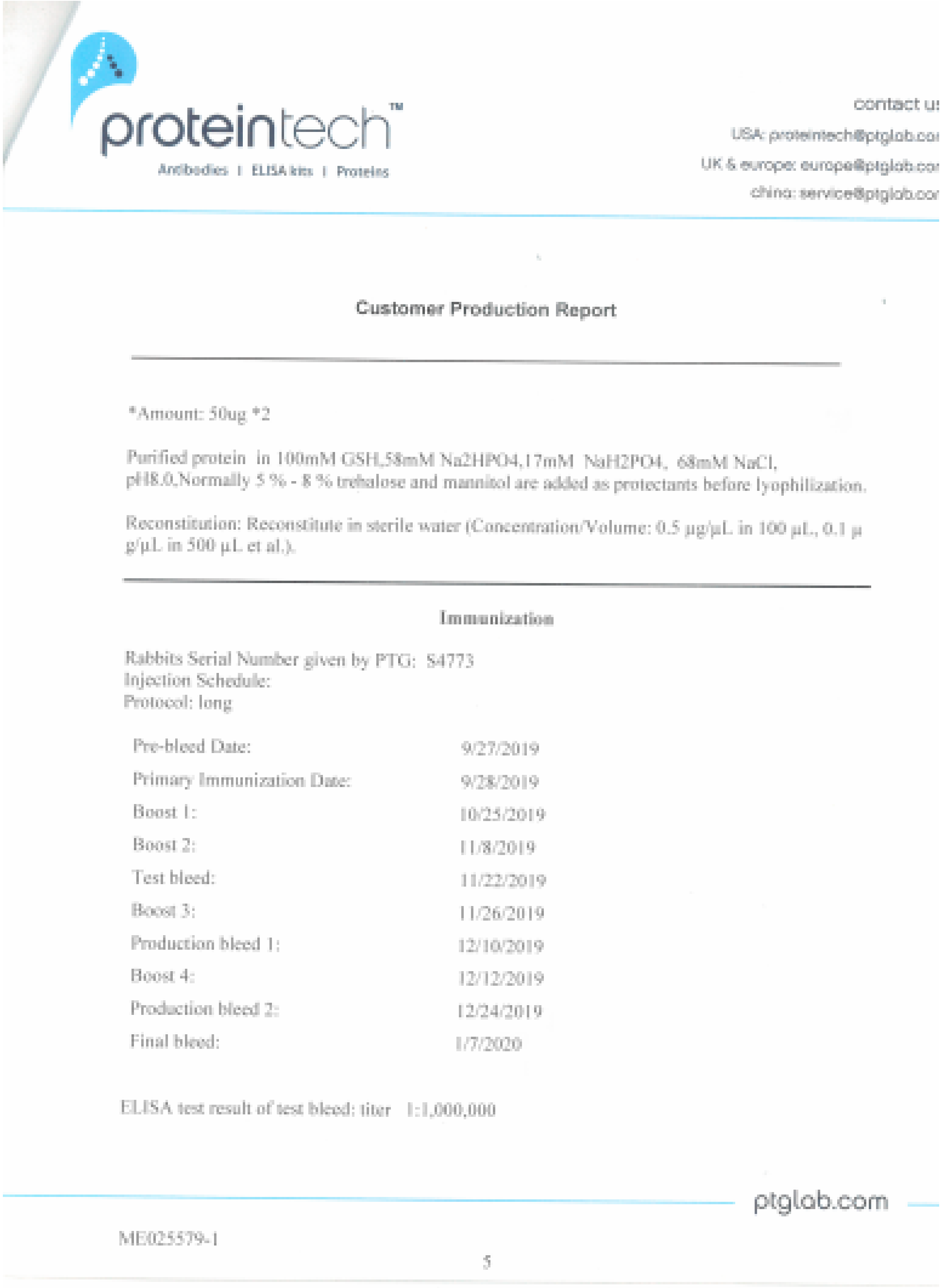

proteintech™
Antibodies | ELISA kits | Proteins

contact u
USA: proteintech@ptglab.co
UK & europe: europe@ptglab.co
china: service@ptglab.co

Customer Production Report

---

*Amount: 50ug *2

Purified protein in 100mM GSH,58mM Na2HPO4,17mM NaH2PO4, 68mM NaCl, pH8.0,Normally 5 % - 8 % trehalose and mannitol are added as protectants before lyophilization.

Reconstitution: Reconstitute in sterile water (Concentration/Volume: 0.5 µg/µL in 100 µL, 0.1 µg/µL in 500 µL et al.).

Immunization

Rabbits Serial Number given by PTG: S4773
Injection Schedule:
Protocol: long

Pre-bleed Date:	9/27/2019
Primary Immunization Date:	9/28/2019
Boost 1:	10/25/2019
Boost 2:	11/8/2019
Test bleed:	11/22/2019
Boost 3:	11/26/2019
Production bleed 1:	12/10/2019
Boost 4:	12/12/2019
Production bleed 2:	12/24/2019
Final bleed:	1/7/2020

ELISA test result of test bleed: titer 1:1,000,000

ptglab.com

proteintech™
Antibodies | ELISA kits | Proteins

contact u
USA: proteintech@ptglab.co
UK & europe: europe@ptglab.co
china: service@ptglab.co

Customer Production Report

ELISA Result Report

11/22/2019 done by Nancy

Ab source: test blood
Incubation Buffer: 5 % milk in PBST

1: Rabbit No. 1
2: Rabbit No. 2

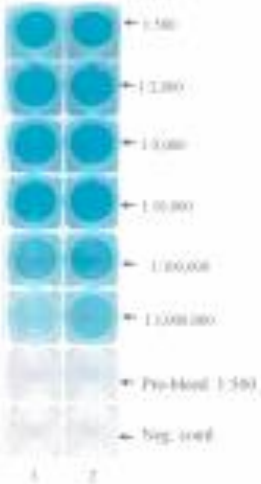
1:500
1:2,000
1:5,000
1:10,000
1:100,000
1:1,000,000
Pre-bleed 1:500
Neg. cont
1
2

Optional Western blot Data of test Bleed: N/A

Serum Volume:
Production Bleed 1: 1# 13ml; 2# 13ml
Production Bleed 2: 1# 15ml; 2# 15ml
Final Bleed: 1# 60ml; 2# 60ml

Affinity Purification

Affinity Ligand: GST-Fusion Protein

Initial serum volume: 15ml/Production Bleed 2(absorbed with GST)

Customer Production Report

Final Purified Antibody Volume: No.1 11ml; No.2 10ml

ELISA: No.1 Initial serum 1:1,000,000 Flow Through 1:2,000 Purified Antibody 1:10,000 ;
No.2 Initial serum 1:1,000,000 Flow Through 1:500 Purified Antibody 1:1,000,000

ELISA Result Report

54773
1st Ab source: 1. Serum
2. Flow through
3. Purified antibody
Incubation Buffer: 5 % milk in PBST

a: Rabbit No.1
b: Rabbit No.2

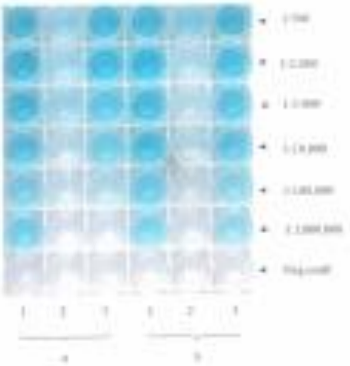
1:500
1:2,000
1:5,000
1:10,000
1:100,000
1:1,000,000
Neg.ctrl
1
2
3
1
2
3
a
b

Estimate antibody concentration by SDS-PAGE:

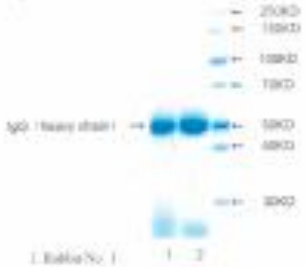
250KD
150KD
100KD
70KD
IgG (heavy chain)
50KD
40KD
30KD
1
2

1. Rabbit No. 1
2. Rabbit No. 2

54773-1: Purified Antibody:450ug/ml
54773-2: Purified Antibody:580ug/ml

Appendix 3.3: Optimisation of transfer membrane for detection of zebrafish ATM by zATM antibodies.

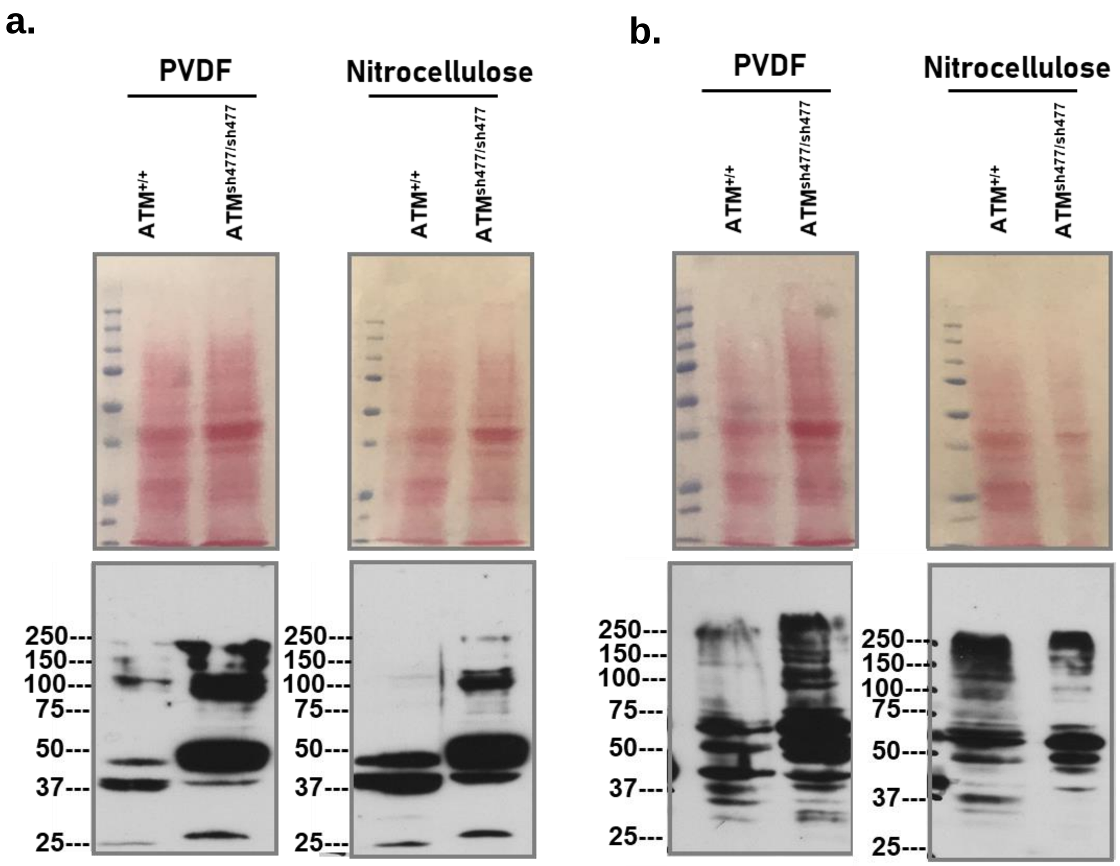
a.
PVDF
Nitrocellulose
ATM+/+
ATMsh477/sh477
ATM+/+
ATMsh477/sh477
250
150
100
75
50
37
25
b.
PVDF
Nitrocellulose
ATM+/+
ATMsh477/sh477
ATM+/+
ATMsh477/sh477
250
150
100
75
50
37
25

Appendix 3.4 Statistical Analysis Corresponding to figure 3.6: ATM$^{sh477/sh477}$ zebrafish develop as male when raised at normal densities.

Figure b. Sex distribution observed within the clutches

Unpaired t test	**P value**	**P value summary**	**Significantly different (P < 0.05)?**	**One- or two-tailed P value?**	**t, df**
Male vs Female	0.8883	Ns	No	Two-tailed	t=0.1496, df=4

Figure c. Sex distribution within the genotypes of the progeny

Two-way ANOVA

Source of Variation	**% of total variation**	**P value**	**P value summary**	**Significant?**
Sex vs Genotype	87.44	<0.0001	****	Yes
Sex	1.447	0.2351	ns	No
Genotype	4.807e-015	>0.9999	ns	No

Tukey's multiple comparisons test	**Mean Diff.**	**95.00% CI of diff.**	**Below threshold?**	**Summary**	**Adjusted P Value**
Male					
ATM$^{+/+}$ vs. ATM$^{+/sh477}$	0.4544	-29.78 to 30.69	No	ns	0.9991
ATM$^{+/+}$ vs. ATM$^{sh477/sh477}$	-67.21	-97.44 to -36.98	Yes	***	0.0002
ATM$^{+/sh477}$ vs. ATM$^{sh477/sh477}$	-67.67	-97.90 to -37.43	Yes	***	0.0002
Female					
ATM$^{+/+}$ vs. ATM$^{+/sh477}$	-0.4544	-30.69 to 29.78	No	ns	0.9991
ATM$^{+/+}$ vs. ATM$^{sh477/sh477}$	67.21	36.98 to 97.44	Yes	***	0.0002
ATM$^{+/sh477}$ vs. ATM$^{sh477/sh477}$	67.67	37.43 to 97.90	Yes	***	0.0002

Šídák's multiple comparisons test Male - Female	**Mean Diff.**	**95.00% CI of diff.**	**Below threshold?**	**Summary**	**Adjusted P Value**
ATM$^{+/+}$	-36.33	-67.72 to -4.932	Yes	*	0.0225
ATM$^{+/sh477}$	-37.23	-68.63 to -5.841	Yes	*	0.0194
ATM$^{sh477/sh477}$	98.10	66.70 to 129.5	Yes	****	<0.0001

Appendix 3.5 Statistical Analysis Corresponding to figure 3.8: ATM$^{sh477/sh477}$ zebrafish morphologically exhibit no increase in their radiosensitivity compared to ATM$^{+/+}$ siblings.

Figure c: quantification of the length of progeny from the ATM$^{+/sh477}$ in-cross

Two way ANOVA

Alpha	*0.05*			
Source of Variation	***% of total variation***	***P value***	***P value summary***	***Significant?***
Irradiation Dose x Genotype	*1.103*	*0.8397*	*ns*	*No*
Irradiation Dose	*14.96*	*0.0001*	*****	*Yes*
Genotype	*0.4906*	*0.7296*	*ns*	*No*

Tukey's multiple comparisons test	***Predicted (LS) mean diff.***	***95.00% CI of diff.***	***Below threshold?***	***Summary***	***Adjusted P Value***
0 Gys vs. 2 Gy	*0.02548*	*-0.3010 to 0.3520*	*No*	*ns*	*0.9812*
0 Gys vs. 8 Gys	*0.4975*	*0.1735 to 0.8215*	*Yes*	****	*0.0012*
2 Gy vs. 8 Gys	*0.4720*	*0.1776 to 0.7664*	*Yes*	*****	*0.0007*

Tukey's multiple comparisons test	***Predicted (LS) mean diff.***	***95.00% CI of diff.***	***Below threshold?***	***Summary***	***Adjusted P Value***
0 Gys					
ATM +/+ vs. ATM$^{+/sh477}$	*-0.04125*	*-0.6906 to 0.6081*	*No*	*ns*	*0.9875*
ATM +/+ vs. ATM$^{sh477/sh477}$	*0.01758*	*-0.5752 to 0.6103*	*No*	*ns*	*0.9973*
ATM$^{+/sh477}$ vs. ATM$^{sh477/sh477}$	*0.05883*	*-0.5339 to 0.6516*	*No*	*ns*	*0.9698*
2 Gys					
ATM +/+ vs. ATM$^{+/sh477}$	*0.2086*	*-0.3088 to 0.7260*	*No*	*ns*	*0.6047*
ATM +/+ vs. ATM$^{sh477/sh477}$	*0.09795*	*-0.4652 to 0.6611*	*No*	*ns*	*0.9101*
ATM$^{+/sh477}$ vs. ATM$^{sh477/sh477}$	*-0.1106*	*-0.5689 to 0.3477*	*No*	*ns*	*0.8343*
8 Gys					
ATM +/+ vs. ATM$^{+/sh477}$	*0.04346*	*-0.4192 to 0.5061*	*No*	*ns*	*0.9729*
ATM +/+ vs. ATM$^{sh477/sh477}$	*-0.1955*	*-0.7418 to 0.3507*	*No*	*ns*	*0.6722*
ATM$^{+/sh477}$ vs. ATM$^{sh477/sh477}$	*-0.2390*	*-0.7420 to 0.2640*	*No*	*ns*	*0.4980*

Appendix 3.6 Statistical analysis corresponding to figure 3.9: H2AX phosphorylation in ATM$^{+/+}$ and ATM$^{sh477/sh477}$ larval zebrafish

Figure b: quantification of the relative area of γH$_2$AX foci/cell

Two way ANOVA					
Alpha	0.05				
Source of Variation	**% of total variation**	**P value**	**P value summary**	**Significant?**	
Irradiation Dose x Genotype	2.792	0.0005	***	Yes	
Irradiation Dose	28.00	<0.0001	****	Yes	
Genotype	0.5734	0.0731	ns	No	

Tukey's multiple comparisons test	**Predicted (LS) mean diff.**	**95.00% CI of diff.**	**Below threshold?**	**Summary**	**Adjusted P Value**
0 Gys vs. 8 Gy	-0.2804	-0.3665 to -0.1943	Yes	****	<0.0001
0 Gys vs. 12 Gys	-0.4289	-0.5093 to -0.3485	Yes	****	<0.0001
8 Gy vs. 12 Gys	-0.1485	-0.2241 to -0.07294	Yes	****	<0.0001

Šídák's multiple comparisons test	**Predicted (LS) mean diff.**	**95.00% CI of diff.**	**Below threshold?**	**Summary**	**Adjusted P Value**
ATM$^{+/+}$ v ATM$^{sh477/sh477}$					
0 Gy	-0.09686	-0.2271 to 0.03342	No	ns	0.2095
8 Gy	-0.1460	-0.2638 to -0.02834	Yes	**	0.0093
12 Gy	0.09171	-0.007708 to 0.1911	No	ns	0.0804

Number of fish analysed for each experimental condition	
ATM$^{+/+}$	
0 Gy	3
8 Gy	9
12 Gy	6
ATM$^{sh477/sh477}$	
0 Gy	3
8 Gy	2
12 Gy	4

Appendix 3.7 Statistical analysis corresponding to figure 3.10: $ATM^{sh477/sh477}$ show no inability to produce immunoglobulins

Mann Whitney test	***P value***	***P value summary***	***Significantly different (P < 0.05)?***	***One- or two-tailed P value?***	***Sum of ranks in column A,B***	***Mann-Whitney U***	***Effect Size***	***No of fish required for 90% power***	***No of fish in esperiment***
IgM *$ATM^{+/+}$ vs $ATM^{sh477/sh477}$*	*0.4206*	*ns*	*No*	*Two-tailed*	*32 , 23*	*8*	*0.7091458*	*90*	*10*
IgD *$ATM^{+/+}$ vs $ATM^{sh477/sh477}$*	*0.5476*	*ns*	*No*	*Two-tailed*	*31 , 24*	*9*	*0.706148*	*92*	*10*
IgZ *$ATM^{+/+}$ vs $ATM^{sh477/sh477}$*	*0.5476*	*ns*	*No*	*Two-tailed*	*31 , 24*	*9*	*0.6955136*	*94*	*10*

Appendix 3.8 Statistical analysis corresponding to figure 3.11: mRNA expression of senescence markers in adult zebrafish

CCNG1

Unpaired t test with Welch's correction	P value	P value summary	Significantly different (P < 0.05)?	One- or two-tailed P value?	Welch-corrected t, df	Effect Size	No of fish required for 90% power	No of fish in esperiment
	0.2638	ns	No	Two-tailed	t=1.202, df=7.956	0.7604003	62	10

p21

Mann Whitney test	P value	Exact or approximate P value?	P value summary	Significantly different (P < 0.05)?	One- or two-tailed P value?	Sum of ranks in column A,B	Mann-Whitney U	Effect Size	No of fish required for 90% power	No of fish in esperiment
	0.4206	Exact	ns	No	Two-tailed	32 , 23	8	0.5164229	168	10

P16

Mann Whitney test	P value	Exact or approximate P value?	P value summary	Significantly different (P < 0.05)?	One- or two-tailed P value?	Sum of ranks in column A,B	Mann-Whitney U	Effect Size	No of fish required for 90% power	No of fish in esperiment
	0.4206	Exact	ns	No	Two-tailed	23 , 32	8	0.5753064	136	10

p53

Unpaired t test with Welch's correction	P value	P value summary	Significantly different (P < 0.05)?	One- or two-tailed P value?	Welch-corrected t, df	Effect Size	No of fish required for 90% power	No of fish in esperiment
	0.7800	ns	No	Two-tailed	t=0.2912, df=6.450	0.1733905	352	10

IL-1β

Mann Whitney test	P value	Exact or approximate P value?	P value summary	Significantly different (P < 0.05)?	One- or two-tailed P value?	Sum of ranks in column A,B	Mann-Whitney U	Effect Size	No of fish required for 90% power	No of fish in esperiment
	0.0556	Exact	ns	No	Two-tailed	18 , 37	3	1.596844	20	10

IL-6

Mann Whitney test	P value	Exact or approximate P value?	P value summary	Significantly different (P < 0.05)?	One- or two-tailed P value?	Sum of ranks in column A,B	Mann-Whitney U	Effect Size	No of fish required for 90% power	No of fish in esperiment
	0.8413	Exact	ns	No	Two-tailed	26 , 29	11	0.4530262	218	10

Appendix 3.9 Statistical analysis corresponding to figure 3.13: Expression of ATR mRNA is not upregulated in ATM$^{sh477/sh477}$ zebrafish

ATM

Mann Whitney test	***P value***	***Exact or approximate P value?***	***P value summary***	***Significantly different (P < 0.05)?***	***One- or two-tailed P value?***	***Sum of ranks in column A,B***	***Mann-Whitney U***	***Effect Size***	***No of fish required for 90% power***	***No of fish in esperiment***
	0.1508	*Exact*	*ns*	*No*	*Two-tailed*	*35 , 20*	*5*	*0.1637558*	*1644*	*10*

ATR

Unpaired t test with Welch's correction	***P value***	***P value summary***	***Significantly different (P < 0.05)?***	***One- or two-tailed P value?***	***Welch-corrected t, df***	***Effect Size***	***No of fish required for 90% power***	***No of fish in esperiment***
	0.7919	*ns*	*No*	*Two-tailed*	*t=0.2750, df=6.502*	*0.1741447*	*1388*	*10*

Appendix 3.10 Statistical analysis corresponding to figure 3.14: Expression of ATR mRNA is not upregulated in ATM$^{sh477/sh477}$ zebrafish after induction of DNA damage

ATM					
Two-way ANOVA					
Alpha	*0.05*				
Source of Variation	***% of total variation***	***P value***	***P value summary***	***Significant?***	
IR Dose x Genotype	*4.248*	*0.4155*	*ns*	*No*	
IR Dose	*48.32*	*0.0200*	***	*Yes*	
Genotype	*1.347*	*0.6417*	*ns*	*No*	
Šídák's multiple comparisons test ATM$^{+/+}$ vs ATM$^{sh477/sh477}$	***Mean Diff.***	***95.00% CI of diff.***	***Below threshold?***	***Summary***	***Adjusted P Value***
0 Gys	*-0.03718*	*-0.4216 to 0.3472*	*No*	*ns*	*0.9590*
8 Gys	*0.1330*	*-0.2514 to 0.5174*	*No*	*ns*	*0.6035*
Šídák's multiple comparisons test IR Dose	***Mean Diff.***	***95.00% CI of diff.***	***Below threshold?***	***Summary***	***Adjusted P Value***
ATM$^{+/+}$ vs ATM$^{+/+}$	*-0.3721*	*-0.7565 to 0.01233*	*No*	*ns*	*0.0572*
ATM^{sh477} vs ATM$^{sh477/sh477}$	*-0.2019*	*-0.5863 to 0.1825*	*No*	*ns*	*0.3400*
ATR					
Two-way ANOVA					
Alpha	*0.05*				
Source of Variation	***% of total variation***	***P value***	***P value summary***	***Significant?***	
IR Dose x Genotype	*2.128*	*0.6297*	*ns*	*No*	
IR Dose	*29.83*	*0.0974*	*ns*	*No*	
Genotype	*0.2695*	*0.8629*	*ns*	*No*	
Šídák's multiple comparisons test ATM$^{+/+}$ vs ATM$^{sh477/sh477}$	***Mean Diff.***	***95.00% CI of diff.***	***Below threshold?***	***Summary***	***Adjusted P Value***
0 Gys	*-0.04218*	*-0.5490 to 0.4646*	*No*	*ns*	*0.9694*
8 Gys	*0.08877*	*-0.4180 to 0.5956*	*No*	*ns*	*0.8731*
Šídák's multiple comparisons test IR Dose	***Mean Diff.***	***95.00% CI of diff.***	***Below threshold?***	***Summary***	***Adjusted P Value***
ATM$^{+/+}$ vs ATM$^{+/+}$	*-0.3106*	*-0.8174 to 0.1962*	*No*	*ns*	*0.2452*
ATM^{sh477} vs ATM$^{sh477/sh477}$	*-0.1797*	*-0.6864 to 0.3271*	*No*	*ns*	*0.5895*

Appendix 3.11 RNA-binding protein motifs found 100 nt of the ATM^{sh477} allele premature stop codon. *Exons 5,6 and 7 of the ATM^{sh477} allele (exons denoted by upper and lower case), bold lettering denotes nucleotides within 100 of the premature stop codon (red). RNA binding motif (pink) directly precedes the premature stop codon (Ray et al., 2013, Lindeboom et al., 2016). Note deletion mutation denoted by a dashed line.*

tttgctggatttgttctgtgggctgtttaataggggaaccaggtcaatcaacagagt
caagtgagtcgtatcatctacacggtggtttggggctgttgtgtccaaacagaggga
ttgtcccacactcttttcaacttctttcttaaagctctgagcaacagcagGGCAGAA
AAACAGCTGATGGTTCTGGAGAATCTGGTATCTGCTGTAAATGTGTTCCT**GCGCTCA**
GTGCTTCTCTCCTGCAGGAAGAGGGTGTGTGGTCTGGGT………GGTCCTGTCAGATAT
GCTGTGCGTTTATACTGGGATGAGACCCAGCTCAGTACTTAAAGAAGAGCTCGTGAA
ATTTTTCCAAATTCAGCTTTTTGTTCATCACCCCAAAGGTGCAAAGACTATTGAGAC
AGgtgcacaggctcaagactgggtgaaatggcgtagtcagctctgcacgctctatga
cgcccttgttagtgagatcagtcagatcggcagcagaggcaaatacgccacaggctc
acgccatatagctgtgaaagaaaatcttattgaactgacagctgatgtatgccacca
g

Appendix 4

Appendix 4.1 Statistical Analysis Corresponding to figure 4.4: Neoplastic Sertoli cell growth disrupts the organisational structure of ATM$^{sh477/sh477}$ testes

Figure b: Contribution of Sertoli and Leydig cells to the makeup of the testes

Sertoli Cells

Welch's t test	***P value***	***P value summary***	***Significantly different (P < 0.05)?***	***One- or two-tailed P value?***	***t, df***
ATM$^{+/+}$ vs ATM$^{sh477/sh477}$	*<0.0001*	****	*Yes*	*Two-tailed*	*t=7.031, df=20.12*

Leydig Cells

Mann Whitney test	***P value***	***P value summary***	***Significantly different (P < 0.05)?***	***One- or two-tailed P value?***	***Mann-Whitney U***
ATM$^{+/+}$ vs ATM$^{sh477/sh477}$	*0.7759*	*ns*	*No*	*Two-tailed*	*177.5*

Appendix 4.2 Method used to quantify the area of H&E stained cells in the testes of ATM$^{+/+}$ and ATM$^{sh477/sh477}$ Automated analysis could not be carried out on binary images **(left panel)** as there was considerable overlap in the cells. Therefore, analysis was carried out by drawing a 10 point perimeter around each cell to be quantified and the area (µm^2) of the cell measured **(right panel)**. Cells to measured were chosen based on morphological resemblance to the cell stage that was being quantified and the ability to draw around easily disenable cell borders. **a.** ATM$^{+/+}$ Primary Spermatocytes **b.** ATM$^{+/+}$ Spermatids and mature spermatozoa **c.** A mixture of overlapping cell types from ATM$^{sh477/sh477}$

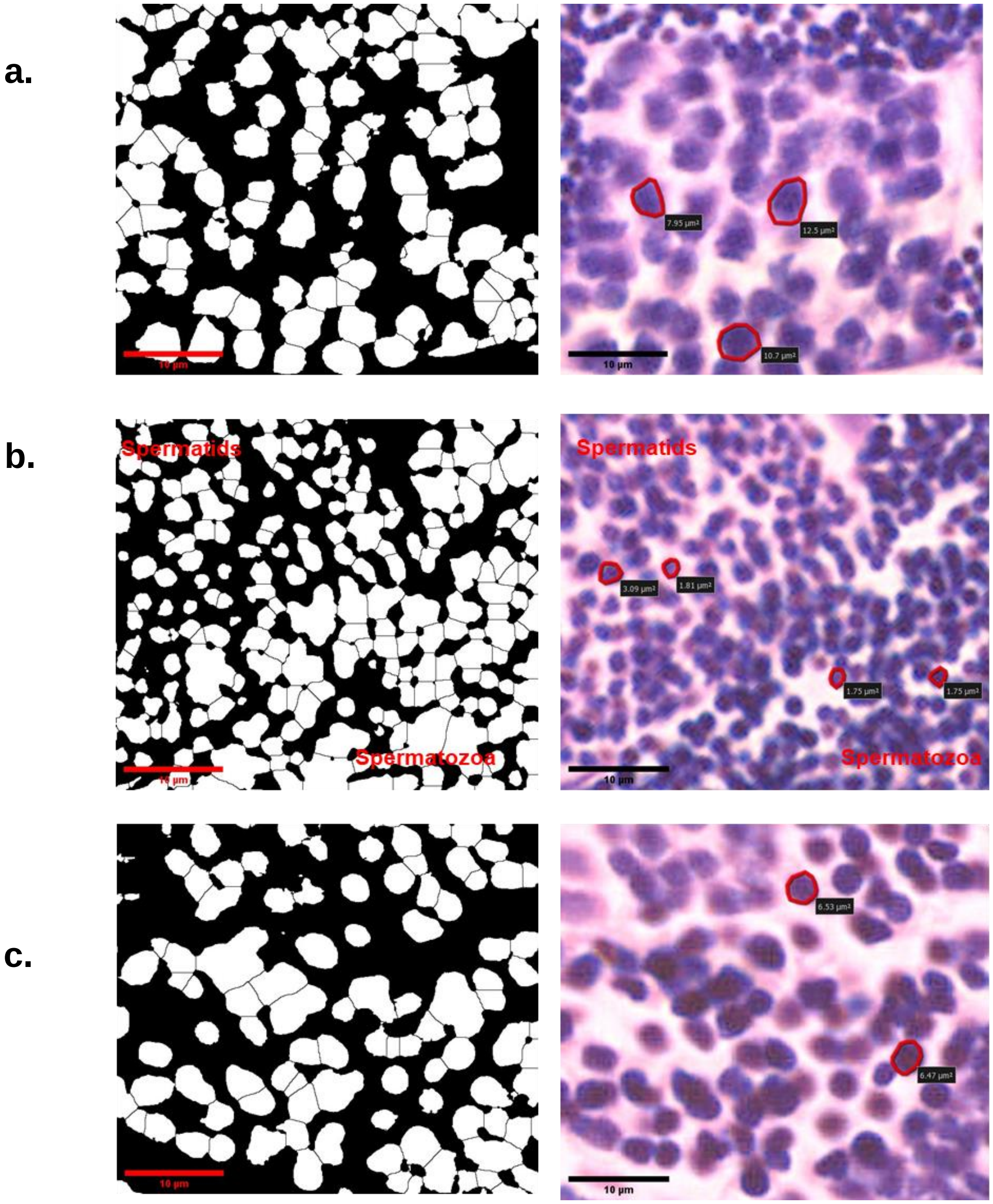
a.
7.95 µm²
12.5 µm²
10.7 µm²
10 µm
10 µm
b.
Spermatids
Spermatozoa
10 µm
Spermatids
3.09 µm²
1.81 µm²
1.75 µm²
1.75 µm²
Spermatozoa
10 µm
c.
6.53 µm²
6.47 µm²
10 µm
10 µm

Appendix 4.3 Statistical analysis corresponding to figure 4.7: Histological comparison of spermatogenesis between ATM$^{+/+}$ and ATM$^{sh477/sh477}$ zebrafish at 3 months

Kruskal-Wallis test	**P value**	**P value summary**	**Do the medians vary signif. (P < 0.05)?**	**Number of groups**	**Kruskal-Wallis statistic**
	<0.0001	****	Yes	5	330.3

Dunn's multiple comparisons test	**Mean rank diff.**	**Significant?**	**Summary**	**Adjusted P Value**
ATM$^{+/+}$ Primary Spermatocytes vs ATM$^{sh477/sh477}$ Primary Spermatocytes	1.707	No	ns	>0.9999
ATM$^{+/+}$ Primary Spermatocyte vs ATM$^{sh477/sh477}$ Late Spermatocytes	113.9	Yes	****	<0.0001
ATM$^{+/+}$ Primary Spermatocytes vs ATM$^{+/+}$Spermatids	186.7	Yes	****	<0.0001
ATM$^{+/+}$ Primary Spermatocytes vs ATM$^{+/+}$ Mature Spermatozoa	256.9	Yes	****	<0.0001
ATM$^{sh477/sh477}$ Primary Spermatocytes vs ATM$^{sh477/sh477}$ Late Spermatocytes	112.2	Yes	****	<0.0001
ATM$^{sh477/sh477}$ Primary Spermatocytes vs ATM$^{+/+}$Spermatids	185.0	Yes	****	<0.0001
ATM$^{sh477/sh477}$ Primary Spermatocytes vs ATM$^{+/+}$ Mature Spermatozoa	255.1	Yes	****	<0.0001
ATM$^{sh477/sh477}$ Late Spermatocytes vs ATM$^{+/+}$Spermatids	72.83	Yes	***	0.0004
ATM$^{sh477/sh477}$ Late Spermatocytes vs ATM$^{+/+}$ Mature Spermatozoa	143.0	Yes	****	<0.0001
ATM$^{+/+}$Spermatids vs ATM$^{+/+}$ Mature Spermatozoa	70.13	Yes	***	0.0007

Appendix 5

Appendix 5.1 Statistical Analysis Corresponding to Figure 5.1: ATM$^{sh477/sh477}$ zebrafish larvae do no exhibit any detectable swimming abnormalities at 5dpf

Figure b: Average distance travelled in dark and light phases

Two-way RM ANOVA

Alpha	*0.05*			
Source of Variation	***% of total variation***	***P value***	***P value summary***	***Significant?***
Light Driving x Genotype	*0.06515*	*0.3700*	*ns*	*No*
Light Driving	*57.86*	*<0.0001*	******	*Yes*
Genotype	*0.02201*	*0.8026*	*ns*	*No*
Subject	*21.91*	*<0.0001*	******	*Yes*

Tukey's multiple comparisons test Genotype v Genotype	***Predicted (LS) mean diff.***	***95.00% CI of diff.***	***Below threshold?***	***Summary***	***Adjusted P Value***
Dark					
ATM$^{+/+}$ vs. ATM$^{+/sh477}$	1.838	-36.97 to 40.64	No	ns	0.9932
ATM$^{+/+}$ vs. ATM$^{sh447/sh447}$	21.51	-22.17 to 65.19	No	ns	0.4800
ATM$^{+/sh477}$ vs. ATM$^{sh447/sh447}$	19.67	-18.16 to 57.50	No	ns	0.4412
Light					
ATM$^{+/+}$ vs. ATM$^{+/sh477}$	5.569	-33.24 to 44.38	No	ns	0.9393
ATM$^{+/+}$ vs. ATM$^{sh447/sh447}$	-2.605	-46.28 to 41.07	No	ns	0.9893
ATM$^{+/sh477}$ vs. ATM$^{sh447/sh447}$	-8.174	-46.00 to 29.65	No	ns	0.8678

Šídák's multiple comparisons test Dark v Light	***Predicted (LS) mean diff.***	***95.00% CI of diff.***	***Below threshold?***	***Summary***	***Adjusted P Value***
ATM$^{+/+}$	376.4	331.1 to 421.8	Yes	****	<0.0001
ATM$^{+/sh477}$	380.2	347.5 to 412.8	Yes	****	<0.0001
ATM$^{sh447/sh447}$	352.3	308.7 to 395.9	Yes	****	<0.0001

Figure d: Average duration of active swimming spent in dark and light phases

Two-way RM ANOVA				
Alpha	*0.05*			
Source of Variation	***% of total variation***	***P value***	***P value summary***	***Significant?***
Light Driving x Genotype	*0.09834*	*0.2179*	*ns*	*No*
Light Driving	*40.92*	*<0.0001*	******	*Yes*
Genotype	*0.008487*	*0.9548*	*ns*	*No*
Subject	*40.32*	*<0.0001*	******	*Yes*

Tukey's multiple comparisons test Genotype v Genotype	***Predicted (LS) mean diff.***	***95.00% CI of diff.***	***Below threshold?***	***Summary***	***Adjusted P Value***
Dark					
ATM$^{+/+}$ vs. ATM$^{+/sh477}$	*-1.090*	*-8.302 to 6.122*	*No*	*ns*	*0.9330*
ATM$^{+/+}$ vs. ATM$^{sh447/sh447}$	*0.8496*	*-7.252 to 8.951*	*No*	*ns*	*0.9671*
ATM$^{+/sh477}$ vs. ATM$^{sh447/sh447}$	*1.940*	*-5.072 to 8.951*	*No*	*ns*	*0.7927*
Light					
ATM$^{+/+}$ vs. ATM$^{+/sh477}$	*1.017*	*-6.195 to 8.229*	*No*	*ns*	*0.9414*
ATM$^{+/+}$ vs. ATM$^{sh447/sh447}$	*-2.359*	*-10.46 to 5.742*	*No*	*ns*	*0.7731*
ATM$^{+/sh477}$ vs. ATM$^{sh447/sh447}$	*-3.376*	*-10.39 to 3.635*	*No*	*ns*	*0.4955*

Šídák's multiple comparisons test Dark v Light	***Predicted (LS) mean diff.***	***95.00% CI of diff.***	***Below threshold?***	***Summary***	***Adjusted P Value***
ATM$^{+/+}$	*47.48*	*41.39 to 53.56*	*Yes*	******	*<0.0001*
ATM$^{+/sh477}$	*49.59*	*45.20 to 53.97*	*Yes*	******	*<0.0001*
ATM$^{sh447/sh447}$	*44.27*	*38.44 to 50.10*	*Yes*	******	*<0.0001*

Appendix 5.2 Statistical Analysis Corresponding to Figure 5.2: ATM$^{sh477/sh477}$ zebrafish larvae on a TDP1$^{sh475/sh475}$ (null) background do no exhibit any detectable swimming abnormalities at 5dpf

Figure b: **Average distance travelled in dark and light phases**

Two-way RM ANOVA				
Alpha	*0.05*			
Source of Variation	***% of total variation***	***P value***	***P value summary***	***Significant?***
Light Driving x Genotype	*0.1015*	*0.3828*	*ns*	*No*
Light Driving	*54.21*	*<0.0001*	******	*Yes*
Genotype	*0.3212*	*0.2107*	*ns*	*No*
Subject	*26.56*	*<0.0001*	******	*Yes*

Tukey's multiple comparisons test Genotype v Genotype	***Predicted (LS) mean diff.***	***95.00% CI of diff.***	***Below threshold?***	***Summary***	***Adjusted P Value***
Dark					
ATM$^{+/+}$ TDP1$^{sh475/sh475}$ vs. ATM$^{+/sh477}$ TDP1$^{sh475/sh475}$	*-27.50*	*-67.86 to 12.86*	*No*	*ns*	*0.2459*
ATM$^{+/+}$ TDP1$^{sh475/sh475}$ vs. ATM$^{sh447/sh447}$ TDP1$^{sh475/sh475}$	*-41.09*	*-87.58 to 5.392*	*No*	*ns*	*0.2459*
ATM$^{+/sh477}$ TDP1$^{sh475/sh475}$ vs. ATM$^{sh447/sh447}$ TDP1$^{sh475/sh475}$	*-13.59*	*-54.16 to 26.97*	*No*	*ns*	*0.2459*
Light					
ATM$^{+/+}$ TDP1$^{sh475/sh475}$ vs. ATM$^{+/sh477}$ TDP1$^{sh475/sh475}$	*-16.05*	*-56.41 to 24.32*	*No*	*ns*	*0.6188*
ATM$^{+/+}$ TDP1$^{sh475/sh475}$ vs. ATM$^{sh447/sh447}$ TDP1$^{sh475/sh475}$	*-9.636*	*-56.12 to 36.85*	*No*	*ns*	*0.8774*
ATM$^{+/sh477}$ TDP1$^{sh475/sh475}$ vs. ATM$^{sh447/sh447}$ TDP1^{sh475}	*6.411*	*-34.15 to 46.98*	*No*	*ns*	*0.9268*

Šidák's multiple comparisons test Dark v Light	***Predicted (LS) mean diff.***	***95.00% CI of diff.***	***Below threshold?***	***Summary***	***Adjusted P Value***
ATM$^{+/+}$ TDP1$^{sh475/sh475}$	*262.0*	*223.0 to 301.1*	*Yes*	******	*<0.0001*
ATM$^{+/sh477}$ TDP1$^{sh475/sh475}$	*273.5*	*245.4 to 301.6*	*Yes*	******	*<0.0001*
ATM$^{sh447/sh447}$ TDP1$^{sh475/sh475}$	*293.5*	*254.2 to 332.8*	*Yes*	******	*<0.0001*

Figure d: Average duration of active swimming spent in dark and light phases

Two-way RM ANOVA

Alpha	*0.05*			
Source of Variation	***% of total variation***	***P value***	***P value summary***	***Significant?***
Light Driving x Genotype	*0.02989*	*0.7469*	*ns*	*No*
Light Driving	*34.29*	*<0.0001*	******	*Yes*
Genotype	*0.2273*	*0.5485*	*ns*	*No*
Subject	*48.89*	*<0.0001*	******	*Yes*

Tukey's multiple comparisons test Genotype v Genotype	***Predicted (LS) mean diff.***	***95.00% CI of diff.***	***Below threshold?***	***Summary***	***Adjusted P Value***
Dark					
ATM$^{+/+}$ TDP1$^{sh475/sh475}$ vs. ATM$^{+/sh477}$ TDP1$^{sh475/sh475}$	*-3.959*	*-12.47 to 4.555*	*No*	*ns*	*0.5189*
ATM$^{+/+}$ TDP1$^{sh475/sh475}$ vs. ATM$^{sh447/sh447}$ TDP1$^{sh475/sh475}$	*-3.105*	*-12.91 to 6.700*	*No*	*ns*	*0.7372*
ATM$^{+/sh477}$ TDP1$^{sh475/sh475}$ vs. ATM$^{sh447/sh447}$ TDP1$^{sh475/sh475}$	*0.8539*	*-7.702 to 9.410*	*No*	*ns*	*0.9701*
Light					
ATM$^{+/+}$ TDP1$^{sh475/sh475}$ vs. ATM$^{+/sh477}$ TDP1$^{sh475/sh475}$	*-2.971*	*-11.48 to 5.543*	*No*	*ns*	*0.6907*
ATM$^{+/+}$ TDP1$^{sh475/sh475}$ vs. ATM$^{sh447/sh447}$ TDP1$^{sh475/sh475}$	*-0.2255*	*-10.03 to 9.580*	*No*	*ns*	*0.9984*
ATM$^{+/sh477}$ TDP1$^{sh475/sh475}$ vs. ATM$^{sh447/sh447}$ TDP1^{sh475}	*2.745*	*-5.811 to 11.30*	*No*	*ns*	*0.7313*

Šídák's multiple comparisons test Dark v Light	***Predicted (LS) mean diff.***	***95.00% CI of diff.***	***Below threshold?***	***Summary***	***Adjusted P Value***
ATM$^{+/+}$ TDP1$^{sh475/sh475}$	*36.00*	*29.47 to 42.52*	*Yes*	******	*<0.0001*
ATM$^{+/sh477}$ TDP1$^{sh475/sh475}$	*36.98*	*32.28 to 41.68*	*Yes*	******	*<0.0001*
ATM$^{sh447/sh447}$ TDP1$^{sh475/sh475}$	*38.87*	*32.30 to 45.45*	*Yes*	******	*<0.0001*

Appendix 5.3 Statistical Analysis Corresponding to Figure 5.3: Optimisation of DMSO treatment at 48 hpf in a 96 well plate for swimming analysis at 5dpf

Figure b: Average distance travelled in dark and light phases

Two-way RM ANOVA

Alpha	*0.05*			
Source of Variation	***% of total variation***	***P value***	***P value summary***	***Significant?***
Light Driving x DMSO Conc.	*4.291*	*0.0003*	*****	*Yes*
Light Driving	*45.29*	*<0.0001*	******	*Yes*
DMSO Conc	*10.27*	*<0.0001*	******	*Yes*
Subject	*21.52*	*0.2446*	*ns*	*No*

Tukey's multiple comparisons test Genotype v Genotype	***Predicted (LS) mean diff.***	***95.00% CI of diff.***	***Below threshold?***	***Summary***	***Adjusted P Value***
Dark					
Untreated vs. 1% DMSO	*318.1*	*194.8 to 441.4*	*Yes*	******	*<0.0001*
Untreated vs. 0.1% DMSO	*-13.83*	*-137.1 to 109.5*	*No*	*ns*	*0.9914*
Untreated vs. 0.01% DMSO	*75.72*	*-47.57 to 199.0*	*No*	*ns*	*0.3855*
1% DMSO vs. 0.1% DMSO	*-331.9*	*-455.2 to -208.7*	*Yes*	******	*<0.0001*
1% DMSO vs. 0.01% DMSO	*-242.4*	*-365.7 to -119.1*	*Yes*	******	*<0.0001*
0.1% DMSO vs. 0.01% DMSO	*89.55*	*-33.73 to 212.8*	*No*	*ns*	*0.2388*
Light					
Untreated vs. 1% DMSO	*93.19*	*-30.09 to 216.5*	*No*	*ns*	*0.2072*
Untreated vs. 0.1% DMSO	*42.53*	*-80.75 to 165.8*	*No*	*ns*	*0.8077*
Untreated vs. 0.01% DMSO	*34.53*	*-88.75 to 157.8*	*No*	*ns*	*0.8865*
1% DMSO vs. 0.1% DMSO	*-50.66*	*-173.9 to 72.63*	*No*	*ns*	*0.7110*
1% DMSO vs. 0.01% DMSO	*-58.66*	*-181.9 to 64.63*	*No*	*ns*	*0.6063*
0.1% DMSO vs. 0.01% DMSO	*-8.001*	*-131.3 to 115.3*	*No*	*ns*	*0.9983*

Figure d: Average duration of active swimming spent in dark and light phases

Two-way RM ANOVA

Alpha	*0.05*			
Source of Variation	***% of total variation***	***P value***	***P value summary***	***Significant?***
Light Driving x DMSO Conc.	*3.539*	*0.0005*	*****	*Yes*
Light Driving	*37.86*	*<0.0001*	******	*Yes*
DMSO Conc	*15.37*	*<0.0001*	******	*Yes*
Subject	*26.39*	*0.0162*	***	*Yes*

Tukey's multiple comparisons test Genotype v Genotype	***Predicted (LS) mean diff.***	***95.00% CI of diff.***	***Below threshold?***	***Summary***	***Adjusted P Value***
Dark					
Untreated vs. 1% DMSO	*56.50*	*36.40 to 76.60*	*Yes*	******	*<0.0001*
Untreated vs. 0.1% DMSO	*3.261*	*-16.84 to 23.36*	*No*	*ns*	*0.9749*
Untreated vs. 0.01% DMSO	*8.675*	*-11.42 to 28.77*	*No*	*ns*	*0.6783*
1% DMSO vs. 0.1% DMSO	*-53.24*	*-73.34 to -33.14*	*Yes*	******	*<0.0001*
1% DMSO vs. 0.01% DMSO	*-47.83*	*-67.93 to -27.73*	*Yes*	******	*<0.0001*
0.1% DMSO vs. 0.01% DMSO	*5.414*	*-14.69 to 25.51*	*No*	*ns*	*0.8976*
Light					
Untreated vs. 1% DMSO	*24.51*	*4.409 to 44.61*	*Yes*	****	*0.0098*
Untreated vs. 0.1% DMSO	*10.00*	*-10.10 to 30.10*	*No*	*ns*	*0.5705*
Untreated vs. 0.01% DMSO	*8.325*	*-11.77 to 28.42*	*No*	*ns*	*0.7059*
1% DMSO vs. 0.1% DMSO	*-14.51*	*-34.61 to 5.591*	*No*	*ns*	*0.2440*
1% DMSO vs. 0.01% DMSO	*-16.18*	*-36.28 to 3.916*	*No*	*ns*	*0.1610*
0.1% DMSO vs. 0.01% DMSO	*-1.675*	*-21.77 to 18.42*	*No*	*ns*	*0.9964*

Appendix 5.4.1 Optimisation 3 of CPT treatment on zebrafish embryos and larvae in a 96 well plate for swimming analysis at 5dpf, distance swum analysis. *Zebrafish larvae were untreated, treated with 0.1% DMSO or 0.1% DMSO and CPT in E3 at 8, 24, 48, 72 and 96 hpf in 96 well plates. At 5dpf, zebrafish were assayed by being subjected to alternating dark and light cycles (light driving phases) for 5 mins each for a total of 30 mins, during which their swimming was tracked.* ***Note: Grey panels in graph represent dark cycles****.* ***a****. embryos treated ar 8 hpf.* ***b****. embryos treated at 24 hpf.* ***c****. embryos treated at 48 hpf.* ***d****. embryos treated at 72 hpf.* ***e****. larvae treated at 96 hpf* ***i****. Average distance travelled by each genotype in each of the light driving phases.* ***ii*** *Average distance travelled in dark and light phases, individual data points represent the mean value per embryo of distance travelled across the 3 dark and 3 light phases. Data was analysed by Two-way ANOVA with RM with a post hoc Tukey's multiple comparisons test. Error bars represent SD. Statistical analysis can be found in* ***appendix 5.5.2*** *and n numbers for each experiment in* ***appendix 5.5.5 b.***

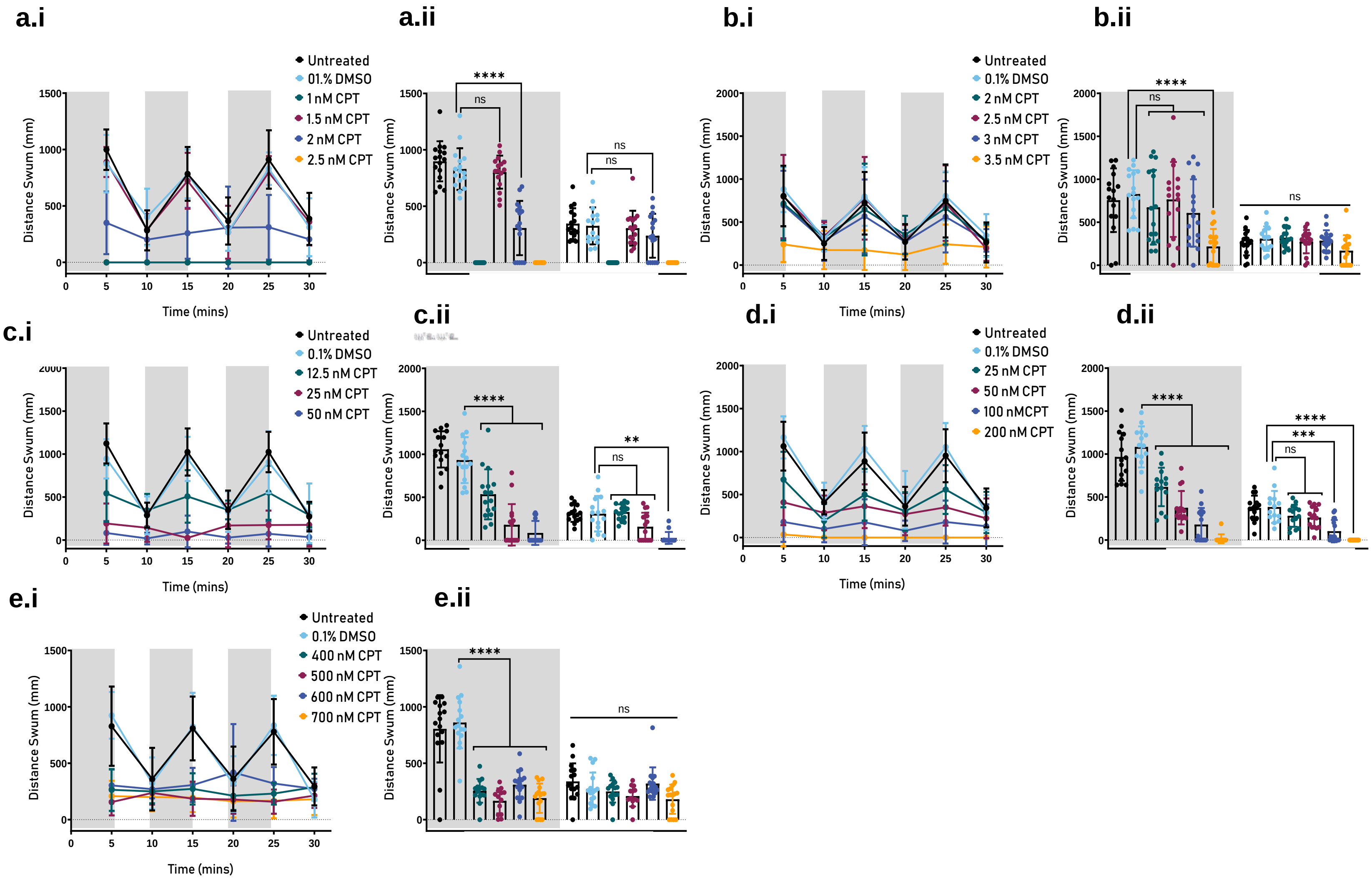

a.i
Untreated
01.% DMSO
1 nM CPT
1.5 nM CPT
2 nM CPT
2.5 nM CPT
Distance Swum (mm)
Time (mins)
a.ii
****
ns
ns
ns
b.i
Untreated
0.1% DMSO
2 nM CPT
2.5 nM CPT
3 nM CPT
3.5 nM CPT
b.ii
****
ns
ns
c.i
Untreated
0.1% DMSO
12.5 nM CPT
25 nM CPT
50 nM CPT
c.ii
****
**
ns
d.i
Untreated
0.1% DMSO
25 nM CPT
50 nM CPT
100 nMCPT
200 nM CPT
d.ii
****
****
***
ns
e.i
Untreated
0.1% DMSO
400 nM CPT
500 nM CPT
600 nM CPT
700 nM CPT
e.ii
****
ns
0
500
1000
1500
2000
0
5
10
15
20
25
30

Appendix 5.4.2 Statistical Analysis of figures a.ii-e.ii in appendix 5.5.1: Optimisation 3 of CPT treatment on zebrafish embryos and larvae in a 96 well plate for swimming analysis at 5dpf, distance swum analysis.

ii. Average distance travelled in dark and light phases

8 hpf treated

Two-way RM ANOVA

Alpha	***0.05***			
Source of Variation	***% of total variation***	***P value***	***P value summary***	***Significant?***
Light Driving x CPT Conc	*12.47*	*<0.0001*	******	*Yes*
Light Driving	*14.74*	*<0.0001*	******	*Yes*
CPT Conc	*54.71*	*<0.0001*	******	*Yes*
Subject	*10.84*	*0.0023*	****	*Yes*

Tukey's multiple comparisons test Light Driving x DMSO Conc	***Predicted (LS) mean diff.***	***Predicted (LS) mean diff.***	***Below threshold?***	***Summary***	***Adjusted P Value***
Dark					
Untreated vs. 01.% DMSO	*68.47*	*-82.69 to 219.6*	*No*	*ns*	*0.7817*
Untreated vs. 1 nM CPT	*898.2*	*744.6 to 1052*	*Yes*	******	*<0.0001*
Untreated vs. 1.5 nM CPT	*95.57*	*-55.59 to 246.7*	*No*	*ns*	*0.4543*
Untreated vs. 2 nM CPT	*591.5*	*440.4 to 742.7*	*Yes*	******	*<0.0001*
Untreated vs. 2.5 nM CPT	*898.2*	*738.6 to 1058*	*Yes*	******	*<0.0001*
01.% DMSO vs. 1 nM CPT	*829.8*	*676.1 to 983.4*	*Yes*	******	*<0.0001*
01.% DMSO vs. 1.5 nM CPT	*27.10*	*-124.1 to 178.3*	*No*	*ns*	*0.9955*
01.% DMSO vs. 2 nM CPT	*523.1*	*371.9 to 674.2*	*Yes*	******	*<0.0001*
01.% DMSO vs. 2.5 nM CPT	*829.8*	*670.1 to 989.4*	*Yes*	******	*<0.0001*
1 nM CPT vs. 1.5 nM CPT	*-802.7*	*-956.3 to -649.0*	*Yes*	******	*<0.0001*

1 nM CPT vs. 2 nM CPT	*-306.7*	*-460.4 to -153.1*	*Yes*	****	*<0.0001*
1 nM CPT vs. 2.5 nM CPT	*0.000*	*-162.0 to 162.0*	*No*	*ns*	*>0.9999*
1.5 nM CPT vs. 2 nM CPT	*496.0*	*344.8 to 647.1*	*Yes*	****	*<0.0001*
1.5 nM CPT vs. 2.5 nM CPT	*802.7*	*643.0 to 962.3*	*Yes*	****	*<0.0001*
2 nM CPT vs. 2.5 nM CPT	*306.7*	*147.1 to 466.3*	*Yes*	****	*<0.0001*
Light					
Untreated vs. 01.% DMSO	*19.30*	*-131.9 to 170.4*	*No*	*ns*	*0.9991*
Untreated vs. 1 nM CPT	*345.4*	*191.7 to 499.0*	*Yes*	****	*<0.0001*
Untreated vs. 1.5 nM CPT	*39.95*	*-111.2 to 191.1*	*No*	*ns*	*0.9735*
Untreated vs. 2 nM CPT	*107.3*	*-43.89 to 258.4*	*No*	*ns*	*0.3213*
Untreated vs. 2.5 nM CPT	*345.4*	*185.7 to 505.0*	*Yes*	****	*<0.0001*
01.% DMSO vs. 1 nM CPT	*326.1*	*172.4 to 479.7*	*Yes*	****	*<0.0001*
01.% DMSO vs. 1.5 nM CPT	*20.66*	*-130.5 to 171.8*	*No*	*ns*	*0.9988*
01.% DMSO vs. 2 nM CPT	*87.97*	*-63.18 to 239.1*	*No*	*ns*	*0.5486*
01.% DMSO vs. 2.5 nM CPT	*326.1*	*166.5 to 485.7*	*Yes*	****	*<0.0001*
1 nM CPT vs. 1.5 nM CPT	*-305.4*	*-459.1 to -151.8*	*Yes*	****	*<0.0001*
1 nM CPT vs. 2 nM CPT	*-238.1*	*-391.8 to -84.46*	*Yes*	***	*0.0002*
1 nM CPT vs. 2.5 nM CPT	*5.684e-014*	*-162.0 to 162.0*	*No*	*ns*	*>0.9999*
1.5 nM CPT vs. 2 nM CPT	*67.31*	*-83.84 to 218.5*	*No*	*ns*	*0.7937*
1.5 nM CPT vs. 2.5 nM CPT	*305.4*	*145.8 to 465.1*	*Yes*	****	*<0.0001*
2 nM CPT vs. 2.5 nM CPT	*238.1*	*78.48 to 397.8*	*Yes*	***	*0.0004*
24 hpf treated					
Two-way RM ANOVA					
Alpha	***0.05***				

Source of Variation	***% of total variation***	***P value***	***P value summary***	***Significant?***
Light Driving x CPT Conc	*5.175*	*0.0001*	*****	*Yes*
Light Driving	*27.23*	*<0.0001*	******	*Yes*
CPT Conc	*11.81*	*0.0002*	*****	*Yes*
Subject	*39.86*	*<0.0001*	******	*Yes*

Tukey's multiple comparisons test Light Driving x DMSO Conc	***Predicted (LS) mean diff.***	***Predicted (LS) mean diff.***	***Below threshold?***	***Summary***	***Adjusted P Value***
Dark					
Untreated vs. 0.1% DMSO	*-71.33*	*-351.2 to 208.5*	*No*	*ns*	*0.9774*
Untreated vs. 2 nM CPT	*82.39*	*-197.4 to 362.2*	*No*	*ns*	*0.9579*
Untreated vs. 2.5 nM CPT	*-8.944*	*-288.8 to 270.9*	*No*	*ns*	*>0.9999*
Untreated vs. 3 nM CPT	*148.1*	*-131.8 to 427.9*	*No*	*ns*	*0.6491*
Untreated vs. 3.5 nM CPT	*537.8*	*257.9 to 817.6*	*Yes*	******	*<0.0001*
0.1% DMSO vs. 2 nM CPT	*153.7*	*-126.1 to 433.6*	*No*	*ns*	*0.6112*
0.1% DMSO vs. 2.5 nM CPT	*62.39*	*-217.4 to 342.2*	*No*	*ns*	*0.9876*
0.1% DMSO vs. 3 nM CPT	*219.4*	*-60.43 to 499.2*	*No*	*ns*	*0.2167*
0.1% DMSO vs. 3.5 nM CPT	*609.1*	*329.3 to 888.9*	*Yes*	******	*<0.0001*
2 nM CPT vs. 2.5 nM CPT	*-91.33*	*-371.2 to 188.5*	*No*	*ns*	*0.9355*
2 nM CPT vs. 3 nM CPT	*65.68*	*-214.2 to 345.5*	*No*	*ns*	*0.9844*
2 nM CPT vs. 3.5 nM CPT	*455.4*	*175.6 to 735.2*	*Yes*	******	*<0.0001*
2.5 nM CPT vs. 3 nM CPT	*157.0*	*-122.8 to 436.8*	*No*	*ns*	*0.5888*
2.5 nM CPT vs. 3.5 nM CPT	*546.7*	*266.9 to 826.6*	*Yes*	******	*<0.0001*
3 nM CPT vs. 3.5 nM CPT	*389.7*	*109.9 to 669.5*	*Yes*	****	*0.0012*
Light					
Untreated vs. 0.1% DMSO	*-46.96*	*-326.8 to 232.9*	*No*	*ns*	*0.9967*
Untreated vs. 2 nM CPT	*-57.62*	*-337.4 to 222.2*	*No*	*ns*	*0.9914*
Untreated vs. 2.5 nM CPT	*-12.29*	*-292.1 to 267.5*	*No*	*ns*	*>0.9999*
Untreated vs. 3 nM CPT	*-22.81*	*-302.6 to 257.0*	*No*	*ns*	*>0.9999*
Untreated vs. 3.5 nM CPT	*92.55*	*-187.3 to 372.4*	*No*	*ns*	*0.9319*
0.1% DMSO vs. 2 nM CPT	*-10.66*	*-290.5 to 269.2*	*No*	*ns*	*>0.9999*
0.1% DMSO vs. 2.5 nM CPT	*34.67*	*-245.2 to 314.5*	*No*	*ns*	*0.9992*
0.1% DMSO vs. 3 nM CPT	*24.14*	*-255.7 to 304.0*	*No*	*ns*	*0.9999*
0.1% DMSO vs. 3.5 nM CPT	*139.5*	*-140.3 to 419.3*	*No*	*ns*	*0.7049*
2 nM CPT vs. 2.5 nM CPT	*45.33*	*-234.5 to 325.2*	*No*	*ns*	*0.9972*
2 nM CPT vs. 3 nM CPT	*34.80*	*-245.0 to 314.6*	*No*	*ns*	*0.9992*
2 nM CPT vs. 3.5 nM CPT	*150.2*	*-129.7 to 430.0*	*No*	*ns*	*0.6351*
2.5 nM CPT vs. 3 nM CPT	*-10.53*	*-290.4 to 269.3*	*No*	*ns*	*>0.9999*
2.5 nM CPT vs. 3.5 nM CPT	*104.8*	*-175.0 to 384.7*	*No*	*ns*	*0.8891*
3 nM CPT vs. 3.5 nM CPT	*115.4*	*-164.5 to 395.2*	*No*	*ns*	*0.8423*

48 hpf treated

Two-way RM ANOVA

Alpha	***0.05***			
Source of Variation	***% of total variation***	***P value***	***P value summary***	***Significant?***
Light Driving x CPT Conc	*15.38*	*<0.0001*	****	*Yes*
Light Driving	*19.11*	*<0.0001*	****	*Yes*
CPT Conc	*41.19*	*<0.0001*	****	*Yes*
Subject	*16.64*	*0.0010*	***	*Yes*

Tukey's multiple comparisons test Light Driving x DMSO Conc	***Predicted (LS) mean diff.***	***Predicted (LS) mean diff.***	***Below threshold?***	***Summary***	***Adjusted P Value***
Dark					
Untreated vs. 0.1% DMSO	*124.9*	*-70.53 to 320.4*	*No*	*ns*	*0.3974*
Untreated vs. 12.5 nM CPT	*523.0*	*330.7 to 715.4*	*Yes*	****	*<0.0001*
Untreated vs. 25 nM CPT	*878.2*	*685.8 to 1071*	*Yes*	****	*<0.0001*
Untreated vs. 50 nM CPT	*972.8*	*773.8 to 1172*	*Yes*	****	*<0.0001*
0.1% DMSO vs. 12.5 nM CPT	*398.1*	*205.7 to 590.5*	*Yes*	****	*<0.0001*
0.1% DMSO vs. 25 nM CPT	*753.3*	*560.9 to 945.6*	*Yes*	****	*<0.0001*
0.1% DMSO vs. 50 nM CPT	*847.8*	*648.9 to 1047*	*Yes*	****	*<0.0001*
12.5 nM CPT vs. 25 nM CPT	*355.1*	*165.9 to 544.4*	*Yes*	****	*<0.0001*
12.5 nM CPT vs. 50 nM CPT	*449.7*	*253.8 to 645.6*	*Yes*	****	*<0.0001*
25 nM CPT vs. 50 nM CPT	*94.56*	*-101.3 to 290.5*	*No*	*ns*	*0.6707*
Light					
Untreated vs. 0.1% DMSO	*3.020*	*-192.4 to 198.5*	*No*	*ns*	*>0.9999*
Untreated vs. 12.5 nM CPT	*-16.92*	*-209.3 to 175.5*	*No*	*ns*	*0.9992*
Untreated vs. 25 nM CPT	*154.6*	*-37.78 to 347.0*	*No*	*ns*	*0.1781*
Untreated vs. 50 nM CPT	*284.9*	*85.98 to 483.8*	*Yes*	**	*0.0011*
0.1% DMSO vs. 12.5 nM CPT	*-19.94*	*-212.3 to 172.4*	*No*	*ns*	*0.9985*
0.1% DMSO vs. 25 nM CPT	*151.6*	*-40.80 to 344.0*	*No*	*ns*	*0.1944*
0.1% DMSO vs. 50 nM CPT	*281.9*	*82.96 to 480.8*	*Yes*	**	*0.0013*
12.5 nM CPT vs. 25 nM CPT	*171.5*	*-17.73 to 360.8*	*No*	*ns*	*0.0954*
12.5 nM CPT vs. 50 nM CPT	*301.8*	*105.9 to 497.7*	*Yes*	***	*0.0004*
25 nM CPT vs. 50 nM CPT	*130.3*	*-65.61 to 326.2*	*No*	*ns*	*0.3562*

72 hpf treated

Two-way RM ANOVA

Alpha	***0.05***			
Source of Variation	***% of total variation***	***P value***	***P value summary***	***Significant?***
Light Driving x CPT Conc	*12.46*	*<0.0001*	****	*Yes*
Light Driving	*17.05*	*<0.0001*	****	*Yes*
CPT Conc	*49.31*	*<0.0001*	****	*Yes*
Subject	*9.865*	*0.7309*	*ns*	*No*

Tukey's multiple comparisons test Light Driving x DMSO Conc	***Predicted (LS) mean diff.***	***Predicted (LS) mean diff.***	***Below threshold?***	***Summary***	***Adjusted P Value***
Dark					
Untreated vs. 0.1% DMSO	*-116.2*	*-304.9 to 72.63*	*No*	*ns*	*0.4851*
Untreated vs. 25 nM CPT	*349.7*	*160.9 to 538.5*	*Yes*	****	*<0.0001*
Untreated vs. 50 nM CPT	*592.1*	*406.6 to 777.6*	*Yes*	****	*<0.0001*
Untreated vs. 100 nMCPT	*787.3*	*604.7 to 969.9*	*Yes*	****	*<0.0001*
Untreated vs. 200 nM CPT	*952.6*	*760.1 to 1145*	*Yes*	****	*<0.0001*
0.1% DMSO vs. 25 nM CPT	*465.9*	*273.9 to 657.9*	*Yes*	****	*<0.0001*
0.1% DMSO vs. 50 nM CPT	*708.2*	*519.4 to 897.0*	*Yes*	****	*<0.0001*
0.1% DMSO vs. 100 nMCPT	*903.4*	*717.5 to 1089*	*Yes*	****	*<0.0001*
0.1% DMSO vs. 200 nM CPT	*1069*	*873.1 to 1264*	*Yes*	****	*<0.0001*
25 nM CPT vs. 50 nM CPT	*242.3*	*53.57 to 431.1*	*Yes*	**	*0.0039*
25 nM CPT vs. 100 nMCPT	*437.6*	*251.7 to 623.5*	*Yes*	****	*<0.0001*
25 nM CPT vs. 200 nM CPT	*602.9*	*407.2 to 798.5*	*Yes*	****	*<0.0001*
50 nM CPT vs. 100 nMCPT	*195.2*	*12.65 to 377.8*	*Yes*	*	*0.0285*
50 nM CPT vs. 200 nM CPT	*360.5*	*168.0 to 553.0*	*Yes*	****	*<0.0001*
100 nMCPT vs. 200 nM CPT	*165.3*	*-24.39 to 355.0*	*No*	*ns*	*0.1263*
Light					
Untreated vs. 0.1% DMSO	*-11.76*	*-200.5 to 177.0*	*No*	*ns*	*>0.9999*
Untreated vs. 25 nM CPT	*90.54*	*-98.24 to 279.3*	*No*	*ns*	*0.7370*
Untreated vs. 50 nM CPT	*112.1*	*-73.37 to 297.6*	*No*	*ns*	*0.5053*
Untreated vs. 100 nMCPT	*269.5*	*86.96 to 452.1*	*Yes*	***	*0.0005*
Untreated vs. 200 nM CPT	*372.7*	*180.2 to 565.2*	*Yes*	****	*<0.0001*
0.1% DMSO vs. 25 nM CPT	*102.3*	*-89.70 to 294.3*	*No*	*ns*	*0.6411*
0.1% DMSO vs. 50 nM CPT	*123.9*	*-64.88 to 312.7*	*No*	*ns*	*0.4103*
0.1% DMSO vs. 100 nMCPT	*281.3*	*95.39 to 467.2*	*Yes*	***	*0.0003*

0.1% DMSO vs. 200 nM CPT	384.5	188.8 to 580.2	Yes	****	<0.0001
25 nM CPT vs. 50 nM CPT	21.59	-167.2 to 210.4	No	ns	0.9995
25 nM CPT vs. 100 nMCPT	179.0	-6.919 to 364.9	No	ns	0.0664
25 nM CPT vs. 200 nM CPT	282.2	86.54 to 477.9	Yes	***	0.0007
50 nM CPT vs. 100 nMCPT	157.4	-25.17 to 340.0	No	ns	0.1342
50 nM CPT vs. 200 nM CPT	260.6	68.11 to 453.1	Yes	**	0.0019
100 nMCPT vs. 200 nM CPT	103.2	-86.47 to 292.9	No	ns	0.6199

96 hpf

Two-way RM ANOVA

Alpha	**0.05**			
Source of Variation	**% of total variation**	**P value**	**P value summary**	**Significant?**
Light Driving x CPT Conc	22.03	<0.0001	****	Yes
Light Driving	9.462	<0.0001	****	Yes
CPT Conc	35.62	<0.0001	****	Yes
Subject	24.40	<0.0001	****	Yes

Tukey's multiple comparisons test Light Driving x DMSO Conc	**Predicted (LS) mean diff.**	**Predicted (LS) mean diff.**	**Below threshold?**	**Summary**	**Adjusted P Value**
Dark					
Untreated vs. 0.1% DMSO	-56.16	-219.6 to 107.3	No	ns	0.9205
Untreated vs. 400 nM CPT	549.2	383.1 to 715.4	Yes	****	<0.0001
Untreated vs. 500 nM CPT	638.6	466.0 to 811.2	Yes	****	<0.0001
Untreated vs. 600 nM CPT	495.1	331.7 to 658.6	Yes	****	<0.0001
Untreated vs. 700 nM CPT	614.6	451.2 to 778.0	Yes	****	<0.0001
0.1% DMSO vs. 400 nM CPT	605.4	439.3 to 771.5	Yes	****	<0.0001
0.1% DMSO vs. 500 nM CPT	694.8	522.2 to 867.4	Yes	****	<0.0001
0.1% DMSO vs. 600 nM CPT	551.3	387.9 to 714.7	Yes	****	<0.0001
0.1% DMSO vs. 700 nM CPT	670.8	507.3 to 834.2	Yes	****	<0.0001
400 nM CPT vs. 500 nM CPT	89.41	-85.76 to 264.6	No	ns	0.6831
400 nM CPT vs. 600 nM CPT	-54.10	-220.2 to 112.0	No	ns	0.9359
400 nM CPT vs. 700 nM CPT	65.36	-100.8 to 231.5	No	ns	0.8666
500 nM CPT vs. 600 nM CPT	-143.5	-316.1 to 29.10	No	ns	0.1633
500 nM CPT vs. 700 nM CPT	-24.05	-196.7 to 148.6	No	ns	0.9986
600 nM CPT vs. 700 nM CPT	119.5	-43.97 to 282.9	No	ns	0.2888
Light					
Untreated vs. 0.1% DMSO	66.16	-97.27 to 229.6	No	ns	0.8520

Untreated vs. 400 nM CPT	*88.85*	*-77.29 to 255.0*	*No*	*ns*	*0.6381*
Untreated vs. 500 nM CPT	*129.6*	*-42.97 to 302.2*	*No*	*ns*	*0.2599*
Untreated vs. 600 nM CPT	*18.88*	*-144.5 to 182.3*	*No*	*ns*	*0.9994*
Untreated vs. 700 nM CPT	*157.9*	*-5.556 to 321.3*	*No*	*ns*	*0.0649*
0.1% DMSO vs. 400 nM CPT	*22.68*	*-143.5 to 188.8*	*No*	*ns*	*0.9988*
0.1% DMSO vs. 500 nM CPT	*63.47*	*-109.1 to 236.1*	*No*	*ns*	*0.8965*
0.1% DMSO vs. 600 nM CPT	*-47.28*	*-210.7 to 116.2*	*No*	*ns*	*0.9608*
0.1% DMSO vs. 700 nM CPT	*91.71*	*-71.72 to 255.1*	*No*	*ns*	*0.5883*
400 nM CPT vs. 500 nM CPT	*40.78*	*-134.4 to 215.9*	*No*	*ns*	*0.9849*
400 nM CPT vs. 600 nM CPT	*-69.96*	*-236.1 to 96.17*	*No*	*ns*	*0.8297*
400 nM CPT vs. 700 nM CPT	*69.03*	*-97.10 to 235.2*	*No*	*ns*	*0.8376*
500 nM CPT vs. 600 nM CPT	*-110.7*	*-283.4 to 61.86*	*No*	*ns*	*0.4372*
500 nM CPT vs. 700 nM CPT	*28.25*	*-144.4 to 200.9*	*No*	*ns*	*0.9971*
600 nM CPT vs. 700 nM CPT	*139.0*	*-24.44 to 302.4*	*No*	*ns*	*0.1449*

Appendix 5.4.3 Optimisation 3 of CPT treatment on zebrafish embryos and larvae in a 96 well plate for swimming analysis at 5dpf duration of active swimming analysis. *Zebrafish larvae were untreated, treated with 0.1% DMSO or 0.1% DMSO and CPT in E3 at 8, 24, 48, 72 and 96 hpf in 96 well plates. At 5dpf, zebrafish were assayed by being subjected to alternating dark and light cycles (light driving phases) for 5 mins each for a total of 30 mins, during which their swimming was tracked.* **Note: Grey panels in graph represent dark cycles***.* ***a****. embryos treated ar 8 hpf.* ***b****. embryos treated at 24 hpf.* ***c****. embryos treated at 48 hpf.* ***d****. embryos treated at 72 hpf.* ***e****. larvae treated at 96 hpf* ***i****. Average duration of active swimming by each genotype in each of the light driving phases.* ***ii****. . Average duration of active swimming spent in dark and light phases, individual data points represent the mean value per embryo of active duration across the 3 dark and 3 light driving phases. Data was analysed by Two-way ANOVA with RM with a post hoc Tukey's multiple comparisons test. Error bars represent SD. Statistical analysis can be found in* ***appendix 5.4.4*** *and n numbers for each experiment in* ***appendix 5.4.5 b.***

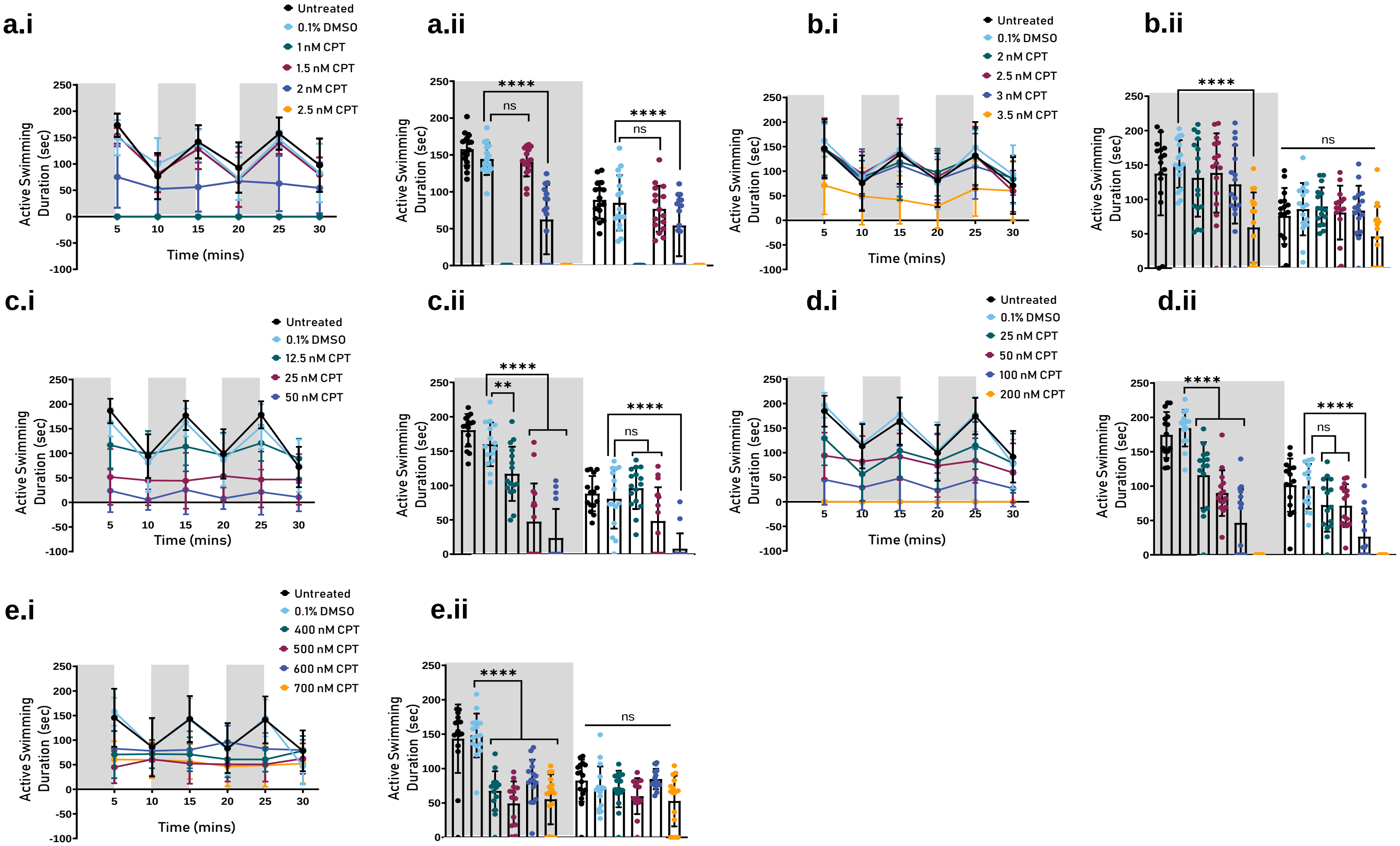
a.i
a.ii
b.i
b.ii
c.i
c.ii
d.i
d.ii
e.i
e.ii
Untreated
0.1% DMSO
1 nM CPT
1.5 nM CPT
2 nM CPT
2.5 nM CPT
3 nM CPT
3.5 nM CPT
12.5 nM CPT
25 nM CPT
50 nM CPT
100 nM CPT
200 nM CPT
400 nM CPT
500 nM CPT
600 nM CPT
700 nM CPT
Active Swimming Duration (sec)
Time (mins)
5
10
15
20
25
30
250
200
150
100
50
0
-50
-100
****
**
ns

Appendix 5.4.4 Statistical Analysis of figures a.ii-e.ii in appendix 5.5.3: Optimisation 3 of CPT treatment on zebrafish embryos and larvae in a 96 well plate for swimming analysis at 5dpf duration of active swimming analysis

ii. Average distance travelled in dark and light phases

8 hpf treated					
Two-way RM ANOVA					
Alpha	***0.05***				
Source of Variation	***% of total variation***	***P value***	***P value summary***	***Significant?***	
Light Driving x CPT Conc	*6.154*	*<0.0001*	****	*Yes*	
Light Driving	*7.187*	*<0.0001*	****	*Yes*	
CPT Conc	*68.74*	*<0.0001*	****	*Yes*	
Subject	*12.45*	*<0.0001*	****	*Yes*	
Tukey's multiple comparisons test Light Driving x DMSO Conc	***Predicted (LS) mean diff.***	***Predicted (LS) mean diff.***	***Below threshold?***	***Summary***	***Adjusted P Value***
Dark					
Untreated vs. 01.% DMSO	*13.14*	*-14.12 to 40.40*	*No*	*ns*	*0.7336*
Untreated vs. 1 nM CPT	*157.7*	*130.4 to 184.9*	*Yes*	****	*<0.0001*
Untreated vs. 1.5 nM CPT	*16.94*	*-10.31 to 44.20*	*No*	*ns*	*0.4741*
Untreated vs. 2 nM CPT	*95.24*	*67.98 to 122.5*	*Yes*	****	*<0.0001*
Untreated vs. 2.5 nM CPT	*157.7*	*128.9 to 186.4*	*Yes*	****	*<0.0001*
01.% DMSO vs. 1 nM CPT	*144.5*	*117.3 to 171.8*	*Yes*	****	*<0.0001*
01.% DMSO vs. 1.5 nM CPT	*3.804*	*-23.45 to 31.06*	*No*	*ns*	*0.9986*
01.% DMSO vs. 2 nM CPT	*82.10*	*54.84 to 109.4*	*Yes*	****	*<0.0001*
01.% DMSO vs. 2.5 nM CPT	*144.5*	*115.7 to 173.3*	*Yes*	****	*<0.0001*
1 nM CPT vs. 1.5 nM CPT	*-140.7*	*-168.0 to -113.5*	*Yes*	****	*<0.0001*
1 nM CPT vs. 2 nM CPT	*-62.42*	*-89.68 to -35.16*	*Yes*	****	*<0.0001*
1 nM CPT vs. 2.5 nM CPT	*2.842e-014*	*-28.79 to 28.79*	*No*	*ns*	*>0.9999*

1.5 nM CPT vs. 2 nM CPT	*78.29*	*51.04 to 105.6*	*Yes*	******	*<0.0001*
1.5 nM CPT vs. 2.5 nM CPT	*140.7*	*111.9 to 169.5*	*Yes*	******	*<0.0001*
2 nM CPT vs. 2.5 nM CPT	*62.42*	*33.63 to 91.21*	*Yes*	******	*<0.0001*
Light					
Untreated vs. 01.% DMSO	*3.967*	*-23.29 to 31.23*	*No*	*ns*	*0.9983*
Untreated vs. 1 nM CPT	*88.98*	*61.72 to 116.2*	*Yes*	******	*<0.0001*
Untreated vs. 1.5 nM CPT	*12.07*	*-15.19 to 39.33*	*No*	*ns*	*0.7979*
Untreated vs. 2 nM CPT	*34.70*	*7.444 to 61.96*	*Yes*	****	*0.0043*
Untreated vs. 2.5 nM CPT	*88.98*	*60.19 to 117.8*	*Yes*	******	*<0.0001*
01.% DMSO vs. 1 nM CPT	*85.01*	*57.75 to 112.3*	*Yes*	******	*<0.0001*
01.% DMSO vs. 1.5 nM CPT	*8.100*	*-19.16 to 35.36*	*No*	*ns*	*0.9562*
01.% DMSO vs. 2 nM CPT	*30.74*	*3.477 to 57.99*	*Yes*	***	*0.0172*
01.% DMSO vs. 2.5 nM CPT	*85.01*	*56.22 to 113.8*	*Yes*	******	*<0.0001*
1 nM CPT vs. 1.5 nM CPT	*-76.91*	*-104.2 to -49.65*	*Yes*	******	*<0.0001*
1 nM CPT vs. 2 nM CPT	*-54.28*	*-81.54 to -27.02*	*Yes*	******	*<0.0001*
1 nM CPT vs. 2.5 nM CPT	*2.842e-014*	*-28.79 to 28.79*	*No*	*ns*	*>0.9999*
1.5 nM CPT vs. 2 nM CPT	*22.64*	*-4.623 to 49.89*	*No*	*ns*	*0.1644*
1.5 nM CPT vs. 2.5 nM CPT	*76.91*	*48.12 to 105.7*	*Yes*	******	*<0.0001*
2 nM CPT vs. 2.5 nM CPT	*54.28*	*25.49 to 83.07*	*Yes*	******	*<0.0001*

24 hpf treated

Two-way RM ANOVA

Alpha	***0.05***			
Source of Variation	***% of total variation***	***P value***	***P value summary***	***Significant?***
Light Driving x CPT Conc	*2.581*	*0.0006*	*****	*Yes*

Light Driving	*17.22*	*<0.0001*	******	*Yes*
CPT Conc	*15.30*	*0.0004*	*****	*Yes*
Subject	*55.22*	*<0.0001*	******	*Yes*

Tukey's multiple comparisons test Light Driving x DMSO Conc	***Predicted (LS) mean diff.***	***Predicted (LS) mean diff.***	***Below threshold?***	***Summary***	***Adjusted P Value***
Dark					
Untreated vs. 0.1% DMSO	*-14.09*	*-61.32 to 33.15*	*No*	*ns*	*0.9556*
Untreated vs. 2 nM CPT	*6.254*	*-40.98 to 53.49*	*No*	*ns*	*0.9989*
Untreated vs. 2.5 nM CPT	*-0.9479*	*-48.18 to 46.28*	*No*	*ns*	*>0.9999*
Untreated vs. 3 nM CPT	*15.64*	*-31.60 to 62.87*	*No*	*ns*	*0.9317*
Untreated vs. 3.5 nM CPT	*78.29*	*31.06 to 125.5*	*Yes*	******	*<0.0001*
0.1% DMSO vs. 2 nM CPT	*20.34*	*-26.89 to 67.57*	*No*	*ns*	*0.8162*
0.1% DMSO vs. 2.5 nM CPT	*13.14*	*-34.09 to 60.37*	*No*	*ns*	*0.9670*
0.1% DMSO vs. 3 nM CPT	*29.72*	*-17.51 to 76.96*	*No*	*ns*	*0.4602*
0.1% DMSO vs. 3.5 nM CPT	*92.38*	*45.15 to 139.6*	*Yes*	******	*<0.0001*
2 nM CPT vs. 2.5 nM CPT	*-7.202*	*-54.43 to 40.03*	*No*	*ns*	*0.9979*
2 nM CPT vs. 3 nM CPT	*9.381*	*-37.85 to 56.61*	*No*	*ns*	*0.9927*
2 nM CPT vs. 3.5 nM CPT	*72.04*	*24.81 to 119.3*	*Yes*	*****	*0.0003*
2.5 nM CPT vs. 3 nM CPT	*16.58*	*-30.65 to 63.82*	*No*	*ns*	*0.9137*
2.5 nM CPT vs. 3.5 nM CPT	*79.24*	*32.01 to 126.5*	*Yes*	******	*<0.0001*
3 nM CPT vs. 3.5 nM CPT	*62.66*	*15.43 to 109.9*	*Yes*	****	*0.0025*
Light					
Untreated vs. 0.1% DMSO	*-9.933*	*-57.17 to 37.30*	*No*	*ns*	*0.9905*
Untreated vs. 2 nM CPT	*-13.76*	*-60.99 to 33.47*	*No*	*ns*	*0.9598*
Untreated vs. 2.5 nM CPT	*-4.973*	*-52.21 to 42.26*	*No*	*ns*	*0.9997*
Untreated vs. 3 nM CPT	*-7.890*	*-55.12 to 39.34*	*No*	*ns*	*0.9968*
Untreated vs. 3.5 nM CPT	*29.90*	*-17.33 to 77.13*	*No*	*ns*	*0.4532*
0.1% DMSO vs. 2 nM CPT	*-3.827*	*-51.06 to 43.41*	*No*	*ns*	*>0.9999*
0.1% DMSO vs. 2.5 nM CPT	*4.960*	*-42.27 to 52.19*	*No*	*ns*	*0.9997*
0.1% DMSO vs. 3 nM CPT	*2.044*	*-45.19 to 49.28*	*No*	*ns*	*>0.9999*
0.1% DMSO vs. 3.5 nM CPT	*39.84*	*-7.397 to 87.07*	*No*	*ns*	*0.1517*
2 nM CPT vs. 2.5 nM CPT	*8.788*	*-38.45 to 56.02*	*No*	*ns*	*0.9946*
2 nM CPT vs. 3 nM CPT	*5.871*	*-41.36 to 53.10*	*No*	*ns*	*0.9992*
2 nM CPT vs. 3.5 nM CPT	*43.66*	*-3.570 to 90.90*	*No*	*ns*	*0.0880*
2.5 nM CPT vs. 3 nM CPT	*-2.917*	*-50.15 to 44.32*	*No*	*ns*	*>0.9999*
2.5 nM CPT vs. 3.5 nM CPT	*34.87*	*-12.36 to 82.11*	*No*	*ns*	*0.2782*
3 nM CPT vs. 3.5 nM CPT	*37.79*	*-9.441 to 85.02*	*No*	*ns*	*0.1975*

48 hpf treated

Two-way RM ANOVA

Alpha	***0.05***			
Source of Variation	***% of total variation***	***P value***	***P value summary***	***Significant?***
Light Driving x CPT Conc	*8.180*	*<0.0001*	******	*Yes*

Light Driving	*10.28*	*<0.0001*	****	*Yes*
CPT Conc	*49.59*	*<0.0001*	****	*Yes*
Subject	*24.87*	*<0.0001*	****	*Yes*

Tukey's multiple comparisons test Light Driving x DMSO Conc	***Predicted (LS) mean diff.***	***Predicted (LS) mean diff.***	***Below threshold?***	***Summary***	***Adjusted P Value***
Dark					
Untreated vs. 0.1% DMSO	*20.45*	*-17.91 to 58.80*	*No*	*ns*	*0.5820*
Untreated vs. 12.5 nM CPT	*63.42*	*25.67 to 101.2*	*Yes*	****	*<0.0001*
Untreated vs. 25 nM CPT	*133.0*	*95.23 to 170.7*	*Yes*	****	*<0.0001*
Untreated vs. 50 nM CPT	*156.9*	*119.1 to 194.6*	*Yes*	****	*<0.0001*
0.1% DMSO vs. 12.5 nM CPT	*42.98*	*5.225 to 80.73*	*Yes*	*	*0.0170*
0.1% DMSO vs. 25 nM CPT	*112.5*	*74.78 to 150.3*	*Yes*	****	*<0.0001*
0.1% DMSO vs. 50 nM CPT	*136.4*	*98.69 to 174.2*	*Yes*	****	*<0.0001*
12.5 nM CPT vs. 25 nM CPT	*69.56*	*32.42 to 106.7*	*Yes*	****	*<0.0001*
12.5 nM CPT vs. 50 nM CPT	*93.47*	*56.33 to 130.6*	*Yes*	****	*<0.0001*
25 nM CPT vs. 50 nM CPT	*23.91*	*-13.23 to 61.05*	*No*	*ns*	*0.3902*
Light					
Untreated vs. 0.1% DMSO	*7.531*	*-30.83 to 45.89*	*No*	*ns*	*0.9827*
Untreated vs. 12.5 nM CPT	*-7.801*	*-45.55 to 29.95*	*No*	*ns*	*0.9791*
Untreated vs. 25 nM CPT	*39.86*	*2.112 to 77.62*	*Yes*	*	*0.0329*
Untreated vs. 50 nM CPT	*80.07*	*42.32 to 117.8*	*Yes*	****	*<0.0001*
0.1% DMSO vs. 12.5 nM CPT	*-15.33*	*-53.08 to 22.42*	*No*	*ns*	*0.7948*
0.1% DMSO vs. 25 nM CPT	*32.33*	*-5.419 to 70.08*	*No*	*ns*	*0.1308*
0.1% DMSO vs. 50 nM CPT	*72.54*	*34.79 to 110.3*	*Yes*	****	*<0.0001*
12.5 nM CPT vs. 25 nM CPT	*47.67*	*10.53 to 84.80*	*Yes*	**	*0.0047*
12.5 nM CPT vs. 50 nM CPT	*87.87*	*50.73 to 125.0*	*Yes*	****	*<0.0001*
25 nM CPT vs. 50 nM CPT	*40.21*	*3.068 to 77.34*	*Yes*	*	*0.0267*

72 hpf treated

Two-way RM ANOVA

Alpha	***0.05***			
Source of Variation	***% of total variation***	***P value***	***P value summary***	***Significant?***
Light Driving x CPT Conc	*5.320*	*<0.0001*	****	*Yes*
Light Driving	*9.244*	*<0.0001*	****	*Yes*
CPT Conc	*61.13*	*<0.0001*	****	*Yes*
Subject	*14.83*	*0.0350*	*	*Yes*

Tukey's multiple comparisons test Light Driving x DMSO Conc	***Predicted (LS) mean diff.***	***Predicted (LS) mean diff.***	***Below threshold?***	***Summary***	***Adjusted P Value***
Dark					
Untreated vs. 0.1% DMSO	*-9.904*	*-46.14 to 26.33*	*No*	*ns*	*0.9693*
Untreated vs. 25 nM CPT	*58.49*	*22.89 to 94.10*	*Yes*	****	*<0.0001*
Untreated vs. 50 nM CPT	*84.54*	*48.94 to 120.1*	*Yes*	****	*<0.0001*

Untreated vs. 100 nMCPT	*127.9*	*92.82 to 162.9*	*Yes*	******	*<0.0001*
Untreated vs. 200 nM CPT	*174.4*	*139.3 to 209.4*	*Yes*	******	*<0.0001*
0.1% DMSO vs. 25 nM CPT	*68.40*	*32.16 to 104.6*	*Yes*	******	*<0.0001*
0.1% DMSO vs. 50 nM CPT	*94.45*	*58.21 to 130.7*	*Yes*	******	*<0.0001*
0.1% DMSO vs. 100 nMCPT	*137.8*	*102.1 to 173.4*	*Yes*	******	*<0.0001*
0.1% DMSO vs. 200 nM CPT	*184.3*	*148.6 to 220.0*	*Yes*	******	*<0.0001*
25 nM CPT vs. 50 nM CPT	*26.05*	*-9.556 to 61.65*	*No*	*ns*	*0.2877*
25 nM CPT vs. 100 nMCPT	*69.37*	*34.32 to 104.4*	*Yes*	******	*<0.0001*
25 nM CPT vs. 200 nM CPT	*115.9*	*80.85 to 150.9*	*Yes*	******	*<0.0001*
50 nM CPT vs. 100 nMCPT	*43.32*	*8.274 to 78.36*	*Yes*	****	*0.0062*
50 nM CPT vs. 200 nM CPT	*89.85*	*54.80 to 124.9*	*Yes*	******	*<0.0001*
100 nMCPT vs. 200 nM CPT	*46.53*	*12.06 to 81.01*	*Yes*	****	*0.0020*
Light					
Untreated vs. 0.1% DMSO	*1.855*	*-34.38 to 38.09*	*No*	*ns*	*>0.9999*
Untreated vs. 25 nM CPT	*29.03*	*-6.578 to 64.63*	*No*	*ns*	*0.1803*
Untreated vs. 50 nM CPT	*29.91*	*-5.696 to 65.51*	*No*	*ns*	*0.1548*
Untreated vs. 100 nMCPT	*74.92*	*39.88 to 110.0*	*Yes*	******	*<0.0001*
Untreated vs. 200 nM CPT	*101.4*	*66.35 to 136.4*	*Yes*	******	*<0.0001*
0.1% DMSO vs. 25 nM CPT	*27.17*	*-9.063 to 63.41*	*No*	*ns*	*0.2614*
0.1% DMSO vs. 50 nM CPT	*28.05*	*-8.181 to 64.29*	*No*	*ns*	*0.2288*
0.1% DMSO vs. 100 nMCPT	*73.07*	*37.39 to 108.8*	*Yes*	******	*<0.0001*
0.1% DMSO vs. 200 nM CPT	*99.54*	*63.86 to 135.2*	*Yes*	******	*<0.0001*
25 nM CPT vs. 50 nM CPT	*0.8822*	*-34.72 to 36.49*	*No*	*ns*	*>0.9999*
25 nM CPT vs. 100 nMCPT	*45.90*	*10.85 to 80.94*	*Yes*	****	*0.0030*
25 nM CPT vs. 200 nM CPT	*72.37*	*37.32 to 107.4*	*Yes*	******	*<0.0001*
50 nM CPT vs. 100 nMCPT	*45.02*	*9.972 to 80.06*	*Yes*	****	*0.0039*
50 nM CPT vs. 200 nM CPT	*71.49*	*36.44 to 106.5*	*Yes*	******	*<0.0001*
100 nMCPT vs. 200 nM CPT	*26.47*	*-8.003 to 60.94*	*No*	*ns*	*0.2371*

96 hpf

Two-way RM ANOVA

Alpha	***0.05***			
Source of Variation	***% of total variation***	***P value***	***P value summary***	***Significant?***
Light Driving x CPT Conc	*15.36*	*<0.0001*	******	*Yes*
Light Driving	*5.387*	*<0.0001*	******	*Yes*
CPT Conc	*28.64*	*<0.0001*	******	*Yes*
Subject	*41.88*	*<0.0001*	******	*Yes*

Tukey's multiple comparisons test Light Driving x DMSO Conc	***Predicted (LS) mean diff.***	***Predicted (LS) mean diff.***	***Below threshold?***	***Summary***	***Adjusted P Value***
Dark					
Untreated vs. 0.1% DMSO	*-4.723*	*-37.85 to 28.40*	*No*	*ns*	*0.9985*
Untreated vs. 400 nM CPT	*75.83*	*42.16 to 109.5*	*Yes*	******	*<0.0001*
Untreated vs. 500 nM CPT	*94.04*	*59.06 to 129.0*	*Yes*	******	*<0.0001*

Untreated vs. 600 nM CPT	61.60	28.47 to 94.72	Yes	****	<0.0001
Untreated vs. 700 nM CPT	88.01	54.88 to 121.1	Yes	****	<0.0001
0.1% DMSO vs. 400 nM CPT	80.55	46.88 to 114.2	Yes	****	<0.0001
0.1% DMSO vs. 500 nM CPT	98.77	63.78 to 133.8	Yes	****	<0.0001
0.1% DMSO vs. 600 nM CPT	66.32	33.19 to 99.45	Yes	****	<0.0001
0.1% DMSO vs. 700 nM CPT	92.73	59.60 to 125.9	Yes	****	<0.0001
400 nM CPT vs. 500 nM CPT	18.21	-17.29 to 53.72	No	ns	0.6785
400 nM CPT vs. 600 nM CPT	-14.24	-47.91 to 19.44	No	ns	0.8274
400 nM CPT vs. 700 nM CPT	12.17	-21.50 to 45.85	No	ns	0.9030
500 nM CPT vs. 600 nM CPT	-32.45	-67.44 to 2.538	No	ns	0.0860
500 nM CPT vs. 700 nM CPT	-6.038	-41.02 to 28.95	No	ns	0.9962
600 nM CPT vs. 700 nM CPT	26.41	-6.717 to 59.54	No	ns	0.2007
Light					
Untreated vs. 0.1% DMSO	11.66	-21.47 to 44.78	No	ns	0.9127
Untreated vs. 400 nM CPT	12.21	-21.47 to 45.88	No	ns	0.9019
Untreated vs. 500 nM CPT	22.65	-12.34 to 57.63	No	ns	0.4269
Untreated vs. 600 nM CPT	-2.177	-35.30 to 30.95	No	ns	>0.9999
Untreated vs. 700 nM CPT	29.68	-3.446 to 62.81	No	ns	0.1072
0.1% DMSO vs. 400 nM CPT	0.5533	-33.12 to 34.23	No	ns	>0.9999
0.1% DMSO vs. 500 nM CPT	10.99	-24.00 to 45.98	No	ns	0.9447
0.1% DMSO vs. 600 nM CPT	-13.83	-46.96 to 19.29	No	ns	0.8347
0.1% DMSO vs. 700 nM CPT	18.03	-15.10 to 51.15	No	ns	0.6206
400 nM CPT vs. 500 nM CPT	10.44	-25.07 to 45.94	No	ns	0.9581
400 nM CPT vs. 600 nM CPT	-14.39	-48.06 to 19.29	No	ns	0.8209
400 nM CPT vs. 700 nM CPT	17.47	-16.20 to 51.15	No	ns	0.6677
500 nM CPT vs. 600 nM CPT	-24.82	-59.81 to 10.16	No	ns	0.3215
500 nM CPT vs. 700 nM CPT	7.034	-27.95 to 42.02	No	ns	0.9923
600 nM CPT vs. 700 nM CPT	31.86	-1.269 to 64.99	No	ns	0.0670

Appendix 5.4.5. Survival of CPT treatment Optimisation 3. *Zebrafish larvae were untreated, treated with 0.1% DMSO or 0.1% DMSO and CPT in E3 at 8, 24, 48, 72 and 96 hpf in 96 well plates. Survival was monitored daily until 4 dpf (96 hpf).* ***a****. Kaplan-Meier plots of survival until 4dpf.* ***i****. 8 hpf treated* ***ii****. 24 hpf treated* ***iii****. 48 hpf treated* ***iv****. 72 hpf treated. Dashed line indicated time of treatment.* ***b****. table indicated n numbers at the time of treatment and at the time of swimming analysis.*

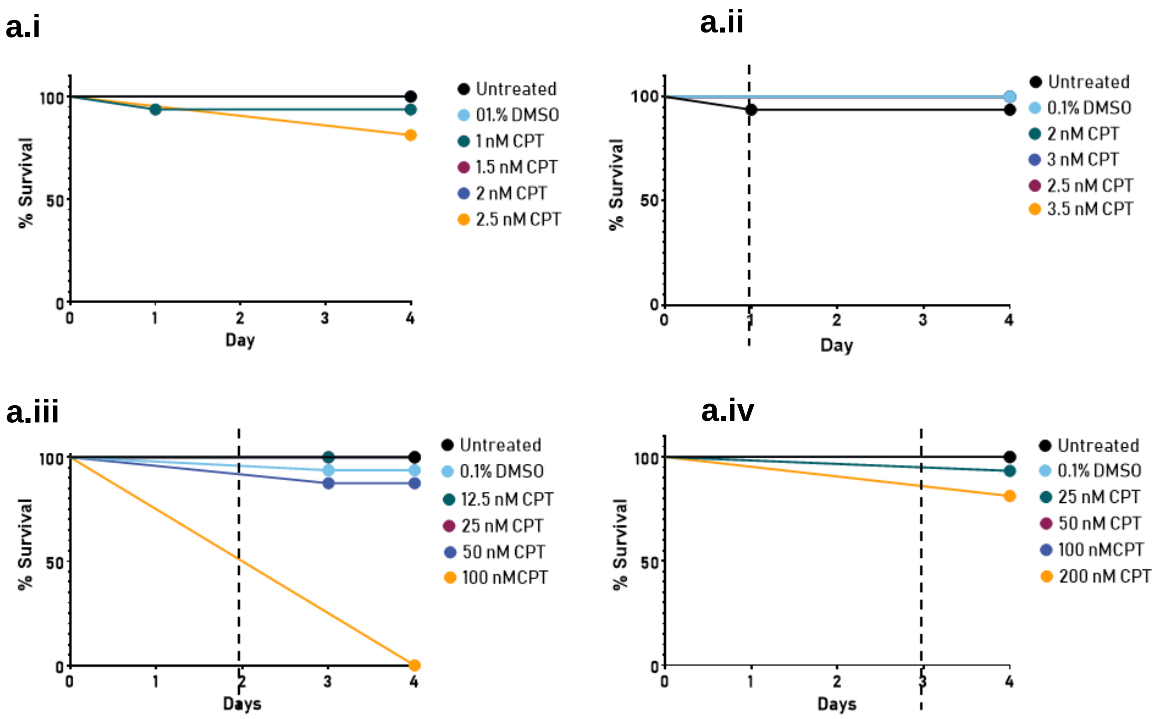
a.i

a.ii

a.iii

a.iv

b

Time/ Dose of CPT Treatment	*Number of fish treated*	*Number of fish survived for swimming analysis*
8 hpf		
Untreated	*16*	*16*
0.1% DMSO	*16*	*16*
1 nM	*16*	*15*
1.5 nM	*16*	*16*
2 nM	*16*	*16*
2.5 nM	*16*	*13*
24 hpf		
Untreated	*16*	*15*
0.1% DMSO	*16*	*16*
2 nM	*16*	*16*
2.5 nM	*16*	*16*
3 nM	*16*	*16*
3.5 nM	*16*	*16*
48 hpf		
Untreated	*15*	*15*
0.1% DMSO	*16*	*15*
12 nM	*16*	*16*
25 nM	*16*	*16*
50 nM	*16*	*14*
100 nM	*16*	*0*
72 hpf		
Untreated	*15*	*15*
0.1% DMSO	*14*	*14*
25 nM	*15*	*14*
50 nM	*15*	*15*
100 nM	*16*	*16*
200 nM	*16*	*13*
96 hpf		
Untreated	*16*	*16*
0.1% DMSO	*16*	*16*
400 nM	*15*	*15*
500 nM	*13*	*13*
600 nM	*16*	*16*
700 nM	*16*	*16*

Appendix 5.5 Statistical Analysis Corresponding to Figure 5.4: Optimisation 4 of CPT treatment on wild type (LWT) zebrafish embryos at 48 hpf in a 96 well plate for swimming analysis at 5dpf.

Figure b: Average distance travelled in dark and light phases

Two way RM ANOVA

Alpha	*0.05*			
Source of Variation	***% of total variation***	***P Value***	***P value summary***	***Significant?***
Light Driving x CPT Conc	*15.17*	*<0.0001*	******	*Yes*
Light Driving	*22.08*	*<0.0001*	******	*Yes*
CPT Conc	*30.91*	*<0.0001*	******	*Yes*
Subject	*22.54*	*<0.0001*	******	*Yes*

Tukey's multiple comparisons test	***Predicted (LS) mean diff.***	***95.00% CI of diff.***	***Below threshold?***	***Summary***	***Adjusted P Value***
Dark					
0.1% DMSO vs. 0.1 nM CPT	*197.6*	*-14.85 to 410.1*	*No*	*ns*	*0.0844*
0.1% DMSO vs. 1 nM CPT	*109.2*	*-99.79 to 318.2*	*No*	*ns*	*0.6611*
0.1% DMSO vs. 12.5 nM CPT	*536.8*	*327.8 to 745.8*	*Yes*	******	*<0.0001*
0.1% DMSO vs. 25 nM CPT	*712.1*	*503.1 to 921.2*	*Yes*	******	*<0.0001*
0.1% DMSO vs. 50 nM CPT	*919.7*	*707.3 to 1132*	*Yes*	******	*<0.0001*
0.1 nM CPT vs. 1 nM CPT	*-88.40*	*-300.9 to 124.1*	*No*	*ns*	*0.8370*
0.1 nM CPT vs. 12.5 nM CPT	*339.1*	*126.7 to 551.6*	*Yes*	*****	*0.0001*
0.1 nM CPT vs. 25 nM CPT	*514.5*	*302.1 to 727.0*	*Yes*	******	*<0.0001*
0.1 nM CPT vs. 50 nM CPT	*722.1*	*506.3 to 938.0*	*Yes*	******	*<0.0001*
1 nM CPT vs. 12.5 nM CPT	*427.5*	*218.5 to 636.6*	*Yes*	******	*<0.0001*
1 nM CPT vs. 25 nM CPT	*602.9*	*393.9 to 811.9*	*Yes*	******	*<0.0001*
1 nM CPT vs. 50 nM CPT	*810.5*	*598.1 to 1023*	*Yes*	******	*<0.0001*
12.5 nM CPT vs. 25 nM CPT	*175.4*	*-33.64 to 384.4*	*No*	*ns*	*0.1558*
12.5 nM CPT vs. 50 nM CPT	*383.0*	*170.5 to 595.4*	*Yes*	******	*<0.0001*
25 nM CPT vs. 50 nM CPT	*207.6*	*-4.860 to 420.1*	*No*	*ns*	*0.0597*
Light					
0.1% DMSO vs. 0.1 nM CPT	*6.222*	*-206.2 to 218.7*	*No*	*ns*	*>0.9999*
0.1% DMSO vs. 1 nM CPT	*82.45*	*-126.6 to 291.5*	*No*	*ns*	*0.8654*
0.1% DMSO vs. 12.5 nM CPT	*99.98*	*-109.0 to 309.0*	*No*	*ns*	*0.7400*
0.1% DMSO vs. 25 nM CPT	*108.6*	*-100.4 to 317.7*	*No*	*ns*	*0.6662*
0.1% DMSO vs. 50 nM CPT	*201.1*	*-11.36 to 413.6*	*No*	*ns*	*0.0750*
0.1 nM CPT vs. 1 nM CPT	*76.23*	*-136.2 to 288.7*	*No*	*ns*	*0.9060*
0.1 nM CPT vs. 12.5 nM CPT	*93.76*	*-118.7 to 306.2*	*No*	*ns*	*0.8001*

0.1 nM CPT vs. 25 nM CPT	102.4	-110.0 to 314.9	No	ns	0.7336
0.1 nM CPT vs. 50 nM CPT	194.9	-20.98 to 410.8	No	ns	0.1023
1 nM CPT vs. 12.5 nM CPT	17.53	-191.5 to 226.5	No	ns	0.9999
1 nM CPT vs. 25 nM CPT	26.19	-182.8 to 235.2	No	ns	0.9992
1 nM CPT vs. 50 nM CPT	118.7	-93.81 to 331.1	No	ns	0.5936
12.5 nM CPT vs. 25 nM CPT	8.660	-200.4 to 217.7	No	ns	>0.9999
12.5 nM CPT vs. 50 nM CPT	101.1	-111.3 to 313.6	No	ns	0.7440
25 nM CPT vs. 50 nM CPT	92.47	-120.0 to 304.9	No	ns	0.8093

Figure d: Average duration spent in active swimming in dark and light phases

Two way RM ANOVA

Alpha	*0.05*			
Source of Variation	***% of total variation***	***P Value***	***P value summary***	***Significant?***
Light Driving x CPT Conc	9.930	<0.0001	****	Yes
Light Driving	12.00	<0.0001	****	Yes
CPT Conc	35.13	<0.0001	****	Yes
Subject	32.37	<0.0001	****	Yes

Tukey's multiple comparisons test	***Predicted (LS) mean diff.***	***95.00% CI of diff.***	***Below threshold?***	***Summary***	***Adjusted P Value***
Dark					
0.1% DMSO vs. 0.1 nM CPT	23.42	-13.07 to 59.90	No	ns	0.4370
0.1% DMSO vs. 1 nM CPT	8.542	-27.35 to 44.43	No	ns	0.9833
0.1% DMSO vs. 12.5 nM CPT	63.06	27.17 to 98.95	Yes	****	<0.0001
0.1% DMSO vs. 25 nM CPT	86.44	50.55 to 122.3	Yes	****	<0.0001
0.1% DMSO vs. 50 nM CPT	133.6	97.13 to 170.1	Yes	****	<0.0001
0.1 nM CPT vs. 1 nM CPT	-14.88	-51.36 to 21.61	No	ns	0.8483
0.1 nM CPT vs. 12.5 nM CPT	39.65	3.162 to 76.13	Yes	*	0.0246
0.1 nM CPT vs. 25 nM CPT	63.02	26.54 to 99.51	Yes	****	<0.0001
0.1 nM CPT vs. 50 nM CPT	110.2	73.13 to 147.3	Yes	****	<0.0001
1 nM CPT vs. 12.5 nM CPT	54.52	18.63 to 90.41	Yes	***	0.0003
1 nM CPT vs. 25 nM CPT	77.90	42.01 to 113.8	Yes	****	<0.0001
1 nM CPT vs. 50 nM CPT	125.1	88.59 to 161.6	Yes	****	<0.0001
12.5 nM CPT vs. 25 nM CPT	23.38	-12.51 to 59.27	No	ns	0.4199
12.5 nM CPT vs. 50 nM CPT	70.55	34.07 to 107.0	Yes	****	<0.0001
25 nM CPT vs. 50 nM CPT	47.18	10.69 to 83.66	Yes	**	0.0035
Light					

0.1% DMSO vs. 0.1 nM CPT	*1.127*	*-35.36 to 37.61*	*No*	*ns*	*>0.9999*
0.1% DMSO vs. 1 nM CPT	*11.13*	*-24.77 to 47.02*	*No*	*ns*	*0.9477*
0.1% DMSO vs. 12.5 nM CPT	*15.45*	*-20.44 to 51.34*	*No*	*ns*	*0.8163*
0.1% DMSO vs. 25 nM CPT	*18.52*	*-17.37 to 54.41*	*No*	*ns*	*0.6731*
0.1% DMSO vs. 50 nM CPT	*48.76*	*12.28 to 85.24*	*Yes*	****	*0.0022*
0.1 nM CPT vs. 1 nM CPT	*9.998*	*-26.49 to 46.48*	*No*	*ns*	*0.9690*
0.1 nM CPT vs. 12.5 nM CPT	*14.33*	*-22.16 to 50.81*	*No*	*ns*	*0.8677*
0.1 nM CPT vs. 25 nM CPT	*17.39*	*-19.09 to 53.88*	*No*	*ns*	*0.7427*
0.1 nM CPT vs. 50 nM CPT	*47.63*	*10.57 to 84.70*	*Yes*	****	*0.0038*
1 nM CPT vs. 12.5 nM CPT	*4.327*	*-31.56 to 40.22*	*No*	*ns*	*0.9993*
1 nM CPT vs. 25 nM CPT	*7.396*	*-28.49 to 43.29*	*No*	*ns*	*0.9913*
1 nM CPT vs. 50 nM CPT	*37.64*	*1.152 to 74.12*	*Yes*	***	*0.0389*
12.5 nM CPT vs. 25 nM CPT	*3.069*	*-32.82 to 38.96*	*No*	*ns*	*0.9999*
12.5 nM CPT vs. 50 nM CPT	*33.31*	*-3.175 to 69.79*	*No*	*ns*	*0.0954*
25 nM CPT vs. 50 nM CPT	*30.24*	*-6.244 to 66.72*	*No*	*ns*	*0.1660*

Appendix 5.6: Statistical Analysis Corresponding to Figure 5.5: Optimisation 5 of CPT treatment on wild type (LWT) zebrafish embryos at 48 hpf in a 96 well plate for swimming analysis at 5dpf.

Figure b: Average distance travelled in dark and light phases

Two way RM ANOVA					
Alpha	***0.05***				
Source of Variation	***% of total variation***	***P Value***	***P value summary***	***Significant?***	
Light Driving x CPT Conc	*2.281*	*0.0385*	***	*Yes*	
Light Driving	*49.40*	*<0.0001*	******	*Yes*	
CPT Conc	*2.587*	*0.1654*	*ns*	*No*	
Subject	*31.08*	*0.0066*	****	*Yes*	
Šídák's multiple comparisons test	***Mean Diff.***	***95.00% CI of diff.***	***Below threshold?***	***Summary***	***Adjusted P Value***
Dark					
0.1% DMSO vs. 1 nM	*141.8*	*-42.05 to 325.6*	*No*	*ns*	*0.1795*
0.1% DMSO vs. 10 nM	*215.6*	*31.80 to 399.4*	*Yes*	***	*0.0160*
1 nM vs. 10 nM	*73.85*	*-110.0 to 257.7*	*No*	*ns*	*0.7005*
Light					
0.1% DMSO vs. 1 nM	*67.06*	*-116.8 to 250.9*	*No*	*ns*	*0.7583*
0.1% DMSO vs. 10 nM	*-6.825*	*-190.6 to 177.0*	*No*	*ns*	*0.9996*
1 nM vs. 10 nM	*-73.89*	*-257.7 to 109.9*	*No*	*ns*	*0.7002*

Figure d: Average duration spent in active swimming in dark and light phases

Two way RM ANOVA					
Alpha	***0.05***				
Source of Variation	***% of total variation***	***P Value***	***P value summary***	***Significant?***	
Light Driving x CPT Conc	*3.588*	*0.0025*	****	*Yes*	
Light Driving	*40.17*	*<0.0001*	******	*Yes*	
CPT Conc	*6.748*	*0.0246*	***	*Yes*	
Subject	*37.69*	*<0.0001*	******	*Yes*	
Tukey's multiple comparisons test	***Mean Diff.***	***95.00% CI of diff.***	***Below threshold?***	***Summary***	***Adjusted P Value***
Dark					
0.1% DMSO vs. 1 nM	*20.31*	*-7.809 to 48.42*	*No*	*ns*	*0.2029*
0.1% DMSO vs. 10 nM	*23.04*	*-5.073 to 51.16*	*No*	*ns*	*0.1300*
1 nM vs. 10 nM	*2.735*	*-25.38 to 30.85*	*No*	*ns*	*0.9708*
Light					

0.1% DMSO vs. 1 nM	*37.40*	*9.284 to 65.52*	*Yes*	****	*0.0059*
0.1% DMSO vs. 10 nM	*-2.221*	*-30.34 to 25.90*	*No*	*ns*	*0.9807*
1 nM vs. 10 nM	*-39.62*	*-67.74 to -11.50*	*Yes*	****	*0.0033*

Appendix 5.7: Statistical Analysis Corresponding to Figure 5.6: ATM$^{sh477/sh477}$ zebrafish larvae exhibit no behavioural abnormalities in response to DNA damaging agent CPT compared to their control siblings.

Figure b: Average distance travelled in dark and light phases

Two way RM ANOVA					
Alpha	***0.05***				
Source of Variation	***% of total variation***	***P Value***	***P value summary***	***Significant?***	
CPT Conc x Genotype	*1.090*	*0.5264*	*ns*	*No*	
CPT Conc	*30.85*	*<0.0001*	******	*Yes*	
Genotype	*0.4404*	*0.3549*	*ns*	*No*	
Tukey's multiple comparisons test Genotype v Genotype	***Predicted (LS) mean diff.***	***95.00% CI of diff.***	***Below threshold?***	***Summary***	***Adjusted P Value***
0.1% DMSO – Dark					
ATM$^{+/+}$ vs. ATM$^{+/sh477}$	*-100.5*	*-281.4 to 80.50*	*No*	*ns*	*0.3917*
ATM$^{+/+}$ vs. ATM$^{sh477/sh477}$	*36.78*	*-173.5 to 247.0*	*No*	*ns*	*0.9106*
ATM$^{+/sh477}$ vs. ATM$^{sh477/sh477}$	*137.2*	*-35.92 to 310.4*	*No*	*ns*	*0.1501*
10 nM CPT -Dark					
ATM$^{+/+}$ vs. ATM$^{+/sh477}$	*45.94*	*-110.5 to 202.3*	*No*	*ns*	*0.7682*
ATM$^{+/+}$ vs. ATM$^{sh477/sh477}$	*106.4*	*-109.7 to 322.5*	*No*	*ns*	*0.4777*
ATM$^{+/sh477}$ vs. ATM$^{sh477/sh477}$	*60.50*	*-144.0 to 265.0*	*No*	*ns*	*0.7652*
0.1% DMSO - Light					
ATM$^{+/+}$ vs. ATM$^{+/sh477}$	*9.064*	*-171.9 to 190.0*	*No*	*ns*	*0.9923*
ATM$^{+/+}$ vs. ATM$^{sh477/sh477}$	*42.03*	*-168.2 to 252.3*	*No*	*ns*	*0.8849*
ATM$^{+/sh477}$ vs. ATM$^{sh477/sh477}$	*32.97*	*-140.2 to 206.1*	*No*	*ns*	*0.8950*
10 nM CPT - Light					
ATM$^{+/+}$ vs. ATM$^{+/sh477}$	*98.24*	*-58.16 to 254.6*	*No*	*ns*	*0.3020*
ATM$^{+/+}$ vs. ATM$^{sh477/sh477}$	*64.03*	*-152.1 to 280.1*	*No*	*ns*	*0.7646*
ATM$^{+/sh477}$ vs. ATM$^{sh477/sh477}$	*-34.20*	*-238.7 to 170.3*	*No*	*ns*	*0.9179*
Tukey's multiple comparisons test 0.1% DMSO v 10 nM CPT (Within Genotypes)	***Predicted (LS) mean diff.***	***95.00% CI of diff.***	***Below threshold?***	***Summary***	***Adjusted P Value***
ATM$^{+/+}$					
0.1% DMSO (D) vs. 10 nM CPT (D)	*40.97*	*-173.3 to 255.2*	*No*	*ns*	*0.9603*
0.1% DMSO (D) vs. 0.1% DMSO (L)	*429.6*	*191.9 to 667.3*	*Yes*	******	*<0.0001*
0.1% DMSO (D) vs. 10 nM CPT (L)	*347.0*	*132.7 to 561.3*	*Yes*	*****	*0.0002*
10 nM CPT (D) vs. 0.1% DMSO (L)	*388.7*	*174.4 to 602.9*	*Yes*	******	*<0.0001*
10 nM CPT (D) vs. 10 nM CPT (L)	*306.0*	*118.1 to 494.0*	*Yes*	*****	*0.0002*
0.1% DMSO (L) vs. 10 nM CPT (L)	*-82.61*	*-296.9 to 131.7*	*No*	*ns*	*0.7514*
ATM$^{+/sh477}$					
0.1% DMSO (D) vs. 10 nM CPT (D)	*187.4*	*35.97 to 338.8*	*Yes*	****	*0.0083*
0.1% DMSO (D) vs. 0.1% DMSO (L[1])	*539.2*	*389.8 to 688.5*	*Yes*	******	*<0.0001*
0.1% DMSO (D) vs. 10 nM CPT (L)	*545.7*	*394.3 to 697.1*	*Yes*	******	*<0.0001*
10 nM CPT (D) vs. 0.1% DMSO (L)	*351.8*	*200.4 to 503.2*	*Yes*	******	*<0.0001*
10 nM CPT (D) vs. 10 nM CPT (L)	*358.3*	*204.9 to 511.8*	*Yes*	******	*<0.0001*
0.1% DMSO (L) vs. 10 nM CPT (L)	*6.563*	*-144.8 to 158.0*	*No*	*ns*	*0.9995*
ATM$^{SH477/SH477}$					
0.1% DMSO (D) vs. 10 nM CPT (D)	*110.6*	*-141.3 to 362.5*	*No*	*ns*	*0.6680*
0.1% DMSO (D) vs. 0.1% DMSO (L)	*434.9*	*211.6 to 658.2*	*Yes*	******	*<0.0001*
0.1% DMSO (D) vs. 10 nM CPT (L)	*374.3*	*122.4 to 626.2*	*Yes*	*****	*0.0009*
10 nM CPT (D) vs. 0.1% DMSO (L)	*324.2*	*72.34 to 576.1*	*Yes*	****	*0.0055*
10 nM CPT (D) vs. 10 nM CPT (L)	*263.6*	*-13.95 to 541.2*	*No*	*ns*	*0.0695*

0.1% DMSO (L) vs. 10 nM CPT (L)	*-60.61*	*-312.5 to 191.3*	*No*	*ns*	*0.9250*
Tukey's multiple comparisons test Total 0.1% DMSO Dark v Total 10 nM CPT Light	*Predicted (LS) mean diff.*	***95.00% CI of diff.***	***Below threshold?***	***Summary***	***Adjusted P Value***
0.1% DMSO (D) vs. 10 nM CPT (D)	*113.0*	*-8.243 to 234.2*	*No*	*ns*	*0.0777*
0.1% DMSO (D) vs. 0.1% DMSO (L)	*467.9*	*348.3 to 587.5*	*Yes*	******	*<0.0001*
0.1% DMSO (D) vs. 10 nM CPT (L)	*422.3*	*301.1 to 543.6*	*Yes*	******	*<0.0001*
10 nM CPT (D) vs. 0.1% DMSO (L)	*354.9*	*233.7 to 476.1*	*Yes*	******	*<0.0001*
10 nM CPT (D) vs. 10 nM CPT (L)	*309.3*	*186.5 to 432.2*	*Yes*	******	*<0.0001*
0.1% DMSO (L) vs. 10 nM CPT (L)	*-45.55*	*-166.8 to 75.69*	*No*	*ns*	*0.7659*

Figure d: Average duration spent in active swimming in dark and light phases

Two way RM ANOVA

Alpha	**0.05**			
Source of Variation	**% of total variation**	**P Value**	**P value summary**	**Significant?**
CPT Conc x Genotype	1.028	0.7336	ns	No
CPT Conc	14.82	<0.0001	****	Yes
Genotype	1.110	0.1471	ns	No

Tukey's multiple comparisons test Genotype v Genotype	**Predicted (LS) mean diff.**	**95.00% CI of diff.**	**Below threshold?**	**Summary**	**Adjusted P Value**
0.1% DMSO – Dark					
ATM$^{+/+}$ vs. ATM$^{+/sh477}$	-2.004	-35.72 to 31.71	No	ns	0.9892
ATM$^{+/+}$ vs. ATM$^{sh477/sh477}$	12.34	-26.83 to 51.50	No	ns	0.7385
ATM$^{+/sh477}$ vs. ATM$^{sh477/sh477}$	14.34	-17.92 to 46.60	No	ns	0.5475
10 nM CPT -Dark					
ATM$^{+/+}$ vs. ATM$^{+/sh477}$	11.55	-17.58 to 40.69	No	ns	0.6190
ATM$^{+/+}$ vs. ATM$^{sh477/sh477}$	23.21	-17.04 to 63.46	No	ns	0.3641
ATM$^{+/sh477}$ vs. ATM$^{sh477/sh477}$	11.66	-26.43 to 49.75	No	ns	0.7510
0.1% DMSO - Light					
ATM$^{+/+}$ vs. ATM$^{+/sh477}$	5.425	-28.29 to 39.14	No	ns	0.9238
ATM$^{+/+}$ vs. ATM$^{sh477/sh477}$	7.263	-31.90 to 46.43	No	ns	0.9001
ATM$^{+/sh477}$ vs. ATM$^{sh477/sh477}$	1.837	-30.42 to 34.10	No	ns	0.9901
10 nM CPT - Light					
ATM$^{+/+}$ vs. ATM$^{+/sh477}$	27.79	-1.340 to 56.93	No	ns	0.0651
ATM$^{+/+}$ vs. ATM$^{sh477/sh477}$	18.35	-21.90 to 58.61	No	ns	0.5307
ATM$^{+/sh477}$ vs. ATM$^{sh477/sh477}$	-9.439	-47.53 to 28.65	No	ns	0.8288

Tukey's multiple comparisons test 0.1% DMSO v 10 nM CPT (Within Genotypes)	**Predicted (LS) mean diff.**	**95.00% CI of diff.**	**Below threshold?**	**Summary**	**Adjusted P Value**
ATM$^{+/+}$					
0.1% DMSO (D[2]) vs. 10 nM CPT (D)	-0.2267	-40.14 to 39.69	No	ns	>0.9999
0.1% DMSO (D) vs. 0.1% DMSO (L[3])	52.68	8.404 to 96.97	Yes	*	0.0123
0.1% DMSO (D) vs. 10 nM CPT (L)	27.68	-12.23 to 67.60	No	ns	0.2790
10 nM CPT (D) vs. 0.1% DMSO (L)	52.91	13.00 to 92.83	Yes	**	0.0039

10 nM CPT (D) vs. 10 nM CPT (L)	27.91	-7.099 to 62.92	No	ns	0.1687
0.1% DMSO (L) vs. 10 nM CPT (L)	-25.00	-64.92 to 14.91	No	ns	0.3694
ATM$^{+/sh477}$					
0.1% DMSO (D[4]) vs. 10 nM CPT (D)	13.33	-14.88 to 41.53	No	ns	0.6136
0.1% DMSO (D) vs. 0.1% DMSO (L[5])	60.11	32.29 to 87.93	Yes	****	<0.0001
0.1% DMSO (D) vs. 10 nM CPT (L)	57.48	29.27 to 85.68	Yes	****	<0.0001
10 nM CPT (D) vs. 0.1% DMSO (L)	46.78	18.58 to 74.99	Yes	***	0.0001
10 nM CPT (D) vs. 10 nM CPT (L)	44.15	15.57 to 72.73	Yes	***	0.0005
0.1% DMSO (L) vs. 10 nM CPT (L)	-2.635	-30.84 to 25.57	No	ns	0.9950
ATM$^{SH477/SH477}$					
0.1% DMSO (D[6]) vs. 10 nM CPT (D)	10.65	-36.28 to 57.57	No	ns	0.9361
0.1% DMSO (D) vs. 0.1% DMSO (L[7])	47.61	6.017 to 89.21	Yes	*	0.0176
0.1% DMSO (D) vs. 10 nM CPT (L)	33.70	-13.22 to 80.63	No	ns	0.2494
10 nM CPT (D) vs. 0.1% DMSO (L)	36.96	-9.962 to 83.89	No	ns	0.1773
10 nM CPT (D) vs. 10 nM CPT (L)	23.05	-28.66 to 74.76	No	ns	0.6573
0.1% DMSO (L) vs. 10 nM CPT (L)	-13.91	-60.84 to 33.01	No	ns	0.8695
Tukey's multiple comparisons test Total 0.1% DMSO Dark v Total 10 nM CPT Light	**Predicted (LS) mean diff.**	**95.00% CI of diff.**	**Below threshold?**	**Summary**	**Adjusted P Value**
0.1% DMSO (D) vs. 10 nM CPT (D)	7.917	-14.67 to 30.50	No	ns	0.8015
0.1% DMSO (D) vs. 0.1% DMSO (L)	53.47	31.20 to 75.74	Yes	****	<0.0001
0.1% DMSO (D) vs. 10 nM CPT (L)	39.62	17.04 to 62.21	Yes	****	<0.0001
10 nM CPT (D) vs. 0.1% DMSO (L)	45.55	22.97 to 68.14	Yes	****	<0.0001
10 nM CPT (D) vs. 10 nM CPT (L)	31.70	8.812 to 54.59	Yes	**	0.0023
0.1% DMSO (L) vs. 10 nM CPT (L)	-13.85	-36.43 to 8.735	No	ns	0.3887

Appendix 5.8: Statistical Analysis Corresponding to Figure 5.7: ATM$^{sh477/sh477}$ zebrafish larvae exhibit no swimming defects in response to exogenous DNA damage induced by IR compared to their control siblings.

Figure b: Average distance travelled in dark and light phases

Two way ANOVA					
Alpha	*0.05*				
Source of Variation	***% of total variation***	***P Value***	***P value summary***	***Significant?***	
IR DOSE X Genotype	*0.2049*	*0.9378*	*ns*	*No*	
IR Dose	*46.75*	*<0.0001*	******	*Yes*	
Genotype	*0.7609*	*0.0371*	***	*Yes*	

Tukey's multiple comparisons test Genotype v Genotype	***Predicted (LS) mean diff.***	***95.00% CI of diff.***	***Below threshold?***	***Summary***	***Adjusted P Value***
0 Gy - Dark					
ATM$^{+/+}$ vs. ATM$^{+/sh477}$	*35.69*	*-45.51 to 116.9*	*No*	*ns*	*0.5560*
ATM$^{+/+}$ vs. ATM$^{sh477/sh477}$	*-26.45*	*-113.0 to 60.15*	*No*	*ns*	*0.7529*
ATM$^{+/sh477}$ vs. ATM$^{sh477/sh477}$	*-62.14*	*-142.7 to 18.43*	*No*	*ns*	*0.1662*
8 Gy - Dark					
ATM$^{+/+}$ vs. ATM$^{+/sh477}$	*-18.44*	*-101.4 to 64.53*	*No*	*ns*	*0.8603*
ATM$^{+/+}$ vs. ATM$^{sh477/sh477}$	*-66.54*	*-161.3 to 28.21*	*No*	*ns*	*0.2253*
ATM$^{+/sh477}$ vs. ATM$^{sh477/sh477}$	*-48.10*	*-137.8 to 41.58*	*No*	*ns*	*0.4179*
0 Gy - Light					
ATM$^{+/+}$ vs. ATM$^{+/sh477}$	*20.10*	*-61.45 to 101.7*	*No*	*ns*	*0.8311*
ATM$^{+/+}$ vs. ATM$^{sh477/sh477}$	*-19.00*	*-105.6 to 67.60*	*No*	*ns*	*0.8636*
ATM$^{+/sh477}$ vs. ATM$^{sh477/sh477}$	*-39.11*	*-120.0 to 41.82*	*No*	*ns*	*0.4922*
8 Gy - Light					
ATM$^{+/+}$ vs. ATM$^{+/sh477}$	*-2.204*	*-85.18 to 80.77*	*No*	*ns*	*0.9979*
ATM$^{+/+}$ vs. ATM$^{sh477/sh477}$	*-34.89*	*-129.6 to 59.86*	*No*	*ns*	*0.6620*
ATM$^{+/sh477}$ vs. ATM$^{sh477/sh477}$	*-32.69*	*-122.4 to 56.99*	*No*	*ns*	*0.6676*

Tukey's multiple comparisons test 0 Gy vs 8 Gy (within Genotype)	***Predicted (LS) mean diff.***	***95.00% CI of diff.***	***Below threshold?***	***Summary***	***Adjusted P Value***
ATM$^{+/+}$					
0 Gy (D) vs. 8Gy (D)	*230.1*	*133.9 to 326.4*	*Yes*	******	*<0.0001*
0 Gy (D) vs. 0 Gy (L)	*327.4*	*231.8 to 423.0*	*Yes*	******	*<0.0001*
0 Gy (D) vs. 8Gy (L)	*404.7*	*308.4 to 501.0*	*Yes*	******	*<0.0001*
8Gy (D) vs. 0 Gy (L)	*97.22*	*0.9229 to 193.5*	*Yes*	***	*0.0468*
8Gy (D) vs. 8Gy (L)	*174.5*	*77.57 to 271.5*	*Yes*	******	*<0.0001*
0 Gy (D) vs. 8Gy (L)	*77.32*	*-18.97 to 173.6*	*No*	*ns*	*0.1644*
ATM$^{+/sh477}$					
0 Gy (D) vs. 8Gy (D)	*176.0*	*92.74 to 259.3*	*Yes*	******	*<0.0001*
0 Gy (D) vs. 0 Gy (L)	*311.8*	*229.4 to 394.2*	*Yes*	******	*<0.0001*
0 Gy (D) vs. 8Gy (L)	*366.8*	*283.5 to 450.1*	*Yes*	******	*<0.0001*
8Gy (D) vs. 0 Gy (L)	*135.8*	*52.06 to 219.5*	*Yes*	*****	*0.0002*
8Gy (D) vs. 8Gy (L)	*190.8*	*106.2 to 275.4*	*Yes*	******	*<0.0001*
0 Gy (D) vs. 8Gy (L)	*55.01*	*-28.69 to 138.7*	*No*	*ns*	*0.3275*

$ATM^{sh477/sh477}$					
0 Gy (D) vs. 8Gy (D)	*190.1*	*87.38 to 292.7*	*Yes*	******	*<0.0001*
0 Gy (D) vs. 0 Gy (L)	*334.8*	*240.5 to 429.1*	*Yes*	******	*<0.0001*
0 Gy (D) vs. 8Gy (L)	*396.2*	*293.6 to 498.9*	*Yes*	******	*<0.0001*
8Gy (D) vs. 0 Gy (L)	*144.8*	*42.08 to 247.4*	*Yes*	****	*0.0018*
8Gy (D) vs. 8Gy (L)	*206.2*	*95.78 to 316.6*	*Yes*	******	*<0.0001*
0 Gy (D) vs. 8Gy (L)	*61.43*	*-41.25 to 164.1*	*No*	*ns*	*0.4128*

Figure d: Average duration spent in active swimming in dark and light phases

Two way ANOVA

Alpha	*0.05*				
Source of Variation	***% of total variation***	***P Value***	***P value summary***	***Significant?***	
IR Dose X Genotype	*0.4219*	*0.7445*	*ns*	*No*	
IR Dose	*41.97*	*<0.0001*	******	*Yes*	
Genotype	*0.2485*	*0.3581*	*ns*	*No*	
Tukey's multiple comparisons test Genotype v Genotype	***Predicted (LS) mean diff.***	***95.00% CI of diff.***	***Below threshold?***	***Summary***	***Adjusted P Value***
0 Gy - Dark					
$ATM^{+/+}$ vs. $ATM^{+/sh477}$	*-3.271*	*-20.02 to 13.47*	*No*	*ns*	*0.8903*
$ATM^{+/+}$ vs. $ATM^{sh477/sh477}$	*-4.296*	*-22.21 to 13.62*	*No*	*ns*	*0.8393*
$ATM^{+/sh477}$ vs. $ATM^{sh477/sh477}$	*-1.025*	*-17.50 to 15.45*	*No*	*ns*	*0.9883*
8 Gy - Dark					
$ATM^{+/+}$ vs. $ATM^{+/sh477}$	*10.19*	*-6.233 to 26.62*	*No*	*ns*	*0.3117*
$ATM^{+/+}$ vs. $ATM^{sh477/sh477}$	*-1.842*	*-20.77 to 17.08*	*No*	*ns*	*0.9715*
$ATM^{+/sh477}$ vs. $ATM^{sh477/sh477}$	*-12.03*	*-30.45 to 6.386*	*No*	*ns*	*0.2749*
0 Gy - Light					
$ATM^{+/+}$ vs. $ATM^{+/sh477}$	*-4.918*	*-21.66 to 11.83*	*No*	*ns*	*0.7691*
$ATM^{+/+}$ vs. $ATM^{sh477/sh477}$	*-4.742*	*-22.66 to 13.17*	*No*	*ns*	*0.8079*
$ATM^{+/sh477}$ vs. $ATM^{sh477/sh477}$	*0.1756*	*-16.30 to 16.65*	*No*	*ns*	*0.9997*
8 Gy - Light					
$ATM^{+/+}$ vs. $ATM^{+/sh477}$	*4.469*	*-11.96 to 20.89*	*No*	*ns*	*0.7983*
$ATM^{+/+}$ vs. $ATM^{sh477/sh477}$	*-3.859*	*-22.78 to 15.06*	*No*	*ns*	*0.8810*
$ATM^{+/sh477}$ vs. $ATM^{sh477/sh477}$	*-8.328*	*-26.75 to 10.09*	*No*	*ns*	*0.5375*
Tukey's multiple comparisons test 0 Gy vs 8 Gy (within Genotype)	***Predicted (LS) mean diff.***	***95.00% CI of diff.***	***Below threshold?***	***Summary***	***Adjusted P Value***
$ATM^{+/+}$					
0 Gy (D) vs. 8Gy (D)	*230.1*	*133.9 to 326.4*	*Yes*	******	*<0.0001*
0 Gy (D) vs. 0 Gy (L)	*327.4*	*231.8 to 423.0*	*Yes*	******	*<0.0001*
0 Gy (D) vs. 8Gy (L)	*404.7*	*308.4 to 501.0*	*Yes*	******	*<0.0001*
8Gy (D) vs. 0 Gy (L)	*97.22*	*0.9229 to 193.5*	*Yes*	***	*0.0468*
8Gy (D) vs. 8Gy (L)	*174.5*	*77.57 to 271.5*	*Yes*	******	*<0.0001*
0 Gy (D) vs. 8Gy (L)	*77.32*	*-18.97 to 173.6*	*No*	*ns*	*0.1644*
$ATM^{+/sh477}$					
0 Gy (D) vs. 8Gy (D)	*176.0*	*92.74 to 259.3*	*Yes*	******	*<0.0001*

0 Gy (D) vs. 0 Gy (L)	*311.8*	*229.4 to 394.2*	*Yes*	******	*<0.0001*
0 Gy (D) vs. 8Gy (L)	*366.8*	*283.5 to 450.1*	*Yes*	******	*<0.0001*
8Gy (D) vs. 0 Gy (L)	*135.8*	*52.06 to 219.5*	*Yes*	*****	*0.0002*
8Gy (D) vs. 8Gy (L)	*190.8*	*106.2 to 275.4*	*Yes*	******	*<0.0001*
0 Gy (D) vs. 8Gy (L)	*55.01*	*-28.69 to 138.7*	*No*	*ns*	*0.3275*
ATM$^{sh477/sh477}$					
0 Gy (D) vs. 8Gy (D)	*190.1*	*87.38 to 292.7*	*Yes*	******	*<0.0001*
0 Gy (D) vs. 0 Gy (L)	*334.8*	*240.5 to 429.1*	*Yes*	******	*<0.0001*
0 Gy (D) vs. 8Gy (L)	*396.2*	*293.6 to 498.9*	*Yes*	******	*<0.0001*
8Gy (D) vs. 0 Gy (L)	*144.8*	*42.08 to 247.4*	*Yes*	****	*0.0018*
8Gy (D) vs. 8Gy (L)	*206.2*	*95.78 to 316.6*	*Yes*	******	*<0.0001*
0 Gy (D) vs. 8Gy (L)	*61.43*	*-41.25 to 164.1*	*No*	*ns*	*0.4128*

Appendix 5.9.1 Statistical Analysis Corresponding to figure 5.9: ATM$^{sh477/sh477}$ zebrafish do not exhibit sensitivity to an ATM inhibitor.

Figure b: Average distance travelled in dark and light phases

Two way ANOVA

Alpha	*0.05*			
Source of Variation	***% of total variation***	***P value***	***P value summary***	***Significant?***
Genotype and IR Dose x ATMi	*1.358*	*0.2199*	*ns*	*No*
Genotype/IR dose	*1.584*	*0.0033*	****	*Yes*
ATMi	*51.38*	*<0.0001*	******	*Yes*

Tukey's multiple comparisons test	***Predicted (LS) mean diff.***	***95.00% CI of diff.***	***Below threshold?***	***Summary***	***Adjusted P Value***
Dark ***1% DMSO***					
ATM$^{+/+}$0 GY vs. ATM$^{sh477/sh477}$0 GY	*-15.25*	*-154.3 to 123.8*	*No*	*ns*	*0.9921*
ATM$^{+/+}$0 GY vs. ATM$^{+/+}$12 GY	*23.49*	*-110.3 to 157.3*	*No*	*ns*	*0.9690*
ATM$^{+/+}$0 GY vs. ATM$^{sh477/sh477}$ 12GY	*-57.24*	*-202.7 to 88.23*	*No*	*ns*	*0.7405*
ATM$^{sh477/sh477}$0 GY vs. ATM$^{+/+}$12 GY	*38.74*	*-78.99 to 156.5*	*No*	*ns*	*0.8309*
ATM$^{sh477/sh477}$ 0 GY vs. ATM$^{sh477/sh477}$ 12GY	*-42.00*	*-172.8 to 88.83*	*No*	*ns*	*0.8410*
ATM$^{+/+}$12 GY vs. ATM$^{sh477/sh477}$ 12GY	*-80.74*	*-206.0 to 44.49*	*No*	*ns*	*0.3445*
10 nM ATMi					
ATM$^{+/+}$ 0 GY vs. ATM$^{sh477/sh477}$0 GY	*100.5*	*-32.40 to 233.5*	*No*	*ns*	*0.2085*
ATM$^{+/+}$ 0 GY vs. ATM$^{+/+}$12 GY	*152.8*	*35.60 to 269.9*	*Yes*	****	*0.0047*
ATM$^{+/+}$ 0 GY vs. ATM$^{sh477/sh477}$ 12GY	*-45.86*	*-165.3 to 73.62*	*No*	*ns*	*0.7549*
ATM$^{sh477/sh477}$ 0 GY vs. ATM$^{+/+}$12 GY	*52.23*	*-82.48 to 186.9*	*No*	*ns*	*0.7492*
HOM 0 GY vs. ATM$^{sh477/sh477}$ 12GY	*-146.4*	*-283.1 to -9.682*	*Yes*	***	*0.0304*
ATM$^{+/+}$ 12 GY vs. ATM$^{sh477/sh477}$ 12GY	*-198.6*	*-320.1 to -77.19*	*Yes*	*****	*0.0002*
Light					
1% DMSO					
ATM$^{+/+}$0 GY vs. ATM$^{sh477/sh477}$0 GY	-26.70	-165.8 to 112.4	No	ns	0.9601
ATM$^{+/+}$0 GY vs. ATM$^{+/+}$12 GY	6.342	-127.5 to 140.2	No	ns	0.9993
ATM$^{+/+}$0 GY vs. ATM$^{sh477/sh477}$ 12GY	-21.97	-167.5 to 123.5	No	ns	0.9799
ATM$^{sh477/sh477}$0 GY vs. ATM$^{+/+}$12 GY	33.04	-84.69 to 150.8	No	ns	0.8874
ATM$^{sh477/sh477}$ 0 GY vs. ATM$^{sh477/sh477}$ 12GY	4.723	-126.1 to 135.5	No	ns	0.9997
ATM$^{+/+}$12 GY vs. ATM$^{sh477/sh477}$ 12GY	-28.31	-153.5 to 96.91	No	ns	0.9370

10 nM ATMi					
ATM$^{+/+}$ 0 GY vs. ATM$^{sh477/sh477}$0 GY	21.19	-111.8 to 154.1	No	ns	0.9765
ATM$^{+/+}$ 0 GY vs. ATM$^{+/+}$12 GY	41.96	-75.21 to 159.1	No	ns	0.7920
ATM$^{+/+}$ 0 GY vs. ATM$^{sh477/sh477}$ 12GY	2.852	-116.6 to 122.3	No	ns	>0.9999
ATM$^{sh477/sh477}$ 0 GY vs. ATM$^{+/+}$12 GY	20.77	-113.9 to 155.5	No	ns	0.9786
HOM 0 GY vs. ATM$^{sh477/sh477}$ 12GY	-18.33	-155.1 to 118.4	No	ns	0.9857
ATM$^{+/+}$ 12 GY vs. ATM$^{sh477/sh477}$ 12GY	-39.10	-160.5 to 82.34	No	ns	0.8398

Tukey's multiple comparisons test	***Predicted (LS) mean diff.***	***95.00% CI of diff.***	***Below threshold?***	***Summary***	***Adjusted P Value***
ATM$^{+/+}$ 0 GY					
1% DMSO vs. 10 nM ATMi (Dark)	*-26.92*	*-162.3 to 108.4*	*No*	*ns*	*0.9559*
1% DMSO light vs. 10 nM ATMi (Light)	*3.153*	*-132.2 to 138.5*	*No*	*ns*	*>0.9999*
ATM$^{sh477/sh477}$ 0 GY					
1% DMSO vs. 10 nM ATMi (Dark)	*88.87*	*-47.85 to 225.6*	*No*	*ns*	*0.3371*
1% DMSO light vs. 10 nM ATMi (Light)	*51.03*	*-13.03 to 217.8*	*No*	*ns*	*0.1024*
ATM$^{+/+}$ 12 GY					
1% DMSO vs. 10 nM ATMi (Dark)	*102.4*	*-13.03 to 217.8*	*No*	*ns*	*0.1024*
1% DMSO light vs. 10 nM ATMi (Light)	*38.77*	*-76.62 to 154.2*	*No*	*ns*	*0.8219*
ATM$^{sh477/sh477}$ 12GY					
1% DMSO vs. 10 nM ATMi (Dark)	*-15.54*	*-146.4 to 115.3*	*No*	*ns*	*0.9900*
1% DMSO light vs. 10 nM ATMi (Light)	*27.98*	*-102.8 to 158.8*	*No*	*ns*	*0.9460*

Figure d: Average duration spent in active swimming in dark and light phases

Two way ANOVA				
Alpha	*0.05*			
Source of Variation	***% of total variation***	***P value***	***P value summary***	***Significant?***
Genotype and IR Dose x ATMi	0.8023	0.7565	ns	No
Genotype/IR dose	2.149	0.0016	**	Yes
ATMi	42.81	<0.0001	****	Yes

Tukey's multiple comparisons test	***Predicted (LS) mean diff.***	***95.00% CI of diff.***	***Below threshold?***	***Summary***	***Adjusted P Value***
Dark					
1% DMSO					
ATM$^{+/+}$0 GY vs. ATM$^{sh477/sh477}$0 GY	-3.448	-25.75 to 18.86	No	ns	0.9785
ATM$^{+/+}$0 GY vs. ATM$^{+/+}$12 GY	7.263	-14.20 to 28.73	No	ns	0.8188
ATM$^{+/+}$0 GY vs. ATM$^{sh477/sh477}$ 12GY	-3.473	-26.81 to 19.86	No	ns	0.9807

ATM$^{sh477/sh477}$0 GY vs. ATM$^{+/+}$12 GY	10.71	-8.172 to 29.59	No	ns	0.4606
ATM$^{sh477/sh477}$ 0 GY vs. ATM$^{sh477/sh477}$ 12GY	-0.02528	-21.01 to 20.96	No	ns	>0.9999
ATM$^{+/+}$12 GY vs. ATM$^{sh477/sh477}$ 12GY	-10.74	-30.82 to 9.349	No	ns	0.5131
10 nM ATMi					
ATM$^{+/+}$ 0 GY vs. ATM$^{sh477/sh477}$0 GY	9.786	-11.54 to 31.11	No	ns	0.6372
ATM$^{+/+}$ 0 GY vs. ATM$^{+/+}$12 GY	22.32	3.527 to 41.11	Yes	*	0.0124
ATM$^{+/+}$ 0 GY vs. ATM$^{sh477/sh477}$ 12GY	-2.924	-22.09 to 16.24	No	ns	0.9793
ATM$^{sh477/sh477}$ 0 GY vs. ATM$^{+/+}$12 GY	12.53	-9.072 to 34.14	No	ns	0.4404
HOM 0 GY vs. ATM$^{sh477/sh477}$ 12GY	-12.71	-34.64 to 9.220	No	ns	0.4412
ATM$^{+/+}$ 12 GY vs. ATM$^{sh477/sh477}$ 12GY	-25.24	-44.72 to -5.765	Yes	**	0.0050
Light					
1% DMSO					
ATM$^{+/+}$0 GY vs. ATM$^{sh477/sh477}$0 GY	-6.205	-28.51 to 16.10	No	ns	0.8900
ATM$^{+/+}$0 GY vs. ATM$^{+/+}$12 GY	3.840	-17.62 to 25.30	No	ns	0.9673
ATM$^{+/+}$0 GY vs. ATM$^{sh477/sh477}$ 12GY	-2.510	-25.84 to 20.82	No	ns	0.9925
ATM$^{sh477/sh477}$0 GY vs. ATM$^{+/+}$12 GY	10.04	-8.838 to 28.93	No	ns	0.5173
ATM$^{sh477/sh477}$ 0 GY vs. ATM$^{sh477/sh477}$ 12GY	3.695	-17.29 to 24.68	No	ns	0.9687
ATM$^{+/+}$12 GY vs. ATM$^{sh477/sh477}$ 12GY	-6.349	-26.43 to 13.74	No	ns	0.8470
10 nM ATMi					
ATM$^{+/+}$ 0 GY vs. ATM$^{sh477/sh477}$0 GY	3.982	-17.34 to 25.30	No	ns	0.9631
ATM$^{+/+}$ 0 GY vs. ATM$^{+/+}$12 GY	12.84	-5.953 to 31.63	No	ns	0.2929
ATM$^{+/+}$ 0 GY vs. ATM$^{sh477/sh477}$ 12GY	1.616	-17.55 to 20.78	No	ns	0.9964
ATM$^{sh477/sh477}$ 0 GY vs. ATM$^{+/+}$12 GY	8.857	-12.75 to 30.46	No	ns	0.7154
HOM 0 GY vs. ATM$^{sh477/sh477}$ 12GY	-2.367	-24.30 to 19.56	No	ns	0.9925
ATM$^{+/+}$ 12 GY vs. ATM$^{sh477/sh477}$ 12GY	-11.22	-30.70 to 8.254	No	ns	0.4464

Tukey's multiple comparisons test	***Predicted (LS) mean diff.***	***95.00% CI of diff.***	***Below threshold?***	***Summary***	***Adjusted P Value***
ATM$^{+/+}$ 0 GY					
1% DMSO vs. 10 nM ATMi (Dark)	3.851	-17.86 to 25.56	No	ns	0.9681
1% DMSO light vs. 10 nM ATMi (Light)	2.633	-19.08 to 24.34	No	ns	0.9894
ATM$^{sh477/sh477}$ 0 GY					
1% DMSO vs. 10 nM ATMi (Dark)	17.09	-4.844 to 39.01	No	ns	0.1859
1% DMSO light vs. 10 nM ATMi (Light)	12.82	-9.108 to 34.75	No	ns	0.4333
ATM$^{+/+}$ 12 GY					
1% DMSO vs. 10 nM ATMi (Dark)	18.91	0.4011 to 37.42	Yes	*	0.0431

1% DMSO light vs. 10 nM ATMi (Light)	11.63	-6.874 to 30.14	No	ns	0.3674
ATM$^{sh477/sh477}$ 12GY					
1% DMSO vs. 10 nM ATMi (Dark)	4.401	-16.58 to 25.38	No	ns	0.9489
1% DMSO light vs. 10 nM ATMi (Light)	6.759	-14.22 to 27.74	No	ns	0.8396

Appendix 5.9.2 Numbers of fish per treatment group in figure 5.9: ATM$^{sh477/sh477}$ zebrafish do not exhibit sensitivity to an ATM inhibitor.

	ATM$^{+/+}$ 0 Gy	***ATM$^{+/+}$ 12 Gy***	***ATM$^{sh477/sh477}$ 0 Gy***	***ATM$^{sh477/sh477}$ 12 Gy***
1 %DMSO	*17*	*32*	*26*	*21*
10 nM ATMi	*30*	*28*	*18*	*26*

Appendix 5.10: Statistical Analysis Corresponding to Figure 5.10: $ATM^{sh477/sh477}$ zebrafish larvae exhibit no swimming defects at 12 dpf.

Figure b: Average distance travelled in dark and light phases

Two way RM ANOVA

Alpha	0.05			
Source of Variation	**% of total variation**	**P value**	**P value summary**	**Significant?**
Light Driving x Genotype	0.4490	0.2623	ns	No
Light Driving	1.074	0.0125	*	Yes
Genotype	2.137	0.3219	ns	No
Subject	81.87	<0.0001	****	Yes

Tukey's multiple comparisons test Genotype v Genotype	**Predicted (LS) mean diff.**	**95.00% CI of diff.**	**Below threshold?**	**Summary**	**Adjusted P Value**
Dark					
$ATM^{+/+}$ vs. $ATM^{+/sh477}$	-40.61	-480.0 to 398.8	No	ns	0.9740
$ATM^{+/+}$ vs. $ATM^{sh477/sh477}$	-182.7	-625.4 to 260.0	No	ns	0.5932
$ATM^{+/sh477}$ vs. $ATM^{sh477/sh477}$	-142.1	-570.1 to 285.8	No	ns	0.7127
Light					
$ATM^{+/+}$ vs. $ATM^{+/sh477}$	-276.1	-715.5 to 163.3	No	ns	0.3004
$ATM^{+/+}$ vs. $ATM^{sh477/sh477}$	-337.8	-780.5 to 104.9	No	ns	0.1713
$ATM^{+/sh477}$ vs. $ATM^{sh477/sh477}$	-61.73	-489.6 to 366.2	No	ns	0.9380

Šídák's multiple comparisons test	**Predicted (LS) mean diff.**	**95.00% CI of diff.**	**Below threshold?**	**Summary**	**Adjusted P Value**
Dark - Light					
$ATM^{+/+}$	279.6	22.95 to 536.2	Yes	*	0.0282
$ATM^{+/sh477}$	44.09	-196.0 to 284.2	No	ns	0.9593
$ATM^{sh477/sh477}$	124.5	-119.4 to 368.4	No	ns	0.5206

Figure d: Average duration spent in active swimming in dark and light phases

Two way RM ANOVA

Alpha	0.05			
Source of Variation	**% of total variation**	**P value**	**P value summary**	**Significant?**
Light Driving x Genotype	0.3017	0.0504	ns	No
Light Driving	0.5061	0.0018	**	Yes
Genotype	1.879	0.4149	ns	No
Subject	93.06	<0.0001	****	Yes

Tukey's multiple comparisons test Genotype v Genotype	**Predicted (LS) mean diff.**	**95.00% CI of diff.**	**Below threshold?**	**Summary**	**Adjusted P Value**
Dark					
$ATM^{+/+}$ vs. $ATM^{+/sh477}$	-8.235	-36.21 to 19.74	No	ns	0.7663
$ATM^{+/+}$ vs. $ATM^{sh477/sh477}$	-9.672	-37.86 to 18.52	No	ns	0.6967
$ATM^{+/sh477}$ vs. $ATM^{sh477/sh477}$	-1.437	-28.68 to 25.81	No	ns	0.9915
Light					
$ATM^{+/+}$ vs. $ATM^{+/sh477}$	-20.54	-48.52 to 7.439	No	ns	0.1950
$ATM^{+/+}$ vs. $ATM^{sh477/sh477}$	-15.20	-43.38 to 12.99	No	ns	0.4116
$ATM^{+/sh477}$ vs. $ATM^{sh477/sh477}$	5.343	-21.90 to 32.59	No	ns	0.8884

Šídák's multiple comparisons test	Predicted (LS) mean diff.	95.00% CI of diff.	Below threshold?	Summary	Adjusted P Value
Dark - Light					
ATM$^{+/+}$	279.6	22.95 to 536.2	Yes	*	0.0282
ATM$^{+/sh477}$	44.09	-196.0 to 284.2	No	ns	0.9593
ATM$^{sh477/sh477}$	124.5	-119.4 to 368.4	No	ns	0.5206

Appendix 5.11.1: Statistical Analysis Corresponding to Figure 5.11: $ATM^{sh477/sh477}$ zebrafish larvae exhibit no swimming defects at 12 dpf after treatment at 48 hpf with ionising radiation.

Figure b: Average distance travelled in dark and light phases

Two way ANOVA

Source of Variation	% of total variation	P value	P value summary	Significant?
Alpha	**0.05**			
IR Dose x Genotype	1.509	0.7317	ns	No
IR Dose	19.14	<0.0001	****	Yes
Genotype	0.07861	0.8351	ns	No

Tukey's multiple comparisons test Genotype v Genotype	Predicted (LS) mean diff.	95.00% CI of diff.	Below threshold?	Summary	Adjusted P Value
0 Gy – Dark					
$ATM^{+/+}$ vs. $ATM^{+/sh477}$	-185.0	-572.1 to 202.2	No	ns	0.4995
$ATM^{+/+}$ vs. $ATM^{SH477/SH477}$	130.8	-314.0 to 575.6	No	ns	0.7683
$ATM^{+/sh477}$ vs. $ATM^{SH477/SH477}$	315.8	-148.8 to 780.4	No	ns	0.2471
2 Gy - Dark					
$ATM^{+/+}$ vs. $ATM^{+/sh477}$	-76.99	-466.0 to 312.0	No	ns	0.8873
$ATM^{+/+}$ vs. $ATM^{SH477/SH477}$	-111.0	-582.5 to 360.5	No	ns	0.8445
$ATM^{+/sh477}$ vs. $ATM^{SH477/SH477}$	-34.01	-495.6 to 427.6	No	ns	0.9836
8 Gy- Dark					
$ATM^{+/+}$ vs. $ATM^{+/sh477}$	113.3	-292.7 to 519.3	No	ns	0.7887
$ATM^{+/+}$ vs. $ATM^{SH477/SH477}$	-1.263	-432.0 to 429.5	No	ns	>0.9999
$ATM^{+/sh477}$ vs. $ATM^{SH477/SH477}$	-114.6	-557.9 to 328.8	No	ns	0.8158
0 Gy – Light					
$ATM^{+/+}$ vs. $ATM^{+/sh477}$	156.9	-230.3 to 544.0	No	ns	0.6066
$ATM^{+/+}$ vs. $ATM^{SH477/SH477}$	-10.89	-455.7 to 433.9	No	ns	0.9982
$ATM^{+/sh477}$ vs. $ATM^{SH477/SH477}$	-167.8	-632.4 to 296.8	No	ns	0.6722
2 Gy - Light					
$ATM^{+/+}$ vs. $ATM^{+/sh477}$	-81.61	-470.6 to 307.4	No	ns	0.8743
$ATM^{+/+}$ vs. $ATM^{SH477/SH477}$	-238.0	-709.5 to 233.5	No	ns	0.4612
$ATM^{+/sh477}$ vs. $ATM^{SH477/SH477}$	-156.4	-617.9 to 305.2	No	ns	0.7050
8 Gy- Light					
$ATM^{+/+}$ vs. $ATM^{+/sh477}$	172.5	-233.5 to 578.6	No	ns	0.5774
$ATM^{+/+}$ vs. $ATM^{SH477/SH477}$	44.44	-386.3 to 475.2	No	ns	0.9680
$ATM^{+/sh477}$ vs. $ATM^{SH477/SH477}$	-128.1	-571.4 to 315.3	No	ns	0.7754

Tukey's multiple comparisons test IR Dose within Genotype	Predicted (LS) mean diff.	95.00% CI of diff.	Below threshold?	Summary	Adjusted P Value
$ATM^{+/+}$					
0 Gy (D) vs. 2 Gy (D)	-145.7	-611.2 to 319.9	No	ns	0.9472
0 Gy (D) vs. 8 Gy (D)	118.9	-341.3 to 579.1	No	ns	0.9768
0 Gy (D) vs. 0 Gy (L)	448.1	5.950 to 890.2	Yes	*	0.0449
0 Gy (D) vs. 2 Gy (L)	272.1	-193.4 to 737.7	No	ns	0.5494
0 Gy (D) vs. 8 Gy (L)	566.1	105.9 to 1026	Yes	**	0.0063
2 Gy (D) vs. 8 Gy (D)	264.6	-218.1 to 747.3	No	ns	0.6186
2 Gy (D) vs. 0 Gy (L)	593.8	128.2 to 1059	Yes	**	0.0040
2 Gy (D) vs. 2 Gy (L)	417.8	-70.03 to 905.6	No	ns	0.1409
2 Gy (D) vs. 8 Gy (L)	711.8	229.1 to 1195	Yes	***	0.0004
8 Gy (D) vs. 0 Gy (L)	329.2	-131.0 to 789.4	No	ns	0.3165
8 Gy (D) vs. 2 Gy (L)	153.2	-329.5 to 636.0	No	ns	0.9440
8 Gy (D) vs. 8 Gy (L)	447.2	-30.37 to 924.8	No	ns	0.0812
0 Gy (L) vs. 2 Gy (L)	-176.0	-641.5 to 289.6	No	ns	0.8880
0 Gy (L) vs. 8 Gy (L)	118.0	-342.2 to 578.2	No	ns	0.9775
2 Gy (L) vs. 8 Gy (L)	294.0	-188.8 to 776.7	No	ns	0.5030
$ATM^{+/sh477}$					
0 Gy (D) vs. 2 Gy (D)	-37.68	-516.9 to 441.5	No	ns	>0.9999
0 Gy (D) vs. 8 Gy (D)	417.2	-87.52 to 921.9	No	ns	0.1703
0 Gy (D) vs. 0 Gy (L)	790.0	291.2 to 1289	Yes	***	0.0001

0 Gy (D) vs. 2 Gy (L)	*375.5*	*-103.7 to 854.7*	*No*	*ns*	*0.2199*
0 Gy (D) vs. 8 Gy (L)	*923.6*	*418.9 to 1428*	*Yes*	*****	*<0.0001*
2 Gy (D) vs. 8 Gy (D)	*454.9*	*-30.50 to 940.2*	*No*	*ns*	*0.0807*
2 Gy (D) vs. 0 Gy (L)	*827.7*	*348.4 to 1307*	*Yes*	*****	*<0.0001*
2 Gy (D) vs. 2 Gy (L)	*413.2*	*-45.64 to 872.0*	*No*	*ns*	*0.1048*
2 Gy (D) vs. 8 Gy (L)	*961.3*	*475.9 to 1447*	*Yes*	*****	*<0.0001*
8 Gy (D) vs. 0 Gy (L)	*372.8*	*-131.9 to 877.5*	*No*	*ns*	*0.2812*
8 Gy (D) vs. 2 Gy (L)	*-41.68*	*-527.1 to 443.7*	*No*	*ns*	*0.9999*
8 Gy (D) vs. 8 Gy (L)	*506.4*	*-4.127 to 1017*	*No*	*ns*	*0.0533*
0 Gy (L) vs. 2 Gy (L)	*-414.5*	*-893.7 to 64.77*	*No*	*ns*	*0.1334*
0 Gy (L) vs. 8 Gy (L)	*133.6*	*-371.1 to 638.3*	*No*	*ns*	*0.9741*
2 Gy (L) vs. 8 Gy (L)	*548.1*	*62.72 to 1033*	*Yes*	***	*0.0166*
$ATM^{sh477/sh477}$					
0 Gy (D) vs. 2 Gy (D)	*-387.5*	*-1025 to 249.7*	*No*	*ns*	*0.5047*
0 Gy (D) vs. 8 Gy (D)	*-13.15*	*-610.2 to 583.9*	*No*	*ns*	*>0.9999*
0 Gy (D) vs. 0 Gy (L)	*306.4*	*-318.9 to 931.7*	*No*	*ns*	*0.7246*
0 Gy (D) vs. 2 Gy (L)	*-96.64*	*-733.8 to 540.6*	*No*	*ns*	*0.9980*
0 Gy (D) vs. 8 Gy (L)	*479.7*	*-117.3 to 1077*	*No*	*ns*	*0.1958*
2 Gy (D) vs. 8 Gy (D)	*374.3*	*-235.2 to 983.8*	*No*	*ns*	*0.4933*
2 Gy (D) vs. 0 Gy (L)	*693.9*	*56.70 to 1331*	*Yes*	***	*0.0238*
2 Gy (D) vs. 2 Gy (L)	*290.8*	*-358.0 to 939.7*	*No*	*ns*	*0.7936*
2 Gy (D) vs. 8 Gy (L)	*867.2*	*257.7 to 1477*	*Yes*	*****	*0.0008*
8 Gy (D) vs. 0 Gy (L)	*319.6*	*-277.5 to 916.6*	*No*	*ns*	*0.6428*
8 Gy (D) vs. 2 Gy (L)	*-83.48*	*-693.0 to 526.0*	*No*	*ns*	*0.9988*
8 Gy (D) vs. 8 Gy (L)	*492.9*	*-74.53 to 1060*	*No*	*ns*	*0.1301*
0 Gy (L) vs. 2 Gy (L)	*-403.0*	*-1040 to 234.1*	*No*	*ns*	*0.4591*
0 Gy (L) vs. 8 Gy (L)	*173.3*	*-423.7 to 770.4*	*No*	*ns*	*0.9615*
2 Gy (L) vs. 8 Gy (L)	*576.4*	*-33.14 to 1186*	*No*	*ns*	*0.0758*

Tukey's multiple comparisons test IR Dose v IR Dose	***Predicted (LS) mean diff.***	***95.00% CI of diff.***	***Below threshold?***	***Summary***	***Adjusted P Value***
0 Gy (D) vs. 2 Gy (D)	*-190.3*	*-498.0 to 117.5*	*No*	*ns*	*0.4855*
0 Gy (D) vs. 8 Gy (D)	*174.3*	*-128.1 to 476.7*	*No*	*ns*	*0.5648*
0 Gy (D) vs. 0 Gy (L)	*514.8*	*210.2 to 819.5*	*Yes*	*****	*<0.0001*
0 Gy (D) vs. 2 Gy (L)	*183.7*	*-124.1 to 491.4*	*No*	*ns*	*0.5261*
0 Gy (D) vs. 8 Gy (L)	*656.5*	*354.1 to 958.9*	*Yes*	*****	*<0.0001*
2 Gy (D) vs. 8 Gy (D)	*364.6*	*59.07 to 670.1*	*Yes*	****	*0.0091*
2 Gy (D) vs. 0 Gy (L)	*705.1*	*397.4 to 1013*	*Yes*	*****	*<0.0001*
2 Gy (D) vs. 2 Gy (L)	*373.9*	*63.11 to 684.8*	*Yes*	****	*0.0083*
2 Gy (D) vs. 8 Gy (L)	*846.8*	*541.2 to 1152*	*Yes*	*****	*<0.0001*
8 Gy (D) vs. 0 Gy (L)	*340.5*	*38.12 to 642.9*	*Yes*	***	*0.0171*
8 Gy (D) vs. 2 Gy (L)	*9.353*	*-296.2 to 314.9*	*No*	*ns*	*>0.9999*
8 Gy (D) vs. 8 Gy (L)	*482.2*	*182.0 to 782.3*	*Yes*	*****	*<0.0001*
0 Gy (L) vs. 2 Gy (L)	*-331.2*	*-638.9 to -23.41*	*Yes*	***	*0.0266*
0 Gy (L) vs. 8 Gy (L)	*141.7*	*-160.7 to 444.1*	*No*	*ns*	*0.7612*
2 Gy (L) vs. 8 Gy (L)	*472.8*	*167.3 to 778.3*	*Yes*	*****	*0.0002*

Figure d: Average duration spent in active swimming in dark and light phases

Two way ANOVA

Alpha	*0.05*			
Source of Variation	***% of total variation***	***P value***	***P value summary***	***Significant?***
IR Dose x Genotype	*1.450*	*0.8022*	*ns*	*No*
IR Dose	*13.83*	*<0.0001*	*****	*Yes*
Genotype	*1.087*	*0.1017*	*ns*	*No*

Tukey's multiple comparisons test Genotype v Genotype	***Predicted (LS) mean diff.***	***95.00% CI of diff.***	***Below threshold?***	***Summary***	***Adjusted P Value***
0 Gy – Dark					
$ATM^{+/+}$ vs. $ATM^{+/sh477}$	*-11.17*	*-40.68 to 18.34*	*No*	*ns*	*0.6463*
$ATM^{+/+}$ vs. $ATM^{SH477/SH477}$	*-5.417*	*-35.94 to 25.11*	*No*	*ns*	*0.9083*
$ATM^{+/sh477}$ vs. $ATM^{SH477/SH477}$	*5.754*	*-27.39 to 38.90*	*No*	*ns*	*0.9121*

2 Gy - Dark					
ATM$^{+/+}$ vs. ATM$^{+/sh477}$	-1.798	-30.22 to 26.62	No	ns	0.9878
ATM$^{+/+}$ vs. ATM$^{SH477/SH477}$	-8.764	-43.21 to 25.68	No	ns	0.8209
ATM$^{+/sh477}$ vs. ATM$^{SH477/SH477}$	-6.965	-40.69 to 26.76	No	ns	0.8779
8 Gy- Dark					
ATM$^{+/+}$ vs. ATM$^{+/sh477}$	17.36	-12.69 to 47.42	No	ns	0.3634
ATM$^{+/+}$ vs. ATM$^{SH477/SH477}$	1.294	-30.75 to 33.34	No	ns	0.9950
ATM$^{+/sh477}$ vs. ATM$^{SH477/SH477}$	-16.07	-49.37 to 17.23	No	ns	0.4927
0 Gy – Light					
ATM$^{+/+}$ vs. ATM$^{+/sh477}$	10.83	-18.67 to 40.34	No	ns	0.6632
ATM$^{+/+}$ vs. ATM$^{SH477/SH477}$	-14.10	-45.21 to 17.01	No	ns	0.5353
ATM$^{+/sh477}$ vs. ATM$^{SH477/SH477}$	-24.94	-58.62 to 8.749	No	ns	0.1910
2 Gy - Light					
ATM$^{+/+}$ vs. ATM$^{+/sh477}$	3.377	-25.04 to 31.80	No	ns	0.9578
ATM$^{+/+}$ vs. ATM$^{SH477/SH477}$	-18.33	-52.78 to 16.11	No	ns	0.4230
ATM$^{+/sh477}$ vs. ATM$^{SH477/SH477}$	-21.71	-55.43 to 12.01	No	ns	0.2849
8 Gy- Light					
ATM$^{+/+}$ vs. ATM$^{+/sh477}$	16.72	-13.34 to 46.78	No	ns	0.3908
ATM$^{+/+}$ vs. ATM$^{SH477/SH477}$	6.145	-25.90 to 38.19	No	ns	0.8938
ATM$^{+/sh477}$ vs. ATM$^{SH477/SH477}$	-10.58	-43.88 to 22.72	No	ns	0.7353

Tukey's multiple comparisons test IR Dose within Genotype	**Predicted (LS) mean diff.**	**95.00% CI of diff.**	**Below threshold?**	**Summary**	**Adjusted P Value**
ATM$^{+/+}$					
0 Gy (D) vs. 2 Gy (D)	-9.665	-43.68 to 24.35	No	ns	0.9648
0 Gy (D) vs. 8 Gy (D)	-0.5280	-34.15 to 33.09	No	ns	>0.9999
0 Gy (D) vs. 0 Gy (L)	28.29	-4.015 to 60.59	No	ns	0.1241
0 Gy (D) vs. 2 Gy (L)	15.21	-18.81 to 49.22	No	ns	0.7953
0 Gy (D) vs. 8 Gy (L)	28.62	-5.001 to 62.24	No	ns	0.1457
2 Gy (D) vs. 8 Gy (D)	9.137	-26.13 to 44.40	No	ns	0.9765
2 Gy (D) vs. 0 Gy (L)	37.95	3.939 to 71.96	Yes	*	0.0188
2 Gy (D) vs. 2 Gy (L)	24.87	-10.77 to 60.51	No	ns	0.3446
2 Gy (D) vs. 8 Gy (L)	38.29	3.018 to 73.55	Yes	*	0.0245
8 Gy (D) vs. 0 Gy (L)	28.81	-4.807 to 62.44	No	ns	0.1404
8 Gy (D) vs. 2 Gy (L)	15.73	-19.53 to 51.00	No	ns	0.7967
8 Gy (D) vs. 8 Gy (L)	29.15	-5.742 to 64.04	No	ns	0.1611
0 Gy (L) vs. 2 Gy (L)	-13.08	-47.09 to 20.93	No	ns	0.8804
0 Gy (L) vs. 8 Gy (L)	0.3337	-33.29 to 33.96	No	ns	>0.9999
2 Gy (L) vs. 8 Gy (L)	13.41	-21.85 to 48.68	No	ns	0.8853
ATM$^{+/sh477}$					
0 Gy (D) vs. 2 Gy (D)	-0.2913	-36.77 to 36.19	No	ns	>0.9999
0 Gy (D) vs. 8 Gy (D)	28.01	-10.71 to 66.73	No	ns	0.3041
0 Gy (D) vs. 0 Gy (L)	50.29	11.08 to 89.51	Yes	**	0.0037
0 Gy (D) vs. 2 Gy (L)	29.75	-6.724 to 66.23	No	ns	0.1820
0 Gy (D) vs. 8 Gy (L)	56.51	17.79 to 95.23	Yes	***	0.0005
2 Gy (D) vs. 8 Gy (D)	28.30	-7.651 to 64.25	No	ns	0.2154
2 Gy (D) vs. 0 Gy (L)	50.58	14.11 to 87.06	Yes	**	0.0012
2 Gy (D) vs. 2 Gy (L)	30.05	-3.476 to 63.57	No	ns	0.1079
2 Gy (D) vs. 8 Gy (L)	56.81	20.86 to 92.75	Yes	***	0.0001
8 Gy (D) vs. 0 Gy (L)	22.29	-16.43 to 61.01	No	ns	0.5664
8 Gy (D) vs. 2 Gy (L)	1.749	-34.20 to 37.70	No	ns	>0.9999
8 Gy (D) vs. 8 Gy (L)	28.51	-9.712 to 66.73	No	ns	0.2706
0 Gy (L) vs. 2 Gy (L)	-20.54	-57.02 to 15.94	No	ns	0.5903
0 Gy (L) vs. 8 Gy (L)	6.221	-32.50 to 44.94	No	ns	0.9974
2 Gy (L) vs. 8 Gy (L)	26.76	-9.188 to 62.71	No	ns	0.2727
ATM$^{sh477/sh477}$					
0 Gy (D) vs. 2 Gy (D)	-13.01	-57.54 to 31.52	No	ns	0.9604
0 Gy (D) vs. 8 Gy (D)	6.183	-35.92 to 48.28	No	ns	0.9983
0 Gy (D) vs. 0 Gy (L)	19.60	-22.50 to 61.70	No	ns	0.7658
0 Gy (D) vs. 2 Gy (L)	2.289	-42.24 to 46.82	No	ns	>0.9999
0 Gy (D) vs. 8 Gy (L)	40.18	-1.916 to 82.28	No	ns	0.0710
2 Gy (D) vs. 8 Gy (D)	19.19	-25.94 to 64.32	No	ns	0.8276
2 Gy (D) vs. 0 Gy (L)	32.61	-12.52 to 77.74	No	ns	0.3051
2 Gy (D) vs. 2 Gy (L)	15.30	-32.11 to 62.71	No	ns	0.9400
2 Gy (D) vs. 8 Gy (L)	53.19	8.064 to 98.32	Yes	*	0.0105
8 Gy (D) vs. 0 Gy (L)	13.42	-29.31 to 56.15	No	ns	0.9464
8 Gy (D) vs. 2 Gy (L)	-3.894	-49.02 to 41.24	No	ns	0.9999
8 Gy (D) vs. 8 Gy (L)	34.00	-8.732 to 76.73	No	ns	0.2050
0 Gy (L) vs. 2 Gy (L)	-17.31	-62.44 to 27.82	No	ns	0.8815

0 Gy (L) vs. 8 Gy (L)	*20.58*	*-22.15 to 63.31*	*No*	*ns*	*0.7390*
2 Gy (L) vs. 8 Gy (L)	*37.89*	*-7.236 to 83.02*	*No*	*ns*	*0.1569*

Tukey's multiple comparisons test IR Dose v IR Dose	***Predicted (LS) mean diff.***	***95.00% CI of diff.***	***Below threshold?***	***Summary***	***Adjusted P Value***
0 Gy (D) vs. 2 Gy (D)	*-7.656*	*-29.94 to 14.63*	*No*	*ns*	*0.9228*
0 Gy (D) vs. 8 Gy (D)	*11.22*	*-10.90 to 33.34*	*No*	*ns*	*0.6939*
0 Gy (D) vs. 0 Gy (L)	*32.73*	*10.73 to 54.72*	*Yes*	***	*0.0004*
0 Gy (D) vs. 2 Gy (L)	*15.75*	*-6.537 to 38.04*	*No*	*ns*	*0.3302*
0 Gy (D) vs. 8 Gy (L)	*41.77*	*19.66 to 63.89*	*Yes*	****	*<0.0001*
2 Gy (D) vs. 8 Gy (D)	*18.88*	*-3.665 to 41.42*	*No*	*ns*	*0.1591*
2 Gy (D) vs. 0 Gy (L)	*40.38*	*17.96 to 62.80*	*Yes*	****	*<0.0001*
2 Gy (D) vs. 2 Gy (L)	*23.41*	*0.6964 to 46.12*	*Yes*	*	*0.0390*
2 Gy (D) vs. 8 Gy (L)	*49.43*	*26.89 to 71.97*	*Yes*	****	*<0.0001*
8 Gy (D) vs. 0 Gy (L)	*21.51*	*-0.7435 to 43.76*	*No*	*ns*	*0.0648*
8 Gy (D) vs. 2 Gy (L)	*4.530*	*-18.01 to 27.07*	*No*	*ns*	*0.9926*
8 Gy (D) vs. 8 Gy (L)	*30.55*	*8.181 to 52.92*	*Yes*	**	*0.0015*
0 Gy (L) vs. 2 Gy (L)	*-16.98*	*-39.40 to 5.444*	*No*	*ns*	*0.2547*
0 Gy (L) vs. 8 Gy (L)	*9.045*	*-13.20 to 31.30*	*No*	*ns*	*0.8532*
2 Gy (L) vs. 8 Gy (L)	*26.02*	*3.482 to 48.56*	*Yes*	*	*0.0132*

Appendix 5.11.2: Number of fish used corresponding to Figure 5.9.

ATM$^{+/+}$	
0 Gy	*28*
2 Gy	*23*
8 Gy	*24*
ATM$^{+/sh477}$	
0 Gy	*22*
2 Gy	*26*
8 Gy	*21*
ATM$^{sh477/sh477}$	
0 Gy	*14*
2 Gy	*13*
8 Gy	*17*

Appendix 5.12 Statistical Analysis Corresponding to Figure 5.11: Adult male ATM$^{sh477/sh477}$ zebrafish show slight differences in their swimming endurance at 7 months of age compared to wild type controls.

Unpaired t test with Welch's correction	**P value**	**P value summary**	**Significantly different (P < 0.05)?**	**One- or two-tailed P value?**	**Welch-corrected t, df**	***Size Effect***	***No of fish total required for 90% Power***	***No of fish in experiment***
Figure a	0.1378	ns	No	Two-tailed	t=1.534, df=24.52	*0.626*	110	*35*
Figure b	0.1919	ns	No	Two-tailed	t=1.343, df=23.70	*0.637*	*106*	35
Figure c	0.1005	ns	No	Two-tailed	t=1.698, df=27.94	*0.661*	*100*	*35*
Figure d	0.0470	*	Yes	Two-tailed	t=2.073, df=29.49	*0.662*	*98*	*35*
Figure e	0.0098	**	Yes	Two-tailed	t=2.740, df=32.98	*0.732*	*82*	*35*

Appendix 5.13: Statistical Analysis Corresponding to Figure 5.13: Investigations into Total Motility of ATM$^{sh477/sh477}$ zebrafish.

Unpaired t test with Welch's correction	**P value**	**P value summary**	**Significantly different (P < 0.05)?**	**One- or two-tailed P value?**	**Welch-corrected t, df**	***Size Effect***	***No of fish total required for 90% Power***	***No of fish in experiment***
Figure b	0.2685	ns	No	Two-tailed	t=1.154, df=13.54	***0.647***	***104***	***17***
Figure d	0.0685	ns	No	Two-tailed	t=1.985, df=13.13	***0.746***	***78***	***17***

Appendix 6

Appendix 6.1 Protein-Protein Blast Sequence Alignment of the rad51 zebrafish and Human Sequences

a. Alignment of the Full Protein Sequence Showing 84% Sequence Identity

Query- Zebrafish   Subject-Human

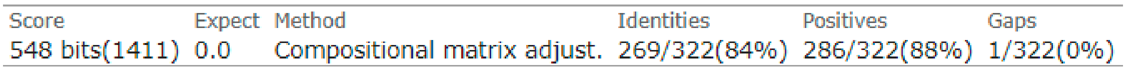

Score	Expect	Method	Identities	Positives	Gaps
548 bits(1411)	0.0	Compositional matrix adjust.	269/322(84%)	286/322(88%)	1/322(0%)

```
Query  19   SFGPQPISRLEQCGINANDVKKLEEAGFHTVEAVAYAPKKELINIKGISEAKADKILTES  78
            +FGPQP+SRLEQ GI+++D+KKLE+ GFHTVEAVAYAPKKEL+NIKGISEAKADKILTE+
Sbjct  20   NFGPQPVSRLEQSGISSSDIKKLEDGGFHTVEAVAYAPKKELLNIKGISEAKADKILTEA  79

Query  79   RSVARLECNSVILVYCTLRLSGSSDSPASASRVVGTTGGIETGSITEMFGEFRTGKTQIC  138
              +  +   +    +   R      S  S        GGIETGSITEMFGEFRTGKTQ+C
Sbjct  80   AKMVPMGFTTAT-EFHQRRAEIIQISTGSKELDKLLQGGIETGSITEMFGEFRTGKTQLC  138

Query  139  HTLAVTCQLPIDRGGGEGKAMYIDTEGTFRPERLLAVAERYGLSGSDVLDNVAYARAFNT  198
             HTLAVTCQLPID+GGGEGKAMYIDTEGTFRPERLLAVAERYGL GSDVLDNVAYARAFNT
Sbjct  139  HTLAVTCQLPIDQGGGEGKAMYIDTEGTFRPERLLAVAERYGLVGSDVLDNVAYARAFNT  198

Query  199  DHQTQLLYQASAMMVESRYALLIVDSATALYRTDYSGRGELSARQMHLARFLRMLLRLAD  258
             DHQTQLLYQASAMM ESRYALLIVDSATALYRTDYSGRGELSARQ HL RFLRMLLRLAD
Sbjct  199  DHQTQLLYQASAMMTESRYALLIVDSATALYRTDYSGRGELSARQGHLGRFLRMLLRLAD  258

Query  259  EFGVAVVITNQVVAQVDGAAMFAADPKKPIGGNIIAHASTTRLYLRKGRGETRICKIYDS  318
             EFGVAVVITNQVVAQVDGAAMF+ADPKKPIGGNI+AHASTTRLYLRKGRGETRICKIYDS
Sbjct  259  EFGVAVVITNQVVAQVDGAAMFSADPKKPIGGNILAHASTTRLYLRKGRGETRICKIYDS  318

Query  319  PCLPEAEAMFAINADGVGDAKD  340
             PCLPEAEAMFAINADGVGDAKD
Sbjct  319  PCLPEAEAMFAINADGVGDAKD  340
```

b. Alignment of the CORE Domain (amino acids 125-225 of the human protein)

Query- Zebrafish   Subject-Human

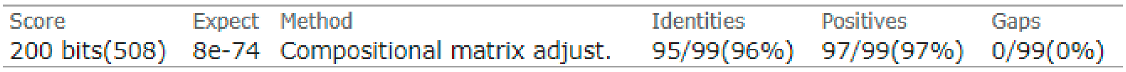

Score	Expect	Method	Identities	Positives	Gaps
200 bits(508)	8e-74	Compositional matrix adjust.	95/99(96%)	97/99(97%)	0/99(0%)

```
Query  1   MFGEFRTGKTQLCHTLAVTCQLPIDQGGGEGKAMYIDTEGTFRPERLLAVAERYGLVGSD  60
           MFGEFRTGKTQ+CHTLAVTCQLPID+GGGEGKAMYIDTEGTFRPERLLAVAERYGL GSD
Sbjct  1   MFGEFRTGKTQICHTLAVTCQLPIDRGGGEGKAMYIDTEGTFRPERLLAVAERYGLSGSD  60

Query  61  VLDNVAYARAFNTDHQTQLLYQASAMMTESRYALLIVDS  99
           VLDNVAYARAFNTDHQTQLLYQASAMM ESRYALLIVDS
Sbjct  61  VLDNVAYARAFNTDHQTQLLYQASAMMVESRYALLIVDS  99
```

Appendix 6.2 Protein-Protein Blast Sequence Alignment of the ATM zebrafish and human sequences

a. *Alignment of the Full Protein Sequence Showing 54% Sequence Identity*

Query- Zebrafish   *Subject-Human*

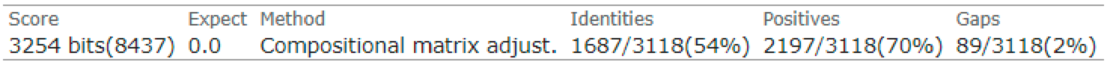

Score	Expect	Method	Identities	Positives	Gaps
3254 bits(8437)	0.0	Compositional matrix adjust.	1687/3118(54%)	2197/3118(70%)	89/3118(2%)

```
Query  1      MSLALHELLVCCRGLENEKATERKKEVDRFRRLICSPDTVEELDRTSGSKGSKQLTWDAV  60
              MSL L++LL+CCR LE+++ATERKKEV++F+RLI  P+T++ LDR S SK  K L WDAV
Sbjct  1      MSLVLNDLLICCRQLEHDRATERKKEVEKFKRLIRDPETIKHLDRHSDSKQGKYLNWDAV  60

Query  61     FRFLQKFLKKETELLQSGKANVSASTQANRQKKMQEISSLMKFFIRCANQRGPRLKCAEL  120
              FRFLQK+++KETE L+  K NVSASTQA+RQKKMQEISSL+K+FI+CAN+R PRLKC EL
Sbjct  61     FRFLQKYIQKETECLRIAKPNVSASTQASRQKKMQEISSLVKYFIKCANRRAPRLKCQEL  120

Query  121    ISHVVEVLQSPFSCVAYGEDYSSILLKNILSVRKYWCEMSQQQWHSLLDLFCGLFNRGTR  180
              ++++++ ++   +   YG D S+ILLK+ILSVRKYWCE+SQQQW  L  ++  L+ + ++
Sbjct  121    LNYIMDTVKDSSNGAIYGADCSNILLKDILSVRKYWCEISQQQWLELFSVYFRLYLKPSQ  180

Query  181    SINRVQVSRIIYTVVWGCCVQTEGLSHTLFNFFLKALSNSRAEKQLMVLENLVSAVNVFL  240
               ++RV V+RII+ V  GCC QT+GL+    +FF KA+  +R EK    L ++++A+ +FL
Sbjct  181    DVHRVLVARIIHAVTKGCCSQTDGLNSKFLDFFSKAIQCARQEKSSSGLNHILAALTIFL  240

Query  241    RSVLLSCRKRVCGLGEEVLSDMLCVYTGMRPSSVLKEELVKFFQIQLFVHHPKGAKTIET  300
              +++ ++ R RVC LG+E+L  +L ++T  R +  LKE +++ FQ+Q+++HHPKGAKT E
Sbjct  241    KTLAVNFRIRVCELGDEILPTLLYIWTQHRLNDSLKEVIIELFQLQIYIHHPKGAKTQEK  300

Query  301    GAQAQDWVKWRSQLCTLYDALVSEISQIGSRGKYATGSRHIAVKENLIELTADVCHQLFN  360
              GA      KWRS L  LYD LV+EIS IGSRGKY++G R+IAVKENLIEL AD+CHQ+FN
Sbjct  301    GAYES--TKWRSILYNLYDLLVNEISHIGSRGKYSSGFRNIAVKENLIELMADICHQVFN  358

Query  361    QSTRVQEVTSSVCRDTQRDSPQ---SCKRRRVELSNWELIRSKLQPHHSDFDMIPWLQVT  417
              + TR  E++ S    TQR+S      CKR+++EL  WE+I+  LQ   +DFD++PWLQ+
Sbjct  359    EDTRSLEISQSYT-TTQRESSDYSVPCKRKKIELG-WEVIKDHLQKSQNDFDLVPWLQIA  416

Query  418    AALISKYPSILLTDDVVPLLGLLCQLQGEQQRRGERAPYVLRCLKELALCHAKSSANSSA  477
                LISKYP+ L   ++ PLL +L QL   QQR GER PYVLRCL E+ALC  K S   S+
Sbjct  417    TQLISKYPASLPNCELSPLLMILSQLL-PQQRHGERTPYVLRCLTEVALCQDKRSNLESS  475

Query  478    CTAELGRLWARVWVLALRGVSSAQTGSLCLELLRIMVQESLVPVDREFWKVFSGAVCKPS  537
                ++L +LW ++W +  RG+SS Q  +    LL  ++Q SLV VDREFWK+F+G+ C+PS
Sbjct  476    QKSDLLKLWNKIWCITFRGISSEQIQAENFGLLGAIIQGSLVEVDREFWKLFTGSACRPS  535

Query  538    LVSALSLTQALLKCSVPKSVHSRDATSVVLTDAGGEPPSLRDSIISWLIMNEQNEETEEN  597
                +   LT AL    VP +V      ++   +      SL++SI+ WL+  +   + E +
Sbjct  536    CPAVCCLTLALTTSIVPGTVKMGIEQNMCEVNRSF---SLKESIMKWLLFYQLEGDLENS  592

Query  598    CRPHLIISRDFPLYLIPRIVVSLTLKDSRAGLTFLMGSLKPDCFSPENSSLTETKATMDE  657
                   I+  +FP  ++ +I+VSLT+K+ +A + F      P+C   E+    + + +  E
Sbjct  593    TEVPPILHSNFPHLVLEKILVSLTMKNCKAAMNFFQSV--PEC---EHHQKDKEELSFSE  647

Query  658    VESLFLQFSFDEAHSSAGFTVDKDSVYSEKPQ----FTVIQALRSKLEHSLLSIAEQLFT  713
              VE LFLQ +FD+      F         EK Q    F+V Q L+  L+  LL ++EQL
Sbjct  648    VEELFLQTTFDKM----DFLTIVRECGIEKHQSSIGFSVHQNLKESLDRCLLGLSEQLLN  703

Query  714    CYSPDSTNTPHECVLRCVSLLIGVLAAYVCIGMLSEEQACLSPLFLKAKALVHEFSHYTS  773
               YS + TN+  E ++RC  LL+GVL  Y  +G+++EE+A  S LF KAK+L+       +
Sbjct  704    NYSSEITNS--ETLVRCSRLLVGVLGCYCYMGVIAEEEAYKSELFQKAKSLMQCAGESIT  761

Query  774    TAKSKLAENETLASVQSVMLLCSDCI--CRREKGDKMSTISRTLFMKTLPVRLLNDLCDM  831
```

```
               K+K  E   + S++++M LC+ C+  C ++  +K   I+   F++ L  +L+ND+ D+
Sbjct  762   LFKNKTNEEFRIGSLRNMMQLCTRCLSNCTKKSPNK---IASGFFLRLLTSKLMNDIADI  818

Query  832   SKQLLSNSGKK-DTIVIESEPVDMQTSRIQVDNQEEIDLFEDGDGTQHITSRPSQSNEEA  890
              K L S   K  D   +ES   D   + ++V++Q  ++LF D     +  S  S +NE
Sbjct  819   CKSLASFIKKPFDRGEVESMEDDTNGNLMEVEDQSSMNLFND-----YPDSSVSDANE-P  872

Query  891   ADSKFITGTKSALSEEHLSKQDLTFLSVLGFLSLCASSELNGGFSFKPLDTQRKLLKLLD  950
              +S+   G  + L+EE+LSKQDL FL +L FL LC ++      SF+  D +RKLL L+D
Sbjct  873   GESQSTIGAINPLAEEYLSKQDLLFLDMLKFLCLCVTTAQTNTVSFRAADIRRKLLMLID  932

Query  951   LADF--SQMLHLQMYLSLLKKLPAEVASLDPEEFNALLRPLADVCSLYRQDQEVCSAILF  1008
              +    ++ LHL MYL LLK+LP E   L  E+   LL+PL++VCSLYR+DQ+VC  IL
Sbjct  933   SSTLEPTKSLHLHMYLMLLKELPGEEYPLPMEDVLELLKPLSNVCSLYRRDQDVCKTILN  992

Query  1009  SLLPSIRCLGLSSSGSEQEEDMADIKGSLLKVISGFCFLGKSGKCTSSVRVALRQCLLAL  1068
              +L  ++ LG S+  SE   +  D +G  L VI  F  L K  K   SVR+AL  CL  L
Sbjct  993   HVLHVVKNLGQSNMDSE---NTRDAQGQFLTVIGAFWHLTKERKYIFSVRMALVNCLKTL  1049

Query  1069  LEADPCCKWAVLTLREEELPVSAVLSSLLADSHQHVCMLTALSVESLFLKKALHSSRKM-  1127
             LEADP  KWA+L +  ++ PV+ V +  LAD+H  V ML A S+  LF      SSR +
Sbjct  1050  LEADPYSKWAILNVMGKDFPVNEVFTQFLADNHHQVRMLAAESINRLFQDTKGDSSRLLK  1109

Query  1128  MLPLKNQQTAFENIYLKAQEGIRRQKN-CPSEDLPDETFNRRATLLKSVSMVMSCSPVCE  1186
              LPLK QQTAFEN YLKAQEG+R   +   + +  DE +NR++ LL  +++V+SCSP+CE
Sbjct  1110  ALPLKLQQTAFENAYLKAQEGMREMSHSAENPETLDEIYNRKSVLLTLIAVVLSCSPICE  1169

Query  1187  KQALFALFQSYKENGIDEQLIKKVLRGISKSLGNRDHKSLINSHLYYLVAEWLNQKQSDS  1246
             KQALFAL +S KENG++  L+KKVL  +S++ G R  +  + SHL YLV EWLN +  D+
Sbjct  1170  KQALFALCKSVKENGLEPHLVKKVLEKVSETFGYRRLEDFMASHLDYLVLEWLNLQ--DT  1227

Query  1247  SYTLQSFPYALLDCCSLEEFFRSSYHVLIPHLVFLNDFEGVKSIGDHLGQDWKQLLAKCF  1306
              Y L SFP+ LL+  ++E+F+RS Y VLIPHLV  + F+ VKSI + + +DWK LL  CF
Sbjct  1228  EYNLSSFPFILLNYTNIEDFYRSCYKVLIPHLVIRSHFDEVKSIANQIQEDWKSLLTDCF  1287

Query  1307  PKIMVNILPHFALAG-QDTHVAQQREKAHRVYDILKNSNCLGKQQIDSLICNNLPDIVVE  1365
             PKI+VNILP+FA  G +D+ +AQQRE A +VYD+LK+ N LGKQ ID L  +NLP+IVVE
Sbjct  1288  PKILVNILPYFAYEGTRDSGMAQQRETATKVYDMLKSENLLGKQ-IDHLFISNLPEIVVE  1346

Query  1366  LLMTLHE----TAGDKGDLQKFTGELDPAPNPPFFSSYVIKATLDYLSKCHSANHKSLVA  1421
             LLMTLHE    +A    DL  F+G+LDPAPNPP F S+VIKAT  Y+S CH    KS++
Sbjct  1347  LLMTLHEPANSSASQSTDLCDFSGDLDPAPNPPHFPSHVIKATFAYISNCHKTKLKSILE  1406

Query  1422  ILSKTPMSIQRILVAVCQKADETTNAYERHRILMMYHLFVSLLLKEVKDGLGGAWAFVLR  1481
             ILSK+P S Q+IL+A+C++A ET N Y++HRIL +YHLFVSLLLK++K GLGGAWAFVLR
Sbjct  1407  ILSKSPDSYQKILLAICEQAAETNNVYKKHRILKIYHLFVSLLLKDIKSGLGGAWAFVLR  1466

Query  1482  DIIYTLIHHINSRSSQQDEVSTRSLSLCCDLLSLVCQTAVEYCDDALESHLQVIVGTLTA  1541
             D+IYTLIH+IN R S   +VS RS SLCCDLLS VCQTAV YC DALE+HL VIVGTL
Sbjct  1467  DVIYTLIHYINQRPSCIMDVSLRSFSLCCDLLSQVCQTAVTYCKDALENHLHVIVGTLIP  1526

Query  1542  QVTEQSAISEQVLSLLRFLVMENPENRMLRKSIPLLEPFPEQPNFAELRAAQHALKYSSG  1601
              V EQ  + +QVL LL++LV++N +N  L  +I LL+PFP+   F +LR  Q  +KYS G
Sbjct  1527  LVYEQVEVQKQVLDLLKYLVIDNKDNENLYITIKLLDPFPDHVVFKDLRITQQKIKYSRG  1586

Query  1602  AFTLRQEIEHFLSVASCDSLPLARLEGLKDLKRQLHSHKQQIGQLLKECHADLDSCILVN  1661
              F+L +EI HFLSV+  D+LPL RLEGLKDL+RQL  HK Q+  +++    +    I+V
Sbjct  1587  PFSLLEEINHFLSVSVYDALPLTRLEGLKDLRRQLELHKDQMVDIMRASQDNPQDGIMVK  1646

Query  1662  LVLNLLQLCKIAANHPGGGDIMKAAGRCLGELGPVDLSSIALHHGKDQLYARAAKLFHNV  1721
             LV+NLLQL K+A NH G  ++++A G CLGE+GP+D S+IA+ H KD  Y +A KLF +
Sbjct  1647  LVVNLLQLSKMAINHTGEKEVLEAVGSCLGEVGPIDFSTIAIQHSKDASYTKALKLFEDK  1706

Query  1722  PHQWIFIILNSMDNALTNHSIAVRQTAGLCIKDILATQSGIEFGEIHKSKRDPLLAYLNP  1781
               QW FI+L  ++N L    + VR  A  C+K+ILAT++G  F EI+K   DP+LAYL P
Sbjct  1707  ELQWTFIMLTYLNNTLVEDCVKVRSAAVTCLKNILATKTGHSFWEIYKMTTDPMLAYLQP  1766
```

```
Query  1782  FRSSKKREPIMAMDVTPESRDRLTSADLWLMQPDGHKDWLKNLCMALLDSGGVRNEALLL  1841
             FR+S+K+   +         + L   +LW+   + H  W+K L  A LDSGG + E L L
Sbjct  1767  FRTSRKKFLEVPRFDKENPFEGLDDINLWIPLSENHDIWIKTLTCAFLDSGGTKCEILQL  1826

Query  1842  TRPLCEVKTDFCQRMLPLFVHDILLGDVDGSWRQLLSTHIQSFFSQCRRPSTPTSRPTTP  1901
              +P+CEVKTDFCQ +LP  +HDILL D + SWR LLSTH+Q FF+ C R  + TSR TTP
Sbjct  1827  LKPMCEVKTDFCQTVLPYLIHDILLQDTNESWRNLLSTHVQGFFTSCLRHFSQTSRSTTP  1886

Query  1902  MLSDSGNTTDAANQCQIDKASLRSMLAVIDHLRQQSRPLAPGSNEYGTVCDSNFWLDLNY  1961
                DS   ++   +C +DK S R+MLAV+D++R+Q RP +      GT+ +  FWLDLNY
Sbjct  1887  ANLDS--ESEHFFRCCLDKKSQRTMLAVVDYMRRQKRPSS------GTIFNDAFWLDLNY  1938

Query  1962  LEVAGAAQMCSAHFTALLYSEIYVDKIRSNMEQNRRSQSRASRRITFEDNSQTLSVSNLN  2021
             LEVA  AQ C+AHFTALLY+EIY DK +S  +Q +RS       + FE+ SQ+ ++S+L+
Sbjct  1939  LEVAKVAQSCAAHFTALLYAEIYADK-KSMDDQEKRS-------LAFEEGSQSTTISSLS  1990

Query  2022  ERSLEDSGFSLQDLLIEVYRCIGEPDSLYGCGGGKLTSPLTRIRTYEHEAMWEKALVSYD  2081
             E+S E++G SLQDLL+E+YR IGEPDSLYGCGGGK+  P+TR+RTYEHEAMW KALV+YD
Sbjct  1991  EKSKEETGISLQDLLLEIYRSIGEPDSLYGCGGGKMLQPITRLRTYEHEAMWGKALVTYD  2050

Query  2082  LHSNLPEVTRQIGIVEGLQNFGLCSILSTYLHGLEKDGMEWGPELRELRFQAAWRSTQWD  2141
             L + +P  TRQ GI++ LQN GLC ILS YL GL+ +  +W PEL EL +QAAWR+ QWD
Sbjct  2051  LETAIPSSTRQAGIIQALQNLGLCHILSVYLKGLDYENKDWCPELEELHYQAAWRNMQWD  2110

Query  2142  CDLPERNEKLKPGINESLFNALQALRDKEFSLFEQTLNYARGREVEELCRGSLEAVSSLY  2201
                    E      +ESL+NALQ+LRD+EFS F ++L YAR +EVEE+C+ SLE+V SLY
Sbjct  2111  HCTSVSKEVEGTSYHESLYNALQSLRDREFSTFYESLKYARVKEVEEMCKRSLESVYSLY  2170

Query  2202  PALCNLQRISELQSVEELFSRPVTDSSLNEVYRKWQQHSDLLTDSDFSLVEPVLALRSSI  2261
             P L  LQ I EL+S+ ELFSR VT   L+EVY KWQ+HS LL DSDFS  EP++ALR+ I
Sbjct  2171  PTLSRLQAIGELESIGELFSRSVTHRQLSEVYIKWQKHSQLLKDSDFSFQEPIMALRTVI  2230

Query  2262  QEALISSETDPDRKNYLISTYSSHLMELCRLARSAGNTQLAERAVFHMKQHNLVMSGSGS  2321
              E L+  E D  ++  +    + HL+EL  LAR+  NTQL ERA+F +KQ+N V  G
Sbjct  2231  LEILMEKEMDNSQRECIKDILTKHLVELSILARTFKNTQLPERAIFQIKQYNSVSCGVSE  2290

Query  2322  SSWAWQLEEAQVFWVKKEHGLALELLKQMIHKLD-DLVCVNPAVVPVYSECLRLCGSWLA  2380
                 WQLEEAQVFW KKE  LAL +LKQMI KLD      NP++   Y+ECLR+CG+WLA
Sbjct  2291  ----WQLEEAQVFWAKKEQSLALSILKQMIKKLDASCAANNPSLKLTYTECLRVCGNWLA  2346

Query  2381  ESCLESPAVILENYLERAVEVIEEHCGGLKSKLQSQKTQAYFSLARFSDAQYQGIENYMK  2440
             E+CLE+PAVI++ YLE+AVEV   + G    +L++ K +A+ SLARFSD QYQ IENYMK
Sbjct  2347  ETCLENPAVIMQTYLEKAVEVAGNYDGESSDELRNGKMKAFLSLARFSDTQYQRIENYMK  2406

Query  2441  SSEFENKHALLEKAKEEVDLMRERKVNNNRYTVKVQRELELDVKALANLQADRNRFLLKA  2500
             SSEFENK ALL++AKEEV L+RE K+  NRYTVKVQRELELD  AL  L+ DR RFL KA
Sbjct  2407  SSEFENKQALLKRAKEEVGLLREHKIQTNRYTVKVQRELELDELALRALKEDRKRFLCKA  2466

Query  2501  VENYIECLELGEEHDTWVFRLASLWLENADVKAVNDKMKSGVKKIPSYKFLPLMYQLAAR  2560
             VENYI CL  GEEHD WVFRL SLWLEN+ V  VN  MK    KIP+YKFLPLMYQLAAR
Sbjct  2467  VENYINCLLSGEEHDMWVFRLCSLWLENSGVSEVNGMMKRDGMKIPTYKFLPLMYQLAAR  2526

Query  2561  MGTKVSSSMASQDVGFHHVLNELICQSSVDHPHHTLFIILALVNANKDDSFS------RS  2614
             MGTK+   +     GFH VLN LI + S+DHPHHTLFIILAL NAN+D+  +      RS
Sbjct  2527  MGTKMMGGL-----GFHEVLNNLISRISMDHPHHTLFIILALANANRDEFLTKPEVARRS  2581

Query  2615  RSSKSSARQPSPLDLERAEVARKIIDVVRKKRAKMVKDIEMLCNAYITLAYMDASRHKTE  2674
             R +K+  +Q S LD +R E A +II  +R +R +MV+ +E LC+AYI LA +DA++ KT+
Sbjct  2582  RITKNVPKQSSQLDEDRTEAANRIICTIRSRRPQMVRSVEALCDAYIILANLDATQWKTQ  2641

Query  2675  KKAIPIPAEQPLMQIKDLEDVIIPTMDIKVDPSGRYEDVVTVRSFKRHFHLAGGVNLPKI  2734
             +K I IPA+QP+ ++K+LEDV++PTM+IKVD +G Y ++VT++SFK  F LAGGVNLPKI
Sbjct  2642  RKGINIPADQPITKLKNLEDVVVPTMEIKVDHTGEYGNLVTIQSFKAEFRLAGGVNLPKI  2701

Query  2735  IDCEGSDGISRRQLVKGQDDLRQDAVMQQVFHMCSTLLQRNAETRKRKLNIRRYKVVPFS  2794
```

```
              IDC GSDG  RRQLVKG+DDLRQDAVMQQVF MC+TLLQRN ETRKRKL I  YKVVP S
Sbjct  2702  IDCVGSDGKERRQLVKGRDDLRQDAVMQQVFQMCNTLLQRNTETRKRKLTICTYKVVPLS  2761

Query  2795  QRSGVLEWCSGTVPIGEFLVDPQKGAHKRFRPQDWANMLCRKKMMEAQRMEFNDKLQAFT  2854
             QRSGVLEWC+GTVPIGEFLV+ + GAHKR+RP D++   C+KKMME Q+  F +K + F
Sbjct  2762  QRSGVLEWCTGTVPIGEFLVNNEDGAHKRYRPNDFSAFQCQKKMMEVQKKSFEEKYEVFM  2821

Query  2855  EVCQNFRPVFRYFCMERFLDPAIWLERRLAYTRSVATSSIVGYIVGLGDRHIQNILIDEQ  2914
             +VCQNF+PVFRYFCME+FLDPAIW E+RLAYTRSVATSSIVGYI+GLGDRH+QNILI+EQ
Sbjct  2822  DVCQNFQPVFRYFCMEKFLDPAIWFEKRLAYTRSVATSSIVGYILGLGDRHVQNILINEQ  2881

Query  2915  TSELVHIDLGVAFEQGKILPTPETVPFRLSRDIVDGMGITGVEGVFRRCCEKTMEVMRSS  2974
             ++ELVHIDLGVAFEQGKILPTPETVPFRL+RDIVDGMGITGVEGVFRRCCEKTMEVMR+S
Sbjct  2882  SAELVHIDLGVAFEQGKILPTPETVPFRLTRDIVDGMGITGVEGVFRRCCEKTMEVMRNS  2941

Query  2975  QEALLTIVEVLLYDPLFDWTMNPLKAFYLQQHDEQAELNATLNPTPGGDEIETHRKASD-  3033
             QE LLTIVEVLLYDPLFDWTMNPLKA YLQQ  E       L+PT   D+ E  R  SD
Sbjct  2942  QETLLTIVEVLLYDPLFDWTMNPLKALYLQQRPED---ETELHPTLNADDQECKRNLSDI  2998

Query  3034  SQSFNKVAERVLLRLQEKLKGVEDGTVLSVGGQVNLLIQQAMDPKNLSRLFPGWQAWV  3091
              QSFNKVAERVL+RLQEKLKGVE+GTVLSVGGQVNLLIQQA+DPKNLSRLFPGW+AWV
Sbjct  2999  DQSFNKVAERVLMRLQEKLKGVEEGTVLSVGGQVNLLIQQAIDPKNLSRLFPGWKAWV  3056
```

b. *Alignment of the TAN Domain showing 64% sequence identity (amino acids 8-165 in the human sequence)*

Query- Zebrafish   Subject-Human

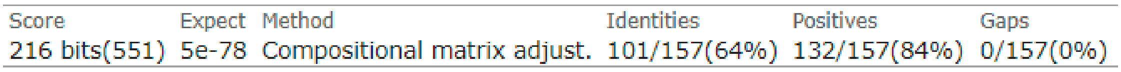

Score	Expect	Method	Identities	Positives	Gaps
216 bits(551)	5e-78	Compositional matrix adjust.	101/157(64%)	132/157(84%)	0/157(0%)

```
Query  1      LLVCCRGLENEKATERKKEVDRFRRLICSPDTVEELDRTSGSKGSKQLTWDAVFRFLQKF  60
              LL+CCR LE+++ATERKKEV++F+RLI  P+T++ LDR S SK  K L WDAVFRFLQK+
Sbjct  1      LLICCRQLEHDRATERKKEVEKFKRLIRDPETIKHLDRHSDSKQGKYLNWDAVFRFLQKY  60

Query  61     LKKETELLQSGKANVSASTQANRQKKMQEISSLMKFFIRCANQRGPRLKCAELISHVVEV  120
              ++KETE L+  K NVSASTQA+RQKKMQEISSL+K+FI+CAN+R PRLKC EL++++++
Sbjct  61     IQKETECLRIAKPNVSASTQASRQKKMQEISSLVKYFIKCANRRAPRLKCQELLNYIMDT  120

Query  121    LQSPFSCVAYGEDYSSILLKNILSVRKYWCEMSQQQW  157
              ++   +   YG D S+ILLK+ILSVRKYWCE+SQQQW
Sbjct  121    VKDSSNGAIYGADCSNILLKDILSVRKYWCEISQQQW  157
```

c. *Alignment of the HEAT Repeat Motifs Showing (amino acids 166-1939 of the human sequence)*

Query- Zebrafish   Subject-Human

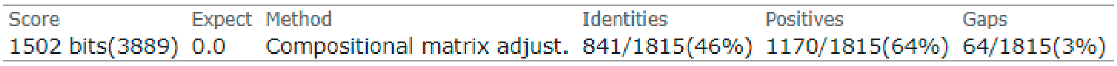

Score	Expect	Method	Identities	Positives	Gaps
1502 bits(3889)	0.0	Compositional matrix adjust.	841/1815(46%)	1170/1815(64%)	64/1815(3%)

```
Query  3      LLDLFCGLFNRGTRSINRVQVSRIIYTVVWGCCVQTEGLSHTLFNFFLKALSNSRAEKQL  62
              L  ++  L+ + ++ ++RV V+RII+ V  GCC QT+GL+    +FF KA+  +R EK
Sbjct  2      LFSVYFRLYLKPSQDVHRVLVARIIHAVTKGCCSQTDGLNSKFLDFFSKAIQCARQEKSS  61

Query  63     MVLENLVSAVNVFLRSVLLSCRKRVCGLGEEVLSDMLCVYTGMRPSSVLKEELVKFFQIQ  122
                L ++++A+ +FL+++ ++ R RVC LG+E+L  +L ++T  R +  LKE +++ FQ+Q
Sbjct  62     SGLNHILAALTIFLKTLAVNFRIRVCELGDEILPTLLYIWTQHRLNDSLKEVIIELFQLQ  121
```

```
Query  123   LFVHHPKGAKTIETGAQAQDWVKWRSQLCTLYDALVSEISQIGSRGKYATGSRHIAVKEN  182
             +++HHPKGAKT E GA      KWRS L  LYD LV+EIS IGSRGKY++G R+IAVKEN
Sbjct  122   IYIHHPKGAKTQEKGAYES--TKWRSILYNLYDLLVNEISHIGSRGKYSSGFRNIAVKEN  179

Query  183   LIELTADVCHQLFNQSTRVQEVTSSVCRDTQRDSPQ---SCKRRRVELSNWELIRSKLQP  239
             LIEL AD+CHQ+FN+ TR  E++ S    TQR+S      CKR+++EL  WE+I+  LQ
Sbjct  180   LIELMADICHQVFNEDTRSLEISQSYTT-TQRESSDYSVPCKRKKIELG-WEVIKDHLQK  237

Query  240   HHSDFDMIPWLQVTAALISKYPSILLTDDVVPLLGLLCQLQGEQQRRGERAPYVLRCLKE  299
               +DFD++PWLQ+   LISKYP+ L   ++ PLL +L QL   QQR GER PYVLRCL E
Sbjct  238   SQNDFDLVPWLQIATQLISKYPASLPNCELSPLLMILSQLL-PQQRHGERTPYVLRCLTE  296

Query  300   LALCHAKSSANSSACTAELGRLWARVWVLALRGVSSAQTGSLCLELLRIMVQESLVPVDR  359
             +ALC  K S   S+  ++L +LW ++W +  RG+SS Q  +    LL  ++Q SLV VDR
Sbjct  297   VALCQDKRSNLESSQKSDLLKLWNKIWCITFRGISSEQIQAENFGLLGAIIQGSLVEVDR  356

Query  360   EFWKVFSGAVCKPSLVSALSLTQALLKCSVPKSVHSRDATSVVLTDAGGEPPSLRDSIIS  419
             EFWK+F+G+ C+PS  +   LT AL    VP +V      ++   +      SL++SI+
Sbjct  357   EFWKLFTGSACRPSCPAVCCLTLALTTSIVPGTVKMGIEQNMCEVNRSF---SLKESIMK  413

Query  420   WLIMNEQNEETEENCRPHLIISRDFPLYLIPRIVVSLTLKDSRAGLTFLMGSLKPDCFSP  479
             WL+  +   + E +     I+  +FP  ++ +I+VSLT+K+ +A + F      P+C
Sbjct  414   WLLFYQLEGDLENSTEVPPILHSNFPHLVLEKILVSLTMKNCKAAMNFFQSV--PEC---  468

Query  480   ENSSLTETKATMDEVESLFLQFSFDEAHSSAGFTVDKDSVYSEKPQ----FTVIQALRSK  535
             E+    + + +  EVE LFLQ +FD+      F         EK Q    F+V Q L+
Sbjct  469   EHHQKDKEELSFSEVE-LFLQTTFDKM----DFLTIVRECGIEKHQSSIGFSVHQNLKES  523

Query  536   LEHSLLSIAEQLFTCYSPDSTNTPHECVLRCVSLLIGVLAAYVCIGMLSEEQACLSPLFL  595
             L+  LL ++EQL   YS + TN+  E ++RC  LL+GVL  Y  +G+++EE+A  S LF
Sbjct  524   LDRCLLGLSEQLLNNYSSEITNS--ETLVRCSRLLVGVLGCYCYMGVIAEEEAYKSELFQ  581

Query  596   KAKALVHEFSHYTSTAKSKLAENETLASVQSVMLLCSDCI--CRREKGDKMSTISRTLFM  653
             KAK+L+       +  K+K  E   + S++++M LC+ C+  C ++  +K   I+   F+
Sbjct  582   KAKSLMQCAGESITLFKNKTNEEFRIGSLRNMMQLCTRCLSNCTKKSPNK---IASGFFL  638

Query  654   KTLPVRLLNDLCDMSKQLLSNSGKK-DTIVIESEPVDMQTSRIQVDNQEEIDLFEDGDGT  712
             + L  +L+ND+ D+ K L S   K  D   +ES   D   + ++V++Q  ++LF D
Sbjct  639   RLLTSKLMNDIADICKSLASFIKKPFDRGEVESMEDDTNGNLMEVEDQSSMNLFND----  694

Query  713   QHITSRPSQSNEEAADSKFITGTKSALSEEHLSKQDLTFLSVLGFLSLCASSELNGGFSF  772
              +  S  S +NE   +S+   G  + L+EE+LSKQDL FL +L FL LC ++      SF
Sbjct  695   -YPDSSVSDANE-PGESQSTIGAINPLAEEYLSKQDLLFLDMLKFLCLCVTTAQTNTVSF  752

Query  773   KPLDTQRKLLKLLDLADF--SQMLHLQMYLSLLKKLPAEVASLDPEEFNALLRPLADVCS  830
             +  D +RKLL L+D +    ++ LHL MYL LLK+LP E   L  E+   LL+PL++VCS
Sbjct  753   RAADIRRKLLMLIDSSTLEPTKSLHLHMYLMLLKELPGEEYPLPMEDVLELLKPLSNVCS  812

Query  831   LYRQDQEVCSAILFSLLPSIRCLGLSSSGSEQEEDMADIKGSLLKVISGFCFLGKSGKCT  890
             LYR+DQ+VC  IL  +L  ++ LG S+  SE   +  D +G  L VI  F  L K  K
Sbjct  813   LYRRDQDVCKTILNHVLHVVKNLGQSNMDSE---NTRDAQGQFLTVIGAFWHLTKERKYI  869

Query  891   SSVRVALRQCLLALLEADPCCKWAVLTLREEELPVSAVLSSLLADSHQHVCMLTALSVES  950
              SVR+AL  CL  LLEADP  KWA+L +  ++ PV+ V +  LAD+H  V ML A S+
Sbjct  870   FSVRMALVNCLKTLLEADPYSKWAILNVMGKDFPVNEVFTQFLADNHHQVRMLAAESINR  929

Query  951   LFLKKALHSSRKM-MLPLKNQQTAFENIYLKAQEGIRRQKN-CPSEDLPDETFNRRATLL  1008
             LF      SSR +  LPLK QQTAFEN YLKAQEG+R   +   + +  DE +NR++ LL
Sbjct  930   LFQDTKGDSSRLLKALPLKLQQTAFENAYLKAQEGMREMSHSAENPETLDEIYNRKSVLL  989

Query  1009  KSVSMVMSCSPVCEKQALFALFQSYKENGIDEQLIKKVLRGISKSLGNRDHKSLINSHLY  1068
               +++V+SCSP CEKQALFAL +S KENG++  L+KKVL  +S++ G R  +  + SHL
Sbjct  990   TLIAVVLSCSP-CEKQALFALCKSVKENGLEPHLVKKVLEKVSETFGYRRLEDFMASHLD  1048

Query  1069  YLVAEWLNQKQSDSSYTLQSFPYALLDCCSLEEFFRSSYHVLIPHLVFLNDFEGVKSIGD  1128
             YLV EWLN +  D+ Y L SFP+ LL+  ++E+F+RS Y VLIPHLV  + F+ VKSI +
Sbjct  1049  YLVLEWLNLQ--DTEYNLSSFPFILLNYTNIEDFYRSCYKVLIPHLVIRSHFDEVKSIAN  1106

Query  1129  HLGQDWKQLLAKCFPKIMVNILPHFALA-GQDTHVAQQREKAHRVYDILKNSNCLGKQQI  1187
              + +DWK LL  CFPKI+VNILP+FA    +D+ +AQQRE A  VYD+LK+ N LGKQ I
Sbjct  1107  QIQEDWKSLLTDCFPKILVNILPYFAYEDAKDSGMAQQREIASTVYDMLKSENLLGKQ-I  1165

Query  1188  DSLICNNLPDIVVELLMTLHE----TAGDKGDLQKFTGELDPAPNPPFFSSYVIKATLDY  1243
             D L  +NLP+IVVELLMTLHE    +A    DL  F+G+LDPAPNPP F S+VIKAT  Y
Sbjct  1166  DHLFISNLPEIVVELLMTLHEPANSSASQSTDLCDFSGDLDPAPNPPHFPSHVIKATFAY  1225

Query  1244  LSKCHSANHKSLVAILSKTPMSIQRILVAVCQKADETTNAYERHRILMMYHLFVSLLLKE  1303
             +S CH    KS++ ILSK+P S Q+IL+A+C++A ET N Y++HRIL +YHLFVSLLLK+
Sbjct  1226  ISNCHKTKLKSILEILSKSPDSYQKILLAICEQAAETNNVYKKHRILKIYHLFVSLLLKD  1285

Query  1304  VKDGLGGAWAFVLRDIIYTLIHHINSRSSQQDEVSTRSLSLCCDLLSLVCQTAVEYCDDA  1363
             +K GLGGAWAFVLRD+IYTLIH+IN R S   +VS RS SLCCDLLS VCQTAV YC DA
Sbjct  1286  IKSGLGGAWAFVLRDVIYTLIHYINQRPSCIMDVSLRSFSLCCDLLSQVCQTAVTYCKDA  1345

Query  1364  LESHLQV-VGTLTAQVTEQSAISEQVLSLLRFLVMENPENRMLRKSIPLLEPFPEQPNFA  1422
             LE+HL V VGTL   V EQ  + +QVL LL++LV++N +N  L  +I LL+PFP+   F
Sbjct  1346  LENHLHVIVGTLIPLVYEQVEVQKQVLDLLKYLVIDNKDNENLYITIKLLDPFPDHVVFK  1405

Query  1423  ELRAAQHALKYSSGAFTLRQEIEHFLSVASCDSLPLARLEGLKDLKRQLHSHKQQIGQLL  1482
             +LR  Q  +KYS G F+L +EI HFLSV+  D+LPL RLEGLKDL+RQL  HK Q+  ++
Sbjct  1406  DLRITQQKIKYSRGPFSLLEEINHFLSVSVYDALPLTRLEGLKDLRRQLELHKDQMVDIM  1465

Query  1483  KECHADLDSCILVNLVLNLLQLCKIAANHPGGGDIMKAAGRCLGELGPVDLSSIALHHGK  1542
             +    +    I+V LV+NLLQL K+A NH G  ++++A G CLGE+GP+D S+IA+ H K
Sbjct  1466  RASQDNPQDGIMVKLVVNLLQLSKMAINHTGEKEVLEAVGSCLGEVGPIDFSTIAIQHSK  1525

Query  1543  DQLYARAAKLFHNVPHQWIFIILNSMDNALTNHSIAVRQTAGLCIKDILATQSGIEFGEI  1602
             D  Y +A KLF +   QW FI+L  ++N L    + VR  A  C+K+ILAT++G  F EI
Sbjct  1526  DASYTKALKLFEDKELQWTFIMLTYLNNTLVEDCVKVRSAAVTCLKNILATKTGHSFWEI  1585

Query  1603  HKSKRDPLLAYLNPFRSSKKREPIMAMDVTPESRDRLTSADLWLMQPDGHKDWLKNLCMA  1662
             +K   DP+LAYL PFR+S+K+   +          + L   +LW+   + H  W+K L  A
Sbjct  1586  YKMTTDPMLAYLQPFRTSRKKFLEVPRFDKENPFEGLDDINLWIPLSENHDIWIKTLTCA  1645

Query  1663  LLDSGGVRNEALLLTRPLCEVKTDFCQRMLPLFVHDILLGDVDGSWRQLLSTHIQSFFSQ  1722
              LDSGG + E L L +P+CEVKTDFCQ +LP  +HDILL D + SWR LLSTH+Q FF+
Sbjct  1646  FLDSGGTKCEILQLLKPMCEVKTDFCQTVLPYLIHDILLQDTNESWRNLLSTHVQGFFTS  1705

Query  1723  CRRPSTPTSRPTTPMLSDSGNTTDAANQCQIDKASLRSMLAVIDHLRQQSRPLAPGSNEY  1782
             C R  + TSR TTP   DS   ++   +C +DK S R+MLAV+D++R+Q RP +
Sbjct  1706  CLRHFSQTSRSTTPANLDS--ESEHFFRCCLDKKSQRTMLAVVDYMRRQKRPSS------  1757

Query  1783  GTVCDSNFWLDLNYL  1797
             GT+ +  FWLDLNYL
Sbjct  1758  GTIFNDAFWLDLNYL  1772
```

d. ***Alignment of FAT Domain showing 73% sequence identity (amino acids 1939-1566 in the human sequence)***

Query- Zebrafish   *Subject-Human*

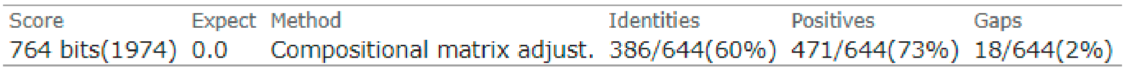

Score	Expect	Method	Identities	Positives	Gaps
764 bits(1974)	0.0	Compositional matrix adjust.	386/644(60%)	471/644(73%)	18/644(2%)

```
Query  1     EVAGAAQMCSAHFTALLYSEIYVDKIRSNMEQNRRSQSRASRRITFEDNSQTLSVSNLNE  60
             EVA  AQ C+AHFTALLY+EIY DK +S  +Q +RS        + FE+ SQ+ ++S+L+E
Sbjct  1     EVAKVAQSCAAHFTALLYAEIYADK-KSMDDQEKRS-------LAFEEGSQSTTISSLSE  52
```

```
Query  61   RSLEDSGFSLQDLLIEVYRCIGEPDSLYGCGGGKLTSPLTRIRTYEHEAMWEKALVSYDL  120
            +S E++G SLQDLL+E+YR IGEPDSLYGCGGGK+  P+TR+RTYEHEAMW KALV+YDL
Sbjct  53   KSKEETGISLQDLLLEIYRSIGEPDSLYGCGGGKMLQPITRLRTYEHEAMWGKALVTYDL  112

Query  121  HSNLPEVTRQIGIVEGLQNFGLCSILSTYLHGLEKDGMEWGPELRELRFQAAWRSTQWDC  180
             + +P  TRQ GI++ LQN GLC ILS YL GL+ +  +W PEL EL +QAAWR+ QWD
Sbjct  113  ETAIPSSTRQAGIIQALQNLGLCHILSVYLKGLDYENKDWCPELEELHYQAAWRNMQWDH  172

Query  181  DLPERNEKLKPGINESLFNALQALRDKEFSLFEQTLNYARGREVEELCRGSLEAVSSLYP  240
                  E      +ESL+NALQ+LRD+EFS F ++L YAR +EVEE+C+ SLE+V SLYP
Sbjct  173  CTSVSKEVEGTSYHESLYNALQSLRDREFSTFYESLKYARVKEVEEMCKRSLESVYSLYP  232

Query  241  ALCNLQRISELQSVEELFSRPVTDSSLNEVYRKWQQHSDLLTDSDFSLVEPVLALRSSIQ  300
             L  LQ I EL+S+ ELFSR VT   L+EVY KWQ+HS LL DSDFS  EP++ALR+ I
Sbjct  233  TLSRLQAIGELESIGELFSRSVTHRQLSEVYIKWQKHSQLLKDSDFSFQEPIMALRTVIL  292

Query  301  EALISSETDPDRKNYLISTYSSHLMELCRLARSAGNTQLAERAVFHMKQHNLVMSGSGSS  360
            E L+  E D  ++  +    + HL+EL  LAR+  NTQL ERA+F +KQ+N V  G
Sbjct  293  EILMEKEMDNSQRECIKDILTKHLVELSILARTFKNTQLPERAIFQIKQYNSVSCGVSE-  351

Query  361  SWAWQLEEAQVFWVKKEHGLALELLKQMIHKLD-DLVCVNPAVVPVYSECLRLCGSWLAE  419
               WQLEEAQVFW KKE  LAL +LKQMI KLD      NP++   Y+ECLR+CG+WLAE
Sbjct  352  ---WQLEEAQVFWAKKEQSLALSILKQMIKKLDASCAANNPSLKLTYTECLRVCGNWLAE  408

Query  420  SCLESPAVILENYLERAVEVIEEHCGGLKSKLQSQKTQAYFSLARFSDAQYQGIENYMKS  479
            +CLE+PAVI++ YLE+AVEV   + G    +L++ K +A+ SLARFSD QYQ IENYMKS
Sbjct  409  TCLENPAVIMQTYLEKAVEVAGNYDGESSDELRNGKMKAFLSLARFSDTQYQRIENYMKS  468

Query  480  SEFENKHALLEKAKEEVDLMRERKVNNNRYTVKVQRELELDVKALANLQADRNRFLLKAV  539
            SEFENK ALL++AKEEV L+RE K+  NRYTVKVQRELELD  AL  L+ DR RFL KAV
Sbjct  469  SEFENKQALLKRAKEEVGLLREHKIQTNRYTVKVQRELELDELALRALKEDRKRFLCKAV  528

Query  540  ENYIECLELGEEHDTWVFRLASLWLENADVKAVNDKMKSGVKKIPSYKFLPLMYQLAARM  599
            ENYI CL  GEEHD WVFRL SLWLEN+ V  VN  MK    KIP+YKFLPLMYQLAARM
Sbjct  529  ENYINCLLSGEEHDMWVFRLCSLWLENSGVSEVNGMMKRDGMKIPTYKFLPLMYQLAARM  588

Query  600  GTKVSSSMASQDVGFHHVLNELICQSSVDHPHHTLFIILALVNA  643
            GTK+   +     GFH VLN LI + S+DHPHHTLFIILAL NA
Sbjct  589  GTKMMGGL-----GFHEVLNNLISRISMDHPHHTLFIILALANA  627
```

e. *Alignment of the Kinase Domain showing 84% sequence identity (amino acids 2712- 2962 in the human sequence)*

Query- Zebrafish *Subject-Human*

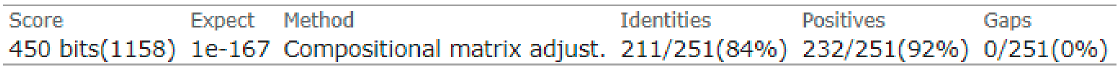

Score	Expect	Method	Identities	Positives	Gaps
450 bits(1158)	1e-167	Compositional matrix adjust.	211/251(84%)	232/251(92%)	0/251(0%)

```
Query  1    RRQLVKGRDDLRQDAVMQQVFQMCNTLLQRNTETRKRKLNIRRYKVVPFSQRSGVLEWCS  60
            RRQLVKGRDDLRQDAVMQQVFQMCNTLLQRNTETRKRKL I  YKVVP SQRSGVLEWC+
Sbjct  1    RRQLVKGRDDLRQDAVMQQVFQMCNTLLQRNTETRKRKLTICTYKVVPLSQRSGVLEWCT  60

Query  61   GTVPIGEFLVDPQKGAHKRFRPQDWANMLCRKKMMEAQRMEFNDKLQAFTEVCQNFRPVF  120
            GTVPIGEFLV+ + GAHKR+RP D++   C+KKMME Q+  F +K + F +VCQNF+PVF
Sbjct  61   GTVPIGEFLVNNEDGAHKRYRPNDFSAFQCQKKMMEVQKKSFEEKYEVFMDVCQNFQPVF  120
```

```
Query  121  RYFCMERFLDPAIWLERRLAYTRSVATSSIVGYIVGLGDRHIQNILIDEQTSELVHIDLG  180
            RYFCME+FLDPAIW E+RLAYTRSVATSSIVGYI+GLGDRH+QNILI+EQ++ELVHIDLG
Sbjct  121  RYFCMEKFLDPAIWFEKRLAYTRSVATSSIVGYILGLGDRHVQNILINEQSAELVHIDLG  180

Query  181  VAFEQGKILPTPETVPFRLSRDIVDGMGITGVEGVFRRCCEKTMEVMRSSQEALLTIVEV  240
            VAFEQGKILPTPETVPFRL+RDIVDGMGITGVEGVFRRCCEKTMEVMR+SQE LLTIVEV
Sbjct  181  VAFEQGKILPTPETVPFRLTRDIVDGMGITGVEGVFRRCCEKTMEVMRNSQETLLTIVEV  240

Query  241  LLYDPLFDWTM  251
            LLYDPLFDWTM
Sbjct  241  LLYDPLFDWTM  251
```

f. *Alignment of the FATC Domain showing 94% sequence identity (amino acids 3023-3056 of the human sequence)*

Query- Zebrafish *Subject-Human*

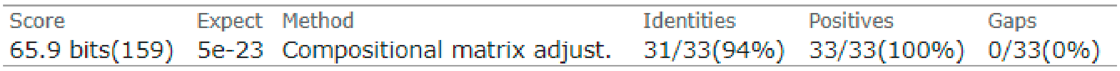

Score	Expect	Method	Identities	Positives	Gaps
65.9 bits(159)	5e-23	Compositional matrix adjust.	31/33(94%)	33/33(100%)	0/33(0%)

```
Query  1    TVLSVGGQVNLLIQQAMDPKNLSRLFPGWQAWV  33
            TVLSVGGQVNLLIQQA+DPKNLSRLFPGW+AWV
Sbjct  1    TVLSVGGQVNLLIQQAIDPKNLSRLFPGWKAWV  33
```

Appendix 6.3 Protein-Protein Blast Sequence Alignment of the TDP1 zebrafish and human sequences

a. ***Alignment of the Full Protein Sequence Showing 55% Sequence Identity***

Query- Zebrafish   Subject-Human

Green – Conserved DNA binding residues, yellow- conserved N-terminal active site residues, pink- conserved C-terminal active site residues

Score	Expect	Method	Identities	Positives	Gaps
693 bits(1788)	0.0	Compositional matrix adjust.	352/638(55%)	445/638(69%)	53/638(8%)

```
Query  1    MSQDSQHGKWSISDSEDEDIIPPTPQKDSVKPIVKPDSQSKPEETPTFLKQEPRLSPKRN  60
            MSQ+  +G+W+IS S++ +   P P K S   ++     +           EPR +
Sbjct  1    MSQEGDYGRWTISSSDESEEEKPKPDKPSTSSLLCARQGAA---------NEPRYT----  47

Query  61   ENSVKTASAPSMGSEARKSAHVNQANPVKYERNAS---PAVKRKRETEEGGWNLSSSDDE  117
                         SEA+K+AH  + +PVK+    S   P  ++    E+ GW LSSSDDE
Sbjct  48   ------------CSEAQKAAHKRKISPVKFSNTDSVLPPKRQKSGSQEDLGWCLSSSDDE  95

Query  118  T--PAPRNEPQKVNISPKRK---------KKTEDKRPPSPHGTSYYKEEPADFFET----  162
                 P+ + +KV I  ++          ++TE+   P+ H      +E  D +ET
Sbjct  96   LQPEMPQKQAEKVVIKKEKDISAPNDGTAQRTENHGAPACHRL----KEEEDEYETSGEG  151

Query  163  ----NLMPTNDIYRFYLNKVTGIPKKYNTGALHIKEILSPMFGTLKESVQFNYCFDIPWM  218
                +++   + ++FYL +V+G+  KYN+GALHIK+ILSP+FGTL  S QFNYCFD+ W+
Sbjct  152  QDIWDMLDKGNPFQFYLTRVSGVKPKYNSGALHIKDILSPLFGTLVSSAQFNYCFDVDWL  211

Query  219  VEQYPPEFRNKPVVLVHGEKRESKACLIEQAKPYPHISFCQAKLDIAFGTHHTKMMLLWY  278
            V+QYPPEFR KP++LVHG+KRE+KA L  QAKPY +IS CQAKLDIAFGTHHTKMMLL Y
Sbjct  212  VKQYPPEFRKKPILLVHGDKREAKAHLHAQAKPYENISLCQAKLDIAFGTHHTKMMLLLY  271

Query  279  EEGFRVIILTSNLIRADWYQKTQGMWMSPLYPRLPQGSPGTAGESLTGFKRDLLEYLEAY  338
            EEG RV+I TSNLI ADW+QKTQG+W+SPLYPR+  G+   +GES T FK DL+ YL AY
Sbjct  272  EEGLRVVIHTSNLIHADWHQKTQGIWLSPLYPRIADGT-HKSGESPTHFKADLISYLMAY  330

Query  339  RAPELANWIERIKQHDLSETRVYLIGSTPGRYQGPAMEKWGHLRLRKLLSEHTQPMQNEE  398
             AP L  WI+ I +HDLSET VYLIGSTPGR+QG   + WGH RL+KLL +H   M N E
Sbjct  331  NAPSLKEWIDVIHKHDLSETNVYLIGSTPGRFQGSQKDNWGHFRLKKLLKDHASSMPNAE  390

Query  399  RWHVLGQFSSIGSMGLDKTKWLAAEFQRTLTTLGKAGKSLASPETQMLLIYPSVENVRTS  458
             W V+GQFSS+GS+G D++KWL +EF+ ++ TLGK  K+       + LIYPSVENVRTS
Sbjct  391  SWPVVGQFSSVGSLGADESKWLCSEFKESMLTLGKESKTPGKSSVPLYLIYPSVENVRTS  450

Query  459  LEGYPAGGSLPYSIQTAQKQLWLHSYFHGWHADVTGRSNAMPHIKTYMRISPDFTQLAWF  518
            LEGYPAGGSLPYSIQTA+KQ WLHSYFH W A+ +GRSNAMPHIKTYMR SPDF+++AWF
Sbjct  451  LEGYPAGGSLPYSIQTAEKQNWLHSYFHKWSAETSGRSNAMPHIKTYMRPSPDFSKIAWF  510

Query  519  LVTSANLSKAAWGALEKNNTQIMVRSYELGVLYLPSAFNMSTFPVEKNVFPACSSSIG-F  577
            LVTSANLSKAAWGALEKN TQ+M+RSYELGVL+LPSAF + +F V++  F      +  F
Sbjct  511  LVTSANLSKAAWGALEKNGTQLMIRSYELGVLFLPSAFGLDSFKVKQKFFAGSQEPMATF  570

Query  578  PVPFDLPPQRYSSKDRPWIWNIPYTQAPDTHGNVWVPS  615
            PVP+DLPP+ Y SKDRPWIWNIPY +APDTHGN+WVPS
Sbjct  571  PVPYDLPPELYGSKDRPWIWNIPYVKAPDTHGNMWVPS  608
```

b. Alignment of the N-terminal regulatory and protein-protein binding domain (amino acids 1-148 in the human sequence)

Query- Zebrafish *Subject-Human*

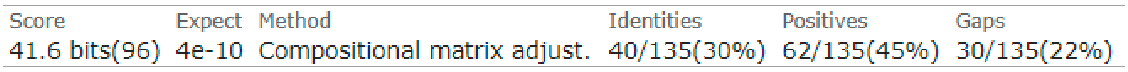

Score	Expect	Method	Identities	Positives	Gaps
41.6 bits(96)	4e-10	Compositional matrix adjust.	40/135(30%)	62/135(45%)	30/135(22%)

```
Query  1    MSQDSQHGKWSISDSEDEDIIPPTPQKDSVKPIVKPDSQSKPEETPTFLKQEPRLSPKRN  60
            MSQ+  +G+W+IS S++ +   P P K S   ++     +           EPR +
Sbjct  1    MSQEGDYGRWTISSSDESEEEKPKPDKPSTSSLLCARQGA---------ANEPRYT----  47

Query  61   ENSVKTASAPSMGSEARKSAHVNQANPVKYERNAS---PAVKRKRETEEGGWNLSSSDDE  117
                         SEA+K+AH  + +PVK+    S   P  ++    E+ GW LSSSDDE
Sbjct  48   ------------CSEAQKAAHKRKISPVKFSNTDSVLPPKRQKSGSQEDLGWCLSSSDDE  95

Query  118  TP--APRNEPQKVNI  130
                 P+ + +KV I
Sbjct  96   LQPEMPQKQAEKVVI  110
```

Appendix 6.4 Protein-Protein Blast Sequence Alignment of the ATR zebrafish and human sequences

Query- Zebrafish   Subject-Human

Score	Expect	Method	Identities	Positives	Gaps
3469 bits(8995)	0.0	Compositional matrix adjust.	1729/2665(65%)	2077/2665(77%)	54/2665(2%)

```
Query  3     EHGLELASMIPALRELGSATPEEYNTVVQKPRQILCQFIDRILTDVNVVAVELVKKTDSQ  62
             E GLE+++MIPAL+EL SA+  EYN  VQKPRQILCQFIDRILTDV+VVA+EL KK+ S+
Sbjct  2     EQGLEMSAMIPALQELASASSVEYNQAVQKPRQILCQFIDRILTDVDVVALELCKKSSSE  61

Query  63    PTSVMLLDFIQHIMKSSPLMFVNVS--GSH--EAKGSCIEFSNWIITRLLRIAATPSCHL  118
             P  VMLLDF+QHI+KSS LMF+N +    H   ++ SC +F+ WII RLLRIAA P C
Sbjct  62    PACVMLLDFVQHIIKSSSLMFINPACLSDHFKNSENSCTDFTKWIINRLLRIAACPECED  121

Query  119   LHKKICEVICSLLFLFKSKSPAIFGVLTKELLQLFEDLVYLHRRNVMGH-AVEWPVVMSR  177
             LH KI  VICSLL LF++K+P +F + + EL+ L +DLV+   +N+M   + +WPVV+ R
Sbjct  122   LHMKISSVICSLLHLFRAKAPVVFSLFSTELICLIQDLVH---KNLMTRPSPQWPVVVER  178

Query  178   FLSQLDEHMGYLQSAPLQLMSMQNLEFIEVTLLMVLTRIIAIVFFRRQELLLWQIGCVLL  237
             F  +  E   YL    LQL S+ + + +  T L VLT +I  +FF R+  ++W   C++L
Sbjct  179   FSIKSGESAVYLTPTILQLSSLSSTQALLATSLRVLTDVIQGLFFPREVGIIWDSTCLML  238

Query  238   EYGSPKIKSLAISFLTELFQLGGLPAQPASTFFSSFLELLKHLVEMDTDQLKLYEEPLSK  297
               GSPK+K++++  LT +  LGG P   +  FFS+FL +L  L   D  +L ++     +
Sbjct  239   SNGSPKLKAVSMVLLTRIVTLGGFPEDHSQPFFSAFLHVLDSLPAFDESELGVFSREFQQ  298

Query  298   LIKTLFPFEAEAYRNIEPVYLNMLLEKLCVMFEDGVLMRLKSDLLKAALCHLLQYFLKFV  357
             L + +F  E  A+   E V+LNML+E+L  +   G L  LK   +KA LC +  + L FV
Sbjct  299   LSRCIFQHEEGAHSRFERVHLNMLMERLEKLVVIGALEHLKVKEVKATLCEVFCFILGFV  358

Query  358   PAGYESALQVRKVYVRNICKALLDVLGIEVDAEYLL-GPLYAALKMESMEIIEEIQCQTQ  416
             P GYE ALQ+RK  V  ICKAL+  +G +   E  L G LYAALK +++  ++++Q
Sbjct  359   PPGYECALQIRKERVAAICKALIKTIGTKDQHEQSLEGYLYAALKTDAIAAMQDVQ----  414

Query  417   QENLSSNSDGISPK-------RRRLSSSLNPSKRAPKQTEEIKHVDMNQKSILWSALKQK  469
                 +S SD   P+        +R + SL    R+  +T+ ++ VDM  +S +W+A+  +
Sbjct  415   ----ASVSDPADPRMYEEELPAKRPNLSLPTQLRSRDKTQPMQ-VDMKSRSEVWAAVDCR  469

Query  470   AESLQISLEYSGLKNPVIEMLEGIAVVLQLTALCTVHCSHQNMNCRTFKDCQHKSKKKPS  529
              E L   +    +    +  ++G+AV+  L ALC+ H         + K  Q   K   S
Sbjct  470   LEELLTQMRNHTVSQ-CVSAVQGLAVIFHLAALCSEH---------SLKGPQRGEKSSES  519

Query  530   VVIT---WMSLDFYTKVLKSCRSLL-ESVQKLDLEATIDKVVKIYDALIYMQVNSSFEDH  585
              V+    W+      +V++SCR++L  +  +  LE  ++ +V+I DA++Y+  NS  +
Sbjct  520   SVVAQLIWLKPQMLAQVVESCRTVLANNYNEEHLEHLVEGIVRILDAVLYLSTNSESDKS  579

Query  586   ILEDLCGMLSLPWIYSHSDDGCLKLTTFAANLLTLSCRISDSYSPQAQSRCVFLLTLFPR  645
                ++C +LS+PW+  HS     +  +F A+L+ LS +++  Y+ Q ++ CVFLL    +
Sbjct  580   FHRNICALLSVPWVLEHSSQSVYQTASFPASLIALSQKLAPVYNAQTRAHCVFLLAPLSK  639

Query  646   RIFLEWRTAVYNWALQSSHEVIRASCVSGFFILLQQQN--SCNRVPKILIDKVKDDSDIV  703
              +  +WR++VY WALQS  E  RAS V GF ILL Q    S + + + L+++++D S  V
Sbjct  640   SVCGDWRSSVYRWALQSKSEAERASAVRGFPILLHQLGVKSNSLIHEALLNRLQDSSTEV  699

Query  704   KKEFASILGQLVCTLHGMFYLTSSLTEPFSEHGHVDLFCRNLKATSQHECSSSQLKASVC  763
             K E A I GQL C L      +S L  P        L C  L  +  H   +S +  S+
Sbjct  700   KTELAGITGQLACCLSE----SSQLQFPQETMPSHQLLCSGLSISDFHSSQTSSIGTSIL  755

Query  764   KPFLFLLKKKIPSPVKLAFIDNLHHLCKHLDFREDETDVKAVLGTLLNLMEDPDKDVRVA  823
              PFL LLK      VK AFI N+ HL KH+D    + D KA++  L+NL+EDPD++VR+
Sbjct  756   TPFLQLLKPVEDMKVKQAFIKNIRHLFKHVDLGNTDPDTKALVNALVNLIEDPDQEVRIM  815

Query  824   FSGNIKHILESLDSEDGFIKELFVLRMKEAYTHAQISRNNELKDTLILTTGDIGRAAKGD  883
             F  NIK++LE  +  +GF+KEL V R+KEAYT+A+ SRNNELK+TLILTTG+IGRAA+G+
Sbjct  816   FGQNIKNLLEFWNG-NGFLKELLVSRLKEAYTNAKTSRNNELKNTLILTTGEIGRAAEGN  874

Query  884   LVPFALLHLLHCLLSKSASVSGAAYTEIRALVAAKSVKLQSFFSQYKKPICQFLVESLHS  943
             LV FALL LLHCLLSKS  VS AAYTEI+AL   + +KLQSFFSQY+ PICQFLVESLHS
Sbjct  875   LVSFALLRLLHCLLSKSNPVSVAAYTEIQALATCRDLKLQSFFSQYRNPICQFLVESLHS  934

Query  944   SQMTALPNTPCQNADVRKQDVAHQREMALNTLSEIANVFDFPDLNRFLTRTLQVLLPDLA  1003
               +TAL  TP Q+++  +++ AHQRE+AL+ LS +A+VFDFPDLNRFL RTLQVLLP LA
Sbjct  935   RHVTALRCTPDQSSEALQEEAAHQRELALDILSHVAHVFDFPDLNRFLNRTLQVLLPFLA  994

Query  1004  AKASPAASALIRTLGKQLNVNRREILINNFKYIFSHLVCSCSKDELERALHYLKNETEIE  1063
             AKASP ASALIRT+ KQLNVNRRE+LINNFKYIFSHLVCSCSK+ELERA HYLKNETEIE
Sbjct  995   AKASPTASALIRTIAKQLNVNRREMLINNFKYIFSHLVCSCSKEELERAFHYLKNETEIE  1054

Query  1064  LGSLLRQDFQGLHNELLLRIGEHYQQVFNGLSILASFASSDDPYQGPRDIISPELMADYL  1123
             LGSLLRQDFQGLHNELLLR+GEHYQQVFNGL+ILASFASSDDPYQGPR+I +P  MADYL
Sbjct  1055  LGSLLRQDFQGLHNELLLRLGEHYQQVFNGLAILASFASSDDPYQGPREITTPGCMADYL  1114

Query  1124  QPKLLGILAFFNMQLLSSSVG-IEDKKMALNSLMSLMKLMGPKHVSSVRVKMMTTLRTGL  1182
             QPKLLGILAFFNMQLLSSS G  E KKMALNSLMSLMKLMGPKH+SSVRVKMMTTLRTGL
Sbjct  1115  QPKLLGILAFFNMQLLSSSAGEKEKKKMALNSLMSLMKLMGPKHISSVRVKMMTTLRTGL  1174

Query  1183  RFKDDFPELCCRAWDCFVRCLDHACLGSLLSHVIVALLPLIHIQPKETAAIFHYLIIENR  1242
             R+KDDFPELCCR WDCFVRCLD + LG LLSHVIVALLPLI IQPKETA I HYLI+ENR
Sbjct  1175  RYKDDFPELCCRTWDCFVRCLDPSYLGPLLSHVIVALLPLISIQPKETAVIMHYLIVENR  1234

Query  1243  DAVQDFLHEIYFLPDHPELKKIKAVLQEYRKETSESTDLQTTLQLSMKAIQHENVDVRIH  1302
             + VQDFLHEIYFLPDHPELK I  VLQ+YRK+TS+STD+Q  LQLSM+AIQHENVDVRIH
Sbjct  1235  EEVQDFLHEIYFLPDHPELKIIHKVLQDYRKQTSKSTDMQAALQLSMRAIQHENVDVRIH  1294

Query  1303  ALTSLKETLYKNQEKLIKYATDSETVEPIISQLVTVLLKGCQDANSQARLLCGECLGELG  1362
             ALTSLKE +YKNQ+ L+K+  DSE VEP+ISQLVTVLL+GCQD N++ARLLCGECLGELG
Sbjct  1295  ALTSLKEMIYKNQDALLKHVLDSEMVEPVISQLVTVLLRGCQDVNTEARLLCGECLGELG  1354

Query  1363  AIDPGRLDFSTTETQGKDFTFVTGVEDSSFAYGLLMELTRAYLAYADNSRAQDSAAYAIQ  1422
             AIDPGRLD S  +TQG   TFV+G++D +FAY LL ELTRA+LAYAD+ RAQD+AAYA+Q
Sbjct  1355  AIDPGRLDLSPADTQGTGSTFVSGIDDPNFAYELLTELTRAFLAYADDVRAQDAAAYAMQ  1414

Query  1423  ELLSIYDCREMETNGPGHQLWRRFPEHVREILEPHLNTRYKSSQKSTDWSGVKKPIYLSK  1482
             ELLS+++CRE  T+  G +LWRRFPE V+EILEPHLNTRYKSSQK  +WS +KKPIYLS
Sbjct  1415  ELLSLFECREGRTDSSGRRLWRRFPEQVQEILEPHLNTRYKSSQKVVNWSKLKKPIYLSS  1474

Query  1483  LGSNFAEWSASWAGYLITKVRHDLASKIFTCCSIMMKHDFKVTIYLLPHILVYVLLGCNQ  1542
              GS F++WSA+WAGYLI+KVRH+LA K+F CCS ++KHD+KVTIYLLPHILVYVL+GC Q
Sbjct  1475  RGSKFSDWSATWAGYLISKVRHELAGKVFNCCSFIIKHDYKVTIYLLPHILVYVLIGCTQ  1534

Query  1543  EDQQEVYAEIMAVLKHDDQHTINTQDIASDLCQLSTQTVFSMLDHLTQWARHKFQALKAE  1602
             E+Q+EV  EIMAVLK  D   +  Q+ AS L QLSTQTVFSMLDHLTQW+RHK Q L
Sbjct  1535  EEQREVTEEIMAVLKEGDPRLVRLQENASSLSQLSTQTVFSMLDHLTQWSRHKLQTLSTN  1594

Query  1603  KCPHSKSNRNKVDSMVSTVDYEDYQSVTRFLDLIPQDTLAVASFRSKAYTRAVMHFESFI  1662
             K    K+ R +  +  + V   +YQSV  FL+ IPQD LA ASFRS+AYTRAVMHFESFI
Sbjct  1595  K-RTGKNAREQPPATGNVVTLVEYQSVVAFLNSIPQDVLAKASFRSRAYTRAVMHFESFI  1653

Query  1663  TEKKQNIQEHLGFLQKLYAAMHEPDGVAGVSAIRKAEPSLKEQILEHESLGLLRDATACY  1722
              EKKQNIQ+HL FLQ LYAAMHEPDGV GV+A+RK EPSL+EQILEHES+GLLR++TACY
Sbjct  1654  REKKQNIQDHLSFLQTLYAAMHEPDGVRGVNALRKEEPSLREQILEHESIGLLRESTACY  1713

Query  1723  DRAIQLEPDQIIHYHGVVKSMLGLGQLSTVITQVNGVHANRSEWTDELNTYRVEAAWKLS  1782
             DRAIQLEPDQ+ HYHGV+ SMLGLGQLSTVITQVNGV A+R  W  +LN YRVEAAWKLS
Sbjct  1714  DRAIQLEPDQLAHYHGVMNSMLGLGQLSTVITQVNGVLASRPRWKSDLNAYRVEAAWKLS  1773

Query  1783  QWDLVENYLAADGKSTTWSVRLGQLLLSAKKRDITAFYDSLKLVRAEQIVPLSAASFERG  1842
             +WDLVE+YLA+D KS+TW VRLGQ+LL+AKK+D  AFY+ LK+ R EQ+VPLSAASFE G
Sbjct  1774  KWDLVEDYLASDCKSSTWGVRLGQMLLAAKKQDSEAFYEKLKIARKEQVVPLSAASFECG  1833
```

```
Query  1843  SYQRGYEYIVRLHMLCELEHSIKPLFQHS--PGDSSQ-EDSLNWVARLEMTQNSYRAKEP  1899
             +YQRGYEYIVRLHMLCELEH    L + S   G S + E  LNW A L MTQNS+RAKEP
Sbjct  1834  TYQRGYEYIVRLHMLCELEHVFTELQKESSEAGRSKKPEPKLNWDAHLLMTQNSFRAKEP  1893

Query  1900  ILALRRALLSLNKRPDYNEMVGECWLQSARVARKAGHHQTAYNALLNAGESRLAELYVER  1959
             +LALRRALLSL+K     E VGECWLQSARVAR+AGHHQTA+NALLNA  S L+EL++E+
Sbjct  1894  VLALRRALLSLSKGSSCEEQVGECWLQSARVARRAGHHQTAFNALLNAENSHLSELFIEK  1953

Query  1960  AKWLWSKGDVHQALIVLQKGVELCFPENETPPEGKNMLIHGRAMLLVGRFMEETANFESN  2019
             AKWLWSKGDVHQALIVLQKGV+ CFP+++T  + K + + + G AMLLVGR+MEETANFESN
Sbjct  1954  AKWLWSKGDVHQALIVLQKGVQQCFPDDQTLTDPKRIQVKGNAMLLVGRYMEETANFESN  2013

Query  2020  AIMKKYKDVTACLPEWEDGHFYLAKYYDKLMPMVTDNKMEKQGDLIRYIVLHFGRSLQYG  2079
             AIMK YKDVT  LPEWEDG+FYLAKYYDK+MPMVTDNK+E+QG+LIRYIV +FG++LQ+G
Sbjct  2014  AIMKTYKDVTTLLPEWEDGNFYLAKYYDKVMPMVTDNKLERQGNLIRYIVTYFGKALQFG  2073

Query  2080  NQFIYQSMPRMLTLWLDYGTKAYEWEKAGRSDRVQMRNDLGKINKVITEHTNYLAPYQFL  2139
             NQ+IYQ+MPRMLTLWLD+G K YE+EKAGRSDRVQMR +L KIN VI++HT+ L+PYQFL
Sbjct  2074  NQYIYQAMPRMLTLWLDFGAKVYEFEKAGRSDRVQMRTELTKINSVISDHTSNLSPYQFL  2133

Query  2140  TAFSQLISRICHSHDEVFVVLMEIIAKVFLAYPQQAMWMMTAVSKSSYPMRVNRCKEILN  2199
             TAFSQLISRICHS +EVF VLMEI+AKVFLAYPQQAMWMMTAVSKSSYP R+NRCKEIL
Sbjct  2134  TAFSQLISRICHSSNEVFAVLMEIVAKVFLAYPQQAMWMMTAVSKSSYPTRMNRCKEILK  2193

Query  2200  KAIHMKKSLEKFVGDATRLTDKLLELCNKPVDGSSSTLSMSTHFKMLKKLVEEATFSEIL  2259
             KAI +  S  KF+GDA RLTDKLLEL NKPVDG+SSTLSMS HFKMLKKLVEE TFS+IL
Sbjct  2194  KAISLNDSFMKFIGDANRLTDKLLELGNKPVDGNSSTLSMSVHFKMLKKLVEEPTFSQIL  2253

Query  2260  IPLQSVMIPTLPSILGTHANHASHEPFPGHWAYIAGFDDMVEILASLQKPKKISLKGSDG  2319
             IPLQSV+IPTLPS  G +     H+ FPGHW Y++GFDD VEILASLQKPKKISLKGSDG
Sbjct  2254  IPLQSVLIPTLPSTGGANPK---HDAFPGHWVYLSGFDDTVEILASLQKPKKISLKGSDG  2310

Query  2320  KFYIMMCKPKDDLRKDCRLMEFNSLINKCLRKDAESRRRELHIRTYAVIPLNDECGIIEW  2379
             KFY MMCKPKDDLRKDCRLMEFN LINK LRKDAESRRR+L IRTYAVIPLN+ECGIIEW
Sbjct  2311  KFYTMMCKPKDDLRKDCRLMEFNCLINKSLRKDAESRRRDLRIRTYAVIPLNEECGIIEW  2370

Query  2380  VNNTAGLRPILTKLYKEKGVYMTGKELRQCMLPKSAALSEKLKVFREFLLPRHPPIFHEW  2439
             VN TAGLR ILTKLYKEKG+Y++G EL++ +LPK+A   EKLK+ ++ L  RHPP+FHEW
Sbjct  2371  VNKTAGLRHILTKLYKEKGIYVSGTELKKLILPKTAPFQEKLKLHKDVLCARHPPVFHEW  2430

Query  2440  FLRTFPDPTSWYSSRSAYCRSTAVMSMVGYILGLGDRHGENILFDSLTGECVHVDFNCLF  2499
             FLRTFPDPTSWY+SRSAYCRSTAVMSMVGYILGLGDRHGENILFDS TGECVHVDFNCLF
Sbjct  2431  FLRTFPDPTSWYNSRSAYCRSTAVMSMVGYILGLGDRHGENILFDSFTGECVHVDFNCLF  2490

Query  2500  NKGETFEVPEIVPFRLTHNMVNGMGPMGTEGLFRRACEVTMRLMRDQREPLMSVLKTFLH  2559
             NKGETF+VPE+VPFRLT NMV+ MGPMGTEGLFR+ACEV +RLMRDQREPLMSVLKTFLH
Sbjct  2491  NKGETFDVPEVVPFRLTQNMVHAMGPMGTEGLFRQACEVILRLMRDQREPLMSVLKTFLH  2550

Query  2560  DPLVEWSKPVKGHSKAPLNETGEVVNEKAKTHVLDIEQRLQGVIKTRNRVTGLPLSIEGH  2619
             DPLVEWSKPVKG SK  +NE+GE++NEKAKTHVLDIEQRLQGVIK RN+V GLPLSIEGH
Sbjct  2551  DPLVEWSKPVKGFSKTQVNESGEILNEKAKTHVLDIEQRLQGVIKNRNKVMGLPLSIEGH  2610

Query  2620  VHYLIQEATDENLLCQMYLGWTPYM  2644
             VHYLIQEATD+NLLC MYLGW PY+
Sbjct  2611  VHYLIQEATDDNLLCMMYLGWGPYL  2635
```

Appendix 6.5 Protein-Protein Blast Sequence Alignment of the DNA-PKcs zebrafish and human sequences

Query- Zebrafish   Subject-Human

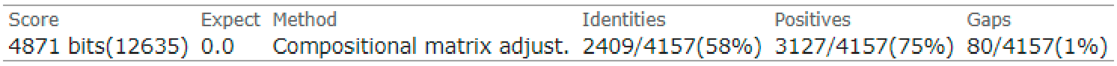

Score	Expect	Method	Identities	Positives	Gaps
4871 bits(12635)	0.0	Compositional matrix adjust.	2409/4157(58%)	3127/4157(75%)	80/4157(1%)

```
Query  6    AGVRCSLLRLQETLSAADRCGAALAGHQLIRGLGQECVLSSSPAVLALQTSLVFSRDFGL  65
             G++  LL+L  +L        A+  H +I  LGQEC+++ +   L LQTSL+F+++ GL
Sbjct  9    GGIQGYLLKLHSSLEDTVSTNVAIVCHDIIGDLGQECMITKNENELVLQTSLLFAKEEGL  68

Query  66   LVFVRKSLNSIEF--------RECREEILKFLCIFLEKMGQKI----APYSVEIKNTCTS  113
            L F+R+SL++ +         RE R EI+ FL  FL++M   +      Y+VE+K+TC
Sbjct  69   LSFLRRSLSTEKLGTTGVEILRETRVEIMNFLGAFLQRMSATVRGWEKNYAVELKDTCIV  128

Query  114  VYTKDRAAKCKIPALDLLIKLLQTFRSSRLMDEFKIGELFSKFYGELALKKKIPDTVLEK  173
            VYTKD++AKC+ PALDLLIK+L   + S +    +IG++F+KFYGEL  K KIPDTVL
Sbjct  129  VYTKDKSAKCRNPALDLLIKILYLTKDSSITQNLRIGDMFNKFYGELCQKHKIPDTVLGC  188

Query  174  VYELLGLLGEVHPSEMINNAENLFRAFLGELKTQMTSAVREPKLPVLAGCLKGLSSLLCN  233
            +YELLG+LGEVHPSEM+NN++ L++A+LGELK QMTS  +EPKLPV+AGCLKG+++L+ N
Sbjct  189  IYELLGVLGEVHPSEMVNNSDKLYKAYLGELKGQMTSTTKEPKLPVVAGCLKGIAALMVN  248

Query  234  FTKSMEEDPQTSREIFNFVLKAIRPQIDLKRYAVPSAGLRLFALHASQFSTCLLDNYVSL  293
            FTKS+EEDP  S+EIF++ LKAI PQ D+KRYAV  AGL+LFA H+SQF +CL+D+Y+S+
Sbjct  249  FTKSVEEDPAASKEIFDYALKAISPQTDIKRYAVIFAGLKLFAKHSSQFGSCLMDHYISI  308

Query  294  FEVLLKWCAHTNVELKKAALSALESFLKQVSNMVAKNAEMHKNKLQYFMEQFYGIIRNVD  353
            F+V+ K C H N ELKK++ +ALESFLKQV+ +VA+N E+HK+KL++FM++F  IIR +D
Sbjct  309  FDVMSKHCGHINAELKKSSYTALESFLKQVATLVAENIELHKSKLKFFMQKFCAIIRTMD  368

Query  354  SNNKELSIAIRGYGLFAGPCKVINAKDVDFMYVELIQRCKQMFLTQTDTGDDRVYQMPSF  413
            S NKELSIAIRGYGLFA PCKV+  +DVD MY ELIQRCKQM+LT++D  DD VYQ+PSF
Sbjct  369  STNKELSIAIRGYGLFAAPCKVVCPQDVDLMYTELIQRCKQMYLTESDRDDDNVYQLPSF  428

Query  414  LQSVASVLLYLDTVPEVYTPVLEHLVVMQIDSFPQYSPKMQLVCCRAIVKVFLALAAKGP  473
            L S+ASVL++LD +PEVYTPVLE L+V+Q+DSFPQYS +MQ   CR+IVKVF+A+A +GP
Sbjct  429  LDSIASVLVHLDRIPEVYTPVLERLLVVQMDSFPQYSQRMQHATCRSIVKVFVAMAVRGP  488

Query  474  VLRNCISTVVHQGLIRICSKPVVLP--KGPESESEDHRASGEVRTGKWKVPTYKDYVDLF  531
            VL +  S+VVHQGLIR+CSKPV+    +G  S       S  VR+GKWKVP+ KDY++LF
Sbjct  489  VLWSFTSSVVHQGLIRVCSKPVLQSDERGVSSGVSQSEDSTLVRSGKWKVPSSKDYLELF  548

Query  532  RHLLSSDQMMDSILADEAFFSVNSSSESLNHLLYDEFVKSVLKIVEKLDLTLEIQTVGEQ  591
            + LL  + + D+   D A  + N +   LN  LYD  V+SV+KIVEKLDL+++  +  ++
Sbjct  549  KGLLDCENLKDTGFVDGAPAAKNYNLRDLNRHLYDALVQSVMKIVEKLDLSVQKVSAADE  608

Query  592  ENGDEAPGVWMIPTSDPAANLHPAKPKDFSAFINLVEFCREILPEKQAEFFEPWVYSFSY  651
               D + G+  + +SDP ANL P KPKDF AFINLV+FC E+LP +  E+F  W++   +
Sbjct  609  VQSDASAGI--VLSSDPTANLMPNKPKDFIAFINLVDFCSELLPSRNPEYFAQWMHPLCH  666

Query  652  ELILQSTRLPLISGFYKLLSITVRNAKKIKYFEGVS--PKSLKHSPEDPEKYSCFALFVK  709
            ELILQS R PL+SGFYKLLS+++  AKK +YF+ V   PK +  S  +    +CF+L  K
Sbjct  667  ELILQSIRFPLVSGFYKLLSLSMGIAKKTQYFQDVKQCPKQVGGSTMEN---ACFSLLAK  723

Query  710  FGKEVAVKMKQYKDELLASCLTFLLSLPHNIIELDVRAYVPALQMAFKLGLSYTPLAEVG  769
            FGKEV V+MKQYKDELLA+CL F+LSL   ++ LD++AY+PALQ A +LGLS+ PLA
Sbjct  724  FGKEVCVRMKQYKDELLAACLMFILSLHPGMVALDIKAYIPALQAALRLGLSHAPLATAA  783

Query  770  LNALEEWSIYIDRHVMQPYYKDILPCLDGYLKTSALSDETKNNWEVSALSRAAQKGFNKV  829
            L+ALE WS +I   ++QP+Y DILP LDGYLKT++ S++  +N EV+ +S  + KG+ +V
Sbjct  784  LDALESWSSFIPAAILQPHYTDILPHLDGYLKTTSSSEKDDSNMEVTFVSTGSSKGYGQV  843
```

```
Query  830   VLKHLKKTKNLSSNEAISLEEIRIRVVQMLGSLGGQINKNLLTVTSSDEMMKSYVAWDRE  889
             +L+ LKK+K  S  +   +  +R RVV++LG LGGQ+N++L+T  S+++MMK +VAWD E
Sbjct  844   LLRLLKKSKRFSLGDESPIAAVRRRVVRLLGHLGGQLNRSLVTAVSAEDMMKRFVAWDCE  903

Query  890   KRLSFAVPFREMKPVIFLDVFLPRVTELALTASDRQTKVAACELLHSMVMFMLGKATQMP  949
             KRLSFAVPF++MKPVI+LD FLPRVTELAL++SDRQTKVAACELLHS+V++M+GK  QM
Sbjct  904   KRLSFAVPFKDMKPVIYLDSFLPRVTELALSSSDRQTKVAACELLHSLVIYMVGKGAQMT  963

Query  950   EGGQGAPPMYQLYKRTFPVLLRLACDVDQVTRQLYEPLVMQLIHWFTNNKKFESQDTVAL  1009
             E  + APPMY L+++ FPVLLRLACDVDQVTRQL+EPLVMQLIHWFTNN+KFESQDTVA+
Sbjct  964   EDDKSAPPMYNLHRKVFPVLLRLACDVDQVTRQLFEPLVMQLIHWFTNNRKFESQDTVAV  1023

Query  1010  LEAILDGIVDPVDSTLRDFCGRCIREFLKWSIKQITPQQQEKSPVNTKSLFKRLYSLALH  1069
             LEAILDGIVDP+DSTLRDF G CI+EF+KWSIKQ TP+QQEKSP N KSLFKR+YSLALH
Sbjct  1024  LEAILDGIVDPLDSTLRDFSGTCIQEFVKWSIKQTTPKQQEKSPANMKSLFKRIYSLALH  1083

Query  1070  PNAFKRLGASLAFNNIYREFREEESLVEQFVFEALVIYMESLALAHADEKSLGTIQQCCD  1129
             P+ FKRLGA+LAFN++YR+FREE SLVEQFVFE LV+++ESLALAH DEKS+GT+QQCC
Sbjct  1084  PSVFKRLGAALAFNSMYRQFREESSLVEQFVFEVLVVFVESLALAHFDEKSVGTVQQCCS  1143

Query  1130  AIDHLCRIIEKKHVSLNKAKKRRLPRGFPPSASLCLLDLVKWLLAHCGRPQTECRHKSIE  1189
             ++DHL RII+ K  SLN   KRR+PRGFP   S+CL ++V WLL  CGRPQTECRHKS+E
Sbjct  1144  SLDHLKRIIKHKADSLNINSKRRIPRGFPADQSVCLSNVVLWLLTQCGRPQTECRHKSME  1203

Query  1190  LFYKFVPLLPGNRSPNLWLKDVLKEEGVSFLINTFEGGGCGQPSGILAQPTLLYLRGPFS  1249
             LF++FVPLLPGN SP +WL + LK+ G  FLI+  EGG      G+L+QPTL  +  PFS
Sbjct  1204  LFFEFVPLLPGNSSPAMWLDEQLKQRGPGFLISCLEGG------GLLSQPTLREIEAPFS  1257

Query  1250  LQATLCWLDLLLAALECYNTFIGERTVGALQVLGTEAQSSLLKAVAFFLESIAMHDIIAA  1309
             ++ TL W+DLLLAAL+CYNTF   R +   ++LGT  +SS L AV FFL  ++M DI AA
Sbjct  1258  IRGTLQWMDLLLAALDCYNTFTNLRCLQLQRILGTCEKSSFLPAVHFFLTELSMQDIQAA  1317

Query  1310  EKCFGTGAAG-NRTSPQEGERYNYSKCTVVVRIMEFTTTLLNTSPEG-WKLLKKDLCNTH  1367
               CF  G AG +  SP+E E+YNYSKC+++VR++EF+T +L   P+  WKL++KD+ N+
Sbjct  1318  RACFRLGNAGQSHFSPRETEQYNYSKCSIIVRMLEFSTMVLQKCPQDLWKLMEKDVFNSS  1377

Query  1368  LMRVLVQTLCEPASIGFNIGDVQVMAHLPDVCVNLMKALKMSPYKDILETHLREKITAQS  1427
             L  ++V  +CEP+SIGFN+ D++VM HLP+VC  L+KAL  +PY+  LE+ +R +IT QS
Sbjct  1378  LFTLVVLAVCEPSSIGFNMADLEVMTHLPEVCFPLLKALASAPYRTQLESCIRMRITKQS  1437

Query  1428  IEELCAVNLYGPDAQVDRSRLAAVVSACKQLHRAGLLHNILPSQSTDLHHSVGTELLSLV  1487
             +EELCA++LY  D +   + +  ++SAC+QLH++GLL+++L SQ      S+G++LL+ V
Sbjct  1438  VEELCAIDLYETDTRNSHASMNLLLSACRQLHQSGLLNSVLHSQDASYGCSLGSKLLTSV  1497

Query  1488  YKGIAPGDERQCLPSLDLSCKQLASGLLELAFAFGGLCERLVSLLLNPAVLSTASLGSSQ  1547
             YK IAPG +R+ LPS+D+  ++LA  L++L+F  G   E+ V LLLN   LS    GS
Sbjct  1498  YKSIAPGTDRKSLPSMDVGSRKLADRLVQLSFCLGDQSEQTVGLLLNTITLSVPLSGSLN  1557

Query  1548  GSVIHFSHGEYFYSLFSETINTELLKNLDLAVLELMQSSVDNTKMVSAVLNGMLDQSFRE  1607
                + FSHGEYFYSLF  ++NTELL+++D +V  L+ S+  N  MVS +LNGMLD SFRE
Sbjct  1558  PHFLSFSHGEYFYSLFQTSLNTELLRSVDRSVPLLLSSANQNPSMVSVLLNGMLDHSFRE  1617

Query  1608  RANQKHQGLKLATTILQHWKKCDSWWAKDSPL---ETKMAVLALLAKILQIDSSVSFNTS  1664
             R+ +K QG +LA  +L+ W     WW  D P    E+K +VL+LLAK+LQIDSSV  NTS
Sbjct  1618  RSVRKSQGSQLAEQVLKGWDLLRPWW--DGPAATPESKTSVLSLLAKVLQIDSSVCSNTS  1675

Query  1665  HGSFPEVFTTYISLLADTKLDLHLKGQAVTLLPFFTSLTGGSLEELRRVLEQLIVAHFPM  1724
             H +F  VFTT+ +LL D  + L+LK QA+ +LPFFT+L    LEELRR LE L+  HFPM
Sbjct  1676  HPAFNAVFTTFTALLTDVSMPLNLKSQALIMLPFFTALPSMPLEELRRALESLVATHFPM  1735

Query  1725  QSREFPPGTPRFNNYVDCMKKFLDALELSQSPMLLELMTEVLCREQQHVMEELFQSSFRR  1784
             QS EFP G+ + NNY+DC++KFL+AL+LSQSP+LL+LM  VLCR+++H+MEELFQ+ F++
Sbjct  1736  QSDEFPRGSLQCNNYMDCIRKFLEALQLSQSPLLLKLMARVLCRDKKHIMEELFQACFQK  1795

Query  1785  IARRGSCVTQVGLLESVYEMFRKDDPRLSFTRQSFVDRSLLTLLWHCSLDALREFFSTIV  1844
```

```
             IA +     QV LL S Y+ F+  +   +F     +DR LL L  HCS  AL +FF + +
Sbjct  1796  IAHQSYLGKQVLLLSSTYQSFQAKEVPSNFMLMGLIDRVLLPLASHCSPQALSQFFISNI  1855

Query  1845  VDAIDVLKSRFTKLNESTFDTQITKKMGYYKILDVMYSRLPKDDVHAKESKINQVFHGSC  1904
              D +  L++RFTK  ES F++QI  K+G  K+L+V+YSRLPK++V++K S INQ F G+
Sbjct  1856  ADIMTTLQTRFTKSVESVFESQIMMKIGCCKLLEVLYSRLPKEEVYSKNSAINQAFCGTG  1915

Query  1905  ITEGNELTKTLIKLCYDAFTENMAGENQLLERRRLYHCAAYNCAISVICCVFNELKFYQG  1964
               EGNEL+K L+K C++AFTENM GE  LLE RR +HCAAYNCAI++I C FNE KFYQG
Sbjct  1916  CAEGNELSKNLLKSCFEAFTENMTGEMVLLELRRQFHCAAYNCAIALISCSFNETKFYQG  1975

Query  1965  FLFSEKPEKNLLIFENLIDLKRRYNFPVEVEVPMERKKKYIEIRKEAREAANGDSDGPSY  2024
             FLF+EKP+KN  IF+NLID +R YNFP+E++VP+ERKKKY+ IRKE     NGD+  P Y
Sbjct  1976  FLFTEKPDKNQFIFDNLIDSQRVYNFPIEIDVPIERKKKYVMIRKEV-SGENGDA--PVY  2032

Query  2025  MSSLSYLADSTLSEEMSQFDFSTGVQSYSYSSQDPRPATGRFRRREQRDPTVHDDVLELE  2084
             +SS SY+ADS+LSEEMSQFDFSTGVQS+SY+SQ+P   +   R RE+++    D+ +ELE
Sbjct  2033  LSSQSYMADSSLSEEMSQFDFSTGVQSFSYNSQNPSGVSSSSRMRERKEVLSQDETVELE  2092

Query  2085  MDELNRHECMAPLTALVKHMHRSLGPPQGEEDSVPRDLPSWMKFLHGKLGNPIVPLNIRL  2144
             MDELN+HECMA +TAL++HM R+   P+ EE   P DLP WMKFL GKL NP  PLNIRL
Sbjct  2093  MDELNQHECMANMTALLRHMQRNNITPKVEEGVRPSDLPPWMKFLQGKLDNPSTPLNIRL  2152

Query  2145  FLAKLVINTEEVFRPYAKHWLSPLLQLAASENNGGEGIHYMVVEIVATILSWTGLATPTG  2204
             F+AKL+INTEE+FRPYAKHWL PL+QL  S +NGGEGIH+MVV+IV T+LSW  +A+P G
Sbjct  2153  FIAKLIINTEEIFRPYAKHWLGPLMQLVVSSSNGGEGIHFMVVDIVVTVLSWASVASPKG  2212

Query  2205  VPKDEVLANRLLNFLMKHVFHPKRAVFRHNLEIIKTLVECWKDCLSIPYRLIFEKFSGKD  2264
               +DEVL NRLL FL K+ FH KRAVFRHNLEII+T+VECWKDCL+IPY LI+E+F+G D
Sbjct  2213  NTRDEVLVNRLLGFLFKNCFHSKRAVFRHNLEIIRTVVECWKDCLTIPYDLIYERFAGTD  2272

Query  2265  PNSKDNSVGIQLLGIVMANDLPPYDPQCGIQSSEYFQALVNNMSFVRYKEVYAAAAEVLG  2324
             PNSKDNSVGIQLLGIVMAN+LPPYD  CGI+   YFQ+L NN+SF+RYKEVY+AAAEV+G
Sbjct  2273  PNSKDNSVGIQLLGIVMANNLPPYDAACGIEHDRYFQSLANNLSFIRYKEVYSAAAEVIG  2332

Query  2325  LILRYVMERKNILEESLCEL-VAKQLKQHQNTMEDKFIVCLNKVTKSFPPLADRFMNAVF  2383
             LIL Y+ ER+N +E +L  + V K +   +  ++DKFIVCL+KV+K FPPL DRF+N VF
Sbjct  2333  LILNYMTERENQIEGTLFNITVTKLMDLRKKEVDDKFIVCLSKVSKHFPPLVDRFINPVF  2392

Query  2384  FLLPKFHGVLKTLCLEVVLCRVEGMTELYFQLKSKDFVQVMRHRDDERQKVCLDIIYKMM  2443
             +LLPK HG+LKT CLE VL R + + E++  LK+K   Q+M H+D+ RQ+VCLDII+K++
Sbjct  2393  YLLPKLHGMLKTHCLECVLSRADVIPEIFLHLKTKGLSQIMSHKDEGRQRVCLDIIHKIL  2452

Query  2444  PKLKPVELRELLNPVVEFVSHPSTTCREQMYNILMWIHDNYRDPESETDNDSQEIFKLAK  2503
               LKP EL+E+L  V  F SHPS  CRE+MY+ILMWI DNY D ES  D+ S E+  +A+
Sbjct  2453  ACLKPEELKEILGAVTAFASHPSPVCRERMYDILMWIQDNYSDSESREDSTSVEVLSVAR  2512

Query  2504  DVLIQGLIDENPGLQLIIRNFWSHETRLPSNTLDRLL-ALNSLYSPKIEVHFLSLATNFL  2562
             + L+QGL DEN GLQL +RNFWSHE+RLP  TL+R+L  L SLYS +IE  FLSLAT+ L
Sbjct  2513  ETLLQGLTDENYGLQLYVRNFWSHESRLPPETLERMLVVLKSLYSSRIEEQFLSLATDLL  2572

Query  2563  LEMTSMSPDYPNPMFEHPLSECEFQEYTIDSDWRFRSTVLTPMFVETQASQGTLQTRTQE  2622
             LEMTS SPD+   MFE PLSEC+FQ+YTIDS+WR RSTVLTPMF+ETQA+QG     +Q
Sbjct  2573  LEMTSHSPDFTRNMFEFPLSECKFQDYTIDSNWRMRSTVLTPMFMETQATQGAEAAGSQA  2632

Query  2623  GSLSARWPVAGQIRATQQQHDF--TLTQTADGRSSFDWLTGSSTDPLVDH---TSPSSDS  2677
              +      V GQIRATQ   +F  TL   A  RS+++WLTGSS D L D+   +   S
Sbjct  2633  AT------VRGQIRATQTSLEFSQTLAPGAGRRSAYNWLTGSSVDTLADYSLSSDSLSSL  2686

Query  2678  LLFAHKRSERLQRAPLKSVGPDFGKKRLGLPGDEVDNKVKGA-AGRTDLLRLRRRFMRDQ  2736
             L+F  KRSER Q A  ++VG  FG KRL    D+ D++       R D+LRLRRRF++D+
Sbjct  2687  LVFDKKRSERPQ-AAWRAVGAGFGSKRLTATSDDTDSRTAAERERRADILRLRRRFLKDK  2745

Query  2737  EKLSLMYARKGVAEQKREKEIKSELKMKQDAQVVLYRSYRHGDLPDIQIKHSSLITPLQA  2796
             EK S+ +A+K +  Q+ E+E +++LK++QDAQV LYRSYR GDLPDIQI+ SSLI PLQA
Sbjct  2746  EKESIKFAKKEIHSQRTERERRADLKIRQDAQVTLYRSYRVGDLPDIQIQFSSLIAPLQA  2805
```

```
Query  2797  VAQRDPIIAKQLFSSLFSGILKEMDKFKTLSEKNNITQKLLQDFNRFLNTTFSFFPPFVS  2856
             +AQRD  +AKQLFSSLF+G+L EM++ K+  E  +I ++L+Q  N FLN +  +FPPF+S
Sbjct  2806  LAQRDATLAKQLFSSLFAGVLVEMERLKSNKETADILKELVQTLNAFLNKSTVYFPPFIS  2865

Query  2857  CIQDISCQHAALLSLDPAAVSAGCLASLQQPVGIRLLEEALLRLLPA--ELPAKRVRGKA  2914
             CIQD+S  H ALL ++P+ VSA CLASLQQP+GI LLEE+LL    A  E P KR RGK
Sbjct  2866  CIQDMSYHHKALLGVEPSLVSATCLASLQQPMGILLLEESLLHGAGASEEPPLKRARGKR  2925

Query  2915  RLPPDVLRWVELAKLYRSIGEYDVLRGIFTSEIGTKQITQSALLAEARSDYSEAAKQYDE  2974
              LPPD  RW+ LAKLYRS+G+YDV+RGIF+ +IGTK IT +AL AEA+SDY+EA K Y+E
Sbjct  2926  ELPPDTERWIHLAKLYRSLGDYDVVRGIFSGKIGTKSITFTALQAEAKSDYAEAVKLYNE  2985

Query  2975  ALNKQDWVDGEPTEAEKDFWELASLDCYNHLAEWKSLEYCSTASIDSENPPDLNKIWSEP  3034
             ALNK+DW DGEPT  EKDFWE+A+L+ YNHL EWKSLEYC+T +ID  +P  L+++W+E
Sbjct  2986  ALNKEDWDDGEPTITEKDFWEIAALEAYNHLTEWKSLEYCATVNIDDSSPIRLDRMWTET  3045

Query  3035  FYQETYLPYMIRSKLKLLLQGEADQSLLTFIDKAMHGELQKAILELHYSQELSLLYLLQD  3094
             FY ETYL YM+RS LK L  GE +Q LL+F+D AM  E  K I+E HYSQELSLLY+LQ+
Sbjct  3046  FYVETYLQYMMRSMLKQLQMGETNQDLLSFVDAAMKTEEHKIIMETHYSQELSLLYILQE  3105

Query  3095  DVDRAKYYIQNGIQSFMQNYSSIDVLLHQSRLTKLQSVQALTEIQEFISFISKQGNLSSQ  3154
             D DRAKYY  N +Q FMQNYSSID LL++SRLT LQSVQALTEIQ+F+++I+   +++S
Sbjct  3106  DYDRAKYYANNCMQVFMQNYSSIDPLLNRSRLTVLQSVQALTEIQDFLNYITGDVSVNS-  3164

Query  3155  VPLKRLLNTWTNRYPDAKMDPMNIWDDIITNRCFFLSKIEEKLTPLPEDNSMNVDQDGDP  3214
               LK ++  WT+ YPDAK+DPMN+WDDIIT+RCFFL KI ++L   PE NSM VD
Sbjct  3165  --LKFMIRRWTSHYPDAKLDPMNVWDDIITSRCFFLDKILKRLKSTPE-NSMEVDGAD--  3219

Query  3215  SDRMEVQEQEEDISSLIRSCKFSMKMKMIDSARKQNNFSLAMKLLKELHKESKTRDDWLV  3274
                   Q   E++  L+++CKF+MK++M DSA KQNNF +A KLLKELH+ +K  D  L+
Sbjct  3220  ------QGSGEELGVLVKTCKFNMKLQMADSAWKQNNFPVASKLLKELHRHAKIDDARLL  3273

Query  3275  SWVQSYCRLSHCRSRSQGCSEQVLTVLKTVSLL-DENNVSSYLSKNILAFRDQNILLGTT  3333
              WV S+ R +H R    G SE++  +LKTV LL D    S  LS  +L  RDQ ILLGTT
Sbjct  3274  RWVHSFSRFTHKRIARLGPSEKINALLKTVPLLKDAERQSEALSARML--RDQRILLGTT  3331

Query  3334  YRIIANALSSEPACLAEIEEDKARRILELSGSSSEDSEKVIAGLYQRAFQHLSEAVQAAE  3393
             Y ++A A    P  L  + E+K ++IL+LS +SS    +V+ GL  +A + L  A   AE
Sbjct  3332  YDLMAGAADRSPFALETLGEEKVQKILQLSQASS--IAQVVEGLQIQALELLRSAACKAE  3389

Query  3394  EEAQPPSWSCGPAAGVIDAYMTLADFCDQQLRKEEENASVIDSAELQAYPALVVEKMLKA  3453
             EE Q  S       G+++AYMT+A+FCD++LR+ E+    I S++LQ+ P  VV+ MLKA
Sbjct  3390  EEEQSFSQQHVNTHGIVEAYMTMANFCDRRLRESEQKEEAI-SSKLQSLPEHVVKMMLKA  3448

Query  3454  LKLNSNEARLKFPRLLQIIERYPEETLSLMTKEISSVPCWQFISWISHMVALLDKDQAVA  3513
             LKL+S EARLKFPRLLQ++E YP ETL LM +E+ SVPCW  I WIS M+ALLDK QA A
Sbjct  3449  LKLSSEEARLKFPRLLQLVEVYPAETLDLMVREVVSVPCWLLIGWISQMMALLDKPQATA  3508

Query  3514  VQHSVEEITDNYPQAIVYPFIISSESYSFKDTSTGHKNKEFVARIKSKLDQGGVIQDFIN  3573
             VQH +EEI + YPQA++YP++ISSE+Y+F+++++G +N+EFV +++S LD+GGVIQ F++
Sbjct  3509  VQHVIEEIAECYPQALIYPYMISSENYTFEESASGQRNREFVEKLESLLDKGGVIQGFVD  3568

Query  3574  ALDQLSNPELLFKDWSNDVRAELAKTPVNKKNIEKMYERMYAALGDPKAPGLGAFRRKFI  3633
             AL QLSNPE+LFKDW ++V+ +L K  ++KK ++  Y  M   LGD K+P  G++RRKFI
Sbjct  3569  ALQQLSNPEMLFKDWWDEVKNQLDKPNLDKKKMKLQY--MTELLGDAKSPRFGSYRRKFI  3626

Query  3634  QTFGKEFDKHFGKGGSKLL-RMKLSDFNDITNMLLLKMNKDSKPPGNLKECSPWMSDFKV  3692
             Q F KE +K  G GGSKL  R K  DF    + ++  M    K PGN+KE SPW+S FK
Sbjct  3627  QKFSKEVEKLLGAGGSKLYERRKDKDFLQQVDRMVQSMRGFQKEPGNMKEYSPWLSSFKA  3686

Query  3693  EFLRNELEIPGQYDGRGKPLPEYHVRIAGFDERVTVMASLRRPKRIIIRGHDEREHPFLV  3752
             E L+NELE+PGQYDG+ KPLPEYH +I GFDERV VM S+RRPKRIIIRG DER++PFLV
Sbjct  3687  ETLKNELEVPGQYDGKSKPLPEYHAKITGFDERVKVMTSIRRPKRIIIRGDDERDYPFLV  3746

Query  3753  KGGEDLRQDQRVEQLFQVMNGILAQDSACSQRALQLRTYSVVPMTSRLGLIEWLENTVTL  3812
```

```
             KGGEDLRQDQR+EQLF VMN IL+QD+ACSQR+L LRTY V+P+TSR+GLIEW+ENT TL
Sbjct  3747  KGGEDLRQDQRIEQLFGVMNMILSQDTACSQRSLALRTYQVIPITSRIGLIEWMENTCTL  3806

Query  3813  KDLLLNTMSQEEKAAYLSDPRAPPCEYKDWLTKMSGK-HDVGAYMLMYKGANRTETVTSF  3871
             KD L +  +++E+         P   Y +W++K++GK   +  Y  +YK A R +TV +F
Sbjct  3807  KDFLSSRRTEQEQKTITR----PNEFYDEWISKVAGKVEGIRRYAELYKKAKRVDTVNNF  3862

Query  3872  RKRESKVPADLLKRAFVRMSTSPEAFLALRSHFASSHALICISHWILGIGDRHLNNFMVA  3931
             R+ E  VP DLLKRAFVRMST+PEAFL+LRSHF+SSHA++CISHWILGIGDRHL+NFM+
Sbjct  3863  RRIEQMVPDDLLKRAFVRMSTTPEAFLSLRSHFSSSHAVLCISHWILGIGDRHLSNFMIN  3922

Query  3932  METGGVIGIDFGHAFGSATQFLPVPELMPFRLTRQFINLMLPMKETGLMYSIMVHALRAF  3991
              ETGG+IGIDFGHAFGSATQFLPVPELMPFRLTRQFINLM P+ E+GL+ S+MVH+LRAF
Sbjct  3923  TETGGMIGIDFGHAFGSATQFLPVPELMPFRLTRQFINLMRPLAESGLIQSVMVHSLRAF  3982

Query  3992  RSDPGLLTNTMDVFVKEPSFDWKNFEQKMLKKGGSWIQEINVAEKNWYPRQKICYAKRKL  4051
             R++P LL NTMDVFVKEPS DWKNFE K LKKGG+W + +N  E NW+P QK+ +A+RKL
Sbjct  3983  RAEPDLLLNTMDVFVKEPSLDWKNFELKQLKKGGTWTESVNTKEINWFPLQKVNFARRKL  4042

Query  4052  AGANPAVITCDELLLGHEKAPAFRDYVAVARGSKDHNIRAQEPESGLSEETQVKCLMDQA  4111
              G NP+VIT +EL LG EK P ++  +AVARG + HNIRA+  +  L+ E QV CL+DQA
Sbjct  4043  EGTNPSVITSEELCLGFEKMPEYKGLLAVARGEEQHNIRARLADKDLTVEDQVDCLLDQA  4102

Query  4112  TDPNILGRTWEGWEPWM  4128
             TDPNILGR W GWEPW+
Sbjct  4103  TDPNILGRVWIGWEPWI  4119
```

Appendix Bibliography

1. Orr HT, Chung MY, Banfi S, Kwiatkowski TJ, Jr., Servadio A, Beaudet AL, et al. Expansion of an unstable trinucleotide CAG repeat in spinocerebellar ataxia type 1. Nat Genet. 1993;4(3):221-6.

2. Banfi S, Servadio A, Chung MY, Kwiatkowski TJ, Jr., McCall AE, Duvick LA, et al. Identification and characterization of the gene causing type 1 spinocerebellar ataxia. Nat Genet. 1994;7(4):513-20.

3. Servadio A, Koshy B, Armstrong D, Antalffy B, Orr HT, Zoghbi HY. Expression analysis of the ataxin-1 protein in tissues from normal and spinocerebellar ataxia type 1 individuals. Nat Genet. 1995;10(1):94-8.

4. Zuhlke C, Dalski A, Hellenbroich Y, Bubel S, Schwinger E, Burk K. Spinocerebellar ataxia type 1 (SCA1): phenotype-genotype correlation studies in intermediate alleles. Eur J Hum Genet. 2002;10(3):204-9.

5. Robitaille Y, Schut L, Kish SJ. Structural and immunocytochemical features of olivopontocerebellar atrophy caused by the spinocerebellar ataxia type 1 (SCA-1) mutation define a unique phenotype. Acta Neuropathol. 1995;90(6):572-81.

6. de Chiara C, Giannini C, Adinolfi S, de Boer J, Guida S, Ramos A, et al. The AXH module: an independently folded domain common to ataxin-1 and HBP1. FEBS Lett. 2003;551(1-3):107-12.

7. Goold R, Hubank M, Hunt A, Holton J, Menon RP, Revesz T, et al. Down-regulation of the dopamine receptor D2 in mice lacking ataxin 1. Hum Mol Genet. 2007;16(17):2122-34.

8. Chen YW, Allen MD, Veprintsev DB, Lowe J, Bycroft M. The structure of the AXH domain of spinocerebellar ataxin-1. J Biol Chem. 2004;279(5):3758-65.

9. Yue S, Serra HG, Zoghbi HY, Orr HT. The spinocerebellar ataxia type 1 protein, ataxin-1, has RNA-binding activity that is inversely affected by the length of its polyglutamine tract. Hum Mol Genet. 2001;10(1):25-30.

10. Lim J, Crespo-Barreto J, Jafar-Nejad P, Bowman AB, Richman R, Hill DE, et al. Opposing effects of polyglutamine expansion on native protein complexes contribute to SCA1. Nature. 2008;452(7188):713-8.

11. de Chiara C, Menon RP, Strom M, Gibson TJ, Pastore A. Phosphorylation of S776 and 14-3-3 binding modulate ataxin-1 interaction with splicing factors. PLoS One. 2009;4(12):e8372.

12. Matilla A, Koshy BT, Cummings CJ, Isobe T, Orr HT, Zoghbi HY. The cerebellar leucine-rich acidic nuclear protein interacts with ataxin-1. Nature. 1997;389(6654):974-8.

13. Tong X, Gui H, Jin F, Heck BW, Lin P, Ma J, et al. Ataxin-1 and Brother of ataxin-1 are components of the Notch signalling pathway. EMBO Rep. 2011;12(5):428-35.

14. Tsai CC, Kao HY, Mitzutani A, Banayo E, Rajan H, McKeown M, et al. Ataxin 1, a SCA1 neurodegenerative disorder protein, is functionally linked to the silencing mediator of retinoid and thyroid hormone receptors. Proceedings of the National Academy of Sciences of the United States of America. 2004;101(12):4047-52.

15. Eto K, Sumi SM, Bird TD, McEvoy-Bush T, Boehnke M, Schellenberg G. Family with dominantly inherited ataxia, amyotrophy, and peripheral sensory loss. Spinopontine atrophy or Machado-Joseph Azorean disease in another non-Portuguese family? Arch Neurol. 1990;47(9):968-74.

16. Babovic-Vuksanovic D, Snow K, Patterson MC, Michels VV. Spinocerebellar ataxia type 2 (SCA 2) in an infant with extreme CAG repeat expansion. Am J Med Genet. 1998;79(5):383-7.

17. Ralser M, Albrecht M, Nonhoff U, Lengauer T, Lehrach H, Krobitsch S. An integrative approach to gain insights into the cellular function of human ataxin-2. J Mol Biol. 2005;346(1):203-14.

18. Satterfield TF, Pallanck LJ. Ataxin-2 and its Drosophila homolog, ATX2, physically assemble with polyribosomes. Hum Mol Genet. 2006;15(16):2523-32.

19. Hallen L, Klein H, Stoschek C, Wehrmeyer S, Nonhoff U, Ralser M, et al. The KRAB-containing zinc-finger transcriptional regulator ZBRK1 activates SCA2 gene transcription through direct interaction with its gene product, ataxin-2. Hum Mol Genet. 2011;20(1):104-14.

20. Li L, Saegusa H, Tanabe T. Deficit of heat shock transcription factor 1-heat shock 70 kDa protein 1A axis determines the cell death vulnerability in a model of spinocerebellar ataxia type 6. Genes Cells. 2009;14(11):1253-69.

21. Buttner N, Geschwind D, Jen JC, Perlman S, Pulst SM, Baloh RW. Oculomotor phenotypes in autosomal dominant ataxias. Arch Neurol. 1998;55(10):1353-7.

22. Takiyama Y, Nishizawa M, Tanaka H, Kawashima S, Sakamoto H, Karube Y, et al. The gene for Machado-Joseph disease maps to human chromosome 14q. Nat Genet. 1993;4(3):300-4.

23. St George-Hyslop P, Rogaeva E, Huterer J, Tsuda T, Santos J, Haines JL, et al. Machado-Joseph disease in pedigrees of Azorean descent is linked to chromosome 14. Am J Hum Genet. 1994;55(1):120-5.

24. Schols L, Vieira-Saecker AM, Schols S, Przuntek H, Epplen JT, Riess O. Trinucleotide expansion within the MJD1 gene presents clinically as spinocerebellar ataxia and occurs most frequently in German SCA patients. Hum Mol Genet. 1995;4(6):1001-5.

25. Shimohata T, Nakajima T, Yamada M, Uchida C, Onodera O, Naruse S, et al. Expanded polyglutamine stretches interact with TAFII130, interfering with CREB-dependent transcription. Nat Genet. 2000;26(1):29-36.

26. Takahashi J, Tanaka J, Arai K, Funata N, Hattori T, Fukuda T, et al. Recruitment of nonexpanded polyglutamine proteins to intranuclear aggregates in neuronal intranuclear hyaline inclusion disease. J Neuropathol Exp Neurol. 2001;60(4):369-76.

27. McCampbell A, Taylor JP, Taye AA, Robitschek J, Li M, Walcott J, et al. CREB-binding protein sequestration by expanded polyglutamine. Hum Mol Genet. 2000;9(14):2197-202.

28. Chai Y, Shao J, Miller VM, Williams A, Paulson HL. Live-cell imaging reveals divergent intracellular dynamics of polyglutamine disease proteins and supports a sequestration model of pathogenesis. Proc Natl Acad Sci U S A. 2002;99(14):9310-5.

29. Evert BO, Araujo J, Vieira-Saecker AM, de Vos RA, Harendza S, Klockgether T, et al. Ataxin-3 represses transcription via chromatin binding, interaction with histone deacetylase 3, and histone deacetylation. J Neurosci. 2006;26(44):11474-86.

30. Wang G, Sawai N, Kotliarova S, Kanazawa I, Nukina N. Ataxin-3, the MJD1 gene product, interacts with the two human homologs of yeast DNA repair protein RAD23, HHR23A and HHR23B. Hum Mol Genet. 2000;9(12):1795-803.

31. Evert BO, Vogt IR, Vieira-Saecker AM, Ozimek L, de Vos RAI, Brunt ERP, et al. Gene expression profiling in ataxin-3 expressing cell lines reveals distinct effects of normal and mutant ataxin-3. Journal of Neuropathology and Experimental Neurology. 2003;62(10):1006-18.

32. Evert BO, Araujo J, Vieira-Saecker AM, de Vos RAI, Harendza S, Klockgether T, et al. Ataxin-3 represses transcription via chromatin binding, interaction with histone deacetylase 3, and histone deacetylation. Journal of Neuroscience. 2006;26(44):11474-86.

33. Araujo J, Breuer P, Dieringer S, Krauss S, Dorn S, Zimmermann K, et al. FOXO4-dependent upregulation of superoxide dismutase-2 in response to oxidative stress is impaired in spinocerebellar ataxia type 3. Hum Mol Genet. 2011;20(15):2928-41.

34. Zhuchenko O, Bailey J, Bonnen P, Ashizawa T, Stockton DW, Amos C, et al. Autosomal dominant cerebellar ataxia (SCA6) associated with small polyglutamine expansions in the alpha 1A-voltage-dependent calcium channel. Nat Genet. 1997;15(1):62-9.

35. Gomez CM, Thompson RM, Gammack JT, Perlman SL, Dobyns WB, Truwit CL, et al. Spinocerebellar ataxia type 6: gaze-evoked and vertical nystagmus, Purkinje cell degeneration, and variable age of onset. Ann Neurol. 1997;42(6):933-50.

36. Ishikawa K, Tanaka H, Saito M, Ohkoshi N, Fujita T, Yoshizawa K, et al. Japanese families with autosomal dominant pure cerebellar ataxia map to chromosome 19p13.1-p13.2 and are strongly associated with mild CAG expansions in the spinocerebellar ataxia type 6 gene in chromosome 19p13.1. Am J Hum Genet. 1997;61(2):336-46.

37. Benomar A, Krols L, Stevanin G, Cancel G, LeGuern E, David G, et al. The gene for autosomal dominant cerebellar ataxia with pigmentary macular dystrophy maps to chromosome 3p12-p21.1. Nat Genet. 1995;10(1):84-8.

38. David G, Abbas N, Coullin P, Stevanin G, Horta W, Gemmill R, et al. The gene for autosomal dominant cerebellar ataxia type II is located in a 5-cM region in 3p12-p13: Genetic and physical mapping of the SCA7 locus. American Journal of Human Genetics. 1996;59(6):1328-36.

39. Lindblad K, Savontaus ML, Stevanin G, Holmberg M, Digre K, Zander C, et al. An expanded CAG repeat sequence in spinocerebellar ataxia type 7. Genome Res. 1996;6(10):965-71.

40. David G, Abbas N, Stevanin G, Durr A, Yvert G, Cancel G, et al. Cloning of the SCA7 gene reveals a highly unstable CAG repeat expansion. Nat Genet. 1997;17(1):65-70.

41. Harding AE. The clinical features and classification of the late onset autosomal dominant cerebellar ataxias. A study of 11 families, including descendants of the 'the Drew family of Walworth'. Brain. 1982;105(Pt 1):1-28.

42. Wieczorek E, Brand M, Jacq X, Tora L. Function of TAF(II)-containing complex without TBP in transcription by RNA polymerase II. Nature. 1998;393(6681):187-91.

43. Brand M, Yamamoto K, Staub A, Tora L. Identification of TATA-binding protein-free TAFII-containing complex subunits suggests a role in nucleosome acetylation and signal transduction. The Journal of biological chemistry. 1999;274(26):18285-9.

44. Martinez E, Kundu TK, Fu J, Roeder RG. A human SPT3-TAFII31-GCN5-L acetylase complex distinct from transcription factor IID. J Biol Chem. 1998;273(37):23781-5.

45. Ogryzko VV, Kotani T, Zhang X, Schiltz RL, Howard T, Yang X-J, et al. Histone-like TAFs within the PCAF Histone Acetylase Complex. Cell. 1998;94(1):35-44.

46. Cancel G, Duyckaerts C, Holmberg M, Zander C, Yvert G, Lebre AS, et al. Distribution of ataxin-7 in normal human brain and retina. Brain. 2000;123 Pt 12:2519-30.

47. Lindenberg KS, Yvert G, Muller K, Landwehrmeyer GB. Expression analysis of ataxin-7 mRNA and protein in human brain: evidence for a widespread distribution and focal protein accumulation. Brain Pathol. 2000;10(3):385-94.

48. Nakamura Y, Tagawa K, Oka T, Sasabe T, Ito H, Shiwaku H, et al. Ataxin-7 associates with microtubules and stabilizes the cytoskeletal network. Hum Mol Genet. 2012;21(5):1099-110.

49. Nakamura K, Jeong SY, Uchihara T, Anno M, Nagashima K, Nagashima T, et al. SCA17, a novel autosomal dominant cerebellar ataxia caused by an expanded polyglutamine in TATA-binding protein. Hum Mol Genet. 2001;10(14):1441-8.

50. Koide R, Kobayashi S, Shimohata T, Ikeuchi T, Maruyama M, Saito M, et al. A neurological disease caused by an expanded CAG trinucleotide repeat in the TATA-binding protein gene: a new polyglutamine disease? Hum Mol Genet. 1999;8(11):2047-53.

51. Ikeda Y, Shizuka M, Watanabe M, Okamoto K, Shoji M. Molecular and clinical analyses of spinocerebellar ataxia type 8 in Japan. Neurology. 2000;54(4):950-5.

52. Ito H, Kawakami H, Wate R, Matsumoto S, Imai T, Hirano A, et al. Clinicopathologic investigation of a family with expanded SCA8 CTA/CTG repeats. Neurology. 2006;67(8):1479-81.

53. Koob MD, Moseley ML, Schut LJ, Benzow KA, Bird TD, Day JW, et al. An untranslated CTG expansion causes a novel form of spinocerebellar ataxia (SCA8). Nat Genet. 1999;21(4):379-84.

54. Daughters RS, Tuttle DL, Gao W, Ikeda Y, Moseley ML, Ebner TJ, et al. RNA gain-of-function in spinocerebellar ataxia type 8. PLoS Genet. 2009;5(8):e1000600.

55. Kuwano A, Morimoto Y, Nagai T, Fukushima Y, Ohashi H, Hasegawa T, et al. Precise chromosomal locations of the genes for dentatorubral-pallidoluysian atrophy (DRPLA), von Willebrand factor (F8vWF) and parathyroid hormone-like hormone (PTHLH) in human chromosome 12p by deletion mapping. Hum Genet. 1996;97(1):95-8.

56. Nagafuchi S, Yanagisawa H, Sato K, Shirayama T, Ohsaki E, Bundo M, et al. Dentatorubral and pallidoluysian atrophy expansion of an unstable CAG trinucleotide on chromosome 12p. Nat Genet. 1994;6(1):14-8.

57. Burke JR, Wingfield MS, Lewis KE, Roses AD, Lee JE, Hulette C, et al. The Haw River syndrome: dentatorubropallidoluysian atrophy (DRPLA) in an African-American family. Nat Genet. 1994;7(4):521-4.

58. Zhang S, Xu L, Lee J, Xu T. Drosophila atrophin homolog functions as a transcriptional corepressor in multiple developmental processes. Cell. 2002;108(1):45-56.

59. Wang L, Rajan H, Pitman JL, McKeown M, Tsai CC. Histone deacetylase-associating Atrophin proteins are nuclear receptor corepressors. Genes Dev. 2006;20(5):525-30.

60. Shen Y, Lee G, Choe Y, Zoltewicz JS, Peterson AS. Functional architecture of atrophins. J Biol Chem. 2007;282(7):5037-44.

61. Wood JD, Nucifora FC, Jr., Duan K, Zhang C, Wang J, Kim Y, et al. Atrophin-1, the dentato-rubral and pallido-luysian atrophy gene product, interacts with ETO/MTG8 in the nuclear matrix and represses transcription. J Cell Biol. 2000;150(5):939-48.

62. Alonso I, Jardim LB, Artigalas O, Saraiva-Pereira ML, Matsuura T, Ashizawa T, et al. Reduced penetrance of intermediate size alleles in spinocerebellar ataxia type 10. Neurology. 2006;66(10):1602-4.

63. Grewal RP, Tayag E, Figueroa KP, Zu L, Durazo A, Nunez C, et al. Clinical and genetic analysis of a distinct autosomal dominant spinocerebellar ataxia. Neurology. 1998;51(5):1423-6.

64. Matsuura T, Achari M, Khajavi M, Bachinski LL, Zoghbi HY, Ashizawa T. Mapping of the gene for a novel spinocerebellar ataxia with pure cerebellar signs and epilepsy. Ann Neurol. 1999;45(3):407-11.

65. Zu L, Figueroa KP, Grewal R, Pulst SM. Mapping of a new autosomal dominant spinocerebellar ataxia to chromosome 22. Am J Hum Genet. 1999;64(2):594-9.

66. Bahl S, Virdi K, Mittal U, Sachdeva MP, Kalla AK, Holmes SE, et al. Evidence of a common founder for SCA12 in the Indian population. Ann Hum Genet. 2005;69(Pt 5):528-34.

67. Holmes SE, O'Hearn EE, McInnis MG, Gorelick-Feldman DA, Kleiderlein JJ, Callahan C, et al. Expansion of a novel CAG trinucleotide repeat in the 5' region of PPP2R2B is associated with SCA12. Nat Genet. 1999;23(4):391-2.

68. Mayer RE, Hendrix P, Cron P, Matthies R, Stone SR, Goris J, et al. Structure of the 55-kDa regulatory subunit of protein phosphatase 2A: evidence for a neuronal-specific isoform. Biochemistry. 1991;30(15):3589-97.

69. Lin CH, Chen CM, Hou YT, Wu YR, Hsieh-Li HM, Su MT, et al. The CAG repeat in SCA12 functions as a cis element to up-regulate PPP2R2B expression. Hum Genet. 2010;128(2):205-12.

70. Nagaoka U, Takashima M, Ishikawa K, Yoshizawa K, Yoshizawa T, Ishikawa M, et al. A gene on SCA4 locus causes dominantly inherited pure cerebellar ataxia. Neurology. 2000;54(10):1971-5.

71. Li M, Ishikawa K, Toru S, Tomimitsu H, Takashima M, Goto J, et al. Physical map and haplotype analysis of 16q-linked autosomal dominant cerebellar ataxia (ADCA) type III in Japan. J Hum Genet. 2003;48(3):111-8.

72. Owada K, Ishikawa K, Toru S, Ishida G, Gomyoda M, Tao O, et al. A clinical, genetic, and neuropathologic study in a family with 16q-linked ADCA type III. Neurology. 2005;65(4):629-32.

73. Amino T, Ishikawa K, Toru S, Ishiguro T, Sato N, Tsunemi T, et al. Redefining the disease locus of 16q22.1-linked autosomal dominant cerebellar ataxia. J Hum Genet. 2007;52(8):643-9.

74. Ohata T, Yoshida K, Sakai H, Hamanoue H, Mizuguchi T, Shimizu Y, et al. A -16C>T substitution in the 5' UTR of the puratrophin-1 gene is prevalent in autosomal dominant cerebellar ataxia in Nagano. J Hum Genet. 2006;51(5):461-6.

75. Sato N, Amino T, Kobayashi K, Asakawa S, Ishiguro T, Tsunemi T, et al. Spinocerebellar ataxia type 31 is associated with "inserted" penta-nucleotide repeats containing (TGGAA)n. Am J Hum Genet. 2009;85(5):544-57.

76. Kobayashi H, Abe K, Matsuura T, Ikeda Y, Hitomi T, Akechi Y, et al. Expansion of intronic GGCCTG hexanucleotide repeat in NOP56 causes SCA36, a type of spinocerebellar ataxia accompanied by motor neuron involvement. Am J Hum Genet. 2011;89(1):121-30.

77. Garcia-Murias M, Quintans B, Arias M, Seixas AI, Cacheiro P, Tarrio R, et al. 'Costa da Morte' ataxia is spinocerebellar ataxia 36: clinical and genetic characterization. Brain. 2012;135(Pt 5):1423-35.

78. Gautier T, Berges T, Tollervey D, Hurt E. Nucleolar KKE/D repeat proteins Nop56p and Nop58p interact with Nop1p and are required for ribosome biogenesis. Mol Cell Biol. 1997;17(12):7088-98.

79. Schols L, Szymanski S, Peters S, Przuntek H, Epplen JT, Hardt C, et al. Genetic background of apparently idiopathic sporadic cerebellar ataxia. Hum Genet. 2000;107(2):132-7.

80. Mallaret M, Synofzik M, Lee J, Sagum CA, Mahajnah M, Sharkia R, et al. The tumour suppressor gene WWOX is mutated in autosomal recessive cerebellar ataxia with epilepsy and mental retardation. Brain. 2014;137(Pt 2):411-9.

81. Chamberlain S, Shaw J, Rowland A, Wallis J, South S, Nakamura Y, et al. Mapping of mutation causing Friedreich's ataxia to human chromosome 9. Nature. 1988;334(6179):248-50.

82. Fujita R, Agid Y, Trouillas P, Seck A, Tommasi-Davenas C, Driesel AJ, et al. Confirmation of linkage of Friedreich ataxia to chromosome 9 and identification of a new closely linked marker. Genomics. 1989;4(1):110-1.

83. Delatycki MB, Knight M, Koenig M, Cossee M, Williamson R, Forrest SM. G130V, a common FRDA point mutation, appears to have arisen from a common founder. Hum Genet. 1999;105(4):343-6.

84. Schmucker S, Argentini M, Carelle-Calmels N, Martelli A, Puccio H. The in vivo mitochondrial two-step maturation of human frataxin. Hum Mol Genet. 2008;17(22):3521-31.

85. Campuzano V, Montermini L, Molto MD, Pianese L, Cossee M, Cavalcanti F, et al. Friedreich's ataxia: autosomal recessive disease caused by an intronic GAA triplet repeat expansion. Science. 1996;271(5254):1423-7.

86. Jacob FD, Ho ES, Martinez-Ojeda M, Darras BT, Khwaja OS. Case of infantile onset spinocerebellar ataxia type 5. J Child Neurol. 2013;28(10):1292-5.

87. Parolin Schnekenberg R, Perkins EM, Miller JW, Davies WI, D'Adamo MC, Pessia M, et al. De novo point mutations in patients diagnosed with ataxic cerebral palsy. Brain. 2015;138(Pt 7):1817-32.

88. Burk K, Zuhlke C, Konig IR, Ziegler A, Schwinger E, Globas C, et al. Spinocerebellar ataxia type 5: clinical and molecular genetic features of a German kindred. Neurology. 2004;62(2):327-9.

89. Ranum LP, Schut LJ, Lundgren JK, Orr HT, Livingston DM. Spinocerebellar ataxia type 5 in a family descended from the grandparents of President Lincoln maps to chromosome 11. Nat Genet. 1994;8(3):280-4.

90. Ikeda Y, Dick KA, Weatherspoon MR, Gincel D, Armbrust KR, Dalton JC, et al. Spectrin mutations cause spinocerebellar ataxia type 5. Nat Genet. 2006;38(2):184-90.

91. Jackson M, Song W, Liu M-Y, Jin L, Dykes-Hoberg M, Lin C-lG, et al. Modulation of the neuronal glutamate transporter EAAT4 by two interacting proteins. Nature. 2001;410(6824):89-93.

92. Clarkson YL, Perkins EM, Cairncross CJ, Lyndon AR, Skehel PA, Jackson M. beta-III spectrin underpins ankyrin R function in Purkinje cell dendritic trees: protein complex critical for sodium channel activity is impaired by SCA5-associated mutations. Hum Mol Genet. 2014;23(14):3875-82.

93. Houlden H, Johnson J, Gardner-Thorpe C, Lashley T, Hernandez D, Worth P, et al. Mutations in TTBK2, encoding a kinase implicated in tau phosphorylation, segregate with spinocerebellar ataxia type 11. Nat Genet. 2007;39(12):1434-6.

94. Worth PF, Giunti P, Gardner-Thorpe C, Dixon PH, Davis MB, Wood NW. Autosomal dominant cerebellar ataxia type III: linkage in a large British family to a 7.6-cM region on chromosome 15q14-21.3. Am J Hum Genet. 1999;65(2):420-6.

95. Herman-Bert A, Stevanin G, Netter JC, Rascol O, Brassat D, Calvas P, et al. Mapping of spinocerebellar ataxia 13 to chromosome 19q13.3-q13.4 in a family with autosomal dominant cerebellar ataxia and mental retardation. Am J Hum Genet. 2000;67(1):229-35.

96. Waters MF, Fee D, Figueroa KP, Nolte D, Muller U, Advincula J, et al. An autosomal dominant ataxia maps to 19q13: Allelic heterogeneity of SCA13 or novel locus? Neurology. 2005;65(7):1111-3.

97. Pyle A, Smertenko T, Bargiela D, Griffin H, Duff J, Appleton M, et al. Exome sequencing in undiagnosed inherited and sporadic ataxias. Brain. 2015;138(Pt 2):276-83.

98. Ghanshani S, Pak M, McPherson JD, Strong M, Dethlefs B, Wasmuth JJ, et al. Genomic organization, nucleotide sequence, and cellular distribution of a Shaw-related potassium channel gene, Kv3.3, and mapping of Kv3.3 and Kv3.4 to human chromosomes 19 and 1. Genomics. 1992;12(2):190-6.

99. Haas M, Ward DC, Lee J, Roses AD, Clarke V, D'Eustachio P, et al. Localization of Shaw-related K+ channel genes on mouse and human chromosomes. Mammalian Genome. 1993;4(12):711-5.

100. Figueroa KP, Minassian NA, Stevanin G, Waters M, Garibyan V, Forlani S, et al. KCNC3: phenotype, mutations, channel biophysics-a study of 260 familial ataxia patients. Hum Mutat. 2010;31(2):191-6.

101. Figueroa KP, Waters MF, Garibyan V, Bird TD, Gomez CM, Ranum LP, et al. Frequency of KCNC3 DNA variants as causes of spinocerebellar ataxia 13 (SCA13). PLoS One. 2011;6(3):e17811.

102. Asai H, Hirano M, Shimada K, Kiriyama T, Furiya Y, Ikeda M, et al. Protein kinase C gamma, a protein causative for dominant ataxia, negatively regulates nuclear import of recessive-ataxia-related aprataxin. Hum Mol Genet. 2009;18(19):3533-43.

103. Yamashita I, Sasaki H, Yabe I, Fukazawa T, Nogoshi S, Komeichi K, et al. A novel locus for dominant cerebellar ataxia (SCA14) maps to a 10.2-cM interval flanked by D19S206 and D19S605 on chromosome 19q13.4-qter. Ann Neurol. 2000;48(2):156-63.

104. Brkanac Z, Bylenok L, Fernandez M, Matsushita M, Lipe H, Wolff J, et al. A new dominant spinocerebellar ataxia linked to chromosome 19q13.4-qter. Arch Neurol. 2002;59(8):1291-5.

105. Chen DH, Brkanac Z, Verlinde CL, Tan XJ, Bylenok L, Nochlin D, et al. Missense mutations in the regulatory domain of PKC gamma: a new mechanism for dominant nonepisodic cerebellar ataxia. Am J Hum Genet. 2003;72(4):839-49.

106. Morita H, Yoshida K, Suzuki K, Ikeda S. A Japanese case of SCA14 with the Gly128Asp mutation. J Hum Genet. 2006;51(12):1118-21.

107. van de Warrenburg BP, Verbeek DS, Piersma SJ, Hennekam FA, Pearson PL, Knoers NV, et al. Identification of a novel SCA14 mutation in a Dutch autosomal dominant cerebellar ataxia family. Neurology. 2003;61(12):1760-5.

108. Johnson KJ, Jones PJ, Spurr N, Nimmo E, Davies J, Creed H, et al. Linkage relationships of the protein kinase C gamma gene which exclude it as a candidate for myotonic dystrophy. Cytogenet Cell Genet. 1988;48(1):13-5.

109. Storey E, Gardner RJ, Knight MA, Kennerson ML, Tuck RR, Forrest SM, et al. A new autosomal dominant pure cerebellar ataxia. Neurology. 2001;57(10):1913-5.

110. Knight MA, Kennerson ML, Anney RJ, Matsuura T, Nicholson GA, Salimi-Tari P, et al. Spinocerebellar ataxia type 15 (sca15) maps to 3p24.2-3pter: exclusion of the ITPR1 gene, the human orthologue of an ataxic mouse mutant. Neurobiol Dis. 2003;13(2):147-57.

111. van de Leemput J, Chandran J, Knight MA, Holtzclaw LA, Scholz S, Cookson MR, et al. Deletion at ITPR1 underlies ataxia in mice and spinocerebellar ataxia 15 in humans. PLoS Genet. 2007;3(6):e108.

112. Hara K, Fukushima T, Suzuki T, Shimohata T, Oyake M, Ishiguro H, et al. Japanese SCA families with an unusual phenotype linked to a locus overlapping with SCA15 locus. Neurology. 2004;62(4):648-51.

113. Matsumoto M, Nakagawa T, Inoue T, Nagata E, Tanaka K, Takano H, et al. Ataxia and epileptic seizures in mice lacking type 1 inositol 1,4,5-trisphosphate receptor. Nature. 1996;379(6561):168-71.

114. Nucifora FC, Jr., Li SH, Danoff S, Ullrich A, Ross CA. Molecular cloning of a cDNA for the human inositol 1,4,5-trisphosphate receptor type 1, and the identification of a third alternatively spliced variant. Brain Res Mol Brain Res. 1995;32(2):291-6.

115. Iwaki A, Kawano Y, Miura S, Shibata H, Matsuse D, Li W, et al. Heterozygous deletion of ITPR1, but not SUMF1, in spinocerebellar ataxia type 16. J Med Genet. 2008;45(1):32-5.

116. Hara K, Shiga A, Nozaki H, Mitsui J, Takahashi Y, Ishiguro H, et al. Total deletion and a missense mutation of ITPR1 in Japanese SCA15 families. Neurology. 2008;71(8):547-51.

117. Duarri A, Jezierska J, Fokkens M, Meijer M, Schelhaas HJ, den Dunnen WF, et al. Mutations in potassium channel kcnd3 cause spinocerebellar ataxia type 19. Ann Neurol. 2012;72(6):870-80.

118. Chung MY, Lu YC, Cheng NC, Soong BW. A novel autosomal dominant spinocerebellar ataxia (SCA22) linked to chromosome 1p21-q23. Brain. 2003;126(Pt 6):1293-9.

119. Verbeek DS, Schelhaas JH, Ippel EF, Beemer FA, Pearson PL, Sinke RJ. Identification of a novel SCA locus (SCA19) in a Dutch autosomal dominant cerebellar ataxia family on chromosome region 1p21-q21. Hum Genet. 2002;111(4-5):388-93.

120. Schelhaas HJ, Verbeek DS, Van de Warrenburg BP, Sinke RJ. SCA19 and SCA22: evidence for one locus with a worldwide distribution. Brain. 127. England2004. p. E6; author reply E7.

121. Kong W, Po S, Yamagishi T, Ashen MD, Stetten G, Tomaselli GF. Isolation and characterization of the human gene encoding Ito: further diversity by alternative mRNA splicing. Am J Physiol. 1998;275(6 Pt 2):H1963-70.

122. Isbrandt D, Leicher T, Waldschutz R, Zhu X, Luhmann U, Michel U, et al. Gene structures and expression profiles of three human KCND (Kv4) potassium channels mediating A-type currents I(TO) and I(SA). Genomics. 2000;64(2):144-54.

123. Dixon JE, Shi W, Wang HS, McDonald C, Yu H, Wymore RS, et al. Role of the Kv4.3 K+ channel in ventricular muscle. A molecular correlate for the transient outward current. Circ Res. 1996;79(4):659-68.

124. Postma AV, Bezzina CR, de Vries JF, Wilde AA, Moorman AF, Mannens MM. Genomic organisation and chromosomal localisation of two members of the KCND ion channel family, KCND2 and KCND3. Hum Genet. 2000;106(6):614-9.

125. Lee YC, Durr A, Majczenko K, Huang YH, Liu YC, Lien CC, et al. Mutations in KCND3 cause spinocerebellar ataxia type 22. Ann Neurol. 2012;72(6):859-69.

126. Devos D, Schraen-Maschke S, Vuillaume I, Dujardin K, Naze P, Willoteaux C, et al. Clinical features and genetic analysis of a new form of spinocerebellar ataxia. Neurology. 2001;56(2):234-8.

127. Delplanque J, Devos D, Huin V, Genet A, Sand O, Moreau C, et al. TMEM240 mutations cause spinocerebellar ataxia 21 with mental retardation and severe cognitive impairment. Brain. 2014;137(Pt 10):2657-63.

128. Bakalkin G, Watanabe H, Jezierska J, Depoorter C, Verschuuren-Bemelmans C, Bazov I, et al. Prodynorphin mutations cause the neurodegenerative disorder spinocerebellar ataxia type 23. Am J Hum Genet. 2010;87(5):593-603.

129. Verbeek DS, van de Warrenburg BP, Wesseling P, Pearson PL, Kremer HP, Sinke RJ. Mapping of the SCA23 locus involved in autosomal dominant cerebellar ataxia to chromosome region 20p13-12.3. Brain. 2004;127(Pt 11):2551-7.

130. Horikawa S, Takai T, Toyosato M, Takahashi H, Noda M, Kakidani H, et al. Isolation and structural organization of the human preproenkephalin B gene. Nature. 1983;306(5943):611-4.

131. Litt M, Buroker NE, Kondoleon S, Douglass J, Liston D, Sheehy R, et al. Chromosomal localization of the human proenkephalin and prodynorphin genes. Am J Hum Genet. 1988;42(2):327-34.

132. Yu GY, Howell MJ, Roller MJ, Xie TD, Gomez CM. Spinocerebellar ataxia type 26 maps to chromosome 19p13.3 adjacent to SCA6. Ann Neurol. 2005;57(3):349-54.

133. Hekman KE, Yu GY, Brown CD, Zhu H, Du X, Gervin K, et al. A conserved eEF2 coding variant in SCA26 leads to loss of translational fidelity and increased susceptibility to proteostatic insult. Hum Mol Genet. 2012;21(26):5472-83.

134. Kaneda Y, Hayes H, Uchida T, Yoshida MC, Okada Y. Regional assignment of five genes on human chromosome 19. Chromosoma. 1987;95(1):8-12.

135. van Swieten JC, Brusse E, de Graaf BM, Krieger E, van de Graaf R, de Koning I, et al. A mutation in the fibroblast growth factor 14 gene is associated with autosomal dominant cerebellar ataxia [corrected]. Am J Hum Genet. 2003;72(1):191-9.

136. Dalski A, Atici J, Kreuz FR, Hellenbroich Y, Schwinger E, Zuhlke C. Mutation analysis in the fibroblast growth factor 14 gene: frameshift mutation and polymorphisms in patients with inherited ataxias. Eur J Hum Genet. 2005;13(1):118-20.

137. Smallwood PM, Munoz-Sanjuan I, Tong P, Macke JP, Hendry SH, Gilbert DJ, et al. Fibroblast growth factor (FGF) homologous factors: new members of the FGF family implicated in nervous system development. Proc Natl Acad Sci U S A. 1996;93(18):9850-7.

138. Cagnoli C, Mariotti C, Taroni F, Seri M, Brussino A, Michielotto C, et al. SCA28, a novel form of autosomal dominant cerebellar ataxia on chromosome 18p11.22-q11.2. Brain. 2006;129(Pt 1):235-42.

139. Cagnoli C, Stevanin G, Brussino A, Barberis M, Mancini C, Margolis RL, et al. Missense mutations in the AFG3L2 proteolytic domain account for approximately 1.5% of European autosomal dominant cerebellar ataxias. Hum Mutat. 2010;31(10):1117-24.

140. Di Bella D, Lazzaro F, Brusco A, Plumari M, Battaglia G, Pastore A, et al. Mutations in the mitochondrial protease gene AFG3L2 cause dominant hereditary ataxia SCA28. Nat Genet. 2010;42(4):313-21.

141. Banfi S, Bassi MT, Andolfi G, Marchitiello A, Zanotta S, Ballabio A, et al. Identification and characterization of AFG3L2, a novel paraplegin-related gene. Genomics. 1999;59(1):51-8.

142. Koppen M, Metodiev MD, Casari G, Rugarli EI, Langer T. Variable and tissue-specific subunit composition of mitochondrial m-AAA protease complexes linked to hereditary spastic paraplegia. Mol Cell Biol. 2007;27(2):758-67.

143. Lobbe AM, Kang JS, Hilker R, Hackstein H, Muller U, Nolte D. A Novel Missense Mutation in AFG3L2 Associated with Late Onset and Slow Progression of Spinocerebellar Ataxia Type 28. Journal of Molecular Neuroscience. 2014;52(4):493-6.

144. Svenstrup K, Nielsen TT, Aidt F, Rostgaard N, Duno M, Wibrand F, et al. SCA28: Novel Mutation in the AFG3L2 Proteolytic Domain Causes a Mild

Cerebellar Syndrome with Selective Type-1 Muscle Fiber Atrophy. Cerebellum. 2017;16(1):62-7.

145. Maltecca F, Baseggio E, Consolato F, Mazza D, Podini P, Young SM, et al. Purkinje neuron Ca2+ influx reduction rescues ataxia in SCA28 model. Journal of Clinical Investigation. 2015;125(1):263-74.

146. Cadieux-Dion M, Turcotte-Gauthier M, Noreau A, Martin C, Meloche C, Gravel M, et al. Expanding the clinical phenotype associated with ELOVL4 mutation: study of a large French-Canadian family with autosomal dominant spinocerebellar ataxia and erythrokeratodermia. JAMA Neurol. 2014;71(4):470-5.

147. Agbaga MP, Brush RS, Mandal MN, Henry K, Elliott MH, Anderson RE. Role of Stargardt-3 macular dystrophy protein (ELOVL4) in the biosynthesis of very long chain fatty acids. Proc Natl Acad Sci U S A. 2008;105(35):12843-8.

148. Wang JL, Yang X, Xia K, Hu ZM, Weng L, Jin X, et al. TGM6 identified as a novel causative gene of spinocerebellar ataxias using exome sequencing. Brain. 2010;133(Pt 12):3510-8.

149. Li M, Pang SY, Song Y, Kung MH, Ho SL, Sham PC. Whole exome sequencing identifies a novel mutation in the transglutaminase 6 gene for spinocerebellar ataxia in a Chinese family. Clin Genet. 2013;83(3):269-73.

150. Guo YC, Lin JJ, Liao YC, Tsai PC, Lee YC, Soong BW. Spinocerebellar ataxia 35: novel mutations in TGM6 with clinical and genetic characterization. Neurology. 2014;83(17):1554-61.

151. Hadjivassiliou M, Aeschlimann P, Strigun A, Sanders DS, Woodroofe N, Aeschlimann D. Autoantibodies in gluten ataxia recognize a novel neuronal transglutaminase. Ann Neurol. 2008;64(3):332-43.

152. Tsoi H, Yu AC, Chen ZS, Ng NK, Chan AY, Yuen LY, et al. A novel missense mutation in CCDC88C activates the JNK pathway and causes a dominant form of spinocerebellar ataxia. J Med Genet. 2014;51(9):590-5.

153. Oshita A, Kishida S, Kobayashi H, Michiue T, Asahara T, Asashima M, et al. Identification and characterization of a novel Dvl-binding protein that suppresses Wnt signalling pathway. Genes Cells. 2003;8(12):1005-17.

154. Coutelier M, Blesneac I, Monteil A, Monin ML, Ando K, Mundwiller E, et al. A Recurrent Mutation in CACNA1G Alters Cav3.1 T-Type Calcium-Channel Conduction and Causes Autosomal-Dominant Cerebellar Ataxia. Am J Hum Genet. 2015;97(5):726-37.

155. Morino H, Matsuda Y, Muguruma K, Miyamoto R, Ohsawa R, Ohtake T, et al. A mutation in the low voltage-gated calcium channel CACNA1G alters the physiological properties of the channel, causing spinocerebellar ataxia. Mol Brain. 2015;8:89.

156. Perez-Reyes E, Cribbs LL, Daud A, Lacerda AE, Barclay J, Williamson MP, et al. Molecular characterization of a neuronal low-voltage-activated T-type calcium channel. Nature. 1998;391(6670):896-900.

157. Jagannathan S, Punt EL, Gu Y, Arnoult C, Sakkas D, Barratt CL, et al. Identification and localization of T-type voltage-operated calcium channel subunits in human male germ cells. Expression of multiple isoforms. J Biol Chem. 2002;277(10):8449-56.

158. Melberg A, Hetta J, Dahl N, Nennesmo I, Bengtsson M, Wibom R, et al. Autosomal dominant cerebellar ataxia deafness and narcolepsy. J Neurol Sci. 1995;134(1-2):119-29.

159. Winkelmann J, Lin L, Schormair B, Kornum BR, Faraco J, Plazzi G, et al. Mutations in DNMT1 cause autosomal dominant cerebellar ataxia, deafness and narcolepsy. Hum Mol Genet. 2012;21(10):2205-10.

160. Yoder JA, Yen RW, Vertino PM, Bestor TH, Baylin SB. New 5' regions of the murine and human genes for DNA (cytosine-5)-methyltransferase. J Biol Chem. 1996;271(49):31092-7.

161. Van Dyke DH, Griggs RC, Murphy MJ, Goldstein MN. Hereditary myokymia and periodic ataxia. Journal of the Neurological Sciences. 1975;25(1):109-18.

162. Gancher ST, Nutt JG. Autosomal dominant episodic ataxia: a heterogeneous syndrome. Mov Disord. 1986;1(4):239-53.

163. Graves TD, Rajakulendran S, Zuberi SM, Morris HR, Schorge S, Hanna MG, et al. Nongenetic factors influence severity of episodic ataxia type 1 in monozygotic twins. Neurology. 2010;75(4):367-72.

164. Litt M, Kramer P, Browne D, Gancher S, Brunt ER, Root D, et al. A gene for episodic ataxia/myokymia maps to chromosome 12p13. Am J Hum Genet. 1994;55(4):702-9.

165. Glaudemans B, van der Wijst J, Scola RH, Lorenzoni PJ, Heister A, van der Kemp AW, et al. A missense mutation in the Kv1.1 voltage-gated potassium channel-encoding gene KCNA1 is linked to human autosomal dominant hypomagnesemia. J Clin Invest. 2009;119(4):936-42.

166. Browne DL, Gancher ST, Nutt JG, Brunt ER, Smith EA, Kramer P, et al. Episodic ataxia/myokymia syndrome is associated with point mutations in the human potassium channel gene, KCNA1. Nat Genet. 1994;8(2):136-40.

167. Eunson LH, Rea R, Zuberi SM, Youroukos S, Panayiotopoulos CP, Liguori R, et al. Clinical, genetic, and expression studies of mutations in the potassium channel gene KCNA1 reveal new phenotypic variability. Ann Neurol. 2000;48(4):647-56.

168. von Brederlow B, Hahn AF, Koopman WJ, Ebers GC, Bulman DE. Mapping the gene for acetazolamide responsive hereditary paryoxysmal cerebellar ataxia to chromosome 19p. Hum Mol Genet. 1995;4(2):279-84.

169. Vahedi K, Joutel A, Van Bogaert P, Ducros A, Maciazeck J, Bach JF, et al. A gene for hereditary paroxysmal cerebellar ataxia maps to chromosome 19p. Ann Neurol. 1995;37(3):289-93.

170. Kordasiewicz HB, Thompson RM, Clark HB, Gomez CM. C-termini of P/Q-type Ca2+ channel alpha1A subunits translocate to nuclei and promote polyglutamine-mediated toxicity. Hum Mol Genet. 2006;15(10):1587-99.

171. Ophoff RA, Terwindt GM, Vergouwe MN, van Eijk R, Oefner PJ, Hoffman SM, et al. Familial hemiplegic migraine and episodic ataxia type-2 are caused by mutations in the Ca2+ channel gene CACNL1A4. Cell. 1996;87(3):543-52.

172. Diriong S, Lory P, Williams ME, Ellis SB, Harpold MM, Taviaux S. Chromosomal localization of the human genes for alpha 1A, alpha 1B, and alpha 1E voltage-dependent Ca2+ channel subunits. Genomics. 1995;30(3):605-9.

173. Escayg A, De Waard M, Lee DD, Bichet D, Wolf P, Mayer T, et al. Coding and noncoding variation of the human calcium-channel beta4-subunit gene CACNB4 in patients with idiopathic generalized epilepsy and episodic ataxia. Am J Hum Genet. 2000;66(5):1531-9.

174. Escayg A, Jones JM, Kearney JA, Hitchcock PF, Meisler MH. Calcium channel beta 4 (CACNB4): human ortholog of the mouse epilepsy gene lethargic. Genomics. 1998;50(1):14-22.

175. Taviaux S, Williams ME, Harpold MM, Nargeot J, Lory P. Assignment of human genes for beta 2 and beta 4 subunits of voltage-dependent Ca2+ channels to chromosomes 10p12 and 2q22-q23. Hum Genet. 1997;100(2):151-4.

176. Jen JC, Wan J, Palos TP, Howard BD, Baloh RW. Mutation in the glutamate transporter EAAT1 causes episodic ataxia, hemiplegia, and seizures. Neurology. 2005;65(4):529-34.

177. de Vries B, Mamsa H, Stam AH, Wan J, Bakker SL, Vanmolkot KR, et al. Episodic ataxia associated with EAAT1 mutation C186S affecting glutamate reuptake. Arch Neurol. 2009;66(1):97-101.

178. Winter N, Kovermann P, Fahlke C. A point mutation associated with episodic ataxia 6 increases glutamate transporter anion currents. Brain. 2012;135(Pt 11):3416-25.

179. Kirschner MA, Arriza JL, Copeland NG, Gilbert DJ, Jenkins NA, Magenis E, et al. The mouse and human excitatory amino acid transporter gene (EAAT1) maps to mouse chromosome 15 and a region of syntenic homology on human chromosome 5. Genomics. 1994;22(3):631-3.

180. Takai S, Yamada K, Kawakami H, Tanaka K, Nakamura S. Localization of the gene (SLC1A3) encoding human glutamate transporter (GluT-1) to 5p13 by fluorescence in situ hybridization. Cytogenet Cell Genet. 1995;69(3-4):209-10.

181. Ferguson FR, Critchley M. A CLINICAL STUDY OF AN HEREDO-FAMILIAL DISEASE RESEMBLING DISSEMINATED SCLEROSIS. Brain. 1929;52(2):203-25.

182. Meijer IA, Hand CK, Grewal KK, Stefanelli MG, Ives EJ, Rouleau GA. A locus for autosomal dominant hereditary spastic ataxia, SAX1, maps to chromosome 12p13. Am J Hum Genet. 2002;70(3):763-9.

183. Grewal KK, Stefanelli MG, Meijer IA, Hand CK, Rouleau GA, Ives EJ. A founder effect in three large Newfoundland families with a novel clinically variable spastic ataxia and supranuclear gaze palsy. Am J Med Genet A. 2004;131(3):249-54.

184. Bourassa CV, Meijer IA, Merner ND, Grewal KK, Stefanelli MG, Hodgkinson K, et al. VAMP1 mutation causes dominant hereditary spastic ataxia in Newfoundland families. Am J Hum Genet. 2012;91(3):548-52.

185. Moreira MC, Barbot C, Tachi N, Kozuka N, Mendonca P, Barros J, et al. Homozygosity mapping of Portuguese and Japanese forms of ataxia-oculomotor apraxia to 9p13, and evidence for genetic heterogeneity. Am J Hum Genet. 2001;68(2):501-8.

186. Barbot C, Coutinho P, Chorao R, Ferreira C, Barros J, Fineza I, et al. Recessive ataxia with ocular apraxia: review of 22 Portuguese patients. Arch Neurol. 2001;58(2):201-5.

187. Criscuolo C, Mancini P, Sacca F, De Michele G, Monticelli A, Santoro L, et al. Ataxia with oculomotor apraxia type 1 in Southern Italy: late onset and variable phenotype. Neurology. 2004;63(11):2173-5.

188. Castellotti B, Mariotti C, Rimoldi M, Fancellu R, Plumari M, Caimi S, et al. Ataxia with oculomotor apraxia type1 (AOA1): novel and recurrent aprataxin mutations, coenzyme Q10 analyses, and clinical findings in Italian patients. Neurogenetics. 2011;12(3):193-201.

189. Date H, Onodera O, Tanaka H, Iwabuchi K, Uekawa K, Igarashi S, et al. Early-onset ataxia with ocular motor apraxia and hypoalbuminemia is caused by mutations in a new HIT superfamily gene. Nat Genet. 2001;29(2):184-8.

190. Sano Y, Date H, Igarashi S, Onodera O, Oyake M, Takahashi T, et al. Aprataxin, the causative protein for EAOH is a nuclear protein with a potential role as a DNA repair protein. Ann Neurol. 2004;55(2):241-9.

191. Whitehouse CJ, Taylor RM, Thistlethwaite A, Zhang H, Karimi-Busheri F, Lasko DD, et al. XRCC1 stimulates human polynucleotide kinase activity at damaged DNA termini and accelerates DNA single-strand break repair. Cell. 2001;104(1):107-17.

192. Moreira MC, Klur S, Watanabe M, Nemeth AH, Le Ber I, Moniz JC, et al. Senataxin, the ortholog of a yeast RNA helicase, is mutant in ataxia-ocular apraxia 2. Nat Genet. 2004;36(3):225-7.

193. Duquette A, Roddier K, McNabb-Baltar J, Gosselin I, St-Denis A, Dicaire MJ, et al. Mutations in senataxin responsible for Quebec cluster of ataxia with neuropathy. Ann Neurol. 2005;57(3):408-14.

194. Bouchard J, Bedard P, Bouchard R. Study of a family with progressive ataxia, tremor and severe distal amyotrophy. Can J Neurol Sci. 1980;7(4):345-9.

195. Nemeth AH, Bochukova E, Dunne E, Huson SM, Elston J, Hannan MA, et al. Autosomal recessive cerebellar ataxia with oculomotor apraxia (ataxia-telangiectasia-like syndrome) is linked to chromosome 9q34. Am J Hum Genet. 2000;67(5):1320-6.

196. Bomont P, Watanabe M, Gershoni-Barush R, Shizuka M, Tanaka M, Sugano J, et al. Homozygosity mapping of spinocerebellar ataxia with cerebellar atrophy and peripheral neuropathy to 9q33-34, and with hearing impairment and optic atrophy to 6p21-23. Eur J Hum Genet. 2000;8(12):986-90.

197. Suraweera A, Lim Y, Woods R, Birrell GW, Nasim T, Becherel OJ, et al. Functional role for senataxin, defective in ataxia oculomotor apraxia type 2, in transcriptional regulation. Hum Mol Genet. 2009;18(18):3384-96.

198. Airoldi G, Guidarelli A, Cantoni O, Panzeri C, Vantaggiato C, Bonato S, et al. Characterization of two novel SETX mutations in AOA2 patients reveals aspects of the pathophysiological role of senataxin. Neurogenetics. 2010;11(1):91-100.

199. Al Tassan N, Khalil D, Shinwari J, Al Sharif L, Bavi P, Abduljaleel Z, et al. A missense mutation in PIK3R5 gene in a family with ataxia and oculomotor apraxia. Hum Mutat. 2012;33(2):351-4.

200. Brock C, Schaefer M, Reusch HP, Czupalla C, Michalke M, Spicher K, et al. Roles of G beta gamma in membrane recruitment and activation of p110 gamma/p101 phosphoinositide 3-kinase gamma. J Cell Biol. 2003;160(1):89-99.

201. Bras J, Alonso I, Barbot C, Costa MM, Darwent L, Orme T, et al. Mutations in PNKP cause recessive ataxia with oculomotor apraxia type 4. Am J Hum Genet. 2015;96(3):474-9.

202. Jilani A, Ramotar D, Slack C, Ong C, Yang XM, Scherer SW, et al. Molecular cloning of the human gene, PNKP, encoding a polynucleotide kinase 3'-phosphatase and evidence for its role in repair of DNA strand breaks caused by oxidative damage. J Biol Chem. 1999;274(34):24176-86.

203. Schurig V, Orman AV, Bowen P. Nonprogressive cerebellar disorder with mental retardation and autosomal recessive inheritance in Hutterites. Am J Med Genet. 1981;9(1):43-53.

204. Glass HC, Boycott KM, Adams C, Barlow K, Scott JN, Chudley AE, et al. Autosomal recessive cerebellar hypoplasia in the Hutterite population. Dev Med Child Neurol. 2005;47(10):691-5.

205. Boycott KM, Flavelle S, Bureau A, Glass HC, Fujiwara TM, Wirrell E, et al. Homozygous deletion of the very low density lipoprotein receptor gene causes autosomal recessive cerebellar hypoplasia with cerebral gyral simplification. Am J Hum Genet. 2005;77(3):477-83.

206. Ozcelik T, Akarsu N, Uz E, Caglayan S, Gulsuner S, Onat OE, et al. Mutations in the very low-density lipoprotein receptor VLDLR cause cerebellar hypoplasia and quadrupedal locomotion in humans. Proc Natl Acad Sci U S A. 2008;105(11):4232-6.

207. Gulsuner S, Tekinay AB, Doerschner K, Boyaci H, Bilguvar K, Unal H, et al. Homozygosity mapping and targeted genomic sequencing reveal the gene responsible for cerebellar hypoplasia and quadrupedal locomotion in a consanguineous kindred. Genome Res. 2011;21(12):1995-2003.

208. Turkmen S, Demirhan O, Hoffmann K, Diers A, Zimmer C, Sperling K, et al. Cerebellar hypoplasia and quadrupedal locomotion in humans as a recessive trait mapping to chromosome 17p. J Med Genet. 43. England2006. p. 461-4.

209. Liu K, Jian Y, Sun X, Yang C, Gao Z, Zhang Z, et al. Negative regulation of phosphatidylinositol 3-phosphate levels in early-to-late endosome conversion. J Cell Biol. 2016;212(2):181-98.

210. Turkmen S, Guo G, Garshasbi M, Hoffmann K, Alshalah AJ, Mischung C, et al. CA8 mutations cause a novel syndrome characterized by ataxia and mild mental retardation with predisposition to quadrupedal gait. PLoS Genet. 2009;5(5):e1000487.

211. Najmabadi H, Hu H, Garshasbi M, Zemojtel T, Abedini SS, Chen W, et al. Deep sequencing reveals 50 novel genes for recessive cognitive disorders. Nature. 2011;478(7367):57-63.

212. Kato K. Sequence of a novel carbonic anhydrase-related polypeptide and its exclusive presence in Purkinje cells. FEBS Lett. 1990;271(1-2):137-40.

213. Bergenhem NC, Sait SS, Eddy RL, Shows TB, Tashian RE. Assignment of the gene for human carbonic anhydrase VIII(CA8) to chromosome 8q11-->q12. Cytogenet Cell Genet. 1995;71(3):299-300.

214. Hirota J, Ando H, Hamada K, Mikoshiba K. Carbonic anhydrase-related protein is a novel binding protein for inositol 1,4,5-trisphosphate receptor type 1. Biochem J. 2003;372(Pt 2):435-41.

215. Onat OE, Gulsuner S, Bilguvar K, Nazli Basak A, Topaloglu H, Tan M, et al. Missense mutation in the ATPase, aminophospholipid transporter protein ATP8A2 is associated with cerebellar atrophy and quadrupedal locomotion. Eur J Hum Genet. 2013;21(3):281-5.

216. Norman RM. PRIMARY DEGENERATION OF THE GRANULAR LAYER OF THE CEREBELLUM: AN UNUSUAL FORM OF FAMILIAL CEREBELLAR ATROPHY OCCURRING IN EARLY LIFE. Brain. 1940;63(4):365-79.

217. Megarbane A, Delague V, Salem N, Loiselet J. Autosomal recessive congenital cerebellar hypoplasia and short stature in a large inbred family. Am J Med Genet. 87. United States1999. p. 88-90.

218. Jobling RK, Assoum M, Gakh O, Blaser S, Raiman JA, Mignot C, et al. PMPCA mutations cause abnormal mitochondrial protein processing in patients with non-progressive cerebellar ataxia. Brain. 2015;138(Pt 6):1505-17.

219. van Bogaert L, Martin L. Optic and cochleovestibular degenerations in the hereditary ataxias. I. Clinico-pathological and genetic aspects. Brain. 1974;97(1):15-40.

220. Spoendlin H. Optic cochleovestibular degenerations in hereditary ataxias. II. Temporal bone pathology in two cases of Friedreich's ataxia with vestibulo-cochlear disorders. Brain. 1974;97(1):41-8.

221. Breedveld GJ, van Wetten B, te Raa GD, Brusse E, van Swieten JC, Oostra BA, et al. A new locus for a childhood onset, slowly progressive autosomal recessive spinocerebellar ataxia maps to chromosome 11p15. J Med Genet. 41. England2004. p. 858-66.

222. Sun Y, Almomani R, Breedveld GJ, Santen GW, Aten E, Lefeber DJ, et al. Autosomal recessive spinocerebellar ataxia 7 (SCAR7) is caused by variants in TPP1, the gene involved in classic late-infantile neuronal ceroid lipofuscinosis 2 disease (CLN2 disease). Hum Mutat. 2013;34(5):706-13.

223. Dy ME, Sims KB, Friedman J. TPP1 deficiency: Rare cause of isolated childhood-onset progressive ataxia. Neurology. 2015;85(14):1259-61.

224. Gros-Louis F, Dupre N, Dion P, Fox MA, Laurent S, Verreault S, et al. Mutations in SYNE1 lead to a newly discovered form of autosomal recessive cerebellar ataxia. Nat Genet. 2007;39(1):80-5.

225. Izumi Y, Miyamoto R, Morino H, Yoshizawa A, Nishinaka K, Udaka F, et al. Cerebellar ataxia with SYNE1 mutation accompanying motor neuron disease. Neurology. 2013;80(6):600-1.

226. Dupre N, Gros-Louis F, Chrestian N, Verreault S, Brunet D, de Verteuil D, et al. Clinical and genetic study of autosomal recessive cerebellar ataxia type 1. Ann Neurol. 2007;62(1):93-8.

227. Zhang Q, Skepper JN, Yang F, Davies JD, Hegyi L, Roberts RG, et al. Nesprins: a novel family of spectrin-repeat-containing proteins that localize to the nuclear membrane in multiple tissues. J Cell Sci. 2001;114(Pt 24):4485-98.

228. Puckelwartz MJ, Kessler E, Zhang Y, Hodzic D, Randles KN, Morris G, et al. Disruption of nesprin-1 produces an Emery Dreifuss muscular dystrophy-like phenotype in mice. Hum Mol Genet. 2009;18(4):607-20.

229. Mollet J, Delahodde A, Serre V, Chretien D, Schlemmer D, Lombes A, et al. CABC1 gene mutations cause ubiquinone deficiency with cerebellar ataxia and seizures. Am J Hum Genet. 2008;82(3):623-30.

230. Aure K, Benoist JF, Ogier de Baulny H, Romero NB, Rigal O, Lombes A. Progression despite replacement of a myopathic form of coenzyme Q10 defect. Neurology. 2004;63(4):727-9.

231. Iiizumi M, Arakawa H, Mori T, Ando A, Nakamura Y. Isolation of a novel gene, CABC1, encoding a mitochondrial protein that is highly homologous to yeast activity of bc1 complex. Cancer Res. 2002;62(5):1246-50.

232. Vermeer S, Hoischen A, Meijer RP, Gilissen C, Neveling K, Wieskamp N, et al. Targeted next-generation sequencing of a 12.5 Mb homozygous region reveals ANO10 mutations in patients with autosomal-recessive cerebellar ataxia. Am J Hum Genet. 2010;87(6):813-9.

233. Balreira A, Boczonadi V, Barca E, Pyle A, Bansagi B, Appleton M, et al. ANO10 mutations cause ataxia and coenzyme Q(1)(0) deficiency. J Neurol. 2014;261(11):2192-8.

234. Doi H, Yoshida K, Yasuda T, Fukuda M, Fukuda Y, Morita H, et al. Exome sequencing reveals a homozygous SYT14 mutation in adult-onset, autosomal-recessive spinocerebellar ataxia with psychomotor retardation. Am J Hum Genet. 2011;89(2):320-7.

235. Fukuda M. Molecular cloning, expression, and characterization of a novel class of synaptotagmin (Syt XIV) conserved from Drosophila to humans. J Biochem. 2003;133(5):641-9.

236. Quintero-Rivera F, Chan A, Donovan DJ, Gusella JF, Ligon AH. Disruption of a synaptotagmin (SYT14) associated with neurodevelopmental abnormalities. Am J Med Genet A. 2007;143a(6):558-63.

237. Herrero-Turrion MJ, Fukuda M, Mollinedo F. Cloning and genomic characterization of sytdep, a new synaptotagmin XIV-related gene. Biochem Biophys Res Commun. 2006;340(2):386-94.

238. Gribaa M, Salih M, Anheim M, Lagier-Tourenne C, H'Mida D, Drouot N, et al. A new form of childhood onset, autosomal recessive spinocerebellar ataxia and epilepsy is localized at 16q21-q23. Brain. 2007;130(Pt 7):1921-8.

239. Bednarek AK, Laflin KJ, Daniel RL, Liao Q, Hawkins KA, Aldaz CM. WWOX, a novel WW domain-containing protein mapping to human chromosome 16q23.3-24.1, a region frequently affected in breast cancer. Cancer Res. 2000;60(8):2140-5.

240. Aqeilan RI, Trapasso F, Hussain S, Costinean S, Marshall D, Pekarsky Y, et al. Targeted deletion of Wwox reveals a tumor suppressor function. Proc Natl Acad Sci U S A. 2007;104(10):3949-54.

241. Chang NS, Doherty J, Ensign A. JNK1 physically interacts with WW domain-containing oxidoreductase (WOX1) and inhibits WOX1-mediated apoptosis. J Biol Chem. 2003;278(11):9195-202.

242. Lise S, Clarkson Y, Perkins E, Kwasniewska A, Sadighi Akha E, Schnekenberg RP, et al. Recessive mutations in SPTBN2 implicate beta-III spectrin in both cognitive and motor development. PLoS Genet. 2012;8(12):e1003074.

243. Elsayed SM, Heller R, Thoenes M, Zaki MS, Swan D, Elsobky E, et al. Autosomal dominant SCA5 and autosomal recessive infantile SCA are allelic conditions resulting from SPTBN2 mutations. Eur J Hum Genet. 2014;22(2):286-8.

244. Stankewich MC, Tse WT, Peters LL, Ch'ng Y, John KM, Stabach PR, et al. A widely expressed betaIII spectrin associated with Golgi and cytoplasmic vesicles. Proc Natl Acad Sci U S A. 1998;95(24):14158-63.

245. Assoum M, Salih MA, Drouot N, H'Mida-Ben Brahim D, Lagier-Tourenne C, AlDrees A, et al. Rundataxin, a novel protein with RUN and diacylglycerol binding domains, is mutant in a new recessive ataxia. Brain. 2010;133(Pt 8):2439-47.

246. Assoum M, Salih MA, Drouot N, Hnia K, Martelli A, Koenig M. The Salih ataxia mutation impairs Rubicon endosomal localization. Cerebellum. 2013;12(6):835-40.

247. Matsunaga K, Saitoh T, Tabata K, Omori H, Satoh T, Kurotori N, et al. Two Beclin 1-binding proteins, Atg14L and Rubicon, reciprocally regulate autophagy at different stages. Nat Cell Biol. 2009;11(4):385-96.

248. Nagase T, Seki N, Ishikawa K, Ohira M, Kawarabayasi Y, Ohara O, et al. Prediction of the coding sequences of unidentified human genes. VI. The coding sequences of 80 new genes (KIAA0201-KIAA0280) deduced by analysis of cDNA clones from cell line KG-1 and brain. DNA Res. 1996;3(5):321-9, 41-54.

249. Shi Y, Wang J, Li JD, Ren H, Guan W, He M, et al. Identification of CHIP as a novel causative gene for autosomal recessive cerebellar ataxia. PLoS One. 2013;8(12):e81884.

250. Shi CH, Schisler JC, Rubel CE, Tan S, Song B, McDonough H, et al. Ataxia and hypogonadism caused by the loss of ubiquitin ligase activity of the U box protein CHIP. Hum Mol Genet. 2014;23(4):1013-24.

251. Synofzik M, Schule R, Schulze M, Gburek-Augustat J, Schweizer R, Schirmacher A, et al. Phenotype and frequency of STUB1 mutations: next-generation screenings in Caucasian ataxia and spastic paraplegia cohorts. Orphanet J Rare Dis. 2014;9:57.

252. Min JN, Whaley RA, Sharpless NE, Lockyer P, Portbury AL, Patterson C. CHIP deficiency decreases longevity, with accelerated aging phenotypes

accompanied by altered protein quality control. Mol Cell Biol. 2008;28(12):4018-25.

253. Ballinger CA, Connell P, Wu Y, Hu Z, Thompson LJ, Yin LY, et al. Identification of CHIP, a novel tetratricopeptide repeat-containing protein that interacts with heat shock proteins and negatively regulates chaperone functions. Mol Cell Biol. 1999;19(6):4535-45.

254. Evers C, Kaufmann L, Seitz A, Paramasivam N, Granzow M, Karch S, et al. Exome sequencing reveals a novel CWF19L1 mutation associated with intellectual disability and cerebellar atrophy. Am J Med Genet A. 2016;170(6):1502-9.

255. Yapici Z, Eraksoy M. Non-progressive congenital ataxia with cerebellar hypoplasia in three families. Acta Paediatr. 2005;94(2):248-53.

256. Nguyen M, Boesten I, Hellebrekers DM, Vanoevelen J, Kamps R, de Koning B, et al. Pathogenic CWF19L1 variants as a novel cause of autosomal recessive cerebellar ataxia and atrophy. Eur J Hum Genet. 2016;24(4):619-22.

257. Burns R, Majczenko K, Xu J, Peng W, Yapici Z, Dowling JJ, et al. Homozygous splice mutation in CWF19L1 in a Turkish family with recessive ataxia syndrome. Neurology. 2014;83(23):2175-82.

258. Hills LB, Masri A, Konno K, Kakegawa W, Lam AT, Lim-Melia E, et al. Deletions in GRID2 lead to a recessive syndrome of cerebellar ataxia and tonic upgaze in humans. Neurology. 2013;81(16):1378-86.

259. Utine GE, Haliloglu G, Salanci B, Cetinkaya A, Kiper PO, Alanay Y, et al. A homozygous deletion in GRID2 causes a human phenotype with cerebellar ataxia and atrophy. J Child Neurol. 2013;28(7):926-32.

260. Lalouette A, Guenet JL, Vriz S. Hotfoot mouse mutations affect the delta 2 glutamate receptor gene and are allelic to lurcher. Genomics. 1998;50(1):9-13.

261. Guissart C, Li X, Leheup B, Drouot N, Montaut-Verient B, Raffo E, et al. Mutation of SLC9A1, encoding the major Na(+)/H(+) exchanger, causes ataxia-deafness Lichtenstein-Knorr syndrome. Hum Mol Genet. 2015;24(2):463-70.

262. Mattei MG, Sardet C, Franchi A, Pouyssegur J. The human amiloride-sensitive Na+/H+ antiporter: localization to chromosome 1 by in situ hybridization. Cytogenet Cell Genet. 1988;48(1):6-8.

263. Franchi A, Perucca-Lostanlen D, Pouyssegur J. Functional expression of a human Na+/H+ antiporter gene transfected into antiporter-deficient mouse L cells. Proc Natl Acad Sci U S A. 1986;83(24):9388-92.

264. Denker SP, Huang DC, Orlowski J, Furthmayr H, Barber DL. Direct binding of the Na--H exchanger NHE1 to ERM proteins regulates the cortical cytoskeleton and cell shape independently of H(+) translocation. Mol Cell. 2000;6(6):1425-36.

265. Thomas AC, Williams H, Seto-Salvia N, Bacchelli C, Jenkins D, O'Sullivan M, et al. Mutations in SNX14 cause a distinctive autosomal-recessive cerebellar ataxia and intellectual disability syndrome. Am J Hum Genet. 2014;95(5):611-21.

266. Sousa SB, Ramos F, Garcia P, Pais RP, Paiva C, Beales PL, et al. Intellectual disability, coarse face, relative macrocephaly, and cerebellar hypotrophy in two sisters. Am J Med Genet A. 2014;164a(1):10-4.

267. Akizu N, Cantagrel V, Zaki MS, Al-Gazali L, Wang X, Rosti RO, et al. Biallelic mutations in SNX14 cause a syndromic form of cerebellar atrophy and lysosome-autophagosome dysfunction. Nat Genet. 2015;47(5):528-34.

268. Carroll P, Renoncourt Y, Gayet O, De Bovis B, Alonso S. Sorting nexin-14, a gene expressed in motoneurons trapped by an in vitro preselection method. Dev Dyn. 2001;221(4):431-42.

269. Shukla A, Upadhyai P, Shah J, Neethukrishna K, Bielas S, Girisha KM. Autosomal recessive spinocerebellar ataxia 20: Report of a new patient and review of literature. European Journal of Medical Genetics. 2017;60(2):118-23.

270. Schmidt WM, Rutledge SL, Schule R, Mayerhofer B, Zuchner S, Boltshauser E, et al. Disruptive SCYL1 Mutations Underlie a Syndrome Characterized by Recurrent Episodes of Liver Failure, Peripheral Neuropathy, Cerebellar Atrophy, and Ataxia. Am J Hum Genet. 2015;97(6):855-61.

271. Kato M, Yano K, Morotomi-Yano K, Saito H, Miki Y. Identification and characterization of the human protein kinase-like gene NTKL: mitosis-specific centrosomal localization of an alternatively spliced isoform. Genomics. 2002;79(6):760-7.

272. Liu SC, Lane WS, Lienhard GE. Cloning and preliminary characterization of a 105 kDa protein with an N-terminal kinase-like domain. Biochim Biophys Acta. 2000;1517(1):148-52.

273. Kawarai T, Tajima A, Kuroda Y, Saji N, Orlacchio A, Terasawa H, et al. A homozygous mutation of VWA3B causes cerebellar ataxia with intellectual disability. J Neurol Neurosurg Psychiatry. 2016;87(6):656-62.

274. Gomez-Herreros F, Schuurs-Hoeijmakers JH, McCormack M, Greally MT, Rulten S, Romero-Granados R, et al. TDP2 protects transcription from abortive topoisomerase activity and is required for normal neural function. Nat Genet. 2014;46(5):516-21.

275. Ledesma FC, El Khamisy SF, Zuma MC, Osborn K, Caldecott KW. A human 5[prime]-tyrosyl DNA phosphodiesterase that repairs topoisomerase-mediated DNA damage. Nature. 2009;461(7264):674-8.

276. Pype S, Declercq W, Ibrahimi A, Michiels C, Van Rietschoten JG, Dewulf N, et al. TTRAP, a novel protein that associates with CD40, tumor necrosis factor (TNF) receptor-75 and TNF receptor-associated factors (TRAFs), and that inhibits nuclear factor-kappa B activation. J Biol Chem. 2000;275(24):18586-93.

277. Duan R, Shi Y, Yu L, Zhang G, Li J, Lin Y, et al. UBA5 Mutations Cause a New Form of Autosomal Recessive Cerebellar Ataxia. PLoS One. 2016;11(2):e0149039.

278. Komatsu M, Chiba T, Tatsumi K, Iemura S, Tanida I, Okazaki N, et al. A novel protein-conjugating system for Ufm1, a ubiquitin-fold modifier. Embo j. 2004;23(9):1977-86.

279. Dou T, Gu S, Liu J, Chen F, Zeng L, Guo L, et al. Isolation and characterization of ubiquitin-activating enzyme E1-domain containing 1, UBE1DC1. Mol Biol Rep. 2005;32(4):265-71.

280. Sanal O, Wei S, Foroud T, Malhotra U, Concannon P, Charmley P, et al. Further mapping of an ataxia-telangiectasia locus to the chromosome 11q23 region. Am J Hum Genet. 1990;47(5):860-6.

281. Woods CG, Taylor AM. Ataxia telangiectasia in the British Isles: the clinical and laboratory features of 70 affected individuals. Q J Med. 1992;82(298):169-79.

282. Savitsky K, Bar-Shira A, Gilad S, Rotman G, Ziv Y, Vanagaite L, et al. A single ataxia telangiectasia gene with a product similar to PI-3 kinase. Science. 1995;268(5218):1749-53.

283. Uziel T, Savitsky K, Platzer M, Ziv Y, Helbitz T, Nehls M, et al. Genomic Organization of the ATM gene. Genomics. 1996;33(2):317-20.

284. Gatti RA, Berkel I, Boder E, Braedt G, Charmley P, Concannon P, et al. Localization of an ataxia-telangiectasia gene to chromosome 11q22-23. Nature. 1988;336(6199):577-80.

285. Hawley RS, Friend SH. Strange bedfellows in even stranger places: the role of ATM in meiotic cells, lymphocytes, tumors, and its functional links to p53. Genes Dev. 1996;10(19):2383-8.

286. Banin S, Moyal L, Shieh S, Taya Y, Anderson CW, Chessa L, et al. Enhanced phosphorylation of p53 by ATM in response to DNA damage. Science. 1998;281(5383):1674-7.

287. Canman CE, Lim DS, Cimprich KA, Taya Y, Tamai K, Sakaguchi K, et al. Activation of the ATM kinase by ionizing radiation and phosphorylation of p53. Science. 1998;281(5383):1677-9.

288. Lim DS, Kirsch DG, Canman CE, Ahn JH, Ziv Y, Newman LS, et al. ATM binds to beta-adaptin in cytoplasmic vesicles. Proc Natl Acad Sci U S A. 1998;95(17):10146-51.

289. Banga SS, Shenkar R, Boyd JB. Hypersensitivity of Drosophila mei-41 mutants to hydroxyurea is associated with reduced mitotic chromosome stability. Mutat Res. 1986;163(2):157-65.

290. Baker BS, Boyd JB, Carpenter AT, Green MM, Nguyen TD, Ripoll P, et al. Genetic controls of meiotic recombination and somatic DNA metabolism in Drosophila melanogaster. Proc Natl Acad Sci U S A. 1976;73(11):4140-4.

291. Hernandez D, McConville CM, Stacey M, Woods CG, Brown MM, Shutt P, et al. A family showing no evidence of linkage between the ataxia telangiectasia gene and chromosome 11q22-23. J Med Genet. 1993;30(2):135-40.

292. Stewart GS, Maser RS, Stankovic T, Bressan DA, Kaplan MI, Jaspers NG, et al. The DNA double-strand break repair gene hMRE11 is mutated in individuals with an ataxia-telangiectasia-like disorder. Cell. 1999;99(6):577-87.

293. Paull TT, Gellert M. The 3' to 5' exonuclease activity of Mre 11 facilitates repair of DNA double-strand breaks. Mol Cell. 1998;1(7):969-79.

294. Trujillo KM, Yuan SS, Lee EY, Sung P. Nuclease activities in a complex of human recombination and DNA repair factors Rad50, Mre11, and p95. J Biol Chem. 1998;273(34):21447-50.

295. Lagier-Tourenne C, Tranebaerg L, Chaigne D, Gribaa M, Dollfus H, Silvestri G, et al. Homozygosity mapping of Marinesco-Sjogren syndrome to 5q31. Eur J Hum Genet. 2003;11(10):770-8.

296. Anttonen AK, Mahjneh I, Hamalainen RH, Lagier-Tourenne C, Kopra O, Waris L, et al. The gene disrupted in Marinesco-Sjogren syndrome encodes SIL1, an HSPA5 cochaperone. Nat Genet. 2005;37(12):1309-11.

297. Senderek J, Krieger M, Stendel C, Bergmann C, Moser M, Breitbach-Faller N, et al. Mutations in SIL1 cause Marinesco-Sjogren syndrome, a cerebellar ataxia with cataract and myopathy. Nat Genet. 2005;37(12):1312-4.

298. Chung KT, Shen Y, Hendershot LM. BAP, a mammalian BiP-associated protein, is a nucleotide exchange factor that regulates the ATPase activity of BiP. J Biol Chem. 2002;277(49):47557-63.

299. Takahata T, Yamada K, Yamada Y, Ono S, Kinoshita A, Matsuzaka T, et al. Novel mutations in the SIL1 gene in a Japanese pedigree with the Marinesco-Sjogren syndrome. J Hum Genet. 2010;55(3):142-6.

300. Tyson JR, Stirling CJ. LHS1 and SIL1 provide a lumenal function that is essential for protein translocation into the endoplasmic reticulum. Embo j. 2000;19(23):6440-52.

301. Dor T, Cinnamon Y, Raymond L, Shaag A, Bouslam N, Bouhouche A, et al. KIF1C mutations in two families with hereditary spastic paraparesis and cerebellar dysfunction. J Med Genet. 2014;51(2):137-42.

302. Bouslam N, Bouhouche A, Benomar A, Hanein S, Klebe S, Azzedine H, et al. A novel locus for autosomal recessive spastic ataxia on chromosome 17p. Hum Genet. 2007;121(3-4):413-20.

303. Novarino G, Fenstermaker AG, Zaki MS, Hofree M, Silhavy JL, Heiberg AD, et al. Exome sequencing links corticospinal motor neuron disease to common neurodegenerative disorders. Science. 2014;343(6170):506-11.

304. Dorner C, Ciossek T, Muller S, Moller PH, Ullrich A, Lammers R. Characterization of KIF1C, a new kinesin-like protein involved in vesicle transport from the Golgi apparatus to the endoplasmic reticulum. J Biol Chem. 1998;273(32):20267-75.

305. Thiffault I, Rioux MF, Tetreault M, Jarry J, Loiselle L, Poirier J, et al. A new autosomal recessive spastic ataxia associated with frequent white matter changes maps to 2q33-34. Brain. 2006;129(Pt 9):2332-40.

306. Bayat V, Thiffault I, Jaiswal M, Tetreault M, Donti T, Sasarman F, et al. Mutations in the mitochondrial methionyl-tRNA synthetase cause a neurodegenerative phenotype in flies and a recessive ataxia (ARSAL) in humans. PLoS Biol. 2012;10(3):e1001288.

307. Spencer AC, Heck A, Takeuchi N, Watanabe K, Spremulli LL. Characterization of the human mitochondrial methionyl-tRNA synthetase. Biochemistry. 2004;43(30):9743-54.

308. Crosby AH, Patel H, Chioza BA, Proukakis C, Gurtz K, Patton MA, et al. Defective mitochondrial mRNA maturation is associated with spastic ataxia. Am J Hum Genet. 2010;87(5):655-60.

309. Wilson WC, Hornig-Do HT, Bruni F, Chang JH, Jourdain AA, Martinou JC, et al. A human mitochondrial poly(A) polymerase mutation reveals the complexities of post-transcriptional mitochondrial gene expression. Hum Mol Genet. 2014;23(23):6345-55.

310. Lapkouski M, Hallberg BM. Structure of mitochondrial poly(A) RNA polymerase reveals the structural basis for dimerization, ATP selectivity and the SPAX4 disease phenotype. Nucleic Acids Research. 2015;43(18):9065-75.

311. Pierson TM, Adams D, Bonn F, Martinelli P, Cherukuri PF, Teer JK, et al. Whole-exome sequencing identifies homozygous AFG3L2 mutations in a spastic ataxia-neuropathy syndrome linked to mitochondrial m-AAA proteases. PLoS Genet. 2011;7(10):e1002325.

312. Muona M, Berkovic SF, Dibbens LM, Oliver KL, Maljevic S, Bayly MA, et al. A recurrent de novo mutation in KCNC1 causes progressive myoclonus epilepsy. Nat Genet. 2015;47(1):39-46.

313. Baets J, Deconinck T, Smets K, Goossens D, Van den Bergh P, Dahan K, et al. Mutations in SACS cause atypical and late-onset forms of ARSACS. Neurology. 2010;75(13):1181-8.

314. Bouchard JP, Barbeau A, Bouchard R, Bouchard RW. Autosomal recessive spastic ataxia of Charlevoix-Saguenay. Can J Neurol Sci. 1978;5(1):61-9.

315. Richter A, Rioux JD, Bouchard JP, Mercier J, Mathieu J, Ge B, et al. Location score and haplotype analyses of the locus for autosomal recessive spastic ataxia of Charlevoix-Saguenay, in chromosome region 13q11. Am J Hum Genet. 1999;64(3):768-75.

316. Parfitt DA, Michael GJ, Vermeulen EG, Prodromou NV, Webb TR, Gallo JM, et al. The ataxia protein sacsin is a functional co-chaperone that protects against polyglutamine-expanded ataxin-1. Hum Mol Genet. 2009;18(9):1556-65.

317. Takashima H, Boerkoel CF, John J, Saifi GM, Salih MA, Armstrong D, et al. Mutation of TDP1, encoding a topoisomerase I-dependent DNA damage repair enzyme, in spinocerebellar ataxia with axonal neuropathy. Nat Genet. 2002;32(2):267-72.

318. El-Khamisy SF, Saifi GM, Weinfeld M, Johansson F, Helleday T, Lupski JR, et al. Defective DNA single-strand break repair in spinocerebellar ataxia with axonal neuropathy-1. Nature. 2005;434(7029):108-13.

319. Pouliot JJ, Yao KC, Robertson CA, Nash HA. Yeast gene for a Tyr-DNA phosphodiesterase that repairs topoisomerase I complexes. Science. 1999;286(5439):552-5.

320. Interthal H, Pouliot JJ, Champoux JJ. The tyrosyl-DNA phosphodiesterase Tdp1 is a member of the phospholipase D superfamily. Proc Natl Acad Sci U S A. 2001;98(21):12009-14.

321. Knight MA, Gardner RJ, Bahlo M, Matsuura T, Dixon JA, Forrest SM, et al. Dominantly inherited ataxia and dysphonia with dentate calcification: spinocerebellar ataxia type 20. Brain. 2004;127(Pt 5):1172-81.

322. Lorenzo DN, Forrest SM, Ikeda Y, Dick KA, Ranum LP, Knight MA. Spinocerebellar ataxia type 20 is genetically distinct from spinocerebellar ataxia type 5. Neurology. 2006;67(11):2084-5.

323. Knight MA, Hernandez D, Diede SJ, Dauwerse HG, Rafferty I, van de Leemput J, et al. A duplication at chromosome 11q12.2-11q12.3 is associated with spinocerebellar ataxia type 20. Hum Mol Genet. 2008;17(24):3847-53.

324. Bisogno T, Howell F, Williams G, Minassi A, Cascio MG, Ligresti A, et al. Cloning of the first sn1-DAG lipases points to the spatial and temporal regulation of endocannabinoid signaling in the brain. J Cell Biol. 2003;163(3):463-8.

325. Ishikawa K, Nagase T, Suyama M, Miyajima N, Tanaka A, Kotani H, et al. Prediction of the coding sequences of unidentified human genes. X. The complete sequences of 100 new cDNA clones from brain which can code for large proteins in vitro. DNA Res. 1998;5(3):169-76.

326. Storey E, Bahlo M, Fahey M, Sisson O, Lueck CJ, Gardner RJ. A new dominantly inherited pure cerebellar ataxia, SCA 30. J Neurol Neurosurg Psychiatry. 2009;80(4):408-11.

327. Nagase T, Kikuno R, Ishikawa K, Hirosawa M, Ohara O. Prediction of the coding sequences of unidentified human genes. XVII. The complete sequences of 100 new cDNA clones from brain which code for large proteins in vitro. DNA Res. 2000;7(2):143-50.

328. Jiang H, Zhu HP, Gomez CM. SCA32: An autosomal dominant cerebellar ataxia with azoospermia maps to chromosome 7q32-q33. Movement Disorders. 2010;25(7):S192-S.

329. Zhu HP, Jiang H, Du XF, Frutiger SA, Pryor JL, Roe CA, et al. Mutation of PODXL, a Cell Surface and Mitochondrial Protein, Underlies Azoospermia and Neurodegeneration in Spinocerebellar Ataxia Type 32 (SCA32). Neurology. 2011;76(9):A21-A.

330. Ray D, Kazan H, Cook KB, Weirauch MT, Najafabadi HS, Li X, et al. A compendium of RNA-binding motifs for decoding gene regulation. Nature. 2013;499(7457):172-7.

331. Lindeboom RGH, Supek F, Lehner B. The rules and impact of nonsense-mediated mRNA decay in human cancers. Nature Genetics. 2016;48(10):1112-8.